METHODS OF BIOCHEMICAL ANALYSIS

Volume 32

Advisory Board

N.G. ANDERSON, *Division of Biological and Medical Research, Argonne National Laboratories, Argonne, IL 60439*

T.H. BÜCHER, *Institute of Physiological Chemistry, and Physical Biochemistry and Cell Biology, University of Munich, 8000 Munich 2, West Germany*

W.E. COHN, *Oak Ridge National Laboratory, Oak Ridge, TN 37830*

P. DOUZOU, *Institute of Physico-Chemical Biology, Edmond de Rothschild Foundation, Paris 75005, France*

S. GATT, *Department of Biochemistry, Hebrew University—Hadassah Medical School, Jerusalem, Israel*

C. JOLICOEUR, *Department of Chemistry, University of Sherbrooke, Sherbrooke, Québec, J1K2R1, Canada*

J.H.R. KÄGI, *Biochemical Institute, University of Zurich, Zurich 8032, Switzerland.*

R.W. LUMRY, *Department of Chemistry, University of Minnesota, Minneapolis, MN 55455*

B.G. MALMSTRÖM, *Department of Biochemistry and Biophysics, Chalmers University of Technology, S-412 96 Göteborg, Sweden*

A. MEISTER, *Department of Biochemistry, Cornell Medical College, New York, NY 10021*

R.S. MELVILLE, *Bureau of Medical Services, Food and Drug Administration, Retired, 11112 Kenilworth, Garrett Park, MD 20896*

M. OTTESEN, *Chemical Department, The Carlsberg Research Center, DK2500 Copenhagen, Valby, Denmark*

J.E. SCOTT, *Department of Medical Biochemistry, University of Manchester, Manchester M139PT, England*

E.C. SLATER, *Laboratory of Biochemistry, B.C.P. Jansen Institute University of Amsterdam, Amsterdam-C., The Netherlands*

B.L. VALLEE, *Center for Biochemical and Biophysical Sciences and Medicine, Harvard University, Boston, MA 02115*

P. VENETIANER, *Institute of Biochemistry, Hungarian Academy of Sciences, Szeged 6701, Hungary*

M. WIKSTRÖM, *Department of Medical Chemistry, University of Helsinki, SF 00170 Helsinki 17, Finland*

K. YAGI, *Institute of Applied Biochemistry, Yagi Memorial Park, Mitake, Gifu 505-01, Japan*

METHODS OF BIOCHEMICAL ANALYSIS

Edited by DAVID GLICK

Cancer Biology Research Laboratory
Stanford University Medical Center
Stanford, California

VOLUME 32

An Interscience Publication
JOHN WILEY & SONS
New York • Chichester • Brisbane • Toronto • Singapore

An Interscience ® Publication

Copyright © 1987 by John Wiley & Sons, Inc.

All rights reserved. Published simultaneously in Canada.

Reproduction or translation of any part of this work beyond that permitted by Section 107 or 108 of the 1976 United States Copyright Act without the permission of the copyright owner is unlawful. Requests for permission or further information should be addressed to the Permissions Department, John Wiley & Sons, Inc.

Library of Congress Catalogue Card Number: 54-7232

ISBN 0-471-82195-0

Printed in the United States of America

10 9 8 7 6 5 4 3 2 1

PREFACE

Annual review volumes dealing with many different fields of science have proved their value repeatedly and are now widely used and well established. These reviews have been concerned not only with the results in the developing fields but also with the techniques and methods employed, and they have served to keep the ever-expanding scene within the view of the investigator, applier, the teacher, and the student.

It is particularly important that review services of this nature should include the area of methods and techniques because it is becoming increasingly difficult to keep abreast of the manifold experimental innovations and improvements which constitute the limiting factor in many cases for the growth of the experimental sciences. Concepts and vision of creative scientists far outrun that which can actually be attained in present practice. Therefore, an emphasis on methodology and instrumentation is a fundamental need in order for material achievement to keep in sight of the advance of useful ideas.

The volumes in this series are designed to try to meet the need in the field of biochemical analysis. The topics to be included are chemical, physical, microbiological, and if necessary, animal assays, as well as basic techniques and instrumentation for the determination of enzymes, vitamins, hormones, lipids, carbohydrates, proteins and their products, minerals, antimetabolites, and so on.

Certain chapters will deal with well-established methods or techniques which have undergone sufficient improvement to merit recapitulation, reappraisal, and new recommendations. Other chapters will be concerned with essentially new approaches which bear promise of great usefulness. Relatively few subjects can be included in any single volume, but as they accumulate, these volumes should comprise a self-modernizing encyclopedia of methods of biochemical analysis. By judicious selection of topics it is planned that most subjects of current importance will receive treatment in these volumes.

The general plan followed in the organization of the individual chapters is a discussion of the background and previous work, a critical evaluation of the various approaches, and a presentation of the procedural

details of the method or methods recommended by the author. The presentation of the experimental details is to be given in a manner that will furnish the laboratory worker with the complete information required to carry out the analysis.

Within this comprehensive scheme the reader may note that the treatments vary widely with respect to taste, and point of view. It is the Editor's policy to encourage individual expression in these presentations because it is stifling to originality and justifiably annoying to many authors to submerge themselves in a standard mold. Scientific writing need not be as dull and uniform as it too often is. In certain technical details a consistent pattern is followed for the sake of convenience, as in the form used for reference citations and indexing.

The success of the treatment of any topic will depend primarily on the experience, critical ability, and capacity to communicate of the author. Those invited to prepare the respective chapters are scientists who either have originated the methods they discuss or have had intimate personal experience with them.

It is the wish of the Advisory Board and the Editor to make this series of volumes as useful as possible and to this end suggestions will be always welcome.

DAVID GLICK

CONTENTS

METHODS OF BIOCHEMICAL ANALYSIS

Volume 32

Methods of Biochemical Analysis, Volume 32
Edited by David Glick
Copyright © 1987 by John Wiley & Sons, Inc.

METHODS OF BIOCHEMICAL ANALYSIS VOLUME 32

Activator Proteins for Lysosomal Glycolipid Hydrolysis

ERNST CONZELMANN AND KONRAD SANDHOFF, *Institut für Organische Chemie und Biochemie der Universität, Bonn, Federal Republic of Germany*

I. INTRODUCTION

In 1964 Mehl and Jatzkewitz (1964) observed that after fractionation by free-flow electrophoresis a crude preparation of porcine arylsulfatase A had lost its ability to hydrolyze sulfatide (sulfogalactosylceramide) in the absence of detergents but remained fully active toward the water-

soluble artificial substrates. Addition of another fraction, which was enzymically inactive, to the assay restored the activity against the glycolipid. This effect could later be attributed to a small, acidic glycoprotein. A similar cofactor that promotes sulfatide catabolism was then shown to exist also in normal human liver as well as in tissues from patients with metachromatic leukodystrophy (Jatzkewitz and Stinshoff, 1973) and was designated as the "activator of cerebroside sulfatase." Although the name may be somewhat misleading because the cofactor does not "activate" the enzyme, such protein cofactors for the degradation of lipid substrates by lysosomal hydrolases are now generally referred to as "activator proteins."

The activator of cerebroside sulfatase (or "sulfatide activator") was purified by Fischer and Jatzkewitz (1975) from human liver and identified as a water-soluble glycoprotein with an isoelectric point at pH 4.3 and a molecular weight of approximately 22,000 Daltons. From kinetic and binding experiments and from the fact that this cofactor stimulated only the degradation of lipid substrates but not of artificial water-soluble ones, these authors concluded that the cofactor serves to solubilize the lipid by binding to it and extracting it from the membrane (or micelle). The resulting activator/lipid complex was assumed to be the true substrate of the enzymic reaction (Fischer and Jatzkewitz, 1977, 1978).

Li and coworkers (Li, Y.-T., et al., 1973; Li, S.-C., and Li, Y.-T., 1976) found that the enzymic hydrolysis of gangliosides G_{M1} and G_{M2} by β-galactosidase and β-hexosaminidase A, respectively, and of globotriaosylceramide by α-galactosidase A also requires the presence of low molecular weight protein cofactors. However, the protein cofactor they isolated was later shown to mediate the degradation of globotriaosylceramide and ganglioside G_{M1} but not of ganglioside G_{M2} and recently turned out to be identical with the sulfatide activator (Inui et al., 1983; Li, S.-C., et al., 1985).

The hydrolysis of ganglioside G_{M2} and related glycosphingolipids (e.g., glycolipid G_{A2}) by β-hexosaminidase A depends on the presence of another activator protein, the "G_{M2} activator" (Conzelmann and Sandhoff, 1978, 1979; Conzelmann et al., 1982), which has similar properties as the sulfatide activator but differs in glycolipid and enzyme specificity. The two proteins are encoded on different chromosomes (G_{M2} activator on chromosome 5 [Burg et al., 1985a], sulfatide activator on chromosome 10 [Inui et al., 1985]) and do not cross-react immunochemically (Li, S.-C., et al., 1979). The G_{M2} activator is also a glycoprotein, with a molecular weight of approximately 22,000 Daltons (Conzelmann et al., 1982; Burg et al., 1985b). On subcellular fractionation it codistributes with the lysosomal marker enzyme β-hexosaminidase

(Banerjee et al., 1984) and, like most other lysosomal proteins studied so far, is synthesized as a form with a slightly higher molecular weight (~ 24,000 Daltons [Burg et al., 1985b]), which is probably the precursor of the mature form.

Studies on the mechanism by which the G_{M2} activator promotes the enzymic degradation of lipid substrates (Conzelmann and Sandhoff, 1979; Conzelmann et al., 1982) demonstrated that this activator binds to ganglioside G_{M2} and solubilizes it as a water-soluble complex with a molar ratio of one glycolipid molecule per protein. Other related glycolipids are also bound but much less strongly. This complex formation is reversible, and hence the G_{M2} activator acts, at least in vitro, also as a glycolipid transfer protein (Conzelmann et al., 1982). Hexosaminidase A does not interact with the membrane-bound ganglioside. Instead, the G_{M2} activator protein binds to the ganglioside G_{M2} and extracts it from the membrane to form a water-soluble complex. This complex then recognizes a specific binding site on the alpha subunit of β-hexosaminidase A (Kytzia and Sandhoff, 1985) and binds in such a way that the terminal *N*-acetylgalactosamine moiety is correctly positioned for the enzymic hydrolysis of the glycosidic bond. The resulting ganglioside G_{M3}/activator complex dissociates then and the activator is set free for another round of catalysis.

The physiological significance of this kind of activator protein is demonstrated by two fatal lipid storage diseases that are caused by deficiencies of activator proteins rather than of the degrading enzymes: variant AB of infantile G_{M2} gangliosidosis results from a defect of the G_{M2} activator protein (Conzelmann and Sandhoff, 1978; Hechtman et al., 1982; Hirabayashi et al., 1983), whereas a deficiency of the sulfatide/G_{M1} activator leads to an atypical variant of juvenile metachromatic leukodystrophy (Stevens et al., 1981; Inui et al., 1983).

The specific interaction between β-hexosaminidase A and the G_{M2} activator has also been taken into account in the development of assay systems for ganglioside G_{M2} hydrolysis by extracts of cultured skin fibroblasts (Erzberger et al., 1980; Conzelmann et al., 1983). With such assays the residual activities in cells from patients with different variants of G_{M2} gangliosidosis could be determined very precisely (Conzelmann et al., 1983).

A basically different type of protein cofactor for lysosomal glycolipid hydrolases was described by Ho and O'Brien (1971) for acid β-glucosidase (glucosylceramidase). This factor accelerates the hydrolysis of glucosylceramide as well as of water-soluble artificial substrates by lysosomal β-glucosidase. It also seems to have an activating effect on acid sphingomyelinase and on galactosylceramide β-galactosidase (Christo-

manou, 1980; Wenger, et al., 1982). Unlike the activator proteins described earlier, this cofactor does not bind to the substrate (Berent and Radin, 1981a) but activates the enzyme itself. However, some controversy still persists as to the nature and the physiological relevance of this type of protein cofactor: the preparations isolated by various groups from different sources differ widely in specific activity (Peters et al., 1977a; Iyer et al., 1983), molecular weight (Ho and O'Brien, 1971; Peters et al., 1977a,b; Wenger and Roth, 1982), and extent and necessity of glycosylation (Ho and O'Brien, 1971; Peters et al., 1977a; Berent and Radin, 1981b).

Recently it was also found that when the natural substrate, glucosylceramide, is incorporated into phospholipid bilayers, together with a certain amount of acidic phospholipids such as phosphatidic acid, a high activity of glucosylceramidase is attained without the need for any activating protein cofactor (Sarmientos et al., 1986).

A new type of glucosylceramidase cofactor has recently been described by Vaccaro et al. (1985). This protein, which seems to be tightly associated with the enzyme, stimulates the hydrolysis of glucosylceramide but not that of the water-soluble substrate. Similarly two small proteins that stimulate specifically lysosomal sphingomyelinase were recently observed by Christomanou and Kleinschmidt (1985). In both cases it is, however, still too early to speculate on the role and significance of these proteins.

II. ASSAYS FOR ACTIVATOR PROTEINS

The quantification of activator proteins is generally based on their capability to stimulate in vitro the degradation of glycolipids by the corresponding hydrolases. The relation between concentration of activator in the assay mixture and resulting reaction rate is linear only within certain limits that depend not only on the reaction catalyzed and on the type of activator protein but also on the precise assay conditions.

Those activator proteins that promote the hydrolysis of glycolipid substrates by water-soluble hydrolases, namely the G_{M2} activator and the sulfatide activator, seem to act by similar mechanisms: they bind the glycolipid and extract it from the membrane to form a water-soluble complex that is the true substrate for the enzyme. Accordingly, the reaction rate depends on the concentration of the activator-lipid complex, with Michaelis-Menten-type saturation kinetics (Conzelmann and Sandhoff, 1979). Such a saturation curve is at no point exactly linear, but for practical purposes sufficient linearity can be assumed at activator concentrations below the K_M value of the enzyme for the respective activator-lipid complex as substrate.

It should also be considered that the formation of the complex between activator and lipid is an equilibrium reaction with a finite dissociation constant. Under the conditions used for the quantification of activators—that is, with pure glycolipid substrates at concentrations well above the K_D of the respective activator-lipid complex—the activator can be assumed to be saturated with the lipid, so that the activator concentration practically equals the concentration of the substrate of the reaction (the activator-lipid complex). However, the presence of other lipids such as phospholipids in the assay mixture may increase the experimental K_D by orders of magnitude since the mixed aggregates formed may be much more stable than the pure glycolipid micelles. (At a large excess of phospholipids as in the case of liposome-bound substrate, the K_D may depend linearly on the phospholipid concentration.) As a consequence the concentration of the activator-lipid complex may be far below the total activator concentration, and the enzymic reaction will accordingly be much slower than with pure glycolipid substrates.

Since, as in simple Michaelis-Menten kinetics, the reaction rate depends linearly on the enzyme concentration, the accuracy of activator determinations depends on the precision with which the enzyme concentration is known. Although it is not necessary to employ pure enzymes for the purpose of activator quantification, problems may arise if several isoenzymes exist of which only one is able to degrade the glycolipid substrate in the presence of the activator but all of them hydrolyze the artificial substrates employed for measuring the enzyme. This is, for example, the case for α-galactosidase, β-hexosaminidase, and arylsulfatase. In these cases separation of the isoenzymes, say by ion-exchange chromatography, is required.

It should also be noted that the Michaelis-Menten equation was derived under the assumption that the substrate concentration is always much higher than the enzyme concentration. This condition may not be met when the substrates involve macromolecules such as proteins. Thus at a low activator or high enzyme concentration some deviation from linearity may be encountered.

The mechanisms by which the cofactors for degradation of glucosylceramide and galactosylceramide stimulate the respective enzymes is not yet known. Quantification of these cofactors by their capacity to enhance enzymic glycolipid hydrolysis in vitro must therefore rely entirely on practical experiences. These will be discussed with the respective assay systems.

As noted before, it is usually not necessary to use highly purified enzymes. In most cases partially purified preparations will do, provided that they are sufficiently concentrated, essentially free of endogenous

activator, and contain only the one isoenzyme that does interact with the activator-lipid complex (or the isoenzyme composition is known, and the results can be corrected for it). For the water-soluble enzymes, satisfactory preparations can be obtained by affinity chromatography on Concanavalin A-Sepharose, followed by ion-exchange chromatography and, in some cases, gel filtration. A major exception is arylsulfatase A, which has to be quite pure since the degradation of sulfatide in the presence of the sulfatide activator is inhibited by many contaminating proteins (Fischer and Jatzkewitz, 1975). The membrane-associated enzymes glucosylceramide β-glucosidase and galactosylceramide β-galactosidase require solubilization with detergents prior to any chromatographic separation.

Activator proteins can also be quantified with immunochemical techniques if suitable antisera are available. Enzyme-linked immunosorbent assays (ELISA) have been developed for the sulfatide/G_{M1} activator (Gardas et al., 1984) and for the G_{M2} activator (Banerjee et al., 1984). The ELISA for the G_{M2} activator was more than 10 times as sensitive as enzymic assays and permitted the precise determination of G_{M2} activator in very dilute samples such as subcellular fractions of cultured skin fibroblasts (Banerjee et al., 1984).

1. Sulfatide/G_{M1} Activator

The sulfatide activator promotes, at least in vitro, several reactions. In principle, any one of them can be used to assay for this cofactor, but the degradation of ganglioside G_{M1} by β-galactosidase is most conveniently used since this reaction proceeds fast enough to permit sensitive measurements of activator content and is the least sensitive to disturbances by impurities. Globotriaosylceramide is much more tedious to prepare in pure form than ganglioside G_{M1}. Degradation of sulfatide by arylsulfatase A is comparatively slow and may be strongly inhibited by contaminating proteins and other compounds so that the assay requires the use of highly purified enzyme and activator. Reliable quantitation of the activator during purification is therefore not possible with this assay (Fischer and Jatzkewitz, 1975).

A. ASSAY WITH GANGLIOSIDE G_{M1}/β-GALACTOSIDASE

1. Substrate. Ganglioside G_{M1} can be purified from brain lipid extracts by any one of several published methods (Svennerholm, 1972; Kundu, 1981; Ledeen and Yu, 1982). The yield of ganglioside G_{M1} can be increased several fold by converting higher gangliosides into ganglioside G_{M1} with sialidase: The crude ganglioside preparation (e.g., the

Folch upper phase [Folch et al., 1957]) is taken to dryness and dissolved in 50 m*M* acetate buffer, pH 5.5, 1 m*M* $CaCl_2$, and incubated overnight with sialidase from clostridium perfringens (10 units/liter) (G. Schwarzmann, personal communication).

For measuring its enzymic degradation, the substrate is most conveniently labeled in the terminal galactose moiety by the galactose oxidase/[^{3}H]borohydride method of Radin (1972a), for example, as modified by Suzuki, K. (1977). (The reduction step of this procedure should be carried out at a pH value below 10. At a more alkaline pH some of the ganglioside G_{M1} is converted to a highly labeled product with the chromatographic mobility of ganglioside G_{M2}.)

Final purification of the labeled product is usually done by column chromatography according to Svennerholm (1972). If only small amounts of labeled ganglioside are needed, purification by preparative thin-layer chromatography is more convenient: the ganglioside solution in organic solvent is applied to a thin-layer plate (e.g., Merck Kieselgel G 60, 0.25 mm thickness) in a 16-cm wide streak. Analytical plates are preferable over preparative ones since they give a much better resolution. Up to 5 mg of lipid can be applied to one plate. The plate is developed in chloroform/methanol/15 m*M* aq $CaCl_2$ (55/45/10 by volume). Radioactive bands are located with a radioscanner, the plate is lightly sprayed with water, and the area containing the [^{3}H]ganglioside G_{M1} is scraped off. (If water is sprayed until the plate starts to become translucent, the lipid may be visible as a white band on a darker background.) The scrapings are suspended in 5 ml chloroform/methanol/water (55/45/10 by volume), packed into a suitable column (e.g., a large Pasteur pipette with glass wool plug) and eluted with 2 × 5 ml of the same solvent. The solvent is then evaporated under a stream of N_2, the dry residue is taken up in distilled water (~1 ml/mg lipid), dialyzed against distilled water and lyophilized.

The specific radioactivity of the product is best determined by measuring sialic acid content, for example, by the modification of Miettinen and Takki-Luukkainen (1959) of the method of Svennerholm (1957). Simply weighing the product may give wrong values due to the presence of some silicic acid.

2. β-Galactosidase. Lysosomal β-galactosidase can be purified from human liver or placenta with conventional methods (Meisler, 1972; Sloan, 1972; Miyatake and Suzuki, 1975) or with affinity chromatography on immobilized *p*-aminophenyl- or 6-aminohexyl-thio-β-D-galactoside (Miller et al., 1977; Lo et al., 1979). The most rapid and convenient procedure seems to be the two-step method of Miller et al. (1977), which is reported to give a more than 20,000-fold purification with 41% yield. The affinity gel is commercially available.

The activity of β-galactosidase is usually measured with the fluorogenic substrate 4-methylumbelliferyl-β-D-galactoside, for example, 1 m*M* in 50 m*M* citrate/0.1 *M* phosphate buffer, pH 4.0, with 0.1 *M* NaCl (Suzuki, K., 1977). (The high ionic strength is needed to stabilize the enzyme.) One unit of β-galactosidase is generally defined as the amount of enzyme that splits 1 μmol of this substrate per minute under the above conditions, at 37°C.

3. Assay. The standard assay mixture for determination of the activator consists of 1 nmol ganglioside G_{M1}, [^{3}H]-labeled in the terminal galactose moiety (~100,000 cpm), 5 mU β-galactosidase and up to 25 μl of the suitably diluted activator sample, in a total volume of 50 μl of 50 m*M* citrate buffer, pH 4.5. The assays are incubated for 1 h at 37°C and then transferred to an ice-bath, and 1 ml of an ice-cold 1 m*M* galactose solution is added. The mixtures are loaded onto small (0.5−1 ml) columns of DEAE-cellulose (in Pasteur pipettes) that have been washed with distilled water. Liberated [^{3}H]galactose is washed out with 2 × 1 ml of 1 m*M* aqueous galactose solution, the combined effluents are collected in scintillation vials, and, after addition of 10 ml of scintillation fluid, their radioactivity is measured in a liquid scintillation counter. Blanks run with water instead of activator solution are subtracted.

The reaction depends almost linearly on the activator concentration up to about 5 μ*M* (~ 5 μg of activator/assay). The K_D of the activator/lipid complex is approximately 3 μ*M* (Vogel, 1985) so that the activator can be assumed to be saturated with the lipid under the preceding conditions.

B. ASSAY WITH SULFATIDE/ARYLSULFATASE A

1. Substrate. Sulfatides are commercially available, but they can also be prepared from crude brain lipid extracts by one of the conventional procedures (Rouser et al., 1969; Kwiterovich et al., 1970; Yu and Ledeen, 1972).

Three different strategies have been proposed for the radiolabeling of sulfatides:

a. Catalytic reduction of the sphingoid base by the method of Schwarzmann (1978), such as modified by Raghavan et al. (1981).

b. Preparation of lysosulfatide (sulfogalactosylsphingosine) by alkaline hydrolysis of sulfatide and reacylation of the sphingosine amino group with a radioactive fatty acid (Dubois et al., 1980).

c. Biosynthetic labeling of sulfatide by injecting [^{35}S]sulfate into the brains of still myelinating laboratory animals and isolation of the sulfatide formed after one or two days (Mehl and Jatzkewitz, 1964; Fluharty et al., 1974).

The product of the latter procedure, [^{35}S]sulfatide, permits a simple quantitation of enzymic sulfatide hydrolysis, by extracting the liberated sulfate into the aqueous phase of a two-phase system. However, the short half-life of ^{35}S (87 days) limits the usefulness of this method.

Of the other two methods, both of which employ long-lived isotopes (^{3}H or ^{14}C), the first one is less tedious and gives better yields.

2. Arylsulfatase A. As noted before, the arylsulfatase A preparations used for assays with sulfatide and the natural activator protein have to be rather pure since contaminating proteins may interfere with this reaction in vitro. A variety of methods have been published for purification of the enzyme from human liver (Draper et al., 1976; James and Austin, 1979), kidney (Stinshoff, 1972), placenta (Gniot-Szulzycka and Komoszynski, 1970), and urine (Breslow and Sloan, 1972; Stevens et al., 1975). In our laboratory the procedure of Stinshoff (1972) is usually followed.

Arylsulfatase activity is usually measured with the chromogenic substrate 4-nitrocatecholsulfate. (A fluorogenic substrate, 4-methylumbelliferylsulfate, is also available but is less frequently used because it is hydrolyzed only very slowly.) The assay system of Baum et al. (1959), which was developed to permit the determination of arylsulfatase A in the presence of the B isoenzyme, is still most widely used. The unusual time course of the hydrolysis of 4-nitrocatecholsulfate by arylsulfatase A (Roy, 1953; Baum et al., 1958; Stinshoff, 1972) may present a problem for standardization of the enzyme preparation and should be taken into account, such as by using short incubation times (15–30 min). The enzyme unit is usually defined as the amount of enzyme that hydrolyzes 1 μmol of this substrate per minute.

3. Assay. The standard assay mixture consists of 5 nmol sulfatide, either ^{3}H-labeled in the sphingoid base or ^{14}C-labeled in the fatty acid, 5 mU arylsulfatase A, and an aliquot of the activator sample to be assayed in a total volume of 100 μl of 0.1 *M* sodium acetate buffer, pH 5.0, with 0.1 *M* NaCl. After incubation for 3 h at 37°C, the reaction is stopped by addition of 400 μl of chloroform/methanol (2:1 by volume), and after thorough mixing, phases are separated by centrifugation. The (aqueous) upper phase is discarded, the organic phase is washed with 200 μl theoretical upper phase (chloroform/methanol/water, 3:48:47 by volume) and then loaded onto a 0.5 ml column of DEAE-cellulose (in a Pasteur pipette) equilibrated with methanol. Unbound lipids are eluted with 2 ml methanol, collected in a scintillation vial, and their radioactivity is quantified by liquid scintillation counting. Blanks that were run with water instead of activator solution are subtracted.

As noted earlier, the reaction is very sensitive to the presence of contaminating proteins and other compounds. Also arylsulfatase A is competitively inhibited by many anions such as phosphate (K_I = 0.6 m*M* [Gniot-Szulzycka, 1974]), sulfate, and others. Precise determination of activator content with this method is therefore very difficult.

C. ASSAY WITH GLOBOTRIAOSYLCERAMIDE/α-GALACTOSIDASE A

1. Substrate. Globotriaosylceramide can be isolated from the neutral lipid fraction of many tissues, including kidney, spleen, and liver. Porcine intestine (Dean and Sweeley, 1977) or erythrocytes (Taketomi and Kawamura, 1972) have been recommended as convenient sources. A particularly rich source is tissue of patients with Fabry's disease (Sweeley and Klionsky, 1963), especially liver and kidney. This disease is rare, however, and autopsy tissue is usually difficult to obtain.

Extraction and purification of globotriaosylceramide follows the usual methods described for neutral glycosphingolipids (Suzuki, C., et al., 1968; Esselman et al., 1972).

For enzymic studies, the glycolipid can be radiolabeled in the terminal galactose moiety by the galactose oxidase/[^{3}H]borohydride method of Radin (1972a), such as described by Suzuki, Y., and Suzuki, K. (1972) or Dean and Sweeley (1977).

2. α-Galactosidase A. The enzyme can be purified from human liver or placenta with conventional techniques (Beutler and Kuhl, 1972; Dean and Sweeley, 1979) or affinity chromatography (Bishop and Desnick, 1981). The enzyme is routinely assayed with the fluorogenic substrate 4-methylumbelliferyl-α-D-galactoside, most assays being modifications of the method of Desnick et al. (1973). Enzyme units (μmol/minute) are usually also defined with this substrate.

3. Assay. For the standard assay for activator protein, 2 nmol globotriaosylceramide, [^{3}H]-labeled in the terminal galactose residue (~22,000 cpm), are incubated with 1 mU α-galactosidase A and a suitable dilution of the sample to be assayed in a total volume of 50 μl of 50 m*M* sodium acetate buffer, pH 4.0, for 1–3 h at 37°C. (Assays with purified activator should contain some 5 μg of bovine serum albumin to prevent unspecific adsorption of protein on surfaces.) The reaction is terminated with 0.6 ml chloroform/methanol (2:1 by volume) and 0.1 ml of 1 m*M* galactose/1 *M* NaCl in water. After thorough mixing and centrifugation for 5 min in a benchtop centrifuge (Eppendorf), the lower phases are removed and discarded, the remaining upper phases are washed with 0.5 ml of theoretical lower phase (chloroform/methanol/water, 86:14:1 by volume) and then transferred to scintillation vials. Radioactivity is quanti-

fied by liquid scintillation counting, after addition of 5 ml scintillation fluid. Blanks run with water instead of activator solution are subtracted. The reaction rate increases linearly with activator concentration up to 2–3 μ*M* (~2–3 μg/assay).

2. G_{M2} Activator

The G_{M2} activator is determined by its ability to promote the hydrolysis of ganglioside G_{M2} by β-hexosaminidase A.

1. Substrate. Ganglioside G_{M2} is found only in traces in most tissues, so purification from normal sources is extremely tedious. The ganglioside is usually isolated by the method of Svennerholm (1972) from brain tissue of patients who died from G_{M2} gangliosidosis. A more readily available source has recently been indicated by Li, Y.-T., et al. (1984) who found that ganglioside G_{M2} constitutes the main ganglioside of striped mullet (Mugil cephalus) roe. Care should however be exercised when using such preparations for kinetic studies since the ceramide moiety of the fish ganglioside differs somewhat from that of the human ganglioside.

The terminal *N*-acetylgalactosamine moiety can be radiolabeled with galactose oxidase/NaB^3H_4 (Suzuki, Y., and Suzuki, K., 1972) by essentially the same procedure as ganglioside G_{M1} (see the preceding section). However, the specific activity attainable is considerably lower than that of ganglioside G_{M1} or other glycolipids, due to an only limited degree of oxidation of the *N*-acetylgalactosamine residue. Unspecific labeling of other parts of the molecule may therefore contribute significantly to the specific activity of the labeled substrate, and it is recommended to reduce the starting material with unlabeled $NaBH_4$ prior to enzymic oxidation (Suzuki, Y., and Suzuki, K., 1972). As in the case of ganglioside G_{M1}, the amounts required for enzymic assays can be finally purified with preparative thin-layer chromatography and their specific radioactivity checked as described in the preceding section.

2. β-Hexosaminidase A. The enzyme can be purified from normal human liver (Sandhoff et al., 1977), placenta (Lee and Yoshida, 1976; Geiger and Arnon, 1978), kidney (Wiktorowicz et al., 1977), brain (Aruna and Basu, 1976), or urine (Marinkovic and Marinkovic, 1978). The enzyme preparation used does not have to be pure but it is essential to remove β-hexosaminidase B (or at least to know the proportions of the two enzymes) since only the A isoenzyme interacts with the activator/lipid complex. A preparation suitable for activator determination can be obtained from liver or placenta extract (20% in water) with chromatography on Concanavalin A-Sepharose 4B as described by Sandhoff et al. (1977),

followed by ion-exchange chromatography on DEAE-cellulose in 10 m*M* phosphate buffer, pH 6.0. (Column vol. ~1 ml per 5 mg protein to be applied.) Hexosaminidase B is first washed out with 2 column volumes of buffer, then hexosaminidase A is eluted with 0.5 *M* NaCl in the same buffer. The preparation must be dialyzed against distilled water before use because the enzymic reaction rate is inversely proportional to the ionic strength (Conzelmann et al., 1982).

The enzyme is most conveniently assayed with the fluorogenic substrate 4-methylumbelliferyl-β-D-*N*-acetylglucosaminide (Leaback and Walker, 1961; Dance et al., 1969; Sandhoff et al., 1977) (1 m*M* in 50 m*M* citrate buffer, pH 4.5). One enzyme unit is usually defined as the amount of enzyme that splits 1 μmol of this substrate per minute under standard conditions.

3. Assay. The standard assay for quantification of the G_{M2} activator contains 5 nmol of [^{3}H]ganglioside G_{M2} (specific radioactivity at least 5–10 Ci/mol), 2.5 μg bovine serum albumin, 100 mU β-hexosaminidase A, and up to 25 μl of the suitably diluted activator sample in a total volume of 40 μl m*M* citrate buffer, pH 4.0, and is incubated for 1–4 h at 37°C. Samples are then transferred to an ice bath and loaded onto 1 ml columns of DEAE-cellulose (in Pasteur pipettes) that have been washed with distilled water. Liberated [^{3}H]*N*-acetylgalactosamine is eluted with 2 × 1 ml of a 1 m*M* aq *N*-acetylgalactosamine solution. The combined effluents are collected in scintillation vials, and after addition of 10 ml scintillation fluid, their radioactivity is measured. Blanks run with water instead of activator solution are subtracted.

The reaction rate is very low without activator and increases practically linearly up to 1 μg of G_{M2} activator/assay, corresponding to a degradation rate of approximately 50 nmol/(h × U hex A). The absolute reaction rate decreases strongly with increasing ionic strength (Conzelmann et al., 1982). Samples should therefore be dialyzed against water when the activator content is to be quantified precisely.

3. Cofactors for Glucosylceramide β-Glucosidase and Galactosylceramide β-Galactosidase

A. ASSAY WITH β-GLUCOSIDASE

1. Substrates. In most normal tissues, glucosylceramide is only a trace component. Tissues of patients with Gaucher's disease (particularly, spleen and liver) contain large amounts of this glycolipid, due to the deficiency of the catabolizing enzyme, and Gaucher spleen is the most frequent source of the glucosylceramide used in enzymic and other studies.

Extraction and purification can be done as described by Radin (1976) or by Peters et al. (1977c).

Glucosylceramide can also be synthesized chemically (Brady et al., 1965; Stoffyn et al., 1971). It has the advantage of yielding homogeneous products with respect to fatty acid and sphingoid base but is, of course, more laborious.

Radioactive labeling can most easily be achieved by catalytic reduction of the sphingosine double bond (Schwarzmann, 1978). Another possibility is amidation of a radioactive fatty acid with glucosylsphingosine prepared from glucosylceramide by alkaline hydrolysis (Erickson and Radin, 1973). However, the most useful substrate for enzymic assays is the one labeled in the glucose moiety. This can be obtained either by chemical synthesis with radioactive glucose or by labeling intact glucosylceramide by the method of McMaster and Radin (1977).

2. Acid β-glucosidase. Like other lysosomal enzymes, glucosylceramide β-glucosidase (acid β-glucosidase) can be isolated from almost any human tissue. Placenta has proved to be a good source that is readily available. The enzyme can be obtained in water-soluble form after extraction of crude preparations with *n*-butanol or other organic solvents (Blonder et al., 1976; Dale et al., 1976). High purity with good yield was reported with conventional techniques (Dale and Beutler, 1976; Furbish et al., 1978) as well as with affinity chromatography (Strasberg et al., 1982; Grabowski and Dagan, 1984).

Acid β-glucosidase is routinely assayed with the fluorogenic 4-methylumbelliferyl-β-D-glucoside. Standardization of enzyme preparations is, however, problematic since the enzyme is stimulated by acidic phospholipids (Ho and Light, 1973; Dale et al., 1976; Peters et al., 1977a) or detergents (Ho, 1973; Dale et al., 1976; Peters et al., 1976) so that the absolute activity depends strongly on the amount and nature of such additions.

3. Assay. Acid β-glucosidase hydrolyzes both water-soluble and lipid substrates. The activity, and hence the activation of this enzyme by cofactors, can therefore be determined with either kind of substrate. Due to the rapidity and convenience of assays with fluorogenic substrates, most workers prefer to use the commercially available 4-methylumbelliferyl-β-D-glucoside. In some cases it may, however, be desirable, or even necessary, to confirm the results with the natural substrate, glucosylceramide. Both types of assays will therefore be described here.

A central problem in both cases is the definition of "optimal" conditions for the quantification of a stimulating cofactor. Generally, conditions must be sought that lead to maximal stimulation of an otherwise

small basal activity. As outlined earlier, β-glucosidase activity depends strongly on the nature and amount of additions to the assay (acidic phospholipids, anionic detergents). It is therefore difficult to define the activator activity in absolute terms such as an increase in the amount of substrate hydrolyzed per enzyme unit. Most workers express the activation therefore as multiples of basal activity ("-fold activation").

The interaction between acid β-glucosidase and activating protein cofactors depends on the presence of acidic lipids (Ho and Light, 1973), so a certain amount of such lipids has to be added to the assay system. (The partially purified enzyme preparations used contain frequently some lipids, including acidic ones.) On the other hand, higher concentrations of acidic lipids may stimulate the enzyme to almost maximal activity (Berent and Radin, 1981a) and may render protein cofactors obsolete.

Assay with 4-methylumbelliferyl-β-D-glucoside: The activator sample to be assayed is incubated with 2 m*M* substrate in 0.2 *M* acetate buffer, pH 5.5 (Peters et al., 1977a,b), or 50 m*M* acetate, pH 4.5 (Berent and Radin, 1981a; Wenger and Roth, 1982), with an appropriate amount of partially purified enzyme and, if necessary, with 5 μg phosphatidylserine, in a total volume of 100 μl. After incubation (1 h, 37°C), the reaction is terminated by the addition of 0.5 ml 0.2 *M* glycine/0.2 *M* sodium carbonate, and the liberated 4-methylumbelliferone is determined fluorimetrically (excitation 365 nm, emission 440 nm).

Assay with glucosylceramide: Assay conditions are essentially the same as with the fluorogenic substrate except that [glucose-6-^{3}H]glucosylceramide is used as substrate, at a concentration of 0.3−0.4 m*M* (Berent and Radin, 1981b; Wenger and Roth, 1982). After incubation, 5 volumes of chloroform/methanol (2:1 by volume) and 0.5 volumes of an aqueous solution of 0.2 *M* glucose/0.2 *M* KCl are added. The mixture is thoroughly vortexed and then centrifuged and the liberated [^{3}H]glucose is measured in an aliquot of the upper phase. (The sensitivity of the method can be improved, if necessary, by washing the upper phase with 2 volumes of theoretical lower phase {chloroform/methanol/water, 64:9:1, by volume}.)

B. ASSAY WITH GALACTOSYLCERAMIDE β-GALACTOSIDASE

1. Substrate. Galactosylceramide can be purified from the neutral fractions of brain lipid extracts (Radin, 1972a). The galactose moiety can easily be tritium-labeled by the galactose oxidase/sodium borohydride method (Radin, 1972a).

2. Enzyme preparation. Wenger et al. (1982) studied the stimulating effect of protein cofactors on galactosylceramide hydrolysis with crude tissue homogenates or extracts as enzyme sources. Purification of

galactosylceramide β-galactosidase, which seems to be somewhat difficult (Suzuki, K., 1977), may therefore not be necessary.

If a more purified preparation is desired, the enzyme, like acid β-glucosidase, can be converted into a water-soluble form by extraction with organic solvents (Tanaka and Suzuki, 1976, 1977). However, the purification protocols published so far (Radin, 1972b; Wenger et al., 1975) rely mainly on extraction with detergents.

3. Assay. The assay method described is that used by Wenger et al. (1982). [^{3}H]Galactosylceramide (10 nmol; specific activity ~1 mCi/mmol) and 25 μg pure phosphatidylserine are dispersed in 0.1 ml 0.1 *M* citrate/0.2 *M* phosphate buffer, pH 4.6, by sonication. Enzyme, activator sample, and distilled water are added to a final volume of 0.2 ml. After incubation at 37°C for 1 h, 1 ml of chloroform/methanol (2:1 by volume) is added, and the liberated [^{3}H]galactose, which partitions into the upper phase, is determined by liquid scintillation counting.

The reaction rate is reported to increase linearly with the amount of cofactor added up to 5–10-fold stimulation (Wenger et al., 1982).

III. PURIFICATION OF ACTIVATOR PROTEINS

1. G_{M2} Activator

The richest source of human G_{M2} activator is kidney tissue (Conzelmann and Sandhoff, 1978, 1979), which contains some 800 ng activator/mg extract protein, as compared to 100 ng/mg for brain and 50 ng/mg for liver (Banerjee et al., 1984). Another, more convenient, source is urine (Li, Y.-T., et al., 1983), with a G_{M2} activator content between 200 and 1400 ng/mg protein (Banerjee et al., 1984).

The following purification scheme from human kidney is a simplified version of the one originally developed in our laboratory (Conzelmann and Sandhoff, 1979). Human urine, concentrated 10-fold by ultrafiltration (exclusion limit ~10,000 Da) may be substituted for the crude kidney extract.

All steps are performed at 4°C unless otherwise stated. Postmortem human kidney (1 kg) obtained within less than 24 h after death and stored frozen (−20°C) is homogenized in 4 volumes of distilled water, with an Ultra-Turrax or a Polytron homogenizer and centrifuged at 13,000 × g (9000 rpm in a Sorvall GSA or GS-3 rotor) for 30 min. The pellet is reextracted with 3 volumes of water.

The combined supernatants are heated to 60°C in a water-bath for 2 h, and precipitated material is removed by centrifugation (as before). The extract is adjusted to pH 3.0 by slow addition of 10% trichloroacetic acid,

under rapid stirring, and then stirred for another 2 h (or overnight). Precipitated protein is spun off, the clear supernatant is dialyzed against 10 m*M* phosphate buffer, pH 6.0. After filtration, the solution is loaded onto a column of DEAE-cellulose (5 × 30 cm) equilibrated with the same phosphate buffer. The column is washed with 1 l phosphate buffer; then the activator is eluted with a linear gradient of NaCl (0–0.5 *M* in 1 l phosphate buffer). Fractions of 20 ml are collected and monitored for G_{M2} activator. Since this step, ion-exchange chromatography, separates the G_{M2} activator from the sulfatide/G_{M1} activator, the latter may also be recovered and further purified as described shortly, if desired.

Fractions containing the G_{M2} activator (usually those with more than 20% of maximal activity) are pooled, dialyzed against distilled water, and lyophilized. At this point several preparations may be combined and processed together if larger quantities of the activator protein are to be prepared.

The dry residue is dissolved in 10–15 ml of 50 m*M* citrate buffer, pH 4.2, and, after removal of insoluble material by centrifugation, is passed over a gel-filtration column (Sephadex G-100; 2.6 × 90 cm) in the same buffer, at a flow rate of approximately 20 ml/h.

Activator-containing fractions are combined and loaded onto an octyl-Sepharose column (10 ml) packed in water. Unbound protein is washed out with 3 volumes 10 m*M* phosphate buffer, pH 6.0; then the activator is eluted with a linear gradient of 0–1% sodium cholate (analytical grade) in 50 ml of the same buffer. Fractions of 1 ml are collected and analyzed for G_{M2} activator. The active fractions are pooled and dialyzed exhaustively against several changes of distilled water and then lyophilized.

At this stage the preparation is approximately 80% pure as judged by analytical HPLC gel filtration. Recovery is approximately 30–50%. If an even purer preparation is desired, final purification can be achieved with HPLC gel filtration on a TSK G 2000 SW column (150 μl per run, on a 13 ml column, in 0.1 *M* phosphate buffer, pH 6.0, flow rate 0.5 ml/min) or HPLC anion-exchange chromatography on a TSK 545 DEAE column (both columns are from LKB, Sweden). In the latter procedure 10 mg of activator (dissolved in 10 m*M* phosphate buffer, pH 6.0) can be applied to a 6-ml column which is then eluted with a linear gradient of 0–0.3 *M* NaCl in 60 ml of the same buffer.

The purity of G_{M2} activator is difficult to assess with electrophoretic methods since the material isolated from tissue or urine appears to have a very heterogeneous carbohydrate portion and runs on SDS electrophoresis as a broad, diffuse band, with an apparent M_R of approximately 22,000 Da.

2. Sulfatide/G_{M1} Activator

Purification of the human sulfatide activator to a preparation that yielded one band in nondenaturing electophoresis was reported by Fischer and Jatzkewitz (1975). Li and Li (1976) purified the G_{M1} activator, which later turned out to be the same protein. Both procedures exploit the unusual thermal stability of this protein which can be heated to 95°C for several minutes without loss of activity. A gentler procedure that allows the simultaneous preparation of both, the sulfatide/G_{M1} activator and the more sensitive G_{M2} activator, was also suggested by Li and Li (1982). Unfortunately neither publication contains information on yield and purity of the final preparations. Also the steps involving chromatography on DEAE-Sephadex A-50 proved to be quite cumbersome in our hands. The method of Fischer and Jatzkewitz appears to give comparatively pure products, with reasonable yields (5.5 mg/kg tissue), but employing acetone precipitation as the first purification step leads to very large volumes that have to be centrifuged.

We use the following procedures. All steps are performed at 4°C unless otherwise stated. The human autopsy tissues used as sources should be obtained within 24 h after death and should be stored at or below −20°C until used.

A. PURIFICATION FROM HUMAN LIVER

Human autopsy liver (500 g) is homogenized in 4 volumes of 10 m*M* phosphate buffer, pH 6.5, with an Ultra-Turrax or Polytron homogenizer for 5 min. The homogenate is centrifuged at 100,000 × g for 30 min. The pellet is reextracted with 4 volumes of the same buffer, and the combined supernatants are filtered through glass wool.

Solid ammonium sulfate is slowly (within 1 h) added with stirring, up to 60% saturation, and stirring is continued overnight. Precipitated material is spun down (13,000 × g, 1 h), redissolved in approximately 100 ml 10 m*M* phosphate buffer, pH 6.5, and dialyzed against two changes of 10 l each of the same buffer. This solution is then loaded onto a DEAE-cellulose column (2.6 × 40 cm) equilibrated with the same phosphate buffer. After washing with 2 column volumes of buffer, the column is eluted with a linear gradient of 0−0.3 *M* NaCl in 1 l phosphate buffer (flow rate 40 ml/h). Fractions of 15 ml are collected and analyzed for activator content. The fractions with an activator concentration of more than 20% of maximum are pooled, dialyzed against distilled water, lyophilized, and then dissolved in 20 ml 10 m*M* phosphate buffer, pH 6.5, with 100 m*M* NaCl. The solution is passed over a Sephadex G-75 sf column

(2.6 × 86 cm) in the same buffer, at a flow rate of 10 ml/h. Fractions of 10 ml are collected.

The activator-containing fractions are loaded onto a 15 ml octyl-Sepharose column packed in 10 m*M* phosphate buffer, pH 6.5. The column is washed with 2 volumes of 50% ethylene glycol in water and eluted with 1% cholic acid (analytical grade) in 10 m*M* phosphate buffer, pH 6.5. The protein-containing fractions are pooled, dialyzed first against 2 × 2 l 10 m*M* phosphate buffer, pH 6.5, then against 2 × 2 l distilled water and finally lyophilized.

The preparation is finally purified with ion-exchange HPLC: the sample is dissolved in 0.5–1 ml of 10 m*M* phosphate buffer, pH 6.0, and after removal of any insoluble material by centrifugation (Eppendorf benchtop centrifuge), up to 10 mg protein per run are loaded onto a 6 ml TSK 545 DEAE column (LKB, Sweden). The column is eluted at room temperature with a linear gradient of 0–0.3 *M* NaCl in the same phosphate buffer (flow rate 0.5 ml/min). Fractions of 0.5 ml are collected and analyzed for activator protein.

The overall yield of this procedure is approximately 15% (30% before HPLC). The final product yields a single symmetrical peak in analytical HPLC gel filtration, whereas on ion-exchange HPLC several peaks can be resolved, all of which have the same specific activity. The existence of these different forms is probably due to heterogeneity of the carbohydrate portion. The electrophoretic purity is difficult to assess since the activator, which according to gel-filtration experiments seems to have a molecular weight of approximately 22,000 Da, consistently yields several bands in the range between 6,000 and 10,000 Da on SDS electrophoresis.

B. PURIFICATION FROM HUMAN KIDNEY AND URINE

1. Kidney. Human autopsy kidney tissue (500 g) is homogenized with an Ultra-Turrax or Polytron homogenizer in 3 volumes of 10 m*M* phosphate buffer, pH 6.0, and then centrifuged at 13,000 × g for 30 min. The supernatant is heated to 60°C for 30 min in a water bath. Precipitated material is removed by centrifugation (13,000 × g, 30 min). The extract is adjusted to pH 4.0 with 1 *M* citric acid and stirred overnight. After removal of precipitated protein by centrifugation, the solution is dialyzed against 10 m*M* phosphate buffer, pH 6.0, concentrated at room temperature with a rotary evaporator to a volume of 40 ml and centrifuged again. The supernatant is applied to a Sephadex G-75 column (2.6 × 60 cm) in portions of 20 ml and chromatographed in 10 m*M* phosphate buffer, pH 6.0. Fractions with activator content of more than 20% of maximum are pooled and loaded onto a DEAE-cellulose column (2.6 × 25 cm) equili-

brated with 10 m*M* phosphate buffer, pH 6.0. After washing with 2 volumes of this buffer, the column is eluted with a linear gradient of 0–0.5 *M* NaCl in 1 l of the same buffer. The activator-containing fractions are pooled and dialyzed overnight against 1% glycine solution.

For isolelectric focusing the sample is mixed into a linear sucrose gradient from 35 to 0% (w/v), containing 5% (by volume) of carrier ampholyte solution, pH 4–7, (equivalent to an ampholyte concentration of 2%, w/v) in a 110-ml electrofocusing column (LKB, Sweden). The cathode space is filled with 1.5% (w/v) of ethylene diamine in a 50% (w/v) sucrose solution; the sample space is topped off with 0.1% aqueous H_2SO_4 as anode solution. Focusing is performed for 72 h at 500 V; then the contents are collected in 3-ml fractions.

Activator-containing fractions are combined and loaded onto a small (1-ml) column of octyl-Sepharose. Ampholytes are washed out with 5 ml of 10 m*M* phosphate buffer, pH 7; then the activator is eluted with 1% cholic acid (analytical grade) in the same buffer. After addition of 0.1 mg cytochrome c/ml (as protection against adsorption of the small amounts of protein onto dialysis tubing and other surfaces) the sample is dialyzed extensively against distilled water and then lyophilized.

The preparation is finally purified by HPLC as described earlier for the liver protein. Yield and purity of the final preparation are comparable to those of the first method.

2. Urine. Freshly voided human urine is filtered through ordinary filter paper in a Büchner funnel, concentrated 10-fold by ultrafiltration (exclusion limit of the membrane 10,000 Da), dialyzed against distilled water, lyophilized, and taken up in 40 ml of distilled water.

Further processing of the sample is as described earlier for the kidney extract, starting with the Sephadex G-75 gel filtration. Yield and quality of the final product are comparable to those of the other methods described earlier.

During this procedure the G_{M2} activator is separated from the sulfatide activator by the ion-exchange chromatography step and can be further purified as described earlier.

3. Co-glucosidase

Since the initial report by Ho and O'Brien (1971) that lysosomal β-glucosidase activity toward water-soluble substrates as well as glucosylceramide (Ho et al., 1973) is greatly stimulated by small nonenzymic protein cofactors that are particularly abundant in Gaucher spleen, such factors have been purified by several groups from human spleen (Ho and O'Brien, 1971; Peters et al., 1977a, b; Chiao et al., 1978; Iyer et

al., 1983) and brain (Wenger and Roth, 1982), and from bovine spleen (Berent and Radin, 1981a, b). Some of these preparations were also tested with other enzymes and were found to stimulate also the hydrolysis of galactosylceramide by the corresponding β-galactosidase (Wenger et al., 1982).

It is, however, very difficult to assess the various purification procedures suggested. A comparison of the products obtained from various sources with different methods (or even with the same method) indicates a tremendous heterogeneity with respect to molecular weight (Ho and O'Brien, 1971; Peters et al., 1977a, b; Wenger and Roth, 1982), specific activity (Peters et al., 1977a; Iyer et al., 1983), and extent and necessity of glycosylation (Ho and O'Brien, 1971; Peters et al., 1977a; Berent and Radin 1981b). Recent evidence (Sarmientos et al., 1986) also suggests that acid β-glucosidase may be able to degrade its membrane-bound glycolipid substrate without the aid of any protein cofactor. (The role of the intrinsic cofactor for glucosylceramide β-glucosidase recently described by Vaccaro et al. [1985] may be different but cannot yet be assigned.)

A convenient method that yields essentially pure products, from human tissue, is that of Peters et al. (1977a).

However, as long as it is not known which of the stimulating factors for glucosylceramide and galactosylceramide degradation, if any, is required in vivo, we feel that it is impossible to decide on which one of the purification methods currently used to recommend.

References

Aruna, R. A. and Basu, D. (1979), *J. Neurochem.*, *80*, 337–339.

Banerjee, A., Burg, J., Conzelmann, E., Carroll, M., and Sandhoff, K. (1984), *Hoppe-Seyler's Z. Physiol. Chem.*, *365*, 347–356.

Baum, H., Dodgson, K. S., and Spencer, B. (1958), *Biochem. J.*, *69*, 567–572.

Baum, H., Dodgson, K. S., and Spencer, B. (1959), *Clin. Chim. Acta*, *4*, 453–455.

Berent, S. L., and Radin, N. S. (1981a), *Biochim. Biophys. Acta*, *664*, 572–582.

Berent, S. L., and Radin, N. S. (1981b), *Arch. Biochem. Biophys.*, *208*, 248–260.

Beutler, E., and Kuhl, W. (1972), *J. Biol. Chem.*, *247*, 7195–7200.

Bishop, D. F., and Desnick, R. J. (1981), *J. Biol. Chem.*, *256*, 1307–1316.

Blonder, E., Klibansky, C., and DeVries, A. (1976), *Biochim. Biophys. Acta*, *431*, 45–53.

Brady, R. O., Kanfer, J. N., and Shapiro, D. (1965), *J. Biol. Chem.*, *240*, 39–43.

Breslow, J. L., and Sloan, H. R. (1972), *Biochem. Biophys. Res. Commun.*, *46*, 919–925.

Burg, J., Conzelmann, E., Sandhoff, K., Solomon, E., and Swallow, D. M. (1985a), *Ann. Hum. Genet.*, *49*, 41–45.

Burg, J., Banerjee, A., and Sandhoff, K. (1985b), *Biol. Chem. Hoppe-Seyler*, *366*, 887–891.

Christomanou, H. (1980), *Hoppe-Seyler's Z. Physiol. Chem.*, *361*, 1489–1502.

Christomanou, H., and Kleinschmidt, T. (1985), *Biol. Chem. Hoppe-Seyler, 366*, 245–256.

Conzelmann, E., and Sandhoff, K. (1978), *Proc. Natl. Acad. Sci.* (USA), *75*, 3979–3983.

Conzelmann, E., and Sandhoff, K. (1979), *Hoppe-Seyler's Z. Physiol. Chem., 360*, 1837–1849.

Conzelmann, E., Burg, J., Stephan, G., and Sandhoff, K. (1982), *Eur. J. Biochem., 123*, 455–464.

Conzelmann, E., Kytzia, H.-J., Navon, R., and Sandhoff, K. (1983), *Am. J. Hum. Genet., 35*, 900–913.

Dale, G. L., and Beutler, E. (1976), *Proc. Natl. Acad. Sci.* (USA), *73*, 4672–4674.

Dale, G.L., Villacorte, D. and Beutler, E. (1976), *Biochem. Biophys. Res. Commun., 71*, 1048–1053.

Dance, N., Price, R. G., Robinson, D., and Stirling, J. L. (1969), *Clin. Chim. Acta, 24*, 189–197.

Dean, K. J., and Sweeley, C. C. (1977), in *Practical Enzymology of the Sphingolipidoses* (R. H. Glew and S. P. Peters, eds.), Alan R. Liss, Inc., New York, pp. 173–216.

Dean, K. J., and Sweeley, C. C. (1979), *J. Biol. Chem., 254*, 9994–10,000.

Desnick, R. J., Allen, K. Y., Desnick, S. J., Raman, M. K., Bernlohr, R. W., and Krivit, W. (1973), *J. Lab. Clin. Med., 81*, 157–171.

Draper, R. K., Fiskum, G. M., and Edmond, J. (1976), *Arch. Biochem. Biophys., 177*, 525–538.

Dubois, G., Zalc, B., LeSaux, F., and Baumann, N. (1980), *Anal. Biochem., 102*, 313–317.

Erickson, J. S., and Radin, N. S. (1973), *J. Lipid Res., 14*, 133–137.

Erzberger, A., Conzelmann, E., and Sandhoff, K. (1980), *Clin. Chim. Acta, 108*, 361–368.

Esselman, W. J., Laine, R. A., and Sweeley, C. C. (1972), *Methods Enzymol., 28*, 140–156.

Fischer, G., and Jatzkewitz, H. (1975), *Hoppe-Seyler's Z. Physiol. Chem., 356*, 605–613.

Fischer, G., and Jatzkewitz, H. (1977), *Biochim. Biophys. Acta, 481*, 561–572.

Fischer, G., and Jatzkewitz, H. (1978), *Biochim. Biophys. Acta, 528*, 69–76.

Fluharty, A. L., Davis, M. L., Kihara, H., and Kritchevsky, G. (1974), *Lipids, 9*, 865–869.

Folch, J., Lees, M., and Sloane Stanley, G. H. (1957), *J. Biol. Chem., 226*, 497–509.

Furbish, F. S., Blair, H. E., Shiloach, J., Pentchev, P. G., and Brady, R. O. (1978), *Methods Enzymol., 50*, 529–532.

Gardas, A., Li, Y.-T., and Li, S.-C. (1984), *Glycoconjugate J., 1*, 37–42.

Geiger, B., and Arnon, R. (1978), *Methods Enzymol., 50*, 547–555.

Gniot-Szulzycka, J. (1974), *Acta Biochim. Polon., 21*, 247–254.

Gniot-Szulzycka, J., and Komoszynski, M. (1970), *Acta Biochim. Polon., 17*, 185–190.

Grabowski, G. A., and Dagan, A. (1984), *Anal. Biochem., 141*, 267–279.

Ho, M. W. (1973), *Biochem. J., 136*, 721–729.

Ho, M. W., and Light, N. D. (1973), *Biochem. J., 136*, 821–823.

Ho, M. W., and O'Brien, J. S. (1971), *Proc. Natl. Acad. Sci.* (USA), *68*, 2810–2813.

Ho, M. W., O'Brien, J. S., Radin, N. S., and Erickson, J. S. (1973), *Biochem. J., 131*, 173–176.

Inui, K., Emmett, M., and Wenger, D. A. (1983), *Proc. Natl. Acad. Sci.* (USA), *80*, 3074–3077.

Inui, K., Kao, F.-T., Fujibayashi, S., Jones, C., Morse, H. G., Law, M. L., and Wenger, D. A. (1985), *Hum. Genet., 69*, 197–200.

Iyer, S. S., Berent, S. L., and Radin, N. S. (1983), *Biochim. Biophys. Acta, 748*, 1–7.

James, G. T., and Austin, J. H. (1979), *Clin. Chim. Acta, 98*, 103–111.

Jatzkewitz, H., and Stinshoff, K. (1973), *FEBS Lett.*, *32*, 129–131.

Kundu, S. K. (1981), *Methods Enzymol.*, *72*, 174–185.

Kwiterovich, P. O., Jr., Sloan, H. R., and Fredrickson, D. S. (1970), *J. Lipid Res.*, *11*, 322–330.

Kytzia, H.-J., and Sandhoff, K. (1985), *J. Biol. Chem.*, *260*, 7568–7572.

Leaback, D. H., and Walker, P. G. (1961), *Biochem. J.*, *78*, 151–156.

Ledeen, R. W., and Yu, R. K. (1982), *Methods Enzymol.*, *83*, 139–191.

Lee, J. E. S., and Yoshida, A. (1976), *Biochem. J.*, *159*, 535–539.

Li, S.-C., and Li, Y.-T. (1976), *J. Biol. Chem.*, *251*, 1159–1163.

Li, S.-C., and Li, Y.-T. (1982), *Methods Enzymol.*, *83*, 588–595.

Li, S.-C., Nakamura, T., Ogamo, A., and Li, Y.-T. (1979), *J. Biol. Chem.*, *254*, 10592–10595.

Li, S.-C., Kihara, H., Serizawa, S., Li, Y.-T., Fluharty, A. L., Mayes, J. S., and Shapiro, L. J. (1985), *J. Biol. Chem.*, *260*, 1867–1871.

Li, Y.-T., Mazzotta, M. Y., Wan, C.-C., Orth, R., and Li, S.-C. (1973), *J. Biol. Chem.*, *248*, 7512–7515.

Li, Y.-T., Muhiudeen, I. A., DeGasperi, R., Hirabayashi, Y., and Li, S.-C. (1983), *Am. J. Hum. Genet.*, *35*, 629–634.

Li, Y.-T., Hirabayashi, Y., DeGasperi, R., Yu, R. K., Ariga, T., Koerner, T. A. W., and Li, S.-C. (1984), *J. Biol. Chem.*, *259*, 8980–8985.

Lo, J.-T., Mukerji, K., Awasthi, Y. C., Hanada, E., Suzuki, K., and Srivastava, S. K. (1979), *J. Biol. Chem.*, *254*, 6710–6715.

Marinkovic, D. V., and Marinkovic, J. N. (1978), *Biochem. Med.*, *20*, 422–433.

McMaster, M. C., Jr., and Radin, N. S. (1977), *J. Label. Comp. Radiopharmaceut.*, *13*, 353–357.

Mehl, E., and Jatzkewitz, H. (1964), *Hoppe-Seyler's Z. Physiol. Chem.*, *339*, 260–276.

Meisler, M. (1972), *Methods Enzymol.*, *28*, 820–824.

Miettinen, T., and Takki-Luukkainen, I.-T. (1959), *Acta Chem. Scand.*, *13*, 856–858.

Miller, A. L., Frost, R. G., and O'Brien, J. S. (1977), *Biochem. J.*, *165*, 591–594.

Miyatake, T., and Suzuki, K. (1975), *J. Biol. Chem.*, *250*, 585–592.

Peters, S. P., Coyle, P., and Glew, R. H. (1976), *Arch. Biochem. Biophys.*, *175*, 569–582.

Peters, S. P., Coyle, P., Coffee, C. J., Glew, R. H., Kuhlenschmidt, M. S., Rosenfeld, L., and Lee, Y. C. (1977a), *J. Biol. Chem.*, *252*, 563–573.

Peters, S. P., Coffee, C. J., Glew, R. H., Lee, R. E., Wenger, D. A., Li, S.-C., and Li, Y.-T. (1977b), *Arch. Biochem. Biophys.*, *183*, 200–297.

Peters, S. P., Glew, R. H., and Lee, R. E. (1977c), in *Practical Enzymology of the Spingolipidoses* (R. H. Glew and S. P. Peters, eds.), Alan R. Liss, Inc., New York, pp. 71–100.

Radin, N. S. (1972a), *Methods Enzymol.*, *28*, 300–306.

Radin, N. S. (1972b), *Methods Enzymol.*, *28*, 834–839.

Radin, N. S. (1976), *J. Lipid Res.*, *17*, 290–293.

Raghavan, S. S., Gajewski, A., and Kolodny, E. H. (1981), *J. Neurochem.*, *36*, 724–731.

Rouser, G., Kritchevsky, G., Yamamoto, A., Simon, G., Galli, C., and Bauman, A. J. (1969), *Methods Enzymol.*, *14*, 272–317.

Roy, A. B. (1953), *Biochem. J.*, *53*, 12–15.

Sandhoff, K., Conzelmann, E., and Nehrkorn, H. (1977), *Hoppe-Seyler's Z. Physiol. Chem.*, *358*, 779–787.

Sarmientos, F., Schwarzmann, G., and Sandhoff, K. (1986), *Eur. J. Biochem.*, in press.

Schwarzmann, G. (1978), *Biochim. Biophys. Acta, 529*, 106–114.

Sloan, H. R. (1972), *Methods Enzymol., 28*, 867–874.

Stevens, R. L., Fluharty, A. L., Skokut, M. H., and Kihara, H. (1975), *J. Biol. Chem., 250*, 2495–2501.

Stevens, R. L., Fluharty, A. L., Kihara, H., Kaback, M. M., Shapiro, L. J., Marsh, B., Sandhoff, K., and Fischer, G. (1981), *Am. J. Hum. Genet., 33*, 900–906.

Stinshoff, K. (1972), *Biochim. Biophys. Acta, 276*, 475–490.

Stoffyn, P., Stoffyn, A., and Hauser, G. (1971), *J. Lipid Res.*, 12, 318–323.

Strasberg, P. M., Lowden, J. A., and Mahuran, D. (1982), *Can. J. Biochem., 60*, 1025–1031.

Suzuki, C., Makita, A., and Yoshizawa, Z. (1968), *Arch. Biochem. Biophys., 127*, 140–149.

Suzuki, K. (1977), in *Practical Enzymology of the Sphingolipidoses* (R. H. Glew and S. P. Peters, eds.), Alan R. Liss, Inc., New York, pp. 101–136.

Suzuki, Y., and Suzuki, K. (1972), *J. Lipid Res., 13*, 687–690.

Svennerholm, L. (1957), *Biochim. Biophys. Acta, 24*, 604–611.

Svennerholm, L. (1972), *Methods Carbohydr. Chem., 6*, 464–474.

Sweeley, C. C., and Klionsky, B. (1963), *J. Biol. Chem., 238*, 3148–3150.

Taketomi, T., and Kawamura, N. (1972), *J. Biochem., 72*, 791–798.

Tanaka, H., and Suzuki, K. (1976), *Arch. Biochem. Biophys., 175*, 332–340.

Tanaka, H., and Suzuki, K. (1977), *Brain Res., 122*, 325–335.

Vaccaro, A. M., Muscillo, M., Gallozzi, E., Salvioli, R., Tatti, M., and Suzuki, K. (1985), *Biochim. Biophys. Acta, 836*, 157–166.

Vogel, A. (1985), Diplom-Arbeit, Universität Bonn.

Wenger, D. A., and Roth, S. (1982), *Biochem. Int., 5*, 705–710.

Wenger, D. A., Sattler, M., and Clark, C. (1975), *Trans. Am. Soc. Neurochem., 6*, 151–151.

Wenger, D. A., Sattler, M., and Roth, S. (1982), *Biochim. Biophys. Acta, 712*, 639–649.

Wiktorowicz, J. E., Awasthi, Y. C., Kurosky, A., and Srivastava, S. K. (1977), *Biochem. J., 165*, 49–53.

Yu, R. K., and Ledeen, R. W. (1972), *J. Lipid Res., 13*, 680–686.

Methods of Biochemical Analysis, Volume 32
Edited by David Glick
Copyright © 1987 by John Wiley & Sons, Inc.

METHODS OF BIOCHEMICAL ANALYSIS VOLUME 32

Isolation and Analysis of Cell Walls from Plant Material

ROBERT R. SELVENDRAN AND MALCOLM A. O'NEILL,* *AFRC Food Research Institute-Norwich, Colney Lane, Norwich, England*

*Present address: Complex Carbohydrate Research Center, Richard B. Russell Agricultural Research Center, Athens, Georgia.

3. Preparation of Cell Walls from Cereal Endosperm
4. Preparation of Rice Endosperm Cell Walls
5. Preparation of Cell Wall Material from Suspension-Cultured Tissues

IV. Sequential Extraction of CWM and Fractionation of Polymers
1. Recommended Methods for the Fractionation of CWM from Parenchymatous Tissues
A. Extraction of Pectic Substances
B. Fractionation of Pectic Substances
C. Extraction of Hemicellulosic Polymers
D. Fractionation of Hemicellulosic Polymers
E. Extraction and Analysis of Hydroxyproline (Hyp)-Rich Glycoprotein(s) (Extensin)
a. Isolation and Analysis of Hyp-Arabinosides
b. Galactosyl-Serine Linkage in Hyp-Rich Glycoprotein
2. Fractionation of CWM from Tissues Containing Some Lignin
3. Cell Wall Material from Heavily Lignified Tissues
A. Solubilization of Lignin-Polysaccharide Complexes
4. Solubilization of Cell Wall Constituents by Enzymic Methods and Fractionation of the Constituents Released
A. Pectic Polysaccharides
B. Hemicellulosic Polysaccharides
a. Xyloglucan and Xyloglucan-Pectic Complexes
b. Glucuronoarabinoxylan
c. Feruloylated Pectins and Feruloylated Oligosaccharides
5. Fractionation of CWM from Parenchymatous and Lignified Tissues of Cereals
A. Cell Walls from Cereal Endosperm
B. CWM from Lignified Tissues (Beeswing Wheat Bran)
a. Isolation of Feruloylated Oligosaccharides

V. Polysaccharide Homogeneity, Molecular Weight, and Conformation
1. Homogeneity
2. Molecular Weight, Shape, and Conformation

VI. Chemical Characterization and Structure Determination of the Polymers
1. Monosaccharide Composition
A. Neutral Sugars
a. Hydrolysis
b. Determination of the Monosaccharides Released
B. Uronic Acids
a. Hydrolysis
b. Determination of Uronic Acids
C. Unusual Sugars
D. Absolute Configuration and Ring Size of Monosaccharides
2. Glycosyl Linkage Analysis
A. Methylation Analysis
a. Neutral Polysaccharides
b. Acidic Polysaccharides
c. Oligomeric Material
d. Hydrolysis of Methylated Material
e. Preparation of Methylated Alditol Acetates
f. Separation of Partially Methylated Alditol Acetates
g. Identification of PMAA by Electron-Impact Mass Spectrometry

I. INTRODUCTION: SOME GENERAL CONSIDERATIONS

Understanding of the role of plant cell wall carbohydrate polymers was restricted before 1965 by the following factors: (1) Most of the detailed

chemical work on cell wall polysaccharides was carried out by chemists, at a time when the significance of the localization of these polymers in the walls of various tissue types was only just being appreciated. The main emphasis was on the elucidation of the major structural features of a great variety of polysaccharides present in a range of plants. (2) The methods developed essentially for the isolation of cell wall polysaccharides from wood were applied to other tissues, indiscriminately, and little consideration was given to material lost in the extraction fluids (e.g., delignification liquors) and in the supernatants after precipitation with aqueous alcohol. (3) Mainly chemical fractionation techniques were used to resolve the polysaccharides; although these methods can give quantitative recovery of the polysaccharides, the resolutions obtained by such methods alone are inadequate. (4) Relatively large amounts of polysaccharides (>100 mg) were required for detailed structural work. (5) Enzymes capable of cleaving specific glycosidic linkages were not available commercially, and there were relatively few good methods for isolating the necessary enzymes. (6) Very little encouragement was given to work on the cell walls of edible plants, because cell walls and products derived from them were regarded as nutritionally unimportant.

The whole scene has, however, changed over the past 15–20 years, probably for the following reasons: (1) Increasing numbers of plant biochemists and plant physiologists have been studying cell walls, often in collaboration with cell wall and carbohydrate chemists. (2) There has been greater interest in the efficient utilization of cell walls from forages, grasses, and so forth, by ruminants. (3) Dietary fiber in food is considered to be more important. (4) There have been improved methods for the isolation and analysis of cell wall material (CWM) from starch- and protein-rich foods, and from suspension cultured tissues. (5) There are now better methods for resolving cell wall polymers by ion-exchange, cellulose and affinity chromatography, gel filtration, electrophoresis, and sedimentation analysis by ultracentrifugation. (6) It has become practicable to use highly purified enzymes to cleave specific glycosidic linkages in cell wall polymers. (7) There have been important recent developments in various techniques for identifying carbohydrate derivatives, for example, the use of improved methods of methylation analysis, coupled with gas liquid chromatography-mass spectrometry (GLC-MS) of the derived products, permits the scale of experiments to be reduced drastically so that only a few mg of material are necessary. (8) Partial acid hydrolysis, acetolysis, and purified enzymes have been used to degrade the polysaccharides (or their derivatives) into fragments that can be identified, after suitable derivatization, by GLC-MS or high performance liquid chromatography-mass spectrometry (HPLC-MS). This makes sequenc-

ing of complex cell wall polysaccharides possible. (9) β-Eliminative degradation studies, originally developed for structural work on extracellular bacterial polysaccharides, have proved useful to determine the mode of occurrence of certain sugar residues in pectic polysaccharides.

This chapter is primarily intended for plant biochemists and nutritionists who are interested in the chemical aspects, but carbohydrate chemists would also benefit from the biochemical approach to cell wall analysis. In general, chemical methods for analyzing polysaccharides will not be described because several reviews dealing with this subject are available (Aspinall, 1973, 1976, 1982a). However, attention will be drawn to certain aspects of the methods that may be of interest in the context of the analysis of specific cell wall polymers.

1. Definition and Mode of Formation of Cell Walls

The plant cell wall is the principal structural component of the cell surrounding the protoplast and exterior to the plasmalemma. This structure is dynamic in that its shape, composition, and properties are constantly changing in response to growth, the stage of differentiation, the environment of the cell, and its activities.

The mode of formation of cell walls is as follows: Upon cell division, a cell plate is formed separating the cells. Pectic substances, particularly the calcium salts of pectins, are deposited on this plate to form the middle lamella, and then cellulose, hemicelluloses, additional pectic substances, some glycoproteins, and phenolics are deposited to form the primary cell wall. The primary cell wall is more organized than the middle lamella. The pectic substances of the middle lamellae, which are usually highly esterified, and the associated Ca^{2+} cement the cells together; removal of Ca^{2+} usually leads to cell separation. The newly formed cells usually increase in length 10- to 20-fold before growth stops. The cellulose is deposited as microfibrils, which are the cell walls' main structural elements. These are embedded in an amorphous matrix of closely associated (or sometimes interlinked) macromolecules of pectic substances, hemicelluloses, glycoproteins, and phenolics bathed in an aqueous medium. In the microfibrils parallel linear chains of cellulose molecules are closely packed by hydrogen bonding into bundles, forming highly ordered structures. Interspersed with these ordered crystalline regions are somewhat disordered amorphous regions in which the chains of cellulose are not closely packed and in which other sugars or polysaccharides may be found.

The α-cellulose fraction isolated from the parenchymatous tissues of most plants usually contains small but significant amounts of nonglucan

polysaccharides and glycoproteins associated with it. This association might occur during the preparation of the material by some adsorption effects, or it might form part of the essential organization of the polysaccharides within the wall. If the latter is true, then the associated polysaccharides probably serve as linking compounds for the entanglement of the cellulose microfibrils with the matrix polysaccharides.

Cells in some regions of the plant, for example, vascular and supporting tissues, become differentiated into specialized structures such as the xylem and phloem bundles, and sclerenchyma. These form the veins and ribs of leaves and continue into the petioles and stems. The xylem cells and sclerenchyma become thickened and hardened by lignification as the plant organ matures. Lignification begins in the primary wall region and then extends outward to the middle lamella and inward into the developing secondary wall, the final concentration of lignin decreasing from the outside to the inside of the wall. Lignin accounts for 15–35% of most lignified tissues and seems to form covalent linkages with some of the hemicelluloses, cementing together the wall polymers into a unified rigid matrix and stratifying the wall. During the growth of secondary (or lignified) walls cellulose, hemicelluloses (mainly acidic xylans in the case of dicotyledons and acidic arabinoxylans in the case of cereals) and lignin are deposited, and the thickening results more from the cellulose than the hemicellulose deposition. The lignified walls thus have cellulose microfibrils dispersed in hemicelluloses and lignin. The relevant information on the biochemical processes that transform primary walls into secondary walls is summarized in reviews by Northcote (1963, 1969).

In contrast to the cell walls of parenchymatous tissues of dicotyledons, those of cereal grains (wheat, barley, etc.) contain very little, or no, pectic substances. The primary walls of most cereal grains have cellulose microfibrils, which are closely associated with glucomannan, and these fibrillar structures are embedded in an amorphous matrix of hemicelluloses, which consists mainly of arabinoxylans and/or β-D-glucans, some of which are cross-linked by phenolic esters and/or proteins (Selvendran, 1983). Rice endosperm walls seem to be intermediate in character between these and parenchyma of dicotyledons in that they contain about 20% (w/w) of the walls as pectic substances and a substantial amount of cellulose (Shibuya and Iwasaki, 1978). These differences in the organization of the wall structure are reflected in their overall composition. For an extended discussion on these aspects, see Selvendran (1983, 1985).

2. Occurrence, Distribution, Structural Features, and Overall Composition

A knowledge of the occurrence, distribution, and structural features of the main cell wall polymers would help us to appreciate, on the one hand,

the experimental problems involved in their analysis and how these may be overcome, and, on the other, the requirements imposed by the diversity of starting materials. Most of the methods have limitations depending on the type of material being analyzed, and these must be borne in mind when interpreting the results.

The main types of tissues comprising the various products, the constituent cell wall polymers and their major structural features are summarized in Tables I and II; for the relevant references, see Table 1 of Selvendran (1985). The relative proportions of the different types of cell wall polymers vary with the type and maturity of the tissue. In addition to

TABLE I

Components of Cell Walls from Different Tissue Types

	TISSUE TYPES	MAIN CONSTITUENTS
Fruits and vegetables	Growing cells and parenchymatous tissues	Cellulose, pectic substances (e.g., arabinans, Rhamnogalacturonans), hemicelluloses (e.g., xyloglucans), and some glycoproteins
	with some lignified tissues	Cellulose, lignin, hemicelluloses (e.g., glucuronoxylans), small amounts of glycoproteins, and pectic substances
Suspension-cultured tissues of dicotyledons	Cells containing mainly primary cell walls	Same as parenchymatous tissues, except that the walls do not contain appreciable amounts of middle lamella pectins but have higher levels of polyphenolics and glycoproteins
Cereals	Parenchymatous and lignified tissues	Hemicelluloses (arabinoxylans and β-D-glucans), cellulose, phenolic esters, and proteoglycans
		Hemicelluloses (e.g., glucuronoarabinoxylans), cellulose, lignin, associated phenolic esters, and proteoglycans
Suspension-cultured tissues of cereal endosperm	Cells containing mainly primary cell walls	Hemicelluloses (mainly acidic arabinoxylans and β-D-glucans) cellulose, some phenolics and phenolic esters, and proteoglycans
Seeds other than cereals	Parenchymatous (e.g., cotyledons of peas) and some cells with thickened endosperm walls (e.g., guar)	Same as parenchymatous tissues of dicotyledons
		Galactomannans and small amounts of cellulose, pectic substances, and glycoproteins

TABLE II

Structural Features of Some Major Cell Wall Polymers

POLYMER	MONOSACCHARIDES		STRUCTURAL FEATURES
	MAJOR	MINOR	
Pectic substances			
Pectic acid, pectin	D-GalA	L-Rha L-Ara D-Gal	α-(1→4)-linked D-Gal*p*A (or methyl esterified Gal*p*A) residues containing (1→2)-linked β-L-Rha*p*; short arabinan and galactan side chains linked to C-4 of Rhap
Arabinan	L-Ara		(1→5)-linked L-Ara*f* residues having branch points through C-3, as well as C-3 and C-2 (doubly branched)
Galactan	D-Gal		Mainly β-(1→4)-linked D-Gal*p* residues, with some (1→4,6)-linked residues
Arabinogalactan-I	D-Gal	L-Ara	β-(1→4)-linked D-Gal*p* residues containing α-L-Ara*f* residues as side chains on C-3 of some of the Gal residues
Hemicelluloses			
Xyloglucans	D-Glc D-Xyl	D-Gal L-Ara L-Fuc	β-(1→4)-linked D-Glc*p* residues containing α-D-Xyl*p* residues as side chains on C-6 of at least half the Glc residues, with some of the Xyl residues being further substituted with β-D-Gal, α-D-Gal, α-L-Ara*f*, and L-Fuc*p* residues
Glucuronoxylans (and 4-*O*-Me glucuronoxylans)	D-Xyl	D-Glc*p*A 4-*O*-Me-D-Glc*p*A L-Ara	β-(1→4)-linked D-Xyl*p* residues with side chains of D-Glc*p*A or 4-*O*-Me Glc*p*A
Arabinoxylans	D-Xyl	L-Ara	β-(1→4)-linked D-Xyl*p* residues, with some of the residues doubly branched; side chains contain mainly L-Ara*f* residues
Glucurono- (and 4-*O*-Me glucurono arabinoxylans)	D-Xyl	L-Ara D-Glc*p*A 4-*O*-Me-D-Glc*p*A	As above but side chains contain in addition small amounts of (1→2)-linked α-D-Glc*p*A or 4-OMe-D-Glc*p*A
β-D-Glucans	D-Glc		β-(1→4) and β(1→3)-linked D-Glc*p* residues
Galactomannans	D-Man	D-Gal	β-(1→4)-linked D-Man*p* residues, with side chains on C-6 containing α-D-Gal*p* residues

TABLE II *(Continued)*

POLYMER	MONOSACCHARIDES		STRUCTURAL FEATURES
	MAJOR	MINOR	
Cellulose	D-Glc		Linear chains of β-(1→4)-linked D-Glc*p* residues
Hydroxyproline-rich glycoproteins	L-Ara	D-Gal	Hydroxyproline tetra- and tri-arabinofuranosides; α-D-Gal*p*-Serine linkage

the polysaccharide and glycoprotein components, the cell walls of unlignified tissues of cabbage, carrots, apples, and runner beans contain about 5–10% of polyphenolic compounds in the form of polysaccharide-protein-polyphenol complexes (Stevens and Selvendran, 1984 b, c, d; O'Neill and Selvendran, 1985). Since the cell wall polymers associated with parenchymatous and lignified tissues are different, it is advisable, where possible, to separate the tissues before analysis. This makes subsequent fractionation of the cell wall polymers easier and more predictable.

Before attempting detailed analysis of cell wall material (CWM), it is useful to get some indication of the nature and amount of polysaccharides present in the preparation. This can be obtained from its overall carbohydrate composition (Table III). In this connection, see also the tables given in Ring and Selvendran (1981), O'Neill and Selvendran (1983, 1985), Stevens and Selvendran (1984a, b, c, d), which describe the results of purifying cell walls and of chemical fractionation studies. From Table III, columns 1–3, it can be inferred that the cell walls of parenchymatous tissues contain mainly cellulose, pectic acid (or more correctly pectinic acid), as well as other pectic substances, and are virtually devoid of (acidic) xylans; the bulk of the xylose arises from xyloglucans. The amount of cellulose can be estimated from the values for glucose released on 1 *M* H_2SO_4- and Saeman-hydrolysis, and the amount of pectic acid can be estimated from the uronic acid content of the preparation (Selvendran et al., 1979). This method has the advantage that it measures the total pectic acid: both chelating agent—soluble and insoluble—pectic acid. It is such analyses that helped us to assess the relative significance of the chelating agent— insoluble pectic acid, and its possible association with other cell wall polymers, particularly the α-cellulose fraction. The bulk of the uronic acid in the cell walls of suspension cultured tissues arises from the pectic polymers of primary cell walls (Table III, columns 4 and 5). In general, the cell walls of suspension cultured tissues of dicotyledons contain much higher levels of pectic arabinans, polyphenolics and hydroxyproline-

TABLE III

Carbohydrate Compositions of Cell Walls from Some Plant Tissues (in g anhydrosugar/100 g CWM)

SUGARS	POTATOES (PARENCHYMA) (1)	RUNNER BEANS (PARENCHYMA) (2)	APPLES (PARENCHYMA) (3)	POTATOES (CULTURE) (1)	SYCAMORE (CULTURE) (4)	RUNNER BEANS (PARCHMENT) (5)
6-Deoxyhexose	2.2	1.9	2.0	1.5	4.4	0.7
Arabinose	4.9	3.5	12.3	10.1	21.0	1.1
Xylose	1.8	1.7	3.3	2.3	7.6	24.0
Mannose	1.0	1.6	4.3	1.0	0.3	0.6
Galactose	28.3	7.5	5.7	4.1	12.8	1.6
Glucose	37.3	31.4	22.7	16.2	23.0	42.0
Uronic acid	17.3	36.7	32.8	17.0	13.4	8.0
Carbohydrate (% w/w)	(92.8)	(84.3)	(83.1)	(52.2)	(82.5)	(78.0)

Sources: (1) R. R. Selvendran and P. Ryden, unpublished results; (2) O'Neill and Selvendran (1980a); (3) Stevens and Selvendran (1984d); (4) Talmadge et al. (1973); (5) Selvendran (1984).

rich glycoproteins compared with those of parenchymatous tissues (Selvendran, 1985; R. R. Selvendran, P. Ryden and A. V. Verne, unpublished results).

In contrast to the cell walls of parenchymatous tissues, those of lignified tissues of runner beans contain mainly cellulose and (acidic) xylans, and they are virtually devoid of pectic substances (Table III, column 6). The validity of these statements depends on the following: (1) the bulk of the neutral sugars from pectic substances and hemicelluloses are released by 1 *M* H_2SO_4-hydrolysis; to release glucose from cellulose Saeman-hydrolysis conditions are required; (2) a large proportion (~90%) of the uronic acid arises from the galacturonic acid of pectic substances; (3) the pectic substances of potatoes are rich in galactose, whereas those of apples and cabbage are rich in arabinose; (4) primary cell walls have little or no "free" glucuronoxylans, which are the predominant hemicelluloses of secondary walls; much of the xylose of primary walls arises from xyloglucans. However, cell walls of parenchymatous tissues of apples and runner beans contain small but significant amounts of acidic arabinoxylans and acidic xylans in combination with pectic polysaccharides, xyloglucans, proteins and polyphenolics (Stevens and Selvendran, 1984d; O'Neill and Selvendran, 1985). A significant amount (~5% of the dry wt. of the cell walls) of glucuronoarabinoxylan has also been isolated from the polyglacturonase treated cell walls of suspension cultured tissues of sycamore callus (Darvill et al., 1980c). In this connection it should be noted that cell walls of cambial tissues contain a significant amount of "free" acidic xylans (Simson and Timell, 1978).

3. Background and Present Significance

The purpose of this review is to discuss the important developments in the methods used for the isolation and analysis of higher plant cell walls since 1965–1970, with special reference to developments in our laboratory on the isolation and analysis of cell walls from parenchymatous and immature tissues of edible plant organs. Some of our results on the characterization of extracellular bacterial polysaccharides are also included because the methods used may well find application in the characterization of cell wall polysaccharides. A much shorter account of the methods used for the analysis of cell walls from edible plants has recently been published (Selvendran et al., 1985). The elegant work of Albersheim and coworkers on the sequencing of complex polysaccharides is not discussed in any detail because their methodology has been reviewed recently (McNeil et al., 1982b). Much of the earlier work has been reviewed by Jermyn (1955), various authors in *Methods in Carbohydrate Chemistry*, vol. 5, Blake et al. (1971), Blake and Richards (1971a, b), Wilkie and Woo (1977), Aspinall (1982a, b), and Wilkie (1979, 1985). In the last four references the authors

have drawn attention to some of the limitations and developments in published methods, and the difficulties and inadequacies of available methods for isolating individual polysaccharides in an undegraded state with particular reference to the following problems: (1) the lack of methods for properly defining the homogeneity of the polymers, (2) the relatively poor recoveries from some of the fractionation procedures, and (3) the deficiencies in the standard techniques for determining structure. In some instances suggestions for overcoming these problems have been discussed. In addition several improved techniques, some involving the use of a combination of chemical and enzymic methods for isolating and characterizing polysaccharides, have been presented. Also modifications of the older methods for determining sugar components have been reported because of the greater sensitivity, specificity, or both, made possible by developments in instrumentation, such as GLC-MS or HPLC-MS, for analyzing carbohydrate derivatives. The present review is concerned primarily with later developments, although we attempt some critical assessment of some of the earlier methods, grouping together where possible fractionation and characterization of cell wall polymers from various tissue types.

Despite the improved methods available for isolating relatively "pure" cell wall polymers, there is still a need for the development of methods for assessing the physical and chemical heterogeneity of closely related molecular species. It is useful, for example, to seek evidence of polydiversity in "neutral" pectic and hemicellulosic polysaccharides. Even with the latest techniques an exact structure of a heteropolysaccharide from the plant cell wall has yet to be fully established. The generalized picture of any polysaccharide given by chemical analysis is an inadequate description of its structure; our knowledge of the three-dimensional structure of a polysaccharide is nothing like as exact as that of proteins. However, the use of highly purified enzymes and the application of methods developed for sequencing oligosaccharides to characterize cell wall polysaccharides offers considerable promise for the future.

An additional complication in studying the polysaccharides of the cell wall is that they can form compounds/complexes with noncarbohydrate compounds such as lignin, polyphenolics that are quite distinct from lignin, and proteins. Such complexes have been isolated from a range of tissues by extraction with a variety of reagents and by suitable fractionation (Selvendran, 1985). These studies suggest that in some of the complexes the polysaccharides and noncarbohydrate components are bound together by covalent links. Attention will also be drawn to some of the recent developments in this area.

II. ISOLATION AND FRACTIONATION OF CELL WALL CONSTITUENTS: METHODS USED AND GENERAL DISCUSSION OF THE EXPERIMENTAL PROBLEMS

The problems associated with the isolation and analysis of cell walls are (1) those arising from the preparation of cell wall material, (2) those associated with the isolation of wall components, (3) those associated with the fractionation of the carbohydrate polymers. There are also problems associated with the determination of the constituent sugars, their mode of occurrence, and fine structural details; these are discussed later. The problems encountered in dietary fiber analysis and lignin determination, and measures for overcoming them, have been discussed at some length in a recent review (Selvendran and Du Pont, 1984) and will not be described in this chapter.

1. Preparation of Cell Wall Material

The purity of the cell wall preparation is very much dependent on the type of plant organ (or tissue) and also on the overall objectives of the investigation. It is more difficult to prepare relatively pure CWM from parenchymatous tissues than with those of lignified tissues, which are usually dead and contain very small amounts of intracellular compounds. The major problem with lignified tissues is usually the subdivision of the long fibers into relatively short ones without recourse to drastic physical methods, such as dry ball-milling, for long periods, which might cause degradation of the cell wall polymers. The nature of the problems associated with parenchymatous tissues is dependent on the type and amount of intracellular compounds present, such as polyphenols, pigments, lipids, nucleic acids, proteins, and reserve polysaccharides (e.g., starch and inulin). In order to study the nature of the cell wall proteins and polyphenolics, every effort must be made to remove the intracellular proteins and polyphenols as completely as possible.

In most of the early work on cell wall analysis, the alcohol insoluble residue (AIR), or the alcohol-benzene extractive free residue, was used as the starting material. Such residues may be suitable for tissues relatively poor in intracellular proteins, polyphenols, and starch, such as grasses and certain fruits and vegetables. Even with these products, interactions between the cell wall polymers occur, due to the dehydration effects of alcohol, resulting in the formation of artifacts. However, for starch- and protein-rich products additional complications arise because of coprecipitation effects. In oats and potatoes, for example, the starch to

proteins to cell wall ratios are about 7.7:1.6:1.0 and 15:0.7:1, respectively (Selvendran and Du Pont, 1980a). Although the bulk of the coprecipitated starch and proteins can be removed by miracloth filtration, and by chemical or enzymic methods, or a combination of both, small but significant amounts of "resistant" starch and proteins tend to remain in the "purified" wall preparations. Such preparations may not be suitable for studies on cell wall proteins but have been effectively used to obtain information on the nature of the major cell wall carbohydrate polymers of wheat (Mares and Stone, 1973a,b) and barley (Fincher, 1975) endosperm. Because of the usefulness of this procedure for cereals, it is described in detail in Section III.3. The intracellular protein contamination of the AIR could vary from as low as 5–6% (w/w) in the case of apple parenchyma to as much as 80% in the case of soyabean cotyledons (Selvendran et al., 1981). Further the protein content of the AIR varies with the maturity of the tissues, high in immature and low in mature tissues. Since pronase tends to degrade some of the hydroxyproline (hyp)-poor cell wall glycoproteins and possibly portions of the hyp-rich glycoproteins, pronase-treated residues may not give as much useful information on wall glycoproteins compared with the alternative methods described in this article.

Although the bulk of the intracellular polyphenols are soluble in aqueous alcohol, a significant amount remains in the AIR, which could obscure the nature of the phenolics associated with the cell wall polymers. It is probable that tissues rich in intracellular polyphenols such as tea shoots and cider apples, contain a relatively higher proportion of polyphenolics associated with the wall polymers, but the nature of these phenolics cannot be obtained using the alcohol-insoluble residues, unless the preparations are extensively purified. The polyphenols appear to be present, to an appreciable extent, in the vacuoles of some of the palisade cells of tea leaves (Selvendran and King, 1976), and this may be true of other tissues. In view of the recent interest in the association of phenolics with some pectic substances, wall proteins, hemicellulosic polymers, and α-cellulose of "primary" cell walls (Fry, 1983; Selvendran, 1985), the foregoing comments may be pertinent.

2. Isolation of Cell Wall Components

The CWM of an organ from a dicotyledonous plant, containing both parenchymatous and lignified tissues, is first depectinated by sequential extraction with hot water and a hot dilute solution of a chelating agent, or by direct extraction with a hot dilute solution of a chelating agent. The depectinated material is usually delignified by treatment with warm sodium chlorite and acetic acid (Wise et al., 1946; Jermyn and Isherwood, 1956), which generates chlorine and chlorine dioxide. The resulting

holocellulose is washed thoroughly with water and then extracted with alkali of increasing strength containing $NaBH_4$, and in some instances borate. The material insoluble in these reagents is called α-cellulose. The α-cellulose fraction isolated from most plant tissues usually contains small but significant amounts of pectic substances and glycoproteins associated with it.

A. PECTIC SUBSTANCES

Pectic substances are by definition those polysaccharides that can be solubilized from the CWM by hot water and by hot aqueous solutions of chelating agents, such as EDTA or ammonium oxalate. The solvent action of the chelating agent depends on its ability to combine with Ca^{2+} and Mg^{2+}, which are usually complexed with the galacturonic acid residues of pectins. The pectic substances extracted with hot water usually have a relatively higher degree of esterification and neutral sugar content compared with the oxalate soluble ones (Ring and Selvendran, 1981). This is because hot water can only partially solubilize some of the pectic substances of the primary cell walls and middle lamellae. The pectic substances in the latter are complexed with relatively higher concentrations of Ca^{2+} (and Mg^{2+}) and therefore require the action of a chelating agent. In the fifties and early sixties the duration of extraction was approximately 10−12 h on a boiling water bath. Subsequent work has shown that these conditions result in considerable breakdown of pectic substances by autohydrolysis and also by transeliminative degradation. Above pH 5, breakdown by transelimination becomes significant at elevated temperatures (Albersheim et al., 1960). Prolonged exposure to hot aqueous solutions was done in the belief that most of the pectic substances could be solubilized by such treatments. However, it is now clear that insoluble pectic material, possibly held by covalent linkages, is present in all types of cell walls, and the amount depends on the type of tissue. With runner beans approximately 80% of the total pectic material is extractable with chelating agents (O'Neill and Selvendran, 1983), whereas with apples it is approximately 50%, and with sugar beet approximately 30% (Selvendran, 1985). Some of the insoluble pectic material is extractable with alkali, but the bulk is found in close association with other cell wall constituents, particularly the α-cellulose fraction.

In view of the degradation of pectins, extraction with hot water is restricted to 1−2 h at pH 5. Even with the shorter extraction period, it is debatable whether extraction with hot water serves any useful purpose. Since the extracted pectic polysaccharides, which are rich in neutral sugars, such as arabinose (in the case of cabbage) and galactose (in the case of potatoes), appear to be breakdown products of more complex highly

esterified pectic polysaccharides (Selvendran, 1985). The less esterified pectins, particularly those complexed with Ca^{2+}, require the use of hot aqueous solutions of chelating agents, such as EDTA (Na salt), ammonium oxalate, or sodium hexametaphosphate. Although EDTA is only really effective above pH 7, which would result in appreciable β-eliminative degradation, Stoddart et al. (1967), using EDTA at pH 4–5, obtained nearly the same yield of apple pectin but over a longer time, as at pH 6.8. In order to maintain good chelating ability with minimum degradation, we have favored the use of 1% (w/v) ammonium oxalate at pH 5 for 2 h at 80°C (Ring and Selvendran, 1981). Other workers (Stoddart et al., 1967) have used 2–3% sodium hexametaphosphate at pH 3.7 for up to 4 h at 90–100°C and claimed that only minimal degradation occurred, although at pH 4.2 Aspinall and Cottrell (1970) found transelimination and de-esterification. We have avoided the use of hexametaphosphate because it could not be completely removed from the isolated polysaccharides.

Cold, dilute alkali has also been used either with, or following extraction by, chelating agents. As with the other methods there is considerable variation, largely dependent on the nature of the tissue, in the proportion of pectin extracted. Voragen et al. (1983) reported that the amounts of uronic acid extracted with cold 0.05 *M* NaOH + 0.005 *M* EDTA were as high as 95% and 97%, of the total uronide that could be solubilized from the AIR of strawberries and cherries, respectively, and 82% for apples (var. Golden Delicious). Using this method, with the cold dilute alkali + EDTA adjusted to pH 10, we could only solubilize 24% of the total uronic acid from a different variety of apple CWM, although polyuronide amounting to 5% of the CWM was solubilized during the preparation of the CWM (Stevens and Selvendran, 1984d).

Recently cyclohexanediamine tetraacetate (CDTA, 0.05 *M*) has been used, apparently very effectively, to solubilize pectic substances at room temperature (20°C), giving yields of pectin comparable to those of the more conventional chelating agents at high temperatures and consequently with reduced degradation (Jarvis et al., 1981; Jarvis, 1982). This procedure has been used to preferentially solubilize pectic substances from the middle lamellae of cell walls from onions (Redgwell and Selvendran, 1986), apples (Selvendran et al., 1985), and potatoes (Selvendran, 1985). Subsequent extraction of the residue with 0.05 *M* Na_2CO_3 at 1°C and then at 20°C was found to solubilize pectic substances from the primary cell walls (Selvendran, 1985). Jarvis et al. (1981) found that, after extraction with chelating agents, 0.1 *M* Na_2CO_3, at room temperature, was efficient for the extraction of galactan-rich pectic material from the CWM of potatoes. More details on the use of modifications of these procedures are given later.

With most tissues some pectic substances are also extracted with the hemicelluloses (Stevens and Selvendran, 1984b, c, d; O'Neill and Selvendran, 1985) but some remain with the α-cellulose residue. Pectic polymers associated with the α-cellulose have been isolated by the use of cellulase (Stevens and Selvendran, 1980; O'Neill and Selvendran, 1983) and have been found to have rhamnose to uronic ratio of approximately 1:6, which is much higher than the corresponding ratios of rhamnose to Gal*p*A in the pectic polymers of the middle lamellae (Selvendran, 1985).

B. Material Solubilized during Delignification

Delignification of the depectinated material is usually carried out by treatment with warm (70°C) Na chlorite-acetic acid for 2–4 h; heavily lignified tissues require longer treatment (Green, 1963). The delignified material is referred to as holocellulose. Despite the fact that the conditions used may effect chemical changes in addition to removal of lignin, and also cause slight depolymerization of some of the polysaccharides containing L-arabinofuranosyl residues, the method is widely used because it is effective. The duration of the delignification treatment can be varied depending on the type of material being analyzed; grass cell walls appear to require a shorter treatment (1 h) (Morrison, 1974a). Delignification of the cell walls from parchment layers of mature runner bean pods for 2 h removed only approximately 60% of the total lignin content (R. R. Selvendran, unpublished results); similar observations have been made with pear cell walls by Jermyn and Isherwood (1956).

During delignification a small proportion (~5–10%) of carbohydrate containing material is solubilized (Buchala et al., 1972; Selvendran et al., 1975). Some of the solubilized polymers may be polysaccharides linked to lignin or cross-linked by phenolics. With runner bean cell walls it was found that treatment with chlorite-acetic acid at 70°C resulted in the solubilization of the bulk of the hydroxyproline (hyp)-rich glycoproteins. The solubilized glycoproteins, which were partially modified, arose mainly from the cell walls of parenchymatous tissues (Selvendran, 1975a, b). Following this work, hyp-rich glycoproteins have been isolated from the cell walls of suspension cultured tissues of tobacco, by treatment with chlorite-acetic acid (Mort and Lamport, 1977). Using a shorter treatment with this reagent, we have isolated less modified wall glycoproteins from parenchymatous tissues of runner beans and have elucidated some of their structural features (O'Neill and Selvendran, 1980).

C. HEMICELLULOSES

Hemicelluloses can be partly extracted from the holocellulose by aqueous solutions of alkali, which may saponify any hemicellulosic ester linkages

between either polysaccharides or hemicelluloses and noncarbohydrate components. Strong alkali solubilizes polysaccharides that are strongly associated with cellulose by hydrogen bonding, such as xyloglucans and glucomannans. Alkaline degradation (peeling) of hemicelluloses can be prevented, or minimized, by reducing latent aldehydic end groups with sodium borohydride. Potassium hydroxide solutions are preferred because the potassium acetate formed on neutralization with HOAc is more soluble than NaOAc in aqueous alcohol. However, to solubilize glucomannans from the holocellulose of gymnosperm wood, NaOH is the preferred solvent (Hamilton and Kircher, 1958; Timell, 1965).

In early work with wood hemicelluloses, Wise and Ratliff (1947) have used a range of concentrations of aqueous KOH (2, 5, 8, 10, 12, 16, and 24%) in an atmosphere of N_2, at 20°C, to solubilize the hemicelluloses; the N_2 atmosphere is required to reduce the danger of aerial alkaline oxidation. Their studies showed that the hemicelluloses are removed rapidly up to 10% KOH concentration, and thereafter the removal was slow. Similar observations have been made, recently, with grass coleoptile cell walls (Carpita, 1983, 1984). Therefore, for practical purposes, Wise and coworkers recommended the use of two strengths of alkali: 5% to solubilize the hemicelluloses which they termed A and 24% to solubilize the fraction B. However, most workers use the term hemicellulose-A to represent the fraction precipitated on neutralization of the alkaline extract (usually 10%) with HOAc, and hemicellulose-B to denote the fraction precipitated by ethanol from the supernatant; this classification will be used in the rest of this chapter. The alcohol supernatant from hemicellulose-B contains some carbohydrate polymers that are not usually recovered. Fractionation of the hemicellulosic polymers from beeswing wheat bran, by graded alcohol precipitation, showed that an appreciable proportion of highly branched acidic arabinoxylans in association with polyphenolics, remained in solution in 90% alcohol (R. R. Selvendran and M. S. Du Pont, unpublished results). Hemicellulose-B usually consists of more highly branched polysaccharides, or in the case of linear polysaccharides those with a relatively lower degree of polymerization, compared with hemicellulose-A, and are generally more soluble in alkali. Hemicelluloses that have acetyl groups, for example, acetylated acidic xylans or glucomannans, can be partially extracted from the holocellulose with DMSO or hot water (Hagglund et al., 1956; Croon et al., 1959; Meir, 1961; Bouveng and Lindberg, 1965).

Based on published work, as well as our experience, a two- or sometimes three-step extraction of the holocellulose, or depectinated cell walls in the case of parenchymatous tissues, is recommended, because it effects partial fractionation of the hemicelluloses. A first extraction with 5%

KOH removes the more soluble polysaccharides and prevents extreme swelling that occurs when the holocellulose is treated directly with 24% KOH; an intermediate 10% KOH extraction could be included in some cases (Carpita, 1983, 1984). The glucuronoxylans with a relatively low degree of polymerization (~100) are dissolved by dilute alkali, whereas the glucuronoxylans with a higher degree of polymerization (~200), glucomannans and xyloglucans, require the stronger alkali (Selvendran et al. 1977; Stevens and Selvendran, 1984d). The effectiveness of the extraction of certain hemicelluloses (e.g., glucomannans) is enhanced by the presence of borate (Croon et al., 1959; Gyaw and Timell, 1965). Presumably the borate forms a complex with the 2,3-cis-hydroxyl groups of D-mannose residues, thus rendering the polymer more acidic and hence more soluble in alkali. Various workers have shown that wood holocellulose residues obtained after extraction with KOH (and NaOH), containing metaborate (addition of 3–4% boric acid), contained fewer mannose units compared with the residues obtained with 16% KOH alone. The preferential solubility of mannose containing polymers has been used extensively in the extraction of glucomannans (Timell, 1965).

D. FRACTIONATION OF CELL WALL POLYMERS

In the study of cell wall polymers one of the first requirements is their purification and fractionation into more or less homogeneous individual polymers. That means further fractionation of the polymer yields only material having the same specific rotations and the same ratio of monosaccharide residues. In *Methods in Carbohydrate Chemistry*, Volume 5, procedures are described for fractionating neutral and acidic polysaccharides. Not all the methods are of preparative value, although they may give information that can be used to interpret or correct results obtained by other means. The hemicelluloses, for example, can be fractionated by a number of methods involving graded alcohol precipitation, formation of iodine and copper complexes, fractionation using $Ba(OH)_2$ and quaternary ammonium salts, and by cellulose column and anion exchange chromatography. For anion exchange chromatography the native (acidic) polysaccharides or the borate complexes of neutral (and acidic) polysaccharides could be used. Some of these methods are applicable for the separation of pectic substances as well.

a. Graded Alcohol Precipitation. Ethanol is most commonly used, but methanol and acetone, and other organic solvents have also found application. To a solution of the polysaccharide in water (or dilute alkali adjusted to pH 6 with HOAc), ethanol is added in a stepwise manner, and the precipitated polysaccharides are removed by centrifugation. If no

precipitation occurs on addition of alcohol, the polysaccharide may be brought out of solution by the addition of potassium acetate. A final salt concentration of <5% is sufficient. It is convenient to add gradually a 4:1 mixture of ethanol and saturated potassium acetate, stirring until precipitation is complete. The acetate is preferred over many other salts because it is highly soluble in ethanol, and consequently there is less risk of precipitating the salt even with a large excess of ethanol. The tendency for coprecipitation of polysaccharides can be partially overcome by repeated fractional precipitations, but unless the solubilities of the components are quite different, the method can produce only a rough separation. With hemicelluloses from beeswing wheat bran, we have found that graded alcohol precipitation (10–90% ethanol) had to precede anion-exchange chromatography for adequate resolution of the polymers (Brillouet et al., 1982; R. R. Selvendran and M. S. Du Pont, unpublished results).

*b. **Precipitation as Iodine Complexes.*** The reaction of a polysaccharide with iodine in a solution of $CaCl_2$ can be used to discriminate between linear and branched polysaccharides; the linear polymer is obtained as a heavy blue precipitate, and the branched polymer remains in solution. Gaillard (1961, 1966) reported that linear polysaccharides are precipitated from 1% solution in 30% aqueous $CaCl_2$ solution by the addition of aqueous iodine in KI, whereas the branched polysaccharides (e.g., arabinogalactans) are not. He has used this method effectively to compare the linear and branched polysaccharides of three Gramineae and three Leguminosae (Gaillard, 1965). The fractionation of corn stalk hemicelluloses by this method compares well with that obtained by graded alcohol precipitation (Gramera and Whistler, 1963). However, the method does not distinguish slightly branched polysaccharides, carrying single terminal branch residues, from linear polysaccharides. The presence of carboxyl groups and the molecular weight of the polymer influence the solubility of the I_2 complex.

*c. **Fractionation Using Copper Complexes and Copper Salts.*** A number of workers have used solutions of copper salts to effect separation of polysaccharides. As is common with most precipitation methods, the copper precipitates are voluminous and jellylike and suffer from the drawbacks of coprecipitation, occlusion, and so forth. Two general methods have been used. One involves the use of Fehling solution or "cuprietheylenediamine" (Jones and Stoodley, 1965; Aspinall and Wilkie, 1956; Aspinall et al., 1977), as in the precipitation of various mannans (Edwards, 1965), presumably through complexation of the cis-2- and 3-hydroxyl groups. The formation of the insoluble copper complexes with xylans (Adams, 1965) is less clear. The copper complex is removed by

either filtration or centrifugation. Usually further fractions can be obtained from the supernatant by the addition of alcohol. The precipitates are then decomposed by an alcoholic solution of acid. This method has been used to purify xyloglucans from rape seed hulls (Aspinall et al., 1977) and potatoes (Ring and Selvendran, 1981). With the material from potatoes, the ratio of polysaccharides from the soluble and insoluble complexes was about 1.1:1, and the molar ratios of the constituent sugars were found to be comparable by sugar and methylation analysis. However, the neutral sugars released on 1 *M* H_2SO_4-hydrolysis accounted for 48 and 94% of the dry weights of the carbohydrate polymers from the soluble and insoluble copper complexes, respectively.

The other method uses only cupric salts, chloride, sulfate, or acetate, to effect the precipitation of the copper complexes; the acetate is generally preferred (Erskine and Jones, 1956; Aspinall et al., 1967; Blake and Richards, 1971a). As before, the formation of the complex depends primarily on interaction between Cu^{2+} and $-OH$ groups of the polysaccharide, although some intermolecular ionic bonding may occur between Cu^{2+} and carboxyl groups of the uronic acid. This method has been used to separate acidic and neutral polysaccharides, but work with pectic substances from cabbage has shown that the method is not as effective as fractionation on DEAE-Sephadex (Stevens and Selvendran, 1984a). Failure to obtain "neutral" pectic polysaccharide from cabbage by the precipitation method may be due to "salting-in" of the first formed precipitate. As more than the optimum amount of salt can inadvertently be added, the procedure has to be based on small-scale solubility curve. For a discussion of the factors involved in the interaction of metal ions with polysaccharides, see Blake and Richards (1971a) and the references therein.

d. Fractionation Using Barium Hydroxide. It has been observed that barium hydroxide in concentrations as low as 0.03 *M* forms insoluble complexes with mannans and glucomannans probably by reaction with the vicinal 2,3-cis hydroxyl groups of the mannose residues (Meier, 1958, 1965). The barium complexes of the mannans and glucomannans are easily soluble in dilute acids. To effect separation of the polysaccharide containing β-(1→4)-linked mannose residues, the hemicelluloses are dissolved in water or in dilute NaOH and saturated $Ba(OH)_2$ solution is added. The precipitate formed is removed by centrifugation and further purified by dissolving it in water or in dilute NaOH and reprecipitating with $Ba(OH)_2$. After centrifugation, the precipitate is dissolved in 2 *M* HOAc, and the mannan is precipitated with ethanol, and washed successively with ethanol-water, ethanol, and ether. Timell (1961) has used the principles underlying this method to isolate glucomannans and

galactoglucomannans from the wood of gymnosperms. It should be noted, however, that galactans containing (1→6)-linked galactose residues, or a high proportion of terminal galactose residues, are also precipitated under the above conditions. This may be because such polysaccharides contain the requisite vicinal cis-hydroxyl groups on carbon atoms 3 and 4 of the galactose residues.

Acidic polysaccharides are also precipitated but at higher concentrations of $Ba(OH)_2$. Meier (1958) found that birch glucuronoxylan was precipitated when the $Ba(OH)_2$ concentration was 0.15 *M*, probably due to the formation of the insoluble barium salt of the acidic xylan. Pectic acid can be separated almost quantitatively from the neutral (pectic) polysaccharides as the insoluble barium salt. Therefore the use of $Ba(OH)_2$ as a precipitant will provide a complement to the other methods.

*e. **Fractionation Using Quaternary Ammonium Salts.*** Quaternary ammonium salts such as cetyltrimethylammonium bromide (Cetavlon, CTAB), cetylpyridinium chloride (CPC), and benzylcetyldimethylammonium chloride react with polyanions to form precipitates that are very insoluble in water. This method was developed by Scott (1955, 1963) and has been used extensively to isolate connective tissue polysaccharides. Neutral polysaccharides do not react except as borate complexes, if these can be formed, or at very high pH, when some of the hydroxyl groups ionize. Acidic polysaccharides can therefore be readily separated from neutral ones by precipitation with CTAB under suitable conditions. There is good evidence to believe that the precipitation involves salt formation. The details of the method and its applications to acidic and neutral polysaccharides are described by Scott (1963, 1965).

The solubility of the cetylpyridinium precipitates is of the order of 1 mg/50 ml. The low solubility of the complexes makes it possible to precipitate polysaccharides even from solutions as dilute as 0.01% or less. For optimum precipitation, however, the polysaccharide concentration should be between 0.1 and 1%. For complete precipitation the polysaccharide is precipitated with three parts of CPC, on a weight basis. The final mixture should contain at least 0.05% of free CPC. The presence of some salt greatly aids the precipitation; NaCl or Na_2SO_4 of 0.02–0.04 *M* is usually satisfactory for this purpose. The cetylpyridinium complexes are converted to sodium salts by dissolving the precipitate in 2 *M* NaCl-ethanol (100:15, v/v), and the polysaccharide is precipitated by the addition of 2–3 volumes of ethanol. Isolated pectins have been separated into fractions of decreasing acidity and increasing neutral sugar content by fractional precipitation with ethanol (Barrett and Northcote, 1965; Foglietti and Percheron, 1968), or, after saponification, with increasing

concentrations (up to 0.22 *M*) of sodium acetate followed by precipitation with ethanol (Zitko and Bishop, 1965; Aspinall et al., 1970; Salimath and Tharanathan, 1982).

f. ***Anion-Exchange Chromatography.*** Several methods have been described for the separation of acidic and neutral cell wall polysaccharides by anion exchange chromatography on polysaccharide fibers (cellulose) or cross-linked gels (dextran in Sephadex or agarose in Sepharose) carrying the required functional groups, for example, *O*-(2-diethylaminoethyl) (Neukom and Kundig, 1965). Certain neutral polysaccharides, such as xyloglucans, can be fractionated as the borate complexes, the requirement being the presence of free cis OH groups that can form the borate complexes (e.g., (1→4)-linked Man*p* or terminal Gal*p* residues). Selective elution from the column is effected by stepwise or gradient elution, using salt solutions or buffers. A variety of ion-exchange materials have been used, including DEAE-cellulose, ECTEOLA-cellulose, DEAE-Sephacel, DEAE-Sephadex, DEAE-Sepharose, and calcium phosphate gels. Despite the extensive literature it is difficult to find information on the optimum conditions for a given separation. Information on the factors influencing abnormal elution patterns and recoveries is likewise difficult to obtain. It is possible to get a better appreciation of some of these problems by considering the basic principles involved in the preparation and use of ion-exchange materials.

The application of anion-exchange chromatography for the separation of acidic polysaccharides has not met with the same general success obtained with smaller acidic molecules. The large size of the molecule prevents its penetration into the adsorbent particle; therefore only the adsorbing sites located at the surface are utilized. To obtain reasonably high adsorption/ion-exchange capacity, the support material (e.g., cellulose used for making DEAE-cellulose) has to be finely subdivided before incorporating the ion-exchange sites on it. Too high a density of ion-exchange sites may result in binding so firm that the conditions required for simultaneous dissociation of all the binding and adsorption sites may be destructive to the integrity of the adsorbed molecules. Also the presence of too many substituents on cellulose interferes with the hydrogen bonding between cellulose chains, which is responsible for the insolubility of the material; a large number of substituents will cause the cellulose derivative to become water soluble like carboxymethylcellulose. The degree of incorporation is controlled to keep the physical properties of the product within the range useful for chromatographic purposes. DEAE-cellulose products containing much more than 1 meq/g exchange capacity have a tendency to be gelatinous, with a high resistance to the flow of

aqueous solvents. This limitation is not serious, for the capacity for acidic polysaccharide adsorption is high, on a mass basis, even when the acid-base capacity of the adsorbent is of the order of 1 meq/g of dry resin, which would correspond to about 200 mg of polysaccharide. However, the actual capacity for polysaccharide is much lower and ranges from 5–25 mg/g of resin, the exact amount depending in part on the nature of the polysaccharide.

Since multiple-site binding is undoubtedly involved in the polysaccharide ion-exchange combination, a low density of binding sites is advantageous, provided that the capacity is adequate, in that it will contribute toward the ease of elution from the column. Alkaline solvents tend to elute glucose containing polymeric material from DEAE-cellulose, which is usually attributed to alkaline degradation of the ion exchanger. Blake and Richards (1971a), however, are of the opinion that this effect is more probably due to slow diffusion of relatively short polymer molecules from the packing. These short molecules are presumably produced during the original processing of the cellulose, particularly the fine subdivision step, and their diffusion into the eluant will be dependent on the extent of the swelling of the particles. In view of this the use of strong alkaline eluants is not recommended for cellulose-based ion exchangers.

Several workers have noted that the recovery of polysaccharides, such as glucuronoxylans and glucuronoarabinoxylans (with a low degree of substitution) from DEAE-cellulose (or cellulose) is poor. This is due to the tendency for strong hydrogen bond formation between the polymer molecules and cellulose, which can be dissociated only with solutions of (strong) alkali or hydrogen bond breaking reagents such as urea. The incorporation of 7 *M* urea in the eluting medium improved the recovery of acidic xylans, but the eluted material was contaminated with glucose containing polymeric material. Furthermore elution of Cellulose CFI with 7 *M* urea or 1 *M* KOH gave polymeric compounds rich in xylose and glucose (yield 10 mg/g of dry cellulose), which presumably arose from "adsorbed" acidic xylans and short β-glucanlike polymer molecules (B. J. H. Stevens and R. R. Selvendran, unpublished results), so the use of cellulose is not recommended unless the use of these solvents can be avoided.

Despite the shortcomings DEAE-cellulose has been used (and often still is) with elution with phosphate buffers, at slightly acid pH (Neukom et al., 1960; Aspinall et al., 1967a). "Neutral" polysaccharides, usually with low levels of uronic acid, are not retained on the column. The bulk of the pectins can be fractionated according to their degree of esterification, the less esterified pectins generally eluting with the higher ionic strength buffers (Deventer-Schriemer and Pilnik, 1976). However, some acidic

polysaccharides adsorb strongly onto the cellulose and require the use of strong chaotropic reagents such as urea, or NaOH up to 0.5 *M*, to release them (Neukom et al., 1960), NaOH causing de-esterification or degradation by β-elimination or both (Knee, 1970). Subsequently another anion-exchange resin based on cellulose, DEAE-Sephacel, has come into use. DEAE-Sephacel is based on a beaded form of cellulose combining the properties of cellulose with the advantage of the high flow rates and nonshrinkage at high ionic strengths. Even with this resin, the recoveries are often poor, sometimes as low as 66% (Stevens and Selvendran, 1984a, b, d). Fractionation of pectic substances on DEAE-Sephacel (chloride form), using NaCl buffers, separates the weakly acidic pectic substances from the strongly acidic ones. Further resolution of both types of pectic substances can be effected by using the anion-exchanger in the acetate form and by using acetate buffers (Stevens and Selvendran, 1984c). The improved resolution may be due to the fact that pectic substances fractionate better in acetate buffers.

The dextran-based ion-exchange materials such as DEAE-Sephadex are also in bead forms and permit higher flow rates, but considerable shrinkage occurs with increasing ionic strength and separation of pectic polysaccharides is no better than on DEAE-cellulose or DEAE-Sephacel. The recovery of pectic substances (Aspinall et al., 1968a; Stevens and Selvendran, 1984a, b) and some of the glucuronoarabinoxylans from beeswing wheat bran (R. R. Selvendran and M. S. Du Pont, unpublished results) on DEAE-Sephadex was seldom more than 60–70%. The relatively poor recovery may be due to shrinking of the resin, during elution, which results in trapping of the larger molecules bound to the interior sites. Another factor responsible for poor recovery may be interaction between the polymers themselves, caused by the close proximity on the column. Such interactions may result in the precipitation of the polymers on the column. Therefore, for preparative work, anion-exchange chromatography should be used in conjunction with the other methods described earlier. In our work with hemicellulosic polysaccharides of beeswing wheat bran, partial fractionation of the polymers was first effected by graded alcohol precipitation, and the separated fractions were then further resolved by chromatography on either DEAE-Sephadex or DEAE-Sephacel (R. R. Selvendran and M. S. Du Pont, unpublished results).

More recently DEAE-Sepharose CL-6B, an agarose-based ion-exchange material with higher exclusion limits than the dextran-based materials, has given improved separations of pectins. Stepwise elution was found to give better and more reproducible separations than gradient elution from the phosphate form (Souty et al., 1981), but in later applica-

tions gradient elution has been used (Barbier and Thibault, 1982; Thibault, 1983). DEAE-Sepharose CL-6B has also been used in the fractionation of hemicellulosic polymers of carrot (Aspinall et al., 1983) and in the separation of xyloglucans from apple cell walls, the borate form provided better resolution and slightly better recoveries than DEAE-Sephacel (Borate) (Ruperez et al., 1985; P. Ruperez, R. R. Selvendran, and B. J. H. Stevens, unpublished results). Macroporous acrylamide polymers have recently become available as ion-exchangers with high ion-exchange capacities and avoiding many of the limitations associated with the polysaccharide-based materials. DEAE-Trisacryl has been used in the purification of pectic arabinans (Joseleau et al., 1983). In our hands, good separation and 85–90% recovery of onion pectic substances and hemicellulosic polymers have been obtained with DEAE-Trisacryl-CM (phosphate form), when the elution was performed with dilute phosphate buffer (0.05 *M*, pH 6.3) containing increasing amounts of NaCl (0.125–0.5 *M*). However, when the elution was performed with acetate buffer (pH 4.5) containing NaCl the recovery was only 51%. The recoveries of onion pectic substances from DEAE-Sephadex and DEAE-Sepharose, both in phosphate forms, using phosphate buffer (pH 6.3) containing NaCl were 59 and 56%, respectively (Redgwell and Selvendran, 1985).

Hydroxyapatite is generally used for fractionating proteins and glycoproteins (Bernadi, 1971) but has been used to fractionate arabinogalactan-proteins (Churms and Stephen, 1984) and proteoglycans from runner bean cell walls (O'Neill and Selvendran, 1985). After an initial fractionation of the runner bean proteoglycans on DEAE-Sephadex (chloride form) fractions were chromatographed on hydroxyapatite. The polymers that were bound and eluted with phosphate buffer were of relatively low carbohydrate content and had significant amounts of protein associated with them. Proteoglycan complexes have also been obtained by fractionating the hemicellulosic polymers of carrot cell walls on DEAE-Sephacel (acetate form) (Stevens and Selvendran, 1984c).

*g. **Affinity Chromatography.*** The reversible noncovalent binding of carbohydrate polymers, most commonly to proteins, provides the basis for affinity chromatography, which takes advantage of the high specificity found in many biological interactions. Carbohydrate binding proteins or lectins have the capacity to bind particular mono- or oligosaccharides and compounds containing such groups. Thus they bind sugars of defined glycosidic configuration and precipitate polysaccharides and glycoproteins specifically. They are usually recognized by their agglutinating effects on erythrocytes (Goldstein and Hayes, 1978). Concanavalin A from jack bean has multiple specificity, especially toward α-D-

mannopyranans and less toward α-D-glucopyranans and precipitates such α-D-glycans from solution. Concanavalin A covalently bound to an inert support such as Sepharose has been used to fractionate *N*-glycosidic glycopeptides containing α-D-mannopyranose residues (Narasimhan et al., 1979 and the references therein). The success of these fractionations is due to variation in the relative affinities of different oligosaccharide structures for Con A-Sepharose. Potato lectin, a glycoprotein containing about 50% carbohydrate and a high proportion of hydroxyproline, was purified by affinity chromatography on an *N*,*N*′,*N*″-triacetylchitotriose-Sepharose matrix (Desai and Allen, 1979). Clarke and coworkers have isolated arabinogalactans and arabinogalactan-protein conjugates using β-D-galactopyranoside-binding lectin from the small giant clam *Tridacna maxima* coupled to Sepharose 4B (Gleeson et al., 1979; Gleeson and Clarke, 1979, 1980). It is very likely that in the near future affinity chromatography will find widespread application for the fractionation of cell wall polysaccharides.

III. METHODS FOR ISOLATING CELL WALLS FROM VARIOUS PLANT TISSUES

The choice of a method for the isolation of cell wall material depends on how necessary it is to isolate the CWM with the minimum contamination of intracellular compounds. In Section II.1 some of the problems involved in the isolation of cell walls have been discussed in general terms. The methods that have been used are illustrated in greater detail by giving some examples of preparing cell walls from different types of tissues. Some of these are subject to the limitations that have been emphasized previously. As representative procedures, however, they indicate the position from which further advances may be made.

A range of methods have been described in the literature, and we shall consider them in the following order: (1) the methods developed at the Food Research Institute-Norwich (FRIN), to isolate cell walls from a range of vegetables and fruits (runner beans, potatoes, cabbage and apples), cereals (oats, wheat and rye) and cereal products (wheat bran and rye biscuits), and lignified tissues (parchment layers of runner bean pods); (2) the special techniques, which may include wet sieving steps, used for the isolation of cell walls from potatoes, wheat endosperm, and wheat and barley aleurone layers; (3) alternative methods for the isolation of cell walls from starch and protein-rich products (rice); and (4) methods used for the isolation of cell walls from suspension-cultured tissues.

1. Preparation of Cell Wall Material from Fresh Tissues (Methods Developed at FRIN)

In our studies coprecipitation effects were avoided by using aqueous inorganic solvents instead of aqueous alcohol. To minimize the formation of oxidation products of polyphenols, 5 m*M* sodium metabisulfite was incorporated into the extraction medium. To achieve "complete" removal of proteins and starch, it was necessary to ensure "complete" disruption of tissue structure and then to use solvents that have a high affinity for these compounds. The first objective was achieved by wet ball-milling the tissue triturated in an aqueous solvent. Proteins were removed by sequential treatment with 1% (w/v) aqueous sodium deoxycholate (SDC) or 1.5% (w/v) aqueous sodium dodecyl sulphate (SDS) and phenol:acetic acid: water (PAW) (2:1:1, w/v/v) (Selvendran, 1975a), and starch was removed with dimethyl sulfoxide containing 10% water (90% aqueous DMSO) (Ring and Selvendran, 1978; Selvendran and Du Pont, 1980; Selvendran et al., 1981). To minimize enzyme activity low temperature extraction, frozen powder (−20°C) was blended with SDC or SDS at 20°C and treatment with PAW was used. As a representative example the preparation of CWM from potatoes is described (Fig. 1).

Preparation of SDC (or SDS)/PAW-Insoluble Residue (Preparation-1). Preparation-1 of potatoes is obtained by sequential treatments of the disintegrated tissues with 1% SDC or 1.5% SDS, 0.5% SDC or SDS and PAW. The tubers are skinned with a sharp knife, sliced into small pieces, dropped into liquid N_2, and ground to a fine powder. The frozen powder is usually stored at −20°C until required. The powder (50 g) or freshly cut material is blended with 100 ml of 1% SDC (or 1.5% SDS) containing 5 m*M* sodium metabisulfite ($Na_2S_2O_5$) in a Waring blender for 2 min and then with an Ultraturrax for a further 3 min; a few drops of octanol are used to minimize frothing. The blended material is filtered through nylon cloth and washed with 2 bed volumes of 0.5% SDC (or 0.5% SDS) containing 3 m*M* $Na_2S_2O_5$ on the filter, and then squeezed to remove the interstitial fluid to give Residue-R_1; from the filtrate the bulk of the SDC-soluble polymers, which are mainly of intracellular origin, could be isolated. The resulting product is quantitatively transferred with approximately 100 ml of 0.5% SDC or SDS containing 3 m*M* $Na_2S_2O_5$ to a Pascall ball-milling pot (500 ml capacity), and ball-milled. Optimal cell disruption is obtained by ball-milling at 60 rev/min for 15 h at 2°C. At the end of the ball-milling period, the suspension is filtered through a nylon sieve (3 mm pore size), and the balls are washed with distilled water. The filtrate (suspension) is centrifuged in the cold (2°C) for 15 min at 23,000 g, and from the supernatant fluid the bulk of the cold SDC- or SDS-soluble cell

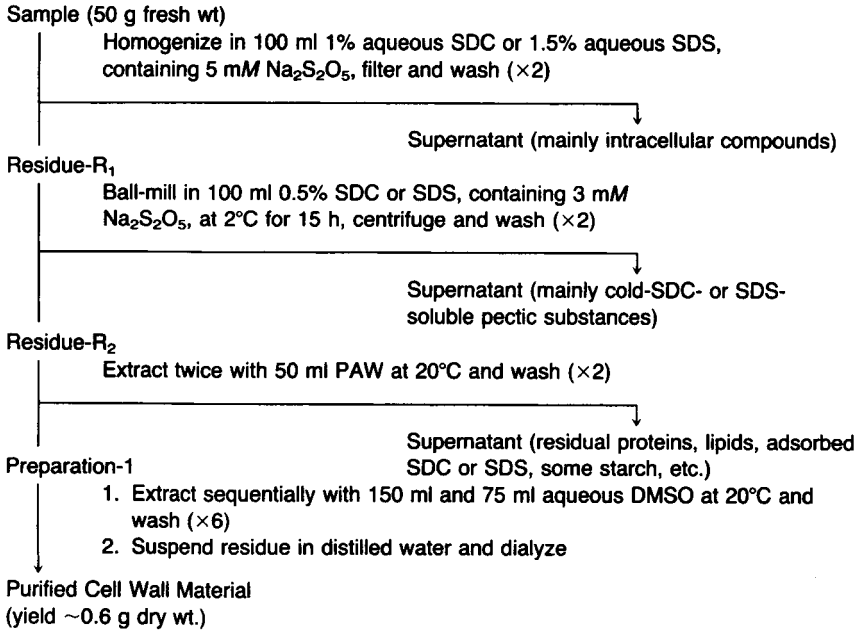

Fig. 1. Scheme for preparation of cell wall material from fresh potatoes.

wall polymers could be isolated. The pellet is washed twice with three bed volumes of distilled water (~100 ml) by centrifugation to give Residue-R_2. The wet residue is then extracted twice with 50 ml of PAW to remove adsorbed SDC (or SDS), residual proteins, pigments, and so on; a short treatment in a blender helps to give a uniform suspension. The residue obtained by centrifugation is washed twice with distilled water on the centrifuge to give the SDC (or SDS)/PAW-residue (Preparation-1). In this connection it should be noted that unless the product is very rich in proteins, such as peas, soybeans, and most cereals, the PAW treatment may be omitted. However, for the products mentioned here, it is essential.

Removal of Starch from Preparation-1. Preparation-1 contains much starch which has to be removed by extraction with 90% (v/v) aqueous DMSO. The wet residue (~20 ml) is blended in 150 ml of aqueous DMSO in a Waring blender and sonicated in a 250 ml round-bottomed flask using an ultrasonic bath (e.g., Bransonic) at maximum output for 10 min. The temperature of the contents of the flask should not be allowed to rise above 30°C. The mixture is then stirred for 16 h (overnight) at 20°C. Centrifugation of the thick emulsion at 15°C for 15 min at 23,000 g yields an opalescent aqueous organic phase that contains mainly (~97%) starch,

and this layer is removed. The residue is dispersed in 75 ml of aqueous DMSO, ultrasonicated for 30 min, stirred for 1 h at 20°C, and centrifuged as before. The insoluble residue is washed six times with distilled water by centrifugation. These treatments resulted in complete removal of starch from potato Preparation-1, as shown by negative reaction with I_2/KI and carbohydrate analysis, so that only cell wall polymers remained. The material thus obtained contains a very small amount of adsorbed DMSO. However, a product completely free of DMSO is obtained by suspending the pellet in distilled water and dialyzing against distilled water for 15 h (Visking, size 2). The residue obtained by centrifugation is defined as the purified cell wall material (CWM): yield approximately 0.6 g dry wt. It is best to freeze-dry an aliquot of the cell wall preparation for analysis of the constituent sugars and amino acids and to store the bulk of it in the frozen state until required for fractionation studies. The procedure can be scaled up for larger quantities provided sufficient ball-milling capacity is available.

Isolation of Polymers from the Extracts. The solvents used for solubilizing the intracellular compounds would also solubilize a small proportion (~6%) of the cell wall polymers from potatoes. These polymers could be isolated from the 1% SDC or 1.5% SDS, 0.5% SDC or SDS, PAW-, and DMSO-extracts.

The SDC- and SDS-extracts are filtered through Whatman No:42 filter paper or glass fiber filter paper GF/C, and dialyzed (Visking, size 7) for 72 h against several changes of distilled water. The dialyzed material is concentrated, and ethanol is added at 20°C to yield a final concentration of 80% ethanol; after 6 h the precipitated polymers are removed by centrifugation. Since some cold water-soluble pectic substances are soluble in 80% ethanol, it is useful to check the supernatant from the water extract for carbohydrate containing material. The contaminating proteins and small amounts of starch in the isolated polymers could be removed enzymically. The polymers from the 1% SDC- or 1.5% SDS-extract are mainly of intracellular origin in the case of fresh potatoes; approximately 1% of cell wall polymers are solubilized. With cooked potatoes, however, significant amounts of pectic polymers are solubilized during SDC extraction. When the disintegrated tissues are ball-milled in 0.5% SDC or SDS, approximately 3–4% of cell wall polymers, mainly of pectic origin, are solubilized in addition to small amounts of starch and proteins.

The PAW extract is diluted with distilled water and dialyzed (Visking, size 7) first against 25% (v/v) acetic acid and then against several changes of distilled water. During dialysis, a flocculent brownish-white precipitate separates in the tubing; this precipitate contains mainly deoxycholic acid

and starch. The polymers are isolated from the supernatant fluid, after concentration, by precipitation with alcohol, as before. PAW treatment solubilized <1% of cell wall polymers from fresh potatoes.

The aqueous DMSO extracts are combined and dialyzed (Visking, size 7) at room temperature against several changes of distilled water for six days. During the latter stages of dialysis, a flocculent gelatinous white precipitate, containing mainly (~98%) starch, separates in the tubing, and this is removed by centrifugation. The supernatant fluid is concentrated and treated with ethanol to precipitate the polymers, which would be mainly starch in the case of potatoes. With potatoes almost pure starch could be obtained from the DMSO extracts. The aqueous DMSO treatments solubilized approximately 2% of cell wall polymers from fresh potatoes.

The contaminating proteins and starch present in these polymers could be removed by sequential treatments with Pronase, and a mixture of pancreatic α-amylase and pullulanase. α-Amylase and pullulanase hydrolyse α-(1→4)- and α-(1→6)-glucosidic linkages, respectively. For details of the enzymic treatments, see Stevens and Selvendran (1980a) for protein removal, and Selvendran and Du Pont (1980a, b) for starch removal.

The total amount of cell wall polymers solubilized by aqueous SDC, water, PAW and aqueous DMSO varied from 6–10% of the purified CWM, in the case of fresh vegetables and unripe fruits (Selvendran, 1975a; Ring and Selvendran, 1978; O'Neill and Selvendran, 1980a; Selvendran et al., 1981; Stevens and Selvendran, 1984a, d) to about 30% in the case of dehulled oats (Selvendran and DuPont, 1980b; Selvendran and DuPont, unpublished results); wheat bran, which contains much lignified tissues, is an exception in that only approximately 2% of the cell wall polymers are solubilized (Ring and Selvendran, 1980; Selvendran et al., 1980). In the case of dehulled oats, and cereal products containing appreciable amounts of endosperm tissues, a significant proportion (~40–50%) of endosperm cell wall β-glucans and arabinoxylans are solubilized mainly during aqueous SDC and aqueous DMSO treatments (Selvendran and DuPont, unpublished results).

Comments. The method described is applicable to starch- and protein-rich tissues. For starch-poor tissues much less aqueous DMSO is required. For protein-poor tissues the PAW treatment may be omitted, but it should be borne in mind that in such cases the adsorbed detergent, some pigments, and small amounts of residual proteins would be removed by the subsequent aqueous DMSO treatment. The yield of CWM depends on the type of tissue; from 100 g fresh parenchymatous (or immature) tissues the yields of dry CWM are as follows: potatoes (1.0–1.2 g), runner beans

(1.1–1.3 g), apples (1.5 g), and cabbage (2.0 g). For lipid-rich products (e.g., certain oil-containing seeds) it is best to defat the products successively with boiling isopropanol and light petroleum (b.p. 60–80°C), prior to aqueous SDC/SDS, PAW, and aqueous DMSO treatments.

Although this method is somewhat long, the final preparation is virtually free of intracellular compounds and therefore enables one to study with greater confidence the nature of the cell wall polymers and their association within the cell wall matrix. Since the method enables one to isolate gram quantities of CWM, appreciable amounts of the individual polymers could be isolated for characterization purposes and also for a study of their properties. Thus xyloglucans have been isolated from potatoes, runner beans, cabbage, and apples; hydroxyproline-rich glycoproteins/proteoglycans from runner beans, cabbage, and apples; hydroxyproline-poor glycoproteins/proteoglycans from runner beans, cabbage, carrot and apples; xyloglucan-pectic-protein and xyloglucan-pectic-protein-polyphenol complexes from cabbage, carrot, and runner beans; and xylan-protein-polyphenol complexes from runner beans (Selvendran, 1985). The last few groups of complexes are interesting in that although they are present in relatively small amounts, they may have an important role in serving as linking compounds within the cell wall matrix. Despite the fact that it is difficult to produce unambiguous evidence for the occurrence of these complexes, our confidence in the findings would have been much less had the starting material contained coprecipitated intracellular proteins, polyphenols, and so on.

Wet Ball-Milling Step. Wet ball-milling is necessary to disintegrate the cell structure and render the contents accessible to solvents. The average time for ball-milling is about 15 h, but for certain tissues, such as apple parenchyma, 7 h is adequate. The tissues should not be ball-milled too fine, as the resulting product does not settle readily on centrifugation. The optimum time for ball-milling should be worked out, for each product, in preliminary experiments. The particle size of the cell wall preparations thus obtained is approximately 50 μm (length) and 5 μm (width) for parenchymatous tissues; for lignified tissues the corresponding sizes are approximately 500 μm and 25 μm, respectively. Suitable checks with potato starch, lysozyme, and bovine serum albumin have shown that these polymers are not degraded to any detectable extent during the wet ball-milling procedure (Ring and Selvendran, 1978; Selvendran et al., 1979). From this it is inferred that the cell wall polymers are unlikely to be degraded under the conditions used in our studies. However, when dry ball-milling is substituted, the cell wall preparations are reduced after 45 h to overall particle size of 5–15 μm. Therefore dry ball-milling may cause some degradation of cell wall polymers, and for this reason it is avoided.

Solvent Solubilization

1. Aqueous detergents and water. In addition to the intracellular compounds, a small amount of cold water-soluble pectic substances (from fresh vegetables and fruits) and significant amounts of β-D-glucans and arabinoxylans (from cereal endosperm) would be solubilized by aqueous SDC (or aqueous SDS). Although both detergents are equally effective for removing such substances as intracellular proteins, in our early work we preferred the use of aqueous SDC because it does not froth as much as aqueous SDS. However, in subsequent work we have found that the cell wall preparations obtained using aqueous SDS were slightly cleaner for certain tissues, such as apple parenchyma. Therefore we now prefer to use aqueous SDS. The amount of cell wall polysaccharides solubilized by the first aqueous detergent treatment when expressed as a percentage of the dry weight of the purified CWM are as follows: fresh potatoes, apples, runner beans, and cabbage approximately 1−2, beeswing wheat bran <1, wheat bran approximately 1, and dehulled oats approximately 6.0. During ball-milling with 0.5% SDC or SDS the cells and walls are teased apart which results in the solubilization of small but significant amounts of cell wall polymers. These account for approximately 4−6% of the dry weight of the CWM for potatoes, apples, runner beans, and cabbage, 1% for wheat bran, and 3% for dehulled oats.

2. Phenol/aceticth acid/water. PAW desorbs residual intracellular proteins, some starch, adsorbed deoxycholate, lipids, and pigments from the SDC-residue. The amount of cell wall polysaccharides solubilized is approximately 1% of the dry weight of the purified CWM for potatoes, runner beans, wheat bran, and oats.

3. Aqueous DMSO. With all the vegetables (potatoes, runner beans, and cabbage) and cereals (oats, rye flour, wheat grains, and wheat bran) which we have examined 90% aqueous DMSO solubilized the remaining starch quantitatively; this starch is >90% of the total starch in the tissue. Evidence to show that aqueous DMSO does not solubilize more than approximately 3% of the CWM in the case of vegetables (potatoes, runner beans, and cabbage) has been reported. However, in the case of oats a significant amount (~15% CWM) of β-glucanlike material is solubilized (Selvendran and DuPont, 1980b). Thus it would appear that the method may not be suitable for cereal endosperm but is highly suitable for beeswing wheat bran and wheat bran. For cereal endosperm the method described in Section III.3 is recommended.

From our experience with a range of plant products it would appear that sequential treatments with aqueous SDC, water, PAW, and aqueous

DMSO are suitable for preparing gram quantities of relatively pure cell walls from vegetables and fruits; about 90% of the total cell wall constituents remain in the final preparation. In the case of products relatively poor in proteins, the PAW treatment could be deleted, but it should be remembered that some of the intracellular proteins (e.g., some chloroplastic proteins) would remain in the final cell wall preparation. The method is also suitable for preparing gram quantities of CWM from lignified tissues of runner bean pods. In the case of lignified tissues the fibers must be first milled to pass through a sieve, and the wet ball-milling period has to be extended to approximately 40–50 h. With lignified tissues the 90% aqueous DMSO treatment solubilizes a small proportion (~5%) of the acidic xylans or acidic arabinoxylans. The amount of hemicelluloses solubilized by absolute DMSO, however, is considerably higher from delignified cell walls (holocellulose), but not from the native walls.

2. An Alternative Method for the Isolation of Gram Quantities of Cell Wall Material from Fresh Potatoes

An alternative method for the isolation of gram quantities of CWM from potatoes involves wet sieving the material triturated in water using the Miracloth filtration apparatus. For details of the method, see Hoff and Castro (1969). Provided the tissue is well disintegrated, Miracloth filtration appears to remove the bulk of the intracellular starch "grains" and proteins. Dr. T. P. Williams and coworkers (Unilever Ltd., Sharnbrook, England) have found that the removal of starch can be considerably enhanced by ensuring that all the cells are broken. They achieved this by replacing the Waring blender cutters with extremely sharp, disposable surgical blades (No. 23), made by Swan Morton Ltd., Sheffield. Each blade is held in position by two small screws, and this arrangement enables the blades to be changed at regular intervals.

It should be noted that in this method a small proportion of cold water-soluble pectic substances, such as galactans, and small fragments of the wall would be lost in the filtration liquor.

3. Preparation of Cell Walls from Cereal Endosperm

A method has been developed by Mares and Stone (1973a) for the isolation of wheat endosperm cell walls using 70% aqueous ethanol as the isolation medium. Aqueous ethanol is used instead of an aqueous medium to minimize loss of water-soluble polymeric components present in the native walls. In this method the cell walls are separated from starch and protein on the basis of their size difference. The endosperm components present in a coarse wheat flour are suspended in 70% aqueous

ethanol and wet sieved on a nylon bolting cloth (linear pore size 75 μm) until only wall fragments are retained on the sieve. Starch-protein aggregates, and starch granules, that adhere to the walls are dislodged by physical and enzymic methods and subsequently removed by further wet sieving. An outline of the procedure for the isolation of wheat endosperm cell walls, from the grains, is shown in Fig. 2.

Comments. Preliminary pearling of the grain removes the germ and much of the outer seed coats. The pearling operation may have to be repeated to ensure that all embryo and husk, and most of the aleurone and pericarp testa, are removed. Some pericarp testa would, however,

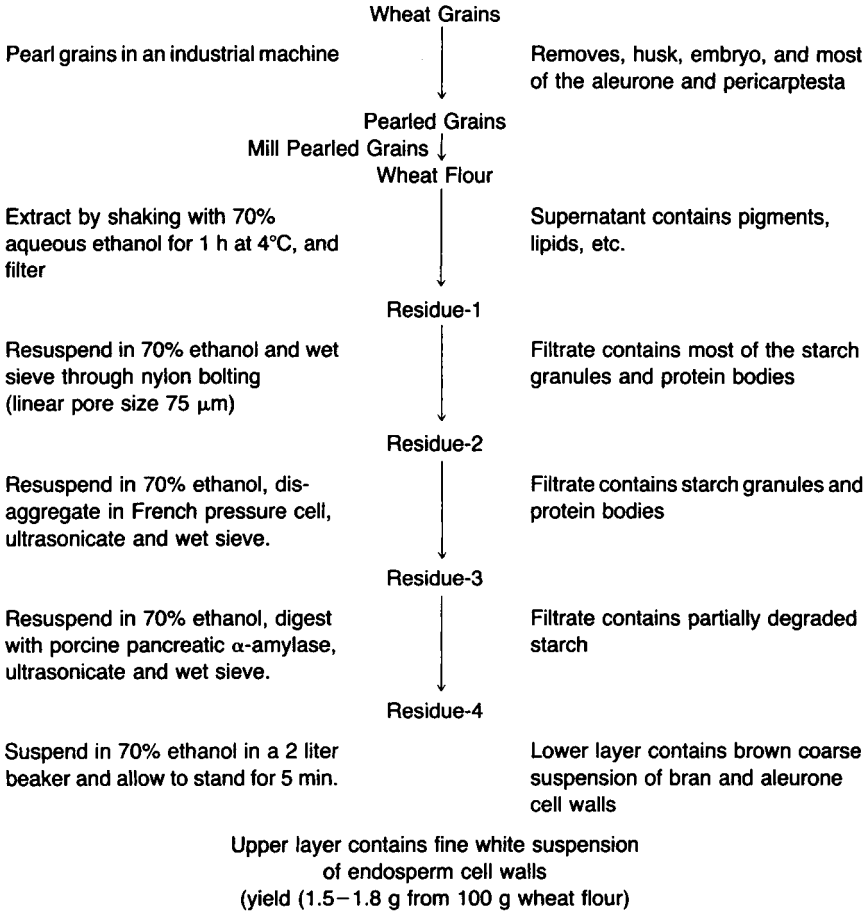

Fig. 2. Procedure for isolation of wheat endosperm cell walls.

remain in the crease region of the grain; these and residual aleurone cell walls are separated from the endosperm walls by differential sedimentation. The milled flour from the pearled grains contains a much reduced quantity of nonendospermic components. Although much of the starch granules and protein bodies could be removed from Residue-1 by wet sieving, sufficient amount of starch remains in Residues-2 and -3 to prevent efficient separation of endosperm walls from the other walls. The adherent starch in Residue-3 has to be removed by salivary (or porcine pancreatic) α-amylase, which retains activity in 70% ethanol. During all wet sieving steps small fragments of wall would be lost through the 75 μm nylon bolting material. Light microscopy has shown that the final preparation of walls from the upper layer contains <4% nonendospermic walls.

A small and variable number of small starch granules could be seen adhering to approximately 3% of the wall fragments. These had resisted α-amylase digestion and loosening by ultrasonic disruption. It is possible that a large proportion of these residual starch grains are actually fused onto the walls. Throughout the isolation procedure light microscopy has to be used to check the progress of purification.

Note. Since 70% aqueous alcohol is used as the extraction medium, some of the intracellular proteins would be coprecipitated onto the cell walls. The coprecipitated proteins cannot be removed completely by wet sieving. Therefore the endosperm walls prepared by the foregoing method cannot be used with any certainty to study the nature of cell wall (glyco) proteins.

For details of the method for the isolation of wheat and barley aleurone cell walls, see Bacic and Stone (1981a).

4. Preparation of Rice Endosperm Cell Walls

Rice endosperm cell walls have been prepared by grinding the rice flour (obtained from the milled grains) to pass through a 50-mesh sieve and then treating the flour sequentially as follows: (1) with cold water and then 1:1 ethanol/ether to defat the flour, (2) with α-amylase to remove starch and isolate the water-soluble polysaccharides from the supernatant fluid, (3) with protease so that the suspension can be passed through a glass bead-bedded filter to yield the cell wall fraction (Shibuya and Iwasaki, 1978).

5. Preparation of Cell Wall Material from Suspension-Cultured Tissues

Albersheim and coworkers have done most of the work on cell walls of cultured sycamore cells, so the method used by this group for preparing

cell walls is outlined (Talmadge et al., 1973). The method involves "complete" disruption of tissue structure and solubilization of the bulk of the intracellular compounds, including proteins and some starch, by the potassium phosphate buffer. The residual starch is then removed with a purified bacterial α-amylase preparation. The details are as follows: the suspension-cultured cells are first washed twice sequentially with 10 volumes (v/w) of cold 100 and 500 m*M* potassium phosphate; throughout the procedure the phosphate is buffered to pH 7. The cells are then suspended in 1 volume (v/w) of 500 m*M* potassium phosphate at 2°C, and the slurry is passed through a French pressure cell at 2000 to 3000 psi to rupture the cells; the resulting suspension is passed into 4 volumes (v/w) of cold 500 m*M* potassium phosphate. Light microscopy showed that this procedure resulted in almost complete disruption of the cells. The suspension is then centrifuged for 10 min at 2000 g, and the pellet is washed twice with 5 volumes (v/w) of 500 m*M* potassium phosphate, followed by 4 washes with 5 volumes (v/w) of distilled water. The resulting pellet is suspended in 5 volumes of 1:1 chloroform/methanol and washed on the sinter three times with 10 volumes of 1:1 $CHCl_3/CH_3OH$, and three times with 10 volumes of acetone. The yield is approximately 1 g of dry CWM from 100 g of fresh cells.

Starch is removed from the preparation by incubating 10 mg of the material, dispersed in 1 ml of 100 m*M* potassium phosphate buffer, pH 7.0, with 40 μg of purified *Bacillus subtilis* α-amylase for 48 h at 25°C.

Comments. In the foregoing procedure the following points should be noted: (1) The initial washing of the cells with phosphate buffer is to remove the "adsorbed" extracellular polymers. (2) The buffer-soluble intracellular and cell wall polymers could be isolated from the extract after disruption of the tissues in the French pressure cell. (3) The disruption of the tissues in the French pressure cell is practically complete. This is because walls of suspension cultured cells are generally thinner compared with most parenchymatous tissues and because the cementing layer between the cells is lacking. Suspension cultured tissues contain mainly primary cell walls and are virtually devoid of middle lamella pectins. (4) Since the α-amylase from *Bacillus subtilis*, which is used to remove starch, is known to have β-glucanase activity, some of the cell wall polymers containing β(1→4)-glucosidic linkages would be lost. The endohydrolase from *B. subtilis* has been reported to cleave 1,4-glucosidic linkages in β-glucans when the glucosyl residue involved in the linkage is substituted at 0-3. The use of "purified" α-amylase from *B. subtilis*, for removing starch from barley aleurone cells, has resulted in considerable losses of the β-glucans from the cell walls preparation: for example, compare the compositions of barley aleurone cell walls obtained by McNeill et al.

(1975) with those obtained by Bacic and Stone (1981b). The "purified" α-amylase from *B. subtilis* may also have some other carbohydrase activity. In view of this it would be advisable to remove the residual starch with either porcine pancreatic α-amylase or human salivary α-amylase. (5) Although phosphate buffers may solubilize most of the intracellular proteins, they are not as effective as aqueous detergents or PAW. Therefore the cell wall preparation may have a proportion of intracellular proteins associated with it.

IV. SEQUENTIAL EXTRACTION OF CWM AND FRACTIONATION OF POLYMERS

To obtain further information on the nature of the carbohydrate polymers constituting the cell wall complex, chemical and enzymic methods have been used. Both types of methods have advantages and disadvantages, and it is best to incorporate them into a unified scheme. First we shall consider the chemical fractionation techniques and some of the more recent developments in this area. When considering chemical fractionation, it is necessary to distinguish between cell wall preparations from organs/tissues that have little or no lignin (e.g., parenchymatous and suspension cultured tissues) from those that have some lignin (e.g., leaves and deseeded pods), or that are heavily lignified (e.g., "strings" and "parchment layers" of mature bean pods).

1. Recommended Methods for the Fractionation of CWM from Parenchymatous Tissues

A. EXTRACTION OF PECTIC SUBSTANCES

The recommended method with the relative amounts of material and solvents used is shown schematically in Fig. 3. This scheme is based on our studies with immature onions, apples, and potatoes (Selvendran et al., 1985). The CWM (1 g) is first extracted with 0.05 *M* CDTA (100 ml), pH 6.5, for 6 h at 20°C. Note that CDTA (free acid) has to be converted to the sodium salt. The suspension is centrifuged, and the residue is further extracted with CDTA for 2 h at 20°C. These treatments solubilize the bulk of the pectins from the middle lamellae that are held by ionic bonds. The CDTA extracts are filtered through GF/C filter paper and concentrated by evaporation under reduced pressure at <35°C to about one-tenth of the original volume. The concentrate is dialyzed for 72 h against deionized water, concentrated, and redialized if necessary (the last traces of CDTA are difficult to remove). Alternatively, the salts can be removed by

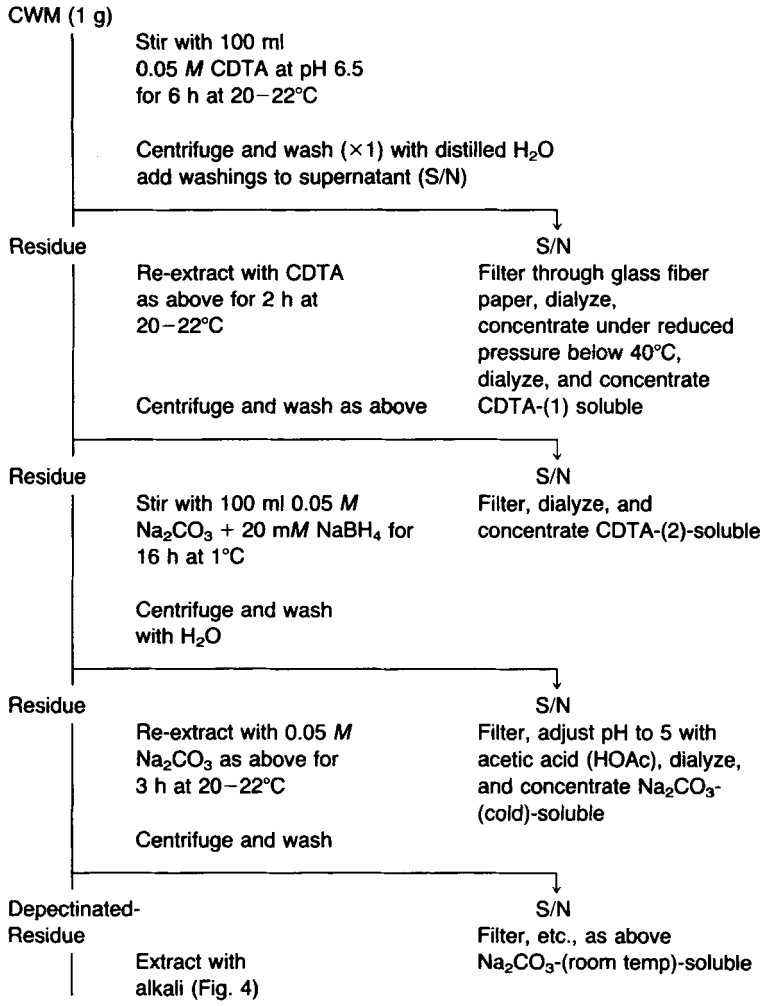

Fig. 3. Scheme for the extraction of pectic substances.

ultrafiltration. The pectins can be recovered by freeze-drying, but it is best to store the bulk of the material in the frozen state for subsequent fractionation studies.

The insoluble residue from CDTA extraction is extracted with 100 ml of 0.05 *M* Na_2CO_3 containing 20 m*M* $NaBH_4$ (pH 10.8) for 16 h at 1°C. The suspension is centrifuged, and the residue is further extracted with 0.05 *M* Na_2CO_3 containing 10 m*M* $NaBH_4$ for 3 h at 20°C. The treatment with Na_2CO_3 at 1°C serves to de-esterify the pectins and thus minimize

transeliminative degradation. These treatments solubilize the bulk of the pectic substances from the "primary cell walls." It should be noted, however, that a clear-cut separation of pectic substances from the middle lamellae and primary cell walls is not possible. With CWM from immature onions it was found that further extraction of the Na_2CO_3-residue with 0.5 *M* KOH for 2 h at 20°C solubilized additional pectic material and only very small amounts of hemicellulosic polymers (Redgwell and Selvendran, 1986). The extracts are filtered, adjusted to pH 5.0 with glacial HOAc and the pectic substances isolated as before. In general, it is better not to combine the Na_2CO_3 extracts.

B. FRACTIONATION OF PECTIC SUBSTANCES

In our earlier studies we fractionated the pectic substances on either DEAE-Sephadex (Cl^-) or DEAE-Sephacel (Cl^- or OAc^-) (see Stevens and Selvendran, 1984a, b, c for details of the procedures). We now prefer an initial fractionation on DEAE-Trisacryl (PO_4^{3-} form) using dilute phosphate buffer (pH 6.3) containing increasing amounts of NaCl (0.125–0.5 *M*) as the eluting medium. The "neutral" and acidic fractions can then be further fractionated on DEAE-Trisacryl (OAc^-) using acetate buffers. Alternatively, the pectic substances can be sequentially fractionated on DEAE-Sepharose in the phosphate and acetate forms. Both DEAE-Trisacryl and DEAE-Sepharose gave better recoveries and separations than the earlier materials, and for onion pectins DEAE-Trisacryl is preferred (Redgwell and Selvendran, 1986).

C. EXTRACTION OF HEMICELLULOSIC POLYMERS

The depectinated residue is extracted with 100 ml of 1 *M* KOH at 1°C for 2 h and then with 100 ml of 1 *M* KOH at 20°C for 2 h. The insoluble residue is extracted with 100 ml of 4 *M* KOH at 20°C for 2 h to solubilize the bulk of the xyloglucans, and then with 4 *M* (or 6 *M*) KOH containing 3–4% boric acid to solubilize additional amounts of the glucomannan-rich fraction. The final residue is referred to as α-cellulose (Fig. 4.). All the alkali extractions are performed in a N_2 or argon atmosphere. In this procedure it should be noted that some glucomannan-enriched fraction could be solubilized from the CDTA-extracted CWM by treatment with 6 *M* guanidinium thiocyanate at 20°C for 20 h (Monro et al., 1976; Stevens and Selvendran, 1984d). The α-cellulose contains small but significant amounts of pectic material and some glycoproteins. This pectic material could be isolated by treatment with cellulase (Stevens and Selvendran, 1980; O'Neill and Selvendran, 1983). With CWM from parenchymatous

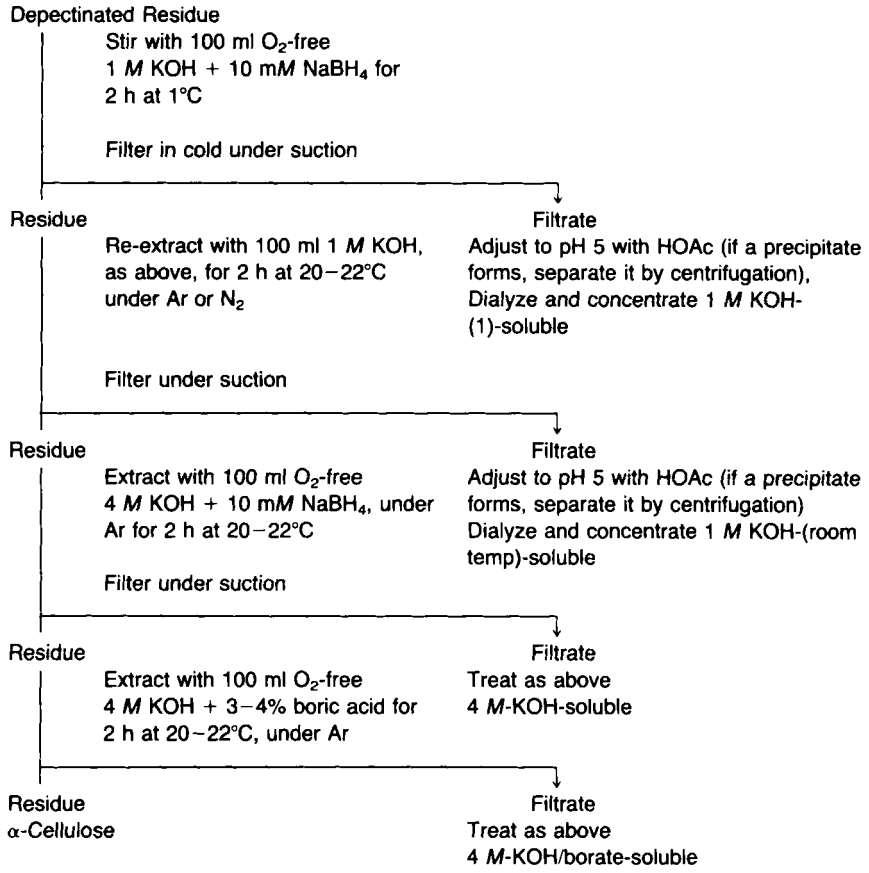

Fig. 4. Scheme for extraction of hemicelluloses.

tissues of runner beans, the bulk of the hydroxyproline-rich glycoproteins remains in the α-cellulose residue from which it can be solubilized by treatment with chlorite/acetic acid (Selvendran, 1975; Selvendran et al., 1977), or obtained as an insoluble residue by treatment with cellulase from *Trichoderma viride* grown with a substrate of ball-milled filter paper (O'Neill and Selvendran, 1983).

The alkaline extracts are acidified to pH 5 with glacial HOAc, dialyzed (or ultrafiltered) to remove salts, and any precipitated polymers (hemicellulose A) are removed by centrifugation. The supernatant fluid is concentrated by evaporation under reduced pressure, redialyzed and concentrated to give a solution of the hemicellulose B fraction; an aliquot is freeze-dried for analytical purposes. Alcohol precipitation is avoided to

minimize loss of polymers in the alcohol supernatant. The precipitates that separate on neutralization of the alkaline extracts, particularly the 1 *M* KOH extracts, are usually defined as hemicellulose A, and we have found that the precipitates from the cell walls of parenchymatous tissues of apples and runner beans contained relatively small amounts of carbohydrate (~30–40% on a dry wt. basis). These precipitates are rich in phenolics and proteins and are probably polysaccharide-protein-polyphenol complexes (O'Neill and Selvendran, 1985).

To solubilize the hemicelluloses, we prefer a two- or three-stage extraction of the depectinated residue because some fractionation of the hemicelluloses could be effected. Thus with CWM from immature cabbage leaves, and parenchymatous tissues of apples and runner beans, 1 *M* KOH solubilized the bulk of the polysaccharide-protein or polysaccharide-protein-polyphenol complexes, some of which precipitated on neutralization. The stronger alkali, on the other hand, solubilized the bulk of the strongly hydrogen-bonded xyloglucans and glucomannans.

D. FRACTIONATION OF HEMICELLULOSIC POLYMERS

The hemicellulosic polymers could be further fractionated by the methods outlined in Section II.2.D, bearing in mind the relative merits of the methods. In our hands the following procedures have given reasonably good separations: (1) ion-exchange chromatography on DEAE-Sephacel (Cl^-), followed by further chromatography of the fractions on either DEAE-Sephacel (OAc^-) or hydroxylapatite, although more recently we have preferred the use of DEAE-Trisacryl (Cl^-) and sequential elution with chloride and dilute alkali for the initial separation, and (2) graded alcohol precipitation followed by chromatography of the fractions on DEAE-Sephacel (Cl^-).

The bulk of the xyloglucans in the 4 *M* KOH-soluble extract could be isolated as the neutral fraction by passing through DEAE-Sephadex or DEAE-Sephacel (Cl^-). Further fractionation of the xyloglucans could be effected on either DEAE-Sephacel or DEAE-Sepharose in the borate form. The neutral fraction from runner bean parenchyma gave only one major xyloglucan peak on further fractionation on DEAE-Sephacel (borate) (O'Neill and Selvendran, 1983), whereas the fraction from apple parenchyma was resolved into two major and five minor components; for details of the procedure, see Ruperez et al. (1985). Fractionation of apple xyloglucans as borate complexes, on DEAE-Sepharose, also gave several components but the major xyloglucans (which accounted for approximately 70% of the total xyloglucans) obtained by both methods were highly comparable. DEAE-Sepharose gave better recoveries of

xyloglucans associated with pectic arabinans (P. Ruperez, R. R. Selvendran, and B. J. H. Stevens, unpublished results).

E. EXTRACTION AND ANALYSIS OF HYDROXYPROLINE (HYP)-RICH GLYCOPROTEIN(S) (EXTENSIN)

Hyp-rich glycoproteins can be solubilized from the depectinated cell walls by treatment with acidified sodium chlorite, a reagent traditionally used for delignification (Selvendran et al., 1975; Selvendran, 1975). The solubilization of the glycoproteins is probably due to the oxidative degradation of the isodityrosine cross-links in the protein moiety (Fry, 1982a) and also phenolic cross-links between the glycoprotein(s) and other wall polymers (O'Neill and Selvendran, 1980b). The following method is essentially based on that described by O'Neill and Selvendran (1980b).

The CWM (1 g) is first depectinated by extraction with 0.05 *M* CDTA at 20°C for 6 h, twice. The insoluble residue is suspended in distilled water (75–100 ml) in a loosely stoppered flask and heated at 70°C. Glacial acetic acid (0.15 ml) and sodium chlorite (0.3 g) are added and the contents stirred for 15 min. The treatment is repeated and the mixture stirred for a further 15 min. To prevent accumulation of chlorine dioxide gas, the contents are continuously flushed with argon. After cooling, the contents are filtered and the residue washed with five bed volumes of distilled water. The filtrate is purged with argon to remove chlorine dioxide, dialyzed, and concentrated to yield the crude chlorite-soluble glycoprotein fraction, and an aliquot is freeze-dried for analysis (yield ~80 mg from 1 g dry CWM of runner beans).

For the initial depectination, extraction with CDTA at 20°C is preferred, because extraction with hot water and oxalate at pH 5, for 2–4 h may cause slight hydrolysis of arabinofuranosidic linkages. Using warm acidified sodium chlorite, hyp-rich glycoproteins have been solubilized from the depectinated CWM of runner beans (O'Neill and Selvendran, 1980b) and suspension cultured tissues of tobacco (Mort and Lamport, 1977; Mort, 1978). Heath and Northcote (1971) and Brown et al. (1974) have used hydrazinolysis to solubilize fragments of hyp-rich glycoproteins from certain cell wall preparations. The crude glycoproteins can be freed from the contaminating pectic substances by chromatography on DEAE-Sephadex (O'Neill and Selvendran, 1980b). However, since some of the glycoproteins may be covalently linked to pectic polysaccharides (Selvendran, 1985), fractionation on DEAE-Trisacryl or DEAE-Sepharose is recommended for better recovery of the complexes from the column.

Treatment of wall glycoproteins with warm acidified chlorite causes

the following changes in the constituent amino acids: (1) isodityrosine cross-links are degraded (Fry, 1982a), (2) most of the tyrosine is destroyed, (3) methionine is oxidized to its sulfoxide and cystine is oxidized to cysteic acid, and (4) most of the lysine is converted to α-aminoadipic acid (Selvendran et al., 1975). Hydroxyproline and proline are not affected. It would appear that treatment of lysozyme with acidified chlorite at 70°C for 30 min does not cleave the molecule into small fragments (O'Neill and Selvendran, 1980b). From this observation it is inferred that the wall glycoproteins are not fragmented by the acidified chlorite treatment.

a. Isolation and Analysis of Hyp-Arabinosides. Hyp-arabinosides can be released from the purified hyp-rich glycoprotein (or native CWM) by hydrolysis with saturated $Ba(OH)_2$ at 90°C for 8 h (Lamport, 1967). We used the foregoing procedure in our work with hyp-rich glycoprotein from runner bean CWM (O'Neill and Selvendran, 1980b). However, in studies with potato lectin, which contains similar hyp-arabinosides, hydrolysis with 5 *M* NaOH at 100°C for 24 h was used (Ashford et al., 1982). After removing the Ba^{2+} as the insoluble sulfate (or neutralization of NaOH with HCl), the hyp-arabinosides can be isolated by sequential chromatography on Bio-Gel P-2 at 20°C and Aminex ion-exchange resin (H^+ form) (Lamport, 1967; O'Neill and Selvendran, 1980b), or by chromatography on Bio-Gel P-2 (−400 mesh) at 65°C; the higher temperature improves the resolution (Ashford et al., 1982). The hyp-arabinosides from potato lectin were subjected to methylation analysis, and the sequences of the sugar residues in the tri- and tetraarabinosides were deduced from the mass spectra of the permethylated hyp-tri- and tetraarabinosides (Ashford et al., 1982). The structural features of the hyp-arabinosides from tobacco CWM have been determined by Akiyama and Kato (1976, 1977).

b. Galactosyl-Serine Linkage in Hyp-Rich Glycoprotein. Methylation analysis of the purified hyp-rich glycoprotein showed the presence of terminal Gal*p* residues (O'Neill and Selvendran, 1980b). Partial acid hydrolysis of the glycoprotein with 20 m*M* oxalic acid at 100°C for 5 h, to remove the arabinose residues, followed by dialysis and treatment with α-D-galactosidase demonstrated that the galactose was α-linked (O'Neill and Selvendran, 1980b). Hydrolysis of the cell walls from suspension cultured tissues of tomato (pH 1, 100°C for 1 h), followed by treatment with trypsin and sequential chromatography of the digest on Sephadex G-25 and Aminex (50W) yielded glycopeptides containing galactose. One of the glycopeptides was deduced to contain galactose-ser linkage (Lamport et al., 1973). The initial mild acid hydrolysis is required to

remove the arabinose residues linked to hyp residues, which are in close proximity to ser-galactose. It would appear that the close proximity of the hyp-arabinosides to the ser-galactose linkage, in addition to restricting the action of trypsin, render the linkage stable to alkaline conditions (Allen et al., 1978; O'Neill and Selvendran, 1980b).

2. Fractionation of CWM from Tissues Containing Some Lignin

CWM from leaves, fruits, and deseeded pods contains some lignin, usually associated with the lignified tissues (veins, vascular tissues, stone cells, and parchment layers). In the past there has been a tendency to delignify the depectinated cell walls from such organs prior to solubilizing the hemicellulosic polysaccharides. Since these organs contain a high proportion of tissues that is not lignified, and because a large proportion of the hemicellulosic polymers present in such tissues can be solubilized with alkali as described before, it would be advisable to extract first the depectinated walls with alkali. The alkali extracted residue can then be thoroughly washed with distilled water, acidified with acetic acid to pH 4, and then delignified prior to further extraction with alkali. This sequence of extractions is recommended because there is growing evidence to suggest that the cell walls of parenchymatous tissues contain small but significant amounts of polysaccharide-protein and polysaccharide-protein-polyphenol complexes. These complexes would be partially (or sometimes completely) modified by the delignification treatment and thus some valuable information lost.

3. Cell Wall Material from Heavily Lignified Tissues

Because very little, if any, pectic material can be solubilized from the CWM of heavily lignified tissues of dicotyledons (e.g., "strings" and "parchment layers" of mature runner bean pods), the depectination stage could be omitted. Such preparations must be delignified prior to extracting the hemicelluloses. The delignified CWM (holocellulose) is thoroughly washed with distilled water, to remove as much as possible of the oxidizing agent, and a small amount (~10–20%) of the hemicelluloses can be solubilized by extraction with hot water (pH 5, 90°C for 2 h). From the hot water-insoluble holocellulose an additional amount (~10–15%) of hemicelluloses can be extracted with absolute DMSO; extraction with DMSO can precede that with hot water. The DMSO-insoluble residue can then be extracted sequentially with 1 *M* and 4 *M* KOH containing 20 m*M* $NaBH_4$, and 4 *M* KOH containing 3–4% H_3BO_3, to solubilize the remaining hemicelluloses, to leave a residue that contains mainly (~98%) cellulose. It may be an advantage to extract the holocellulose with DMSO

and then extract the residue with 0.01 *M* KOH at 1°C for 16 h, prior to extraction with the stronger alkali at room temperature. The low temperature extraction may minimize β-eliminative degradation of glucuronic acid esters.

From the delignification liquor, which has been purged with nitrogen, some degraded lignin associated with hemicelluloses, and modified wall glycoproteins can be isolated. The hemicelluloses extracted with hot water and DMSO are usually acetylated, and the degree of polymerization of the polysaccharides extracted with the stronger alkali, in general, tend to be higher.

A. SOLUBILIZATION OF LIGNIN-POLYSACCHARIDE COMPLEXES

To solubilize lignin-polysaccharide complexes from the CWM, it is necessary to finely subdivide the fibers by ball-milling the (dry) CWM in toluene for up to 7 days (Morrison, 1973); the particle size of the fibers is usually reduced to approximately 5–10 μm. Since ball-milling the CWM in nonaqueous solvents for extended periods may degrade the polymers, it is advisable to ball-mill at 1°C. Even then some degradation of the polymers may occur. To reduce the particle size, some researchers have Vibromilled the ethanol/benzene (1:2) extracted wood meal, for 48 h under nitrogen with external cooling by tap water (Azuma et al., 1981). Fine-milling can also be accomplished by using a cryo-mill with liquid nitrogen (Lomax et al., 1983); this procedure might minimize the degradation of the polymers due to the low temperature used.

From the finely milled grass cell wall preparations, small amounts of lignin-polysaccharide complexes (~1–7% of CWM) can be solubilized by stirring with either DMSO, dimethylformamide, or guanidine hydrochloride (4 *M*) for 7 days in a stoppered flask, or by ultrasonic treatment (MSE 100 W instrument operated at frequency of 20,000 Hz) for 30 min at temperatures below 40°C; the sample to solvent ratio is 1:20 (w/v). Extraction with *M* NaOH solubilized much higher levels of the complexes (~20–25% of CWM), but the ester linkages are hydrolyzed (Morrison, 1973). Das et al. (1981) have used *M* KBH_4 at room temperature to solubilize the lignin-carbohydrate complex from jute fiber. Azuma et al. (1981) have preferred extraction with 80% aqueous 1,4-dioxane at room temperature for 48 h to solubilize the complexes, using a sample to solvent ratio 1:10 (w/v).

The lignin-carbohydrate complexes can be fractionated by conventional methods and also by sequential chromatography on Sephadex G-50 and DEAE-Sephadex (Morrison, 1974). Azuma et al. (1981) have used sequential chromatography on Sepharose 4B and Phenyl-Sepharose Cl-

4B or Octyl-Sepharose Cl-4B to fractionate the complexes from milled wood.

4. Solubilization of Cell Wall Constituents by Enzymic Methods and Fractionation of the Constituents Released

As an alternative to chemical fractionation of primary cell walls, enzymic degradation of the walls followed by fractionation of the released (degraded) polymers have been used (Talmadge et al., 1973; Bauer et al., 1973; Keegstra et al., 1973; Darvill et al., 1978; McNeil et al., 1980; Spellman et al., 1983a, b; Ishii, 1981). A prime requisite for this type of methodology is the availability of highly purified cell wall degrading enzymes, such as endopolygalacturonase and endoglucanase. As Albersheim and coworkers have pioneered most of the work on the analysis of cell walls using purified enzymes, their work will be discussed in some detail. Fry (1982b, 1983) has used "Driselase" to release fragments of cell wall polymers associated with hydroxycinnamic acids. Although the "Driselase" used in Fry's work was not pure, his investigations have opened up new areas of cell wall studies, particularly those in which phenolic and phenolic ester cross-links are involved. It should be borne in mind, however, that both chemical and enzymic methods of cell wall analysis have advantages and disadvantages, and our view is that a combination of both types of methodology is required to get a better understanding of cell wall architecture. The investigations of Pilnik's group on apple cell walls, where the pectic polymers extracted by mild chemical methods, have been degraded by treatment with both pectin and pectate lyases (De Vries et al., 1982), and also galactanase (De Vries et al., 1983a, b), serve as pointers for the methods of choice in the future.

A. PECTIC POLYSACCHARIDES

Fragments of pectic polysaccharides can be solubilized from primary cell walls by treatment with endopolygalacturonase. Albersheim and coworkers have used a highly purified endopolygalacturonase (polygalacturonide glycanhydrolase EC 3.2.1.15), from cultures of *Colletotrichum lindemuthianum*, to solubilize fragments of polymers, mostly from the cell walls of suspension-cultured sycamore cells. The endopolygalacturonase was purified by ion exchange (DEAE-Cellulose), gel filtration (Bio-Gel P-150), and Agarose affinity chromatography (English et al., 1972). The enzyme had optimum activity at pH 5, an apparent molecular weight as determined by gel filtration of approximately 70,000, and preferred polygalacturonic acid to pectin as substrate. The enzyme hydrolyzed only

1% of the glycosidic bonds, reduced the viscosity of polygalacturonic acid by 50%, and hydrolyzed the bulk of the pectins in 1–2 h. The initial as well as the final products of polygalacturonic acid hydrolysis were predominantly tri- and digalacturonic acid, and some monogalacturonic acid. The enzyme was shown to be free of β-1,4-galactanase, β-1,4-glucanase and arabanase activity. One unit of the enzyme relased 1 μmole of reducing sugar per hour from 1 mg of polygalacturonic acid, when the reaction was carried out at 28°C in 1.1 ml of 50 m*M* NaOAc at pH 5.2. In order to release pectic fragments, 5 mg of sycamore cell walls were incubated with 20 units of endopolygalacturonase for 1–3 h, when approximately 16% of CWM was solubilized (Talmadge et al., 1973). The longer times (2–3 h) of incubation were used in their studies on Rhamnogalacturonan-I and -II (Darvill et al., 1978; McNeil et al., 1980; Spellman et al., 1983a). Although Talmadge et al. (1973) have stated that de-esterification of the CWM, by treatment with base, before endopolygalacturonase treatment did not alter the amount of pectic polymers solubilized, the conditions of base treatment are not given. Presumably the base-catalyzed de-esterification was carried out at pH 12 at 0°C for 2 h (English et al., 1972). In our studies with base-catalysed de-esterification of pectic polymers from apples, cabbage, and onions, treatment with dilute NaOH (pH 12, 1°C for 2 h) resulted in incomplete de-esterification (R. R. Selvendran, B. J. H. Stevens and M. O'Neill, unpublished results). Most pectins, particularly the highly esterified ones, require 8–20 h treatment for "complete" de-esterification. The foregoing comment is pertinent because the action of endopolygalacturonase on the cell walls, in the work of Talmadge et al. (1973), might have been enhanced if the pectic polymers were "completely" de-esterified in the first instance. The pH of the de-esterified material should be adjusted to 5.0, with HOAc, before enzymic treatment.

In their initial studies Albersheim and coworkers fractionated the solubilized pectic fragments (~16% CWM) first on Bio-Gel P2, and then refractionated the large molecular weight fraction that voided the column (~7.5% CWM) on DEAE-Sephadex to obtain neutral (0.5% CWM) and acidic (7.0% CWM) fractions. The acidic fraction was subjected to mild acid hydrolysis and further fractionated on DEAE-Sephadex, and the resulting fractions were further resolved on Bio-Gel P2, to give a range of pectic fragments, some of which contained small but significant amounts of xyloglucan (Talmadge et al., 1973).

In their later work Albersheim and coworkers released larger amounts of pectic material from 3.6 g of CWM by successive treatments with endopolygalacturonase (8,400 units of enzyme were used for the first two

treatments and 4,200 units for the third treatment). The solubilized pectic material was filtered through GF/C glass fiber filter paper and dialyzed against distilled water to yield approximately 12% of original CWM. The pectic material was sequentially fractionated on DEAE-Sephadex, Agarose, and Bio-Gel P10, and from the slower running peaks, on DEAE-Sephadex, they isolated Rhamnogalacturonan-I (RG-I) (McNeil et al., 1980) and Rhamnogalacturonan-II (RG-II) (Darvill et al., 1978). RG-I and RG-II accounted for 7% and 3–4% of the dry weight of the CWM, respectively. The methods used to elucidate the structural features of RG-I and RG-II will be discussed later.

B. HEMICELLULOSIC POLYSACCHARIDES

a. Xyloglucan and Xyloglucan-Pectic Complexes. From the endopolygalacturonase pretreated CWM some hemicellulosic polymers, particularly xyloglucan and xyloglucan associated with pectic polymers, were solubilized with 0.5 *M* NaOH (Bauer et al., 1973). Fractionation of these polymers was effected on DEAE-Sephadex. It should be noted that 0.5 *M* NaOH solubilized only approximately 30–35% of the total xyloglucan content of the walls. In our studies with potatoes (Ring and Selvendran, 1981), runner beans (O'Neill and Selvendran, 1983), cabbage, and apples (Stevens and Selvendran, 1984b and d), we found that the bulk of the "free" xyloglucans could only be solubilized with 4 *M* KOH. Lower strength of alkali (1 *M* KOH), however, solubilized small but significant amounts of xyloglucans, xylans, and arabinoxylans in combination with varying amounts of pectic polymers, proteins, and phenolics (Stevens and Selvendran, 1984b, d; O'Neill and Selvendran, 1985; Selvendran, 1985).

Treatment of the endopolygalacturonase-treated sycamore cell walls with partially purified endo-glucanase from *Trichoderma viride* solubilized significant amounts of degraded xyloglucan and degraded xyloglucan associated with pectic polymers (Keegstra et al., 1973). This procedure may prove useful to isolate fragments of xyloglucan that are acetylated. The acetyl groups associated with the xyloglucans are removed by the alkali treatment used in the traditional methods.

b. Glucuronoarabinoxylan. In their later work Albersheim and coworkers have solubilized a glucuronoarabinoxylan, in addition to the polymers discussed earlier, from the endopolygalacturonase pretreated cell walls of suspension cultured sycamore cells, using 0.5 *M* NaOH (Darvill et al., 1980). The enzyme-treated cell walls (3.2 g) were suspended in 640 ml of 0.5 *M* NaOH containing 1 mg/ml of $NaBH_4$ and stirred for 24 h at 2°C. The insoluble residue was removed by centrifugation and the

supernatant was filtered through GF/C glass fiber paper. The filtrate was neutralized with 1 *M* HOAc and dialyzed against distilled water for 24 h. The base-solubilized material was first fractionated on DEAE-Sephadex, and a portion of the fast-moving fraction was refractioned on Bio-Gel P-100 to give a major polysaccharide fraction. This fraction was further resolved by chromatography on Agarose A-1.5 m to give two peaks. From the faster-moving (major) peak a glucuronarabinoxylan was isolated and partially characterized. The glucuronarabinoxylan constituted approximately 5% of the dry weight of the cell walls.

*c. **Feruloylated Pectins and Feruloylated Oligosaccharides.*** The cell walls of parenchymatous tissues of most grasses and some dicotyledons exhibit ultraviolet (uv) fluorescence (Harris and Hartley, 1981). The cell walls isolated from rapidly growing spinach cultures showed NH_3-enhanced uv fluorescence (Fry, 1982b). We have found that the cell walls of parenchymatous (and lignified) tissues of sugar beet (root) and beetroot exhibited uv fluorescence. The cell walls isolated from parenchymatous tissues of beetroot also showed uv fluorescence. In contrast the cell walls of parenchymatous tissues of runner bean pods did not show uv fluorescence (R. R. Selvendran and P. Ryden, unpublished results). It would appear that the pectins (and other wall polymers) associated with ferulic and *p*-coumaric acids could be extracted from the cell walls of parenchymatous tissues (of dicotyledons) which exhibit uv fluorescence.

Treatment of cell walls from rapidly growing spinach cultures with partially purified Driselase liberated low molecular weight oligosaccharides: 4-*O*-(6-*O*-feruloyl-β-D-galactopyranosyl)-D-galactose and 3?-*O*-(3-*O*-feruloyl-α-L-arabinopyranosyl)-L-arabinose (Fry, 1982b). Driselase (from Kyowa Hakko Europe G.m.b.H., Düsseldorf, Germany) is a fungal enzyme preparation containing polysaccharide exo- and endo-hydrolases including cellulase, pectinase, galactanase, β-D-glucosidase, and α- and β-D-galactosidases. Partial purification of Driselase by $(NH_4)_2SO_4$ precipitation was carried out to remove phenolic contaminants (Fry, 1982b).

In subsequent work, Fry (1983) incubated the cell walls with Driselase under conditions that specifically inhibited galactanase and galactosidases, and obtained galactose containing feruloyl tri- to pentasaccharides, in which the feruloyl groups were on the nonreducing termini. The inhibition of the above enzymes was effected by incorporating 40 m*M* D-galactose in the incubation medium. In the same study some feruloylated pectins were extracted from the cell walls with hot 2% hexametaphosphate (pH 3.7), 6% oxalic acid (pH adjusted to 3.7 or 4.7 with NH_4OH), and 0.2 *M* NaH_2PO_4 (pH 6.8). The extractions were performed with 50 mg CWM suspended in 5 ml extractant, in sealed tubes at

100°C for 1 – 16 h. Although these conditions did not appear to hydrolyze glycosidic linkages, it should be borne in mind that the spinach cell walls have high levels of phenolic and ester cross-linkages, which may influence the stability of the glycosidic linkages and the release of the "liberated sugars" into the medium.

In our studies with CWM of parenchymatous tissues of runner beans, detectable amounts of ferulic and *p*-coumaric acids could not be released from the cell walls by treatment with 1 *M* KOH at room temperature (O'Neill and Selvendran, 1980b). However, small but significant amounts of polysaccharide-protein-polyphenol complexes were isolated from the alkaline extract (O'Neill and Selvendran, 1985). We were able to release significant amounts of ferulic and *p*-coumaric acids from the CWM of sugar beet (root) by treatment with alkali. Following the procedure described by Fry (1982b, 1983), using Driselase, we have released from sugar beet CWM, a series of oligosaccharides containing arabinose associated with ferulic and *p*-coumaric acids (B. J. H. Stevens and R. R. Selvendran, unpublished results). From the ammonium oxalate depectinated sugar beet CWM a significant amount of pectic material was solubilized by treatment with chlorite/HOAc. Much less pectic material was solubilized from the ammonium oxalate depectinated CWM by treatment with 0.05 *M* NaOH at 20°C for 4 h (R. R. Selvendran and B. J. H. Stevens, unpublished results; Selvendran, 1985). Comparable results were obtained with depectinated CWM from parenchymatous tissues of cider apples (R. R. Selvendran, P. Hillman, and M. A. O'Neill, unpublished results). These results suggest that in addition to phenolic ester linkages, phenolic ether linkages are also involved in cross-linking the pectic polymers of sugar beet and cider apples.

5. Fractionation of CWM from Parenchymatous and Lignified Tissues of Cereals

A. CELL WALLS FROM CEREAL ENDOSPERM

Since the cell walls from most cereal endosperm contain little or no pectic substances, extraction with a chelating agent could be omitted. Various workers have used different schemes for extraction (Mares and Stone, 1973a; Anderson and Stone, 1973; Fincher, 1975; Ballance and Manners, 1978), so it is difficult to make firm recommendations. However, the following sequential treatments of the CWM (1 g) may prove useful to effect partial fractionation of the polymers: (1) The loosely held polysaccharides could be solubilized by incubation with 100 ml of 10 m*M* NaOAc, pH 5, at 40°C for 2 h three times. If the CWM is not completely free of

starch, salivary α-amylase and amyloglucosidase may be incorporated in the incubation medium. (2) A proportion of the polysaccharides held by noncovalent bonds could be solubilized by extraction with 8 *M* urea (100 ml) at 20°C for 20 h. (3) A proportion of the polysaccharides held by covalent bonds, probably phenolic ester linkages, may be solubilized with 0.05 *M* KOH (100 ml), containing 20 m*M* $NaBH_4$, at 20°C for 16 h. (4) A large proportion of the noncellulosic polysaccharides may be solubilized with *M* KOH containing 20 m*M* $NaBH_4$, at 20°C for 4 h (two or three times). In the case of barley endosperm cell walls it is better to carry out the second and third extractions at 55°C. (5) The remaining polysaccharides, which are strongly associated with "cellulose-glucomannan" fibrils, may be extracted with 4 *M* KOH at 20°C. (6) A glucomannan-enriched fraction may be solubilized with 4 or 6 *M* KOH containing 0.8 *M* H_3BO_3, to leave a residue that contains mainly (~80%) cellulose. The cellulose content of most endosperm cell walls is very low (~3–5%). The alkaline extracts are neutralized with HOAc to pH 5, dialized, and concentrated for further fractionation.

Since most of the polymers from cereal endosperm cell walls contain only very small amounts of uronic acid(s) associated with them, further fractionation of the polymers is usually effected on the basis of molecular size differences using either graded alcohol precipitation, gel filtration (Bio-Gel P-2 or Sepharose 4B), or both. Mares and Stone (1973b) have used ammonium sulfate precipitation to effect partial fractionation of some of the polymers prior to gel filtration. In this connection it is interesting to note that Neukom and coworkers have isolated arabinoxylans associated with ferulic acid and proteins from wheat flour by anion-exchange chromatography (Kündig et al., 1961; Neukom et al., 1964) and have shown that a particular arabinoxylan-ferulic acid complex from wheat germ undergoes oxidative dimerization in the presence of H_2O_2 and peroxidase (Markwalder and Neukom, 1976).

Unlike wheat and barley endosperm cell walls, rice endosperm cell walls contain significant amounts of galacturonic acid containing pectic substances rich in arabinose and xylose (~10% CWM), acidic and neutral arabinoxylans, a complex containing xyloglucan, β-glucan, and arabinoxylan, and appreciable amounts of cellulose (Shibuya and Iwasaki, 1978, 1979; Shibuya and Misaki, 1978). In this case initial depectination with chelating agent is recommended. The 4 *M* KOH-soluble fraction from the depectinated rice endosperm cell walls, when fractionated on DEAE-cellulose, gave three fractions, and the component that eluted with 0.2 *M* NaOH was further fractionated on DEAE-Sephadex and shown to contain a complex composed of a xyloglucan, an arabinoxylan, and a β-glucan, in firm association.

B. CWM FROM LIGNIFIED TISSUES (BEESWING WHEAT BRAN)

Beeswing wheat bran consists mainly of the outer coating of the wheat grain and is about 3–4 cells thick, containing the epidermis, hypodermis, and cross cells. The walls of these cells have phenolic ester cross-links and some of the walls are lignified. The bulk (~60–70%) of the glucuronoarabinoxylans present in the CWM could be extracted by sequential treatments with *M* KOH containing 20 m*M* $NaBH_4$ (20°C, 3 h, three times) and 4 *M* KOH (20°C for 3 h), without prior delignification of the walls. As with heavily lignified tissues it may be an advantage to give a prior extraction with 0.01 *M* KOH at 1°C for 16 h. The alkali-extracted residue contains significant amounts of acidic arabinoxylans, lignin, and cellulose. A proportion (~50%) of the acidic arabinoxylans associated with the alkali-insoluble residue could be solubilized after delignification with chlorite/HOAc at 70°C for 2 h, using 1 *M* KOH at 20°C (R. R. Selvendran and M. S. Du Pont, unpublished results). It is important to ensure that the alkali-extracted residue is thoroughly washed with distilled water, and the pH adjusted to approximately 4.0 with HOAc before delignification. By not subjecting the native CWM to the delignification step, significant amounts of complexes containing acidic arabinoxylans, phenolics, and proteins could be obtained from the *M* KOH extracts, in addition to the major acidic arabinoxylan(s) of the walls. The polymers solubilized by alkali can be initially fractionated by graded alcohol precipitation, prior to further fractionation on DEAE-Sephadex or DEAE-Sephacel. During aqueous alcohol precipitation the acidic arabinoxylans with a relatively high degree of substitution tend to remain in solution. In fact from the 1 *M* KOH-soluble fraction, about 50% of the polymeric material, which contained very highly substituted arabinoxylans, was recovered from the 90% aqueous alcohol supernatant. The recovery of the polysaccharides (and complexes) from both anion-exchangers was very much dependent on the degree of substitution of the acidic arabinoxylans and the presence of phenolics and proteins in the complexes. The recovery of highly substituted arabinoxylans (arabinose: xylose ratio ≥ 1) was generally >80%. But the recovery of less substituted arabinoxylans (arabinose:xylose ratio ≤ 0.7) was <50%, and the recovery of arabinoxylan-protein-phenolic complexes was usually <30% (R. R. Selvendran and M. S. Du Pont, unpublished results).

a. Isolation of Feruloylated Oligosaccharides. Small amounts of feruloylated oligo- (and "poly"-)saccharides could be solubilized from the CWM of beeswing wheat bran by treatment with partially purified Driselase. The amount of material solubilized could be increased by subjecting the CWM to partial acid hydrolysis (20 m*M* oxalic acid at 100°C

for 2 h), prior to Driselase treatment. The acid treatment hydrolyzes some of the arabinofuranosidic cross-linkages in the walls and thus exposes more sites for the enzymatic action. The released fragments can be fractionated by sequential chromatography on Bio-Gel and DEAE-Sephadex columns. Recently Kato and Nevins (1985) have used a combination of partial acid hydrolysis and Driselase treatment to examine the cell walls of *Zea* shoots and have identified *O*-(5-*O*-feruloyl-α-L-arabinofuranosyl)-(1→3)-*O*-β-D-xylopyranosyl-(1→4)-xylopyranose as the major feruloyl compound released. Smith and Hartley (1983) have isolated 2-*O*-[5-*O*-(trans-feruloyl)-β-L-arabinofuranosyl]-D-xylopyranose from the "cellulase" digest of wheat bran cell walls. In earlier work Hartley and Jones (1976a) have reported the release of a range of oligosaccharides associated with ferulic and *p*-coumaric acids from the cell walls of *Lolium multiflorum*, by treatment with partially purified cellulase. Hartley and Jones (1976b) have also released diferulic acid(s) from the cell walls of *Lolium multiflorum* by treatment with alkali.

V. POLYSACCHARIDE HOMOGENEITY, MOLECULAR WEIGHT, AND CONFORMATION

A complete description of a polysaccharide requires a knowledge of the homogeneity, molecular weight, and conformation, but even with modern analytical techniques such information may be difficult to obtain. These aspects are discussed briefly.

1. Homogeneity

Unlike proteins, the biosynthesis of polysaccharides does not involve a mRNA template; therefore monodisperse polysaccharides are rarely, if ever, found. Generally, a polysaccharide will show chemical or physical inhomogeneity. If the variations in chemical and physical parameters are continuous, the polymer is polydisperse. If the polymer is chemically homogeneous but physically "heterogeneous," it is termed polymolecular. The latter situation arises with polysaccharides composed of identical repeating units but whose molecular weights vary. With plant polysaccharides that have less regular structures, there may be differences in chemical composition, the types of linkages, degree of branching, and molecular weight. Since the cell wall is a dynamic entity, the molecular variations may also be due to the age and stage of differentiation of the tissue from which the polymer is extracted. Furthermore the process of extraction can result in inhomogeneity due to the cleavage of sensitive linkages. For a discussion of the problems in assessing the homogeneity of

polysaccharides, the reader should consult Banks and Greenwood (1963) and Aspinall (1982b).

The practical problem of establishing the purity of a polysaccharide is to show the absence of contaminants and the consistency of chemical composition and physical properties after repeated fractionations. Chromatographic procedures including gel-filtration (Andrews, 1970), ion-exchange, or bio-affinity chromatography may be used to demonstrate a polysaccharide homogeneity. It has been shown that antibodies raised against a *Rhizobium* extracellular polysaccharide, when coupled to an inert matrix (Sepharose 6B), were capable of resolving the polysaccharides from *Xanthomonas campestris* and *Enterobacter aerogenes* into pyruvate-rich and pyruvate-poor fractions (Sutherland, 1981).

Zone electrophoresis on glass fiber strips or powdered glass columns (Northcote, 1965) can provide evidence for charge heterogeneity arising from ionizable groups in acidic/basic polysaccharides or suitable complexes (e.g., borate) of neutral polysaccharides. Zone electrophoresis of pectic polysaccharides on glass fiber strips has met with limited success (Barrett and Northcote, 1965) due to high endo-osmotic flow. By using silylated glass fiber and the addition of surfactants to the electrophoretic buffer, Jarvis et al. (1977) have found that electro-endo-osmosis could be eliminated. Dudman and Bishop (1968) have reported the electrophoretic separation of polysaccharides on cellulose acetate strips. However, a range of buffers may be required to achieve satisfactory resolution (Breen et al., 1970). Although polyacrylamide gel electrophoresis is limited, Pavlenko and Ovodov (1970) have claimed a satisfactory resolution of a number of dyed polysaccharides on 4.6% polyacrylamide gels using buffers containing borate, Tris and EDTA at pH 9.2. Microheterogeneity in commercial pectin samples has been demonstrated, but due to the high molecular weight and shape of the polysaccharides, penetration of the gel can take place only to a limited extent (Pavlenko and Ovodov, 1970). Furthermore the harsh extraction procedures used to obtain commercial pectins (e.g., treatment with hot dilute nitric acid) would result in heterogeneity.

Sedimentation analysis in the ultracentrifuge is a widely used criterion for the absence of heterogeneity. However, the detection of multiple peaks does not distinguish between chemical and physical heterogeneity.

2. Molecular Weight, Shape, and Conformation

Methods for the determination of the molecular weight of a polysaccharide include gel-filtration (Andrews, 1970), ultracentrifugation, light scattering, and osmotic pressure determinations (Banks and Greenwood,

1963; Bettelheim, 1970; Rees et al., 1982). Of the techniques, gel filtration is the simplest and the introduction of high performance gel-permeation chromatography is gaining acceptance as a rapid method (Barth and Smith, 1981; Himmel and Squire, 1981). Since the separations are based on shape as well as molecular weight, it is important that the column be calibrated with the appropriate standards. The use of neutral dextrans to calibrate a column used for the separation of highly charged polysaccharides (e.g., pectins) may give doubtful values (Andrews, 1970). It is also essential that the appropriate eluting buffer is used so as to prevent molecular aggregation. Estimates of molecular weights can also be obtined by light scattering (Smith and Stainsby, 1977; Plaschina et al., 1985).

A number of techniques are available for the determination of molecular shape and conformation in both solution and the solid state, and for a recent review, the reader should consult Rees et al. (1982).

VI. CHEMICAL CHARACTERIZATION AND STRUCTURE DETERMINATION OF THE POLYMERS

1. Monosaccharide Composition

The polysaccharides of plant cell walls contain a range of monosaccharides linked by a variety of glycosidic linkages (Darvill et al., 1980b; Dey and Brinson, 1984) that differ in their susceptibility to acid hydrolysis (Aspinall, 1973). Therefore a single hydrolytic procedure cannot give quantitative hydrolysis of every linkage. Furthermore the monosaccharides released differ in their stability to hot acid, and a compromise between maximum depolymerization and minimum destruction of sugars must be achieved (Aspinall, 1982a).

A. NEUTRAL SUGARS

a. Hydrolysis. A range of hydrolytic procedures has been employed for the release of neutral sugars from plant cell walls. A high proportion of the neutral noncellulosic polysaccharides can be hydrolyzed quantitatively using 1 *M* H_2SO_4 for 2.5 h at 100°C (Selvendran et al., 1979), or 2 *M* trifluoroacetic acid for 2 h at 120°C (Albersheim et al., 1967).

Quantitative release of glucose from cellulose requires a pretreatment with 72% H_2SO_4 (Jermyn, 1955), and the details of the method as applied to α-cellulose from pear cell walls have been described by Jermyn and Isherwood (1954). Essentially, quantitative release of the monosaccharides from purified cell walls has been achieved by treatment with 72%

H_2SO_4 for 3 h at 20°C prior to dilution to 1 *M* acid and heating at 100°C for 2 h (Selvendran et al., 1979). However, Rasper et al. (1981) have reported that for pentose-rich material a 2 h pretreatment with 72% H_2SO_4 is preferable.

b. Determination of the Monosaccharides Released. A number of relatively nonspecific colorimetric methods have been developed (Dische, 1962). The estimation of hexoses by the anthrone method is complicated by galactose, mannose, and glucose giving different color yields (Ashwell, 1957). Similarly the estimation of pentoses with phloroglucinol is unreliable when the hexose to pentose ratio is >10:1 (Selvendran et al., 1979), and hexuronic acids also contribute to the color yield (Jermyn and Isherwood, 1949; Selvendran and DuPont, 1984). It is possible to correct for such interfering reactions but this requires a prior knowledge of the carbohydrate composition of the material.

Because of the problems of quantifying mixtures of monosaccharides by direct colorimetric procedures, techniques have been developed whereby the components are separated prior to their detection. Initially paper or thin-layer chromatography was used for the separation of sugar mixtures (Hough, 1954), but this was subsequently superseded by anion-exchange chromatography of the sugars as the borate complexes (Spiro, 1972; Davies et al., 1974; Kennedy and Fox, 1980). Over the last two decades gas-liquid chromatography (GLC) of the sugar derivatives has proved to be the method of choice (Bishop, 1962; Laine, 1972; Dutton, 1973). Recent developments in high performance liquid chromatography allow the rapid separation of certain mixtures of sugars, but there are still difficulties in achieving satisfactory resolution of the sugars found in plant cell walls (Slavin and Marlett, 1983).

GLC is a versatile and widely used method for the separation of volatile sugar derivatives. Although a number of derivatives have found application, the most commonly used derivative is the alditol acetate which gives a single peak for each sugar (Sawardeker et al., 1965). The monosaccharides commonly found in plant cell walls can, as their alditol acetates, be separated readily on a number of commercially available liquid phases such as OV-225 (Selvendran et al., 1979) and SP-2330 (Englyst et al., 1982). In our laboratory we routinely use columns (3 m × 2.2 mm) containing 3% w/w OV-225 at 200°C to obtain baseline resolution of the acetylated derivatives of rhamnitol, arabinitol, xylitol, mannitol, galactitol, and glucitol in approximately 45 min (Selvendran et al., 1979). With high quality columns containing OV-225, it may also be possible to achieve partial resolution of the acetylated derivatives of rhamnitol and fucitol.

Developments in capillary columns for GLC have improved the resolution of the individual components with a concomitant reduction of elution times. Neeser and Schweizer (1984) have separated the *O*-methyloxime acetates of several sugars using a fused-silica Carbowax 20M capillary column. Although alditol acetates can be separated by capillary GLC (Blakeney et al., 1982), this method is more suitable for separating complex mixtures of partially methylated alditol acetates derived from methylation analysis. It has been reported that phthalic esters interfere with the determination of alditol acetates by GLC (Dudman and Whittle, 1976) on conventional packed columns. This problem can be overcome to some extent by the use of capillary columns with polar phases (Henry et al., 1983) or by using high quality reagents.

Recent developments in high performance liquid chromatography (HPLC) offer considerable promise for the direct and rapid determination of monosaccharides. A number of column types and eluants including Bondapak AX/Corasil with ethyl acetate/isopropanol/water (Linden and Lawhead, 1975), chemically modified silica with acetonitrile/water (Mopper and Johnson, 1983), anion exchange with borate buffers (Honda et al., 1983), and heavy-metal cation exchange with water (Slavin and Marlett, 1983) have been used. However, a single system that can adequately resolve all the neutral monosaccharides commonly found in plant cell walls has not yet been developed. A further limitation of the HPLC of sugars is that monosaccharides do not possess a specific absorption maximum. This necessitates the use of refractive index detectors that are only moderately sensitive (Pryde and Gilbert, 1979). Detection limits can be increased by the use of pre- (Lehrfield, 1976) or postcolumn (Honda et al., 1981) derivitization.

Although HPLC may eventually become the method of choice for separating and quantifying neutral monosaccharides, it is at present unable to achieve the resolution of GLC. HPLC does offer considerable promise for the separation of oligosaccharides and their derivatives (see Section VI).

B. URONIC ACIDS

a. Hydrolysis. Due to the stability of the glycosyluronic acid linkage to acid hydrolysis, it is difficult to achieve quantitative hydrolysis of acidic polysaccharides (Roden et al., 1972). Conrad et al. (1966) demonstrated that the linkage (Glc*p*A-(1→3)-Fuc*p* was 30 times more stable to acid hydrolysis than the linkage β-D-Glc*p*-(1→4)-Glc*p*. Incomplete hydrolysis and the apparent loss of xylose has been observed with acidic xylans and arabinoxylans, which has been attributed to the accumulation of 2-*O*-(4-

O-methyl-α-D-Glc*p*A)-D-Xyl*p* in the hydrolysate (Whistler and Richards, 1958). Similarly the slow release of rhamnose during acid hydrolysis of pectins in vegetable cell walls could be attributed to the stability of α-D-Gal*p*A-(1→2)-L-Rha*p*. The recovery of rhamnose may be increased by extending the period of hydrolysis to 5 h (Selvendran et al., 1979), but the degradation of other monosaccharides may become significant. Neeser and Schweizer (1984) have obtained better recoveries of rhamnose (and other sugars) from cell wall polysaccharides when the hydrolysis was performed with 4 *M* trifluoroacetic acid at 125°C for 1 h, provided the concentration of the sugars in the acidic solution was $\leq 2.5 \times 10^{-3}$ *M*.

The analysis of acidic cell wall polymers (notably pectins) can also be complicated by their tendency to precipitate in acidic media. Jermyn and Isherwood (1956) found that aqueous solutions of pectic polymers from pear cell walls precipitated on the addition of nitric acid. If, however, the sample was warmed prior to the slow addition of acid, precipitation could be avoided. Ford (1982) has shown that quantitative analysis of water-soluble pectic polysaccharides can be improved by depolymerization with a poly-(1,4-α-D-galacturonide)-glycanohydrolase (EC 3.2.1.15). This treatment can also be used prior to acid hydrolysis to prevent polymer aggregation. Although the recovery of neutral monosaccharides is increased, the stability of the glycosiduronic linkage still prevents its complete hydrolysis.

In order to eliminate the stability of the glycosiduronic linkage, the carbodiimide-activated carboxyl groups of water-soluble acidic polysaccharides can be reduced with $NaBH_4$ to convert the uronic acid residues to the corresponding neutral sugars, thus replacing the acid resistant glycosiduronic linkages with the more acid-labile glycosyl bonds (Taylor and Conrad, 1972). However, the efficiency of such reductions for pectic polysaccharides may be low (Aspinall and Jiang, 1974; Aspinall and Fanous, 1984). Furthermore, if the pectic polysaccharide is rich in galactose, care must be taken to distinguish between the native galactose and galactose derived from Gal*p*A, which can be dideutero-labeled by performing the reduction with NaB^2H_4.

b. Determination of Uronic Acids. Dische (1962) has described a relatively specific and sensitive assay for uronic acids involving their reaction with carbazole in acidic media. The sensitivity and stability of the assay were improved by the use of H_2SO_4 containing sodium tetraborate (Bitter and Muir, 1962). However, the method was still sensitive to the presence of hexoses and pentoses and required the use of correction factors (Selvendran et al., 1979). By replacing carbazole with *m*-hydroxydiphenyl, the sensitivity of the assay was increased and interfer-

ence by neutral sugars effectively eliminated (Blumenkrantz and Asboe-Hansen, 1973). This has become the method of choice in our own (Selvendran and DuPont, 1984) and many other laboratories.

As with neutral monosaccharides the analysis of uronic acids by paper (PC) and thin-layer chromatography (TLC) are qualitative or semiquantitative. For the separation of uronic acids by PC, acidic solvents such as EtOAc/HOAc/H_2O or BuOH/HOAc/H_2O have been used (Jermyn and Isherwood, 1949). By incorporating formic acid in the solvent, the resolution of the components can be improved (Barrett and Northcote, 1965). It should be noted that in such solvents galactose and galacturonic acid tend to cochromatograph unless extended periods of development are employed (Partridge, 1948; Jermyn and Isherwood, 1949, 1956). Similar problems have also been encountered with TLC in acidic solvents (Lewis and Smith, 1969).

Acidic monosaccharides can be separated by an ion-exchange chromatography, and several automated systems have been developed (Spiro, 1977; Davies et al., 1974). However, their application to the analysis of uronic acids in plant cell walls has been limited (Selvendran, 1975b; Selvendran et al., 1975).

Attempts to separate and quantify uronic acids by GLC have had limited success, and some of the problems encountered in the analysis have been studied by Blake and Richards (1970), who have suggested measures for overcoming them. The major problem with the analysis of hexuronic acids by GLC is the preparation of suitable derivatives. Treatment of the uronic acid with $NaBH_4$ followed by evaporation in the presence of HCl generates mainly the aldono-1,4-lactone (Perry and Hulyalkar, 1965). Attempts to convert the aldono-1,4-lactone to the corresponding alditol have shown that repeated reductions are required (Sjostrom et al., 1966; Jones and Albersheim, 1972), and even then the recoveries are not quantitative (Blake and Richards, 1970). Ford (1982) has proposed a method whereby Gal*p*A, released from water-soluble pectins by treatment with polygalacturonase, is converted to the aldonolactone and silylated. GLC of the trimethylsilyl derivative has given satisfactory resolution of glucuronic and galacturonic acids. Work in our laboratory with Gal*p*A (P. Ryden and R. R. Selvendran, unpublished results) has shown that the conditions of lactonization given by Ford (vacuum-dried sample treated with 0.8 *M* methanolic-HCl at 60°C for 4 h) resulted in multiple peaks on analysis by GLC. This was shown by GLC-MS of the trimethylsilyl derivatives to be partly due to the formation of the aldono-1,5-lactone and incomplete lactonization. These problems could be overcome by performing the lactonization with 6 *M* HCl (Perry and Hulyalkar, 1965), but the response for the Gal*p*A derivative was only 0.6

of that of the 6-deoxyglucose derivative (P. Ryden and R. R. Selvendran, unpublished results). We found that it was essential to ensure that the ratio of sample to silylating agent was 1:60 on a molar basis.

Hexuronic acids can be separated by conventional ion-exchange chromatography, but the elution times may be relatively long (Spiro, 1977). Voragen et al. (1982) have shown that galacturonic, mannuronic, and guluronic acids can be separated by HPLC on strong anion-exchange columns. However, the columns were found to have low stability and short lifetimes (6 months). Attempts to separate acidic monosaccharides on amine modified silica or reverse-phase columns have been unsuccessful (Voragen et al., 1982).

For an extended discussion on some of the aspects considered in Sections VI.1.A and B, the reader should consult Selvendran and Du Pont (1984).

C. UNUSUAL SUGARS

With developments in analytical techniques such as capillary GLC, HPLC, mass spectrometry (MS), and nuclear magnetic resonance (NMR), it is possible to isolate and characterize small amounts of unusual sugars. This is illustrated by the work of Albersheim and colleagues who have isolated and partially characterized the pectic polysaccharide Rhamnogalacturonan-II. This unusual and complex macromolecule contains 2-*O*-methyl fucose, 2-*O*-methyl xylose and apiose (Darvill et al., 1978) as minor components. Subsequently this polymer has also been shown to contain the unusual sugar 3-C-carboxy-5-deoxy-L-xylose (Spellman et al., 1983a) which has been given the name "aceric acid." Using selective acid hydrolysis followed by ion-exchange chromatography and gel filtration, a heptasaccharide was isolated from Rhamnogalacturonan-II (Spellman et al., 1983b) and shown to contain aceric acid. This confirmed that the unusual branched sugar was an integral component of RG-II. Recently another unusual sugar (for plant cell walls), 3-deoxy-D-manno-2-octulosonic acid (KDO) has also been shown to be a component of RG-II (York et al., 1985). The KDO is probably substituted through position 5 with α-L-Rhamnose.

The unusual sugars such as apiose, aceric acid, or KDO require special techniques for their detection and characterization. However, *O*-methylated sugars can be characterized by GLC-MS of their alditol acetates (Darvill et al., 1978). Mono-*O*-methylated derivatives elute faster than their completely acetylated homologues. This can be illustrated by comparison of the retention times (on a SP-1000 glass capillary column) of the acetylated derivatives of xylitol (R-0.71) and 4-*O*-methylxylitol (R-

0.55) and mannitol (R-1.00) and 6-*O*-methylmannitol (0.77) (Gerwig et al., 1984).

There have been reports (Roberts et al., 1972) that plant cell walls contain amino sugars (2-deoxy-2-amino-D-hexose). As with glycosiduronic linkages amino sugars are resistant to acid hydrolysis (Aspinall, 1973). Hydrolysis is generally performed with 2–4 *M* HCl at 100°C for 4–6 h and the released amino sugars can be quantified colorimetrically or separated using a conventional amino acid analyzer (Spiro, 1972). Amino sugars are also amenable to analysis by GLC of their *O*-trimethylsilyl (Laine, 1972) or *O*-acetylated derivatives (Wong et al., 1980).

D. ABSOLUTE CONFIGURATION AND RING SIZE OF MONOSACCHARIDES

In most studies of the structure of cell wall polysaccharides the absolute configuration of the monosaccharides is assumed—rhamnose, fucose, and arabinose are L, whereas mannose, galactose, glucose, glucuronic, and galacturonic acid are D. However, for a complete characterization it is essential to determine the absolute configurations experimentally.

Up to the mid-seventies the absolute configuration of sugars was determined from the optical rotation of the purified sugar or by enzymic methods such as D-galactose oxidase which specifically oxidizes D-galactose. In the former case relatively large amounts of pure sugars are required, and in the latter enzymes with a high degree of specificity are required. Spellman et al. (1983a) have used a combination of periodate oxidation and beef heart L-(+)-lactic dehydrogenase to establish the absolute configuration of aceric acid (3-C-carboxy-5-deoxy-L-xylose) an unusual monosaccharide component of Rhamnogalacturonan-II.

Recently GLC methods have been developed to determine the absolute configuration of sugar residues (Gerwig et al., 1978; Leontein et al., 1978). These methods are based on the formation of the glycosides of chiral alcohols ((−)-2-butanol or (+)-2-octanol) which are derivatized (silylation or acetylation) and separated by capillary GLC. From the relative retention times of the derivatives, the appropriate absolute configuration can be assigned. Using these methods, the absolute configurations of the neutral monosaccharides in Rhamnogalacturonan-I (McNeil et al., 1980) and a glucuronoarabinoxylan (Darvill et al., 1980c) from the cell walls of suspension-cultured sycamore cells have been determined.

The ring forms (furanose or pyranose) of a monosaccharide can, to a limited extent, be inferred from the stability of the sugar to acid hydrolysis. The rates of hydrolysis of furanosides may be $10-10^3$ times greater than those of the corresponding pyranosides (Aspinall, 1973). Terminal, nonreducing sugars can be characterized by methylation analysis as

furanose or pyranose from the positions of *O*-methyl substitution. For interchain sugar residues this distinction may not be clear-cut, (1→4)-hex*p* residues will give the same pattern of *O*-methyl substitution as (1→5)-hex*f* residues. Darvill et al. (1980a) have developed a procedure to determine ring sizes, which is based on the following sequence of reactions: (1) methylation, (2) partial hydrolysis, (3) reduction, (4) realkylation (*O*-ethylation), (5) complete hydrolysis, and (6) analysis of the alkylated alditol acetates by GLC-MS. From the pattern of *O*-methylation/*O*-ethylation the ring size of each sugar can be deduced. For a scheme showing the application of this procedure to interchain hexopyranose and hexofuranose residues, see Darvill et al. (1980a); Selvendran and Stevens (1986) have outlined the scheme for interchain Ara*f* and Ara*p* residues. This method has been used to determine the ring sizes of the sugars in Rhamnogalacturonan-I (McNeil et al., 1980) and a glucurono-arabinoxylan (Darvill et al., 1980c) from the cell walls of suspension-cultured sycamore cells.

2. Glycosyl Linkage Analysis

A. METHYLATION ANALYSIS

Methylation analysis is the most important procedure for linkage analysis in carbohydrate-containing polymers (Lindberg, 1972). The procedure requires that all free hydroxyl in the oligo- or polysaccharide are etherified. Following depolymerization of the methylated material, the monomers are separated, identified, and quantified. The free hydroxyl groups in the partially methylated monomers mark the position(s) at which the sugar residues were substituted.

The once widely used Haworth and/or Purdie procedures employing reagents such as sodium hydroxide, dimethyl sulfate, and silver oxide and/or methyl iodide (Bouveng and Lindberg, 1960) have been replaced by the method developed by Hakomori (1964). Hakomori methylation is more rapid than Haworth methylation and, except for glycans having uronic acid residues, goes to completion in a single two-step treatment. The differences in speed between the Haworth and Hakomori procedures are normally attributed to the relative strengths of the bases affecting ionization. The base used in the latter procedure, sodium methylsulfinylmethanide (dimsyl anion, which is the conjugate base of dimethyl sulfoxide) in DMSO is much more efficient in removing protons than aqueous alkali. In this procedure the polysaccharide dissolved, or swollen, in DMSO is treated with the dimsyl anion in DMSO to ionize the hydroxyls fully so that they will be converted to methyl ethers when methyl iodide

is added. Complete methylation of neutral (or slightly acidic) polysaccharides is generally achieved with one treatment. For details of the procedures the reader should consult Lindberg (1972), Lindberg and Lonngren (1978), and the experimental guide prepared by Lindberg's group (Jansson et al., 1976). In the case of acidic polysaccharides, if the methylation is not completed after one such treatment, then it is normally considered desirable to reject the material and repeat the process. However, since the degradative changes that occur during subsequent Hakomori methylation are largely understood, some useful structural information may be obtained by repeated Hakomori methylation of acidic glycans. Applications of this procedure to some acidic polysaccharides and methods for overcoming problems associated with methylation analysis of acidic cell wall polysaccharides (e.g., pectins) will be discussed later.

The methylated polymer is isolated and hydrolyzed, and the partially methylated monomers are characterized. Originally these derivatives were separated by partition chromatography on paper (Binkley, 1955), but this requires a relatively large amount of material. Subsequently the methylated monomers were separated by GLC as their methyl glycosides (Bishop, 1964), trimethylsilyl derivatives (Petersson and Samuelson, 1968), or preferably as their alditol acetates (Lindberg, 1972). Partially methylated alditol acetates (PMAA) have proved particularly suitable for GLC-MS, since only a single derivative is formed from each methylated sugar and the mass spectral fragmentation patterns of the PMAA are relatively easy to interpret (Lindberg, 1972).

*a. **Neutral Polysaccharides.*** The dry polysaccharide (2–10 mg) in dry dimethylsulfoxide (2 ml) is treated with the base sodium methylsulfinylmethanide (2 ml) for 12 h at room temperature under argon (Jansson et al., 1976). To the cooled mixture (+2°C) is added, dropwise, an excess of methyl iodide (3 ml). The mixture is sonicated and left to clear (2–4 h room temperature). The methylated polymer can be isolated either by extraction into chloroform or gel-permeating chromatography on Sephadex (LH-20 with acetone or methanol/chloroform (Talmadge et al., 1973). Alternatively, the methylation mixture can be mixed with methanol/chloroform (1:1 v/v), filtered, and dialyzed against aqueous 50% ethanol (Ring and Selvendran, 1978).

The extent (completeness) of the methylation reaction can be monitored by methoxyl determination if sufficient material is available or on a microscale by the absence of O-H stretching vibrations (~3400 cm^{-1}) in the infrared spectrum. If the extent of undermethylation is significant the methylation procedure ought to be repeated. The points of undermethylation can be located by using deuterated methyl iodide or ethyl

iodide as the alkylating reagent. In many cases undermethylation can be traced to the polysaccharides being only partially soluble in DMSO. This is especially so when whole cell wall preparations are subjected to methylation analysis (O'Neill and Selvendran, 1980a). Undermethylation can, however, be overcome by (1) grinding the material to a fine powder using a cryo-mill with liquid nitrogen (Lomax et al., 1983), (2) warming the sample in DMSO to 60°C with concomitant sonication, (3) acetylating the polymer prior to methylation to increase its solubility, (4) using potassium methylsulfinylmethanide instead of the Na base (Darvill et al., 1978; Valent et al., 1980), (5) using a *N*-methylmorpholine *N*-oxide-DMSO mixture instead of DMSO (Joseleau et al., 1981), and (6) using tetramethyl urea (Narui et al., 1982) to improve dissolution of the polymer.

b. Acidic Polysaccharides. Essentially, the procedure for the methylation of acidic polysaccharides is similar to that described earlier. However, there are several drawbacks that must be noted. Esterified uronic acids (commonly found in cell wall pectins) on treatment with the strong base will undergo base-catalyzed β-elimination (Lawson et al., 1969), and significant degradation may occur (Lindberg et al., 1975). It is essential that methyl-esterified acidic polysaccharides are de-esterified (0.01 *M* NaOH, 12 h at +2°C) prior to their methylation. The de-esterification is performed at low temperature to minimize β-elimination. The solubility in DMSO of acidic bacterial polysaccharides may be improved by converting them to their hydrogen form. Uronic acids, even after methylation, are well known to have acid-resistant glycosiduronic linkages that result in the units being released as methylated derivatives of aldobiouronic acids (Jones and Wise, 1952; Roy and Timell, 1968). It should be noted that during the second part of the methylation (addition of methyl iodide), all the hydroxyl groups and carboxylic groups will be etherified and esterified, respectively, and some residues may undergo β-elimination before the base is destroyed by the excess of methyl iodide added.

Unlike neutral polysaccharides undermethylated acidic polysaccharides cannot be realkylated directly. The Hakomori procedure leads to esterification of uronic acid residues that on further treatment with base will undergo extensive β-elimination. Therefore the methylated acidic polymer should be carboxyl-reduced with $LiAl^2H_4$ prior to realkylation. This is illustrated by our work (O'Neill et al., 1986a) on the extracellular polysaccharide produced by *Alcaligenes* (ATCC 31555). After a single methylation an excess of branch points was observed which indicated incomplete methylation of position 2 of (1→3)-linked glucose residues. To confirm this, the methylated polysaccharide was carboxyl-reduced, ethylated, and the alkylated alditol acetates analyzed by GLC-MS. The

ratio of nonreducing terminal to branch-point residues became unity and the presence of 1,3,5-tri-*O*-acetyl-2,*O*-ethyl-4,6-di-*O*-methylglucitol (**1**) confirmed incomplete methylation at position 2 of (1→3)-linked Glc*p*. It should be emphasized that with complex polysaccharides such as pectins the possibility of undermethylation must not be overlooked. However, with such molecules, the large number of derivatives obtained after methylation analysis may make the task of detecting undermethylation difficult.

Methylation analysis of acidic polysaccharides is facilitated by reduction of the acidic sugar(s) to the corresponding neutral residues before or after methylation. By performing the reduction with a deuterated reagent, the methyl ethers derived from the uronic acid can easily be distinguished by GLC-MS (Lindberg, 1972). If the polysaccharide is water soluble its carbodiimide-activated intermediate can be reduced with NaB^2H_4 (Taylor and Conrad, 1972). For the reaction to be successful, careful maintenance of pH is required necessitating the use of a pH stat (Taylor et al., 1973). Recently Anderson and Stone (1985) have described the use of 2-(*N*-morpholino) ethane sulfonic acid (MES) and Tris buffers to maintain the appropriate pH values. Generally, the procedure is efficient, although for complex acidic polysaccharides from plants it has been reported that repeated treatments were required (De Vries et al., 1983a). We have found that kiwi fruit gum which contains alternating Glc*p*A and Man*p* residues in its backbone required three separate treatments with the carbiodiimide reagent to achieve 90% reduction of the four-linked Glc*p*A residues (Redgwell et al., 1986a). There may also be some loss of material after reduction and dialysis (to remove the reagents and salts). In some cases recoveries may be as low as 50% (Gowda et al.,

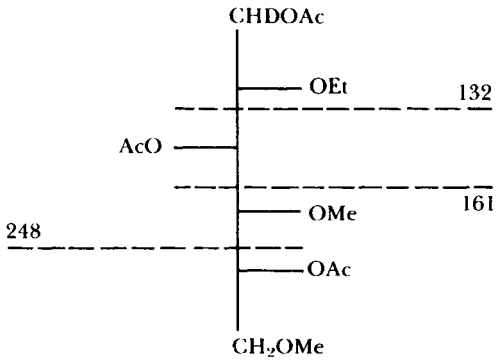

1

1982). For a flowchart showing the application of the method for the methylation analysis of a branched pectic polysaccharide, see Selvendran and Stevens (1986).

Methyl-esterified, and to a lesser extent carboxyl, residues in methylated acidic polysaccharides can be reduced with $LiAlH_4$ (or $LiAl^2H_4$) by refluxing in organic solvents such as tetrahydrofuran or dichloromethane-ether (Lindberg, 1972; Lindberg and Lonngren, 1978). In our experience the latter solvent mixture gives more reproducible results. Losses of polymer may occur by adsorption on to the insoluble salts formed when the excess reducing agent is destroyed. Such losses can be minimized by thoroughly washing the precipitate with chloroform-methanol (1:1 v/v). For details of the method as applied to pectin, see Selvendran and Stevens (1986). By using $LiBH_4$ (LiB^2H_4), the formation of precipitates is avoided, but it is essential that the carboxyl groups are fully esterified. Stevens and Selvendran (1984a) compared the reduction of methylated pectins with $LiAl^2H_4$ and LiB^2H_4 and found both methods were effective, although there were significant losses of galacturonic acid residues because the starting material was not de-esterified. Incomplete reduction of the Gal*p*A residues would also account for the loss in recoveries after methylation analysis.

Valent et al. (1980) have reported that carboxyl reduction can be achieved with $NaBH_4$ (NaB^2H_4) in an ethanol-tetrahydrofuran mixture. However, the reduction of esters under these conditions may be accompanied by ester hydrolysis (Aspinall, 1973), thus requiring two or three cycles of esterification and reduction.

*c. **Oligomeric Material.*** Oligomeric material is methylated in an identical manner to polymeric samples. To avoid base-catalyzed degradation from the reducing terminus (Aspinall, 1973), a prior reduction step ($NaBH_4$ or NaB^2H_4) is required. After methylation the derivatized oligomers are extracted from a DMSO-water mixture by partitioning into chloroform or dichloromethane (Jansson et al., 1976). Recently, the use of C_{18} reverse-phase extraction cartridges (Sep-Pak, Waters Assocs.) has been reported (Waeghe et al., 1983). The DMSO-water mixture containing the methylated oligomers is rendered free of CH_3I and passed through the cartridge where the methylated derivatives are adsorbed. The excess reagents are washed off with water and low concentrations ($\leq$20%) of aqueous acetonitrile, and the methylated oligomers are eluted with aqueous 60% acetonitrile or aqueous methanol (Mort et al., 1983). These cartridges may also be used to isolate some methylated polysaccharides but require 100% methanol or methanol/chloroform (1:1 v/v) for their elution (Mort et al., 1983).

*d. **Hydrolysis of Methylated Material.*** Methylated oligo- or polysaccharides are insoluble in aqueous acids and hydrolysis is therefore preceded by formolysis (Lindberg, 1972). Although the glycosidic linkages of methylated polysaccharides are more readily hydrolyzed than those of the native polymer, their quantitative hydrolysis will vary with the type of linkages involved. With acidic polysaccharides that have not been carboxyl-reduced, the stability of the glycosiduronic linkage prevents the quantitative release of the monosaccharide linked to it (Dutton and Merrifield, 1982). We have found that the hydrolysis conditions described by Lindberg (1972) are suitable for polysaccharides from plant cell walls (Ring and Selvendran, 1978). It should be noted, however, that other researchers have obtained effective hydrolysis of methylated polysaccharides using aqueous trifluoroacetic acid with (Darvill et al., 1978) or without (Dutton and Karunaratne, 1984) formolysis. This can be attributed to the partial solubility of the methylated material in the organic acid.

*e. **Preparation of Methylated Alditol Acetates.*** The monomers released by acid hydrolysis are converted by reduction to their corresponding alditols. By performing the reduction with NaB^2H_4, the alditol is deuterium-labeled at C1. This greatly aids mass spectral interpretation especially where derivatives such as 1,4,5-tri-*O*-acetyl-2,3-di-*O*-methyl- and 1,2,5-tri-*O*-acetyl-3,4-di-*O*-methylpentitol give similar fragmentation patterns (Lindberg, 1972). By incorporating deuterium at C1 the primary fragments of these derivatives are at *m/z* 118, 162, and 189 and at 117, 161, and 190, respectively. The methylated alditols are generally converted to their acetylated derivatives by heating with acetic anhydride/pyridine (1:1 v/v) for 20 min at 120°C (Selvendran et al., 1979). Alternatively, the inclusion of 1-methylimidazole as a catalyst allows acetylation to proceed without the removal of borate ions (Blakeney et al., 1983). With this latter procedure repeated, evaporations under diminished pressure are eliminated, and the loss of extremely volatile derivatives (e.g., 1,5-di-*O*-acetyl-2,3,4-tri-*O*-methyl-6-deoxyhexitols) is minimized.

*f. **Separation of Partially Methylated Alditol Acetates.*** The most suitable method for separating and quantifying partially methylated alditol acetates is GLC. Although several stationary phases have been used, the most versatile ones are OV-225 and ECNSS-M (Lindberg, 1972). Although the latter phase suffers from column bleed at high temperatures, it has proved useful for separating 2,3- and 3,4-di-*O*-methyl xylitol derivatives from the 2,3,4,6-tetra-*O*-methyl galactitol derivative (Jansson et al., 1976). The relative retention times of a number of PMAA have been tabulated by Jansson et al. (1976). However, these values should only be used as a guide because the columns obtained from different manufactur-

ers may give values that vary to a small extent. The elution sequence of a number of PMAA from cabbage pectin and an extracellular anionic polysaccharide produced by *Alcaligenes* (ATCC 31555) (S130; O'Neill et al., 1986a) on OV-225 are shown in Figs. 5 and 6, respectively; Table 4 shows the relative retention times and primary fragment ions of the PMAA from cabbage pectin.

The complex mixtures of methylated alditol acetates, often obtained after methylation analysis, cannot be adequately resolved on conventional packed GLC columns. The fractionation of large numbers of these derivatives now can be achieved using capillary columns (Geyer et al., 1982). It is unlikely that a single column can adequately resolve all the derivatives from the methylation analysis of plant cell walls (Lomax et al., 1985). A combination of different liquid phases and coating procedures, namely wall-coated (WCOT), support-coated (SCOT), and permanently bonded (BP) phases will be required (Geyer et al., 1982; Lomax et al., 1985). As an alternative to PMAA, partially ethylated alditol acetates may be used

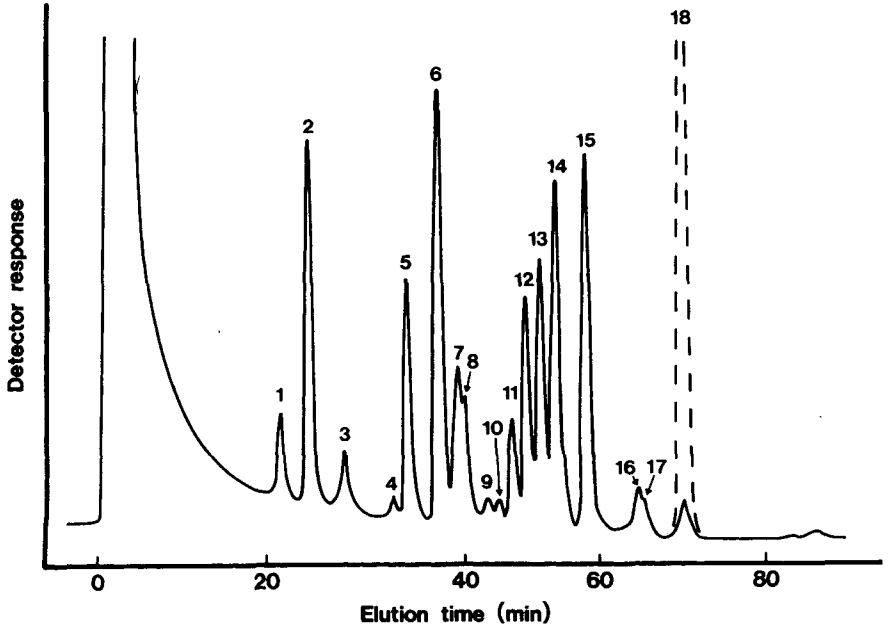

Fig. 5. Separation of the PMAA from cabbage pectin, before (——) and after (– – –) carboxyl-reduction of methylated pectin, on OV-225; initial temperature 150°C, isothermal for 5 min, and then temperature programmed at 1°C/min up to 220°C.

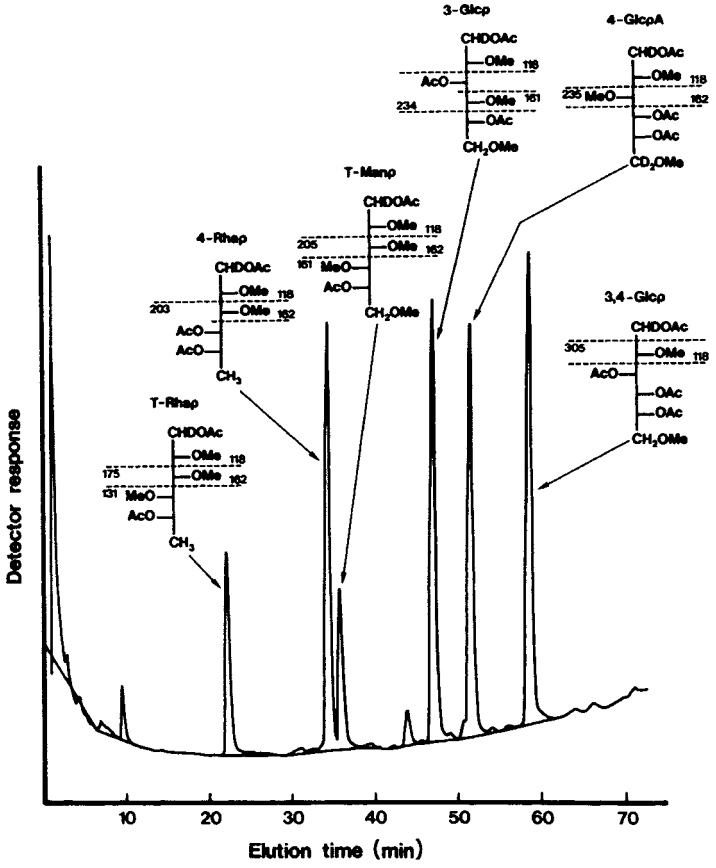

Fig. 6. Separation of the PMAA from S130, after carboxyl reduction. Separation was achieved on OV-225; GLC conditions as for Fig. 5.

when separation difficulties are encountered with particular combinations of the corresponding methylated derivatives (Sweet et al., 1974, 1975). For details of the application of capillary GLC for separating a range of PMAA derived from grass cell walls, the reader should consult Lomax and Conchie (1982) and Lomax et al. (1985). For a comparison of the elution sequence of PMAA derived from a cell wall proteoglycan from runner bean on packed and WCOT OV-225 capillary columns, see Selvendran et al. (1985). Unless very precise chromatographic conditions can be maintained, it is doubtful whether retention data alone can be used for unambiguous identification of PMAA.

TABLE IV

Relative Retention Times and Main Diagnostic Ions of PMAA from a Cabbage Pectin

PEAK NUMBER	RT[a]	ALDITOL ACETATE[b]	DIAGNOSTIC PRIMARY FRAGMENT IONS[c]
1	0.36	?	Unidentified component (nonsugar)
2	0.44	2,3,5-Me_3-Ara	118(100), 161(28), 162(4)
3	0.57	2,3,4-Me_3-Xyl	117(100), 118(94), 161(25), 162(19)
4	0.80	3,5-Me_2-Ara	161(57), 190(35)
5	0.87	3,4-Me_2-Rha	131(100), 190(19)
6	1.07	2,3-Me_2-Ara	118(100), 189(14)
7	1.19	2,3,4,6-Me_4-Gal[e]	118(100), 233(45), 162(14)
		2,3-Me_2-Xyl	118(100), 189(18)
		3,4-Me_2-Xyl	117(100), 190(20)
8	1.26	?	
9	1.37	2-Me-Rha	118(100), 275(5)
10	1.57	4-Me-Rha	131(100), 262(17)
11	1.67	3-Me-Rha	190(39), 203(32)
12	1.83	2-Me-Ara	118(100), 261(4)
13	2.01	3-Me-Xyl	189(34), 190(25)
	2.15	3,4,6-Me_3-Gal	161(42), 190(22)
14	2.22	2,3,6-Me_3-Gal	118(100), 162(14), 233(45)
15	2.60	Arabinitol	115(100), 103(42), 145(72), 187(43)
	2.89	2,3,4-Me_3-Gal	118(100), 162(18), 189(18), 233(14)
	3.14	2,6-Me_2-Gal	118(100), 305(4)
16	3.57	Xylitol	115(100), 103(82), 145(67)
17	3.60	3,6-Me_2-Gal	190(48), 233(22)
18	4.70	2,3-Me_2-Gal	118(100), 261(17)
		2,3-Me_2-6,6'-[^{2}H]-Gal[d]	118(100), 263(15)
		2-Me-Gal	118(100)
		3-Me-Gal	190(30), 261(15)

[a]Retention time is given relative to 1,5-di-*O*-acetyl-2,3,4,6-tetra-*O*-methyl glucitol on OV-225 at 170°C.

[b]2,3,5-Me_3-Ara = 1,4-di-*O*-acetyl-2,3,5-tri-*O*-methylarabinitol, etc.

[c]The galactitol and xylitol derivatives can be separated on ECNSS-M at 170°C.

[d]Obtained after carboxyl reduction of (1→4)-linked galacturonic acid with $LiAl^2H_4$.

[e]Typical relative intensities are given in parentheses.

In addition to the problem of resolving large numbers of PMAA the accurate quantitation may be difficult. This may be attributed to (1) loss of highly volatile derivatives, (2) loss of certain derivatives on sample injection or adsorption on to active sites on the GLC column, and (3) variation in detector responses. By carefully manipulating the experimental procedures the difficulties encountered with (1) and (2) can be minimized. Although detector response values for a number of PMAA have been reported (Sweet et al., 1975), it is questionable whether these can be

directly used with other GLC systems. It is preferable to calibrate the detector responses for an individual chromatographic system, but this may be a time-consuming task.

g. Identification of PMAA by Electron-Impact Mass Spectrometry. The mass spectral fragmentation patterns of PMAA have been discussed in detail by Lindberg (1972) and Aspinall (1982a) and examples of typical mass spectra have been published (Jansson et al., 1976). Generally molecular or pseudomolecular ions are absent. Primary fragment ions are formed by α-cleavage of carbon-carbon bonds in the alditol chain with ions of low molecular mass being dominant (Table 4). The scission of the alditol chain occurs more readily between adjacent methoxylated carbon atoms than between methoxylated and acetoxylated carbons. In the latter case the fragment with the methoxyl group carries the positive charge. Fragmentation between adjacent acetoxylated carbons does not occur to any great extent. Primary fragment ions undergo a series of subsequent eliminations to give secondary fragments. This may occur by a single or consecutive loss of acetic acid (*m/z* 60), methanol (*m/z* 32), ketene (*m/z* 42), or formaldehyde (*m/z* 30). Acetic acid and methanol are lost by β-elimination, although under certain circumstances acetic acid but not methanol can be lost by α-elimination. There is little tendency for scission to take place adjacent to a deoxygenated carbon, but the presence of a deoxysugar derivative is readily recognized by the primary fragments (Table 4).

h. Possible Sources of Error and Misinterpretation. In principle, methylation analysis of a highly branched polysaccharide should give equimolar proportions of nonreducing terminal groups and branch points. However, it is not uncommon to find an excess of branch points. This may be indicative of undermethylation and can be examined by realkylation using C^2H_3I or C_2H_5I. In some plant polysaccharides (e.g., arabinans) the presence of mono-*O*-methyl pentitol-tetraacetate and pentitol-pentacetate was considered as evidence for the occurrence of doubly and triply substituted arabinose residues in the polysaccharide (Stevens and Selvendran, 1980b; Stevens and Selvendran, 1984a). The presence of terminal residues with no corresponding branch points can be indicative of covalent attachment of sugars to hydroxyamino acids of glycoproteins, as has been shown for the hydroxyproline-rich glycoproteins from runner bean cell walls (O'Neill and Selvendran, 1980b) and potato lectin (Ashford et al., 1982).

It was stated earlier that some volatile derivatives may be lost on sample workup. We have found that nonreducing terminal xylose derivatives are underestimated with most of the xyloglucans that we have examined.

This became apparent after methylation of the disaccharide Xyl*p*-(1→6)-Glc*p* (isoprimeverose) when only 50% of the expected yield of the xylose derivative was obtained (O'Neill and Selvendran, 1986). The reason(s) for this loss remain unclear.

A number of polysaccharides, of microbial origin, contain nonsugar substituents, such as ketals of pyruvic acid, that are stable under the conditions of methylation analysis but are acid labile. Unless precautions are taken, such groups can easily lead to the misidentification of branch-point residues. However, most plant cell wall polysaccharides contain noncarbohydrate substituents that are either alkali labile (e.g., *O*-acetyl and phenolic esters) or stable to base and acid hydrolysis (e.g., *O*-methyl ethers). The detection and location of *O*-methyl ethers can be achieved by performing the methylation with deuterated methyl iodide (Ring and Selvendran, 1980; Selvendran, 1983b) or ethyl iodide.

i. ***Controlled Partial Acid Hydrolysis Studies.*** Controlled partial acid hydrolysis in combination with methylation analysis has been used to determine the point of attachment of acid-labile sugars (Lindberg and Lonngren, 1978; O'Neill and Selvendran, 1983). The method is particularly valuable when a polysaccharide contains a limited number of acid-labile glycosidic linkages, which may be cleaved without significant hydrolysis of other glycosidic linkages. Likewise the methylated polysaccharide may be partially hydrolyzed and remethylated with tri-deuteriomethyl iodide (or ethylated). This method yields similar but more detailed information on the positions of the acid-labile sugars. For applications of this method to determine the point of attachment of terminal Ara*f* residues in potato xyloglucan and arabinan side chains in a cabbage pectic polysaccharide, see Ring and Selvendran (1981), Stevens and Selvendran (1984a), and Selvendran and Stevens (1986).

B. OXIDATIVE CLEAVAGE OF POLYSACCHARIDES WITH PERIODATE

The oxidative cleavage of 1,2-diol and 1,2,3-triol groups in polysaccharides with periodate has been extensively reviewed (Bobbit, 1956; Guthrie, 1961). Although the technique may provide information about the type(s) of end groups and glycosidic linkages, caution is required in the interpretation of the results. With complex heteropolysaccharides it is not possible to interpret the results unambiguously without supporting evidence (Aspinall, 1982a). Furthermore, unless careful control of the reaction conditions is maintained, the possibility of overoxidation and less frequently underoxidation may arise (Aspinall, 1982a).

The sequence of reactions known as the Smith degradation (Goldstein et al., 1965), where the oxidized polysaccharide is reduced with $NaBH_4$ to

yield a polyalcohol and then treated with dilute mineral acid, has found extensive application. This procedure takes advantage of the fact that under the hydrolytic conditions used, selective cleavage of acyclic linkages is achieved. However, acetal migration during the hydrolytic step may occur (Goldstein et al., 1965; Gorin and Spencer, 1965). To overcome this problem, Lindberg et al. (1973a) developed a modified procedure whereby the polyalcohol is methylated prior to acid hydrolysis. Realkylation with C^2H_3I or C_2H_5I can then be used to locate the positions to which the oxidatively cleaved sugar residues were originally attached.

3. Glycosyl Sequence Determination

Due to their variety the monosaccharides and linkages present in most cell wall polysaccharides cannot be sequenced with the same degree of certainty as proteins (Walsh et al., 1981) or nucleic acids (Sanger, 1981; Gilbert, 1981). However, during the past two decades, considerable advances have been made in the development of methods that allow the sequence of sugars in a polysaccharide to be determined (Lindberg et al., 1975; Lindberg and Lonngren, 1978; Aspinall, 1982a; Ginsburg, 1982).

For polysaccharides composed of repeating units consisting of 3–8 glycosyl residues, as in most bacterial polysaccharides, procedures are available that may lead to a complete description of the primary structure (Kenne and Lindberg, 1983). For more complex plant polysaccharides, which apparently have less ordered sequences, only an average structure may be obtained (Stephen, 1983). In both cases the procedures involve (1) degrading the polysaccharide (or its derivative) into oligomeric fragments preferably with a d.p. ≤ 6; (2) separating the oligomers by chromatographic methods and identifying them, and (3) piecing together the (overlapping) oligomers to define the structure of the parent polysaccharide. A generalized outline of the procedures used are summarized in Fig. 7.

A. APPLICATIONS OF MASS SPECTROMETRY FOR CHARACTERIZING OLIGOSACCHARIDE DERIVATIVES

Mass spectrometry (MS) has become an important and versatile technique in structural carbohydrate chemistry (Kochetkov and Chizhov, 1966; Hanessian, 1971; Lonngren and Svensson, 1974; DeJongh, 1980). For details of the technical aspects of mass spectrometry, the reader should consult West (1974) and Waller and Dermer (1980), and for an account of the applications of mass spectrometry for the examination of pectic polysaccharides, see Selvendran and Stevens (1986).

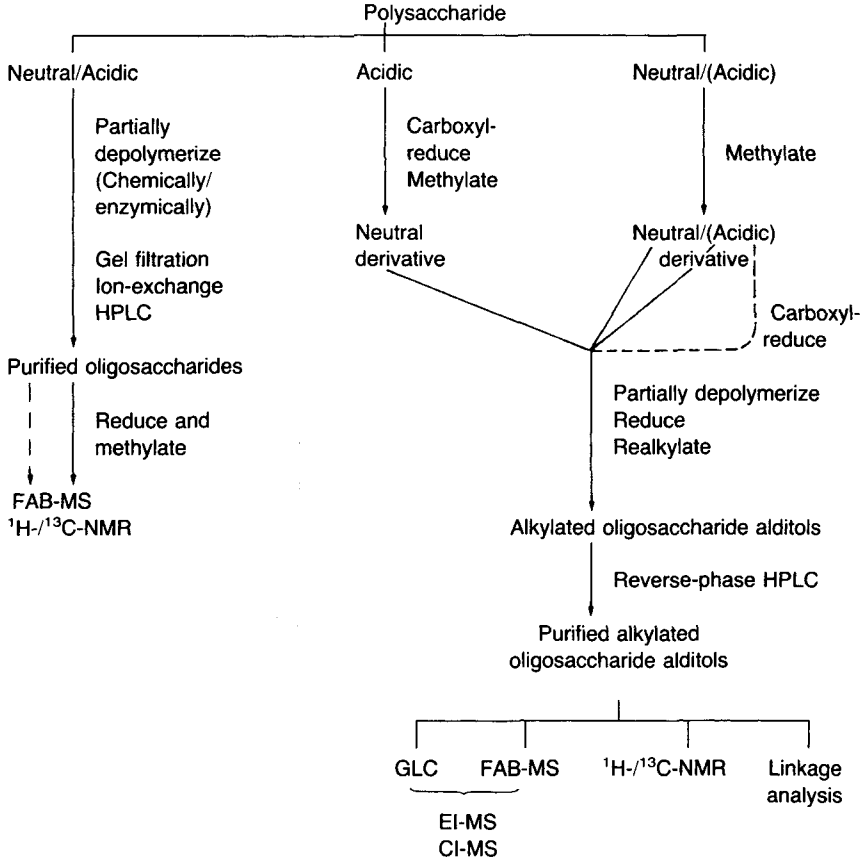

Fig. 7. Flow chart for the sequencing of neutral and acidic polysaccharides.

Most underivatized oligosaccharides are thermally unstable and nonvolatile and therefore unsuitable for most MS analysis. To overcome these problems, a number of volatile derivatives have been used, including *O*-acetyl, *O*-tri-methylsilyl, and *O*-methyl, the last being the most common. With reducing oligosaccharides reduction with NaB^2H_4 prior to derivatization facilitates the distinction between nonreducing and reducing termini (Karkkainen, 1970).

Samples can be introduced into the mass spectrometer through a direct probe inlet or GLC interface (West, 1974). Combined GLC-MS has become increasingly important for oligosaccharide derivatives. However, the resolution of mixtures containing tetra- or larger saccharides may not

be satisfactory (O'Neill and Selvendran, 1986). The recent introduction of liquid chromatography inlets (LC-MS) has great potential as a number of structurally similar oligosaccharide derivatives can be separated and analyzed (McNeil et al., 1982b).

There are several ways of generating the ionization and fragmentation of the sample molecules. For oligosaccharide derivatives, electron impact (EI-MS) gives diagnostic fragment ions, although molecular or pseudomolecular ions are generally absent. Softer methods of ionization including chemical ionization (CI-MS) using reagent gases such as isobutane or isobutane/ammonia (Chizhov et al., 1976), and field desorption (Moor and Waight, 1974) give molecular or pseudomolecular ions. Generally these techniques give a greater abundance of ions in the higher mass range (>400 *m/z*) but provide less structural information. It should be noted that CI-MS of oligosaccharide derivatives using isobutane may cause elimination of internal glycosyl residues (McNeil, 1983), producing fragment ions containing one glycosyl residue less than the parent oligosaccharide-alditol derivative, and this may cause ambiguities in the interpretation. Molecular weights may also be determined using fast atom bombardment (FAB-MS) where the sample is ionized with energetic beams (8 kV) of argon or xenon (Barber *et al.*, 1981). This method has the advantage that it can also be applied to underivatized, nonvolatile oligosaccharides. With FAB-MS, molecular or pseudomolecular ions are dominant, although in favorable cases sequence information may be obtained (Dell and Ballou, 1983; Nothnagel et al., 1983). Depending on the type of mass spectrometer masses up to 6600 daltons may be obtained (Dell and Ballou, 1983).

a. Interpretation of Mass Spectral Data. Several review articles have dealt with the general aspects of interpreting EI-MS data obtained from mono- and oligosaccharide derivatives (Kochetkov and Chizhov, 1966; Lonngren and Svensson, 1974). Although the EI-MS may be relatively complex, a number of primary and secondary fragments are obtained that give valuable structural information. Generally, the fragment ions are classified according to the nomenclature of Kochetkov and Chizhov (1966). However, there is no agreement as to the designation of the sugar rings and alditol moiety (see Nilson and Zopf, 1982; McNeil et al., 1982b). In this article the nonreducing terminal sugar ring will be referred to as *a* and the alditol moiety as *ald* (**2**). The most easily recognizable fragment ions are those from nonreducing terminal residues (aA_1 in **2**). Methylated hexosyl, pentosyl, 6-deoxyhexosyl, and hexuronosyl acids give aA_1 ions at *m/z* 219, 175, 189, and 233, respectively. The corresponding alditol fragment ($aldJ_2$ in **2**) masses, assuming monodeuteration at C1, are *m/z* 236,

192, 206, and 250. Internal glycosyl residues substituted with a single sugar (residue *b* in **2**) are 15 mu less than the corresponding nonreducing terminal residue From these ions information on the sequence of sugar residues in an oligosaccharide-alditol derivative can be deduced.

Ions of the A series arise from cleavage of the glycosyl (C1-)-oxygen bond. These ions undergo a number of fragmentations and eliminations with the loss of the substituent on *O*-3 being the predominant one. If the nonreducing terminal residue (*a* in **2**) is linked to C-3 of the internal residue (*b*), then the relative abundance of the *ba*A ions would be $baA_1 > baA_2 > baA_3$. However, if the residue *a* is attached to C-2 of the internal residue, then the relative abundance would be $baA_2 >> baA_1 > baA_3$ (Karkkainen, 1971; Moor and Waight, 1975). These principles have been used in the sequencing of oligosaccharide derivatives from cell wall polysaccharides (Selvendran, 1983b).

The formation of J_1 ion (shown in **3**) is of particular significance in the mass spectra of oligosaccharide-alditol derivatives, and requires the pres-

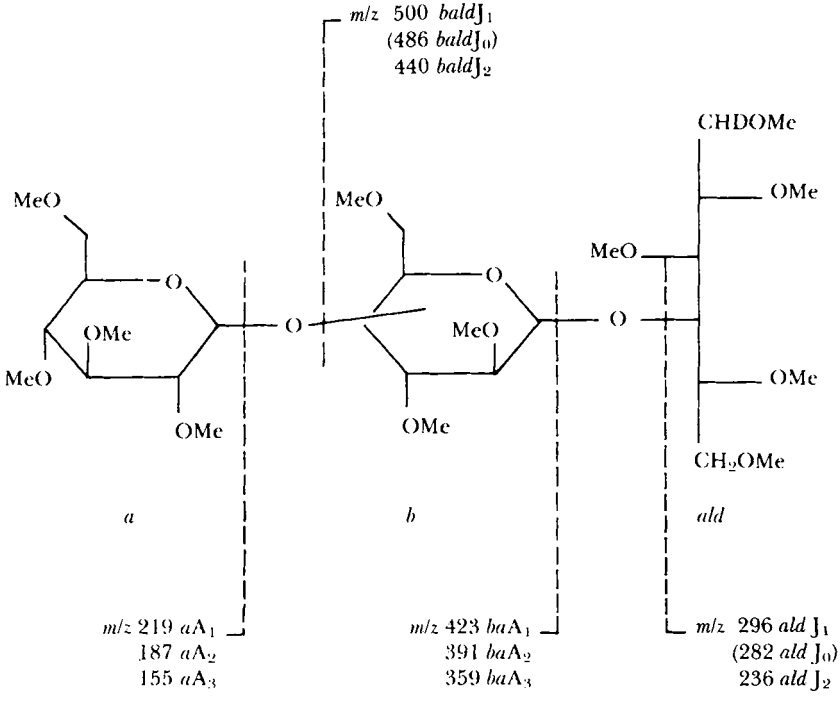

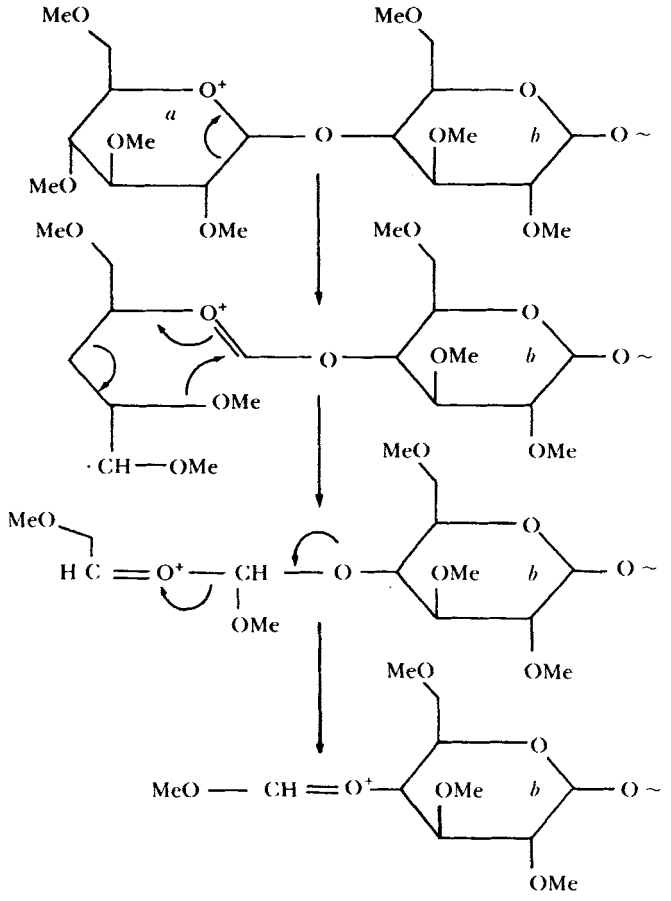

3

ence of an *O*-alkyl (e.g., OCH_3) group on position 3 of the ring sugar (Kochetkov and Chizov, 1966). Loss of 60 mu from the J_1 ion gives rise to the J_2 ion. The absence of an ion of relatively high intensity at the *m/z* values 296 (*ald*J_1 in **2**) provides strong evidence for the presence of a glycosyl substituent on C-3 of ring *b*. Recently Sharp and Albersheim (1984) have shown that 3-*O*-substituted residues give a diagnostic ion and have proposed that it is formed via D_1- and J_1-like fragment ions. If ring *a* in **2** was linked through position 3 of ring *b*, the *m/z* value of the J_0 ion would be 282.

4. Applications of ^{1}H-NMR

High resolution ^{1}H-NMR is a valuable technique for determining the anomeric nature of glycosidic linkages (Perlin and Casu, 1981). Generally the spectrum of oligo- or polysaccharides are similar to the monosaccharides, albeit somewhat more complex. Vliegenthart et al. (1983) have used the term "structural reporter groups" to define particular types of proton resonances. Anomeric protons generally give signals in the region δ 4.2–5.5 ppm with the α-linked protons occurring downfield (i.e., δ 4.9–5.5 ppm) from β-linked protons (δ 4.2–4.9 ppm). Ring protons resonate in the region δ 3.2–4.5 ppm with methyl and acetyl resonances occurring around δ 1.5 ppm and δ 2.0–2.2 ppm, respectively.

The $J_{1,2}$ coupling constants of anomeric protons are dependent on the dihedral angle between the anomeric and C-2 proton. When the angle approaches 180°, large couplings are observed. For β-linked glucosyl residues $J_{1,2}$ is approximately 8 Hz, whereas α-linked glucosyl residues have $J_{1,2}$ approximately 3.5 Hz. Sugars with dihedral angles of approximately 60°C such as α- or β-linked mannose and rhamnose generally have $J_{1,2}$ values $\leq$3 Hz. Therefore from a detailed investigation of chemical shifts (δ) and coupling constants ($J_{1,2}$), it is possible to assign anomeric configurations of both native and derivatized oligo- and polysaccharides. In the case of reducing oligosaccharides, interpretation of the spectrum is facilitated by reduction to the alditols to eliminate the equilibrium effect of the reducing termini (Usui et al., 1974; Di Fabio et al., 1984).

High resolution ^{1}H-NMR has also been used to sequence a number of glycoconjugates, but this is outside the scope of this article; the reader should consult Vliegenthart et al. (1983).

5. Degradation of Native Polysaccharides

A. PARTIAL ACID HYDROLYSIS

Two approaches can be used for partial acid hydrolysis studies. Conditions can be chosen to remove selectively acid-labile residues or, alternatively, the hydrolytic conditions can be such that only residues retaining acid-resistant linkages remain intact. In this section we shall concentrate on methods used to obtain and characterize acid-stable oligosaccharides.

Hydrolysis of acidic polysaccharides with 0.5 *M* H_2SO_4 for 4 h at 100°C is generally sufficient to hydrolyze most neutral sugar linkages while leaving aldobiouronic acids intact (Conrad et al., 1966). With this procedure in combination with ion-exchange chromatography the aldobiouronic acids from *Phaseolus coccineus* pectin (O'Neill and

Selvendran, unpublished) and *Pseudomonas elodea* gum (O'Neill et al., 1983) were isolated. A combination of monosaccharide analysis, CI- and EI-MS of the methylated disaccharide-alditol methyl esters (Fig. 8) allowed the structure of the aldobiouronic acids to be determined.

The molecular weights of the derivatives and ions of the A and J types demonstrated that the pectic aldobiouronic acid derivative contained hexuronosyl and 6-deoxyhexitol residues, and the *P. elodea* derivative was composed of hexuronosyl and hexitol residues (Fig. 8*B*). The abundance ratio $aA_2/aA_1 \simeq 1$ for the derivative from galacturonic acid and >4 for the derivative from glucuronic acid (Kovacik et al., 1968; Ring and Selvendran, 1980). Therefore from the intensities of the aA_1 and aA_2 ions, it could be inferred that the derivatives derived from pectin and bacterial gum contained galacturonic acid and glucuronic acid, respectively. From the fragmentation of carbon-carbon bonds in the alditol moieties, it could be deduced that the deoxyhexitol residue in the pectic aldobiouronic acid was 2-*O*-substituted. Using the same principles, the hexitol residue of the aldobiouronic acid from gellan gum was shown to be 4-*O*-substituted.

Partial acid hydrolysis (0.2 *M* trifluoroacetic acid for 2 h at 100°C) of beeswing wheat bran cell walls followed by ion-exchange chromatography gave an acidic fraction that accounted for 6% of the material (Ring and Selvendran, 1980). The acidic fraction was reduced with NaB^2H_4, methylated with C^2H_3I and the alkylated oligosaccharide-alditol methyl esters separated by GLC on OV-1. Two major components which eluted in the regions for di- and trisaccharide derivatives in the ratio 1.0:2.0 were detected. EI-MS established that the disaccharide had the structure Glc*p*A-(1→2)-Xyl*p*. Because the methylation was performed with C^2H_3I, it was possible to deduce from the relative intensities of the aA_1 ions (*m/z* 245 and 242) that approximately 25% of the glucuronic acid was present as its 4-*O*-methyl analogue (Ring and Selvendran, 1980; Selvendran, 1983b).

GLC-MS of the component eluting in the trisaccharide-alditol region gave ions at *m/z* 49 (16.3%), 96 (16.4%), 143 (9.9%), 204 ($aldJ_2$, 100%), 245 (aA_1, 7.7%), 267 ($aldJ_1$, 0.4%), 370 ($baldJ_2$, 2.6%), 411 (baA_1, 0.2%), 433 ($baldJ_1$, 1.6%), and 582 (M-49, 0.2%). The presence of ions at *m/z* 96 and 143 demonstrated that the pentitol moiety was substituted through position 4. The ratios of the *ba*A series of ions, $baA_2 > baA_3 > baA_1$, suggested that the internal pentosyl residue was linked through position 2 (**4**). These data in combination with monosaccharide analysis established the structure of the acidic trisaccharide as Glc*p*A-(1→2)-Xyl*p*-(1→4)-Xyl*p*. As with the disaccharide approximately 25% of the Glc*p*A residues were endogenously methylated at position 4. These studies were consistent

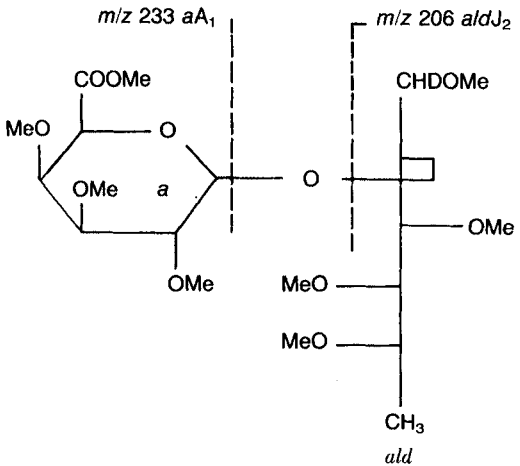

Fig. 8a. Chemistry to go with table.

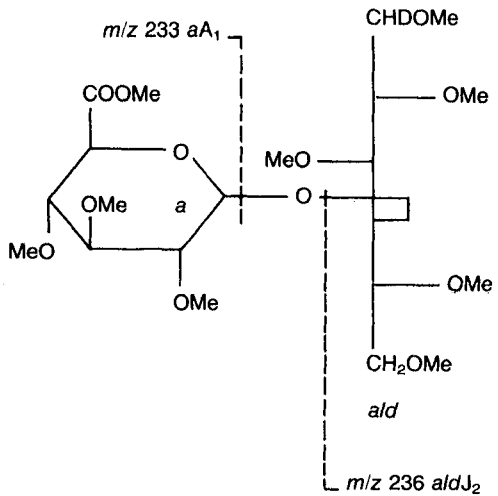

Fig. 8b. Chemistry to go with table.

A.

ION (M/Z)	INTENSITY (/)		FRAGMENT
473	6.2	CI-MS	M+18
456	1.1		M+1
266	8.5		$aldJ_1$
233	51.9		aA_1
206	100.0		$aldJ_2$
201	67.6		aA_2
169	9.3		aA_3

B.

ION (M/Z)	INTENSITY (/)		FRAGMENT
503	4.4	CI-MS	M+18
486	1.3		M+1
296	1.4		$aldJ_1$
236	17.3		$aldJ_2$
233	22.3		aA_1
201	100.0		aA_2
169	10.2		aA_3

Fig. 8. MS fragmentation patterns of methylated aldobiouronic acids (after reduction with NaB^2H_4) from pectic *(A)* and *P. elodea* gum *(B)*.

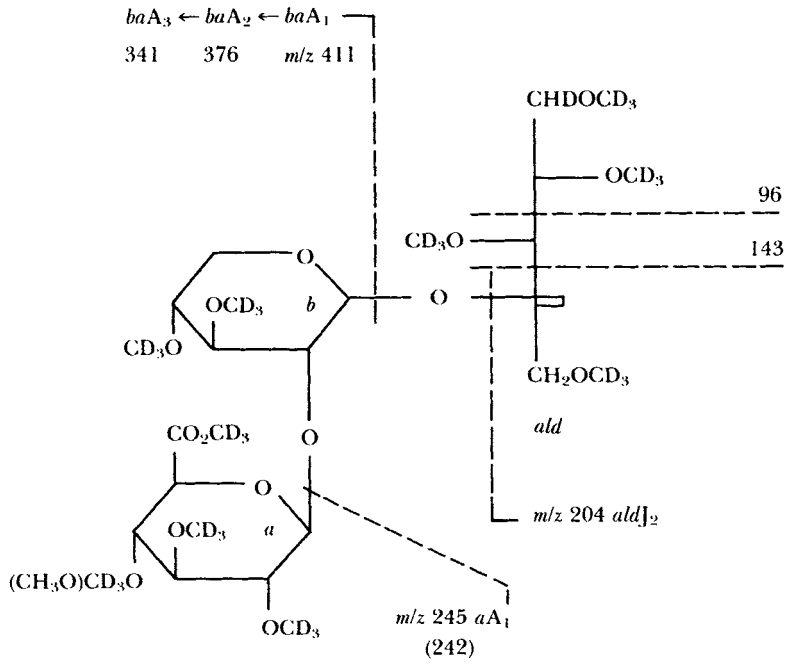

4

with earlier work on acidic arabinoxylans from corn hull (Montgomery et al., 1956), wheat bran (Adams and Bishop, 1956), birch (Rosell and Svensson, 1975), and larch (Shimizu et al., 1978).

Although GLC (on packed columns) can adequately resolve oligosaccharide derivatives containing 3-4 glycosyl residues, derivatives of higher oligosaccharides tend to coelute. Furthermore the high boiling points of these latter derivatives may cause them to condense on the GLC-MS interface and not enter the ion source. These difficulties can be overcome to a certain extent by using capillary columns that can resolve oligosaccharide derivatives containing five glycosyl residues, and as they pass directly into the ion source of the mass spectrometer (Nilsson and Zopf, 1982, 1983), condensation of the material is eliminated.

Recently we found that methylated oligosaccharide-alditol methyl esters can be resolved by reverse-phase HPLC (O'Neill et al., 1986a, b, c). The technique has been applied to the separation and characterization of acidic tri-, tetra-, and pentasaccharide derivatives from a number of bacterial polysaccharides (O'Neill et al., 1986a, b, c). A similar procedure can be used to establish the structural features of cell wall polysaccharides

and plant gums that contain acidic sugars (e.g., pectins, glucuronoarabinoxylans, and glucuronomannans). The technique has the advantage that the derivatives can be collected and further examined by FAB-MS, CI-MS, EI-MS, and ^{1}H-NMR. This allows not only the glycosyl sequences to be determined but also provides information on the anomeric nature of the glycosidic linkages.

This can be illustrated by our work (O'Neill et al., 1986a) on the extracellular anionic polysaccharide produced by *Alcaligenes* (ATCC 31555) species. The polysaccharide was hydrolyzed for 1.5 h with 0.2 *M* trifluoroacetic acid and the acidic oligosaccharides isolated by ion-exchange chromatography. Following reduction and methylation, the methylated oligosaccharide-alditol methyl esters were separated by reverse-phase HPLC (Fig. 9). Two major and one minor components were isolated and characterized by FAB-MS, EI-MS, and ^{1}H-NMR.

FAB-MS of the compound in fraction A (Fig. 9) gave an ion at *m/z* 690, corresponding to $[M+1]^+$ from a methylated oligosaccharide alditol methyl ester containing hexosyl, hexuronosyl, and hexitol residues. EI-MS gave ions at *m/z* 219 (*a*A_1, 13.3%), 236 (*ald*J_2, 47.4%), 296 (*ald*J_1, 3.0%), 437 (*ba*A_1, 0.5%), 454 (*bald*J_2, 0.8%), and 514 (*bald*J_1, 0.5%) confirming the trisaccharide nature of the derivative **(5)**. The ^{1}H-NMR spectrum of **5** contained signals for anomeric protons at δ 4.27 ($J_{1,2}$ 7.6 Hz) and 4.52 ($J_{1,2}$ 7.3 Hz) and were assigned to β-linked sugars with the *gluco*-configuration. These results established the structure of the oligosaccharide as β-D-Glc*p*-(1→4)-β-D-Glc*p*A-(1→4)-D-Glc*p*.

FAB-MS of the derivative in fraction C (Fig. 9) gave an ion at *m/z* 864, corresponding to $[M+1]^+$ from a tetrasaccharide alditol containing two hexosyl, hexuronosyl, and 6-deoxyhexitol residues. EI-MS gave ions at *m/z* 206 (*ald*J_2, 72.0%), 219 (*a*A_1, 18.8%), 266 (*ald*J_1, 20.6%), 410 (*cald*J_2, 1.4%), 437 (*ba*A_1, 1.1%), 470 (*cald*J_1, 0.3%), 628 (*bcald*J_2, 0.2%), 641 (*cab*A_1, 0.1%), and 688 (*bcald*J_1, 0.8%) confirming the tetrasaccharide nature of the derivative **6**. The ^{1}H-NMR spectrum of **6** contained signals for anomeric protons at δ 4.24 ($J_{1,2}$ 7.7 Hz), δ 4.29 ($J_{1,2}$, 7.9 Hz) and δ 4.45 ($J_{1,2}$, 7.9 Hz) which were consistent with two β-linked hexosyl and one β-linked hexuronosyl with the *gluco*-configuration. These data in combination with methylation analysis of the polysaccharide established the structure of the tetrasaccharide as β-D-Glc*p*-(1→4)-β-D-Glc*p*A-(1→4)-β-D-Glc*p*-(1→4)-L-Rha*p*. Using the same procedures, the minor component (peak B, Fig. 9) was found to be derived from the oligosaccharide β-D-Glc*p*A-(1→4)-β-D-Glc*p*-(1→4)-L-Rha*p*. These studies established the sequence of glycosyl residues in the polymer backbone. However, none of the oligosaccharides contained nonreducing terminal rhamnose or mannose which are present in the native polymer. The points of attachment of

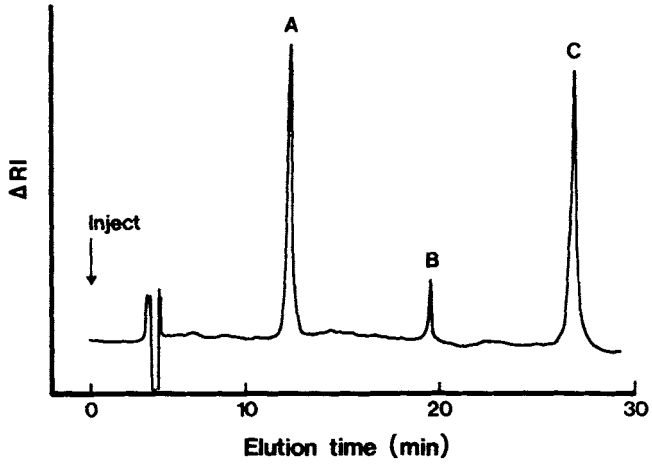

Fig. 9. HPLC elution profile of the acidic oligosaccharides, derived from partial acid hydrolysis of S130, as their reduced and methylated derivatives.

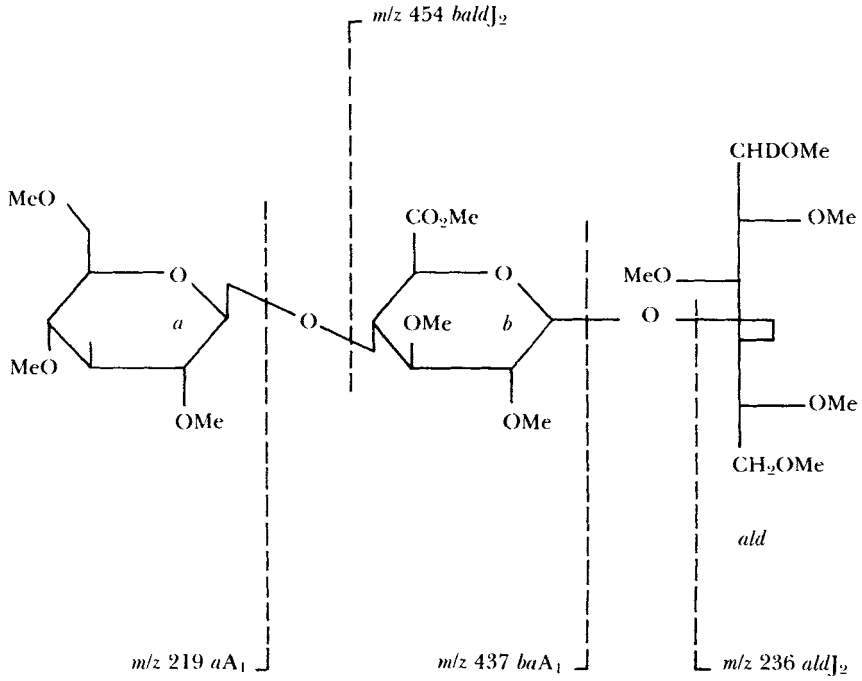

5

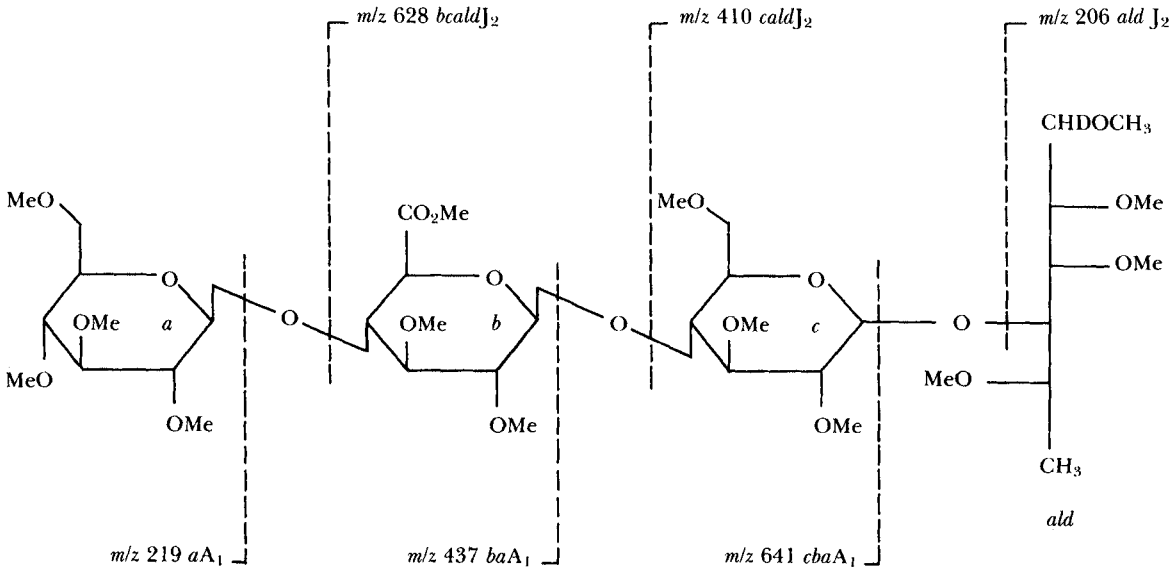
m/z 628 bcaldJ2
m/z 410 caldJ2
m/z 206 ald J2
CHDOCH3
OMe
OMe
MeO
CO2Me
MeO
MeO
OMe a
OMe b
OMe c
O
O
O
O
O
O
OMe
OMe
OMe
MeO
CH3
ald
m/z 219 aA1
m/z 437 baA1
m/z 641 cbaA1

6

these residues were established by using β-eliminative degradation, which is discussed in Section VI.6.E.

B. AUTOHYDROLYSIS

Polysaccharides containing glycosyluronic acid residues may be subjected to graded hydrolysis by heating aqueous 1% solutions of the purified polysaccharide. Autohydrolysis provides controlled hydrolysis of acid-labile linkages from the outer chains of a polysaccharide with minimal degradation of the interior chains. Aspinall et al. (1969) employed autohydrolysis in structural studies on the polysaccharide leiocarpan A from *Anogeissus leiocarpan*. All the arabinose and approximately 50% of the xylose were liberated and a number of oligosaccharides were isolated and characterized. These data in combination with related studies (Aspinall and McNab, 1969; Aspinall and Carlyle, 1969) enabled the overall structure of the polysaccharide to be to be determined.

The acidic polysaccharide from the cell walls of *Lemna minor* which contains apiobiose attached to a galacturonan chain undergoes autohydrolysis at pH 4.5 (Hart and Kindel, 1970). It has been suggested that intramolecular catalysis involving the free carboxyl groups of galacturonic acid results in the cleavage of the apiobiose side chains.

C. PARTIAL DEPOLYMERIZATION OF COMPLEX ACIDIC POLYSACCHARIDES

With complex acidic polysaccharides (pectins and gums) a single degradative technique, such as partial acid hydrolysis may give low yields of oligosaccharides thereby giving limited information on structure. The work of Aspinall and colleagues in the late 1960s illustrates how a number of chemical and enzymic degradations were required to obtain partial structures. This work also demonstrates the difficulties involved in isolating and characterizing oligosaccharides without the aid of modern analytical techniques.

Using a combination of partial acid hydrolysis and acetolysis, Aspinall's group characterized a range of acidic polysaccharides from soybean meal (Aspinall et al., 1967b), soybean hulls (Aspinall et al., 1967c), lemon peel (Aspinall et al., 1968a), and lucerne (Aspinall et al., 1968b). A comparison of the neutral and acidic oligosaccharides from soybean hull and meal showed that partial acid hydrolysis generates a series of acidic oligosaccharides and a limited number of neutral fragments. Conversely, acetolysis yields a range of neutral fragments with lesser amounts of acidic oligosaccharides.

Studies on lemon peel pectin illustrate the value of combining data from chemical and enzymic studies. Partial acid hydrolysis and acetolysis

produced the oligosaccharides (1) Gal*p*A-(1→4)-Gal*p*A-(1→4)-Gal*p*A, (2) Gal*p*A-(1→4)-Gal*p*A, (3) Gal*p*A-(1→2)-Rha*p*, (4) Gal*p*A-(1→2)-Rha*p*-((1→4)-Gal*p*A, and (5) Gal*p*A-(1→2)-Rha*p*-(1→2)-Rha*p*. Oligosaccharide (5), which contains the acid-labile Rha*p*-(1→2)-Rha*p* linkage, could only be obtained by acetolysis. Enzymic degradation produced, albeit in relatively low yields, oligosaccharides composed of Gal*p*A-(1→2)-Rha*p*-(1→4)-Gal*p*A (6), 2-*O*-(4-deoxy-β-L-hex-4-enopyranosyluronic acid)-L-rhamnose (7), and Xyl*p*-(1→3)-Gal*p*A (8). The presence of the 4,5-unsaturated oligosaccharide (7) suggested that the pectic-degrading enzyme(s) contained lyase activity. The presence of the pseudoaldobiouronic acid (8) shows that some of the Gal*p*A residues are substituted through position 3 with xylose and are an integral part of the pectic molecule.

Studies on the complex pectic polysaccharide Rhamnogalacturonan-II have shown the presence of the unusual sugar aceric acid (3-C-carboxy-5-deoxy-L-xylose) (Spellman et al., 1983a). By using mild acid hydrolysis (0.1 *M* trifluoroacetic acid 40°C for 24 h) two complex heptasaccharides (**7** and **8**), one of which contains aceric acid, have been obtained from Rhamnogalacturonan-II (Spellman et al., 1983b; McNeil et al., 1984). The structures of these complex oligosaccharides were established using methylation, partial acid hydrolysis, and subsequent separation of the alkylated oligosaccharide alditols by HPLC, which were characterized by a combination of FAB-MS, EI-MS, and ^{1}H-NMR.

D. PARTIAL ALKALINE DEGRADATION

Partial alkaline degradations have been used for the release of glycopeptides from the hydroxyproline-rich cell wall glycoprotein(s). Lamport (1967) isolated a series of glycopeptides from tomato cell walls and found that they contained hydroxyproline glycosylated with (1→4) arabinose re-

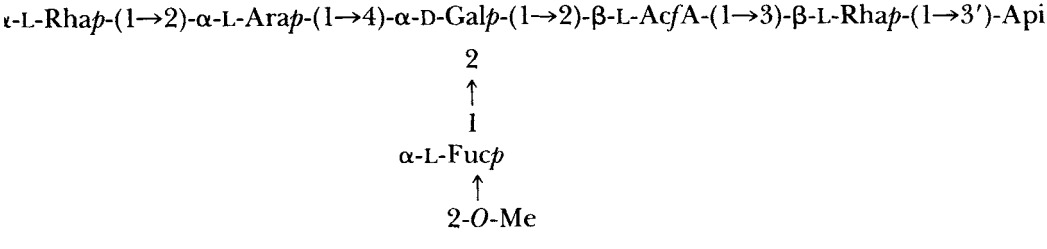

Ac*f*-A = aceric acid
Api = apiose

7

α-Gal*p*A
1
↓
2
α-Gal*p*-(1→2)-β-Glc*p*A-(1→4)-α-Fuc*p*-(1→4)-β-Rha*p*-(1→3′)-Api
3
↑
1
β-Gal*p*A

Api = apiose

8

sidues. Subsequently partial alkaline hydrolysis has been applied to a range of plant cell walls to assess the extent of glycosylation of hydroxyproline (Lamport and Miller, 1972). Detailed studies of hydroxyprolyl-arabinosides obtained after alkaline degradation of suspension-cultured tobacco cell walls (Akiyama and Kato, 1976, 1977; Akiyama et al., 1980) established the structures of the tri- and tetraarabinosides **(9)**. The major hydroxyproline-rich glycoprotein of runner bean cell walls was shown to contain hydroxyproline glycosylated with tri- and tetraarabinosides in the ratio 3:2, and terminal Gal*p* residues α-linked to serine (O'Neill and Selvendran, 1980b).

Hydroxyproline glycosylated with 1→4 arabinose residues has also been released by alkaline degradation of the chitobiose-specific lectin from potato (Allen et al., 1978). Using a combination of optical rotation measurements, CI- and EI-MS (Ashford et al., 1982), it was established that the hydroxyproline of potato lectin is glycosylated with identical sequences **(9)** of arabinose residues as found in tobacco and runner bean cell wall glycoprotein.

Hydroxyprolyl glycopeptides have also been found in lower plants such as ferns and algae (Lamport and Miller, 1972). In the green algae *Chlamydomonas reinhardii* the pattern of glycosylation is different (O'Neill

α-L-Ara*f*-(1→3)-β-L-Ara*f*-(1→2)-β-L-Ara*f*-(1→2)-β-L-Ara*f*-(1→ Hyp

β-L-Ara*f*-(1→2)-β-L-Ara*f*-(1→2)-β-L-Ara*f*-(1→ Hyp

9

and Roberts, 1981). The arabinogalactan-proteins obtained from mono- and dicotyledonous plants also contain hydroxyproline which unlike the cell wall glycoprotein from dicots is substituted with galactose residues (Strahm et al., 1981; McNamara and Stone, 1981).

E. DEGRADATIONS USING PERIODATE

The use of controlled periodate oxidation in structural polysaccharide chemistry has been reviewed (Lindberg et al., 1975). In this section only its general application to plant cell walls will be considered.

A prerequisite for this technique is that a portion of the sugars are resistant to periodate oxidation. The most commonly used procedure is the Smith degradation (Goldstein et al., 1965) where the periodate oxidized polysaccharide is reduced to the polyalcohol and then subjected to mild acid hydrolysis. Acyclic acetals are hydrolyzed more rapidly than glycosidic linkages; thus it is possible to generate oligomeric products that can be isolated and characterized.

Periodate oxidation has been extensively used for the structural characterization of oat (1→3)-,(1→4)-linked β-D-glucans (Goldstein et al., 1965). The major product of the controlled degradation, 2-*O*-β-D-Glc*p*-D-erythritol, suggested alternating (1→3)- and (1→4)-linkages. However, the presence of erythritol indicated adjacent (1→4)-linkages and small proportions of 2-*O*-β-laminaribi-, tri-, and tetra-osyl-D-erythritol are consistent with regions of continuous (1→3)-linkages (Goldstein et al., 1965). Periodate oxidation studies of barley β-glucans suggested that these polysaccharides are composed of cellotriosyl and cellotetraosyl residues separated by a single (1→3)-linkage (Luchsinger et al., 1965; Woodward et al., 1983). Blocks containing 5−11 β-(1→4)-linkages also appear to be present. However, the presence or absence of adjacent (1→3)-linkages has not been resolved. To some extent this may be dependent on the source of the polysaccharide and the care taken to control the oxidation and hydrolysis steps (Woodward et al., 1983).

Periodate oxidation has been used to obtain information on the distribution of (1→3)- and (1→5)-linked arabinosyl residues in the branched arabinan from apple cell walls (Aspinall and Fanous, 1984). Smith degradation yielded a mixture of *O*-glycosylglycerols that was characterized as arabinofuranosylglycerol and two isomeric arabinobiosylglycerols, one with a (1→5)- and the other a (1→3)-intersugar linkage. These results in combination with other data suggest the arabinan is highly branched with regions showing a high degree of multiple branching (Aspinall and Fanous, 1984).

6. Degradations of Polysaccharide Derivatives

A. PARTIAL ACID HYDROLYSIS OF ACIDIC DERIVATIVES

Two procedures have been described for the production of oligosaccharide fragments from methylated acidic polysaccharides. Bjorndal et al. (1973) employed partial formolysis of the methylated material followed by reduction with $LiAl^2H_4$, and realkylation with C^2H_3I. The subsequent separation and characterization of the oligosaccharide-alditol derivatives was performed by GLC-MS. Alternatively, the methylated acidic polysaccharide can be carboxyl-reduced prior to formolysis. After reduction and ethylation, the alkylated oligosaccharide alditols can be separated by reverse-phase HPLC and characterized (Valent et al., 1980). The introduction of *O*-ethyl groups considerably improves the resolution of the derivatives by reverse-phase HPLC. The fractionated oligosaccharide-alditols are subjected to a complete hydrolysis and the partially methylated alditol acetates analysed by GLC-MS. Subsequently, McNeil et al. (1982b) have analyzed the alkylated oligosaccharide-alditols fractionated by HPLC using probe-insertion MS or GLC-MS in the electron impact mode and directly obtained sequence information. The same group have also introduced a portion (3−5%) of the eluant from the HPLC column directly into the mass spectrometer (LC-MS). The acetonitrile in the eluant behaves as a reagent gas giving spectra similar to those obtained by conventional CI-MS. Essentially the same technique has been used by Spellman et al. (1983b) to characterize a complex heptasaccharide from Rhamnogalacturonan-II.

Recently, Lau et al. (1985) used the procedures developed by McNeil et al. (1982b) to characterize a portion of Rhamnogalacturonan-I solubilized from sycamore cell walls by an endo-1,4-α-polygalacturonase. The purified pectic fragment was carboxyl-reduced with NaB^2H_4 in ^2H_2O by the method of Taylor and Conrad (1972), methylated, and formolyzed. Following reduction, the methylated oligosaccharide-alditols were alkylated ($C_2{}^2H_5I$) and separated by reverse-phase HPLC. Pentadeuteroethyl labeling was chosen to avoid ambiguities in the interpretation of the mass spectral data. The alkylated oligosaccharide-alditols were characterized by LC-MS, GLC-MS, ^{1}H-NMR, and glycosyl-linkage composition. The combined data suggest that Rhamnogalacturonan-I backbone is composed of long regions of the repeating unit **10**. For a flowchart showing the methodology used to establish the structural features of Rhmanogalacturonan-I, see Selvendran and Stevens (1986). Studies by Aspinall et al. (1968a) on lemon peel pectin (which was not degraded with endopolygalacturonase) also suggested the presence of alternating α-D-Gal*p* and α-L-Rha*p* residues in the molecule. However, the acidic oligosaccharide

→4)-α-D-Gal*p*A-(1→2)-α-L-Rha*p*-(1→

10

Gal*p*A-(1→2)-Rha*p*-(1→2)-Rha*p* detected in lemon peel pectin was not reported to be present in Rhamnogalacturonan-I.

B. PARTIAL ACID HYDROLYSIS OF NEUTRAL METHYLATED POLYSACCHARIDES

The methods of Valent et al. (1980) and McNeil et al. (1982b) have been applied to the rigorous characterization of a nonasaccharide derived from the enzymic degradation of sycamore cell wall xyloglucan. Following partial acid hydrolysis and workup, 16 alkylated oligosaccharide-alditols were isolated by reverse-phase HPLC, but only 12 were sufficiently pure to be unambiguously characterized.

It is clear that reverse-phase HPLC in combination with mass spectrometry offers considerable promise for the rapid sequencing of relatively small amounts of polysaccharides. It should be emphasized that degradations other than partial acid hydrolysis also yield oligosaccharides that are amenable to this type of analysis. We have recently found that penta- and hexasaccharide fractions produced by enzymic digestion of *Phaseolus coccineus* cell wall xyloglucan can also be separated, as their methylated oligosaccharide-alditols (O'Neill and Selvendran, 1985b). Similarly, alkylated oligosaccharides produced by base catalyzed β-elimination of a methylated microbial polysaccharide could be separated by HPLC and characterized by FAB-MS, EI-MS, and ^{1}H-NMR spectroscopy (O'Neill et al., 1986a).

It is probable that the combination of reverse-phase and ion-exchange HPLC with conventional chromatographic procedures will allow a greater resolution of complex mixtures of oligosaccharides (Sharp et al., 1984; Redgwell et al., 1986a, b).

C. ACETOLYSIS

Acetolysis provides a complementary technique to partial acid hydrolysis. The relative rates of cleavage of glycosidic linkages are quite different from those found with acids (Guthrie and McCarthy, 1967; Lindberg et al., 1975).

Acetolysis is generally performed by dissolving the acetylated glycan in a mixture of acetic anhydride/acetic acid/sulfuric acid at 0°C. The reaction mixture is kept at room temperature for 1−10 days after which the

reaction is terminated by the addition of ice-cold water and adjustment to pH 3.5 with $NaHCO_3$. The acetylated derivatives are extracted into chloroform and can be fractionated directly or deacetylated and fractionated.

Various reaction conditions and times have been employed for both acetylation and depolymerization. Acetylation has been performed with pyridine/acetic anhydride for 8 h at 100°C (Kocourek and Ballou, 1969), two days at room temperature (Kooiman, 1961), a combination of ambient and high temperatures (O'Neill and Selvendran, 1983) or with the inclusion of dimethyl formamide (Stewart et al., 1968). The xyloglucan from the cell walls of runner bean was acetylated with acetic anhydride-pyridine (1:1 v/v) for 12 h at 20°C followed by 8 h at 100°C (O'Neill and Selvendran, 1983). Acetolysis has been carried out in glacial acetic acid/acetic anhydride/concentrated sulfuric acid (1:1:0.1 v/v) for 13 h at 40°C (Kocourek and Ballou, 1969) or with acetic anhydride/concentrated sulfuric acid for 1 h at 0°C followed by two weeks at 50°C (Kooiman, 1961). Acetolysis of the acetylated xyloglucan derived from runner bean cell walls was performed with acetic anhydride-glacial acetic acid-concentrated sulfuric acid (1:1:0.1 v/v) for 12 h at 37°C, and a number of fragments was characterized (O'Neill and Selvendran, 1983). For a discussion of the relative merits of the different procedures for acetolysis, the reader should consult Stewart et al. (1968).

The products of acetolysis with or without deacetylation can be separated by gel filtration (Kocourek and Ballou, 1969) and characterized by methylation analysis (Stewart et al., 1968). Oligosaccharides derived from acetolysis can be separated by chromatography on charcoal-celite columns and monitored by sugar analysis and optical rotation. The partially purified derivatives can be characterized by GLC-MS of the methylated oligosaccharide alditols (Aspinall et al., 1977). If only small amounts (<10 mg) of material are available, the deacetylated oligosaccharides can be reduced, methylated, and analyzed by GLC-MS (O'Neill and Selvendran, 1983). However, for this latter procedure a prior knowledge of both sugar and linkage composition of the original polymer is required to facilitate identification of the derivatives.

Acetolysis of the xyloglucan isolated from *P. coccineus* cell walls followed by reduction, methylation, and GLC gave five major peaks that were characterized by GLC-MS in the EI and CI modes (**11**) (O'Neill and Selvendran, 1983).

Oligosaccharide-4 (**11**) established that the acid-labile fucosyl residue was attached to galactose. Although oligosaccharide-1 (**11**) was only found in small amounts, presumably because the Ara*f* residues are not as stable as 6-deoxyhexose to acetolysis, its presence suggests that it is an

		Ratios
1.	Araf-(1→2)-Xylp	1.0
2.	Galp-(1→2)-Xylp	13.0
3.	Glcp-(1→4)-Glcp	4.0
4.	Fucp-(1→2)-Galp-(1→2)-Xylp	6.0
5.	Glcp-(1→4)-Glcp-(1→4)-Glcp	1.3

11

integral part of the xyloglucan. The presence of oligosaccharides-3 and -5 (**11**), derived from the (1→4)-linked β-D-glucan backbone are consistent with the results of acetolysis of cellulose (Braun, 1943). It should be emphasized that although acetolysis provides information about the nature of the oligosaccharides attached to the β-(1→4)-linked D-glucan backbone of xyloglucans, it cannot be used to deduce their relative distribution. Such information can, however, be obtained using enzymic depolymerization (see Section VI.7.A).

D. CHROMIUM TRIOXIDE OXIDATION OF ACETYLATED POLYSACCHARIDES

Chromium trioxide oxidation of fully acetylated aldopyranosides has been generally used for the determination of anomeric configurations, as the equatorial aglycones (the β-anomer) are preferentially degraded (Angyal and James, 1970). However, the work of Hoffman and Lindberg (1980) suggests that the results must be treated with caution.

Polysaccharides containing chromium trioxide resistant residues may be specifically degraded to yield structural information (Hoffman and Lindberg, 1980). Since this procedure has found limited application in the study of plant polysaccharides, it will not be considered further.

E. METHODS BASED ON β-ELIMINATION REACTIONS

Hakomori methylation of polysaccharides containing uronic acid residues results in their complete esterification. The ester group in the esterified residue (A in **12**) is electron-withdrawing, allowing the hydrogen attached to C5 to become sufficiently acidic that on treatment with base it is eliminated giving the 4,5-unsaturated residue (B in **12**). If the uronic acid is 4-linked, the substituent at C-4 is eliminated (Lindberg et al., 1975).

The β-elimination reaction of methylated polysaccharides containing hexuronic acid residues has been extensively used in structural studies and is discussed in detail by Lindberg et al. (1975) and Lindberg and

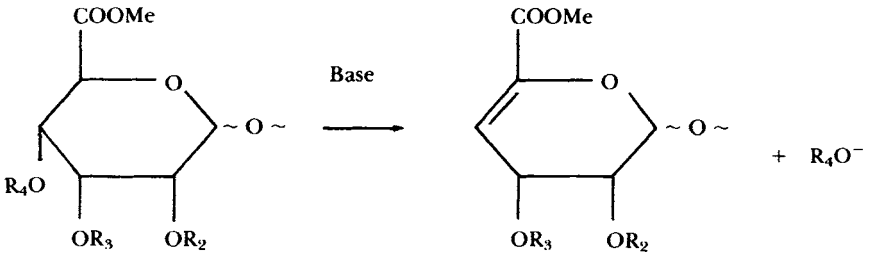

A *B*

12

Lonngren (1978). If the uronic acid residue occupies a nonreducing terminal position, its point of attachment can be readily determined using β-eliminative degradation, mild acid hydrolysis, and realkylation (Lindberg et al., 1973b). However, if the uronic acid is interchain the products of β-elimination (R_4O in **12**) are dependent on the type(s) of substitution and may undergo further degradations (Lindberg et al., 1975).

With the original procedure developed by Lindberg et al. (1973b), the β-eliminated material was subjected to mild acid hydrolysis to cleave selectively the terminal hex-4-enopyranosyluronic acid residues (B in **12**). Subsequently Aspinall and Rosell (1977) have demonstrated that the acid hydrolysis could be omitted and that, without workup, the β-eliminated product could be directly realkylated, thereby labeling the site(s) to which uronic acid residues were attached. For applications of base catalyzed β-elimination reactions, see Aspinall (1982a).

In Rhamnogalacturonan-I McNeil and coworkers using base-catalyzed reactions have determined the neutral glycosyl residues to which the galacturonosyl residues are linked and also the glycosyl residues that are attached to 0-4 of 2,4-linked Rha*p* residues. The former is discussed first. For a flowchart illustrating both aspects, see Selvendran and Stevens (1986). Base-catalyzed degradation of methylated Rhamnogalacturonan-I followed by ethylation, workup, and GLC-MS demonstrated that the *O*-ethyl groups were mainly attached to position 2 of (1→2) and (1→2,4)-linked rhamnose residues. Small amounts of *O*-ethylated derivatives of arabinose and galactose were also found, suggesting that these may also have been attached to galacturonic acid. However, it is conceivable that some of the latter derivatives may have arisen from incomplete methylation of Rhamnogalacturonan-I. It was also established that (1→2)-linked

rhamnose was linked to position 4 of galacturonic acid as the former residue decreased considerably after β-elimination. Surprisingly, the (1→2,4)-linked rhamnose residues remained intact. This led the authors to suggest that the (1→2)- and (1→2,4)-linked rhamnose residues in Rhamnogalacturonan-I are not in the same relative position (McNeil et al., 1980). Subsequently the same group (McNeil et al., 1982a) have established that approximately 90% of the (1→2,4)-linked rhamnosyl residues released on treatment with base are not themselves degraded but form an equilibrium mixture of anomeric alkyl glycosides. The mechanism for this reaction is not known but has also been reported to occur with acidic polysaccharides produced by *Rhizobium* species (McNeil et al., 1982b) which contain branched glucosyl residues attached to position 4 of glucuronic acid.

Degradations involving β-elimination have been performed with a glucuronoarabinoxylan isolated from suspension cultured sycamore cell walls (Darvill et al., 1980c). Glucuronic acid and its 4-*O*-methyl analogue were found to be attached mainly to position 2 of (1→4)-linked xylose with a small proportion attached to position 4 of nonreducing terminal xylose. However, these results must be treated with caution as the number of xylose residues labeled with *O*-ethyl groups after β-elimination was in considerable excess of the content of uronosyl groups. Again, it is conceivable that incomplete methylation of position 2 of 4-linked xylose may explain this result.

Using the conditions of β-elimination described here, the residue eliminated from the uronic acid has an unsubstituted reducing group at C1. In the open-chain form, the carbonyl group, in the presence of strong base, may undergo further elimination reactions (Lindberg et al., 1975). This may, depending on the types of linkages present, result in considerable degradation of the polysaccharide. In an alternative procedure developed by Aspinall et al. (1975) the methylated acidic polysaccharide in benzene-acetic anhydride is heated with the organic base 1,5-diazabicyclo[5.4.0]-undec-5-ene (DBU). The free reducing groups produced by the β-elimination are acetylated and thus protected from further degradation. This degradation has been employed in structural studies of the plant gum leiocarpan A (Aspinall and Chaudhari, 1975). This degradation is complicated by the problems associated with the removal of excess reagents and the recent observation (O'Neill et al., 1986a) that if the residue released from the uronic acid is itself 3-linked, a proportion of the substituent attached to position 3 may be eliminated **(13)**. The scheme proposed in **13** was established from structural studies of the anionic extracellular polysaccharide produced by *Alcaligenes* (ATCC 31555) **(14)**. The methylated polymer was treated with DBU in

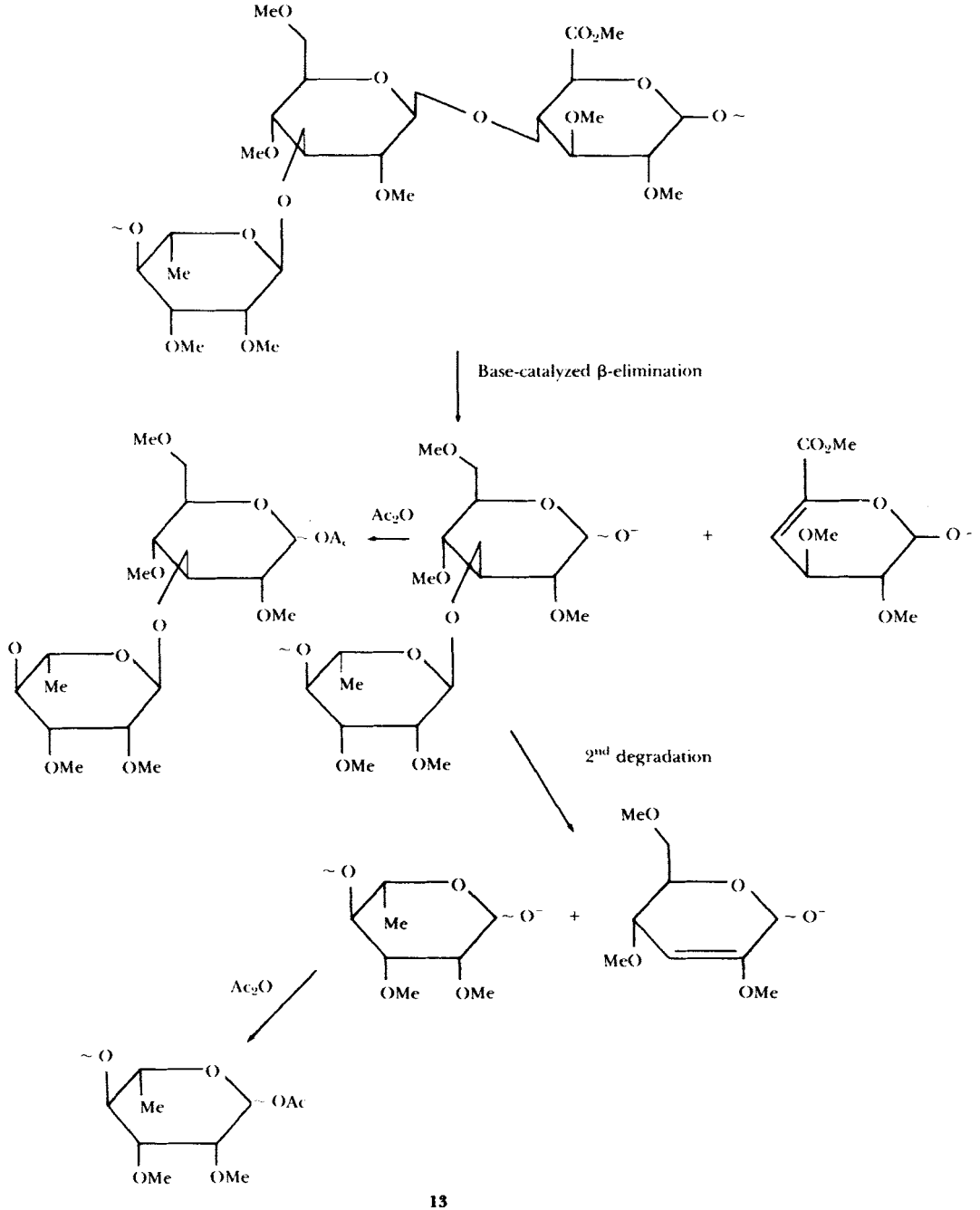
MeO
CO2Me
OMe
Me
OMe
OMe
Base-catalyzed β-elimination
Ac2O
2nd degradation

13

benzene-acetic anhydride and after workup the methylated oligosaccharide alditols were ethylated and fractionated by reverse-phase HPLC (O'Neill et al., 1986a). Two tetra- and two trisaccharide alditol derivatives were obtained and characterized by FAB-MS, EI-MS, and ^{1}H-NMR spectroscopy. The structures of two of the oligosaccharide alditol derivatives are described here because the method may find application in structural studies of some acidic polysaccharides.

FAB-MS of the tetrasaccharide (see Fig. 4, O'Neill et al., 1986a) gave an ion at *m/z* 892, corresponding to $[M+1]^+$ from an alkylated derivative containing two hexosyl, 6-deoxyhexosyl, and hexitol residues. EI-MS gave ions at *m/z* 219 (*a*A_1, 69.8%), 264 (*ald*J_2, 38.5%), 437 (*ba*A_1, 4.0%), 438 (*cald*J_2, 3.6%), 611 (*cba*A_1, 0.2%), and 656 (*bcald*J_2, 0.7%) that define the sequence hex*p*→hex*p*→6-deoxyhex*p*→hexitol.

The mass of the *ba*A_1 ion (*m/z* 437) showed that it contained a single *O*-ethyl group. From partial acid hydrolysis studies it was established that the Glc*p*A residue was attached to position 4 of glucose. Therefore the *O*-ethyl group is located at position 4 of residue b **(15)** as this is exposed during the β-eliminative degradation. Similarly the mass of the *ald*J_2 ion (*m/z* 264) and ions at *m/z* 103 (30.4%) and 147 (6.8%) demonstrated the presence of a hexitol residue containing *O*-ethyl groups at positions 1 and 5 **(15)**.

The absence of an ion at *m/z* 498 (*cald*J_1) and the presence of an ion at *m/z* 484 (*cald*J_0, 1.1%) are consistent with the nonreducing terminal residue (*a* in **15**) being attached to position 3 of the internal hexosyl residue (Sharp and Albersheim, 1984). The ^{1}H-NMR spectrum of the tetrasaccharide alditol derivative contained signals for anomeric protons at δ 4.63 ($J_{1,2}$ 7.9 Hz), δ 5.40 ($J_{1,2}$ 2.1 Hz), and δ 5.49 ($J_{1,2}$ 1.3 Hz). These were assigned to β-linked glucosyl and α-linked rhamnosyl and mannosyl, respectively, and establish the structure of the parent oligosaccharide **16**.

→4)-β-D-Glc*p*A-(1→4)-β-D-Glc*p*-(1→4)-α-L-Rha*p*-(1→3)-β-D-Glc*p*-(1→

3
↑
1
R

R = α-L-Man*p* and α-L-Rha*p*

14

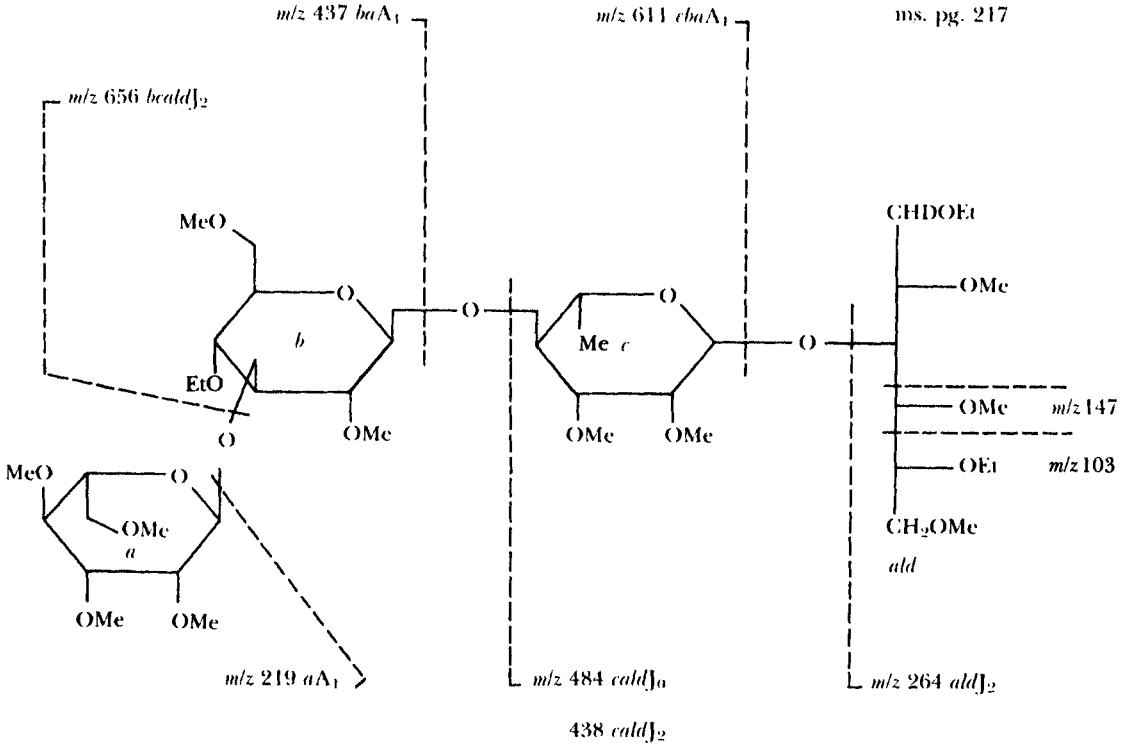
m/z 437 baA1
m/z 611 cbaA1
ms. pg. 217
m/z 656 bcaldJ2
MeO
O
b
EtO
O
OMe
O
O
O
Me c
O
OMe
OMe
O
CHDOEt
OMe
OMe
m/z 147
OEt
m/z 103
CH2OMe
ald
MeO
O
OMe
a
OMe
OMe
m/z 219 aA1
m/z 484 caldJa
438 caldJ2
m/z 264 aldJ2

→4)-β-D-Glc*p*-(1→4)-α-L-Rha*p*-(1→3)-D-Glc*p*-(1→

3
↑
1

α-L-Man*p*

16

Using the principles described previously, the trisaccharide (See Fig. 7, O'Neill et al., 1986a) was shown to have the structure **17**. Comparable tetra- and trisaccharides in which the terminal α-L-Man*p* residue was replaced by terminal α-L-Rha*p* were also detected in the products of β-elimination. The two trisaccharides are probably formed by a β-eliminative degradation of the corresponding tetrasaccharides (see **16** and **17**).

Using the β-eliminative degradation with DBU, it was possible to establish the points of attachment of nonreducing terminal rhamnosyl and mannosyl residues and their anomeric configurations in the polysaccharide from *Alcaligenes*. This information could not be obtained by partial-acid hydrolysis studies since both residues are readily hydrolyzed. From these complementary techniques a series of overlapping fragments was characterized which demonstrated that the polysaccharide was composed of a branched pentasaccharide repeating unit. It should be emphasized that using the preceding methods, the relative distributions of the nonreducing terminal residues could not be determined.

Rosell and Svennson (1975) described a procedure whereby a methylated polysaccharide that contained a limited number of free hydroxyls at specific positions could be selectively degraded. Using a dimethylsulfoxide-chlorine complex (Corey and Kim, 1973), the free hydroxyls are oxidized to keto (or aldehyde) groups. Treatment of the oxidized material with base results in the elimination of glycosyl or methoxyl substituents β to the activated group, and the resultant α,β-unsaturated

→4)-β-D-Glc*p*-(1→4)-L-Rha*p*-(1→

3
↑
1

α-L-Man*p*

17

residues can be selectively removed by mild acid hydrolysis exposing the site(s) to which they were attached. These can be located by alkylation with a deuterated reagent. For the details of the procedure, see Svensson (1978). Using the foregoing series of reactions, Rosell and Svensson (1975) have determined the distribution of 4-*O*-methyl-D-glucuronic acid residues in birch xylan.

A similar series of reactions has also been used by McNeil et al. (1982a) to determine the nature of the sugar residues linked to position 4 of rhamnose residues in Rhamnogalacturonan-I. The reactions employed were (1) de-esterification, (2) methylation, (3) β-elimination of the methylated material using dimsyl anion, (4) oxidation, and (5) β-elimination with DBU. For a flowchart of the reactions, see McNeil et al. (1982a) and Selvendran and Stevens (1986). This procedure showed that seven differently linked glycosyl residues were attached to position 4 of (1→2)-linked rhamnose and has illustrated the complexity of Rhamnogalacturonan-I. A further demonstration of the complexity of pectic polysaccharides has been provided by the work of De Vries et al. (1981, 1982, 1983a) on apple polyuronides, which suggests that the molecules are composed of blocks of homogalacturonan ("smooth regions") and blocks of rhamnogalacturonans substituted with neutral sugar side chains ("hairy regions"). It would appear that some of the arabinogalactan side chains are attached to the rhamnogalacturonan backbone via xylose residues. The same group (De Vries et al., 1983b) has also suggested that the distribution of esterified galacturonic acid in the galacturonan is random (or irregular).

Thus it is clear that pectic polysaccharides isolated from plant cell walls are a family of complex macromolecules. Recent work by Albersheim and associates suggests that the pectic polymers may not serve solely as structural polymers. Fragments of pectic polymers have been implicated in host-pathogen interactions (Darvill and Albersheim, 1984) and plant morphogenesis (Tran Thanh Van et al., 1985). Thus these polysaccharides still provide considerable challenges to both chemists, biochemists, and physiologists in determining their structures and functions.

7. Enzymic Degradations of Cell Wall Polysaccharides

To overcome the limitations of chemical degradations such as low yields of oligosaccharides, low specificity and complicating side reactions, the use of specific enzymes offers great potential in structural polysaccharide chemistry. Probably the most successful application of enzymes has been the use of bacteriophage endoglycanases (Rieger-Hug and Stirm, 1981) for the structural analysis of *Klebsiella* polysaccharides (Dutton et al., 1981; Dutton and Merrifield, 1982).

Polysaccharide degrading enzymes are classified as *endo-* and *exo-*hydrolysases. The former are linkage and monosaccharide specific and fragment polysaccharides into a number of oligosaccharides. *Exo-*hydrolases are specific for both monosaccharide and anomeric configuration but may or may not show aglycone specificity. These enzymes cleave polysaccharides by sequential removal of residues from the nonreducing termini. Kennedy and White (1979) have listed a range of enzymes that may be used in structural analysis of polysaccharides. For a detailed discussion of the use of enzymes for structural characterization of polysaccharides, the reader should consult Matheson and McCleary (1984).

In the following sections we shall briefly illustrate the types of cell wall polysaccharides that have been enzymically degraded as an aid to structural analysis.

A. XYLOGLUCANS

Xyloglucans (amyloids) are a major class of hemicellulosic polysaccharides found mainly in dicotyledonous plants (Darvill et al., 1980b). Xyloglucans have also been found as minor components in the cell walls of monocotyledons (Shibuya and Iwasaki, 1978). Since all xyloglucans are composed of a substituted (1→4)-linked β-D-glucan, they are susceptible to depolymerization with cellulase (EC 3.2.1.4; (1→4)-β-D-glucan 4-glucanohydrolase). By selecting a suitable time (24−48 h) for enzymic treatment a range of oligosaccharides can be obtained. These can be purified by gel filtration or preparative paper chromatography and characterized by sugar and methylation analysis and mass spectrometry (O'Neill and Selvendran, 1985b).

Cellulase digestion of runner bean xyloglucan followed by gel filtration on Biogel P-2 produced a number of oligosaccharides. The oligosaccharides with d.p. ≤ 6 were reduced to their alditols and methylated. Derivatives containing ≤ 4 glycose residues could be adequately separated by GLC and characterized by GLC-MS (EI and CI). For an account of the applications of GLC-MS to characterize oligosaccharides, from cell wall polysaccharides, containing up to four sugar residues, see Selvendran (1983b). However, attempts to characterize oligosaccharides with d.p. 5−6 by GLC-MS were unsuccessful (O'Neill and Selvendran, 1985b). To overcome this problem, the penta- and hexasaccharides were reduced with $NaBD_4$, methylated, and separated by reverse-phase HPLC, and five of the components were identified (see Fig. 2, O'Neill and Selvendran, 1985b). The major peak (peak 1 Fig. 2 of O'Neill and Selvendran, 1985b) gave in FAB-MS an ion at *m/z* 1010, corresponding to $[M+1]^+$ from a methylated derivative containing deoxyhexosyl, pentosyl, two hexosyl,

and hexitol residues. EI-MS gave ions at *m/z* 189 (*a*A_1, 33.7%), 236 (*ald*J_2, 26.6%), 296 (*ald*J_1, 1.3%), 393 (*ba*A_1, 2.4%), 440 (*dald*J_2, 0.2%), 500 (*cdald*J_1, 0.2%), 553 (*cba*A_1, 0.1%), 600 (*cdald*J_2, 0.1%), 660 (*cdald*J_1, 0.9%), 804 (*bcdald*J_2, 0.1%), and 864 (*bcdald*J_1, 0.1%), which are consistent with the sequence **18**. These ions in combination with the intensity ratios of the *ba*A (*ba*A_2>*ba*A_3>*ba*A_1) and *cba*A (*cba*A_2>*cba*A_3>*cba*A_1) series of ions, and methylation analysis, established the structure of the oligosaccharide as Fuc*p*-(1→2)-Gal*p*-(1→2)-Xyl*p*-(1→4)-Glc*p*-(1→4)-Glc*p*.

The second major component obtained after HPLC (peak 5 of Fig. 2, O'Neill and Selvendran, 1985b) on FAB-MS gave an ion at *m/z* 1200, corresponding to $[M+1]^+$ from a methylated alditol derivative containing two pentosyl, three hexosyl, and one hexitol residues. Using the principles outlined earlier, the sequence of the derivative was established

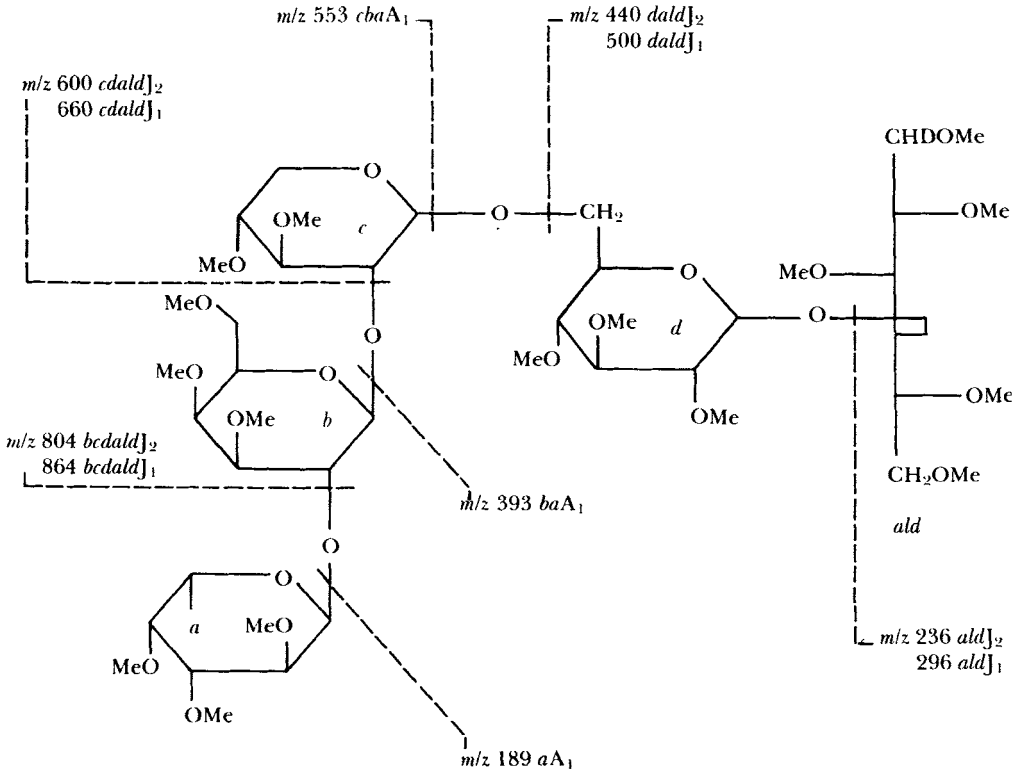

18

as **19**. These data in combination with methylation analysis and acetolysis (O'Neill and Selvendran, 1983) established that the oligosaccharide contained a cellotriosyl backbone substituted through position 6 of the nonreducing terminal residue with Gal*p*-(1→2)-Xyl*p* and through position 6 of the interchain residue with Xyl*p*.

The minor oligosaccharides separated by reverse-phase HPLC (peaks 2–4 of Fig. 2, O'Neill and Selvendran, 1985b) gave on FAB-MS ions at *m/z* 996 (peak 2) 1214, 1170 (peak 3), and 1156 (peak 4). The combined data provided evidence for the occurrence of the following oligosaccharides: (1) cellobiose substituted with Gal*p*-(1→2)-Xyl*p* and Xyl*p* (peak 2), (2) cellotriose substituted with Fuc*p*-(1→2)-Gal*p*-(1→2)-Xyl*p* and cellobiose substituted with both Fuc*p*-(1→2)-Gal*p*-(1→2)-Xyl*p* and Xyl*p* (peak 3), and (3) cellotriose substituted with three Xyl*p* residues (peak 4).

From the results of cellulase digestion and the characterization of a number of oligosaccharides, an improved partial structure for the runner bean cell wall xyloglucan was proposed (O'Neill and Selvendran, 1985b). It would appear that the xyloglucan does not contain a simple repeating unit but is composed of a block-type structure that is commonly encountered in plant polysaccharides (Stephen, 1983).

Although xyloglucans from various plants possess common structural features, the degree and type of side-chain substitution may differ considerably. Xyloglucans isolated from *Annona muricata* seeds have a (1→4)- to (1→4,6)-linked glucose ratio of 1.0:0.3, and the polymer is soluble only in 0.1 *M* alkali (Kooiman, 1967). Xyloglucans from most parenchymatous tissues have considerably lower ratios of (1→4)- to (1→4,6)-linked glucose residues, and these polymers are water soluble. It has been suggested that the degree of substitution of the backbone may regulate cell wall-xyloglucan or xyloglucan-xyloglucan interactions (Bauer et al., 1973). Furthermore the lower degree of substitution of seed xyloglucans may reflect their role as "storage" polysaccharides (Meier and Reid, 1982). The degree of substitution of the glucan backbone can also determine the type(s) of oligosaccharide produced on enzymic degradation (Kooiman, 1961, 1967). Hydrolysis of mung bean xyloglucan with a *Trichoderma viride* cellulase gave hepta-, nona-, and decasaccharides, which accounted for 71% of the polymer (Kato and Matsuda, 1980a). Degradation of the same polymer with a cellulase preparation from *Aspergillus oryzae* gave oligosaccharides with d.p. 2–5 accounting for 50% of the polymer (Kato and Matsuda, 1980b). In contrast, treatment of runner bean xyloglucan with a *T. viride* cellulase gave oligosaccharide fractions of d.p. 2–5 and approximately 10, accounting for 57% and 32% of the polymer, respectively (O'Neill and Selvendran, 1986).

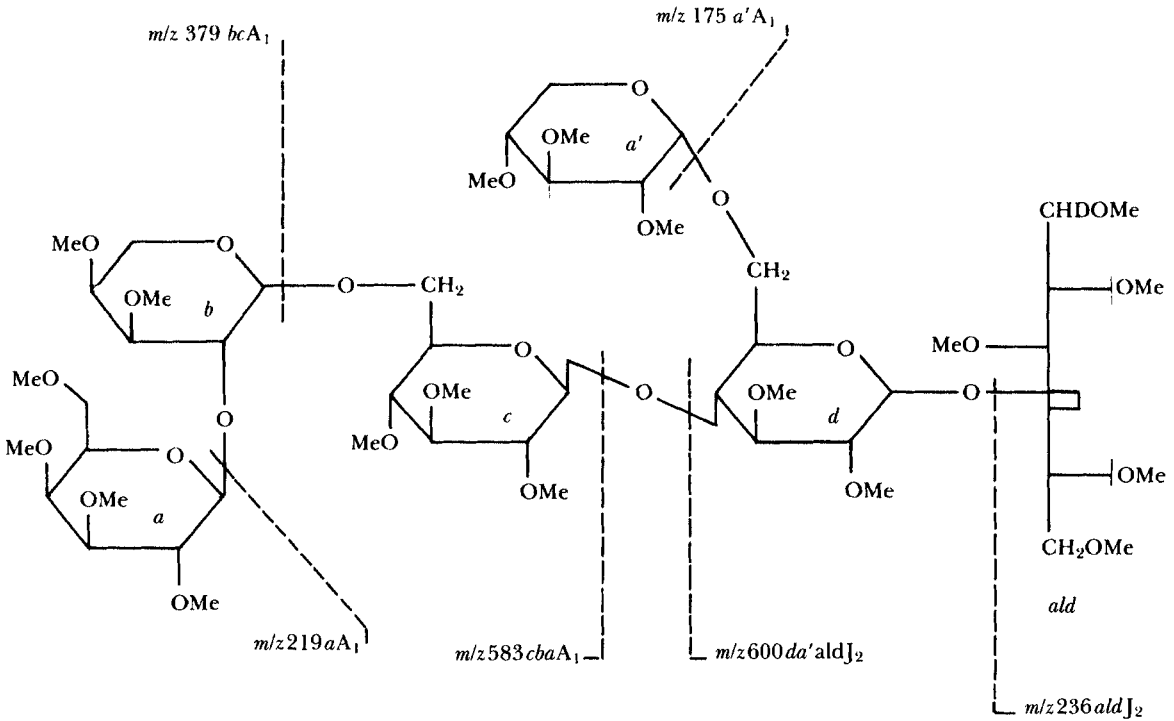
m/z 379 bcA1
m/z 175 a'A1
MeO
OMe
a'
OMe
O
CH2
CHDOMe
OMe
MeO
b
OMe
MeO
c
OMe
OMe
d
OMe
MeO
a
OMe
OMe
OMe
CH2OMe
ald
m/z219aA1
m/z583cbaA1
m/z600da'aldJ2
m/z236aldJ2

19

B. MIXED LINKAGE β-D-GLUCANS

The (1→3), (1→4)-linked β-D-glucans extracted from barley grain is the major component of the endosperm cell wall (Fincher, 1975; Ballance and Manners, 1978). They are linear polymers containing (1→3)- and (1→4)-linked β-D-glucopyranosyl residues in the ratio 1:2.3 (Parrish et al., 1960). Using both chemical and enzymic methods, it has been shown that most water-soluble β-glucans contain predominantly cellotriosyl and cellotetraosyl residues separated by a single (1→3)-linkage (Parrish et al., 1960). Structural analysis of barley β-glucans has been greatly aided by the use of a purified (1→3), (1→4)-β-D-glucan 4-glucanohydrolase (EC 3.2.1.73) from germinating barley (Woodward et al., 1983). The oligosaccharides produced by enzymic hydrolysis were separated by gel filtration and analyzed by methylation analysis (Woodward et al., 1983). Gel filtration of the water-soluble products revealed oligosaccharides of d.p. 2–6 with tri- and tetrasaccharides predominating. These latter oligosaccharides were shown to be 3-*O*-β-D-cellobiosyl-D-glucose and 3-*O*-β-D-cellotriosyl-D-glucose, respectively. During enzymic treatment a small proportion (~5%) of the material precipitated and contained mainly glucose (70%), but with small amounts of arabinose, xylose, galactose, and mannose. From methylation data the oligoglucosides were shown to have an average d.p. of 9–10 with a (1→3)-linkage adjacent to the reducing termini. These data suggest that small proportions of barley β-glucans may contain regions of 5–11 (1→4)-linked glucose residues (Woodward et al., 1983). Statistical analysis of these results (Staudte et al., 1983) suggest that the cellotriosyl and cellotetraosyl units are arranged in an essentially random manner. However, this approach can only define the sequence dependence of adjacent tri- and tetramers; larger repeating sequences would not be detected.

C. XYLANS AND ARABINOXYLANS

Although considerable effort has gone into the chemical characterization of arabinoxylans, the fine structural details have only been obtained using enzymic degradations.

Degradation of wheat straw xylan with a purified cellulolytic enzyme from *Myrothecium verrucaria* gave a range of xylo-oligosaccharides containing arabinose, thereby establishing the linkage of the latter sugar to the xylan backbone (Bishop and Whitaker, 1955). Subsequently a trisaccharide was isolated and characterized as L-Ara*f*-(1→3)-β-D-Xyl*p*-(1→4)-D-Xyl*p* (Bishop, 1956). The same trisaccharide was also isolated from rye flour and cocksfoot grass arabinoxylans after degradation with a commercial "hemicellulase" (Aspinall et al., 1960). Using a xylanase

preparation from *Streptomyces*, a tetrasaccharide was obtained, purified, and characterized as α-L-Ara*f*-(1→3)-β-D-Xyl*p*-(1→4)-β-D-Xyl*p*-(1→4)-Xyl*p* (Goldschmid and Perlin, 1963). Takenishi and Tsujisaka (1973) have reported the isolation of tri- and tetrasaccharides from an enzymic digest of rice-straw arabinoxylan, in which the α-L-Ara*f* residues were linked to position 3 of the xylose at the reducing ends. The results are contrary to the findings of Aspinall et al. (1960) and Goldschmid and Perlin (1963). The preceding observations suggest that the xylanase from *Aspergillus niger* has a different mode of action to that of *M. verracaria* and *Streptomyces*.

Dekker and Richards (1975) have studied the mode of action of a xylanase produced by *Ceratocystis paradoxa* and suggested that xylotriose was the lowest homologue degraded by the enzyme. Although the presence of arabinosyl substituents may not impede enzyme binding to the substrate, the xylosidic linkage to the "right" of the substituent is resistant to hydrolysis. Therefore the sequence L-Ara*f*-(1→3)-Xyl*p*-(1→4)-Xyl*p* is stable to enzymic hydrolysis. To explain fully all the observations on the mode of action of this enzyme, Dekker and Richards (1975) have suggested that there is a tendency for preferential attack at highly substituted regions. This releases less substituted regions of the xylans that associate and precipitate out of solution and thus become further resistant to enzymic degradation.

Early studies employing enzymic degradations of acidic arabinoxylans were conducted by Timell (1962) who isolated a number of neutral and acidic oligosaccharides. The neutral material consisted of (1→4)-linked xylose oligomers (d.p. 2–5). The acidic fraction contained mainly aldotetrao- to aldooctaouronic acids. No aldobio- or aldotriouronic acids were detected, indicating that the acidic sidechains inhibit enzymic degradation. Of the acidic oligosaccharides characterized three were shown to be 4-*O*-Me-α-D-Glc*p*A-(1→2)-Xyl*p*-(1→4)-[Xyl*p*]$_n$, where n=2–4. More recently Comtat et al. (1974) isolated neutral and acidic oligosaccharides from an enzymic digest of Aspen 4-*O*-methyl-D-glucurono-D-xylan. The purified oligosaccharides were analyzed by methylation analysis and probe MS and gave essentially the same results as those of Timell (1962). It was also observed that, independent of the nature of the substituents, the enzymic cleavage led preferentially to oligosaccharides substituted at the nonreducing termini. Similar observations have been made with purified endo-(1→4)-β-D-xylanases from the fungus *Trametes hirsuta* (Kubackova et al., 1979). It has been claimed (Kubackova et al., 1979) that willow glucuronoxylan has a regular distribution of glucuronic acid side chains, whereas redwood glucuronoxylan has an irregular distribution (Comtat et al., 1974). The GLC-MS and HPLC-MS methods that we have

used to elucidate the structural features of runner bean xyloglucan would help to resolve such problems.

D. GALACTOMANNANS

The endosperm cell walls of the seeds of the *Leguminosae* family are a rich source of galactomannans. These polysaccharides are composed of a (1→4)-linked β-D-mannan backbone substituted, to varying degrees, through position 6 with single α-D-galactopyranosyl residues. Several reviews are available describing their chemical structure and interactions (Dea and Morrison, 1975), biochemistry (Meier and Reid, 1982), and problems associated with fine structure determination (Painter, 1982).

Although chemical techniques have provided a considerable amount of data on the structure of galactomannans, it has required the use of highly purified enzymes to determine the distribution of the side chains. Studies using α-D-galactosidases have indicated that the galactomannans from *Gleditsia ferox* and locust bean have a different distribution of α-D-Gal*p* residues (Courtois and Le Dizet, 1966).

Degradation of galactomannans with endo-mannanases usually liberates both linear and branched oligosaccharides. The branched oligosaccharides contain (1→4)-linked-β-D-mannose residues with a single α-D-Gal*p* residue (Courtois and Le Dizet, 1968). Recently McCleary et al. (1985), using computer analysis of the amounts and structures of the oligosaccharides released on enzymic hydrolysis of carob and guar galactomannans, have attempted to determine the distribution of the α-D-Gal*p* residues. In both cases the galactose distribution was nonregular, but the polymers from different varieties of seed have the same fine structure.

Detailed studies by McCleary and Matheson (1983) on the mannanase from *A. niger* and lucerne seeds have shown that for significant enzymic hydrolysis to occur, at least four unsubstituted mannose residues are required. They also established that both enzymes could act as transglycosylases in a similar fashion to the fenugreek seed mannanase (Clermont-Beaugraud and Percheron, 1968).

Although a considerable amount of effort has gone into the determination of the fine structure of galactomannans, a complete structure has not yet been established.

E. PECTIC POLYSACCHARIDES

Pectic polysaccharides from plant cell walls are rarely simple (1→4)-linked α-D-galacturonans but contain varying proportions of neutral monosaccharides. L-Rhamnose is the only neutral sugar present in the

polymer backbone, others being found exclusively in oligosaccharide side chains.

Two major groups of pectin degrading enzymes are the hydrolases (EC 3.2.1.15), which hydrolyse the galacturonan moiety, and the lyases (EC 4.2.2.3), which act by β-elimination (Rexova-Benkova and Markovic, 1976). For effective hydrolysis with endo-polygalacturonase, the pectin must be de-esterified. Little appears to be known about the hydrolytic cleavage of rhamnosyl residues, although the fungus *Corticium rolfsii* is known to secrete an α-L-rhamnosidase (Kaji and Ichimi, 1973). Degradation of the side chains of pectins may be achieved with a number of enzymes including endo-β-1,4-galactanase, exo-β-1,4-galactanase, β-1,4-galactosidase and exo-α-L-arabinofuranosidase (Bateman, 1976).

A major source of pectin degrading enzymes are microbial plant pathogens (Rexova-Benkova and Markovic, 1976). However, even when the microorganisms are grown on defined media, several types of enzymic activity may be present, and it is therefore inadvisable to use crude culture filtrates, without extensive fractionation. The fungus *Colletotrichum lindemuthianum* when grown on citrus pectin produces *exo*-polygalacturonase and arabinosidase activity (Keegstra et al., 1972). *Sclerotinia fructigena* grown on polypectate produces similar enzymic activity (Fielding and Byrde, 1969). To purify the appropriate enzyme by conventional procedures (gel filtration, ion-exchange chromatography) may be time-consuming. However, the purification of an endopolygalacturonase, in a single step, has been achieved using insoluble pectic acid cross-linked with epichlorohydrin (Rexova-Benkova and Tibensky, 1972). Similarly, an α-L-arabinosidase has been affinity purified from a commercial pectinase preparation on columns of immobilized arabinan (Waibel et al., 1980). The techniques of affinity chromatography therefore offer a rapid and relatively simple method for obtaining highly purified, specific enzymes.

Albersheim and coworkers have made extensive use of pectic degrading enzymes for their studies on suspension-cultured sycamore cell walls (Talmadge et al., 1973). Using a combination of pectic enzymes, gel filtration and ion-exchange chromatography, the released polymers have been resolved into Rhamnogalacturonan-I and -II (McNeil et al., 1980, 1982a). These polymers have subsequently been studied in great detail, but their structures and functions are only now being unraveled.

Ishii (1981) has reported that a purified endo-polygalacturonase from *Aspergillus japonicus* solubilizes 95% of the total uronides from potato discs. After purification, three polymers were obtained of which the first two appeared to be Rhamnogalacturonans substituted with linear arabinans and galactans. The third fraction was highly branched and

resembled Rhamnogalacturan-II (Darvill et al., 1978), but it was claimed that apiose, methyl xylose, methyl fucose, and glucuronic acid were absent. Whether this is due to difficulties in detecting small amounts of these unusual sugars or differences between tissues from free-growing plants and suspension-cultured tissues is unclear.

Enzymic degradation of a partially acid hydrolyzed pectin from soy sauce using endo-polygalacturonase and pectic lyase gave a number of acidic fragments. In addition to galacturonic acid and its dimer and trimer, oligosaccharides containing xylose were characterized as β-D-Xyl*p*-(1→3)-D-Gal*p*A and β-D-Xyl*p*-(1→3)-α-D-Gal*p*A-(1→4)-D-Gal*p*A (Kikuchi and Sugimoto, 1976). A high molecular weight component remaining after enzymic depolymerization contained GalpA and Xylp in the ratio 2:1. These results in combination with previous data (Kikuchi and Yokotsuka, 1973a,b) suggest that the xylose is attached to position 3 of galacturonic acid and is in agreement with the work of Aspinall and Jiang (1974).

In a series of studies with purified apple pectins in which both enzymic and chemical degradations were employed (De Vries et al., 1981, 1982, 1983a), it was observed that more than 90% of the uronic acid residues could be isolated as homogalacturonan chains (smooth region). Neutral sugars (arabinose, galactose, and xylose) were present as side chains on the Rhamnogalacturonan backbone (hairy regions), and it was claimed that the rhamnose residues were unevenly distributed along the pectin molecule (however see Lau et al., 1985). The uronic acid residues in the hairy regions appear to be highly esterified.

F. EXOGLYCOSIDASES

Sequential exoglycosidase digestion has become an indispensable technique for the structural analysis of the carbohydrate moieties of glycoproteins (Kobata, 1979). Due to the lack of suitable enzymes, this approach has had only limited use in the characterization of plant cell wall polysaccharides. However, exoglycosidase digestions have been used with some success in the analysis of the carbohydrate moieties of potato lectin (Allen et al., 1978; Ashford et al., 1982), hydroxyproline-rich cell wall glycoprotein (O'Neill and Selvendran, 1980b), and wheat endosperm arabinogalactan peptide (McNamara and Stone, 1981).

Using an α-L-fucosidase from beef kidney, it was possible to remove approximately 85% of the fucose from the xyloglucan from runner bean cell wall (O'Neill and Selvendran, 1983). However, attempts to hydrolyse terminal galactose residues with either α or β-galactosidases were unsuccessful. Kato and Matsuda (1980a,b) found that the exo-β-D-galactosidase

from *Charonia lampas* could remove nonreducing terminal galactose from oligosaccharides derived from a cellulase digest of mung bean xyloglucan. This suggests that steric hindrance in the intact polymer may restrict enzymic action. A similar observation was made on the activity of a β-D-galactosidase toward glycopeptides and glycoproteins (Spiro, 1962).

8. Noncarbohydrate Substituents of Cell Walls

Plant cell walls contain in addition to polysaccharides a number of noncarbohydrate substituents. These include free or ionically bound enzymes, the basic structural protein that is rich in hydroxyproline, and lignin as the high molecular weight components. Certain sugars in polysaccharides are substituted with *O*-methyl groups, such as Rhamnogalacturonan-II (Darvill et al., 1978), or carboxyl groups in pectins may be methyl esterified (Doesburg, 1966), whereas other sugars may be *O*-acetylated (Bacon et al., 1975). Recent evidence suggests that in both mono- and dicotyledonous plants cell wall polysaccharides are esterified with phenolic acids such as ferulic and *p*-coumaric acids (Fry, 1985). Methods for determining the relative proportions of these noncarbohydrate substituents are well established. However, little definitive information is available on the nature of the sugar residue and which of its carbon atoms is *O*-acetylated or *O*-feruloylated. Further the distribution of the methyl esterified carboxyl groups in pectins has not been adequately resolved (Tuerena et al., 1982).

A. CELL WALL PROTEINS

It is well established that cell walls contain protein, and for a detailed discussion the reader should consult Lamport and Catt (1981), Selvendran and O'Neill (1982), and Fry (1985). In this section we will briefly consider the available methods for determining the protein content and amino acid composition of cell walls.

An estimate of the protein content of a cell wall preparation can be obtained by multiplying the percentage of nitrogen by 6.25. Alternatively, the protein content can be estimated by summation of the individual amino acids. Amino acids can be liberated from cell walls by hydrolysis with 6 *M* HCl (24 h at 110°C). The free amino acids are adsorbed on a cation exchange column and eluted with 7 *M* ammonium hydroxide. Quantitative determination of the amino acids can be performed by conventional analysis using ion-exchange chromatography (Benson and Patterson, 1971) or after derivatization by GLC (Coulter and Hann, 1971; Mackenzi, 1981). An advantage of the GLC procedure is that it can readily resolve hydroxyproline, which is commonly found in plant cell walls. This

can also be achieved with ion-exchange chromatography using special eluting buffers (Benson and Patterson, 1971).

We routinely determine the amino acid content of cell walls by the GLC method of March (1975). In this procedure the liberated amino acids are sequentially treated with propanol-HCl and heptafluorobutyric anhydride. The common amino acids, including hydroxyproline, as their *n*-propyl heptafluorobutyryl derivatives, can be separated in less than one hour. It should be noted, however, that the removal of coprecipitated proteins from alcohol insoluble residues of cabbage with pronase in tris buffer complicates amino acid analysis by GLC (Stevens and Selvendran, 1980a). Tris was found to bind strongly to the cell wall material and, following acid hydrolysis and derivatization, eluted in the same region as the alanine and glycine derivatives. It is therefore advisable to use citrate buffers instead of Tris for pronase digestion.

Recently the presence of the oxidatively coupled dimer of tyrosine in plant cell walls has been described (Fry, 1982a). This component, designated isodityrosine, is a diphenyl ether **(20)** that is stable to acid hydrolysis and can be quantitatively released by hydrolyzing the CWM with 6 *M* HCl (containing 10 m*M* phenol) in a sealed tube at 100°C for 24 h and detected after paper electrophoresis at pH 2.0 (Fry, 1982a). The amount of isodityrosine in the cell wall appears to be proportional to the amount of hydroxyproline. Isodityrosine has been suggested to function as a cross-linking agent in the primary cell wall (Fry, 1982a, 1985).

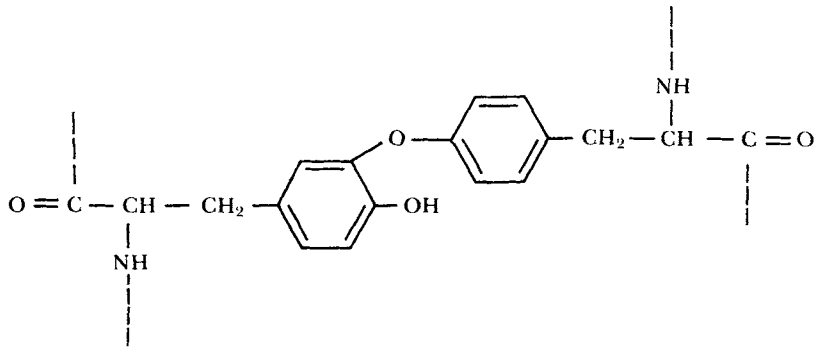

20

B. LIGNIN

Lignin is a very complex aromatic polymer deposited during secondary thickening of cell walls. Due to its complex nature it is difficult to determine accurately the lignin content of cell walls (Sarkanen and Ludwig,

1971). For an assessment of the methods used for the estimation of lignin in vegetable and cereal cell walls, see Selvendran and DuPont (1984).

C. PHENOLIC ESTERS

Certain cell wall polysaccharides, notably arabinoxylans in grass leaves (Hartley and Jones, 1976) and cereal grains (Fulcher et al., 1972) and pectic polysaccharides from suspension cultures of some dicotyledonous plants (Fry, 1983), have been shown to be substituted with phenolic esters. Some of the pectic polysaccharides from sugar beet have also been shown to be associated with phenolic esters (B. J. H. Stevens and R. R. Selvendran, unpublished results; Selvendran, 1985). Usually these phenolics are esters of ferulic and/or coumaric acids, although esters of diferulic acid have also been detected in enzymic digests of grass cell walls (Hartley and Jones, 1976a; Markwalder and Neukom, 1976). There are also reports of complex, oxidatively coupled, phenols in cell walls (Fry, 1984) which may be part of a polysaccharide-protein complex (O'Neill and Selvendran, 1985).

Esterified phenolic residues are readily released by treatment with alkali (1 *M*) at room temperature. The free liberated phenolic acids can be extracted into an organic solvent (ether) and analyzed by TLC (Egger, 1969), GLC (Hartley and Jones, 1975), or HPLC (Shibuya, 1984).

Using a combination of chemical and enzymic methods, Fry (1983) has established that the feruloylated oligomers **(20)** released from the cell walls of suspension-cultured tissues of spinach leaves are probably derived from pectic polymers, whereas in monocotyledons the phenolic esters are associated with arabinoxylans (Hartley and Jones, 1976).

D. DEGREE OF METHYL ESTERIFICATION OF PECTINS

Pectins from plant cell walls contain partially methyl esterified α-D-galacturonic acid (Doesburg, 1966), and several methods are available for the determination of their methyl ester content (Doesburg, 1966).

In our laboratory we have used two methods, both of which involve saponification with alkali to yield methanol. The released methanol can be analyzed colorimetrically after oxidation to formaldehyde with potassium permanganate, and reaction of the formaldehyde with pentan-2,4-dione, to yield a chromophore with λmax 412 nm (Wood and Siddiqui, 1971). Alternatively, the methanol produced can be converted to its nitrite ester by reaction with sodium nitrite and analyzed by GLC (Litchman and Upton, 1972; Versteeg, 1979). For the latter procedure to be reliable, careful timing of the reactions is required (Litchman and Upton, 1972).

Although the determination of the degree of methyl esterification is straightforward, the relative distribution of these groups in native pectins remains unknown. De Vries et al. (1983b) have claimed that uronic acid residues in the highly branched (hairy) portion of the pectic molecule are highly esterified, but the distribution is irregular or random. Tuerena et al. (1982) have studied the distribution of carboxyl groups in pectins of various degrees of esterification (5–70%) by a combination of chemical derivatization (glycolation of free carboxyl groups) and enzymic hydrolysis. All the samples had a significant proportion of free carboxyl regions with a d.p. > 10 and would be consistent with a nonrandom, block distribution of free and esterified carboxyl groups. For a brief discussion concerning the intramolecular distribution of carboxyl groups in low methoxyl pectins, see Taylor (1982).

E. DEGREE OF *O*-ACETYLATION

The *O*-acetyl content of a cell wall preparation of polysaccharide can readily be determined after saponification with alkali by colorimetric or GLC methods.

In our laboratory we use the colorimetric procedure of McComb and McCready (1952) where the released acetic acid is reacted with hydroxylamine hydrochloride to give a chromophore with λmax 520 nm.

Free acetic acid can be determined by GLC (Shelley et al., 1963). An estimate of *O*-acetyl content can be obtained from IR spectrometry (Bacon et al., 1975). However, if the preparation examined also contains esterified uronic acids, IR spectroscopy is of limited value as both carboxylate and *O*-acetyl esters absorb at the same wavelength (1730 cm^{-1}).

A major problem with the analysis of *O*-acetylated sugars is the determination of the site(s) of *O*-acetylation. DeBelder and Norman (1968) have developed a method in which the *O*-acetylated polysaccharide is treated with methyl vinyl ether to yield mixed acetals. These are stable to base and methylation of the protected polymer alkylates the position(s) of *O*-acetylation. Treatment with mild acid hydrolyzes the mixed acetals with minimal cleavage of glycosidic linkages and the polymer can be realkylated with C^2H_3I or C_2H_5I. After workup, and GLC-MS the point(s) of *O*-acetylation can be established from the mass spectral fragmentation pattern of the appropriate derivative(s). Although this technique has been employed with some success, difficulties in obtaining complete acetalation have led to ambiguous results (Dutton and Karunaratne, 1985). However, the procedure appears to work well with partially *O*-acetylated oligosaccharides (Dutton and Karunaratne, 1985).

Alternative methods for locating *O*-acetyl groups in oligosaccharides

employ ^{1}H-NMR, ^{13}C-NMR (Perlin and Casu, 1981), and FAB-MS (Dell et al., 1983).

Although the reasons for partial *O*-acetylation of naturally occurring polysaccharides are unknown, recent work in our laboratory may provide some insight. The polysaccharide produced by *Enterobacter* (NCIB 11870) species gives cation-dependent thermally reversible gels. Using a combination of chemical and enzymic methods, it was established (O'Neill et al., 1986c) that this polysaccharide contained an oligosaccharide repeating unit that was identical with the capsullar polysaccharide produced by *Klebsiella aerogenes* K54 (Dutton and Merrifield, 1982). However, the alternate repeating units of the K54 polysaccharide are mono-*O*-acetylated, and the polymer does not gel, but can be made to gel after de-*O*-acetylation. These results, in combination with X-ray fiber diffraction studies (M. J. Miles, V. J. Morris, and M. A. O'Neill, unpublished results; P. Attwool and E. D. T. Atkins, personal communication) suggest that *O*-acetyl groups hinder the formation of crystalline junction zones by regulating the secondary structure of the polysaccharide. Therefore *O*-acetyl groups may play an important role in influencing the conformation of polysaccharides in nature. In the context of the recent findings by Albersheim's group concerning the biological activity of plant cell wall fragments (Darvill and Albersheim, 1984; Tran Thanh Van, 1985), it would be of interest to determine whether *O*-acetylation plays a role in influencing the biological activity of "oligosaccharins." It has been established that xyloglucans (York et al., 1984) and Rhamnogalacturonan-II (Spellman, 1983b) contain *O*-acetyl groups, but their location and function(s) are unknown.

9. Anomeric Configurations of Monosaccharides

In addition to determining the monosaccharide composition, linkage types, and sequence of residues in a cell wall polysaccharide, it is also essential to determine the anomeric configuration of the glycosyl residues. As with determining the sequence of glycosyl residues, the method of choice, be it chemical, enzymic, or physical, are dependent on the type of material under investigation and the amount available.

A. ENZYMIC DIGESTION

In an earlier section the use of enzymes as an aid for structural investigation was discussed. Provided the specificity of the enzyme is known, its ability to degrade a particular polymer may give information on the anomeric nature of the linkage(s). For instance, the degradation of

galactomannans with β-D-mannanases and α-D-galactosidases confirms the presence of β-D-Man*p* and α-D-Gal*p*, respectively (Matheson and McCleary, 1984). Similarly the ability of α-D-galacturonases to degrade pectins and cellulases to hydrolyze xyloglucans show that these polymers contain α-D-Gal*p*A and β-D-Glc*p*, respectively, in their backbones. Exoglycosidase digestions have established the anomeric nature of fucose (O'Neill and Selvandran, 1983) and galactose (Kato and Matsuda, 1980a, b) in xyloglucans. Using a purified α-L-arabinosidase, it was established that the nonreducing terminal Ara*f* residue attached to hydroxyprolyl-tetraarabinosides was α-linked (Ashford et al., 1982).

B. CHEMICAL DEGRADATIONS

In many cases specific enzymes may not be available and specific chemical degradations have been used. It has been shown that β-linked acetylated aldopyranosides are readily degraded by oxidation with chromium trioxide, whereas the α-anomers are stable (Angyal and James, 1970). In the case of aldofuranosides both the α- and β-anomers are degraded. Using this technique, it is therefore possible to determine the anomeric nature of glycopyranosides. It should be emphasized that to obtain unambiguous results, the polymer must be fully acetylated and the reaction time for the oxidation carefully selected. Generally, a 2 h oxidation is sufficient, but we have found with the microbial polysaccharide gellan gum (O'Neill et al., 1983) that after 2 h oxidation a proportion of the β-linked aldopyranosides remained intact.

C. PHYSICAL METHODS

Optical rotation measurements of homopolysaccharides can indicate the type of anomeric linkage. If the polysaccharide is complex, unambiguous interpretation of such data is difficult. Optical rotation values can be of considerable value for determining the anomeric configurations of oligosaccharides, although similar problems arise as for the polysaccharides. Measurement of the optical rotation of the disaccharide, D-Xyl*p*-(1→6)-D-Glc*p*, derived from the enzymic digest of runner bean xyloglucan established the xylose to be α-linked (O'Neill and Selvendran, 1986). In an attempt to determine the anomeric nature of the arabinose residues attached to hydroxyproline in potato lectin by optical rotation, Allen et al. (1978) were led to suggest that all the arabinose residues were β-linked. In subsequent work it was found that the $[\alpha]_{ara}$ and $[M]_{ara}$ for Hyp-Ara_4 were less than that expected for a glycopeptide containing all β-linkages. The observed and theoretical values were consistent with one

α- and three β-linkages (Ashford et al., 1982). Using a purified *exo*-α-L-arabinofuranosidase, it was established that the nonreducing terminal Ara*f* residue was α-linked (Ashford et al., 1982).

Probably the most suitable methods for determining anomeric configurations are high resolution ^{1}H- and ^{13}C-NMR. The signals of anomeric protons or carbons are readily distinguished from their ring counterparts. Therefore by careful measurement of chemical shift (δ) values and coupling constants (for ^{1}H-NMR: $J_{1,2}$), it is possible to determine the anomeric nature of each glycosidic linkage in a polymer. For details of the applications of NMR to the study of carbohydrates, the reader should consult Perlin and Casu (1981), Gorin (1981), and Vliegenthart et al. (1982).

VII. CONCLUDING REMARKS

In this chapter an attempt has been made to discuss the methods available for the isolation and analysis of higher plant cell walls. Because the structures and properties of the cell wall polymers from various tissue types show considerable differences, it is emphasized that, where possible, separation of the tissues in a plant organ prior to preparation of the cell walls is desirable. Attention is drawn to the problems associated with coprecipitation of intracellular compounds with cell wall polymers, particularly in view of the occurrence of small amounts of proteoglycan and proteoglycan-polyphenol complexes in the walls and the covalent attachment of phenolics and phenolic esters with some of the cell wall polymers of parenchymatous and suspension-cultured tissues. The preparation of gram quantities of relatively pure cell walls from starch- and protein-rich tissues is discussed at some length because of the importance of dietary fiber in human nutrition and an understanding of the composition, structure, and properties of dietary fiber would be hampered without such methods (Selvendran, 1984).

The methods that have been used to extract sequentially polymers from cell walls are critically and objectively assessed, and attention is drawn to the advantages and disadvantages of chemical and enzymic methods for solubilizing the polymers. It is hoped that the comments and suggestions would provide the necessary stimulus for researchers to devise improved schemes for fractionating various types of cell walls. A number of methods available for fractionating cell wall polymers is discussed, and the shortcomings in the available methods are indicated. In order to cover the points mentioned here effectively, we have drawn from the experience of our group. Various methods available for degrading the purified polymers (or their derivatives) to fragments are discussed,

and the characterization of partially methylated alditol acetates and methylated oligosaccharide alditols are discussed in some detail. The use of improved methods of methylation analysis, coupled with GLC-MS, HPLC-MS, FAB-MS, and ^{1}H-NMR of the derivatives permits the scale of experiments to be reduced so drastically that a few milligrams can be made to yield much more information than could be gained previously from work with quantities hundreds of times larger. We have discussed the characterization of fragments from cell wall and microbial polysaccharides on which we have worked because (1) they illustrate specific features and possible potential applications, (2) the relevant information is scattered in the literature, and (3) some of the points on structural characterization are too briefly discussed in the journals to be of much use to the average worker. The methods for sequencing complex polysaccharides by the procedures developed by Albersheim's group are not discussed in detail because they have been adequately reviewed recently (McNeil et al., 1982b).

In addition to the applications of NMR discussed in the text, in the near future ^{1}H- and ^{13}C-NMR will be used increasingly in cell wall studies to obtain a "fingerprint" of the main types of polymers present in the walls (Joseleau and Chambat, 1984), on the one hand, and to determine the nature and mode of attachment of noncarbohydrate substituents in the polymers (Kato and Nevins, 1985), on the other. NMR can be used to distinguish the crystalline and amorphous types of polymers present in the wall matrix and also the nature of the association of the matrix polymers (MacKay et al., 1982). The technique may also serve to monitor certain subtle changes in the cell wall structure in response to external stimuli, without disrupting the wall structure. Coupled with detailed structural studies and immunocytochemistry, such methods may help us to formulate plausible models for cell walls from which further advances can be made. A proper knowledge of cell wall structure would enhance our understanding of vegetables and fruits, fresh or cooked, and the changes that occur in plant tissues during maturation and senescence.

More recently attention has been drawn to the fact that fragments of cell wall polymers can act as regulatory molecules (McNeil et al., 1984; Tran Thanh Van et al., 1985). These studies show that the cell wall matrix is not just a structural component of the plant and is far from being inert. We hope that this chapter will increase the reader's awareness of the exciting possibilities for future research.

Acknowledgments

The authors thank Susan Du Pont, Verena Verne and Barry Stevens for editorial help and for some of their unpublished results, John Eagles and

Keith Parsley for help and advice with GLC-MS analysis, Steve Tanner for NMR spectroscopy, and Hazel Chesters for her conscientious typing of the manuscript.

References

Adams, G. A., and Bishop, C. T. (1956), *J. Amer. Chem. Soc.*, *78*, 2842–2844.

Adams, G. A. (1965), *Methods Carbohydr. Chem.*, *5*, 170–175.

Akiyama, Y., and Kato, K. (1976), *Agric. Biol. Chem.*, *40*, 2343–2348.

Akiyama, Y., and Kato, K. (1977), *Agric. Biol. Chem.*, *41*, 79–81.

Akiyama, Y., Mori, M., and Kato, K. (1980), *Agric. Biol. Chem.*, *44*, 2487–2489.

Albersheim, P., Neukom, H., and Deuel, H. (1960), *Arch. Biochem. Biophys.*, *90*, 46–51.

Albersheim, P., Nevins, D. J., English, P. D., and Karr, A. (1967), *Carbohydr. Res.*, *5*, 340–345.

Allen, A. K., Desai, N. N., Neuberger, A. A., and Creeth, J. M. (1978), *Biochem. J.*, *171*, 665–674.

Anderson, R. L., and Stone, B. A. (1973), *Aust. J. Biol. Sci.*, *26*, 135–150.

Anderson, M. A., and Stone, B. A. (1985), *Carbohydr. Polymers*, *5*, 115–129.

Andrews, P. (1970), *Methods Biochem. Anal.*, *18*, 1–53.

Angyal, S. J., and James, K. (1970), *Carbohydr. Res.*, *12*, 147–153.

Ashford, D. A., Desai, N. N., Allen, A. K., Neuberger, A., O'Neill, M. A., and Selvendran, R. R. (1982), *Biochem. J.*, *201*, 199–208.

Ashwell, G. (1957), *Methods Enzymol.*, *3*, 73–105.

Aspinall, G. O. (1973), in *Techniques of Chemistry: Elucidation of Organic Structures by Physical and Chemical Methods*, Vol. 4 (K. W. Bentley and G. W. Kirby, eds.), Wiley-Interscience, New York, pp. 379–450.

Aspinall, G. O. (1976), in *MTP International Review of Science, Organic Chemistry Series Two: Carbohydrates*, Vol. 7 (G. O. Aspinall, ed.), Butterworths, Boston, pp. 201–222.

Aspinall, G. O. (1982a), in *The Polysaccharides*, Vol. 1 (G. O. Aspinall, ed.), Academic Press, New York, pp. 35–131.

Aspinall, G. O. (1982b), in *The Polysaccharides*, Vol. 1 (G. O. Aspinall, ed.), Academic Press, New York, pp. 19–34.

Aspinall, G. O., and Carlyle, J. J. (1969), *J. Chem. Soc., C*, 851–856.

Aspinall, G. O., and Chaudhari, A. S. (1975), *Can. J. Chem.*, *53*, 2189–2193.

Aspinall, G. O., and Cottrell, J. W. (1970), *Can. J. Chem.*, *48*, 1283–1289.

Aspinall, G. O., and Fanous, H. K. (1984), *Carbohydr. Polymers*, *4*, 193–214.

Aspinall, G. O., and Jiang, K. S. (1974), *Carbohydr. Res.*, *38*, 247–255.

Aspinall, G. O., and McNab, J. M. (1969), *J. Chem. Soc., C*, 845–851.

Aspinall, G. O., and Rosell, K.-G. (1977), *Carbohydr. Res.*, *57*, C23–C27.

Aspinall, G. O., and Wilkie, K. C. B. (1956), *J. Chem. Soc.*, 1072–1076.

Aspinall, G. O., Begbie, R., Hamilton, A., and Whyte, J. N. C. (1967a), *J. Chem. Soc., C*, 1065–1070.

Aspinall, G. O., Cairncross, I. M., Sturgeon, R. J., and Wilkie, K. C. B. (1960), *J. Chem. Soc., C*, 3881–3885.

Aspinall, G. O., Carlyle, J. J., McNab, J. M., and Rudowski, A. (1969), *J. Chem. Soc., C*, 840–845.

Aspinall, G. O., Cottrell, I. W., Egan, S. V., Morrison, I. M., and Whyte, J. N. C. (1967b), *J. Chem. Soc., C*, 1071–1080.

Aspinall, G. O., Craig, J. W. T., and Whyte, J. L. (1968a), *Carbohydr. Res., 7*, 442–452.

Aspinall, G. O., Fanous, H. K., and Sen, A. K. (1983), in *Unconventional Sources of Dietary Fibre* (I. Furda, ed.), Washington, D.C.: American Chemical Society, pp. 33–48.

Aspinall, G. O., Gestetner, B., Molloy, J. A., and Uddin, M. (1968b), *J. Chem. Soc., C*, 2554–2559.

Aspinall, G. O., Hunt, K., and Morrison, I. M. (1967c), *J. Chem. Soc., C*, 1080–1086.

Aspinall, G. O., Krishnamurthy, T. N., Mitura, W., and Funabashi, M. (1975), *Can. J. Chem., 53*, 2182–2188.

Aspinall, G. O., Krishnamurthy, T. N., and Rosell, K. G. (1977), *Carbohydr. Res.., 55*, 11–19.

Azuma, J.-I., Takahashi, N., and Koshijima, T. (1981), *Carbohydr. Res., 93*, 91–104.

Bacic, A., and Stone, B. A. (1981a), *Aust. J. Plant Physiol., 8*, 453–474.

Bacic, A., and Stone, B. A. (1981b), *Aust. J. Plant Physiol., 8*, 475–495.

Bacon, J. S. D., Gordon, A. H., and Morris, E. J. (1975), *Biochem. J., 149*, 485–487.

Ballance, G. M., and Manners, D. J. (1978), *Carbohydr. Res., 61*, 107–118.

Banks, W. and Greenwood, C. T. (1963), *Adv. Carbohydr. Chem., 18*, 357–398.

Barber, M., Bordoli, R. S., Sedgwick, R. D., and Tyler, A. N. (1981), *Nature, 293*, 270–275.

Barbier, M., and Thibault, J.-F. (1982), *Phytochem., 21*, 111–115.

Barrett, A. J., and Northcote, D. H. (1965) *Biochem. J., 94*, 617–627.

Barth, H. G., and Smith, D. A. (1981), *J. Chromatogr., 206*, 410–415.

Bateman, D. F. (1976), in *Biochemical Aspects of Plant-Parasite Relationships* (J. Friend and D. R. Threlfall, eds.), Academic Press, London, pp. 79–103.

Bauer, W. D., Talmadge, K. W., Keegstra, K., and Albersheim, P. (1973), *Plant Physiol., 51*, 174–187.

Benson, J. W., and Patterson, J. A. (1971), in *New Techniques in Amino Acid, Peptide and Protein Analysis* (A. Niederweiser and G. Pataki, eds.), Ann Arbor Pub. Co., Michigan, pp. 1–73.

Bernardi, G. (1971), *Methods Enzymol., 22*, 325–339.

Bettelheim, F. A. (1970), in *The Carbohydrates, Chemistry and Biochemistry*, Vol. IIA (W. Pigman and D. Horton, eds.), Academic Press, New York, pp. 383–394.

Binkley, W. W. (1955), *Adv. Carbohydr. Chem., 10*, 55–94.

Bishop, C. T. (1956), *J. Amer. Chem. Soc., 78*, 2840–2841.

Bishop, C. T. (1962), *Methods Biochem. Anal., 10*, 1–42.

Bishop, C. T. (1964), *Adv. Carbohydr. Chem., 19*, 95–147.

Bishop, C. T., and Whitaker, D. R. (1955), *Chemistry and Industry*, 119.

Bitter, T., and Muir, H. M. (1962), *Anal. Biochem., 4*, 330–334.

Björndal, H., Lindberg, B., Lönngren, J., Meszaros, M., Thompson, J. L., and Nimmich, W. (1973), *Carbohydr. Res., 31*, 93–100.

Blake, J. D., and Richards, G. N. (1970), *Carbohydr. Res., 14*, 375–387.

Blake, J. D., and Richards, G. N. (1971a), *Carbohydr. Res., 17*, 253–268.

Blake, J. D., and Richards, G. N. (1971b), *Carbohydr. Res., 18*, 11–21.

Blake, J. D., Murphy, P. T., and Richards, G. N. (1971), *Carbohydr. Res.*, *16*, 49–57.

Blakeney, A. B., Harris, P. J., Henry, R. J., Stone, B. A., and Norris, T. (1982), *J. Chromatogr.*, *249*, 180–182.

Blakeney, A. B., Harris, P. J., Henry, R. J. and Stone, B. A. (1983), *Carbohydr. Res.*, *113*, 291–299.

Blumenkrantz, N., and Asboe-Hansen, G. (1973), *Anal. Biochem.*, *54*, 484–489.

Bobbit, J. M. (1956), *Adv. Carbohydr. Chem.*, *17*, 1–41.

Bouveng, H. O., and Lindberg, B. (1960), *Adv. Carbohydr. Chem.*, *15*, 53–89.

Bouveng, H. O., and Lindberg, B. (1965), *Methods Carbohydr. Chem.*, *5*, 147–150.

Braun, G. (1943), *Org. Synthesis, Coll.*, *2*, 122–130.

Breen, M., Weinstein, H. G., Andersen, M., and Veis, A. (1970), *Anal. Biochem.*, *35*, 146–159.

Brillouet, J.-M., Joseleau, J.-P., Utille, J.-P., and Lelievre, D. (1982), *J. Agric. Food Chem.*, *30*, 488–495.

Brown, R. G., Kimmins, W. C., and Lindberg, B. (1974), *Acta Chem. Scand.*, *B29*, 4–13.

Buchala, A. J., Fraser, C. G., and Wilkie, K. C. B. (1972), *Phytochem.*, *11*, 1249–1254.

Carpita, N. C. (1983), *Plant Physiol.*, *72*, 515–521.

Carpita, N. C. (1984), *Phytochem.*, *23*, 1089–1093.

Chizhov, O. S., Kadentsev, V. I., Solovyov, A. A., Levonowich, P. F., and Dougherty, R. C. (1976), *J. Org. Chem.*, *41*, 3425–3428.

Churms, S. C., and Stephen, A. M. (1984), *Carbohydr. Res.*, *133*, 105–123.

Clermont-Beaugraud, S., and Percheron, F. (1968), *Bull. Soc. Chim. Biol.*, *30*, 633–639.

Comtat, J., Joseleau, J.-P., Bosso, C., and Barnoud, F. (1974), *Carbohydr. Res.*, *38*, 217–224.

Conrad, H. E., Bamburg, J. R., Epley, J. D., and Kindt, T. J. (1966), *Biochemistry*, *5*, 2808–2817.

Corey, E. J., and Kim, C. U. (1973), *Tetrahedron Lett.*, *12*, 919–922.

Coulter, J. R., and Hann, C. S. (1971), in *New Techniques in Amino Acid, Peptide and Protein Analysis* (A. Niederweiser and G. Pataka, eds.), Ann Arbor Pub. Co., Michigan, pp. 75–128.

Courtois, J. E., and Le Dizet, P. (1966), *Carbohydr. Res.*, *3*, 141–151.

Courtois, J. E., and Le Dizet, P. (1968), *Bull. Soc. Chim. Biol.*, *50*, 1695–1709.

Croon, I., Lindberg, B., and Meier, H. (1959), *Acta Chem. Scand.*, *13*, 1299–1304.

Darvill, A. G., and Albersheim, P. (1984), *Ann. Rev. Plant Physiol.*, *35*, 243–275.

Darvill, A. G., McNeil, M., and Albersheim, P. (1978), *Plant Physiol.*, *62*, 418–422.

Darvill, A. G., McNeil, M., and Albersheim, P. (1980a), *Carbohydr. Res.*, *86*, 309–315.

Darvill, A. G., McNeil, M., Albersheim, P., and Delmer, D. P. (1980b), in *The Biochemistry of Plants*, Vol. 1 (N. E. Tolbert, ed.), Academic Press, New York, pp. 92–162.

Darvill, J. E., McNeil, M., Darvill, A. G., and Albersheim, P. (1980c), *Plant Physiol.*, *66*, 1135–1139.

Das, N. S., Das, S. C., Dutt, A. S., and Roy, A. (1981), *Carbohydr. Res.*, *94*, 73–82.

Davies, A. M. C., Robinson, D. S., and Couchman, R. (1974), *J. Chromatog.*, *101*, 307–314.

Dea, I. C. M., and Morrison, A. (1975), *Adv. Carbohydr. Chem. Biochem.*, *31*, 241–312.

De Belder, A. N., and Norrman, B. (1968), *Carbohydr. Res.*, *8*, 1–6.

De Jongh, D. C. (1980), in *The Carbohydrates*, Vol. IB (W. Pigman and D. Horton, eds.), Academic Press, New York, pp. 1327–1353.

Dekker, R. F. H., and Richards, G. N. (1975), *Carbohydr. Res.*, *42*, 107–123.

Dell, A., and Ballou, C. E. (1983), *Carbohydr. Res.*, *120*, 95–111.

Dell, A., Dutton, G. G. S., Jansson, P. E., Lindberg, B., Lindquist, U., and Sutherland, I. W. (1983), *Carbohydr. Res.*, *122*, 340–343.

Desai, N. N., and Allen, A. K. (1979), *Anal. Biochem.*, *93*, 88–90.

Deventer-Schriemer, W. H., and Pilnik, W. (1976), *Lebensmittel-Wissenschaft & Technologie*, *9*, 42–44.

De Vries, J. A., Voragen, A. G. J., Rombouts, F. M., and Pilnik, W. (1981), *Carbohydr. Polymers*, *1*, 117–127.

De Vries, J. A., Rombouts, F. A., Voragen, A. G. J., and Pilnik, W. (1982), *Carbohydr. Polymers*, *2*, 25–33.

De Vries, J. A., Den Uijl, C. H., Voragen, A. G. J., Rombouts, F. M., and Pilnik, W. (1983a), *Carbohydr. Polymers*, *3*, 193–205.

De Vries, J. A., Rombouts, F. M., Voragen, A. G. J., and Pilnik, W. (1983b), *Carbohydr. Polymers*, *3*, 245–258.

Dey, P. M. and Brinson, K. (1984), *Adv. Carbohydr. Chem. Biochem.*, *42*, 265–382.

Di Fabio, J. L., Dutton, G. G. S., and Parolis, H. (1984), *Carbohydr. Res.*, *133*, 125–133.

Dische, Z. (1962), *Methods Carbohydr. Chem.*, *1*, 477–514.

Doesburg, J. J. (1966), *Pectic Substances in Fresh and Preserved Fruits and Vegetables, I.B.V.T. Communication*, *25*, Wageningen, The Netherlands.

Dudman, W. F., and Bishop, C. T. (1968), *Can. J. Chem.*, *46*, 3099–4006.

Dudman, W. F., and Whittle, C. P. (1976), *Carbohydr. Res.*, *46*, 267–272.

Dutton, G. G. S. (1973), *Adv. Carbohydr. Chem. Biochem.*, *28*, 11–160.

Dutton, G. G. S., and Merrifield, E. H. (1982), *Carbohydr. Res.*, *105*, 189–203.

Dutton, G. G. S., and Karunaratne, D. N. (1984), *Carbohydr. Res.*, *134*, 103–114.

Dutton, G. G. S., and Karunaratne, D. N. (1985), *Carbohydr. Res.*, *138*, 277–291.

Dutton, G. G. S., Di Fabio, J. L., Leek, D. M., Merrifield, E. H., Nunn, J. R., and Stephen, A. M. (1981), *Carbohydr. Res.*, *97*, 127–138.

Edwards, T. E. (1965), *Methods Carbohydr. Chem.*, *5*, 176–179.

Egger, K. (1969), in *Thin-Layer Chromatography* (E. Stahl, ed.), George Allen and Unwin, London, pp. 687–706.

English, P. D., Maglothin, A., Keegstra, K., and Albersheim, P. (1972), *Plant Physiol.*, *49*, 293–297.

Englyst, H., Wiggins, H. S., and Cummings, J. H. (1982), *Analyst*, *107*, 307–318.

Erskine, A. J., and Jones, J. K. N. (1956), *Can. J. Chem.*, *34*, 821–826.

Fielding, A. H., and Byrde, R. J. W. (1969), *J. Gen. Microbiol.*, *58*, 73–84.

Fincher, G. B. (1975), *J. Instit. Brewing*, *81*, 116–122.

Foglietti, M. J., and Percheron, F. (1968), *Carbohydr. Res.*, *7*, 146–155.

Ford, C. W. (1982), *J. Sci. Food Agric.*, *33*, 318–324.

Fry, S. C. (1982a), *Biochem. J.*, *204*, 449–455.

Fry, S. C. (1982b), *Biochem. J.*, *203*, 493–504.

Fry, S. C. (1983), *Planta*, *157*, 111–123.

Fry, S. C. (1984), *Phytochem.*, *23*, 59–64.

Fry, S. C. (1985), in *Oxford Surveys of Plant Molecular and Cell Biology*, Vol. 2 (B. Miflin, ed.), Oxford University Press, pp. 1–42.

Fulcher, R. G., O'Brien, T. P., and Lee, J. W. (1972), *Aust. J. Biol. Sci.*, *25*, 23–34.

Gaillard, B. D. E. (1961), *Nature*, *191*, 1295–1296.

Gaillard, B. D. E. (1965), *Phytochem.*, *4*, 631–634.

Gaillard, B. D. E. (1966), *Nature*, *212*, 202–203.

Gerwig, G. J., Kamerling, J. P., and Vliegenthart, J. F. G. (1978), *Carbohydr. Res.*, *62*, 349–357.

Gerwig, G. J., Kamerling, J. P., Vliegenthart, J. F. G., Homan, W. L., Van Egmond, P., and Vanden Ende, H. (1984), *Carbohydr. Res.*, *127*, 245–251.

Geyer, R., Geyer, H., Kühnhardt, S., Mink, W., and Stirm, S. (1982), *Anal. Biochem.*, *121*, 263–274.

Gilbert, W. (1981), *Science*, *214*, 1305–1312.

Ginsburg, V., (1982), *Methods Enzymol.*, *83*, 3–260.

Gleeson, P. A., and Clarke, A. E. (1979), *Biochem. J.*, *181*, 607–621.

Gleeson, P. A., and Clarke, A. E. (1980), *Phytochem.*, *19*, 1777–1782.

Gleeson, P. A., Jermyn, M. A., and Clarke, A. E. (1979), *Anal. Biochem.*, *92*, 41–45.

Goldschmid, H. R., and Perlin, A. S. (1963), *Can. J. Chem.*, *41*, 2272–2277.

Goldstein, I. J., and Hayes, C. E. (1978), *Adv. Carbohydr. Chem. Biochem.*, *35*, 127–340.

Goldstein, I. J., Hay, C. W., Lewis, B. A., and Smith, F. (1965), *Methods Carbohydr. Chem.*, *5*, 361–370.

Gorin, P. A. J. (1980), *Adv. Carbohydr. Chem. Biochem.*, *38*, 13–104.

Gorin, P. A. J., and Spencer, J. F. T. (1965), *Can. J. Chem.*, *43*, 2978–2984.

Gowda, D. S., Reuter, G., and Schauer, R. (1982), *Phytochem.*, *21*, 2297–2300.

Gramera, R. E., and Whistler, R. L. (1963), *Arch. Biochem. Biophys.*, *101*, 75–80.

Green, J. W. (1963), *Methods Carbohydr. Chem.*, *3*, 9–21.

Guthrie, R. D. (1961), *Adv. Carbohydr. Chem.*, *16*, 105–158.

Guthrie, R. D., and McCarthy, J. F. (1967), *Adv. Carbohydr. Chem.*, *22*, 11–23.

Gyaw, M. O., and Timell, T. E. (1960), *Can. J. Chem.*, *38*, 1957–1966.

Hagglund, E., Lindberg, B., and McPherson, J. (1956), *Acta Chem. Scand.*, *10*, 1160–1164.

Hakomori, S. (1964), *J. Biochem. (Tokyo)*, *55*, 205–208.

Hamilton, J. K., and Kircher, H. W. (1958), *J. Am. Chem. Soc.*, *80*, 4703–4708.

Hanessian, S. (1971), *Methods of Biochem. Anal.*, *19*, 105–228.

Harris, P. J., and Hartley, R. D. (1980), *Biochem. Syst. Ecol.*, *8*, 153–160.

Hart, D. A., and Kindel, P. K. (1970), *Biochem.*, *9*, 2190–2196.

Hartley, R. D., and Jones, E. C. (1975), *J. Chromatogr.*, *107*, 213–218.

Hartley, R. D., and Jones, E. C. (1976a), *Phytochem.*, *15*, 305–307.

Hartley, R. D., and Jones, E. C. (1976b), *Phytochem.*, *15*, 1157–1160.

Heath, M. F. and Northcote, D. H. (1971), *Biochem. J.*, *125*, 953–961.

Henry, R. J., Blakeney, A. B., Harris, P. J., and Stone, B. A. (1983), *J. Chromatogr.*, *256*, 419–427.

Himmell, M. E., and Squire, P. G. (1981), *J. Chromatogr., 210*, 443–452.

Hoff, J. E., and Castro, M. D. (1969), *J. Agric. Food Chem., 17*, 1328–1331.

Hoffman, J., and Lindberg, B. (1980), *Methods Carbohydr. Chem., 8*, 117–122.

Honda, S., Takahashi, M., Kakehi, K., and Ganno, S. (1981), *Anal. Biochem., 113*, 130–138.

Honda, S., Takahashi, M., Shimada, S., Kakehi, K., and Ganno, S. (1983), *Anal. Biochem., 128*, 429–437.

Hough, L. (1954), *Methods of Biochem. Anal., 1*, 205–242.

Ishii, S. (1981), *Phytochem., 20*, 2329–2333.

Jansson, P. E., Kenne, L., Liedgren, H., Lindberg, B., and Lönngren, J. (1976), *Chem. Commun.* Univ. Stockholm, Sweden, pp. 1–76.

Jarvis, M. C. (1982), *Planta, 154*, 344–346.

Jarvis, M. C., Hall, M. A., Threlfall, D. R., and Friend, J. (1981), *Planta, 152*, 93–100.

Jarvis, M. C., Threlfall, D. R., and Friend, J. (1977), *Phytochem., 16*, 849–852.

Jermyn, M. A. (1955), in *Modern Methods of Plant Analysis*, Vol. 2 (K. Paech and M. V. Tracey, eds.), Springer-Verlag, Berlin, pp. 197–225.

Jermyn, M. A., and Isherwood, F. A. (1949), *Biochem. J., 44*, 402–407.

Jermyn, M. A., and Isherwood, F. A. (1956), *Biochem. J., 64*, 123–133.

Jones, T. M., and Albersheim, P. (1972), *Plant Physiol., 49*, 926–936.

Jones, J. K. N., and Stoodley, R. J. (1965), *Methods Carbohydr. Chem., 5*, 36–38.

Jones, J. K. N., and Wise, L. E. (1952), *J. Chem. Soc.*, 3389–3393.

Joseleau, J.-P., and Chambat, G. (1984), *Physiol. Veg., 22*, 461–470.

Joseleau, J.-P., Chambat, G., and Chumpitazi-Hermoza, B. (1981), *Carbohydr. Res., 90*, 339–344.

Joseleau, J.-P., Chambat, G., and Lanvers, M. (1983), *Carbohydr. Res., 122*, 107–113.

Kaji, A., and Ichimi, T. (1973), *Agric. Biol. Chem., 37*, 431–432.

Kärkkäinen, J. (1970), *Carbohydr. Res., 14*, 27–33.

Kärkkäinen, J. (1971), *Carbohydr. Res., 17*, 1–10.

Kato, Y., and Matsuda, Y. (1980a), *Agric. Biol. Chem., 44*, 1751–1758.

Kato, Y., and Matsuda, Y. (1980b), *Agric. Biol. Chem., 44*, 1759–1766.

Kato, Y., and Nevins, D. J. (1985), *Carbohydr. Res., 137*, 139–150.

Keegstra, K., English, P. D., and Albersheim, P. (1972), *Phytochem., 11*, 1873–1880.

Keegstra, K., Talmadge, K. W., Bauer, W. D., and Albersheim, P. (1973), *Plant Physiol., 51*, 188–196.

Kenne, L., and Lindberg, B. (1983), in *The Polysaccharides*, Vol. 2 (G. O. Aspinall, ed.), Academic Press, New York, pp. 287–363.

Kennedy, J. F., and White, C. A. (1979), in *Comprehensive Organic Chemistry* (D. Barton and W. D. Ollis, eds.), Pergamon Press, Oxford, p. 755.

Kennedy, J. F., and Fox, J. E. (1980), *Methods Carbohydr. Chem., 8*, 3–12.

Kikuchi, T., and Yokotsuka, T. (1973a), *Agric. Biol. Chem., 37*, 973–979.

Kikuchi, T., and Yokotsuka, T. (1973b), *Agric. Biol. Chem., 37*, 2473–2477.

Kikuchi, T., and Sugimoto, H. (1976), *Agric. Biol. Chem., 40*, 87–92.

Knee, M. (1970), *J. Exp. Bot., 21*, 651–662.

Kobata, A. (1979), *Anal. Biochem., 100*, 1–14.

Kocourek, J., and Ballou, C. E. (1969), *J. Bacteriol., 100*, 1175–1181.

Kooiman, P. (1961), *Receuil Trav. Chim. Pays-Bas, 80*, 849–852.

Kooiman, P. (1967), *Phytochem., 6*, 1665–1673.

Kochetkov, N. K., and Chizhov, O. S. (1966), *Adv. Carbohydr. Chem., 21*, 39–93.

Kovacik, V., Bauer, S., Rosik, J., and Kovac, P. (1968), *Carbohydr. Res., 8*, 282–290.

Kubackova, M., Karacsonyi, S., Bilisics, L., and Tomán, R. (1979), *Carbohydr. Res., 76*, 177–188.

Kündig, W., Neukom, H., and Deuel, H. (1961), *Helv. Chim. Acta, 44*, 823–829.

Laine, R. A., Esselman, W. J., and Sweeley, C. C. (1972), *Methods Enzymol., 28*, 159–178.

Lamport, D. T. A. (1967), *Nature, 216*, 1322–1324.

Lamport, D. T. A., and Miller, D. H. (1971), *Plant Physiol., 48*, 454–456.

Lamport, D. T. A., and Catt, J. W. (1981), in *Encyclopedia of Plant Physiology*, Vol. 13B (W. Tanner and F. A. Loewus, eds.), Springer-Verlag, Berlin, pp. 133–165.

Lamport, D. T. A., Katona, L., and Roerig, S. (1973), *Biochem. J., 133*, 125–131.

Lau, J. M., McNeil, M., Darvill, A. G., and Albersheim, P. (1985), *Carbohydr. Res., 137*, 111–125.

Lawson, C. J., McCleary, C. W., Nakada, H. I., Rees, D. A., Sutherland, I. W., and Wilkinson, C. F. (1969), *Biochem. J., 115*, 947–958.

Lehrfield, J. (1976), *J. Chromatogr., 120*, 141–147.

Leontein, K., Lindberg, B., and Lönngren, J. (1978), *Carbohydr. Res., 62*, 359–362.

Lewis, B. A., and Smith, F. (1969), in *Thin-Layer Chromatography* (E. Stahl, ed.), Allen and Unwin, London, pp. 807–837.

Lindberg, B. (1972), *Methods Enzymol., 28*, 178–195.

Lindberg, B., and Lönngren, J. (1978), *Methods Enzymol., 50*, 3–33.

Lindberg, B., Lönngren, J., Nimmich, W., and Ruden, U. (1973a), *Acta Chem. Scand., 27*, 3787–3790.

Lindberg, B., Lönngren, J., and Thompson, J. L. (1973b), *Carbohydr. Res., 28*, 351–357.

Lindberg, B., Lönngren, J., and Svensson, S. (1975), *Adv. Carbohydr. Chem. Biochem., 31*, 185–240.

Linden, J. C., and Lawhead, C. L. (1975), *J. Chromatogr., 105*, 125–133.

Litchman, M. A., and Upton, R. P. (1972), *Anal. Chem., 44*, 1495–1497.

Lomax, J. A., and Conchie, J. (1982), *J. Chromatogr., 236*, 385–394.

Lomax, J. A., Gordon, A. H., and Chesson, A. (1983), *Carbohydr. Res., 122*, 11–22.

Lomax, J. A., Gordon, A. H., and Chesson, A. (1985), *Carbohydr. Res., 138*, 177–188.

Lönngren, J., and Svensson, S. (1974), *Adv. Carbohydr. Chem. Biochem., 29*, 41–106.

Luchsinger, W. W., Chen, S.-C., and Richards, A. W. (1965), *Arch. Biochem. Biophys., 112*, 524–530.

MacKenzie, S. L. (1981), *Methods Biochem. Anal., 27*, 1–88.

MacKay, A. L., Bloom M., Tepfer, M., and Taylor, I. E. P. (1982), *Biopolymers, 21*, 1521–1534.

March, J. F. (1975), *Anal. Biochem., 69*, 420–442.

Mares, D. J., and Stone, B. A. (1973a), *Aust. J. Biol. Sci., 26*, 793–812.

Mares, D. J., and Stone, B. A. (1973b), *Aust. J. Biol. Sci., 26*, 813–830.

Markwalder, H. U., and Neukom, H. (1976), *Phytochem., 15*, 836–837.

Matheson, N. K., and McCleary, B. V. (1984), in *The Polysaccharides*, Vol. 3 (G. O. Aspinall, ed.), Academic Press, New York, pp. 1–105.

McCleary, B. V., and Matheson, N. K. (1983), *Carbohydr. Res., 119*, 191–219.

McCleary, B. V., Clarke, A. H., Dea, I. C. M., and Rees, D. A. (1985), *Carbohydr. Res., 139*, 237–260.

McComb, E. A., and McCready, R. M. (1952), *Anal. Chem., 24*, 1630–1632.

McNamara, M. K., and Stone, B. A. (1981), *Lebensmit, Wiss. Technol., 14*, 182–187.

McNeil, M. (1983), *Carbohydr. Res., 123*, 31–40.

McNeil, M., Albersheim, P., Taiz, L., and Jones, R. L. (1975), *Plant Physiol., 55*, 64–68.

McNeil, M., Darvill, A. G., and Albersheim, P. (1980), *Plant Physiol., 66*, 1128–1134.

McNeil, M., Darvill, A. G., and Albersheim, P. (1982a), *Plant Physiol., 70*, 1586–1591.

McNeil, M., Darvill, A. G., Åman, P., Franzén, L.-E., and Albersheim, P. (1982b), *Methods Enzymol., 83*, 3–45.

McNeil, M., Darvill, A. G., Fry, S. C., and Albersheim, P. (1984), *Ann. Rev. Biochem., 53*, 625–663.

Meier, H. (1958), *Acta Chem. Scand., 12*, 144–146.

Meier, H. (1961), *Acta Chem. Scand., 15*, 1381–1385.

Meier, H. (1965), *Methods Carbohydr. Chem., 5*, 45–46.

Meier, H., and Reid, J. S. G. (1982), in *Encylopedia of Plant Physiology*, Vol. 13A (F. A. Loewus and W. Tanner, eds.), Springer-Verlag, Berlin, pp. 418–471.

Menzies, I. S., and Seakins, J. W. T. (1969), in *Chromatographic and Electrophoretic Techniques*, Vol. 1 (I. Smith, ed.), William Heinemann, London, pp. 310–329.

Monro, J. A., Bailey, R. W., and Penny, D. (1976), *Phytochem., 15*, 175–181.

Montgomery, R., Smith, F., and Srivastava, H. C. (1956), *J. Am. Chem. Soc., 78*, 2837–2839.

Moor, J., and Waight, E. S. (1974), *Org. Mass Spectrom., 9*, 903–912.

Moor, J., and Waight, E. S. (1975), *Biomed. Mass Spectrom., 2*, 36–43.

Mopper, K., and Johnson, L. (1983), *J. Chromatogr., 256*, 27–38.

Morrison, I. M. (1973), *Phytochem., 12*, 2979–2984.

Morrison, I. M. (1974a), *Phytochem., 14*, 505–508.

Morrison, I. M. (1974b), *Biochem. J., 139*, 197–204.

Mort, A. J. (1978), Ph.D. Dissertation, University of Michigan.

Mort, A. J., and Lamport, D. T. A. (1977), *Anal. Biochem., 82*, 289–309.

Mort, A. J., Parker, S., and Kuo, W.-S. (1983), *Anal. Biochem., 133*, 380–384.

Narasimhan, S., Wilson, J. R., Martin, E., and Schachter, H. (1979), *Can. J. Biochem., 57*, 83–96.

Narui, T., Takahashi, K., Kobayashi, M., and Shibata, S. (1982), *Carbohydr. Res., 103*, 293–301.

Neeser, J. R., and Schweizer, T. F. (1984), *Anal. Biochem., 142*, 58–67.

Neukom, H., and Kundig, W. (1965), *Methods Carbohydr. Chem., 5*, 14–17.

Neukom, H., Deuel, H., Heri, W. J., and Kundig, W. (1960), *Helv. Chim. Acta, 43*, 64–71.

Neukom, H., Providoli, L., Gremli, H., and Hui, P. A. (1964), *Cereal Chem., 44*, 238–244.

Nilsson, B., and Zopf, D. (1982), *Methods Enzymol.*, *83*, 46–58.

Nilsson, B., and Zopf, D. (1983), *Arch. Biochem. Biophys.*, *222*, 628–648.

Northcote, D. H. (1963), in *Symp. Soc. Exp. Biol.*, Vol. 17, Cambridge University Press, pp. 157–174.

Northcote, D. H. (1965), *Methods Carbohydr. Chem.*, *5*, 201–210.

Northcote, D. H. (1969), in *Essays in Biochemistry*, Vol. 5, pp. 89–137.

Nothnagel, E. A., McNeil, M., Albersheim, P., and Dell, A. (1983), *Plant Physiol.*, *71*, 916–926.

O'Neill, M. A., and Selvendran, R. R. (1980a), *Carbohydr. Res.*, *79*, 115–124.

O'Neill, M. A., and Selvendran, R. R. (1980b), *Biochem. J.*, *187*, 53–63.

O'Neill, M. A., and Roberts, K. (1981), *Phytochem.*, *20*, 25–28.

O'Neill, M. A., and Selvendran, R. R. (1983), *Carbohydr. Res.*, *111*, 239–255.

O'Neill, M. A., and Selvendran, R. R. (1985a), *Biochem. J.*, *227*, 475–481.

O'Neill, M. A., and Selvendran, R. R. (1985b), *Carbohydr. Res.*, *145*, 45–58.

O'Neill, M. A., Selvendran, R. R., and Morris, V. J. (1983), *Carbohydr. Res.*, *124*, 123–133.

O'Neill, M. A., Selvendran, R. R., Morris, V. J., and Eagles, J. (1986a), *Carbohydr. Res.*, *147*, 295–313.

O'Neill, M. A., Morris, V. J., and Selvendran, R. R. (1986b), in *Gums and Stabilisers for the Food Industry*, Vol. 3 (G. O. Phillips and D. A. Wedlock, eds.), Pergamon Press, Oxford, pp. 29–38.

O'Neill, M. A., Morris, V. J., Selvendran, R. R., Sutherland, I. W., and Taylor, I. T. (1986c), *Carbohydr. Res.*, *148*, 63–69.

Painter, T. J. (1982), *Lebensm. Wiss. Technol.*, *15*, 57–61.

Parrish, F. W., Perlin, A. S., and Reese, E. T. (1960), *Can. J. Chem.*, *38*, 2094–2104.

Partridge, S. M. (1948), *Biochem. J.*, *42*, 238–250.

Pavlenko, A. F., and Ovodov, Y. S. (1970), *J. Chromatogr.*, *52*, 165–168.

Perlin, A. S., and Casu, B. (1982), in *The Polysaccharides*, Vol. 1 (G. O. Aspinall, ed.), Academic Press, New York, pp. 133–193.

Perry, M. B., and Hulyalkar, R. K. (1965), *Can. J. Biochem.*, *43*, 573–584.

Peterson, G., and Samuelson, O. (1968), *Svensk Papperstidn.*, *71*, 77–84

Plaschina, I. G., Semenova, M. G., Braudo, E. E., and Tolstoguzow, V. B. (1985), *Carbohydr. Polymers*, *5*, 159–179.

Pryde, A., and Gilbert, M. T. (1979), *Applications of High Performance Liquid Chromatography*, Chapman Hall, London.

Rasper, V. F., Brillouet, J. M., Bertrand, D., and Mercier, C. (1981), *J. Food Sci.*, *46*, 559–563.

Redgwell, R. J., and Selvendran, R. R. (1986), *Carbohydr. Res.*, *157*, 183–199.

Redgwell, R. J., O'Neill, M. A., Selvendran, R. R., and Parsley, K. (1986a), *Carbohydr. Res.*, *153*, 97–106.

Redgwell, R. J., O'Neill, M. A., Selvendran, R. R., and Parsley, K. (1986b), *Carbohydr. Res.*, *153*, 107–118.

Rees, D. A., Morris, E. R., Thorn, D., and Madden, J. K. (1982), in *The Polysaccharides*, Vol. 1 (G. O. Aspinall, ed), Academic Press, New York, pp. 195–290.

Rexova-Benkova, L., and Markovic, O. (1976), *Adv. Carbohydr. Chem. Biochem.*, *33*, 323–385.

Rexova-Benkova, L., and Tibensky, V. (1972), *Biochim. Biophys. Acta, 268*, 187–193.

Rieger-Hug, D., and Stirm, S. (1981), *Virology, 113*, 363–378.

Ring, S. G., and Selvendran, R. R. (1978), *Phytochem., 17*, 745–752.

Ring, S. G., and Selvendran, R. R. (1980), *Phytochem., 19*, 1723–1730.

Ring, S. G., and Selvendran, R. R. (1981), *Phytochem., 20*, 2511–2519.

Roberts, R. M., Cetorelli, J. J., Kirby, E. G., and Ericson, M. (1972), *Plant Physiol., 50*, 531–535.

Roden, L., Baker, J. R., Cifonelli, J. A., and Mathews, M. B. (1972), *Methods Enzymol., 28*, 73–140.

Rosell, K.-G., and Svensson, S. (1975), *Carbohydr. Res., 42*, 297–304.

Ruperez, P., Selvendran, R. R., and Stevens, B. J. H. (1985), *Carbohydr. Res., 142*, 107–113.

Salimath, P. V., and Tharanathan, R. N. (1982), *Carbohydr. Res., 106*, 251–257.

Sanger, F. (1981), *Science, 214*, 1205–1210.

Sarkanen, K. V., and Ludwig, C. H., eds. (1971), *Lignins*, Wiley-Interscience, New York.

Sawardeker, J. S., Sloneker, J. H., and Jeanes, A. (1965), *Anal. Chem., 37*, 1602–1604.

Scott, J. E. (1955), *Chem. and Ind.*, pp. 168–169.

Scott, J. E. (1963), *Methods Biochem. Anal., 8*, 145–197.

Scott, J. E. (1965), *Methods Carbohydr. Chem., 5*, 38–44.

Selvendran, R. R. (1975a), *Phytochem., 14*, 1011–1017.

Selvendran, R. R. (1975b), *Phytochem., 14*, 2175–2180.

Selvendran, R. R. (1983a), in *Dietary Fibre* (G. G. Birch and K. J. Parker, eds.), Applied Science Publishers, London, pp. 95–147.

Selvendran, R. R. (1983b), in *Recent Developments in Mass Spectrometry in Biochemistry, Medicine and Environmental Research*, Vol. 8 (A. Frigerio, ed.), Elsevier Scientific, Amsterdam, pp. 159–176.

Selvendran, R. R. (1984), *Am. J. Clin. Nutr., 39*, 320–337.

Selvendran, R. R. (1985), *J. Cell Sci. Suppl., 2*, 51–88.

Selvendran, R. R., and Du Pont, M. S. (1980a), *J. Sci. Food Agric., 31*, 1173–1182.

Selvendran, R. R., and Du Pont, M. S. (1980b), *Cereal Chem., 57*, 278–283.

Selvendran, R. R., and Du Pont, M. S. (1984), in *Developments in Food Analysis Techniques*, Vol. 3 (R. D. King, ed.), Elsevier Applied Science, New York, pp. 1–68.

Selvendran, R. R., and King, N. R. (1976), *Annals Applied Biology, 83*, 463–473.

Selvendran, R. R., and O'Neill, M. A. (1982), *Encyclopedia of Plant Physiology*, Vol. 13A (F. A. Loewus and W. Tanner, eds.), Springer-Verlag, Berlin, Heidelberg, pp. 515–583.

Selvendran, R. R., and Stevens, B. J. H. (1986), in *Modern Methods of Plant Analysis*, Vol. 3 (H.-F. Linskens and J. F. Jackson, eds.), Springer-Verlag, Berlin, New York, pp. 23–46.

Selvendran, R. R., Davies, A. M. C., and Tidder, E. (1975), *Phytochem., 14*, 2169–2174.

Selvendran, R. R., March, J. F., and Ring, S. G. (1977), in *Cell Wall Biochemistry*, (B. Solheim and J. Raa, eds.), Universitats-forlaget, Bergen, pp. 115–117.

Selvendran, R. R., March, J. F., and Ring, S. G. (1979), *Anal. Biochem., 96*, 282–292.

Selvendran, R. R., Ring, S. G., and Du Pont, M. S. (1979), *Chem. Ind.*, 225–230.

Selvendran, R. R., Ring, S. G., and Du Pont, M. S. (1981), in *The Analysis of Dietary Fibre in Food* (W. P. T. James and O. Theander, eds.), Dekker, New York, pp. 95–121.

Selvendran, R. R., Stevens, B. J. H., and O'Neill, M. A. (1985), in *Biochemistry of Plant Cell Walls: SEB Seminar Series*, Vol. 28 (C. T. Brett and J. R. Hillman, eds.), Cambridge University Press, pp. 39–78.

Sharp, J. K., and Albersheim, P. (1984), *Carbohydr. Res., 128*, 193–202.

Sharp, J. K., Valent, B., and Albersheim, P. (1984), *J. Biol. Chem., 259*, 11312–11320.

Shelley, R. N., Salwin, H., and Horowitz, W. (1963), *J. Assoc. Anal. Chem., 46*, 486–493.

Shibuya, N. (1984), *Phytochem., 23*, 2233–2237.

Shibuya, N., and Iwasaki, T. (1978), *Agric. Biol. Chem., 42*, 2259–2266.

Shibuya, N., and Misaki, A. (1978), *Agric. Biol. Chem., 42*, 2267–2274.

Shimizu, K., Hashi, M., and Sakurai, K. (1978), *Carbohydr. Res., 62*, 117–126.

Simson, B. W., and Timell, T. E. (1978), *Cellul. Chem. Technol., 12*, 79–84.

Sjostrom, E., Haglund, P., and Janson, J. (1966), *Acta Chem. Scand., 20*, 1718–1719.

Slavin, J. L., and Marlett, J. A. (1983), *J. Agric. Food Chem., 31*, 467–471.

Smith, J. E., and Stainsby, G. (1977), *Brit. Polymer J., 9*, 284–290.

Smith, M. M., and Hartley, R. D. (1983), *Carbohydr. Res., 118*, 65–80.

Smith, M. M., and Stone, B. A. (1973), *Phytochem., 12*, 1361–1367.

Souty, M., Thibault, J. F., Navarro-Garcia, G., Lopez-Roca, J. M., and Breuils, L. (1981), *Science des Aliments, 1*, 67–80.

Spellman, M. W., McNeil, M., Darvill, A. G., Albersheim, P., and Henrick, K. (1983a), *Carbohydr. Res., 122*, 115–129.

Spellman, M. W., McNeil, M., Darvill, A. G., Albersheim, P., and Dell, A. (1983b), *Carbohydr. Res., 122*, 131–153.

Spiro, M. J. (1977), *Anal. Biochem., 82*, 348–352.

Spiro, R. G. (1962), *J. Biol. Chem., 237*, 646–651.

Spiro, R. G. (1972), *Methods Enzymol., 28*, 3–43.

Staudte, R. G., Woodward, J. R., Fincher, G. B., and Stone, B. A. (1983), *Carbohydr. Polymers, 3*, 299–312.

Stephen, A. M. (1983), in *The Polysaccharides*, Vol. 2 (G. O. Aspinall, ed.), Academic Press, New York, pp. 97–193.

Stevens, B. J. H., and Selvendran, R. R. (1980a), *J. Sci. Food Agric., 31*, 1257–1267.

Stevens, B. J. H., and Selvendran, R. R. (1980b), *Phytochem., 19*, 559–561.

Stevens, B. J. H., and Selvendran, R. R. (1984a), *Carbohydr. Res., 135*, 155–166.

Stevens, B. J. H., and Selvendran, R. R. (1984b), *Phytochem., 23*, 339–347.

Stevens, B. J. H., and Selvendran, R. R. (1984c), *Carbohydr. Res., 128*, 321–333.

Stevens, B. J. H., and Selvendran, R. R. (1984d), *Phytochem., 23*, 107–115.

Stewart, T. S., Mendershausen, P. B., and Ballou, C. E. (1968), *Biochem., 7*, 1843–1854.

Stoddart, R. W., Barrett, A. J., and Northcote, D. H. (1967), *Biochem. J., 102*, 194–204.

Strahm, A., Amado, R., and Neukom, H. (1981), *Phytochem., 20*, 1061–1063.

Sutherland, I. W. (1981), *J. Chromatogr., 213*, 301–306.

Svensson, S. (1978), *Methods Enzymol., 50*, 33–38.

Sweet, D. P., Albersheim, P., and Shapiro, R. H. (1975), *Carbohydr. Res., 40*, 199–216.

Sweet, D. P., Shapiro, R. H., and Albersheim, P. (1974), *Biomed. Mass Spectrom., 1*, 263–268.

Takenishi, S., and Tsujisaka, Y. (1973), *Agric. Biol. Chem., 37*, 1385–1391.

Talmadge, K. W., Keegstra, K., Bauer, W. D., and Albersheim, P. (1973), *Plant Physiol., 51*, 158–173.

Taylor, A. J. (1982), *Carbohydr. Polymers, 2*, 9–17.

Taylor, R. L., and Conrad, H. E. (1972), *Biochemistry, 11*, 1383–1388.

Taylor, R. L., Shirely, J. E., Conrad, H. E., and Cifonelli, J. A. (1973), *Biochemistry, 12*, 3633–3637.

Thibault, J. F. (1983), *Phytochem., 22*, 1567–1571.

Timell, T. E. (1962), *Svensk Papperstidn., 65*, 435–447.

Timell, T. E. (1965), *Adv. Carbohydr. Chem. Biochem., 20*, 409–483.

Tran Thanh Van, K., Toubart, P., Cousson, P., Darvill, A. G., Gollin, D. J., Chelf, P., and Albersheim, P. (1985), *Nature, 314*, 615–617.

Tuerena, C. E., Taylor, A. J., and Mitchell, J. R. (1982), *Carbohydr. Polymers, 2*, 193–203.

Usui, T., Yokoyama, M., Yamaoka, N., Matsuda, K., Tuzimura, K., Sugiyama, H., and Seto, S. (1974), *Carbohydr. Res., 33*, 105–116.

Valent, B., Darvill, A. G., McNeil, M., Robertson, B. K., and Albersheim, P. (1980), *Carbohydr. Res., 79*, 165–192.

Versteeg, C. (1979), Ph.D. Dissertation, Agricultural University Wageningen, The Netherlands.

Vliegenthart, J. F. G., Dorland, L., and Van Hahlbeek, H. (1983), *Adv. Carbohydr. Chem. Biochem., 41*, 209–374.

Voragen, A. G. J., Schols, H. A., De Vries, J. A., and Pilnik, W. (1982), *J. Chromatogr., 244*, 327–336.

Voragen, A. G. J., Timmers, J. P. H., Linssen, J. P. H., Schols, H. A., and Pilnik, W. (1983), *Zeitschrift für Lebensmittel-Untersuchung und Forschung, 177*, 251–256.

Waeghe, T. J., Darvill, A. G., McNeil, M., and Albersheim, P. (1983), *Carbohydr. Res., 123*, 281–304.

Waibel, R., Amado, R., and Neukom, H. (1981), *J. Chromatogr., 197*, 86–91.

Waller, G. R., and Dermer, O. C., eds. (1980), *Biochemical Applications of Mass Spectrometry*, Suppl. Vol., Wiley, New York.

Walsh, K. A., Ericson, L. H., Parmalee, D. C., and Titani, K. (1981), *Ann. Rev. Biochem., 50*, 261–284.

West, A. R., ed. (1974), *Adv. Mass Spectrom.*, Vol. 6, Applied Science, London.

Whistler, R. L., and Richards, G. N. (1958), *J. Am. Chem. Soc., 80*, 4888–4892.

Wilkie, K. C. B. (1979), *Adv. Carbohydr. Chem. Biochem., 36*, 215–264.

Wilkie, K. C. B. (1985), in *Biochemistry of Plant Cell Walls:* SEB Seminar Series, Vol. 28 (C. T. Brett and J. R. Hillman, eds.), Cambridge University Press, pp. 1–37.

Wilkie, K. C. B., and Woo, S.-L. (1977), *Carbohydr. Res., 57*, 145–162.

Wise, L. E., Murphy, M., and D'Addieco, A. A. (1946), *Paper Trade Journal, 122*, 35–43.

Wise, L. E., and Ratliff, E. K. (1947), *Anal. Chem., 19*, 459–462.

Wong, C. G., Sung, S.-S. J., and Sweeley, C. C. (1980), *Methods Carbohydr. Chem., 8*, 55–65.

Wood, P. J., and Siddiqui, I. R. (1971), *Anal. Biochem., 39*, 418–428.

Woodward, J. R., Fincher, G. B., and Stone, B. A. (1983), *Carbohydr. Polymers, 3*, 207–225.

York, W. S., Darvill, A. G., and Albersheim, P. (1984), *Plant Physiol., 75*, 295–297.

York, W. S., Darvill, A. G., McNeil, M., and Albersheim, P. (1985), *Carbohydr. Res., 138*, 109–126.

Zitko, V., and Bishop, C. T. (1965), *Can. J. Chem., 43*, 3206–3214.

Methods of Biochemical Analysis, Volume 32
Edited by David Glick
Copyright © 1987 by John Wiley & Sons, Inc.

METHODS OF BIOCHEMICAL ANALYSIS VOLUME 32

Electro-Optical Reflection Methods for Studying Bioactive Substances at Electrode-Solution Interfaces—An Approach to Biosurface Behavior

KIYOKO TAKAMURA AND FUMIYO KUSU, *Tokyo College of Pharmacy, Horinouchi, Hachioji, Tokyo, Japan*

I. INTRODUCTION

Bio- and electrochemists have come to give increasing attention to the interface between a charged surface and aqueous electrolyte solution in recent years. Many bioactive substances are known to be localized at particular points on biosurfaces where they perform various functions in vivo. The complex formation of an enzyme and its substrate, the specific binding of an antigen and its antibody, and the attachment of a neurotransmitter at a site on a biomembrane are typical cases of specific interaction on biosurfaces.

Such substances may initially be attracted to biosurfaces mainly through electrostatic interactions and then sometimes become closely linked to specific sites in a particular orientation or conformation state. Such attachment may be essential to the expression of their biological

functions. However, the structural complexity of a biosurface and the virtual impossibility of identifying interactions at the molecular level prevent basic study of interfacial behavior in vivo. It would be of considerable interest to know how to determine the mechanism involved in the function of substances at biosurfaces.

A biomembrane surface-biological fluid interface may be regarded as a solid-liquid interface exhibiting electrical behavior similar to that at an electrode-electrolyte solution interface (Pilla, 1974). Similarities between electrode interfaces and biomembranes in contact with aqueous solutions have recently been noted (Berry et al., 1985; Bowden et al., 1985).

When a potential is applied on a metal electrode in contact with an electrolyte solution, any excess charge on the electrode resides on its surface. Ions, solvent molecules, and other species in the solution interact with this charged surface to form a structured interfacial region generally called an electrical double layer. The net charge on the solution side of the double layer is opposite in sign to the excess charge on the metal. Although biomembranes are considerably more complex than electrode surfaces, they are also charged surfaces whose polar phospholipid head groups are situated at the surface of the biomembrane of a bilayer structure. Because of the charged surface, opposing charged species exist near the surface of the membrane, as in the case of an electrode-solution interface.

Another similarity is the existence of an ordered (structured) water layer at the respective surfaces. Some water molecules are associated with each lipid head group of phosphatidylcholine bilayers (Hauser, 1975) and exhibit properties different from bulk phase water but qualitatively similar to those of interfacial water at metal electrode surfaces.

Electrode surfaces can thus be expected to resemble biosurfaces with respect to charged surfaces in contact with electrolyte solutions. A study of the electrochemical behavior of bioactive substances should provide useful information regarding biosurface behavior.

In general, two important types of processes occur at the electrode surface in contact with electrolyte solution containing electroactive substances when an appropriate potential is applied: a charge (electron) transfer process that causes oxidation or reduction of the substances and an adsorption-desorption process in which adsorbable species from the solution phase are attached to the electrode surface through replacement of preadsorbed species such as solvent molecules. Electrochemical adsorption is characterized by competitive processes depending on the electrode potential. Furthermore the adsorbed state of a species, particularly its orientation to the electrode surface, affects redox reactivity. In situ studies on the adsorption of bioactive substances on an electrode surface are thus of great interest from a bioelectroanalytical standpoint.

Adsorption studies at the electrode-electrolyte solution interfaces require tools for detecting and characterizing trace amounts (in general, less than monolayer formation) of adsorbed species with high sensitivity and specificity. There are many useful techniques for the study of solid surfaces in vacuo, such as LEED, ESCA, and Auger spectroscopy. However, these are not available for the in situ observation of an electrode surface under actual conditions. That is, an electrode surface in contact with an electrolyte solution becomes polarized on application of a potential, causing a current to flow through the medium. Thus, for an understanding of the interfacial states of an electrode surface under actual conditions, nondestructive methods for the in situ observation are necessary.

In situ electro-optical reflection is a very promising means for meeting this need. There are two such methods, internal and external reflection methods; the latter includes specular reflection spectroscopy, ellipsometry, IR reflection spectroscopy, and surface enhanced Raman scattering (SERS).

In the internal reflection method a light ray is incident from the interior side of an electrode to the interface. Optically transparent electrodes (OTE), such as tin oxide, metal film electrodes in the visible region, are used to obtain absorption spectra of adsorbed species by multiple reflection (Hansen, 1973; Heineman et al., 1984; Kuwana and Winograd, 1974; Mark and Randall, 1970).

In the external method, a light ray strikes the electrode surface from the solution phase. On hitting a well-polished electrode surface, the light is reflected from the interface back to the solution. A quantitative comparison is then made of the properties of the incidental and reflected light. It should be noted that the reflection causes change in the properties of the light, that is, in amplitude and phase, so that the reflected light provides information about the interface.

Although the application of ellipsometry to bioelectrochemistry was anticipated by many workers (Cuypers et al., 1980; Davis et al., 1980; Kruger, 1973; Vroman and Adams, 1969), only a few papers have been published on the adsorption studies of bioactive substances at electrodes by this method (Humphreys and Parsons, 1977; Kinoshita et al., 1977b; Kunimatsu and Parsons, 1979; Stenbery et al., 1977). Since the first attempt was made in 1970 (Takamura et al., 1970), the usefulness of the specular reflection method in the visible region in in situ observation of an electrode-solution interface during electrolysis has frequently been noted by the authors. Excellent reviews are available on the background of the theory and techniques of specular reflection spectroscopy. (McIntyre, 1973a; Takamura and Takamura, 1978). More recently the application of

IR reflection (Bewick, 1983; Habib and Bockris, 1984) and SERS (Cotton et al., 1980; Ervin et al., 1980; Fleischmann and Hill, 1983; Koglin and Séquaris, 1983) has been examined and is expected to find future development in the field of surface electrochemistry.

In this chapter the techniques and experimental procedures of the specular reflection method are discussed in detail. Its application to the study of the adsorption of various biologically important substances to electrode surfaces is presented, and an attempt is made to elucidate the biosurface behavior of these substances.

II. PRINCIPLE

1. Specular Reflection of Light at an Electrode-Solution Interface

A. REFLECTIVITY CHANGE ARISING FROM AN ADSORBED LAYER ON AN ELECTRODE SURFACE

Figure 1 shows a solid electrode surface covered by an optically uniform film in contact with an electrolyte solution. The "film" actually corresponds to an adsorbed layer on the surface. When a light beam passing through the solution is reflected at the surface, the reflectivity is defined as the ratio of reflected light intensity to that of the incident beam. Because of the difficulty in measuring absolute reflectivity, relative reflectivity denoted as R/R_0 is conveniently obtained and is the ratio of the reflectivities in the presence and absence of the film. R/R_0 is simply "reflectivity" in this review.

The difference in the optical properties of the film and those of other phases such as the solution results in change in reflectivity at the surface. Provided that the film is extremely thin compared to the wavelength of the light, McIntyre and Aspnes (1971) derived the following relation on the basis of the Drude equation of reflectivity for a three-phase model (Fig. 1); that is, an uniform thin film is "sandwiched" between two different bulk dielectrics. This assumption practically holds for an adsorbed monolayer several angstroms thick. The reflectivity change $\Delta R/R_0$ at the monolayer coverage (i.e., surface coverage $\theta = 1$) observed by the perpendicularly polarized light (designated by the subscript $\perp$) is given by (1),

$$\left(\frac{\Delta R}{R_0}\right)_{\perp,\theta=1} = \frac{8\pi d\, n_s \cos\phi}{\lambda} \operatorname{Im}\left(\frac{\hat{\varepsilon}_{ad} - \hat{\varepsilon}_M}{n_s^2 - \hat{\varepsilon}_M}\right) \tag{1}$$

where d is the thickness of the adsorbed layer, ϕ the incidental angle, λ the wavelength of the incident light ray, and n_s the refractive index of the

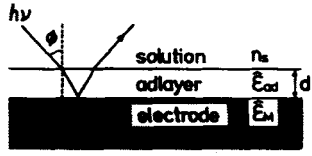

Fig. 1. Three-phase model of electrode-solution interface.

bulk electrolyte solution. $\hat{\varepsilon}_{ad}$ and $\hat{\varepsilon}_M$ are the complex dielectric constants of the adsorbed layer and metal substrate, respectively.

The following equations are generally obtained:

$$\hat{\varepsilon} = \varepsilon' - i\varepsilon'' \qquad (i = \sqrt{-1}) \tag{2}$$

$$\varepsilon' = n^2 - k^2 \tag{3}$$

$$\varepsilon'' = 2nk \tag{4}$$

where k is the extinction coefficient. It should be noted that equation (1) is important for indicating the proportionality between $\Delta R/R_0$ and d; the coefficient includes the optical constants of each phase.

B. ADSORPTION STUDY BASED ON REFLECTIVITY CHANGE

When the amount of adsorption is less than monolayer coverage, the change in reflectivity due to adsorption at θ is expressed as (McIntyre, 1973; McIntyre and Aspnes, 1971)

$$\left(\frac{\Delta R}{R_0}\right)_{\perp,\theta} = \left(\frac{\Delta R}{R_0}\right)_{\perp,\theta=1} \cdot \theta \tag{5}$$

provided $\hat{\varepsilon}_{ad}$ and $\hat{\varepsilon}_M$ are not altered during adsorption. Equation (5) refers to the proportionality between the observed values of reflectivity change and surface coverage, indicating the applicability of the reflection technique to the study of adsorption.

2. Electrode Processes

Application of the foregoing relations to the study of adsorption at electrode surfaces requires an understanding of the electrochemical processes at electrode-solution interfaces. Consider an electrode in contact with a solution containing electroactive species along with supporting electrolytes. Two important processes occur at the electrode surface: a *faradaic* process in which electrons are transferred across the electrode-solution interface (oxidation-reduction reaction). As a result of these reactions current flows through the medium. Adsorption-desorption is

another process that occurs. Both generally occur when an electrode reaction takes place.

An overall electrode reaction may be expressed as

$$\text{Oxid.} + ne \rightleftharpoons \text{Red.}$$

in which the oxidized species (Oxid.), dissolved in solution, is converted by the number of electrons *(ne)* to its reducted form, Red. In general, the reaction proceeds as follows:

1. Mass transfer of Oxid. and Red. from the bulk solution to the electrode surface.
2. Electron transfer at the electrode surface.
3. Adsorption and desorption at the electrode surface.

Adsorption and desorption phenomena often actually take place at the electrode surface (Fig. 2). Generally, adsorption from solution is characterized by competition between solute and solvent molecules. The electrode-solution interface can thus be assumed to conform to the illustration in Fig. 3, where electroactive species are adsorbed through replacement of preadsorbed solvent molecules.

The simplest reactions of nonadsorbed species involve only mass and electron transfers. However, more complex reactions involve chemical reactions preceeding or following electron transfer, such as protonation, dimerization, or tautomerization.

3. In Situ Observation of Adsorption by the Specular Reflection Method

A. OBSERVATION OF REFLECTIVITY CHANGE DURING A POTENTIAL SCAN

When a potential applied to an electrode is scanned at a constant rate from a negative to positive potential side, or vice versa (so-called linear sweep voltammetry), adsorption and desorption may occur at the electrode-solution interface. Consider an organic species adsorbed onto an electrode surface at a given potential range. That the molecular refractive index of organic species is generally larger than that of the water molecule makes it possible to predict $n_{ad} > n_s$. In cases where the adsorbed layer exhibits no light absorption (i.e., $k_{ad} \approx 0$), (6) can be derived from (1)–(4):

$$\left(\frac{\Delta R}{R_0}\right)_{\perp,\theta=0} = \frac{-8\pi d n_s \cos\phi}{\lambda} \cdot \frac{\varepsilon''_M (n_{ad}^2 - n_s^2)}{(n_s^2 - \varepsilon'_M)^2 + \varepsilon''^2_M} \tag{6}$$

The right-hand side of (6) takes a negative value; that is, $(\Delta R/R_0)_{\perp,\theta=1}$ is negative. This suggests that the adsorption of organic species causes a

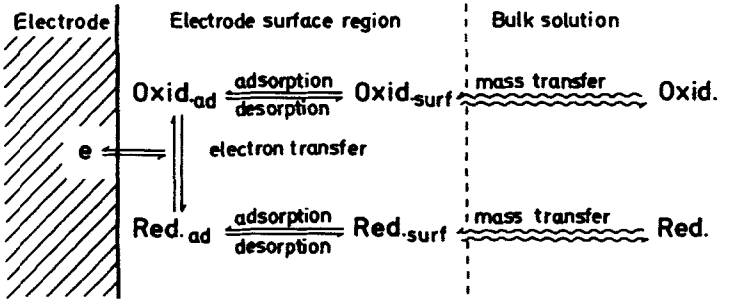

Fig. 2. Electrochemical processes at electrode-solution interface.

decrease in reflectivity, as has been verified experimentally in many cases of organic adsorption on solid electrodes (Kusu, 1985a; Takamura et al., 1973, 1974, 1979).

The mode of reflectivity change observed with the scanning of applied potential E ($R/R_0 - E$ curve) is schematically depicted in Fig. 4. Typical results for solutions with or without organic species are shown in Fig. 4, from which it is evident that R/R_0 drops in value in the potential range where adsorption takes place.

B. REFLECTIVITY CHANGE AT ADSORPTION EQUILIBRIUM

Quantitative analysis of adsorption requires determination of $\Delta R/R_0$ values in the equilibrium state at a fixed potential. In cases of organic

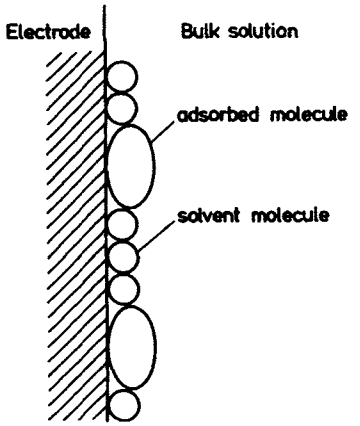

Fig. 3. Proposed model of electrode-solution interface.

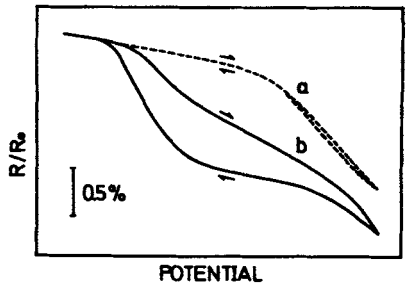

Fig. 4. Reflectivity versus potential curves obtained with solutions with and without organic species.

adsorption, ample time is generally required for establishment of equilibrium. Attainment of adsorption equilibrium can be confirmed experimentally by R/R_0 versus time measurements (see Fig.5). The electrode potential is first set at E_1, where the presence of organic species in solution gives no change in R/R_0 (indicating no adsorption of organic species to take place at E_1). Then the potential is stepped up to E_2, and the R/R_0 -time curve is recorded until the R/R_0 takes on a constant value (i.e., adsorption is equilibrated at E_2). The same procedure is applied to the supporting electrolyte solution as a reference. Then the difference between the magnitudes of reflectivity decrease of the former and the latter, denoted as $\Delta R/R_0$, can be obtained.

C. POTENTIAL AND CONCENTRATION DEPENDENCE OF ADSORPTION

In electromechanical adsorption, the surface coverage of adsorbed molecules is effected not only by the bulk concentration of solute but by electrode potential. Since $(\Delta R/R_0)_{\perp,\theta}$ is proportional to θ, $\Delta R/R_0$ as a function of potential as well as concentration provides significant information regarding adsorption characteristics.

The mode of potential dependence of adsorption is characterized with

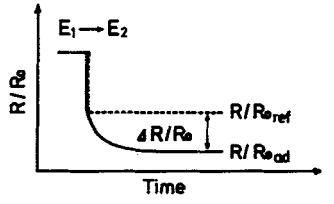

Fig. 5. Reflectivity change versus time relation in the potential step method.

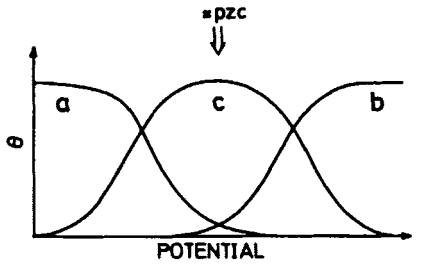

Fig. 6. Potential dependence of adsorption.

respect to the ionic properties of the adsorbed species. In general, cationic and anionic adsorption become predominant in negative and positive potential regions, respectively (Fig. 6*a* and *b*). In contrast, adsorption of neutral molecules favorably occurs around point of zero charge (pzc), and their adsorptivity is gradually lowered as the electrode potential deviates from pzc, as a result of competition with ionic species for adsorption sites on the electrode surface. According, θ versus E is a bell-type relation having a maximum at pzc (Fig. 6*c*).

Increasing the bulk concentration results in increased adsorption, and consequently, enhancement of reflectivity change, but $\Delta R/R_0$ becomes saturated at a sufficiently high concentration. A typical example is shown in Fig. 7, where the magnitude of $\Delta R/R_0$, $|\Delta R/R_0|$, versus concentration exhibits a Langmuir-like isotherm. Analysis of the relation on the basis of an appropriate isotherm equation offers fundamental data on adsorption, such as area occupied by one adsorbed molecule and the free energy change in adsorption.

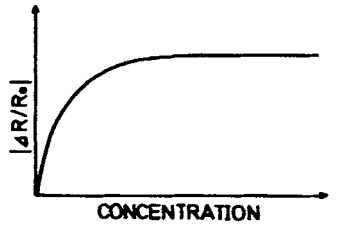

Fig. 7. Concentration dependence of reflectivity change.

D. ELECTROREFLECTANCE SPECTRUM

In the electroreflectance or electromodulation method (McIntyre, 1973b), the electrode potential can be modulated by superposing a sinusoidal wave alternating potential of small amplitude $\pm\Delta E$ on the applied scanning potential for electrolysis (Fig. 8). The resulting reflectivity changes can be detected by a lock-in technique and electroreflectance signal $(1/R_0)(\partial R/\partial E)$ at a fixed wavelength versus the E relation is obtained. This relation, corresponding to a differential form of the $R/R_0 - E$ curve, makes it possible to detect minor changes in reflectivity by as much as $10^{-2}\%$.

Observation of $(1/R_0)(\partial R/\partial E)$ at a fixed potential as a function of incident light wavelength gives an electroreflectance spectrum. When the adsorbed species are light absorbing, the electroreflectance spectrum at times exhibits characteristic peaks at the wavelengths of absorption maxima, thus providing further information on the adsorbed states of the species.

III. EXPERIMENTAL TECHNIQUES

Instrumental specifications for specular reflection spectroscopy have been reviewed in detail by McIntyre (1973a). Typical apparatus, electro-optical cells, and electrodes for specular reflection spectroscopy and measurement procedures used in the spectroscopy are described in this section.

1. Apparatus

Figure 9 shows a block diagram of the apparatus for specular reflection spectroscopy. Specular reflection measurements were carried out in conjunction with conventional electrochemical methods; the potential was

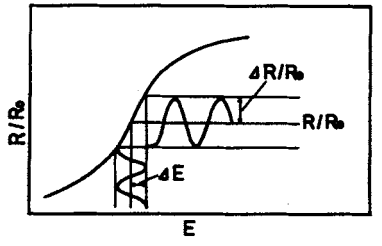

Fig. 8. Electromodulation for electroreflectance method.

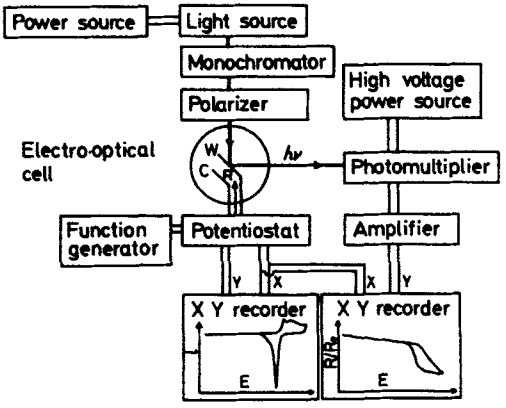

Fig. 9. Block diagram of apparatus for specular reflection spectroscopy

applied from a potentiostat connected to a function generator. In the figure monochromatic light passes through a polarizer to render it linearly polarized, and the optical axis is set either perpendicular or parallel to the plane of incidence. The light is then directed to the working electrode surface. The intensity of the reflected beam is monitored by a photomultiplier. The relative reflectivity, R/R_0, the ratio of the intensity of the reflected beam to that of the reference beam, is recorded as a function of the applied potential, E, or time, t, on an XY recorder. A current-potential, $i - E$, curve is usually recorded simultaneously on another XY recorder.

In the electroreflectance method a sinusoidal wave alternating potential (about 10 − 100 Hz) is superimposed on a conventional linear potential generally used in specular reflection measurements. A lock-in amplifier is used to detect resulting changes in which reflected light intensities are proportional to $\partial R/\partial E$. The response of $1(1/R_0)(\partial R/\partial E)$ is recorded as a function of the linear potential on an XY recorder.

Commercial spectrophotometers provided with adequately large sample compartments are suitable for specular reflection measurements, although an electro-optical cell setting assembly must be fitted to the sample compartment and both equipped with a polarizer. An example of such an optical system is shown in Fig. 10. The main features are a light source (LS, a halogen lamp for the visible range), slit systems ($S1$, $S2$), a monochromator, polarizer ($O2$), a semitransparent mirror ($M5$), and two photomultipliers (PM_1, PM_2). The bar A is designed so as to control the angle of incidence. The electro-optical cell (E) is placed at the center of the

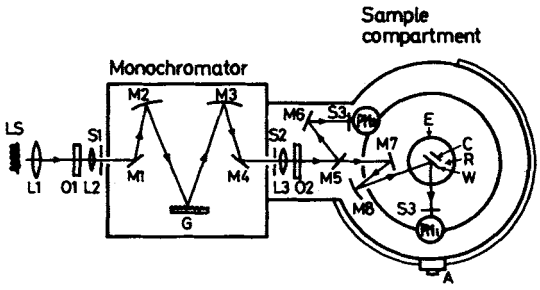

Fig. 10. Optical system of apparatus for specular reflection spectroscopy: *LS*, light source; *M5*, semitransparent mirror; *O2*, polarizer; PM_1 and PM_2, photomultipliers; *G*, grating; *A*, bar for changing the incidental angle; *W*, working electrode; *R*, reference electrode, *C*, counter electrode; *E*, electro-optical cell. (From Kusu and Takamura, 1985b, with permission.)

circular sample compartment on the bar, and the reflected beam from the working electrode surface is always directed to the photomultiplier (PM_1) for any incidental angle. The light paths are indicated by arrows.

2. Electro-Optical Cell

An example of a single-reflection electro-optical cell is shown in Fig. 11. A polished metal plate (e.g., gold) used as a working electrode *(W)* is fixed to a Teflon holder *(a)*. This assembly, after being fixed vertically to the Teflon lid *(c)*, is inserted into a quartz cell *(b)* provided with cylindrical optics; the angle of incidence is variable. Compartments *e* and *f* are joined to the main compartment of the cell by means of fritted glass discs. Compartment *f* with a Luggin capillary *(d)* contains the reference electrode *(R)*, such as an Ag/AgCl or saturated calomel electrode, and the other, counter electrode *(C)*, such as an Au plate or Pt wire. The tip of the Luggin capillary is placed near the working electrode but is kept out of the optical path. The Teflon lid *(c)* covers the quartz cell so that the cell compartment is airtight during operation under an inert atmosphere, such as that of argon gas. This lid has several holes *(h)* near its perimeter to enable the cell to be fixed at the center of the sample compartment. Two holes are for the gas inlet *(i)* and outlet *(j)*.

3. Working Electrodes

To ensure optically smooth and flat surfaces, vacuum-evaporated or sputtered metal films on smooth substrates are recommended for specu-

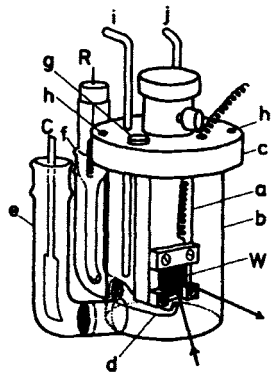

Fig. 11. Electro-optical cell: *W*, working electrode; *R*, reference electrode; *C*, counter electrode; *a*, Teflon holder; *b*, cylindrical quartz cell; *c*, Teflon lid; *d*, Luggin capillary; *e*, compartment for counter electrode; *f*, compartment for reference electrode; *g*, sample inlet; *h*, screw hole; *i*, gas inlet; *j*, gas outlet. (From Kusu and Takamura, 1985b, with permission.)

lar reflection spectroscopy (McIntyre, 1973a). In doing so, certain problems may be encountered such as the peeling of film, used as working electrodes, from the substrates due to repeated electrolysis. Rolled metal plates, polished to a mirror surface, are easier to prepare and use in routine electrolysis. Although various metals such as Au, Pt, Pd, and Ag can be used for working electrodes in specular reflection spectroscopy, gold is best from an electroanalytical standpoint in view of its electrochemical inertness over a wide potential range.

The area of an working electrode is determined by the size of the incident light beam. Gold plates of high purity are generally used and range from 1–3 cm on edge and 0.2–0.5 mm in thickness.

To ensure maximum specular reflectivity and avoid a situation where signals cannot be read accurately due to the presence of contaminating substances on the electrode surface, great care must be taken in the surface preparation, and contaminating substances must not be allowed to settle on the surface. Thus the electrodes must be carefully cleaned before use in order to obtain reproducible specular reflection data. For this purpose, various procedures for cleaning solid electrodes are recommended (Bewick and Thomas, 1975; Droog et al., 1979; Gardner and Woods, 1977; Hinnen et al., 1983; Woods, 1976). In bioanalytical studies, the following cleaning procedure should prove adequate: polishing the gold plate mechanically with 0.3 μm alumina powder, thoroughly wash-

ing it with redistilled water, and finally cleaning it electrochemically by applying a scanning potential in a supporting electrolyte solution.

4. Procedure

The present authors generally perform the following procedure to obtain $R/R_0 - E$ and $R/R_0 - t$ curves:

1. Establish proper optical conditions in regard to wavelength, polarization, and incidental angle of light.
2. Pipette a certain amount of supporting electrolyte solution, prepared by dissolving reagents in highly pure water, into the electro-optical cell provided with a clean gold plate as the working electrode. The amount of supporting electrolyte solution will vary according to electro-optical cell and working electrode size and electrode position. The working electrode must be completely immersed in the supporting electrolyte solution.
3. Remove dissolved oxygen from the supporting electrolyte solution by bubbling pure argon gas through it.
4. Create proper electrolysis conditions in regard to initial potential, potential range and potential sweep rate so as to record the $i - E$ curves and/or $R/R_0 - E$ curves. For a detailed procedure of linear sweep voltammetry, consult references Adams (1969), Bard and Faulkner (1980), Elving et al. (1973), and Nicholson (1965).
5. Measure both $R/R_0 - E$ and $i - E$ at the same time, and/or $R/R_0 - t$ of the gold electrode in the supporting electrolyte solution.

For measurement of $R/R_0 - t$, the potential step method is frequently used: the electrode potential is first set at a potential where no adsorption of the sample occurs and then stepped up to the second potential where adsorption does occur. The $R/R_0 - t$ curve continues to be recorded until no further change in R/R_0 takes place.

6. The sample is then added to the supporting electrolyte solution through which argon gas is being bubbled, accompanied by gentle stirring.
7. The operation in step 5 is repeated but in a solution containing the sample.

IV. ADSORPTION OF DNA-RELATED SUBSTANCES

In recent years adsorption of nucleic acid bases and their derivatives on a gold electrode has been investigated by the present authors (Takamura et al., 1979; 1981a). This section deals first with the adsorption of adenine

for a typical example to show how the optical reflection method can be applied to the observation of its interfacial behavior and then with an extension of the method to its related substances. All the data cited here were obtained under such experimental conditions that wavelength and angle of incidental light were fixed at 500 nm and 15°, respectively, so as to get maximal signals for the reflectivity changes.

1. Adsorption of Adenine and Observed Reflectivity Change

Figure 12 shows $i-E$ and R/R_0-E curves of gold measured simultaneously in the supporting electrolyte (0.1 M $NaClO_4$) solution containing different concentrations of adenine. The potential scan was started from -1.1 V to the positive potential side and reversed at 0.4 V with a sweep rate of 100 mV s^{-1}. As seen in the figure, the supporting electrolyte gives only a flat double layer region on the $i-E$ curve over whole potential range investigated (curve a, dashed line), but the R/R_0-E curve is characterized by two approximately linear portions with different slopes intersecting at about -0.1 V for the sweep in either the anodic or cathodic direction (curve c). This potential value corresponds to pzc for gold in neutral solutiosn (Bodé et al., 1967; Damaskin et al., 1971); therefore the electrode is negatively (or positively) charged at the potentials that are more negative (more positive) than this potential.

When adenine was added to the solution, no appreciable change was found on the $i-E$ curve (Figure 12, curve b, solid line), although the marked decrease in reflectivity was observed on the R/R_0-E curves in the potential region more positive than -0.8 V (curves d, e, and f in Fig. 12, in which the R/R_0-E curves are drawn separately to avoid their overlap). The reflectivity change was enhanced with the increase in the adenine concentration, but it tended to be saturated when the adenine concentration was more than 1×10^{-4} M.

Such a trend suggests that the adsorption of adenine takes place on the gold electrode surface, because the adsorption of organic compounds usually produces the decrease in reflectivity, as stated earlier. The hysteresis on the R/R_0-E curve, which is most evident in the intermediate concentration, may be associated with the slow adsorption-desorption of adenine, as is known in some cases (Takamura et al., 1971, 1974).

2. Adsorption Characteristics of Adenine

In order to know the potential dependence of the adenine adsorption, $\Delta R/R_0$ at adsorption equilibrium was obtained from the R/R_0 versus t measurement by a potential step method with the solutions containing different concentrations of adenine. The potential was first set at -0.1 V,

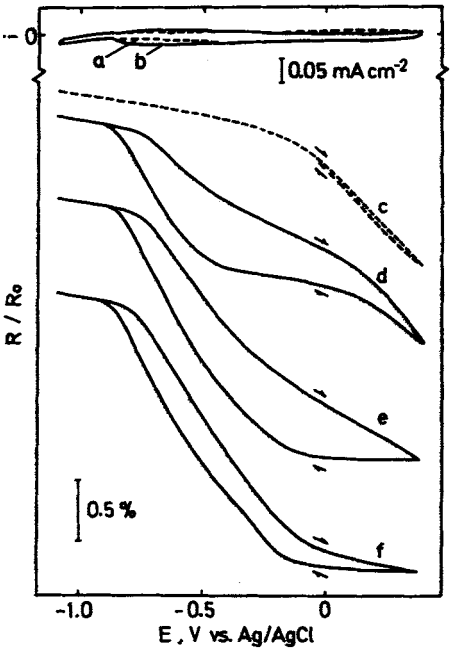

Fig. 12. Current versus potential and reflectivity versus potential curves of Au in 0.1 *M* $NaClO_4$ in the absence and presence of adenine. Adenine concentration: (*a* and *c*) 0, (*b* and *f*) 1.2×10^{-4}, (*d*) 9.0×10^{-6}, (*e*) 3.6×10^{-5} *M*. Wavelength: 500 nm. Potential sweep rate: 100 mV sec^{-1}. (From Takamura et al., 1979, with permission.)

where no adsorption of adenine is expected, and then stepped to a more positive value, and the subsequent decay of R/R_0 was recorded until there was no further decrease in R/R_0. The magnitude of $\Delta R/R_0$, $|\Delta R/R_0|$, is plotted against the electrode potential in Fig. 13, in which the $|\Delta R/R_0|-E$ curves are of a quasi-bell type having a maximum at -0.1 V. It is clearly seen that the adsorption of adenine occurs in a more positive potential region than -0.8 V and atains its maximum at -0.1 V. This potential agrees with the pzc observed in the supporting electrolyte solution. When the concentration of adenine is more than 1.0×10^{-4} *M*, the $|\Delta R/R_0|$ at -0.1 V tends to a limiting value, indicating saturation of the adsorption. The $|\Delta R/R_0|$ versus concentration plots at given potentials (Fig. 14) show a Langmuir-like isotherm. No point of discontinuity is found in both the relations of $|\Delta R/R_0|$ versus E and $|\Delta R/R_0|$ versus concentration, suggesting that no orientational change takes place at least in the potential region observed.

Quantitative analysis of the adsorption isotherm of adenine can be made by the procedure stated earlier. The value of θ can be calculated according to (5), assuming the limiting value of $|\Delta R/R_0|$ at pzc to correspond to the reflectivity change at $\theta = 1$. Since the adsorption behavior of adenine observed in Figs. 13 and 14 is very similar to those in the adsorption of aromatic hydrocarbons on a gold electrode studied by Dahms and Green (1963), the present data were analyzed based on the same isotherm that they used. The isotherm is represented by (7):

$$\frac{\theta}{(1-\theta)^p} = cK \tag{7}$$

where p is the number of water molecules being replaced by one molecule of adsorbed species, and c is the concentration in bulk solution. The constant K is the adsorption coefficient given by (8):

$$K = \exp\left(-\frac{\Delta G^0_{ad}}{RT} + \frac{\alpha F \bar{E}}{RT}\right) \tag{8}$$

where ΔG^0_{ad} is the standard free energy change of adsorption at the pzc, α a constant, and $\bar{E}$ the potential difference between the pzc and the potential at which the observation is made. Equation (7) is found to hold in the potential region where the orientation of the adsorbed solvent molecules is independent of potential.

The use of equation (7) enables us to know the area occupied by

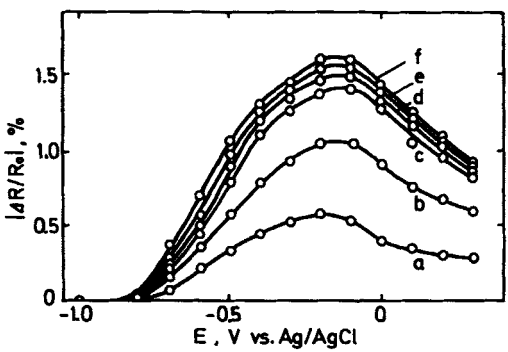

Fig. 13. Potential dependence of the reflectivity change due to the adsorption of adenine. Adenine concentration: *(a)* 1.8×10^{-6}, *(b)* 3.6×10^{-6}, *(c)* 9.0×10^{-6}, *(d)* 1.8×10^{-5}, *(e)* 3.6×10^{-5}, *(f)* 1.2×10^{-4} *M*. Wavelength: 500 nm. (From Takamura et al., 1979, with permission.)

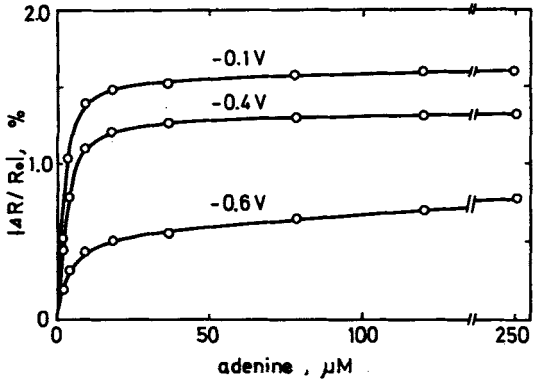

Fig. 14. Concentration dependence of the reflectivity change due to the adsorption of adenine.

adsorbed adenine on the electrode surface in terms of p. Combination of equations (7) and (8) leads to (9):

$$2.30 \log\left(\frac{\theta}{c}\right) = 2.30\, p \log(1-\theta) - \frac{\Delta G^0_{ad}}{RT} + \frac{\alpha F \bar{E}}{RT} \qquad (9)$$

Then the determination of p and ΔG^0_{ad} can be made using the data in Fig. 13 according to the following procedure: The potential range is restricted to the negatively polarized region (i.e., between -0.1 and -0.8 V) when the pzc remains unchanged throughout the measurement. A linear relation between $\log c$ and $\bar{E}$ is obtained at constant $|\Delta R/R_0|$ (i.e., at constant θ) from which the value of $\alpha F/2.3RT$ is calculated to be 11.2. Assuming that the limiting value of $|\Delta R/R_0| = 1.7\%$ in Fig. 13 corresponds to the reflectivity change at the monolayer coverage of adenine, the numerical values of p and ΔG^0_{ad} can be obtained using equation (9). The parameter p can be determined from either $\log(\theta/c)$ versus $\log(1-\theta)$ plot at a constant potential or $\log\theta - (\alpha F\bar{E}/2.3RT)$ versus $\log(1-\theta)$ plot in a given concentration.

Examples of these two plots are shown in Figs. 15 and 16, respectively. Both the plots give straight lines and the values of p obtained from Figs. 15 and 16 are 4.7 and 4.8, respectively. The linearity of these plots, as well as the coincidence in p values obtained by the different methods, suggests that the present treatment based on equation (7) is valid. The intercept of $\log(\theta/c)$ versus $\log(1-\theta)$ gives the value of ΔG^0_{ad} as -58.6 kJ mol^{-1}.

From the value of p the area occupied by one adenine molecule on the electrode surface can be calculated to be approximately 0.42 nm^2, assum-

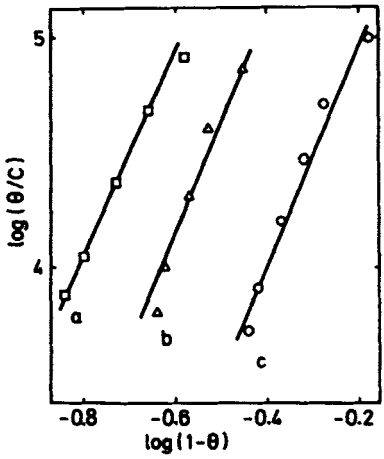

Fig. 15. Plots of $\log(\theta/c)$ versus $\log(1-\theta)$ for adenine adsorption. The values of θ were calculated using the values of $\Delta R/R_0$ at *(a)* −0.3, *(b)* −0.4, and *(c)* −0.5 V in Fig. 13. (From Takamura et al., 1979, with permission.)

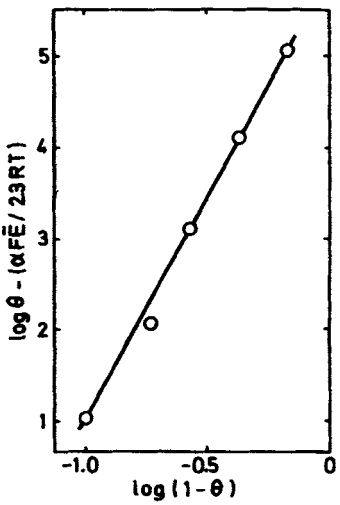

Fig. 16. Plot of $\log\theta - (\alpha F\bar{E}/\,2.3\,RT)$ versus $\log(1-\theta)$ for adenine adsorption using the curve *e* in Fig. 13. (From Takamura et al., 1979, with permission.)

ing that of adsorbed water to be 0.09 nm^2. The value for adsorbed adenine is in fair agreement with the value 0.42 nm^2, which is the planar area of the molecule estimated from the crystal structure of adenine reported by Donohue (1968). Then it is quite likely that adenine is adsorbed in a flat orientation on the negatively charged electrode surface. This value is also close to that of the area occupied by adenine on a mercury electrode (Kinoshita et al., 1977a, b).

3. Nucleic Acid Bases and Their Nucleosides and Nucleotides

A. REFLECTIVITY-POTENTIAL CURVES

The procedure described here was extended to the analysis of adsorption of other nucleic acid bases and their nucleosides and nucleotides on a gold electrode.

When the bases were present in solution, no appreciable change in the $i - E$ curve was observed, however, a marked decrease in reflectivity was observed for the R/R_0-E curves in potential regions more positive than -0.8 V when guanine was present (Fig. 17, curve *d*), and at regions more positive than about -0.5 V when thymine or cytosine was present (curves *f* and *g*). The R/R_0-E curve for adenine is inserted for comparison in Fig. 17, in which the R/R_0-E curves are drawn separately as in Fig. 12. As with adenine, the change in reflectivity increased with an increase in base concentration and reached a limiting value at higher concentrations, suggesting that a state of saturation had been reached. This result suggests that the adsorption of guanine, thymine, and cytosine also takes place on the gold electrode surface.

A comparison of the R/R_0-E curves shows that adenine and guanine begin to be adsorbed at more negative potentials than thymine and cytosine. This suggests that the purine bases having both pyrimidine and imidazole rings are more readily adsorbed than pyrimidine bases. The same tendency was observed for adsorption of nucleic acid bases at a mercury electrode by Brabec et al. (1978). Adsorptivity should increase according to the number of rings in the heterocyclic compounds. Such a finding has been reported by Takamura et al. (1974) for the adsorption of aromatic hydrocarbons, such as benzene, naphthalene, and anthracene on gold; that is, the adsorptivity of hydrocarbon molecules increases with the number of aromatic rings.

The $i-E$ and the R/R_0-E curves of gold were also measured simultaneously in the presence of deoxynucleosides and deoxynucleotides of these bases. The presence of these derivatives caused no appreciable change in the $i-E$ curves, whereas it led to a remarkable reflectivity

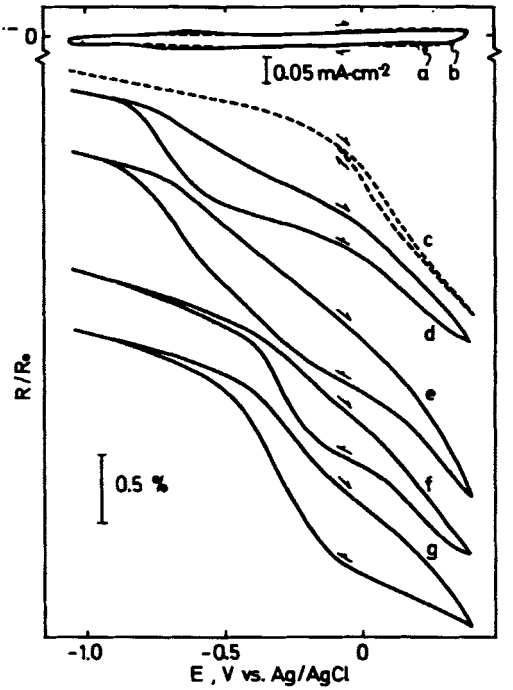

Fig. 17. Current versus potential (*a* and *b*) and reflectivity versus potential (*c* ~*g*) curves of Au in 0.1 *M* $NaClO_4$ in the absence (*a* and *c*) and the presence (*b* and *d*) of 1.0×10^{-5} *M* adenine, *(e)* 1.8×10^{-6} *M* guanine, *(f)* 2.5×10^{-5} *M* thymine, *(g)* 1.1×10^{-5} *M* cytosine. (From Takamura et al., 1981a, with permission.)

decrease as shown in the R/R_0-E curves, indicating that these derivatives are also adsorbed on a gold electrode.

B. POTENTIAL AND CONCENTRATION DEPENDENCE OF THE ADSORPTION

In Figs. 18 and 19 the experimentally obtained $|\Delta R/R_0|$ values due to the adsorption of nucleic acid bases and their derivatives are plotted against the applied potential. Here $|\Delta R/R_0|$ increases with increasing potentials from about -0.8 or -0.5 V to near the pzc where the maximum $|\Delta R/R_0|$ is obtained. The curves at negative potential regions reveal various shapes depending on the adsorbed compound and its concentration. The higher the concentration, the larger is $|\Delta R/R_0|$ value. However, a point of saturation is eventually reached. The saturation concentration for each compound was used in obtaining curves marked *b* in Figs. 18 and 19.

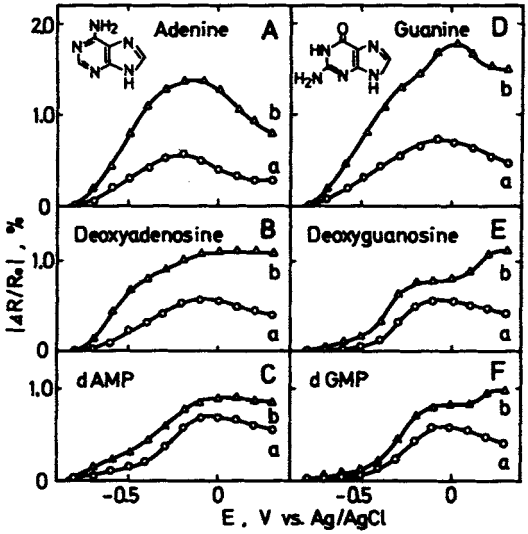

Fig. 18. Potential dependence of the reflectivity change obtained with 0.1 *M* $NaClO_4$ solutions containing adenine, guanine, and their derivatives. Concentration: A (a) 1.8, (b) 18.0; B (a) 1.4, (b) 14.0; C (a) 2.7, (b) 14.0; D (a) 0.9, (b) 19.3; E (a) 0.9, (b) 10.0; F (a) 2.0, (b) 9.4×10^{-5} *M*. (From Takamura et al., 1981a, with permission.)

C. ADSORPTION OF PURINE DERIVATIVES

The $|\Delta R/R_0|-E$ plots obtained for adenine, guanine, and their derivatives are shown in Fig. 18. In the case of adenine (Fig. 18*A*), the $|\Delta R/R_0|-E$ curves are of a quasi-bell type having a maximum at −0.1 V. The maximum value of $|\Delta R/R_0|$ increased with increasing adenine concentration but tended to a limiting value at concentrations $>1.0 \times 10^{-4}$ *M*. The $|\Delta R/R_0|-E$ relation gives a smooth curve for any concentration, suggesting that the orientation of the adsorbed adenine molecules changes very little in the observed potential region.

In general, adsorption of neutral molecules at the electrode surface depends on the electrode potential, and the amount adsorbed shows a so-called bell-type dependence on the potential having a maximum at pzc. The adsorption of adenine is regarded as an example of such a case. Contrary to this, deoxyadenosine and dAMP give no simple bell-type $|\Delta R/R_0|-E$ relations (see Fig. 18*B* and *C*); that is, the decrease in $|\Delta R/R_0|$ is not as significant as for adenine at potentials more positive than −0.1 V.

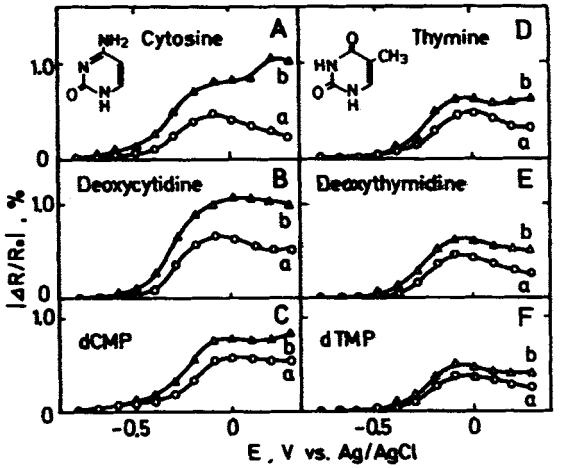

Fig. 19. Potential dependence of the reflectivity change obtained with 0.1 *M* $NaClO_4$ solutions containing cytosine, thymine and their derivatives. Concentration: *A (a)* 0.7, *(b)*, 11.3; *B (a)* 1.3, *(b)* 10.3; *C (a)* 1.4, *(b)* 14.3; *D (a)* 1.2, *(b)* 12.3; *E (a)* 1.1, *(b)* 10.0; *F (a)* 1.0, *(b)* 9.0 × 10^{-5} *M*. (From Takamura et al., 1981a, with permission.)

This seems to indicate that the deoxyribose and phosphate groups participate in the adsorption process, especially in the positive potential region.

For guanine, $|\Delta R/R_0|$ increases at potentials more positive than −0.8 V, and a bell-type $|\Delta R/R_0|-E$ curve is given only at lower concentration (see curve *a* in Fig. 18*D*); however, the shape of this curve becomes somewhat complex at high concentrations, with a round hump around zero V (see curve *b*). The increase in $|\Delta R/R_0|$ near zero V is relatively small compared to the size of $|\Delta R/R_0|$, and the $|\Delta R/R_0|$ versus the concentration relation obtained at the potentials does not show a stepped-shaped curve suggesting multilayer adsorption. Thus the characteristic change in the $|\Delta R/R_0|-E$ curve around zero V is not due to formation of a multilayer. From these results it would be expected that guanine is adsorbed differently at different potentials and concentrations. For example, the reorientation of the molecule from parallel to perpendicular to the electrode surface, and/or the stacking and dimerization of adsorbed molecules, may occur beyond a certain concentration of guanine. The structure of guanine seems to be capable of the formation of intermolecular hydrogen bonding, NH····O. It seems likely that guanine takes an associated form, since the energy of self-association of guanine calculated by Pullman et al.

(1966) is two or more times larger than that of adenine, and the structure of hydrogen-bonded guanine dimer has been referred to in the crystallographic study (Iball and Wilson, 1963).

In the $|\Delta R/R_0|-E$ curves of deoxyguanosine and dGMP (Fig. 18*E* and *F*), the potential at which $|\Delta R/R_0|$ begins to increase is about -0.5 V, which is less negative than for guanine. Owing to the repulsion between their substituent groups and the negatively charged electrode surface, the adsorptivity of the derivatives in the negative potential region seems to be less than for guanine. The curves of deoxyguanosine and dGMP at lower concentration reveal quasi-bell-type shaped curves. However, the features of the curves change with concentration; that is, further increase in $|\Delta R/R_0|$ is observed at potentials more positive than 0.1 V with increase in concentration. This behavior, which is different from that of guanine, suggests that the participation of deoxyribose and phosphate groups in the adsorption is strongly dependent on the surface concentration and charge. The adsorptivity of deoxyguanosine and dGMP in the positive potential region would be intensified by the interaction between the substituent groups and the electrode surface. The somewhat abrupt increase in $|\Delta R/R_0|$ near 0.2 V of curve *b* in Fig. 18*E*, and *F* suggests a change of interfacial orientation and/or an increase in the amount adsorbed due to the interaction of negative charges contributed by deoxyribose and phosphate with the positively charged electrode surface.

Guanine, having $-NH_2$ and $=O$ as substituents, shows more complex adsorption behavior than adenine, with only the $-NH_2$ group as a substituent. Deoxyribose and phosphate moieties of guanine and adenine derivatives seem to participate in their adsorption processes, mainly in the positive potential region.

D. ADSORPTION OF PYRIMIDINE DERIVATIVES

Figure 19 shows the $|\Delta R/R_0|-E$ curves of cytosine, thymine, and their derivatives. In the case of cytosine, $|\Delta R/R_0|$ begins to increase at about -0.5 V. The curve shows a quasi-bell shape having a maximum at the pzc at lower concentrations but aquires a somewhat more complex shape at higher concentration, with some increase in $|\Delta R/R_0|$ at potentials more positive than 0.1 V (curve *b* in Fig. 19*A*). This seems to indicate that the adsorption process is accompanied by reorientation or formation of the cytosine dimer on the positively charged surface. Since such complicated shapes are observed only in the curves of cytosine and guanine, having the same substituent groups, the interaction of $-NH_2$ and $=O$ may be partly responsible for their complicated behavior on the electrode surface.

No irregular shaped curves were observed for deoxycytidine and

dCMP; that is, $|\Delta R/R_0|$ increases monotonically from -0.5 to -0.1 V and decreases slightly from -0.1 to 0.3 V (Fig. 19*B* and *C*). The amount of adsorption of deoxycytidine and dCMP seems to increase gradually from -0.5 V to the pzc and remains approximately constant within the positive potential region. In the adsorption of these compounds also, the interaction of the deoxyribose and phosphate groups with the positively charged electrode surface appears to be a possibility.

The $|\Delta R/R_0|-E$ curves of thymine have smooth shapes at all concentrations (Fig. 19*D*). The decrease in $|\Delta R/R_0|$ is not as significant at potentials more positive than the pzc, indicating that thymine still remains adsorbed at these potentials. The adsorptivity in the positive region due to the interaction between the =O group of thymine and the positively charged electrode surface is so strong that reorientation of the adsorbed molecule may not occur at higher concentrations. From a comparison of the curve of thymine with that of cytosine, the presence of substituent groups on the pyrimidine ring seems to influence the adsorption state at high concentrations.

Deoxythymidine and dTMP give a $|\Delta R/R_0|-E$ relation similar to thymine (Fig. 19*E* and *F*). It is likely that the participation of the deoxyribose and phosphate parts in the adsorption of deoxythymidine and dTMP is not significant, in contrast with that of deoxycytidine and dCMP.

4. Orientation Models

In order to discuss the adsorbed state and adsorptivity for the substances investigated, the values of p and ΔG^0_{ad} were obtained based on the same isotherm given by equation (7). The results are listed in Table 1, in which the p values serve to estimate the areas covered by one adsorbed molecule by comparison with that of an adsorbed water molecule.

As stated, the p value for adenine corresponds to 0.42 nm^2, implying a flat orientation on the negatively charged electrode surface. Similar values of p obtained for deoxyadenosine and dAMP suggest that both derivatives are adsorbed primarily lying with the purine moiety flat to the electrode surface. These values correspond to the projected areas of 0.48 and 0.33 nm^2 for deoxyadenosine and dAMP, respectively, from which configurations in their adsorbed states can be deduced: in the former case the deoxyribose group lies perpendicularly in close vicinity of the electrode surface (the *anti*-conformation), and in the latter the deoxyribose-phosphate group is directed to the solution side away from the electrode surface (the *syn*-conformation).

For thymine, deoxythymidine, and dTMP, a planar area of about 0.41 nm^2 was also calculated from p. The planar area of the thymine molecule

TABLE I

Adsorption Parameters of Adenine, Thymine, and Their Derivatives in the Negative Potential Region on Au

COMPOUND	p	ΔG°_{ad} (kJ mol^{-1})
Adenine	4.7 ± 0.2	−58.6 ± 1.6
Deoxyadenosine	5.3 ± 0.3	−56.1 ± 0.8
dAMP	3.7 ± 0.3	−41.4 ± 1.2
Thymine	4.6 ± 0.3	−42.7 ± 1.2
Deoxythymidine	4.6 ± 0.1	−45.2 ± 1.2
dTMP	4.6 ± 0.3	−43.5 ± 2.4

Source: From Takamura et al. (1981a), Reprinted with permission.

Note: Standard states 1 mol l^{-1} in solution and a value of θ for with $\theta/(1-\theta)^p = 1$ on the surface.

was estimated as 0.38 nm^2, using its crystal structural data reported by Donohue (1968). It is likely that these molecules are adsorbed with their pyrimidine moieties in contact with the electrode surface, directing the deoxyribose group of deoxythymidine (the *anti*-conformation) and the deoxyribose-phosphate group of dTMP (the *anti*-conformation) to the solution side away from the electrode surface. Such conformations have been pointed out by Brabec et al. (1978).

Comparing the ΔG^0_{ad} values of adenine and thymine, the latter is about 16 kJ mol^{-1} smaller than the former, suggesting that thymine is not as strongly adsorbed. Possibly this is due to the repulsive interaction between the =O group of thymine and the negatively charged surface, in addition to the fact that the adsorptivity of the pyrimidine ring is less than that of the purine ring. In the adenine series dAMP has the smallest adsorption energy, that is, the lowest adsorptivity. This fact seems to result from the hydrophilic property of the phosphate group and its repulsive interaction with the negative charges on the electrode surface (Brabec, 1979). On the other hand, both the values for p and ΔG^0_{ad} in the thymine series are essentially equal, implying only minor effects of the phosphate group on the adsorption of dTMP. This fact is probably attributable to the presence of negative =O groups in the thymine moiety, as a result of which the effect of the phosphate group may be screened from the electrode surface.

Based on these results, possible models to show the orientation of both the adenine and the thymine series in their adsorption on the negatively charged electrode surface are given in Fig. 20.

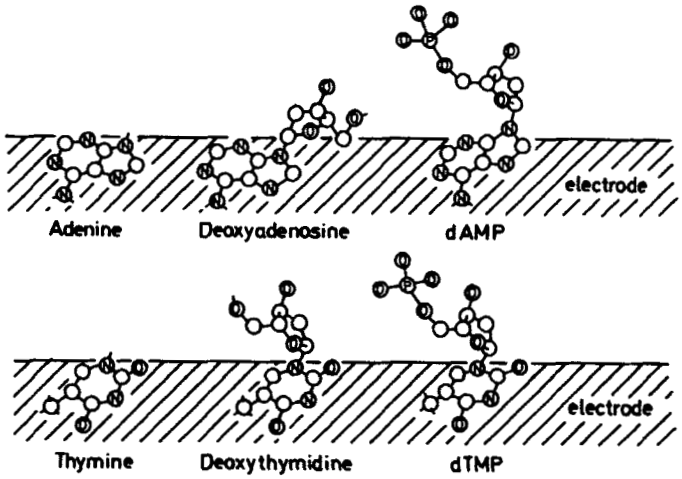

Fig. 20. Possible orientation of adenine, thymine, and their derivatives adsorbed at the negatively charged surface of a Au electrode.

In addition quantititative treatment of adsorption in the positive potential range cannot be made because of oxide formation on the electrode surface; however, we can estimate from the $|\Delta R/R_0|-E$ curves in Figs. 18 and 19 that a similar orientation exists, even in the observed positive potential range. Adenine gives a monotonic decrease in $|\Delta R/R_0|$ with increasing electrode potential, indicating that gradual desorption takes place. Deoxyadenosine and dAMP exhibit somewhat larger $|\Delta R/R_0|$ values than adenine. This fact indicates that deoxyribose and phosphate groups begin to interact with the surface at this range. In the thymine series the $|\Delta R/R_0|-E$ relations suggest that an interaction between two negative =O groups and the positively charged surface prevents desorption to some extent.

V. ADSORPTION OF SOME BIOACTIVE SUBSTANCES

In the preceding section the procedure of adsorption analysis was dealt with based on the reflection method. The procedure has been extended in this section to some bioactive substances such as redox coenzymes and neurotransmitters.

These substances are known to localize at the particular sites of biosurfaces in their respective states in vivo and exert their functions through their own processes. Taking possible analogies between adsorp-

tion layers of some organic compounds and biomembranes (Srinivasan et al., 1977) into account, the behavior of these substances at the electrode surfaces is expected to bear a resemblance to that at the biosurfaces. Therefore the studies of their interfacial behavior at an electrode solution would provide some suggestions in finding their biological significance at biosurfaces. However, such behavior, especially surface orientation, has scarcely been discussed so far from the standpoint of an approach in the field of bioelectrochemistry.

Because of structural complexity of these substances, the $|\Delta R/R_0|-E$ and $|\Delta R/R_0|-$concentration data cannot always be analyzed using the simple isotherm as used for nucleic acid bases. Even in such cases significant information still can be drawn by a comparison of the data obtained with their constituent groups. Some of the experimental results of our recent studies will be described shortly, in which the reflection data were obtained for a gold electrode at the fixed wavelength of 500 nm with an angle of incidence of 15°, unless otherwise noted.

1. Redox Coenzymes Involved in an Electron-Transport Chain

A. NICOTINAMIDE ADENINE DINUCLEOTIDE (NAD^+)

NAD^+ is a well-known coenzyme that enables the dehydrogenase enzymes to play an important part in redox processes in biological systems. NAD^+ is reduced at the 4-position of carbon in the pyridine ring in vivo. Similarly pyridine and its derivatives such as NMN^+ and nicotinamide are also reduced at the same position in vitro (Elving et al., 1973; Schemakel et al., 1974); however, none of them appear to be biologically active. In our voltammetric study of NAD^+, NMN^+, and nicotinamide at a gold electrode, it was found that they were reduced at different potentials. The study of the interfacial behavior of such compounds at the charged electrode surface in relation to the difference in their reducibility becomes of great interest.

a. Electroreduction of NAD^+ and Its Components. Linear sweep voltammograms at a gold electrode in phosphate buffer solution (pH 8.30) containing different concentrations of NAD^+ are shown in Fig. 21. The potential scan started from 0.4 V, proceeded to the negative potential side and reversed at −1.0 V. The sweep rate was 20 mV s^{-1}. The reduction current that appears at potentials more negative than −0.8 V increases with an increase in NAD^+ concentration. In addition to the reduction peaks of NAD^+, the rounded peaks are observed in the voltammograms around the pzc of gold in phosphate buffer solution (−0.2 V), corresponding to the capacitive currents due to the formation of an electric double layer at the surface.

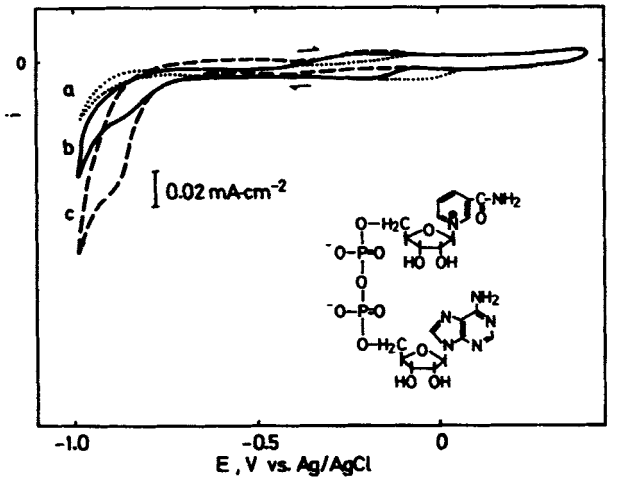

Fig. 21. Current versus potential curves for NAD^+ at Au in 0.05 *M* phosphate buffer (pH 8.30). NAD^+ concentration: *(a)* 0; *(b)* 4.1×10^{-4}; *(c)* 1.0×10^{-3} *M*. Potential sweep rate: 20 mv sec^{-1} (From Takamura et al., 1981b, with permission.)

In order to know the electroreduction products, the controlled-potential electrolysis of NAD^+ was examined in the phosphate buffer solution at −0.9 V, and ultraviolet absorption spectra of the electrolytic solution were determined before and after the electrolysis. Before the electrolysis the solution showed a single absorption peak having a maximum at 260 nm. This peak decreased during the electrolysis and a new peak appeared at about 340 nm. The latter peak increased with time of the electrolysis, indicating that it was due to electrolysis products. Enzymatic analysis using ADH showed that 41% of enzymatically active NADH was present among the products; however, other products gave no indication of coenzymatic activity. The products were separated into two fractions by a high-pressure liquid chromatograph with ODS column. One of these was found to contain NADH and its isomer in the 7:3 ratio by comparison with the standard retention time for NADH. The other seems to contain the 4,4′-dimer of NAD, taking into account the reports of Schmakel et al. (1975), that NAD^+ presumably undergoes a one-electron reduction on a mercury electrode, with the formation of free radicals which dimerize at the position 4 of the pyridine ring (Fig. 22). Burnett and Underwood (1968) proposed that the isolated product was the 4,4′-dimer which showed ultraviolet absorption peaks at 259 and 340 nm.

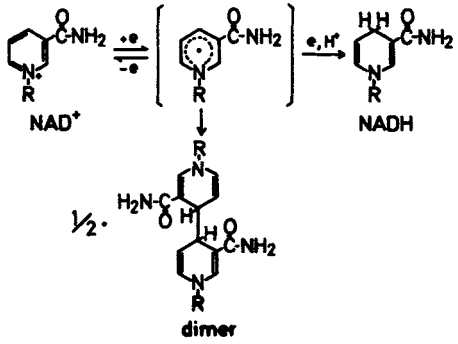

Fig. 22. Reaction paths for the electrochemical behavior of NAD^+. (Taken with modification from Schmakel et al., 1975.)

On the voltammograms of NMN^+, as well as nicotinamide in a phosphate buffer, a well-defined cathodic peak is no longer observed at -0.9V, the observed reduction potential of NAD^+. However, the voltammogram of NMN^+ shows only a slight cathodic current at about -0.1 V. The voltammetry of NAD^+, NMN^+, and nicotinamide was further examined in solutions with higher pH values in order to observe the reduction of their nicotinamide moieties (Fig. 23).

Figure 24 shows the voltammograms of these compound obtained at pH 10.0. NAD^+ and NMN^+ are reduced at about -0.9 and -1.0 V (Fig. 24, curves *a* and *b*), respectively; however, nicotinamide was not reduced in the observed potential range (curve *c*). The ultraviolet spectrum of the NMN^+ solution after controlled-potential electrolysis at -1.0 V showed the characteristic peak of 1,4-dihydropyridine structure at 340 nm, indicating that the nicotinamide moiety in NMN^+ is also reduced on a gold electrode. From these results the order of reducibility can be given as follows: $NAD^+ > NMN^+ >$ nicotinamide. The fact that NMN^+ **(1)** is more easily reduced than nicotinamide **(2)** is probably due to the presence of the pyridinium ionic form (Fig. 23). The relative reducibility of NAD^+ will be discussed later.

b. Adsorption of NAD^+ and Its Components

Reflectivity-Potential Curve. R/R_0–E curves of gold in a phosphate buffer solution (pH 8.30) containing two different concentrations of NAD^+ are shown in Fig. 25. Addition of NAD^+ to the solution scarcely affects the R/R_0 values between -0.8 and -1.0 V but causes a marked decrease in reflectivity in potential regions more positive than about -0.8 V (curves *b* and *c* in Fig. 25, in which the curves are drawn separately as in

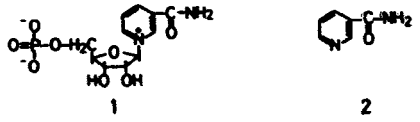

1 2

Fig. 23. Formulas for NMN^+ (**1**) and nicotinamide (**2**).

Fig. 12). The magnitude of the decrease was enhanced with the increase in NAD^+ concentration and tended to the limiting value.

The R/R_0-E curves of NAD^+ components such as NMN^+, nicotinamide, adenine, and adenosine are shown in Fig. 26, in which the curves are drawn separately as in Fig. 12. Compared with measurements using only the phosphate buffer (curve *a*), the presence of these components also causes a decrease in reflectivity as shown by the R/R_0-E curves (curves $b-e$). These observations suggest that NAD^+ and its components are adsorbed on the electrode surface. Other electrochemical data (e.g., differential capacitance) are consistent with this suggestion.

Potential and Concentration Dependence of Adsorption. The $\Delta R/R_0$ values due to the adsorption of NAD^+ and its components were obtained in the same way as described earlier, using solutions containing different concentrations of each compound. The $|\Delta R/R_0|$ is plotted as a function of the applied potential in Fig. 27. From the features of the relations in Fig. 27, NAD^+ is found to be adsorbed on a gold electrode at potentials more positive than about -0.8 V (Fig. 27*A*) and NMN^+, nicotinamide, adenine,

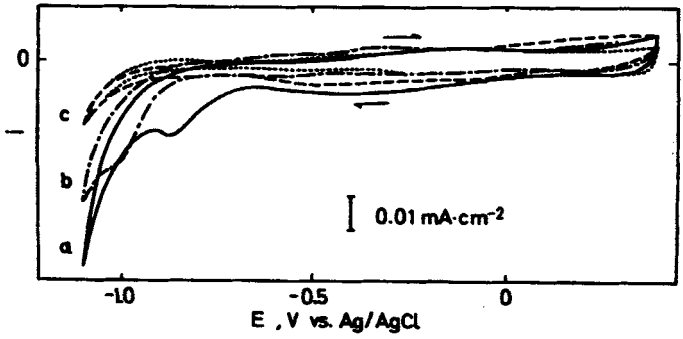

Fig. 24. Current versus potential curves at Au in 0.05 *M* carbonate buffer (pH 10.0) in the absence (· · · ·) and in the presence of *(a)* 2.0×10^{-4} *M* NAD^+; *(b)* 1.4×10^{-4} *M* NMN^+; *(c)* 1.2×10^{-4} *M* nicotinamide. Potential sweep rate: 20 mV sec^{-1}. (From Takamura et al., 1981b, with permission.)

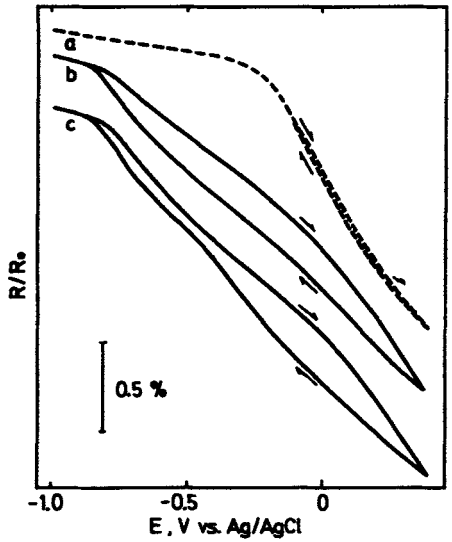

Fig. 25. Reflectivity versus potential curves of Au in 0.05 *M* phosphate buffer (pH 8.30) in the absence and in the presence of NAD^+. NAD^+ concentration: *(a)* 0; *(b)* 5.3×10^{-6}; *(c)* 1.9×10^{-5} *M*. Wavelength: 500 nm. Potential sweep rate: 100 mV sec^{-1}. (From Takamura et al., 1981b, with permission.)

and adenosine, more positive than −0.7 V, −0.6 V, −0.8 V, and −0.8 V, respectively (*B*, *C*, *D*, and *E*).

The adsorbed amount of these substances increases with increasing potentials up to the pzc, where it reaches a maximum value. It is noteworthy that the potential range of adsorption and the shape of $|\Delta R/R_0|-E$ curves for NAD^+ are very similar to those of adenosine. This seems to suggest the contribution of the adenosine moiety to the adsorption of NAD^+. On the other hand, the potential ranges of adsorption of NAD^+, NMN^+, and nicotinamide were found to be different from each other.

*c. **Orientation of Adsorbed Molecules at the Negatively Charged Electrode Surface.*** In order to know the orientation of adsorbed molecules, an investigation was made of the adsorption phenomena using equation (7).

The $|\Delta R/R_0|$ values obtained at the pzc for all these compounds increase with increasing concentrations and tend to limiting values at sufficiently high concentrations, indicating that the adsorption reaches saturation (see Fig. 27). In the potential regions more negative than the pzc, the $|\Delta R/R_0|-E$ curves are smooth, indicating that there is no change in the

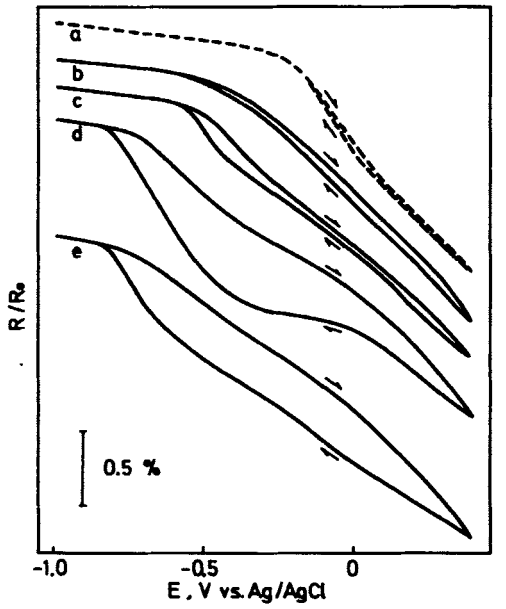

Fig. 26. Reflectivity versus potential curves of Au in 0.05 *M* phosphate buffer (pH 8.30) in the absence *(a)* and in the presence of *(b)* 1.4×10^{-5} *M* NMN^+; *(c)* 1.1×10^{-5} *M* nicotinamide; *(d)* 1.3×10^{-5} *M* adenine; *(e)* 1.4×10^{-5} *M* adenosine. Wavelength: 500 nm. Potential sweep rate: 100 mV sec^{-1}. (From Takamura et al., 1981b, with permission.)

orientation of the adsorbed molecule. From this, θ can be calculated from the $|\Delta R/R_0|$ value according to equation (5). The values of p and ΔG^0_{ad} evaluated from equation (7) for nicotinamide, adenine and adenosine are listed in Table 2. In the cases of NAD^+ and NMN^+ the effects of their reduction prevented the estimation of the $|\Delta R/R_0|$ values at saturation, and the preceding calculations could not be performed for these compounds.

Approximate orientation of the adsorbed molecule can be determined by comparison of the area occupied by one adsorbed molecule estimated from p, with that estimated using a molecular model. Results indicate that nicotinamide is adsorbed with either its pyridine ring or both N(**1**) of the pyridine and the $-NH_2$ group in contact with the electrode. For adenine and adenosine, the p values are approximately equal to 4, implying that they are adsorbed lying with the purine moiety flat against the electrode. Considering its molecular structure, NMN^+ is thought to be adsorbed with either the nicotinamide moiety only or the nicotinamide moiety and a

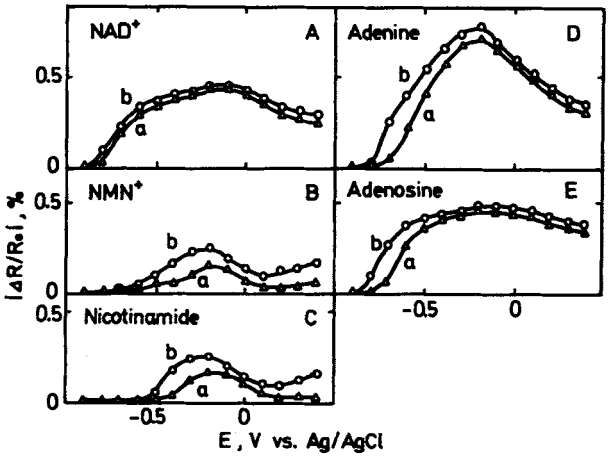

Fig. 27. Potential dependence of the reflectivity change obtained with 0.05 *M* phosphate buffer (pH 8.30) containing NAD^+ and its components. Concentration: *A (a)* 1.9, *(b)* 10.3; *B (a)* 1.4, *(b)* 12.7; *C (a)* 1.1, *(b)* 10.9; *D (a)* 1.3, *(b)* 11.7; *E (a)* 1.4, *(b)* 21.1×10^{-5} *M*. (From Takamura et al., 1981b, with permission.)

TABLE II

Adsorption Parameters of Nicotinamide, Adenine, and Adenosine on Au from 0.05 *M* Phosphate Buffer (pH 8.3)

COMPOUND	p	ΔG°_{ad} (kJ mol^{-1})
Nicotinamide	2.2 ± 0.1	−31.0 ± 1.3
Adenine	4.4 ± 0.4	−49.8 ± 0.9
Adenosine	3.8 ± 0.1	−49.4 ± 0.9

Source: From Takamura et al. (1981b). Reprinted with permission.
Note: Standard state 1 mol l^{-1} in solution and value of θ for with $\theta/(1-\theta)^p = 1$ on the surface.

part of the ribose moiety in contact with the electrode, since the sugar moiety participates in the adsorption process in the negative potential region to a minor degree (Takamura et al., 1979).

Although it is difficult to obtain the p value of NAD^+, it can be reasonably assumed that this compound is adsorbed on negatively charged electrodes with either its nicotinamide or adenine moiety in

contact with the electrode surface, since the ribose moiety takes a minor part in the adsorption and phosphate groups will be repelled from the surface. Such orientation is very similar to that obtained at a mercury electrode by Brabec (1978, 1979). However, the result of reflectivity measurement for NAD^+ resembles that of adenosine more closely than that of NMN^+. In addition the ΔG^0_{ad} values in Table 2 suggest a higher adsorptivity for adenine than for nicotinamide. It can be concluded from these results that NAD^+ is adsorbed with the adenine moiety predominantly in contact with the electrode surface, and a possible model for the adsorbed NAD^+ is shown in Fig. 28.

d. Consideration of the Role of Adsorption in the Reduction of NAD^+. Now it seems worthwhile to consider how the adsorption of NAD^+ affects its reducibility. As stated earlier, NAD^+ is reduced at less negative potentials than NMN^+ and nicotinamide, even though these compounds are all reduced through virtually the same mechanism, namely through the pyridine ring. During the cathodic scan, NAD^+ remains adsorbed on the electrode surface until its reduction takes place, whereas NMN^+ and nicotinamide are desorbed at potentials where no reduction occurs.

From the proposed model for the adsorbed NAD^+ on the electrode surface, it can readily be seen that the nicotinamide moiety is favorably located in the vicinity of the surface, as shown in Fig. 28 in which its adenine moiety is attached to the surface. Access of NAD^+ to the surface will result in expulsion of preadsorbed species such as water molecules or ionic species, and consequently this situation will be expected to facilitate the reduction of NAD^+. Thus the proposed model provides an explanation of how the adsorption of NAD^+ serves to make its reduction easier than that of NMN^+ and nicotinamide.

B. FLAVIN MONONUCLEOTIDE (FMN) AND FLAVIN ADENINE DINUCLEOTIDE(FAD)

Flavin coenzymes are electron transferring and serve as the prosthetic groups of respiratory enzymes—flavoproteins. A number of studies on the electrochemical behavior of FMN and FAD relating to the adsorption have so far been made (Dryhurst, 1977; Elving et al., 1973; Janik and Elving, 1968; Kakutani et al., 1981, 1983), but little has been known about the adsorbed states (Hartley and Wilson, 1966; Kakutani et al., 1983).

The adsorbed states of FMN and FAD formed on the gold electrode surface were investigated in relation to their redox reactions by the reflection method. Besides FMN(**3**) and FAD(**4**), riboflavin(**5**) and adenosine-5′-phosphate (AMP)(**6**) are taken for comparison (see Fig. 29).

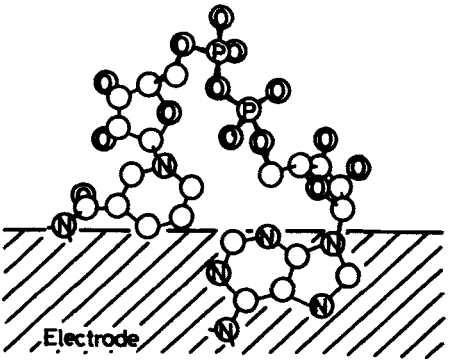

Fig. 28. Possible orientation of NAD^+ at the negatively charged surface of a Au electrode. (From Takamura et al., 1981b, with permission.)

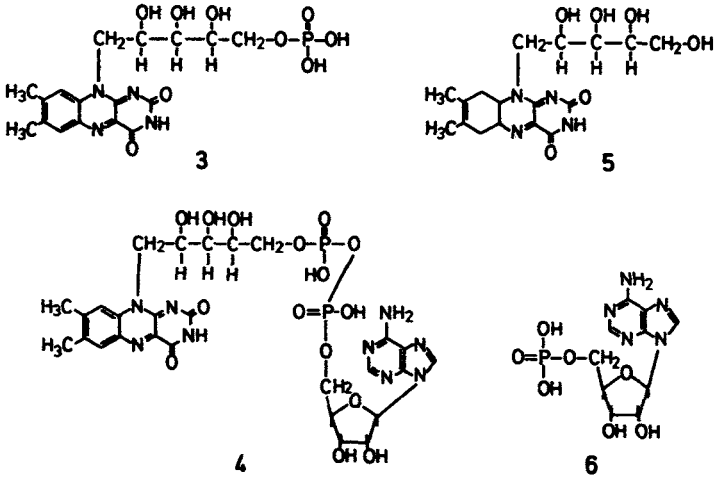

Fig. 29. Formulas for FMN (3), FAD (4), riboflavin (5), and AMP (6).

a. Redox Reactions of FMN and FAD. $i-E$ curves obtained in carbonate buffer (0.05 M, pH 10.0) in the absence and the presence of FMN are shown in Fig. 30. FMN exhibits cathodic and anodic peaks at about -0.5 V (curves b and c in Fig. 30). The former is attributed to the reduction of FMN, and the latter to the oxidation of the electroreduction product of FMN. Both peak currents increased with increase of FMN concentration.

Like FMN, both FAD and riboflavin give well-defined redox peaks on the $i-E$ curves at approximately the same potentials as FMN, suggesting that the isoalloxazine moieties of these compounds participate in the electron transport. Since AMP itself exhibits no redox peak in the potential range investigated, it is assumed that the AMP moiety of FAD is not reduced. Thus the reaction mechanisms for the redox reactions of FMN and FAD (Elving et al., 1973; Janik and Elving, 1968) can be given as in Fig. 31.

b. Adsorption of FMN and FAD.

Reflectivity Versus Potential Curve. The R/R_0-E curves for FMN measured simultaneously with the $i-E$ curves are shown in Fig. 32, in which the wavelength of the light is chosen at 560 nm to avoid direct excitation of FMN, FAD, and riboflavin. Addition of FMN causes a marked decrease in reflectivity in the potential region more positive than about -0.8 V (curves $b-d$, where the curves are drawn separately as in Fig. 12), The reflectivity change is enhanced with increase of FMN concentration but tends to saturation and reaches the limiting value at approximately 5×10^{-4} M. Such changes in reflectivity are observed in the potential region either more positive or more negative than -0.5 V. This result suggests that both FMN and its reduction product ($FMNH_2$) are adsorbed on the gold electrode.

The results obtained for FAD, as well as for riboflavin and AMP, are similar to those for FMN, except for the absence of a redox reaction for AMP in the potential range investigated.

Potential and Concentration Dependence of Adsorption. The $|\Delta R/R_0|$ values obtained for FMN are plotted against the applied potentials in Fig. 33*A*. The $|\Delta R/R_0|$ value at each potential increases with the increase in the FMN concentration and approaches the limiting value at sufficiently high concentration, indicating saturation of the adsorption. In the potential region from approximately -0.8 to -0.5 V, $|\Delta R/R_0|$ increases with increasing potential, suggesting increase in the amount of adsorbed $FMNH_2$. In the region more positive than -0.5 V, $|\Delta R/R_0|$ also increases with increasing potential and attains the maximum value at pzc, but no appreciable change is observed at more positive potentials ($|\Delta R/R_0|$ slightly decreases with increasing potential only when the concentration is

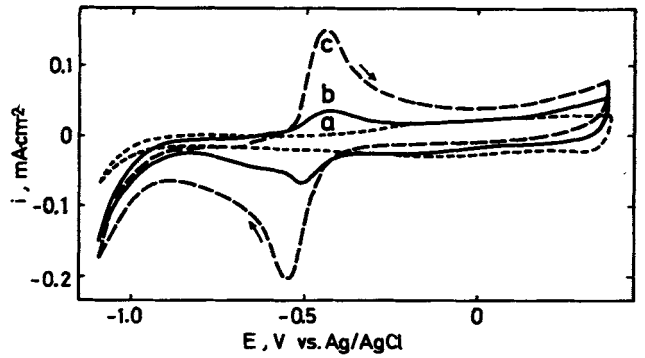

Fig. 30. Current versus potential curves obtained for FMN on a Au electrode in 0.05 *M* carbonate buffer solution. FMN concentration: *(a)* 0; *(b)* 5.1×10^{-5}; *(c)* 4.8×10^{-4} *M*. Potential sweep rate: 100 mV sec^{-1}. (From Takamura et al., 1981d, with permission.)

very low (Fig. 33*A*, curve *a*), suggesting that the adsorbed FMN is gradually desorbed by competitive adsorption of supporting electrolyte anion).

The $|\Delta R/R_0|-E$ relation for FAD is plotted in Fig. 33*B*, in which the $|\Delta R/R_0|$ value at each potential also increases and approaches the limiting value with increasing concentration. The $|\Delta R/R_0|-E$ curves for riboflavin as well as for AMP are also shown in Fig. 33*C* and *D* for comparison.

c. Consideration of the Orientation of Adsorbed Molecules.

The Oxidized Form. The adsorption parameters, p and ΔG^0_{ad}, obtained for FMN and FAD are listed in Table 3, together with those for riboflavin and AMP for comparison.

The p value of FMN is essentially equal to that of riboflavin, suggesting that FMN is adsorbed on the surface via its isoalloxazine and/or ribitol moieties. Strong adsorptivity of the ribitol moiety, however, seems unlikely because of its hydrophilic property. Assuming that an adsorbed water molecule occupies an area of 0.09 nm^2, the area occupied by one

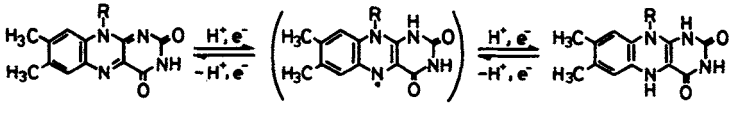

Fig. 31. Electrochemical reaction of FMN or FAD. (Adapted from Elving et al., 1973.)

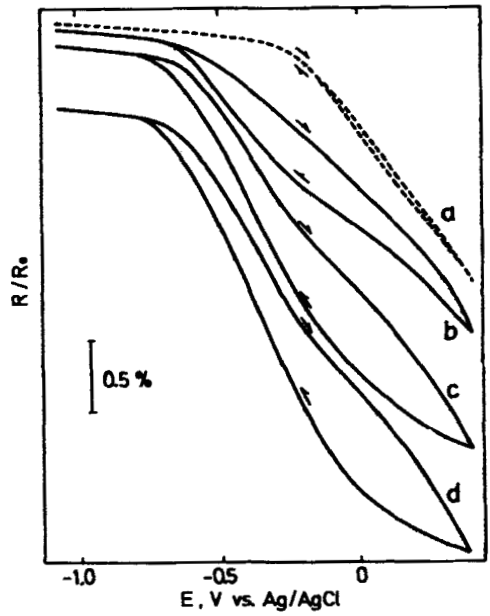

Fig. 32. Reflectivity versus potential curves obtained for FMN on a Au electrode in 0.05 *M* carbonate buffer solution. FMN concentration: *(a)* 0; *(b)* 5.0×10^{-6}; *(c)* 5.1×10^{-5}; *(d)* 4.8×10^{-4} *M*. Wavelength: 560 nm. Potential sweep rate: 100 mV sec^{-1}. (From Takamura et al., 1981d, with permission.)

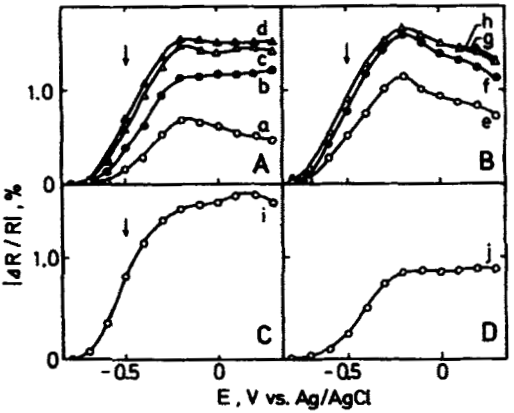

Fig. 33. Potential dependence of the reflectivity change obtained for FMN *(A)*, FAD *(B)*, Riboflavin *(C)*, and AMP *(D)*. Concentration: *(a)* 1.5×10^{-6}; *(b)* 1.5×10^{-5}; *(c)* 1.5×10^{-4}; *(d)* 4.8×10^{-4}; *(e)* 1.5×10^{-6}; *(f)* 1.6×10^{-5}; *(g)* 1.6×10^{-4}; *(h)* 3.5×10^{-4}; *(i)* 1.5×10^{-4}; *(j)* 1.4×10^{-4} *M*. The arrow shows the redox potential. (From Takamura et al., 1981d, with permission.)

TABLE III

Adsorption Parameters of FMN, FAD, Riboflavin, and AMP on Au from 0.05 *M* Carbonate Buffer Solution (pH 10.0)

COMPOUND	p	ΔG°_{ad} (kJ mol^{-1})
FMN	5.3 ± 0.4	−44.7 ± 1.7
FAD	6.7 ± 0.4	−62.3 ± 0.9
Riboflavin	5.1 ± 0.4	−49.3 ± 1.7
AMP	3.6 ± 0.3	−38.0 ± 0.9

Source: From Takamura et al. (1981d). Reprinted with permission.

adsorbed FMN molecule is calculated to be about 0.48 nm^2. The projected area of the isoalloxazine moiety can be estimated by using a molecular model and taking into account the data on the crystal structure of riboflavin (Tanaka et al., 1969), that is, 0.68−0.71 nm^2 for the flat orientation and approximately 0.23 nm^2 (in contact with two methyl groups of the isoalloxazine moiety) or 0.34 nm^2 (in contact with the methyl group of C(**7**) and the oxygen of C(**4**)) for the perpendicular orientation. Comparison of the area obtained from our experiments with these values suggests that the adsorbed FMN lies on the electrode with its isoalloxazine plane inclined relative to the electrode surface. Phosphate and ribitol moieties of FMN would be directed to the solution side because of their hydrophilic property and the small repulsive interaction between the negative charge of these groups and the electrode surface. Based on the preceding discussion, a possible model of the orientation of FMN adsorbed in the potential region from −0.5 V to pzc is schematically drawn in Fig. 34*A*.

In the potential region more positive than pzc, the $|\Delta R/R_0|-E$ relation (Fig. 33*A*) suggests that FMN remains adsorbed on the positively charged electrode surface. It has been reported that some sugars interact weakly with the electrode surface mainly at more positive potentials than pzc, especially when they are bound to phosphate groups (Brabec et al., 1978). This suggests that the presence of ribitol and phosphate groups makes the release of FMN from the electrode surface difficult.

The area occupied by one adsorbed FAD molecule in the potential region from −0.5 V to pzc was calculated to be about 0.60 nm^2 from its p value of 6.7 ± 0.4. This area is larger than those of FMN and AMP, probably implying that the FMN and the AMP moieties of FAD both participate in its adsorption. However, preferential adsorption of the

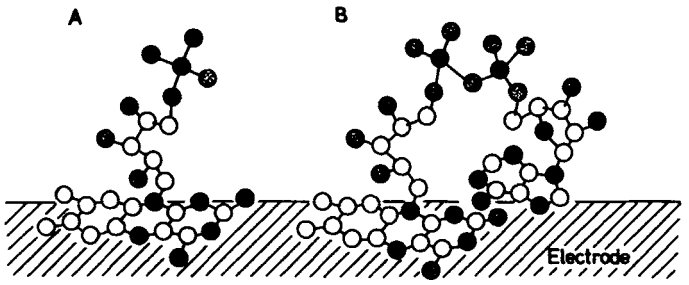

Fig. 34. Possible models of FMN *(A)* and FAD *(B)* adsorbed on a Au electrode in the potential region from −0.5 V to pzc. (From Takamura et al., 1981d, with permission.)

FMN moiety is suggested by comparison of the ΔG^{υ}_{ad} values of FMN and AMP.

The area of an adsorbed molecule of AMP calculated from P is about 0.32 nm^2, which is somewhat smaller than the 0.42 nm^2 planar area of adenine but is larger than the approximately 0.22 nm^2 perpendicular area estimated from the crystal structure (Donohue, 1968). Thus AMP is regarded as being adsorbed primarily with its adenine moiety nearly flat relative to the surface. The ribose-phosphate moiety of AMP may be directed to the solution side, in analogy with the cases of deoxynucleotides (Takamura et al., 1979, 1981c).

It seems most reasonable to consider that FAD is adsorbed with its isoalloxazine ring nearly flat relative to the surface and with a part of the adenine moiety in contact with the surface. Such an orientation is depicted by the model in Fig. 34B. The finding that the ΔG^{0}_{ad} of FAD is about 16 kJ mol^{-1} larger than that of FMN also supports the participation of the adenine moiety in the adsorption.

In the potential region more positive than pzc, the $|\Delta R/R_0|-E$ relation is somewhat different from that for FMN. The relation (Fig. 33*B*) indicates that FAD is desorbed with increase in electrode potential. Its sugar (ribitol and ribose) and phosphate groups may not be able to approach the surface easily because of steric hindrance.

The Reduction Form. The same treatment as described here cannot be applied to $FMNH_2$ and $FADH_2$ in the potential region between −0.8 and −0.5 V, since $|\Delta R/R_0|$ at $\theta = 1$ is difficult to obtain. The isoalloxazine moieties in these reduced forms no longer have the planar structure but a bent one as a result of hydrogenation at their N(**1**) and N(**5**) positions (Tanaka et al., 1969). However, the $|\Delta R/R_0|-E$ curves are smooth over

the potential range from −0.8 V to pzc (see Fig. 34*A* and *B*), implying that both $FMNH_2$ and $FADH_2$ are adsorbed with essentially the same orientation as their oxidized forms.

To sum up, FMN and FAD are adsorbed in both the oxidized and reduced forms on the gold electrode surface. Their isoalloxazine moieties appear principally to come into contact with the surface, and it can therefore be expected that electron transport is accomplished through these moieties.

C. COENZYME Q (CoQ)

The present method was applied further to the adsorption study of CoQ on a gold electrode. Electrochemical behavior of CoQ is characterized by the redox reaction of its quinone moiety (see Fig. 35) accompanying the adsorption of its isoprenoid side chain. Observation was made for CoQ_{10} (ubiquinone-10), and also for squalene and duroquinone for comparison, in 80% ethanol solution containing 0.1 *M* $NaClO_4$ because of their poor solubility in water. The wavelength of the light was fixed at 560 nm.

a. Redox Reaction of CoQ. The pH of the test solutions was adjusted to 6.3 ± 0.2 during the measurements. Voltammograms obtained in the absence (curve *a*) and the presence (curve *b*) of CoQ are shown in Fig. 36. The cathodic and anodic peaks at about −0.3 V increases with an increase in CoQ concentration. Ultraviolet absorption spectra of the test solution measured before and after the controlled-potential electrolysis at −0.4 V shows that the characteristic peak of the quinoid structure of CoQ at 275 nm decreased throughout the electrolysis. Since the voltammogram of squalene (a six-unit isoprene polymer, which is adopted as an analogous compound to the side chain in CoQ) exhibits no redox peak in the potential range from −0.2 to −1.1 V, the side-chain moiety of CoQ would not participate in any redox reaction. From these observations the cathodic and anodic peaks are attributed to the redox reaction of its quinone moiety (Fig. 35). Such a redox reaction with two-electron transport has already been confirmed for ubiquinone at a mercury electrode (Hart and Catterall, 1980; Moret et al., 1961).

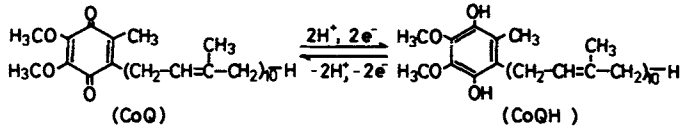

Fig. 35. Electrochemical reaction of CoQ.

b. Adsorption of CoQ

Reflectivity Versus Potential Curve. The R/R_0-E curves for CoQ measured simultaneously with the $i-E$ curves are also shown in Fig. 36. The addition of CoQ caused a marked decrease in reflectivity on the R/R_0-E curve in the potential region more positive than about -0.7 V (curve b'), compared with that obtained for the supporting electrolyte (curve a'). Such a trend is enhanced with increasing CoQ concentration up to approximately 5×10^{-6} M and then approaches the limiting curve. These results indicate that the adsorption of CoQ on the electrode surface takes place at potentials more positive than approximately -0.7 V.

Potential Dependence of Adsorption. The $|\Delta R/R_0|$ values for CoQ are plotted against the applied potentials in Fig. 37*A*, in which the arrow indicates the redox potential of CoQ. At each potential the $|\Delta R/R_0|$ value increases with the increase of CoQ concentration and approaches the limiting value at about 5×10^{-6} M, indicating the saturation of adsorption. In the potential region from approximately -0.7 to -0.4 V, the $|\Delta R/R_0|$ increases with increasing potentials but does not change appreciably at more positive potentials.

In order to know what part of the CoQ molecule contacts the electrode surface on the adsorption, the reflectivity measurements were also carried out for squalene and duroquinone (2,3,5,6-tetramethyl benzoquinone). The latter has a somewhat analogous structure to the quinone moiety of CoQ. The $|\Delta R/R_0|-E$ relation for squalene was plotted in Fig. 37*B*, in which the $|\Delta R/R_0|$ value increases with increasing potential from approximately -0.7 to -0.4 V and does not appreciably change at more positive potentials. On the other hand, the change in reflectivity is scarcely observed for duroquinone (Fig. 37*C*), suggesting that duroquinone is not adsorbed under the present conditions. The results for CoQ are similar to those for squalene.

c. Surface Orientation of CoQ. As seen in Fig. 37, the $|\Delta R/R_0|-E$ relation for CoQ is similar to that not for duroquinone but for squalene. Consequently it can be concluded that the adsorption of CoQ, as well as its reduction product, is essentially due to the attraction between the long side chain and the electrode surface. Such a conclusion is similar to that obtained for the adsorption of ubiquinone-6 at a mercury electrode by O'Brien and Oliver (1961). The conclusion implies that the adsorbed CoQ is reduced, and the resulting product remains adsorbed at the electrode surface; that is, CoQ participates in electron transport in the adsorbed state on the surface.

A possible model to show the orientation of adsorbed coenzyme in its oxidized form on the electrode surface is schematically drawn in Fig. 38. CoQ would be adsorbed by means of its isoprenoid chain. By considering

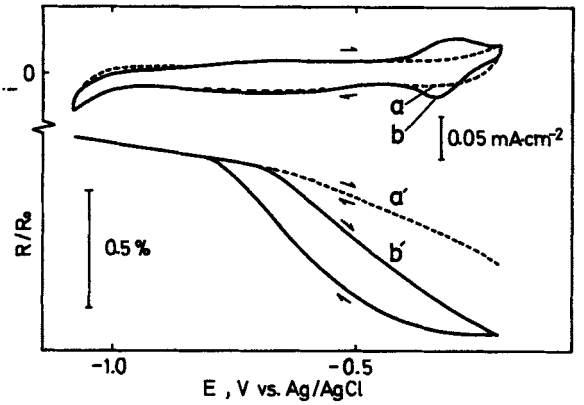

Fig. 36. Current versus potential and reflectivity versus potential curves for CoQ in 0.1 *M* $NaClO_4$—80% ethanol solution. Concentration of CoQ: (*a* and *a'*) 0; (*b* and *b'*) 1.25×10^{-5} *M*. Sweep rate: 100 mV sec^{-1}.

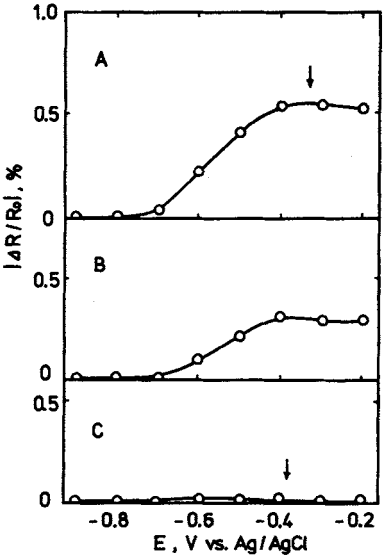

Fig. 37. Potential dependence of the reflectivity change obtained with 0.1 *M* $NaClO_4$—80% ethanol solutions containing *(A)* 4.3×10^{-6} *M* CoQ, *(B)* 4.7×10^{-6} *M* squalene, and *(C)* 8.1×10^{-6} *M* duroquinone. The arrow shows the reduction potential.

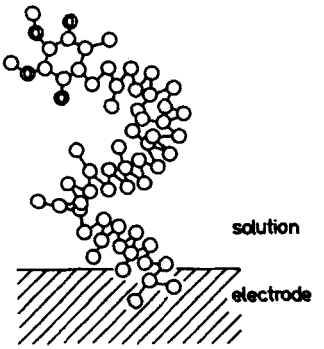

Fig. 38. Possible orientational model of adsorbed CoQ at the Au electrode surface.

the orientation of other quinone derivatives having a long side chain (Takamura and Hayakawa, 1974) and adsorption behavior of higher alcohols (Damaskin et al., 1971), it can reasonably be assumed that the terminal part of the isoprenoid chain of CoQ is mainly in contact with the surface. Since the chain would be conformationally flexible, the quinone moiety of the adsorbed molecule may easily approach the surface.

D. ANALOGY BETWEEN THE BEHAVIOR OF THE COENZYMES AT THE INNER MITOCHONDRIAL MEMBRANE AND THAT AT THE ELECTRODE-SOLUTION INTERFACE

The mitochondrial respiratory chain consists of several components that catalyze the reduction of molecular oxygen in vivo. In the respiratory chain, electrons are transported through a series of electron carriers as shown in Fig. 39. This concept has been deduced based on their standard reduction potentials. The order of the reduction potentials of the coenzymes investigated here i.e., CoQ>FMN and FAD>NAD^+ is found to be consistent with the sequence of these coenzymes in the respiratory chain. In the reduction of these coenzymes, the parts being reduced at the electrode surface are the same as those in vivo.

These coenzymes are localized in the inner mitochondrial membrane in their respective states and take part in electron transport through their own processes. CoQ is located in the hydrocarbon phase of the inner membrane and serves as a mobile carrier of electrons. FMN and FAD are the prosthetic groups of membrane-linked respiratory enzymes, namely flavoproteins. Both the coenzymes are tightly bound to the apoproteins

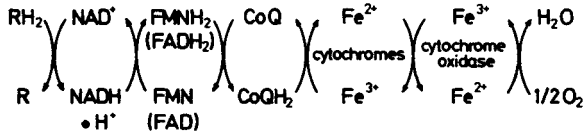

Fig. 39. Electron-transport chain. RH_2 and R denote the reduced and oxidized forms of substrate, respectively.

and cause electron transport in this condition. NAD^+ is suspended in the matrix portion. Enzymatically produced NADH in the matrix approaches the inner membrane and is oxidized by NADH dehydrogenase at the membrane surface. The resulting NAD^+ is then removed from the surface.

The behavior of these coenzymes at the electrode surface seems to resemble their function in mitochondria in some respects. CoQ, as well as $CoQH_2$, is adsorbed on the electrode surface. The adsorbed layer composed of a long hydrocarbon chain may be analogous to a part of the lipid layer of the inner membrane. FMN (or FAD) is adsorbed in both the oxidized and reduced forms on the electrode surface with approximately the same orientation. This result is consistent with the characteristics of these coenzymes as prosthetic groups. The adsorbed layer formed on the electrode surface, in which hydrophilic phosphate and sugar groups would be directed to the solution side, seems to be analogous to the flavoproteins located in the matrix side of the inner membrane in contact with aqueous phase. In the case of NAD^+ the simultaneous occurrence of the reduction and desorption of adsorbed NAD^+ seems to be an indication of its interfacial behavior as a mobile electron carrier in mitochondria, that is, the approach to the inner membrane and elimination from the membrane associated with electron transport. In addition the adsorption effect observed for NAD^+ on its reducibility of nicotinamide moiety might give some suggestions about the necessity of its adenine moiety for the coenzymatic activity. Such a characteristic effect of the adenine moiety was not observed for FAD in its electroreduction. This result corresponds to the fact that the flavocoenzymes exhibit their activity as redox coenzymes irrespective of the presence of the adenine moiety.

The behavior of a series of coenzymes at the electrode surface observed by the reflection method is found to have some analogy with that at the inner membrane. Thus the information about the behavior of redox coenzymes obtained from electrochemical studies is expected to give some clues in understanding their mode of action at biological surfaces.

E. CYTOCHROMES c

The electron transfer reactions between electrodes and cytochromes c have been extensively studied (Betso et al., 1972; Heineman et al., 1975; Hinnen et al., 1983; Ranweiler and Wilson, 1976; Yeh and Kuwana, 1977). It has been noted that both cytochrome c and c_3 adsorb strongly on electrodes from aqueous solutions and that the adsorbed cytochromes play an important role in the electrode reactions of these heme proteins.

Recently Hinnen et al. (1983) observed the nature of the adsorbed cytochrome on a gold electrode by electroreflectance technique. On the voltammograms of cytochromes c and c_3 in a NaF solution, the redox peaks appear near -0.5 V versus SCE (denoted as E_p) corresponding to the electron transfer reaction of adsorbed cytochromes. The electroreflectance spectra for adsorbed cytochrome c_3 molecules obtained at E_p are characteristic of a pronounced bipolar feature near 410 nm (Fig. 40). The amplitude of the spectrum depends strongly on the nature of the supporting electrolyte and pH. A qualitative understanding of the spectrum was made in considering the change in the light absorbing properties of cytochrome resulting from oxidation of the ferrous cytochrome (λ_{max} 418 nm) to ferric (λ_{max} 404 nm). If such a redox conversion occurs between adsorbed species in the potential region near E_p, an electroreflectance effect may be caused.

When adsorbed species on the electrode surface is light absorbing, the electroreflectance technique seems to be effective in detecting them with high sensitivity. Furthermore the technique will serve as a tool for obtaining knowledge of the adsorbed species at the molecular level since the electroreflectance spectrum indicates the electronic states of the species.

2. Neurotransmitters and Drugs

As a type of interaction of neurotransmitters and their related substances with a charged surface, adsorption of acetylcholine and cholinergic and anticholinergic drugs on to a gold electrode has been examined by the reflection method (Kusu and Takamura, 1984). Such drugs are called "structurally specific drugs" whose pharmacological action results essentially from their chemical structure.

Acetylcholine is a natural intercellular effector in nervous transmission systems, and its importance has promoted considerable research on the interaction of this molecule, as well as that of cholinergic drugs, with cholinergic receptors in the peripheral nervous system. The nature of drug–receptor interaction has been deduced primarily from the biological effects produced by drugs, on the basis of the relationship between

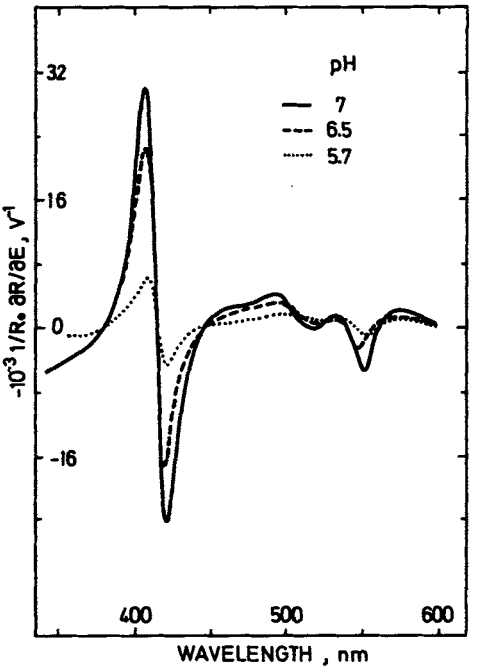

Fig. 40. Influence of pH on the amplitude of the electroreflectance spectra for adsorbed cytochrome c_3 on a Au electrode in 0.02 *M* NaF solution. (——) pH = 7; (– – –) pH = 6.5; (· · · ·) pH = 5.7. (From Hinnen et al., 1983, with permission.)

chemical structure and mode of action (Ariëns , 1971; Ariëns and Simonis, 1967; Mayer, 1980; Taylor, 1980; Weiner, 1980). However, basic studies on the interaction between drug and receptor in vivo are difficult due to the structural complexity of the receptor and the virtual impossibility of identifying the interaction at the submolecular level.

Recently adsorption of acetylcholine chloride and polycyclic ganglionic blocking drugs as quaternary ammonium salts on a mercury electrode in the negatively charged region was examined by a polarographic technique, and the results are consistent with the effects of ganglionic blocking agents in vivo (Sakura, 1981). Considering possible analogies between adsorption layers of organic compounds and signal-transmitting biomembranes (Jehring et al., 1979), observation of the adsorption behavior of drug molecules on an electrode may be expected to provide information on orientational preferences at receptor sites. This expectation prompted an extention of the present method to the adsorption study of drugs.

A. ADSORPTION BEHAVIOR

The $i-E$ curves of acetylcholine chloride and its related drugs, except nicotine, gave a flat region from -1.1 to 0.3 V and agreed well with the curve of the supporting electrolyte solution (0.1 M $NaClO_4$), indicating that no redox reaction takes place in this region of potential. Therefore the adsorption behavior was examined in this potential region. For nicotine, the potential was restricted to the range from -1.1 to 0 V since this drug is oxidized at a positive potential exceeding 0.04 V.

On the R/R_0-E curves of the solution containing acetylcholine chloride and its related drugs, a decrease in reflectivity was observed in a certain region of potential for the R/R_0-E curves, suggesting that the adsorption of these drugs takes place on the electrode-electrolyte interface.

The values of $|\Delta R/R_0|$ at adsorption equilibrium were plotted against the applied potentials (Figs. 41–44). The $|\Delta R/R_0|-E$ plots for the drugs exhibit three types of the potential profiles of adsorption. On the basis of the profiles of potential, the drugs studied are divided into three groups: (I) acetylcholine, carbamylcholine, and methacholine, (II) tetraethylammonium ion and hexamethonium, and (III) nicotine, atropine, scopolamine, and pilocarpine. The profiles are described in detail next.

a. Acetylcholine, Carbamylcholine, and Methacholine (Group I)

Acetylcholine and Its Components. As shown in Fig. 41*a*, an increase in acetylcholine concentration results in an increase in $|\Delta R/R_0|$ and, at the same time, a shift toward more negative values of the potential at which the increase in $|\Delta R/R_0|$ starts. This observation suggests that the adsorption of acetylcholine chloride occurs over a fairly wide range of potential more positive than about -0.9 V.

The distribution of the electronic charges on acetylcholine, as studied by Pullman et al. (1971), indicates the nearly neutral character of the quaternary nitrogen, the distribution of a large fraction of the formal positive charge of this nitrogen onto surrounding methyl groups to produce a large cationic globe, and the near equivalence of the net total negative charge on the two oxygen atoms of acetylcholine.

As can be seen from Fig. 41*b–d*, choline chloride, NaCl, and tetramethylammonium perchlorate are adsorbed in the potential ranges between -0.9 and 0.3 V, -0.4 and 0.3 V, and -1.0 and 0 V, respectively.

Taking into account the electronic properties of acetylcholine and comparing the adsorption potential for acetylcholine with its components, we can roughly estimate the electrode potentials at which each moiety of the acetylcholine molecule is in contact with the electrode

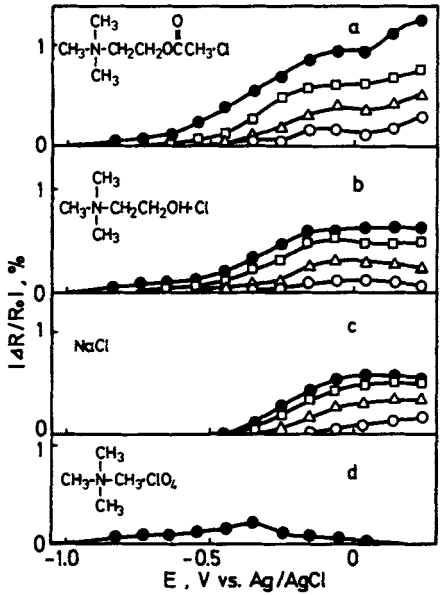

Fig. 41. Potential dependence of the reflectivity change obtained with 0.1 *M* $NaClO_4$ solutions containing *(a)* acetylcholine chloride; *(b)* choline chloride; *(c)* NaCl; *(d)* tetramethylammonium perchlorate. Concentrations: (○) 1.1×10^{-4}; (△) 1.0×10^{-3}; (□) 7.6×10^{-3}; (●) 3.8×10^{-2} *M*. (From Kusu and Takamura, 1984, with permission.)

surface. The trimethylammonium cation head is in contact with the negatively charged electrode surface and the acetyl ester part, as well as Cl^-, is attached to the positively charged surface. Owing to the conformational flexibility of the acetylcholine molecule, conformational changes in the molecules on the electrode surface may occur easily, depending on the surface charge.

Carbamylcholine and Methacholine. The potential dependence of $|\Delta R/R_0|$ in the cases of carbamylcholine chloride and methacholine chloride (Fig. 42) is similar to that for acetylcholine chloride. Thus the adsorption behavior of these molecules is probably similar to that of acetylcholine.

b. Tetraethylammonium Ion and Hexamethonium (Group II). The potential dependence of $|\Delta R/R_0|$ for tetraethylammonium perchlorate is shown in Fig. 43*a*, in which two-stepped curves are obtained at higher concentration of the drug. The large $|\Delta R/R_0|$ values near 0 V, in contrast to the small value for tetramethylammonium ion (see Fig. 41*d*) whose

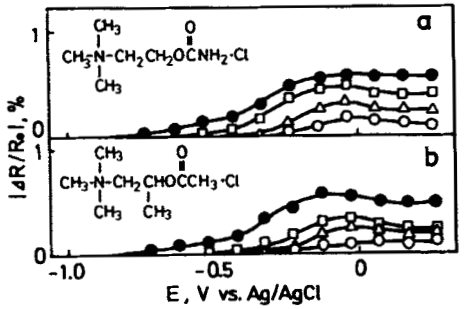

Fig. 42. Potential dependence of the reflectivity change obtained with 0.1 *M* $NaClO_4$ solutions containing *(a)* carbamylcholine chloride and *(b)* methacholine chloride. Concentrations: *(a)* (○) 9.2×10^{-5}, (△) 3.9×10^{-4}, (□) 1.7×10^{-3}, (●) 9.5×10^{-3}; *(b)* (○) 8.8×10^{-5}, (△) 6.0×10^{-4}, (□) 1.4×10^{-3}, (●) 1.1×10^{-2} *M*. (From Kusu and Takamura, 1984, with permission.)

methyl groups form a kind of large ball of delocalized positive charge, appear to be due to the adsorption of the hydrocarbon chain of the ethyl groups. On the other hand, the values of $|\Delta R/R_0|$ at potentials more negative than −0.4 V suggests that the cationic part in the vicinity of nitrogen preferentially interacts with the negatively charged electrode surface. Thus the shape of the curves probably indicates the formation of

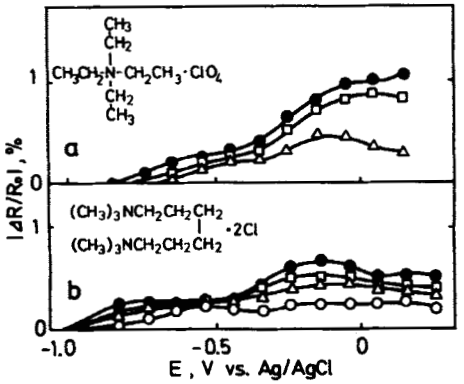

Fig. 43. Potential dependence of the reflectivity change obtained with 0.1 *M* $NaClO_4$ solutions containing *(a)* tetraethylammonium perchlorate and *(b)* hexamethonium chloride. Concentrations: *(a)* (△) 3.4×10^{-3}, (□) 7.7×10^{-3}, (●) 1.8×10^{-2}; *(b)* (○) 5.3×10^{-5}, (△) 2.6×10^{-4}, (□) 7.4×10^{-4}, (●) 2.9×10^{-3} *M*. (From Kusu and Takamura, 1984, with permission.)

two or more orientations of the adsorbed tetraethylammonium ions on the electrode surface, depending on the electrode potential.

Similar behavior may be expected for hexamethonium, since its $|\Delta R/R_0|-E$ curves (Fig. 43*b*) are also two-stepped in shape. The cationic parts of the molecule, that is, the quaternary ammonium groups, seem to be adsorbed at negative potentials ranging about -1.05 to -0.4 V but to keep away from the positively charged electrode surface. The other alkyl parts are probably adsorbed on the electrode surface near pzc.

*c. **Nicotine, Atropine, Scopolamine, and Pilocarpine (Group III).*** The $|\Delta R/R_0|-E$ curves for nicotine, atropine, scopolamine hydrochloride, and pilocarpine hydrochloride have a bell-like form with maxima near to the pzc (Fig. 44). The maximum value of $|\Delta R/R_0|$ increases with increasing drug concentration but tends to take on a constant value when the concentration exceeds 6×10^{-4} *M*. The dependence on potential of $|\Delta R/R_0|$ suggests that the adsorption of these drugs may be regarded as examples of the adsorption of neutral organic compounds. It should be noted that these drugs give larger values of $|\Delta R/R_0|$ even at lower concentrations as compared to the drugs of groups I and II. The $|\Delta R/R_0|-E$ plots (Fig. 44) give smooth curves for any concentration in the potential region more negative than pzc, suggesting that no reorientation of the adsorbed drug molecules takes place.

B. DRUG ACTION AND ADSORPTION BEHAVIOR

In the steps involved in neurohumoral transmission, acetylcholine diffuses across the synaptic or junctional cleft and combines with cholinergic receptors on the postjunctional membrane; this results generally in a localized, nonpropagated increase in the ionic permeability, or conductance, of the membrane. A generalized increase in permeability to Na^+ and K^+, leads to a localized depolarization of the membrane, that is, an excitatory postsynaptic potential. When a molecule of cholinergic or anticholinergic drug combines with a cholinergic receptor, one of the following two effects may appear: the same effect that acetylcholine exerts (i.e., cholinomimetic), or no apparent direct effect but, by occupation of the receptor site, prevention of the action of endogenous acetylcholine (i.e., cholinergic blockage) (Mayer, 1980).

Group I includes cholinergic drugs that act on effector cells in vivo to produce effects similar to those brought about by acetylcholine. Groups II and III include anticholinergic drugs.

The drugs of group II, that is, the tetraethylammonium ion and hexamethonium, are nondepolarizing competitive ganglionic blocking agents. They block the transmission in autonomic ganglia without producing any preceding or concomitant change in the membrane potentials

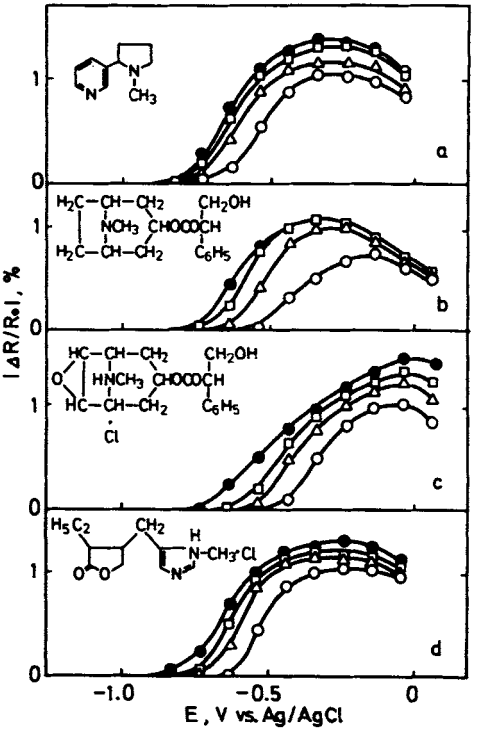

Fig. 44. Potential dependence of the reflectivity change obtained with 0.1 *M* $NaClO_4$ solutions containing *(a)* nicotine, *(b)* atropine, *(c)* scopolamine hydrochloride, and *(d)* pilocarpine hydrochloride. Concentrations: *(a)* (○) 1.3×10^{-5}, (△) 9.0×10^{-5}, (□) 2.8×10^{-4}, (●) 6.5×10^{-4}; *(b)* (○) 2.5×10^{-5}, (△) 1.3×10^{-4}, (□) 2.7×10^{-4}, (●) 5.9×10^{-4}; *(c)* (○) 4.5×10^{-6}, (△) 2.7×10^{-5}, (□) 1.6×10^{-4}, (●) 3.6×10^{-4}; *(d)* (○) 1.4×10^{-5}, (△) 8.1×10^{-5}, (□) 2.1×10^{-4}, (●) 1.1×10^{-3} *M*. (From Kusu and Takamura, 1984, with permission.)

of ganglion cells. In general, they do not modify the conduction of impulses in preganglionic or postganglionic fibers and do not prevent release of acetylcholine by preganglionic impulses. They produce ganglionic blockade by occupying receptor sites and by stabilizing the postsynaptic membranes against the action of acetylcholine (Taylor, 1980).

For the drugs of group III, nicotine is a depolarizing ganglionic blocking agent, and atropine and scopolamine are cholinergic blocking agents. Nicotine initially stimulates the ganglia by an acetylcholine like action and then blocks the ganglion because of a persistent depolarization. Pro-

longed application of nicotine results in desensitization of the cholinergic receptor site and continual blockade (Taylor, 1980). Atropine and scopolamine inhibit the actions of acetylcholine on autonomic effectors innervated by postganglionic cholinergic nerves; that is, they antagonize the muscarinic actions of acetylcholine (Weiner, 1980). These cholinergic blocking agents combine at the cholinoceptive sites with relatively high selectivity but have no important effect directly; their effects are due to blockade of the approach of acetylcholine or cholinomimetic agents. Pilocarpine produces muscarinic effects as a cholinergic agent and competes with muscarinic agonists, such as atropine, for identical binding sites on muscarinic receptors. On the other hand, nicotine produces nicotinic effects that are blocked by tetraethylammonium ions (Ariëns, 1971).

The correspondence between the type of the adsorption potential profile and the type of drug action suggests that the adsorption of drugs on a charged electrode surface reflects partly the occurrence of important events, such as drug attacks on cholinergic receptor sites, in revealing the effect of drugs in vivo.

Cholinergic blocking agents block the activity of acetylcholine by removing it from the cholinergic receptor site, but this requires a high concentration of cholinergic agent (Ariëns, 1971). The order of adsorptivity was found to be group I < group II < group III, by a comparison of the lower concentration limits at which drugs are adsorbed on a electrode surface. These facts suggest that the binding strengths of these drugs at the receptor site can be explained in relation to their adsorptivity.

The action of acetylcholine, and some of its related drugs, at the junctions of various cholinergic nerve endings with their effector organs or postsynaptic sites, terminates as it is enzymatically destroyed. Thus cholinergic or anticholinergic effects of drugs depends not only on their binding strength with receptor sites but also on their enzymatic destruction rates. Unfortunately the information available from adsorption studies is restricted to a measure of the binding strength.

Acetylcholine and its antagonists are clearly quite stereospecific at the postjunctional membrane; that is, the cholinergic receptor is stereoselective, especially muscarinic receptor (Ariëns, 1971; Ariëns and Simonis, 1967). From the results of electrochemical adsorption some knowledge of this stereospecificity can be obtained. However, it should be noted that the experimental evidence for the adsorption of acetylcholine and drugs onto a charged surface provides information of the competitive inhibitory effects on the attachment of acetylcholine to the cholinergic receptor site.

C. OTHER DRUGS

The findings observed for acetylcholine and its agonist and antagonists appear quite interesting in connection with the pharmacological hypothesis concerning the structure and activity relationship of drugs. The extension of the present method is worth applying to other series of not only structurally specific but structurally nonspecific drugs.

Adrenergic drugs (norepinephrine, epinephrine, etc.) and adrenergic blocking drugs (ergotamine, propranolol, etc.), which are other examples of structurally specific drugs, gave results similar to those for the acetylcholine series.

In contrast with these two series, barbiturates are drugs in which pharmacological action is not directly related to chemical structure. Such drugs exert a hypnotic effect on the central nervous system, and their biological responses are known to relate closely to their permeability of lipid-containing structures in vivo. Later we dealt, using the same procedure, with the adsorption behavior of six kinds of barbiturates (Takamura and Kusu, 1983), such as allobarbital, amobarbital, barbital, cyclobarbital, hexobarbital, and phenobarbital. Although they differ from one another in chemical structure, they were similar in their $|\Delta R/R_0|-E$ relations. This fact is in marked contrast to the findings for acetylcholine and norepinephrine and their related drugs.

Nevertheless, the results obtained for the three series of drugs investigated showed a good correlation between the type of the adsorption-potential profile and the type of drug action. Therefore the reflection method seems to have the advantage of affording clues to the binding of drugs to their receptor sites.

VI. FUTURE DEVELOPMENT

This chapter discussed the application of the electro-optical reflection method in the in situ observation of the adsorption and desorption of bioactive substances at an electrode surface acting as a simple model of charged sites at a biosurface. This method should find extensive application in various bioelectrochemical fields as a potent means of surface analysis. Electrode surfaces, though much simpler than biosurfaces, still provide data reflecting actual occurrences at biosurfaces in some respects. Electro-optical studies on the behavior of bioactive substances at electrode surfaces should provide some indication of how such substances behave at biosurfaces.

Further application of this method to biochemistry will require im-

proved model surfaces for approximating actual biomembranes. Modified electrodes may facilitate solution of this problem. Many attempts have been made recently to modify electrode surfaces so as to select biofunctionally significant electrode processes (Murray, 1984; Oyama and Anson, 1979). Electrodes coated with biological substances such as lipids and enzymes appear adequate to serve as improved models for this purpose. Our future research shall employ a laser source to ensure greater measurement sensitivity.

The specular reflection spectroscopy is being applied extensively in our research, but it provides only limited data on the molecular level. Thus SERS, IR, or internal reflection spectroscopy used in conjunction with the present method should help to obviate this problem.

Acknowledgment

We wish to thank Dr. A. Shinohara for her technical assistance. This research was supported in part by Grants-in-Aid for Scientific Research from the Japanese Ministry of Education, Science and Culture.

References

Adams, R. N. (1969), in *Electrochemistry at Solid Electrodes*, Dekker, New York, pp. 115–162.

Ariëns, E. J., and Simonis A. M. (1967) *Ann. N.Y. Acad. Sci.*, *144*, 842–868.

Ariëns, E. J. (1971) in *Drug Design*, Academic Press, New York, pp. 162–193.

Bard, A. J., and Faulkner L. R. (1980) in *Electrochemical Methods*, Wiley, New York, pp. 213–243.

Berry, M. N., Grivell, A. R., and Wallace, P. G. (1985), in *Comprehensive Treatise of Electrochemistry*, Vol. 10 (S. Srinivasan, Y. A. Chizmadzhev, J. O'M. Bockris, B. E. Conway, and E. Yeager, eds.), Plenum Press, New York, pp. 347–356.

Betso, S. R., Klapper, M. H., and Anderson, L. B. (1972) *J. Am. Chem. Soc.*, *94*, 8197–8204.

Bewick, A. (1983), *J. Electroanal. Chem.*, *150*, 481–493.

Bewick, A., and Thomas, B. (1975), *J. Electroanal. Chem.*, *65*, 911–931.

Bodé, D. D., Andersen, T. N., and Eyring, H. (1967), *J. Phys. Chem.*, *71*, 792–797.

Bowden, E. F., Hawkridge, F. M., and Blount, H. N. (1985), in *Comprehensive Treatise of Electrochemistry*, Vol. 10 (S. Srinivasan, Y. A. Chizmadzhev, J. O'M. Bockris, B. E. Conway, and E. Yeager, eds.), Plenum Press, New York, pp. 297–306.

Brabec, V., Christian, S. D., and Dryhurst, G. (1978), *J. Electrochem. Soc.*, *125*, 1236–1244.

Brabec, V., Kim, M. H., Christian, S. D., and Dryhurst, G. (1979), *J. Electroanal. Chem.*, *100*, 111–133.

Burnett, R. W., and Underwood, A. L. (1968), *Biochemistry*, *7*, 3328–3333.

Cotton, T. M., Schultz, S. G., and van Duyne, R. P. (1980), *J. Am. Chem. Soc.*, *102*, 7960–7962.

Cuypers, P. A., Janssen, M. P., Kop, J. M. M., Hermens, W. T., and Hemker, H. C. (1980), *Surface Sci.*, *96*, 555–563.

Dahms, H. and Green, M. (1963), *J. Electrochem. Soc.*, *110*, 1075–1080.

Damaskin, B. B., Petrii, O. A., and Batrakov, V. V. (1971), in *Adsorption of Organic Compounds on Electrodes*, Plenum Press, New York, pp. 175–485.

Davis, R. B., Azzam, R. M. A., and Holtz, G. (1980), *Surface Sci.*, *96*, 539–554.

Donohue, J. (1968), *Arch. Biochem. Biophys.*, *128*, 591–594.

Droog, J. M. M., Alderliesten, P. T., and Bootsma, G. A. (1979), *J. Electroanal. Chem.*, *99*, 173–186.

Dryhurst, G. (1977), in *Electrochemistry of Biological Molecules*, Academic Press, New York, pp. 365–391.

Elving, P. J., O'Reilly, J. E. and Schmakel, C. O. (1973) in *Methods of Biochemical Analysis*, Vol. 21 (D. Glick, ed.), Interscience, New York, pp. 287–465.

Ervin, K. M., Koglin, E., Sequaris, J. M., Valenta, P., and Nürnberg, H. W. (1980), *J. Electroanal. Chem.*, *114*, 179–194.

Fleischmann, M., and Hill, I. R. (1983), *J. Electroanal. Chem.*, *146*, 367–376.

Gardner, J. R., and Woods, R. (1977), *J. Electroanal. Chem.*, *81*, 285–290.

Habib, M. A., and Bockris, J. O'M. (1984), *J. Electroanal. Chem.*, *180*, 287–306.

Hansen, W. N. (1973) in *Advances in Electrochemistry and Electrochemical Engineering*, Vol. 9 (P. Delahay and C. W. Tobias, eds.), Wiley-Interscience, New York, pp. 1–60.

Hart, J. P., and Catterall, A. (1980) in *Electroanalysis in Hygiene, Environmental, Clinical and Pharmaceutical Chemistry* (E. F. Smith, ed.), Elsevier, New York, pp. 145–153.

Hartley, A. M., and Wilson, G. S. (1966), *Anal. Chem.*, *38*, 681–687.

Hauser, H. (1975) in *Water—A Comprehensive Treatise*, Vol. 4 (F. Franks, ed.), Plenum Press, New York, pp. 209–303.

Heineman, W. R., Norris, B. J., and Goelz, J. F. (1975), *Anal. Chem.*, *47*, 79–84.

Heineman, W. R., Hawkridge, F. M., and Blount, H. N. (1984), in *Electroanalytical Chemistry*, Vol. 13 (A. J. Bard, ed.), Dekker, New York, pp. 1–113.

Hinnen, C., Parsons, R., and Niki, K. (1983), *J. Electroanal. Chem.*, *147*, 329–337.

Humphreys, M. W., and Parsons, R. (1977), *J. Electroanal. Chem.*, *75*, 427–436.

Iball, J., and Wilson, H. R. (1963), *Nature*, *198*, 1193–1195.

Janik, B., and Elving, P. J. (1968), *Chem. Rev.*, *68*, 295–319.

Jehring, H., Huyen, N. V. Gian, T. X., Horn, E., and Hirche, C. (1979), *J. Electroanal. Chem.*, *100*, 13–22.

Kakutani, T., Kano, K., Ando, S., and Senda, M. (1981), *Bull. Chem. Soc. Jpn.*, *54*, 884–890.

Kakutani, T., Katasho, I., and Senda, M. (1983), *Bull. Chem. Soc. Jpn.*, *56*, 1761–1767.

Kinoshita, H., Christian, S. D., and Dryhurst, G. (1977a), *J. Electroanal. Chem.*, *83*, 151–166.

Kinoshita, H., Christian, S. D., Kim, M. H., Baker, J. G., and Dryhurst, G. (1977b), in *Electrochemical Studies of Biological Systems* (D. T. Sawyer, ed.), American Chemical Society, Washington, D.C., pp. 113–142.

Koglin, E., and Séquaris, J. M. (1983), *J. de Phys.*, *10*, 487–490.

Kruger, J. (1973), in *Advances in Electrochemistry and Electrochemical Engineering*, Vol. 9 (P. Delahay and C. W. Tobias, eds.), Wiley-Interscience, New York, pp. 227–280.

Kunimatsu, K., and Parsons, R. (1979), *J. Electroanal. Chem.*, *100*, 335–363.

Kusu, F., and Takamura, K. (1984), *J. Electroanal. Chem.*, *161*, 169–180.

Kusu, F., and Takamura, K. (1985a), *Surface Sci.*, *158*, 633–643.

Kusu, F., and Takamura, K. (1985b), Denki Kagaku, 53, 361–365.

Kuwana, T., and Winograd, N. (1974) in *Electroanalytical Chemistry,* Vol. 7 (A. J. Bard, ed.), Dekker, New York, pp. 1–78.

Mark, H. B., and Randall, E. N. (1970), *Symposia Faraday Soc., 4,* 157–172.

Mayer, S. E. (1980) in *The Pharmacological Basis of Therapeutics* (A. G. Gilman, L. S. Goodman, and A. Gilman, eds.) 6th ed., Macmillan, New York, pp. 56–90.

McIntyre, J. D. E. (1973a), in *Advances in Electrochemistry and Electrochemical Engineering,* Vol. 9 (P. Delahay and C. W. Tobias eds.) Wiley-Interscience, New York, pp. 61–166.

McIntyre, J. D. E. (1973b), *Surface Sci., 37,* 658–682.

McIntyre, J. D. E., and Aspnes, D. E. (1971), *Surface Sci., 24,* 417–434.

Moret, V., Pinamonti, S., and Fornasari, E. (1961) *Biochem. Biophys. Acta, 54,* 381–383.

Murray, R. W. (1984), in *Electroanalytical Chemistry,* Vol. 13 (A. J. Bard, ed.), Dekker, New York, pp. 191–368.

Nicholson, R. S. (1965), *Anal. Chem., 37,* 1351–1354.

O'Brien, F. L., and Oliver, J. W. (1961), *Anal. Chem., 41,* 1810–1813.

Oyama, N. and Anson, F. C. (1979), *J. Am. Chem. Soc., 101,* 739–741, 3450–3456.

Pilla, A. A. (1974), *Bioelectrochem. Bioenerg., 1,* 227–243.

Pullman, B., Claverie, P., and Caillett, J. (1966), *Proc. Natl. Acad. Sci. USA 55,* 904–912.

Pullman, B., Courriere, P., and Coubeils, J. L. (1971), *Mol. Pharmacol., 7,* 397–405.

Ranweiler, J. S., and Wilson, G. S. (1976), *Bioelectrochem. Bioenerg., 3,* 113–122.

Sakura, S. (1981), *Bioelectrochem. Bioenerg., 8,* 43–48.

Schmakel, C. O., Santhanam, K. S. V., and Elving, P. J. (1974), *J. Electrochem. Soc., 121,* 345–353, 1033–1045.

Schmakel, C. O., Santhanam, K. S. V., and Elving, P. J. (1975), *J. Am. Chem. Soc., 97,* 5083–5092.

Srivivasan, S., Cahen, G. L., Jr., and Sloner, G. E. (1977), in *Electrochemistry* (H. Bloom and F. Gutmann, eds.), Plenum Press, New York, pp. 57–70.

Stenberg, M., Arwin, H., and Nilsson, A. (1979), *J. Colloid Interface Sci., 72,* 255–264.

Takamura, K., and Hayakawa, Y. (1974), *J. Electroanal. Chem., 49,* 133–140.

Takamura, K., and Kusu, F. (1983), *Denki Kagaku, 51,* 141–142.

Takamura, T., and Takamura, K. (1978), in *Surface Electrochemistry* (T. Takamura and A. Kozawa, eds.), Japan Scientific Societies Press, Tokyo, pp. 179–241.

Takamura, T., Takamura, K., Nippe, W., and Yeager, E. (1970) *J. Electrochem. Soc., 117,* 626–630.

Takamura, T., Takamura, K., and Yeager, E. (1971), *J. Electroanal. Chem., 29,* 279–291.

Takamura, T., Takamura, K., and Hayakawa, Y. (1973), *Denki Kagaku, 41,* 823–827.

Takamura, T., Takamura, K., and Watanabe, F. (1974), *Surface Sci., 44,* 93–108.

Takamura, K., Mori, A., and Watanabe, F. (1979), *J. Electroanal. Chem., 102,* 109–116.

Takamura, K., Mori, A., and Watanabe, F. (1981a), *Bioelectrochem. Bioenerg., 8,* 125–136.

Takamura, K., Mori, A., and Kusu, F. (1981b), *Bioelectrochem. Bioenerg., 8,* 229–238.

Takamura, K., Mori, A., and Kusu, F. (1981c), *Chem. Pharm. Bull., 29,* 1810–1818.

Takamura, K., Mori, A., and Kusu, F. (1981d), *Chem. Pharm. Bull., 29,* 3083–3089.

Takamura, K., Mori, A., and Kusu, F. (1982), *Bioelectrochem. Bioenerg., 9,* 499–508.

Tanaka, N., Ashida, T., Sasada, Y., and Kakudo, M. (1969), *Bull. Chem. Soc. Jpn.*, *42*, 1546–1554.

Taylor, P. (1980), in *The Pharmacological Basis of Therapeutics* (A. G. Gilman, L. S. Goodman and A. Gilman, eds.) 6th ed., Macmillan, New York, pp. 211–219.

Vroman, L., and Adams, A. L. (1969), *Surface Sci.*, *16*, 438–446.

Weiner, N. (1980) in *The Pharmacological Basis of Therapeutics* (A. G. Gilman, L. S. Goodman, and A. Gilman, eds.) 6th ed., Macmillan, New York, pp. 120–137.

Woods, R. (1976) in *Electroanalytical Chemistry*, Vol. 9 (A. J. Bard, ed.), Dekker, New York, pp. 20–27.

Yeh, P., and Kuwana T. (1977), *Chem. Lett.*, 1145–1148.

Methods of Biochemical Analysis, Volume 32
Edited by David Glick
Copyright © 1987 by John Wiley & Sons, Inc.

METHODS OF BIOCHEMICAL ANALYSIS VOLUME 32

Isoelectric Focusing in Immobilized pH Gradients: Theory and Newer Methodology

PIER GIORGIO RIGHETTI AND ELISABETTA GIANAZZA, *Faculty of Pharmaceutical Sciences and Department of Biomedical Sciences and Technologies, University of Milano, Milano, Italy*

I. INTRODUCTION

The technique of immobilized pH gradients (IPG) in isoelectric focusing was first announced to the scientific community at a meeting of the International Electrophoresis Society in Athens, April 1982, as the result of an intensive collaborative effort (Righetti et al., 1983c; Bjellqvist et al., 1983; Görg et al., 1983). It seems extraordinary that in only two and one-half years the method was developed to such an extent as to call for an extensive review. When conventional isoelectric focusing (IEF) was developed in 1960 (Svensson, 1961, 1962), it took a full decade before the scientific community became aware of it.

We start this review with a list of fundamental references in the field of IPG noting all the important developments concerning this new electrophoretic technique.

1. The milestone article of the foundations of IPGs (Bjellqvist et al., 1982)
2. Description of extended pH intervals, spanning 2–6 pH units (computer programs and formulations: Dossi et al., 1983; Gianazza et al., 1983a; Gianazza et al., 1984a; Gianazza et al., 1985a, b).
3. Strategy for optimizing preparative runs (manipulations of gel thickness, pH gradient width, buffering power, ionic strength, the discovery of the high loading capacity of "soft gels"; retrieval of proteins from Immobiline matrices) (Ek et al., 1983; Gelfi and Righetti, 1983; Righetti and Gelfi, 1984; Casero et al., 1985; Bartels and Bock, 1984).
4. Copolymerization kinetics of Immobilines into polyacrylamide gels; swelling kinetics of dried IPG gels and stability of Immobilines and precast IPG gels (Righetti et al., 1984a; Gelfi and Righetti, 1984; Pietta et al., 1985).
5. The first two-dimensional (2-D) maps and the use of urea and detergents in IPG systems (Westermeier et al., 1983; Gianazza et al., 1984b; Gianazza et al., 1983b).
6. Early reviews in the field of IPG and 2-D maps (Righetti, 1983a, b; Righetti et al., 1983a; Righetti, 1984; Righetti et al., 1984b).
7. An artifact with the IPG technique (Righetti et al., 1983b).
8. Zymograms and substrate gradients in IPGs (Görg et al., 1985).

II. THE EVOLUTION OF AN IDEA

To follow the development of the isoelectric focusing concept from a somewhat shaky origin to the present stage, we must start in the 1950s when two scientists independently worked on focusing ions or proteins in a pH gradient: Schumacher (1957) in Switzerland and Kolin (1958) in the US. Kolin's work is well known, but there has been hardly a single mention of Schumacher's work. One of Schumacher's coworkers (Dr. W. Thormann) having brought this to our attention, we are happy to repair this injustice and give credit for his excellent work. Kolin's system was incredibly advanced, conceptually and methodologically, for those early days of electrophoresis. He used the term "isoelectric spectrum" to denote a distribution pattern established by a sorting process in a pH gradient. This pattern was generated by placing the substance to be separated at the interface between an acidic and a basic buffer, in a Tiselius-like apparatus, and allowing diffusion to proceed in an electric field. In these "artificial" pH gradients Kolin was able to obtain isoelectric line spectra of dyes, proteins, cells, microorganisms, and viruses on a time scale from 40 sec to a few minutes, a rapidity still unmatched in this field. Along with the pH gradient, a density gradient, an electrical conductivity gradient, and a vertical temperature gradient were applied in the separation cell. Later on Kolin (1977) broadened the scope of IEF into a concept, termed "isoperichoric focusing" (Fig. 1), which encompassed such condensation phenomena as isopycnic-, isoconductivity-, isodielectric-, isomagnetic-, isoparamagnetic-, and isodiamagnetic-focusing.

A second evolutionary event followed when Svensson (1961) introduced the concept of "natural" pH gradients and established the theoretical basis of conventional IEF. Svensson synthesized the minimum basic requirement for stable pH gradients in an electric field in the "carrier ampholyte." That is, the buffers used in this system required two fundamental properties: (1) amphoterism so that they could reach an equilibrium position along the separation column and (2) "carrier" ability. This last concept is more subtle but just as fundamental. Any ampholyte cannot be used for IEF, only a carrier ampholyte, that is, a compound capable of carrying the current (a good conductor) and capable of carrying the pH (a good buffer). With this notion, and with Vesterberg's (1969) elegant synthesis of such ampholytes, present-day conventional IEF was born (Fig. 2). The gestation period was summarized in a superb review (Haglund, 1971). In breadth and depth it was unsurpassed for many years, and at that time it was a *Summa Theologica* of all the knowledge available in the field: it served in training a generation of biochemists.

Over about 25 years, conventional IEF served superbly, as

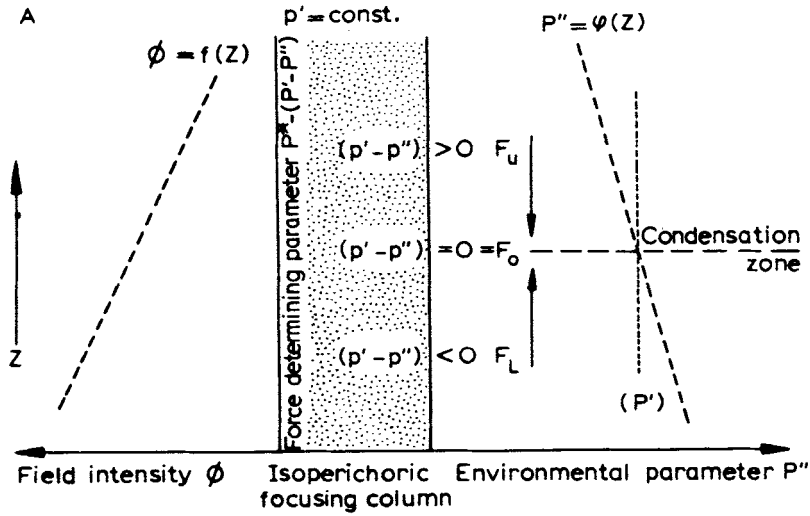

Fig. 1. Isoperichoric focusing. A chemical environment is generated in which an environmental property described by parameter p'' is changing from point to point along the z-axis [$p'' = \phi(z)$]. A species of particles characterized by the parameter value p', corresponding to the parameter p'' of the suspension fluid, is dispersed with an arbitrary distribution in the fluid column. It is assumed that there is a point within the gradient of the p'' distribution, at which p'-p''-O, where the particle parameter equals the environmental parameter (focusing or condensation zone). (From Kolin, 1977. Reproduced with permission of the publisher.)

documented by more than 5000 articles (Righetti and Caravaggio, 1976; Righetti et al., 1981a). The need to improve the technique arose because of (1) cathodic drift (2) lack of even conductivity and buffering capacity, (3) extremely low and unknown ionic strength *(I)*, and (4) limited load capacity, mostly due to isoelectric precipitation caused by the low *I* environment. Immobilized pH gradients, the latest step in the evolutionary process and a new, revolutionary concept, have solved these problems.

III. THE CHEMICALS: THE IMMOBILINE MATRIX

1. General Properties of Immobilines

IPGs are based on the principle that the pH gradient, which exists prior to the IEF run itself, is copolymerized, and thus insolubilized, within the fibers of the polyacrylamide matrix. This is achieved by using, as buffers,

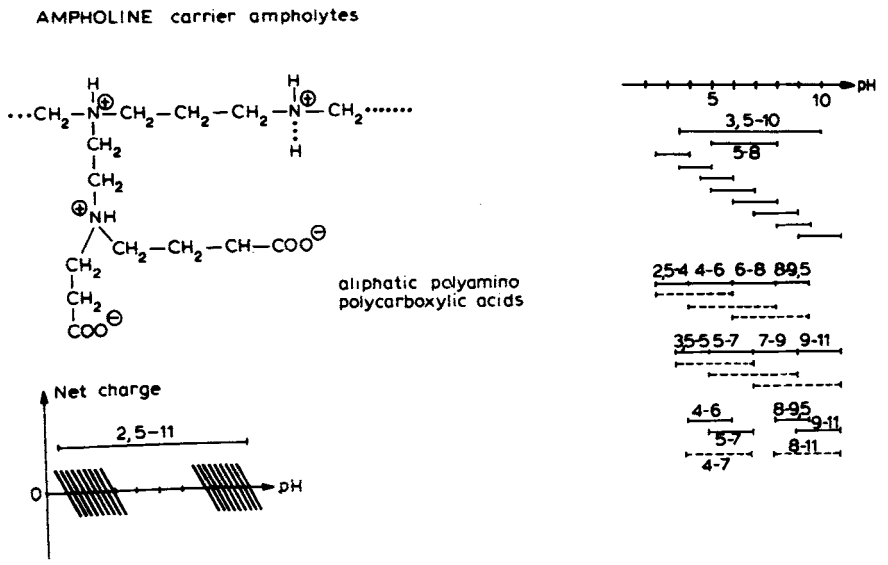

Fig. 2. Composition of Svensson-type (1961) carrier ampholytes, as synthesized by Vesterberg (1969). On the upper left side a representative chemical formula is shown (aliphatic oligo amino oligo carboxylic acids). On the lower left side, portions of hypothetical titration curves of Ampholines are depicted. Right: different pH cuts for wide and narrow range carrier ampholytes. (Courtesy of LKB Produkter AB, Bromma. Reproduced with permission of the publisher.)

a set of seven nonamphoteric, weak acids and bases, having the following general chemical composition: $CH_2{=}CH{-}CO{-}NH{-}R$, where R denotes either three different weak carboxyls, with p*K*s 3.6, 4.4, and 4.6 or four tertiary amino groups, with p*K*s 6.2, 7.0, 8.5, and 9.3 (Table I). During gel polymerization, these buffering species are efficiently incorporated into the gel (84–86% conversion efficiency at 50°C for 1 h) (Righetti et al., 1984a). Immobiline-based pH gradients can be cast in the same way as conventional polyacrylamide gradient gels, by using a density gradient to stabilize the Immobiline concentration gradient, with the aid of a standard, two-vessel gradient mixer. As shown in the formula, these buffers are no longer amphoteric, as in conventional IEF but are bifunctional: at one end of the molecule is located the buffering group, and at the other the acrylic double bond, which will disappear during the grafting process. The three carboxyl Immobilines have rather small temperature coefficients (dpK/dT) in the 10–25°C range, due to their small standard heats of ionization, (~1 kcal/mol) and thus exhibit negligible p*K*

TABLE I

Apparent pK Values[a], I-[2]

	H_2O		Polyacrylamide gel [b] T = 5%, C = 3%		Polyacrylamide gel [b] T = 5%, C = 3% glycerol 25% (w/v)		Physical state at room temperature
	10°C	25°C	10°C	25°C	10°C	25°C	
Acids with carboxyl as buffering group							
Immobiline pK 3.6	3.57	3.58	–	–	3.68 ± 0.02	3.75 ± 0.02	solid
Immobiline pK 4.4	4.39	4.39	4.30 ± 0.02	4.36 ± 0.02	4.40 ± 0.03	4.47 ± 0.03	solid
Immobiline pK 4.6	4.60	4.61	4.51 ± 0.02	4.61 ± 0.02	4.61 ± 0.02	4.71 ± 0.03	solid
Bases with tertiary amine as buffering group							
Immobiline pK 6.2	6.41	6.23	6.21 ± 0.05	6.15 ± 0.03	6.32 ± 0.08	6.24 ± 0.07	solid
Immobiline pK 7.0	7.12	6.97	7.06 ± 0.07	6.96 ± 0.05	7.08 ± 0.07	6.95 ± 0.06	solid
Immobiline pK 8.5	8.96	8.53	8.50 ± 0.06	8.38 ± 0.06	8.66 ± 0.09	8.45 ± 0.07	liquid
Immobiline pK 9.3	9.64	9.28	9.59 ± 0.08	9.31 ± 0.07	9.57 ± 0.06	9.30 ± 0.05	liquid

[a] pK values measured with glass surface electrode without any corrections.
[b] Mean values of 10 determinations. Due to the slow response of the electrode the pK values for the amines are uncertain.

variations in this temperature interval. On the other hand, the four basic Immobilines exhibit rather large ΔpKs (as much as $\Delta pK = 0.44$ for the pK 8.5 species) due to their larger heats of ionization (6–12 kcal/mol). Therefore, for reproducible runs and pH gradient calculations, all the experimental parameters have been fixed at 10°C. Temperature is not the only variable that affects Immobiline pKs (and therefore the actual pH gradient generated): for the corrections to be made, additives in the gel that change the water structure (chaotropic agents, e.g., urea) or lower its dielectric constant, and the ionic strength of the solution, alter their pK values (Gianazza et al., 1983b). The list of seven Immobilines is not exhaustive. For generation of extended pH gradients, with a two-chamber mixer, there might be a need for two additional ones: a strongly acidic ($pK < 1$) and a strongly basic ($pK > 12$) compound with pKs well outside the desired pH range. It is not unreasonable to predict that they will contain a sulphate and a quaternary amino group, respectively.

Figure 3 depicts a segment of a hypothetical structure of an Immobiline matrix (lower tracing) as compared with the partial formula of a carrier ampholyte molecule. (In the matrix the long strings represent the polyacrylamide coils, and the short, vertical segments are the cross-links.) Since they are copolymerized within the matrix, the Immobiline buffers no longer migrate in the electric field: this means that the pH gradient is stable indefinitely, though this condition has to be established before the onset of polymerization, and can only be destroyed if and when the polyacrylamide gel is hydrolyzed. At the matrix concentration normally used (5%T) and at the standard Immobiline levels (approximately 10 mM buffering ion) there is about one buffering group (or titrant) every 47 acrylamide residues, which means that statistically there are about 94 carbon atoms between two adjacent Immobiline species. This is extremely important for the ionic strength of the system, as compared with conventional IEF (Righetti et al., 1983a).

2. Stability of Immobilines with pH and Temperature

Given such a sophisticated and highly reproducible methodology, the first true example of "pH gradient engineering," it is important to know how to handle the Immobiline chemicals for optimum performance run after run. As shown in Table I, the first five species are solids, whereas the two most alkaline ones are in a liquid state. In general, troubles arise from the pKs 8.5 and 9.3 chemicals; in fact, we are told (Dr. B. Bjellqvist) that presently they are added with traces of inhibitors. These chemicals could degrade through two major pathways: (1) autopolymerization (a simple check for it is that the solution becomes slightly opalescent) or (2) hydrolysis along the amide bond, thus splitting the acrylamide moiety from the

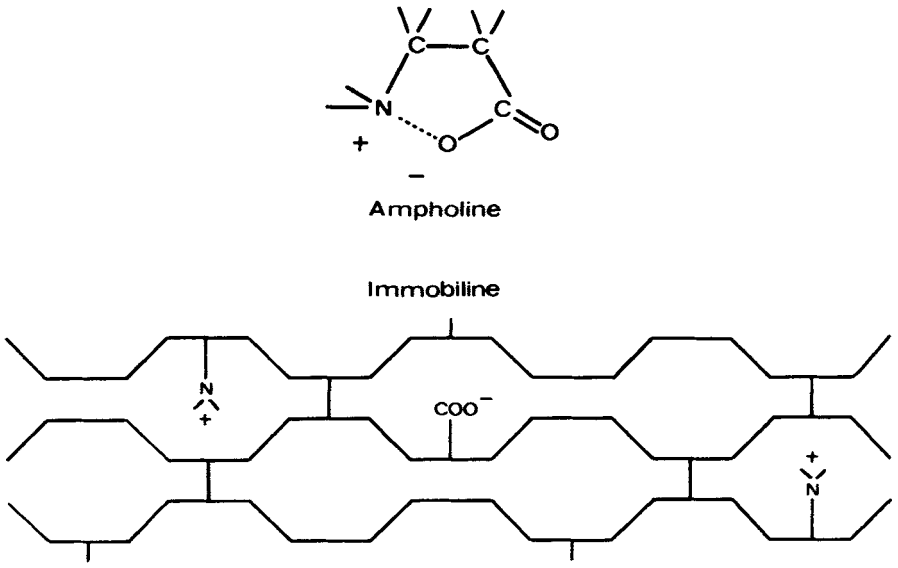

Fig. 3. Comparison between ionic strength in Ampholine and Immobiline gels. The upper drawing depicts a segment of an isoelectric Ampholine molecule, and the lower tracing shows a portion of an Immobiline gel. An Ampholine molecule, at its p*I*, is likely to form an inner salt, which does not contribute to the ionic strength of the system. The fixed charges in the Immobiline gel, being spaced approximately 47 carbon atoms apart, are believed to behave as point charges in the surrounding space, thus effectively contributing to the ionic strength of the milieu. (From Righetti et al., 1983a. Reproduced with permission of the publisher.)

buffering group at the other extremity of the molecule. In both cases the results of an IPG experiment would fail. From the point of view of storage we reconstitute the powders (or liquids) with 25 g of distilled water (i.e., we prepare stock solutions by weight rather than by volume, the former being more accurate) thus obtaining 0.2 *M* solutions of each species. They are then dispensed in 5 ml aliquots and stored frozen at −20°C. Each 5 ml aliquot was found to have a shelf life at +4°C of at least four weeks; the frozen batches being stable for at least six months. As this information was not available, we have now studied the stability with time of Immobiline solutions and of precast Immobiline gels as a function of pH and temperature (Pietta et al., 1985). The results are summarized in Fig. 4*A* and *B*. Temperature seems to affect these chemicals most: whatever degradation occurs at 20°C within a few weeks time, it is operative at 60°C within a few

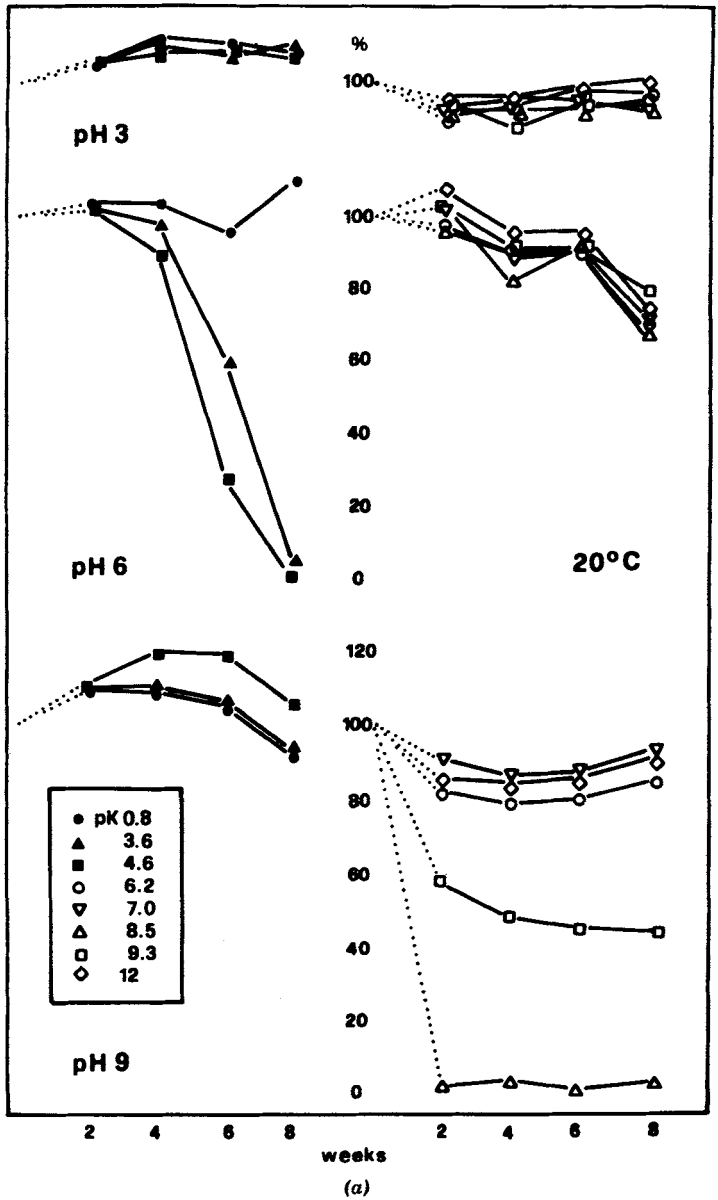

Fig. 4. Kinetics of Immobiline degradation upon storage at 20°C *(a)* or at 60°C *(b)*, 200 µl of a solution 2.5 m*M* in each Immobiline at pH 3 (top), 6 (middle), or 9 (bottom) were sealed in vials and kept at 20°C or at 60°C for various lengths of time; quantitation of the remaining Immobiline was then performed by HPLC, by reverse phase on a microBondapak C18 column and isocratic elution for the acidic monomers (data plotted on the left) or by cation exchange on a Zorbax SCX300 column under isocratic elution for the basic monomers (on the right). Symbols are listed in the inset. (From Pietta et al., 1985. Reproduced with permission of the publisher.)

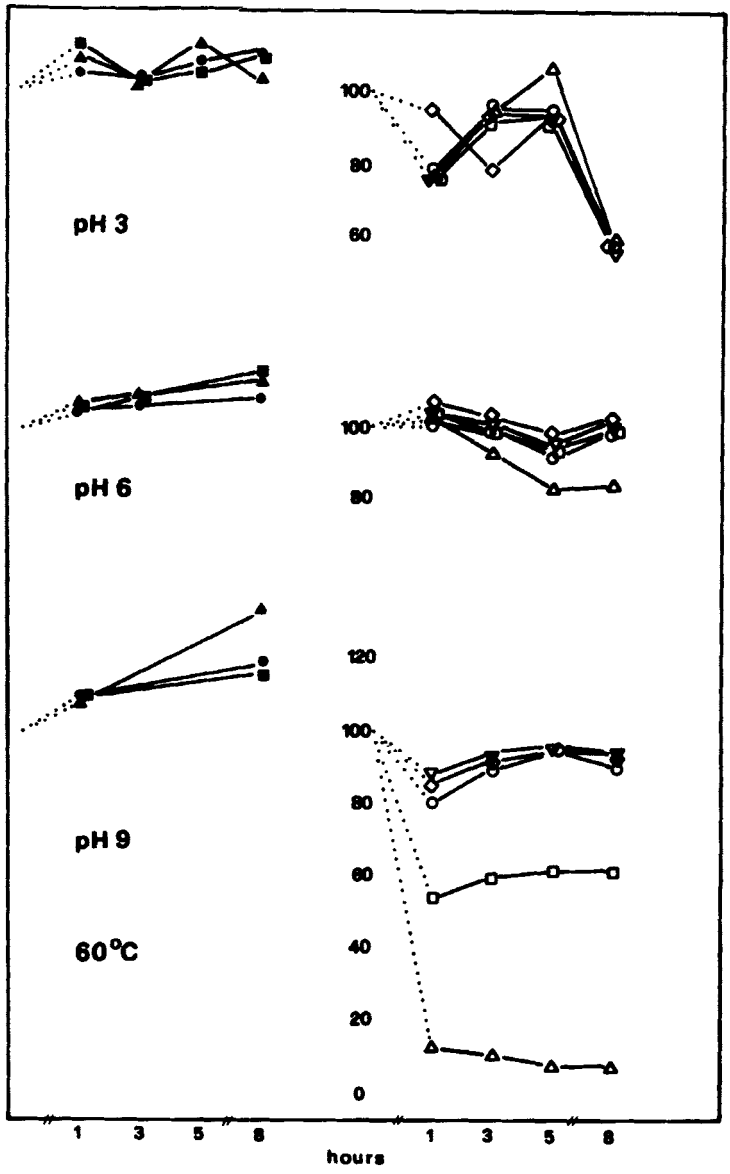

(b)

Fig. 4. *(Continued)*

hours. pH alters these buffers in different ways: acidic Immobilines (p*K*s 3.6 and 4.6) are extensively degraded around neutrality (pH 6), whereas basic species (especially p*K*s 8.5 and 9.3) are fully destroyed in alkaline solutions (pH 9), acidic pH values (pH 3–4) ensuring maximum stability for all Immobiline chemicals. In medium-term storage of precast gels, wet matrices exhibit least degradation if titrated to pH 4, formic acid being the best titrant because it can be efficiently removed during the focusing step with formation of the narrowest salt front at the anode. Dry matrices have much longer stability (>2 months) but should be stored under somewhat humid conditions to prevent the plastic support from cracking and peeling off, which occurs in the absence of humidity. A practical way of dealing with the instablity of Immobilines p*K*s 8.5 and 9.3 at pH 9.0 and 60°C (i.e., 85% destruction within 1 h!) is to maintain the reaction temperature of 50°C for 1 h, which allows similar reactivity and optimal incorporation of all species in the gel matrix (Righetti et al., 1984a), while controlling the pH of the gelling mixture for any desired pH gradient and keeping it around pH 7–7.5 (by suitable titration with acids or bases); see Section VI.3.

IV. NARROW AND ULTRANARROW pH GRADIENTS

We define the gradients from 0.1 to a 1 pH unit as narrow and ultranarrow gradients. Within these limits we work on a "tandem" principle—that is we choose a "buffering" Immobiline such as a base or an acid with its p*K* within the pH interval we want to generate, and a "nonbuffering" Immobiline such as an acid or a base with its p*K* at least 2 pH units removed from either the minimum or maximum of our pH range. The titrant will provide equivalents of acid or base to titrate the buffering group but will not itself buffer in the desired pH interval. For these calculations, we used to resort to modified Henderson-Hasselbalch equations (Bjellqvist et al., 1982) and to rather complex nomograms found in the LKB Application Note No. 321. Things are much easier now. In Note No. 324 you will find no less than 58, 1 pH unit wide gradients, starting with the pH 3.8–4.8 interval and ending with the pH 9.5–10.5 range, separated by 0.1 pH unit increments. In Table II are the relative recipes giving the Immobiline volumes (for 15 ml of mixture) needed in the acidic (mixing) chamber to obtain pHmin and the corresponding volumes for the basic (reservoir) chamber of the gradient mixer needed to generate pHmax of the desired pH interval. We work on the "troika" principle only between pH 4.6–5.1 (pHmin) and 7.2–7.4 (pHmin) for in these regions there are wide gaps in the p*K*s of neighboring Immobilines.

TABLE II

1-pH Unit Gradients: Volumes of Immobiline for 15 ml Each of Starting Solution (2 gels)

Control pH at 20°C	Volume (µl) 0.2 M Immobiline pK Acidic dense solution 3.6	4.4	4.6	6.2	7.0	8.5	9.3	pH range	mid point	Control pH at 20°C	Volume (µl) 0.2 M Immobiline pK Basic light solution 3.6	4.4	4.6	6.2	7.0	8.5	9.3
3.84±0.03	–	750	–	–	–	–	159	3.8– 4.8	4.3	4.95±0.06	–	750	–	–	–	–	591
3.94±0.03	–	710	–	–	–	–	180	3.9– 4.9	4.4	5.04±0.07	–	810	–	–	–	–	667
4.03±0.03	–	–	755	–	–	–	157	4.0– 5.0	4.5	5.14±0.06	–	–	745	–	–	–	584
4.13±0.03	–	–	713	–	–	–	177	4.1– 5.1	4.6	5.23±0.07	–	–	803	–	–	–	659
4.22±0.03	–	–	689	–	–	–	203	4.2– 5.2	4.7	5.33±0.08	–	–	884	–	–	–	753
4.32±0.03	–	–	682	–	–	–	235	4.3– 5.3	4.8	5.42±0.10	–	–	992	–	–	–	871
4.42±0.03	–	–	691	–	–	–	275	4.4– 5.4	4.9	5.52±0.12	–	–	1133	–	–	–	1021
4.51±0.04	–	–	716	–	–	–	325	4.5– 5.5	5.0	5.61±0.14	–	–	1314	–	–	–	1208
4.64±0.05	562	–	600	863	–	–	–	4.6– 5.6	5.1	5.69±0.04	–	–	863	863	–	–	105
4.75±0.05	458	–	675	863	–	–	–	4.7– 5.7	5.2	5.79±0.04	–	–	863	863	–	–	150
4.86±0.04	352	–	750	863	–	–	–	4.8– 5.8	5.3	5.90±0.04	–	–	863	863	–	–	202
4.96±0.03	218	–	863	863	–	–	–	4.9– 5.9	5.4	5.99±0.03	–	–	863	863	–	–	248
5.07±0.03	158	–	863	863	–	–	–	5.0– 6.0	5.5	6.09±0.04	–	–	863	803	–	–	338
5.17±0.04	113	–	863	863	–	–	–	5.1– 6.1	5.6	6.20±0.04	–	–	863	713	–	–	443
5.24±0.18	1251	–	–	1355	–	–	–	5.2– 6.2	5.7	6.34±0.04	337	–	–	724	–	–	–
5.33±0.12	1055	–	–	1165	–	–	–	5.3– 6.3	5.8	6.43±0.03	284	–	–	694	–	–	–
5.43±0.12	899	–	–	1017	–	–	–	5.4– 6.4	5.9	6.53±0.03	242	–	–	682	–	–	–
5.52±0.09	775	–	–	903	–	–	–	5.5– 6.5	6.0	6.63±0.03	209	–	–	686	–	–	–
5.62±0.07	676	–	–	817	–	–	–	5.6– 6.6	6.1	6.73±0.03	182	–	–	707	–	–	–
5.71±0.06	598	–	–	755	–	–	–	5.7– 6.7	6.2	6.82±0.03	161	–	–	745	–	–	–
5.81±0.06	536	–	–	713	–	–	–	5.8– 6.8	6.3	6.92±0.03	144	–	–	803	–	–	–
5.91±0.05	486	–	–	689	–	–	–	5.9– 6.9	6.4	7.02±0.03	131	–	–	884	–	–	–
6.01±0.05	447	–	–	682	–	–	–	6.0– 7.0	6.5	7.12±0.03	120	–	–	992	–	–	–
6.10±0.04	416	–	–	691	–	–	–	6.1– 7.1	6.6	7.22±0.03	112	–	–	1133	–	–	–
6.11±0.11	972	–	–	–	1086	–	–	6.2– 7.2	6.7	7.21±0.03	262	–	–	–	686	–	–
6.21±0.09	833	–	–	–	956	–	–	6.3– 7.3	6.8	7.31±0.03	224	–	–	–	682	–	–
6.30±0.08	722	–	–	–	857	–	–	6.4– 7.4	6.9	7.41±0.03	195	–	–	–	694	–	–
6.40±0.07	635	–	–	–	783	–	–	6.5– 7.5	7.0	7.50±0.03	171	–	–	–	724	–	–

6.49±0.06	565	—	—	—	732	—	—	**6.6— 7.6**	**7.1**	7.60±0.03	152	—	—	—	771	—	—
6.59±0.05	509	—	—	—	699	—	—	**6.7— 7.7**	**7.2**	7.70±0.03	137	—	—	—	840	—	—
6.69±0.05	465	—	—	—	683	—	—	**6.8— 7.8**	**7.3**	7.80±0.03	125	—	—	—	934	—	—
6.78±0.04	430	—	—	—	684	—	—	**6.9— 7.9**	**7.4**	7.90±0.03	116	—	—	—	1058	—	—
6.88±0.04	403	—	—	—	701	—	—	**7.0— 8.0**	**7.5**	8.00±0.03	108	—	—	—	1217	—	—
6.98±0.04	381	—	—	—	736	—	—	**7.1— 8.1**	**7.6**	8.09±0.03	103	—	—	—	1422	—	—
7.21±0.06	1028	—	—	—	750	750	—	**7.2— 8.2**	**7.7**	8.36±0.05	548	—	—	—	750	750	—
7.31±0.06	983	—	—	—	750	750	—	**7.3— 8.3**	**7.8**	8.46±0.05	503	—	—	—	750	750	—
7.41±0.05	938	—	—	—	750	750	—	**7.4— 8.4**	**7.9**	8.56±0.05	458	—	—	—	750	750	—
7.66±0.15	1230	—	—	—	—	1334	—	**7.5— 8.5**	**8.0**	8.76±0.04	331	—	—	—	—	720	—
7.75±0.12	1037	—	—	—	—	1149	—	**7.6— 8.6**	**8.1**	8.85±0.03	279	—	—	—	—	692	—
7.85±0.10	885	—	—	—	—	1004	—	**7.7— 8.7**	**8.2**	8.95±0.03	238	—	—	—	—	682	—
7.94±0.08	764	—	—	—	—	893	—	**7.8— 8.8**	**8.3**	9.05±0.06	206	—	—	—	—	687	—
8.04±0.07	667	—	—	—	—	810	—	**7.9— 8.9**	**8.4**	9.14±0.06	180	—	—	—	—	710	—
8.13±0.06	591	—	—	—	—	750	—	**8.0— 9.0**	**8.5**	9.24±0.06	159	—	—	—	—	750	—
8.23±0.06	530	—	—	—	—	710	—	**8.1— 9.1**	**8.6**	9.34±0.06	143	—	—	—	—	810	—
8.33±0.05	482	—	—	—	—	687	—	**8.2— 9.2**	**8.7**	9.44±0.06	130	—	—	—	—	893	—
8.43±0.04	443	—	—	—	—	682	—	**8.3— 9.3**	**8.8**	9.54±0.06	119	—	—	—	—	1004	—
8.52±0.04	413	—	—	—	—	692	—	**8.4— 9.4**	**8.9**	9.64±0.06	111	—	—	—	—	1149	—
8.62±0.04	389	—	—	—	—	720	—	**8.5— 9.5**	**9.0**	9.74±0.06	105	—	—	—	—	1334	—
8.40±0.14	1208	—	—	—	—	—	1314	**8.6— 9.6**	**9.1**	9.50±0.06	325	—	—	—	—	—	716
8.49±0.12	1021	—	—	—	—	—	1133	**8.7— 9.7**	**9.2**	9.59±0.06	275	—	—	—	—	—	691
8.59±0.10	871	—	—	—	—	—	992	**8.8— 9.8**	**9.3**	9.69±0.06	235	—	—	—	—	—	682
8.68±0.08	753	—	—	—	—	—	884	**8.9— 9.9**	**9.4**	9.79±0.06	203	—	—	—	—	—	689
8.78±0.07	659	—	—	—	—	—	803	**9.0—10.0**	**9.5**	9.88±0.06	177	—	—	—	—	—	713
8.87±0.06	584	—	—	—	—	—	745	**9.1—10.1**	**9.6**	9.98±0.06	157	—	—	—	—	—	755
8.97±0.05	525	—	—	—	—	—	707	**9.2—10.2**	**9.7**	10.08±0.06	141	—	—	—	—	—	817
9.07±0.04	478	—	—	—	—	—	686	**9.3—10.3**	**9.8**	10.18±0.06	129	—	—	—	—	—	903
9.16±0.07	440	—	—	—	—	—	682	**9.4—10.4**	**9.9**	10.28±0.06	119	—	—	—	—	—	1017
9.26±0.07	410	—	—	—	—	—	694	**9.5—10.5**	**10.0**	10.38±0.06	111	—	—	—	—	—	1165

From LKB Application Note No. 324 (1984). The pH range (given in the middle two columns) is the one existing in the gel during the run at 20°C. For controlling the pH of the starting solutions, the values (control pH) are given at 20°C.

As an example, take the pH 4.6–5.6 interval: there are no available Immobilines with p*K*s within this pH region, so the nearest species, p*K*s 4.6 and 6.2, will act as both partial buffers and partial titrants; then there is needed a third Immobiline in each vessel, a true titrant that will bring the pH to the desired value (as titrant we will use for pHmin p*K* 3.6 and for pH max p*K* 9.3).

If a narrower pH gradient is needed, it can be derived from any of the 58 pH intervals tabulated by a simple linear interpolation of intermediate Immobiline molarities. Suppose that from a pH 6.8–7.8 range, which is excellent for most hemoglobin (Hb) analyses, we want to obtain a pH gradient of 7.1 to 7.5, which will resolve neutral mutants that cofocus with HbA. Figure 5 shows the graphic method: the limiting molarities of the two Immobilines in the 1 pH unit interval are joined by a straight line (because the pouring of the gradient is done linearly), and then the new

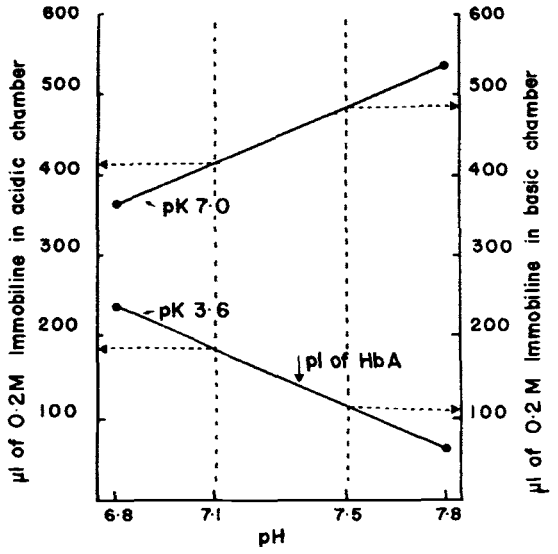

Fig. 5. Graphic representation of the preparation of narrow (up to 1 pH unit) IPG gradients on the "tandem" principle. The limiting molarities of p*K* 7.0 (buffering species) and p*K* 3.6 (titrant) Immobilines needed to generate a pH 6.8–7.8 interval, as obtained directly from Table II, are plotted in a graph. These points are joined by straight lines, and the new molarities needed to generate any narrower pH gradient within the stated pH intervals are then obtained by simple linear interpolation (broken vertical and horizontal lines). In this example a narrow pH 7.1–7.5 gradient is graphically derived. (From Rochette et al., 1984. Reproduced with permission of the publisher.)

pH interval is defined according to experimental needs (in our case pH 7.1–7.5). Two lines are drawn from the two new limits of the pH interval, parallel to the ordinates (broken vertical lines). Where they intersect the two sloping lines defining the two Immobiline molarities, four new lines (dashed lines) are drawn parallel to the abscissa and four new molarities of the Immobilines defining the new pH interval are read directly on the ordinates. This process can be repeated for any desired pH interval down to ranges as narrow as 0.1 pH units.

V. EXTENDED pH GRADIENTS

1. Formulations with Strong Titrants

Now we mix several buffering species, and the situation becomes considerably more complex. However, computer programs have been designed specifically for this purpose (Dossi et al., 1983; Gianazza et al., 1983a; Righetti et al., 1984b). The basic findings are: (1) for generating a linear pH gradient, the buffering power has to be constant throughout the desired pH interval, and (2) to avoid deviations from linearity, the titrants should have pKs well outside pH min and pH max of the desired pH range (in general, at least 2 pH units removed from the limits of the pH interval). As a consequence for pH ranges wider than 3 pH units, two additional Immobilines are needed as titrants: one strongly acidic ($pK < 1$) and one strongly basic ($pK > 12$).

In Table III are recipes for 2- and 3-pH unit wide gradients whose intervals can be generated without the aid of strongly acidic and basic titrants. In Table IV are computed the remianing pH units, 4 and 5 pH unit gradients and pH 4–10, which spans the widest possible pH interval. The two formulas show, on the left side, identical molarities of the buffering Immobiline which are used in the two chambers of the gradient mixer and then titrated with strong acid and bases to the two two extremes, and, on the right side, the buffering species present in unequal amounts in the two vessels (designed as Cham 1 and Cham 2) which will generate a gradient of buffering species. By computer modeling, we could demonstrate the rationale behind these two approaches, that linear pH gradients are obtained by arranging for an even buffering power throughout. The latter could be ensured only by ideal buffers spaced apart by $\Delta pK = 1$. In practice, since there are only 6 Immobiline species rather than 7—the p*K*s 4.4 and 4.6 should never be mixed together—there are two ways to smooth the β power along the pH scale. In one approach (constant buffer concentration, Fig. 6*A*), the concentration of each buffer is kept constant throughout the span of the pH gradient and

TABLE III

Broad pH Gradients: Volumes of Immobiline for 15 ml of Each Starting Solution

CONTROL pH AT 20°C	VOLUME (µl) 0.2 *M* IMMOBILINE pK ACIDIC DENSE SOLUTION							pH RANGE	MID POINT	CONTROL pH AT 20°C	VOLUME (µl) 0.2 *M* IMMOBILINE pK BASIC LIGHT SOLUTION						
	3.6	4.4	4.6	6.2	7.0	8.5	9.3				3.6	4.4	4.6	6.2	7.0	8.5	9.3
3.53 ± 0.06	299	—	223	157	—	—	—	3.5– 5.0	4.25	5.06 ± 0.07	212	—	310	465	—	—	—
4.00 ± 0.06	569	—	99	439	—	—	—	4.0– 6.0	5.0	6.09 ± 0.14	390	—	521	276	—	—	722
4.54 ± 0.06	415	—	240	499	—	—	—	4.5– 6.5	5.5	6.53 ± 0.05	—	—	570	244	235	—	297
5.08 ± 0.03	69	—	428	414	—	—	—	5.0– 7.0	6.0	7.01 ± 0.06	—	—	474	270	219	—	320
5.56 ± 0.03	—	—	450	354	113	—	—	5.5– 7.5	6.5	7.51 ± 0.09	347	—	—	236	287	284	—
6.06 ± 0.08	435	—	—	323	208	44	—	6.0– 8.0	7.0	8.11 ± 0.09	286	—	—	174	325	329	—
6.56 ± 0.13	771	—	—	276	185	538	—	6.5– 8.5	7.5	8.66 ± 0.06	192	—	—	153	278	362	—
7.03 ± 0.24	1349	—	—	—	272	372	845	7.0– 9.0	8.0	8.94 ± 0.07	484	—	—	—	232	189	546
7.50 ± 0.11	668	—	—	—	445	226	348	7.5– 9.5	8.5	9.37 ± 0.06	207	—	—	—	925	139	346
8.10 ± 0.07	399	—	—	—	364	355	94	8.0–10.0	9.0	9.89 ± 0.05	91	—	—	—	329	366	289
4.01 ± 0.05	578	—	110	450	—	—	—	4.0– 7.0	5.5	7.02 ± 0.14	302	—	738	151	269	—	876
5.03 ± 0.12	702	—	254	416	133	346	—	5.0– 8.0	6.5	8.12 ± 0.07	175	—	123	131	345	346	—
6.04 ± 0.14	779	—	—	402	93	364	80	6.0– 9.0	7.5	9.01 ± 0.06	241	—	—	161	449	237	225
6.98 ± 0.07	542	—	—	—	378	351	—	7.0–10.0	8.5	9.88 ± 0.05	90	—	—	—	324	350	280

From LKB Application Note No. 324 (1984). See also footnote to Table II.

TABLE IV

4,5 and 6-pH-Unit-Wide Immobilized pH Gradients

4–8

Initial pH	: 4.000				Initial pH	: 4.015			
Final pH	: 8.000				Final pH	: 8.008			
Notes	: 4.068–8.153(7.813):4.084–8.004(7.689)				Notes	: 4.076–8.112 : 4.091–7.986			
Buffer concentrations					Buffer concentrations				
n. 1 pK	0.80	Cham 1	11.085	Cham 2 0.000	n. 1 pK	0.80	Cham 1	8.643	Cham 2 0.000
n. 2 pK	3.57	Cham 1	0.864	Cham 2 0.864	n. 2 pK	3.57	Cham 1	1.420	Cham 2 0.000
n. 3 pK	4.51	Cham 1	5.259	Cham 2 5.259	n. 3 pK	4.51	Cham 1	4.560	Cham 2 6.519
n. 4 pK	6.21	Cham 1	4.167	Cham 2 4.167	n. 4 pK	6.21	Cham 1	5.222	Cham 2 1.975
n. 5 pK	7.06	Cham 1	2.379	Cham 2 2.379	n. 5 pK	7.06	Cham 1	2.326	Cham 2 4.586
n. 6 pK	8.50	Cham 1	6.432	Cham 2 6.432	n. 6 pK	8.50	Cham 1	3.276	Cham 2 3.822
n. 8 pK	12.00	Cham 1	0.000	Cham 2 0.924	n. 8 pK	12.00	Cham 1	0.000	Cham 2 3.130

4–9

Initial pH	: 4.000				Initial pH	: 4.019			
Final pH	: 9.000				Final pH	: 8.996			
Notes	: 4.071–9.086(8.007):4.088–8.925(7.876)				Notes	: 4.067–8.980 : 4.081–8.825			
Buffer concentrations					Buffer concentrations				
n. 1 pK	0.80	Cham 1	11.649	Cham 2 0.000	n. 1 pK	0.80	Cham 1	11.793	Cham 2 0.000
n. 2 pK	3.57	Cham 1	0.657	Cham 2 0.657	n. 2 pK	3.57	Cham 1	2.832	Cham 2 4.130
n. 3 pK	4.51	Cham 1	5.394	Cham 2 5.394	n. 3 pK	4.51	Cham 1	4.253	Cham 2 7.780
n. 4 pK	6.21	Cham 1	3.888	Cham 2 3.888	n. 4 pK	6.21	Cham 1	5.353	Cham 2 2.635
n. 5 pK	7.06	Cham 1	2.943	Cham 2 2.943	n. 5 pK	7.06	Cham 1	0.585	Cham 2 4.252
n. 6 pK	8.50	Cham 1	4.734	Cham 2 4.734	n. 6 pK	8.50	Cham 1	4.814	Cham 2 3.056
n. 7 pK	9.59	Cham 1	1.857	Cham 2 1.857	n. 7 pK	9.59	Cham 1	4.196	Cham 2 4.654
n. 8 pK	12.00	Cham 1	0.000	Cham 2 3.399	n. 8 pK	12.00	Cham 1	0.000	Cham 2 7.415

5–9

Initial pH	: 5.000				Initial pH	: 5.022			
Final pH	: 9.000				Final pH	: 9.037			
Notes	: 5.076–9.086(7.544):5.085–8.926(7.457)				Notes	: 5.100–9.080 : 5.110–8.921			
Buffer concentrations					Buffer concentrations				
n. 1 pK	0.80	Cham 1	7.527	Cham 2 0.000	n. 1 pK	0.80	Cham 1	11.404	Cham 2 0.000
n. 3 pK	4.51	Cham 1	7.089	Cham 2 7.089	n. 3 pK	4.51	Cham 1	7.989	Cham 2 3.498
n. 4 pK	6.21	Cham 1	3.408	Cham 2 3.408	n. 4 pK	6.21	Cham 1	3.102	Cham 2 3.493
n. 5 pK	7.06	Cham 1	3.180	Cham 2 3.180	n. 5 pK	7.06	Cham 1	1.908	Cham 2 2.933
n. 6 pK	8.50	Cham 1	4.683	Cham 2 4.683	n. 6 pK	8.50	Cham 1	11.020	Cham 2 4.091
n. 7 pK	9.59	Cham 1	1.839	Cham 2 1.839	n. 7 pK	9.59	Cham 1	1.694	Cham 2 2.692
n. 8 pK	12.00	Cham 1	0.000	Cham 2 4.464	n. 8 pK	12.00	Cham 1	0.000	Cham 2 0.438

5–10

Initial pH	: 5.000				Initial pH	: 4.993			
Final pH	: 10.000				Final pH	: 10.034			
Notes	: 5.076–9.892(8.171):5.086–9.745(8.034)				Notes	: 5.068–9.933 : 5.075–9.779			
Buffer concentrations					Buffer concentrations				
n. 1 pK	0.80	Cham 1	9.102	Cham 2 0.000					
n. 3 pK	4.51	Cham 1	7.179	Cham 2 7.179	n. 1 pK	0.80	Cham 1	7.605	Cham 2 0.295
n. 4 pK	6.21	Cham 1	3.210	Cham 2 3.210	n. 3 pK	4.51	Cham 1	6.260	Cham 2 0.805
n. 5 pK	7.06	Cham 1	3.531	Cham 2 3.531	n. 4 pK	6.21	Cham 1	4.044	Cham 2 0.454
n. 6 pK	8.50	Cham 1	3.729	Cham 2 3.729	n. 5 pK	7.06	Cham 1	3.717	Cham 2 5.677
n. 7 pK	9.59	Cham 1	4.275	Cham 2 4.275	n. 6 pK	8.50	Cham 1	3.088	Cham 2 4.197
n. 8 pK	12.00	Cham 1	0.000	Cham 2 5.922	n. 7 pK	9.59	Cham 1	1.730	Cham 2 3.687

6–10

Initial pH	: 6.000				Initial pH	: 5.994			
Final pH	: 10.000				Final pH	: 9.996			
Notes	: 6.039–9.886 : 5.988–9.733				Notes	: 6.035–9.876 : 5.986–9.723			
Buffer concentrations					Buffer concentrations				
n. 1 pK	0.80	Cham 1	12.060	Cham 2 0.000					
n. 1 pK	0.80	Cham 1	1.323	Cham 2 1.323	n. 2 pK	3.57	Cham 1	12.919	Cham 2 1.370
n. 4 pK	6.21	Cham 1	3.351	Cham 2 3.351	n. 4 pK	6.21	Cham 1	3.748	Cham 2 4.583
n. 5 pK	7.06	Cham 1	3.603	Cham 2 3.603	n. 5 pK	7.06	Cham 1	3.339	Cham 2 4.962
n. 6 pK	8.50	Cham 1	3.711	Cham 2 3.711	n. 6 pK	8.50	Cham 1	3.585	Cham 2 3.283
n. 7 pK	9.59	Cham 1	4.299	Cham 2 4.299	n. 7 pK	9.59	Cham 1	3.891	Cham 2 4.475
n. 8 kP	12.00	Cham 1	0.000	Cham 2 0.000					

4–10

Initial pH	: 4.000				Initial pH	: 4.026			
Final pH	: 10.000				Final pH	: 9.968			
Notes	: 4.079–9.891(8.658):4.097–9.742(8.502)				Notes	: 4.105–9.826 : 4.121–9.675			
Buffer concentrations					Buffer concentrations				
n. 1 pK	0.80	Cham 1	13.656	Cham 2 0.000	n. 1 pK	0.80	Cham 1	15.849	Cham 2 0.000
n. 3 pK	4.51	Cham 1	5.712	Cham 2 5.712	n. 3 pK	4.51	Cham 1	4.740	Cham 2 2.446
n. 4 pK	6.21	Cham 1	3.609	Cham 2 3.609	n. 4 pK	6.21	Cham 1	6.645	Cham 2 0.000
n. 5 pK	7.06	Cham 1	3.342	Cham 2 3.342	n. 5 pK	7.06	Cham 1	0.000	Cham 2 6.799
n. 6 pK	8.50	Cham 1	3.765	Cham 2 3.765	n. 6 pK	8.50	Cham 1	6.633	Cham 2 1.977
n. 7 pK	9.59	Cham 1	4.305	Cham 2 4.305	n. 7 pK	9.59	Cham 1	3.776	Cham 2 5.641
n. 8 pK	12.00	Cham 1	0.000	Cham 2 4.431	n. 8 pK	12.00	Cham 1	0.000	Cham 2 0.715

From Gianazza et al. (1984a). The "same concentration" formulations are listed in the left column, the ones with "different concentrations" on the right. In each mixture record: initial and final pHs in the gel phase, at 10°C. Notes: pH of the limiting solutions (and of the buffer mixture, prior to the addition of titrants) at 20°C (figures before) and at 25°C (figures after the colon). Buffer concentrations: expressed as mM/L (to convert into μL/mL, for 0.2 *M* Immobiline concentration, multiply by 5).

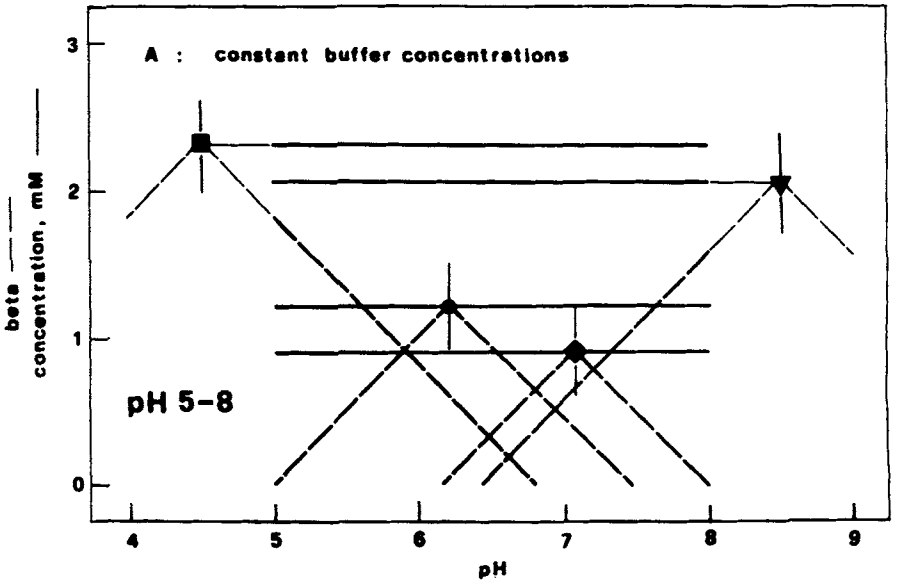

Fig. 6. Illustration of the alternative methods for the preparation of IPGs. *(a)* same concentration of each buffer in both chambers; *(b)* varying buffer concentration between the chambers. The same 5–8 pH gradient is taken as an example in both cases. The concentrations of the various Immobilines are represented with continuous thick lines (horizontal in panel *a*, slanted in panel *b*) within the span of the gradient, and with thin lines when extrapolated outside it. The buffering power (β) courses are approximated by wedges (broken lines) with apexes centered at the p*K*s of the different Immobilines (the scale of beta power is in arbitrary units). The solid symbols refer to the position of the apparent p*K*s under the actual gradient conditions, and the barred open symbols to conditions of ideal titration (when distinct from above). The identification between the various symbols and the different Immobilines is given in panel *B*. (From Gianazza et al., 1984b. Reproduced with permission of the publisher.)

"holes" of buffering power are filled by increasing the amounts of the buffering species bordering the largest Δp*K*s; in the other approach (varying buffer concentration, Fig. 6*B*) the variation in concentration of different buffers along the width of the desired pH gradient results in a shift in each buffer's apparent p*K*, along with the Δp*K* values evening out. These recipes ensure that preparation of any Immobiline gel will be trouble free, for all the complex computing routines have already been performed and no further calculations are required.

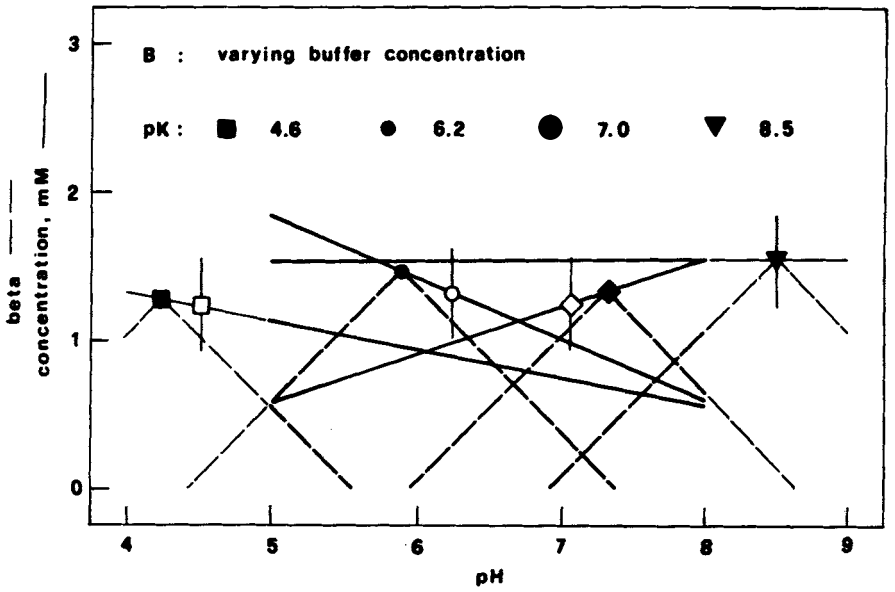

Fig. 6. *(Continued)*

2. Formulations with Only the Commercially Available Immobilines

From the recipes given in Tables II–IV it would appear that the entire know-how on IPGs was completely codified. However, these data (Righetti et al., 1984a) of the two Immobilines with strong titrants (an acid, pK 0.8 and a base, pK > 12, required for all gradients 4 pH units or more) were not generally available, and there were no immediate plans for marketing them. Even without these two strong titrants, the generation of extended IPGs would still be possible if a multichamber apparatus is used (Dossi et al., 1983). Yet such a device would not be practical for laboratories that routinely use two-chamber mixers. To solve this dilemma, we have recalculated and listed in Table V (A to F) all gradients between 4 and 6 pH units along with formulations for the six available Immobiline buffers. The "pedigree" of each pH interval is given in Fig. 7 *(A–F)*: it shows the buffering power (β, left scale), the ionic strength (μ, right scale), and the deviation from linearity (central scale) expressed in the nominal range extremes and as a percentage of the gradient span. The same set of data from comparable ranges, prepared with a two-chamber mixer but using strong titrants, is plotted at at the right side of each panel. The curves correspond to the equivalent pH spans given in

TABLE V

4,5 and 6-pH-Unit-Wide Gradients Prepared with Only Six Available Immobiline

A 4–8, NO TITRANTS					
Initial pH			: *4.090*		
Final pH			: *8.010*		
Notes			: *pH in solution at 25°C: 4.12–7.97*		
Buffer concentrations					
pK	3.57	Cham 1	7.850	Cham 2	0.000
pK	4.51	Cham 1	3.380	Cham 2	7.384
pK	6.21	Cham 1	3.136	Cham 2	4.792
pK	7.06	Cham 1	1.564	Cham 2	1.894
pK	8.50	Cham 1	2.261	Cham 2	4.454
pK	9.59	Cham 1	0.000	Cham 2	3.838
B 5–9, NO TITRANTS					
Initial pH			: *5.060*		
Final pH			: *9.040*		
Notes			: *pH in solution at 25°C: 5.13–8.91*		
Buffer concentrations					
pK	3.57	Cham 1	11.059	Cham 2	0.000
pK	4.51	Cham 1	7.759	Cham 2	3.317
pK	6.21	Cham 1	2.903	Cham 2	3.510
pK	7.06	Cham 1	1.835	Cham 2	2.833
pK	8.50	Cham 1	10.601	Cham 2	3.892
pK	9.59	Cham 1	1.630	Cham 2	3.071
C 6–10, NO TITRANTS					
Initial pH			: *5.980*		
Final pH			: *10.000*		
Notes			: *pH in solution at 25°C: 5.97–9.72*		
Buffer concentrations					
pK	3.57	Cham 1	12.546	Cham 2	1.329
pK	6.21	Cham 1	3.634	Cham 2	4.446
pK	7.06	Cham 1	3.237	Cham 2	4.813
pK	8.50	Cham 1	3.471	Cham 2	3.185
pK	9.59	Cham 1	3.761	Cham 2	4.341
D 4–9, NO TITRANTS					
Initial pH			: *4.140*		
Final pH			: *8.920*		
Notes			: *pH in solution at 25°C: 4.18–8.65*		
Buffer concentrations					
pK	3.57	Cham 1	11.048	Cham 2	1.964
pK	4.51	Cham 1	3.138	Cham 2	5.656
pK	6.21	Cham 1	3.092	Cham 2	4.801
pK	7.06	Cham 1	0.298	Cham 2	3.952
pK	8.50	Cham 1	3.336	Cham 2	0.942
pK	9.59	Cham 1	2.951	Cham 2	8.834

TABLE V *(Continued)*

E 5–10, NO TITRANTS

Initial pH		:	*5.040*		
Final pH		:	*10.040*		
Notes		:	*pH in solution at 25°C: 5.11–9.79*		
Buffer concentrations					
pK	3.57	Cham 1	7.505	Cham 2	0.286
pK	4.51	Cham 1	6.178	Cham 2	0.788
pK	6.21	Cham 1	3.970	Cham 2	0.447
pK	7.06	Cham 1	3.646	Cham 2	5.593
pK	8.50	Cham 1	3.027	Cham 2	4.138
pK	9.59	Cham 1	1.689	Cham 2	3.637

F 4–10, NO TITRANTS

Initial pH		:	*4.150*		
Final pH		:	*9.950*		
Notes		:	*pH in solution at 25°C: 4.16–9.66*		
Buffer concentrations					
pK	3.57	Cham 1	14.699	Cham 2	0.000
pK	4.51	Cham 1	0.000	Cham 2	1.523
pK	6.21	Cham 1	6.073	Cham 2	0.667
pK	7.06	Cham 1	1.187	Cham 2	6.503
pK	8.50	Cham 1	4.452	Cham 2	2.089
pK	9.59	Cham 1	0.000	Cham 2	4.763

G 3–10, SAME CONCENTRATION

Initial pH		:	*3.000*		
Final pH		:	*10.000*		
Notes : *pH in solution at 25°C: 3.02–9.75 (mixture: 7.76)*					
Buffer concentrations					
pK	0.80	Cham 1	14.211	Cham 2	0.000
pK	3.57	Cham 1	4.137	Cham 2	4.137
pK	4.51	Cham 1	3.764	Cham 2	3.764
pK	6.21	Cham 1	4.017	Cham 2	4.017
pK	7.06	Cham 1	3.041	Cham 2	3.041
pK	8.50	Cham 1	3.780	Cham 2	3.780
pK	9.59	Cham 1	4.278	Cham 2	4.278
pK	12.00	Cham 1	0.000	Cham 2	6.647

H 3–10, DIFFERENT CONCENTRATIONS

Initial pH		:	*2.970*		
Final pH		:	*9.960*		
Notes		:	*pH in solution at 25°C: 3.00–9.66*		
Buffer concentrations					
pK	0.80	Cham 1	17.083	Cham 2	0.000
pK	3.57	Cham 1	2.252	Cham 2	0.000
pK	4.51	Cham 1	5.013	Cham 2	2.596
pK	6.21	Cham 1	6.688	Cham 2	0.000
pK	7.06	Cham 1	0.000	Cham 2	7.115
pK	8.50	Cham 1	6.931	Cham 2	2.072
pK	9.59	Cham 1	3.946	Cham 2	5.899
pK	12.00	Cham 1	0.000	Cham 2	0.747

From Gianazza et al. (1985b). See also footnote to Table 4.

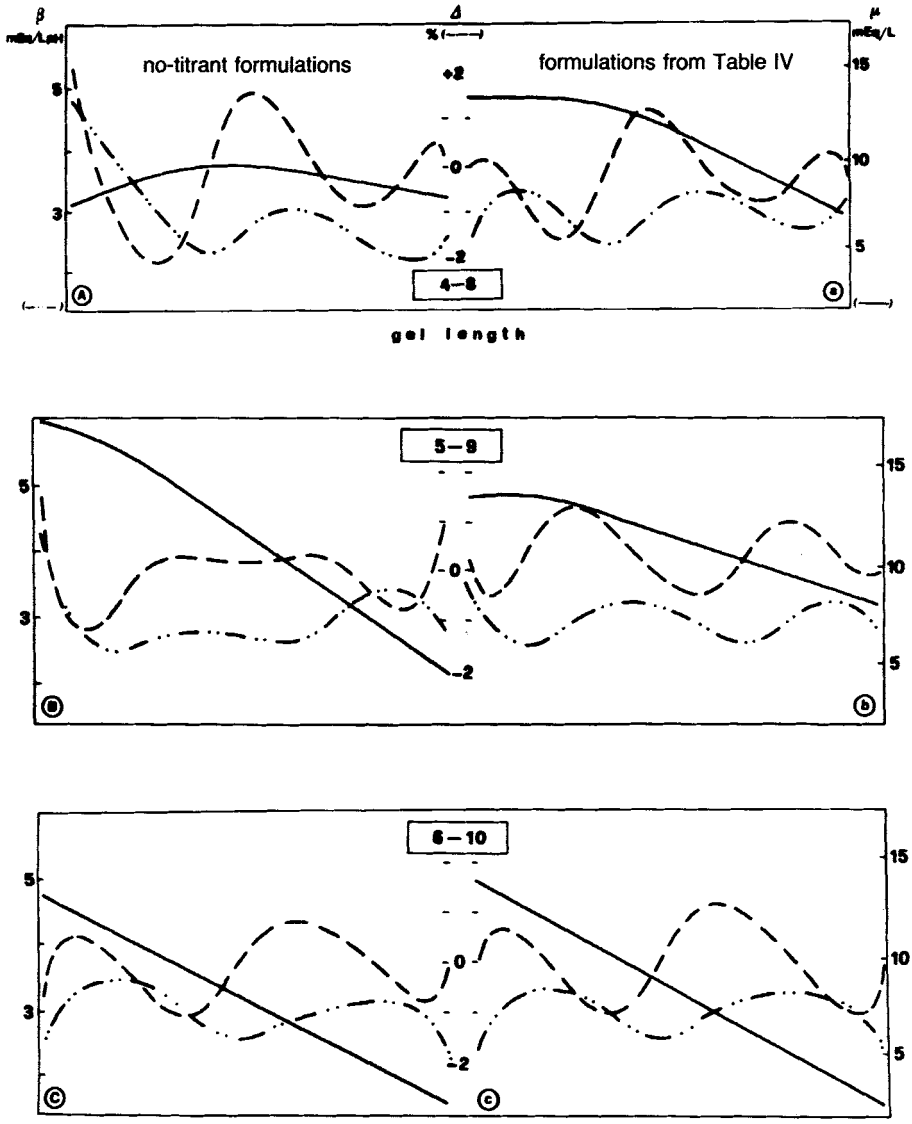

Fig. 7. Plot of the parameters: buffering power (β — · · —), left scale), deviation from the linear regression between the stated pH extremes, expressed as percentage over the gradient span (Δ — —, middle scale), and ionic strength (μ — — —, right scale) for the IPGs listed in Table V (left side) (sections *A*–*F*, on the left) and for the corresponding ranges computed according to the "same concentration" approach and listed in Table IV (sections *a*–*f*, on the right). (From Gianazza et al., 1985a. Reproduced with permission of the publisher.)

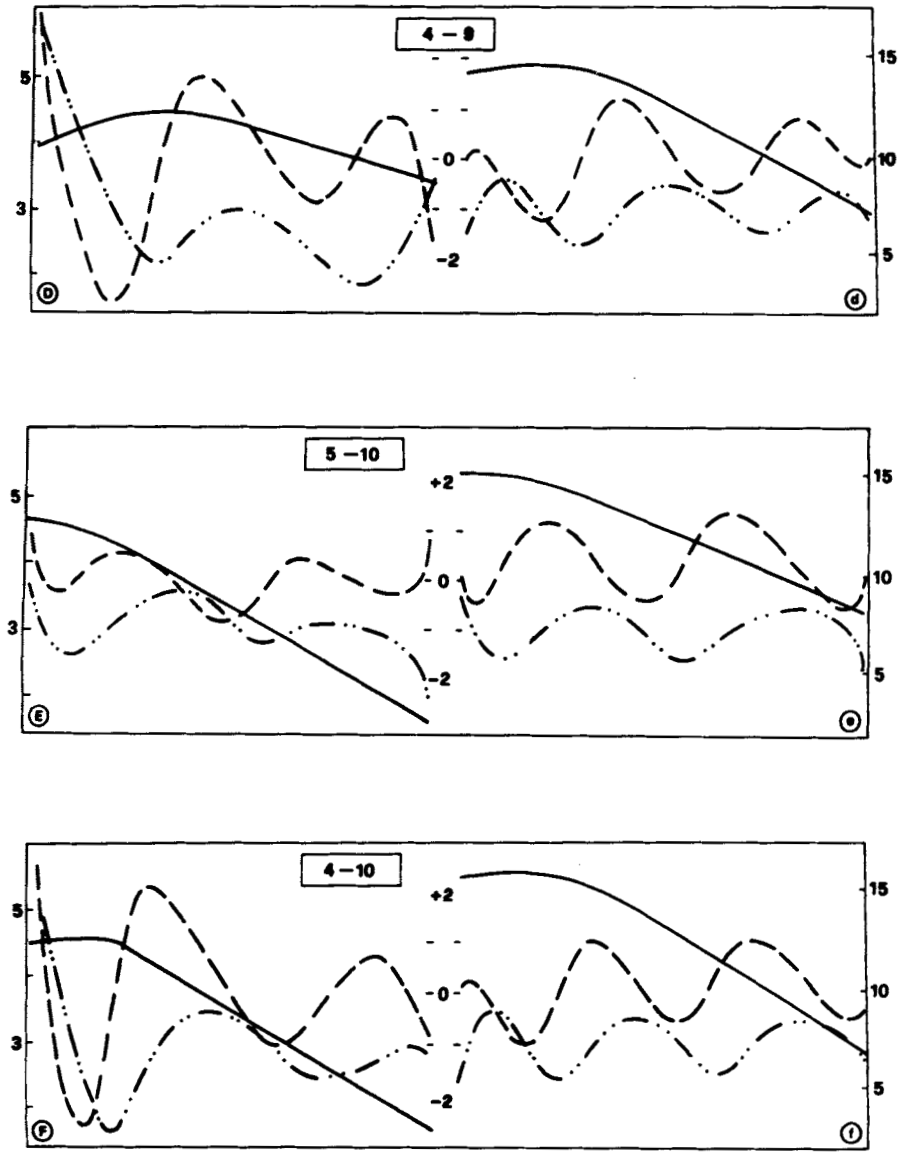

Fig. 7. *(Continued)*

Table IV (left side, same concentration formulations). These formulations will be useful until the p*K*s 0.8 and 12 chemicals are generally available. How can the recipes in Tables IV and V be compared? In terms of linearity of the pH course, the quality of the gradients is comparable for the pH 5–9, 6–10, and 5–10 intervals. Much worse results are observed, however, with the pH 4–8, 4–9, and 4–10 gradients (standard deviations 2–3 times larger in Table V than in Table IV). In fact, the largest deviations are to be found in the acidic portion of the gradient, between pH 4 and 6 (Fig. 7*A*–*F*). In addition, since all formulations are normalized to give the same average value of $\beta=3.0$ mequiv. Liter^{-1} pH^{-1}, the average ionic strength of the formulations in Table V is in most cases lower (by about 20%) than the corresponding ones in Table IV. Despite these shortcomings the recipes listed in Table V are fully acceptable: given a standard deviation below 5% (in Table IV a standard deviation not exceeding 1% of the operative pH interval was achieved), it is still possible to measure p*I* values with good accuracy and, in any event, obtain completely reproducible pH gradients from run to run.

In Table V (entries G and H) formulations are given for the widest possible IPG span, a pH 3–10 interval, prepared with a two-chamber mixer either according to the "same concentration" (G) or to the "different concentration" (H) approaches (Gianazza et al., 1985a). For recipe G, the courses of β, μ, and the pH gradient deviation from linearity between the stated range extremes are plotted in Fig. 8. Both formulations (G and H) performed well and with practically identical results in the analysis of complex protein mixtures. It should be noted, however, that in neither case could such a wide pH range be created without resorting to strong titrants.

3. Nonlinear, Extended pH Gradients

Up to now IPG formulations have been given only in terms of rigorously linear pH gradients. Although this has been the only solution adopted so far, it might not be the optimal one in some cases. The pH slope might need to be altered in pH regions that are overcrowded with proteins. In conventional IEF, flattening of the gradient slope in some regions was obtained in three different ways: (1) by adding an amphoteric spacer (separator IEF of Brown et al., 1977), (2) by changing the gel thickness ("thickness-modified" slope of Altland and Kaempfer, 1980), and (3) by changing the concentration of carrier ampholytes ("concentration-modified" slope of Låås and Olsson, 1981).

Table VI gives two examples of a nonlinear, pH 4–10 interval, obtained without titrants (left part) or with only a strongly acidic titrant (right part). This has been calculated for a general case involving the

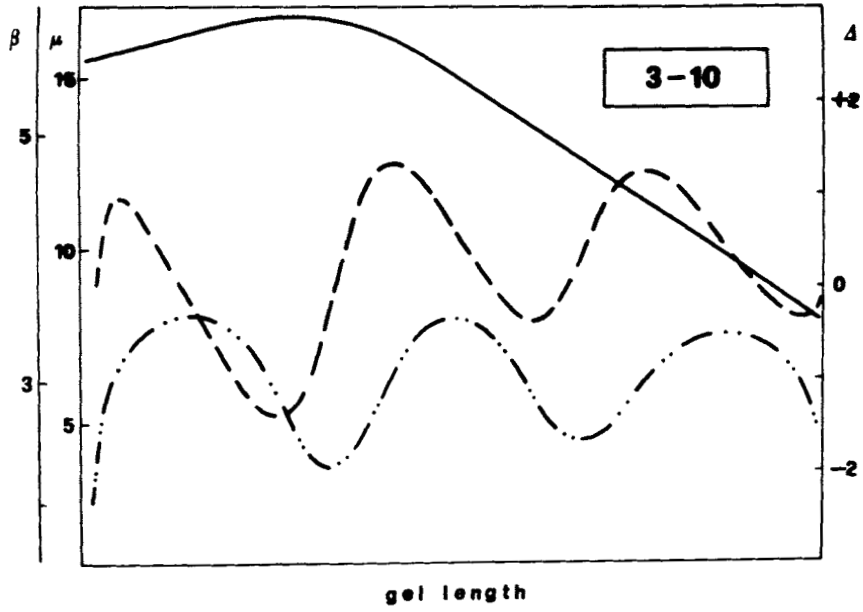

Fig. 8. Plot of β, pH deviation from linearity (Δ), and μ for formulation *G* in Table V (pH gradient 3–10, "same concentration" approach). Symbols as in Fig. 7. (From Gianazza et al., 1985a. Reproduced with permission of the publisher.)

separation of proteins in a complex mixture, such as a cell lysate. Gianazza and Righetti (1980) have computed the statistical distribution of the pI's of the water-soluble proteins given in the histogram shown in Fig. 9. With the relative abundance of different species, it is clear that an optimally resolving pH gradient should have a gentler slope in the acidic portion and a steeper course in the alkaline region. Such a general course has been calculated by assigning to each 0.5 pH unit interval in the pH 3.5–10 region a slope inversely proportional to the relative abundance of proteins in that interval: by such a procedure the ideal curve (dotted line) in Fig. 9 was obtained. Of the two formulations given in Table VI, the one including the strongly acidic titrant followed most closely the theoretically predicted course (solid line). In a separation of a crude lysate of *Klebsiella pneumoniae*, a great improvement in resolution for the acidic cluster of bands, without loss of the basic portion of the pattern, was obtained (Gianazza et al., 1985b). What is also important here is the establishment of a new principle in IPG technology, namely that the pH gradient and the density gradient stabilizing it need not be colinear, because the pH can be adjusted by localized flattening for increased resolution while leaving

TABLE VI

Nonlinear 4–10 Immobilized pH Gradient

"IDEAL" 4–10					
Initial pH			: *4.190*		
Final pH			: *9.980*		
Notes			: *pH in solution at 25°C: 4.24–9.70*		
Buffer concentrations			*(no titrants)*		
pK	3.57	Cham 1	9.321	Cham 2	0.577
pK	4.51	Cham 1	4.327	Cham 2	0.000
pK	6.21	Cham 1	8.943	Cham 2	2.596
pK	7.06	Cham 1	0.000	Cham 2	3.173
pK	8.50	Cham 1	0.000	Cham 2	1.154
pK	9.59	Cham 1	0.000	Cham 2	1.846
"IDEAL" 4–10					
Initial pH			: *4.040*		
Final pH			: *9.880*		
Notes			: *pH in solution at 25°C: 4.13–9.61*		
Buffer concentrations			*(with acidic titrant)*		
pK	0.80	Cham 1	7.028	Cham 2	0.910
pK	4.51	Cham 1	7.659	Cham 2	0.000
pK	6.21	Cham 1	9.010	Cham 2	2.703
pK	7.06	Cham 1	0.000	Cham 2	3.604
pK	8.50	Cham 1	0.000	Cham 2	1.352
pK	9.59	Cham 1	0.000	Cham 2	2.523

From Gianazza et al. (1985b). See also footnote to Table IV.

the density gradient unaltered. Though we have considered only the example of an extended pH gradient, narrower pH intervals can be treated in the same fashion.

VI. GENERAL THEORETICAL CONSIDERATIONS

1. Buffering Capacity and Ionic Strength

In contrast to conventional IEF, where the ionic strength *(I)* during separation is uncertain (in 2% focused Ampholine estimated to be approximately 1 mequiv Liter^{-1}; Righetti, 1980), in IPGs the *I* value becomes a true physicochemical parameter amenable to full experimental control. For the buffering power (β) the discrepancies between the two systems are less pronounced because the β can be determined with accu-

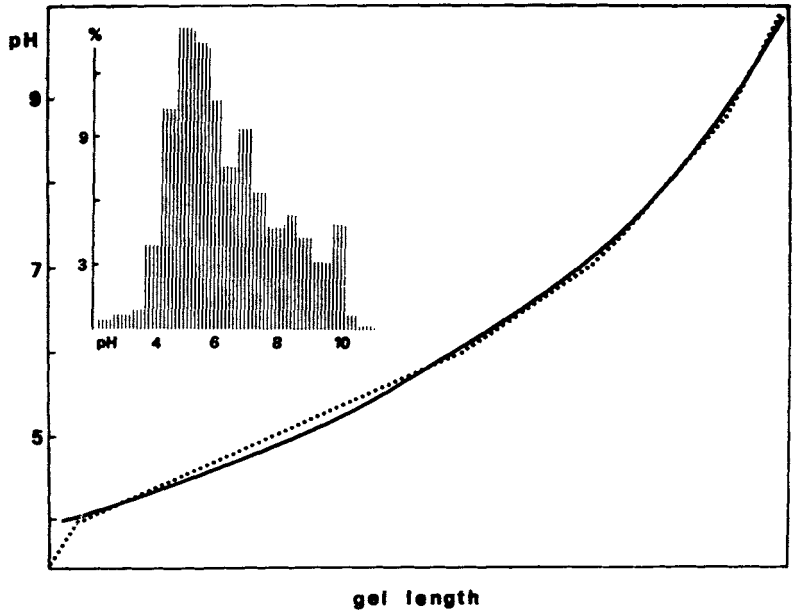

Fig. 9. Nonlinear 4–10 pH gradient: "ideal" (.....) and actual (——, formulation *D*, including acidic titrant from Table 4) courses. The shape for the "ideal" profile was computed from data on the statistical distribution of protein p*I*s (Gianazza and Righetti, 1980). The relevant histogram is redrawn in the figure inset. (From Gianazza et al., 1985b. Reproduced with permission of the publisher.)

racy and is comparable in both systems. However, in conventional IEF, the *I* and β values can be subjected to great variations in peaks and valleys within adjacent, focused Ampholine zones, that is, distances of 10–50 μm along the separation track. This is of no minor consequence, for through its influence on activity factors the ionic strength will affect the pK values of ionizable groups in proteins. In IPGs, given a known molarity of grafted buffers and titrants, the ionic strength in the gel can simply be calculated by the following relationship:

$$I = \sum C_{A_i} \frac{10^{(\mathrm{pH}-\mathrm{p}K_{A_i})}}{10^{(\mathrm{pH}-\mathrm{p}K_{A_i})} + 1} = \sum C_{B_i} \frac{1}{10^{(\mathrm{pH}-\mathrm{p}K_{B_i})} + 1} \qquad (1)$$

where C_{A_i} is the concentration of acidic Immobiline with $\mathrm{p}K = \mathrm{p}K_{A_i}$, and C_{Bi} is the concentration of basic Immobiline with $\mathrm{p}K = \mathrm{p}K_{Bi}$. It should be noted that the pK values of the Immobilines also vary with the ionic

strength. From the Debye-Hückel (1924) law, the variation for Immobiline can be given approximately by

$$pK = pK_0 - 0.5Z^2\sqrt{I} \quad (2)$$

where pK_0 is the pK value at an I of zero and Z is equal to -1 for acids and $+1$ for bases; thus the pK increases with I for acids and decreases for bases. When Immobilines are used according to recommendations, these pK variations, which are less than 0.03 pH unit, can be neglected. However, they should be considered when using extremely narrow pH gradients (approximately 0.01 pH unit/cm) or high Immobiline molarities (e.g., 30 m*M*), for in these cases the band positions might be affected.

The β power is another quantity that is well defined in an Immobiline pH gradient. As for any solution containing weak monofunctional acids and bases, the buffering capacity is given by the equation

$$\beta = 2.3 \sum_{i=1}^{l+m} C_i \frac{K_i[H^+]}{(K_i + [H^+])^2} \quad (3)$$

where C_i is the molar concentration of the ith Immobiline having a dissociation constant of K_i. Equations (1) and (3) are part of our computer program for extended pH gradients (Dossi et al., 1983) which, given a mixture of Immobilines in any pH range, will automatically simulate and optimize the generated pH gradient and calculate the accompanying I and β values. Equations (1) and (3) can also be used to calculate the I and β power courses with a pocket calculator, usually at 0.1 pH unit increments.

The buffering capacity must be high enough to make the pH gradient insensitive to impurities (e.g., acrylic acid from the acrylamide and Bis monomers), and it should also be even in order to minimize the effects of small disturbances in forming the gradient when casting the gel. For analytical purposes, a β value of 3–5 mequiv. $Liter^{-1}$ pH^{-1} will give well-functioning pH gradients. A higher buffering capacity will give more sharply focused bands (Gelfi and Righetti, 1983). However, such gels will start to swell during the staining and destaining steps if the total molar concentration of Immobilines exceeds 30 m*M*. The example shown in Fig. 10 is a computer-derived graph on the courses of pH gradient, ionic strength *(I)* and buffering power (β) of the pH 6.8–7.8 immobilized pH gradient routinely used for Hb separation (the molarities of the buffering ion and titrant are plotted in Fig. 5). Recently we have developed a more sophisticated program that allows us to arrange for constant I values, if necessary, and for a smoother β course (i.e., decreased deviation from linearity of the pH gradient course). In any case once the working pH

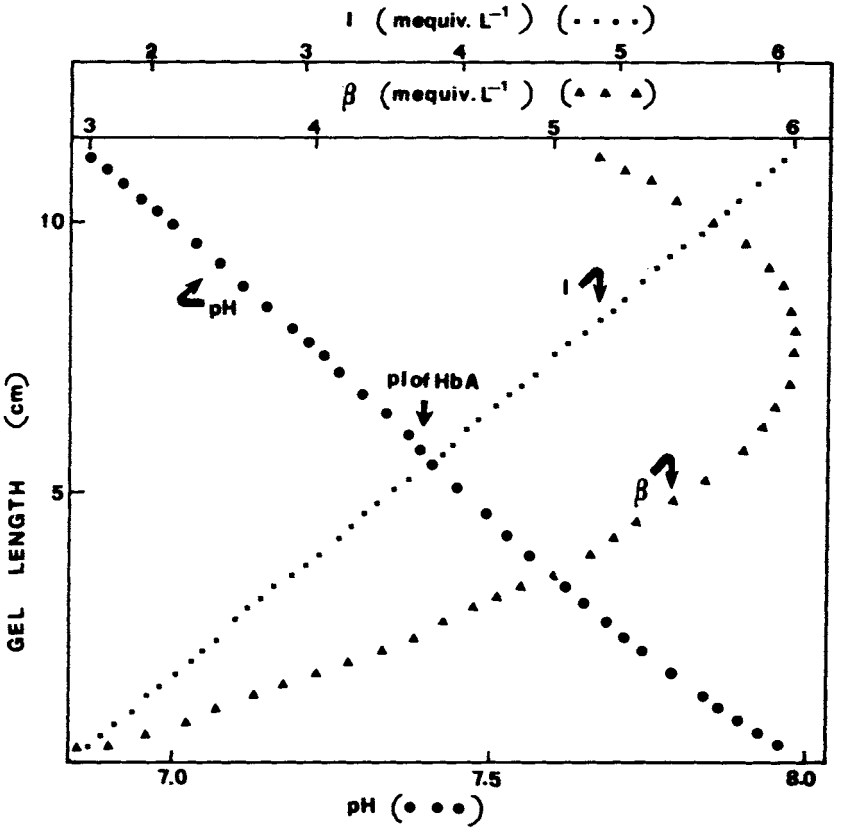

Fig. 10. Computer simulation of pH, β, *I* courses in the pH 6.8–7.8 Immobiline gradient for hemoglobin analysis, having the limiting composition plotted in Fig. 5. The same data could be calculated with the aid of equations (1) and (3) and, for the pH gradient, by eluting fractions from the gradient mixer and reading the pH in solution of 0.5 ml eluates. The p*I* position of HbA is marked by a vertical arrow. (From Gelfi and Righetti, 1983. Reproduced with permission of the publisher.)

interval and the molarities of buffer and titrant are known (Tables II to VI), the experimental parameters of a separation (*I*, β) can also be calculated from equations (1) and (3).

2. Electroendosmosis

Electroendosmosis is not usually a problem in Immobiline pH gradients, for the gel does not have any net charge after traces of the catalysts and

nonincorporated Immobilines have been electrophoretically transported away. Generally, at low and high pH values the presence of H^+ and OH^- ions means that the matrix adopts a net charge that will result in water transport toward the cathode at low pH and toward the anode at high pH. A trough could form close to the electrode at the extreme pH ranges, and eventually the gel could dry out and burn. As a rule this phenomenon will not occur within the pH ranges for which Immobiline is recommended, but it is wise to include glycerol (20%) in the washing step in gels below pH 5 and above pH 9.

Carbon dioxide from the air is also expected to cause electroendosmosis. Delincée and Radola (1978) were the first to describe the effect of CO_2. Gaseous CO_2 dissolves in the gel, especially at pH > 6.3 (the solubility of carbon dioxide increases with pH), forming HCO_3^- ions as follows:

$$CO_2 + H_2O \longrightarrow H^+ + HCO_3^-$$

This acidification, in conventional IEF, causes the part of the pH gradient above pH 6.3 to drift toward the cathode, by charging and mobilizing electrophoretically the focused carrier ampholytes (possibly by salt formation). However, it cannot act on IPGs by the same mechanism; it will certainly alter the slope of the theoretical pH gradient depending on the local ratio (HCO_3^-)/(Immobiline), which is like introducing a new buffer with p*K* 6.3 in the immobilized pH gradient. The HCO_3^- ion migrates electrophoretically (Fig. 11) from the cathodic side toward the anode. At pH 6.3, carbon dioxide gas starts to form and is liberated from the gel. At the same time OH^- is formed according to the equation

$$HCO_3^- \longrightarrow OH^- + CO_2$$

The gas released at the anodic gel side can be readsorbed at the cathode and thus recirculated through the system as depicted in Fig. 11. By analogy, volatile amines will cause the same disturbance but in the opposite direction (therefore ethanolamine, ethylendiamine, etc., should not be used as catholytes). Even in IPG a very marked effect on band sharpness is observed in alkaline pH ranges if carbon dioxide is excluded from the system. For this, the IEF cell should be airtight, flushed with inert gas (denser than air, such as argon; nitrogen is lighter and will float!) and/or covered on the gel-free space with sponges impregnated with NaOH or $Ca(OH)_2$. A note of caution when working with 2-D techniques: the 2-mercaptoethanol added to the sample will behave in a similar way to CO_2; it is in fact a buffer with p*K* 9.5. This compound ionizes at the basic gel end and is driven electrophoretically along the pH gradient. The remedy is to apply the sample at the anodic-gel end: below pH 7 the $-SH$ group will not buffer or be ionized (Righetti et al., 1982).

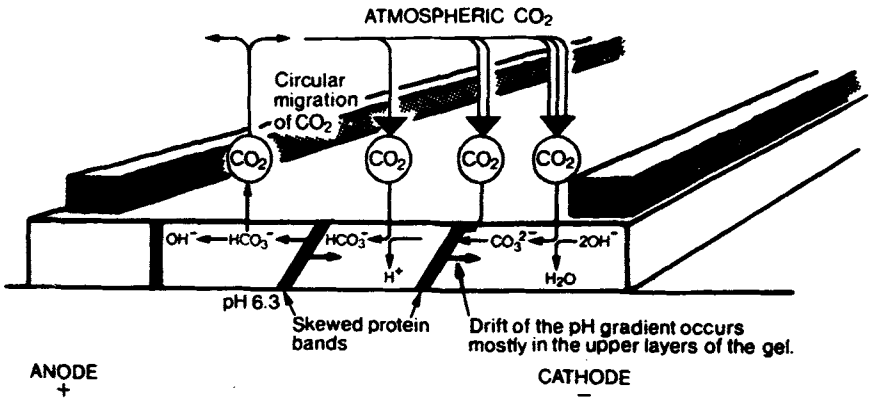

Fig. 11. Diagram illustrating the principle of interference by atmospheric carbon dioxide at high pH. Hypothetical cross section of a gel. Note that at pH 10.3 and above, the CO_3^{-2} ion predominates, whereas between pH 6.3 and 10.3 the HCO_3^- ion predominates. (Courtesy of Dr. P. Burdett, Pharmacia Fine Chemicals, Uppsala. Reproduced with permission of the publisher.)

Finally, we have also found a strong electroendosmotic flow when trying to cast Immobiline gels onto porous membranes for direct protein blots, after the IEF step, while the gel is still on the supporting foil. Several potential candidates: denitrated cellulose nitrate, cellulose acetate (including the best IEF brands), cellophane, porous polyethylene, Zeta Probe, Pall Biodyne, among others, have all failed. It is not understood why IPGs should be so sensitive to porous membranes and what mechanism causes this electroendosmotic flow, but at present IPGs and porous supports seem to be incompatible. For protein blots there is a simple solution (Bos et al., 1984): instead of casting the gel onto the hydrophilic side of Gel Bond PAG, to which it adheres rather strongly, it may be cast onto the hydrophobic side, from which it can be peeled away easily at the end of the IPG run.

3. Polymerization Kinetics

In copolymerization chemistry it is often reported that the composition of the copolymer formed differs from the initial input composition because the monomers differ in reactivity toward free radical addition. Thus with less than 100% incorporation of monomers into the polymer, there is a possibility that the concentration ratios between the Immobilines built into the gel will differ from the ratios in the starting solution. This could have serious effects on the pH gradient generated, for instance, change its

slope and the theoretically computed pH interval. To minimize this effect, all Immobilines are derived from acrylamide, but despite this the resulting pH values will still depend to some extent on polymerization efficiency. Using techniques described by Gelfi and Righetti (1981a, b) and Righetti et al. (1981b), we have studied the effects of the following parameters on Immobiline gels: (1) level of persulfate, from 0.015 to 0.058%, (2) level of TEMED, from 0.024 to 0.096%, and (3) temperature range, from 20 to 60°C. The optimum polymerization efficiency (in the range 84–88% incorporation for the seven Immobilines) was found at 0.047% TEMED, 0.033% persulphate, 50°C, and pH > 7. Figure 12 gives an example of the effect of temperature on the extent and rate of reaction of Immobilines: as the temperature is lowered, the reactivity rate diverges greatly for the different Immobiline chemicals, with a consequent lowering of the incorporation levels in the gel matrix. Curiously, at 60°C the incorporation efficiency is lowered slightly for some species (the alkaline ones). Polymerization for 1 h at 50°C, as previously suggested, appears to be the right solution: all Immobilines seem to come to a confluence point at this temperature, by exhibiting very similar reactivity ratios and incorporation efficiencies (Righetti et al., 1984). Another important finding of these experiments is that when casting extended pH gradients (e.g., pH, 3.0–10, the widest possible with Immobiline chemicals), it is imperative that the acidic end of the pH gradient be titrated (with NaOH) around pH 7–7.5 to ensure a uniform reactivity ratio between the two pH extremes. The alkaline extreme of the gradient should be titrated (with formic acid) to pH 7–7.5 to avoid the massive destruction of Immobilines p*K* 8.5 and 9.3 that takes place at pH 9 and above and at 60°C (Fig. 4B). In fact, given recent findings (Pietta et al., 1985), we now arrange for polymerization conditions at pH 7–7.5 for any possible pH interval, from the most acidic to the most alkaline ranges.

When Immobiline gradients are cast by standard techniques, with a gradient mixer equilibrated in air, an 84–88% incorporation efficiency is the best that can be achieved, and this for most practical applications will be adequate. However, if better than 96% incorporation is required for some special experiments, this can be achieved by completely excluding oxygen from the polymerization mixture. We have achieved this by building a gradient mixer that provides for anaerobic conditions; however, the experimental manipulations are more complex.

A word of caution: the procedure must be followed carefully, for we are trying to copolymerize, possibly with the same efficiency, as many as nine different chemicals at one time (in extended pH gradients, seven Immobilines + acrylamide and Bis). Deviations do not work. For example, when we tried to make highly cross-linked (i.e., highly porous) gels by

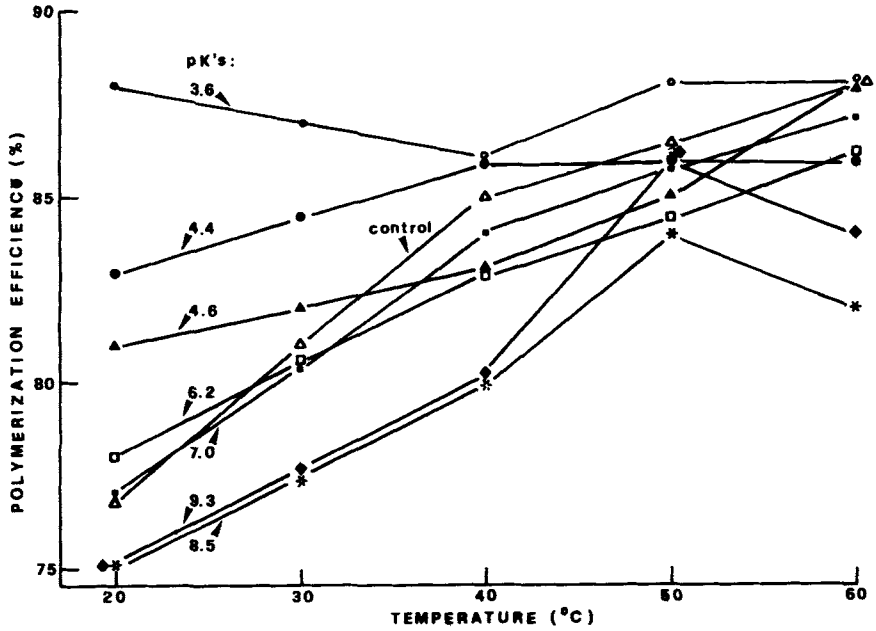

Fig. 12. Polymerization efficiency of the seven Immobiline species as a function of temperature. The percentage incorporation into the matrix is putative, as it is based on the ratio between initial and final absorbancies at 285 nm (disappearance of double bonds). The best convergence (similar reactivity ratios) is only obtained at 50°C. Note that the critical parameter is not so much a 100% incorporation efficiency, but the achievement of a ratio of incorporation between the buffering ion and the titrant as close as possible to unity. (From Righetti et al., 1984a. Reproduced with permission of the publisher.)

using 20% Bis or more, we found we had the porous structure but not the Immobilines bound to it! Even trying to change the cross-linker can often be troublesome (e.g., acrylaide gave us blurred and highly distorted patterns). Composite agarose (the best IEF brand)-acrylamide gels are also besieged with difficulties and give extremely poor results, possibly because the incorporation of Immobilines into the polyacrylamide is impeded by the onset of agarose gelation.

4. Alternatives for "Buffer Focusing"

In a way IPGs can be regarded as a system for performing isoelectric focusing in nonamphoteric buffers (NAB-IEF), and as such they would seem to go back to Kolin's (1958) "artificial" pH gradients. In reality

Kolin's approach was ineffective because it did not allow control of the pH gradient slope with time: upon prolonged electrolysis, the buffers and titrants would collect at the anode and cathode, forming strongly acidic and basic solutions with a great pH drop in between. By insolubilizing our nonamphoteric buffers, and titrating them near their pKs, unlimited stability with time and the needed buffering capacity coupled to the correct ionic strength is ensured. Over the years other laboratories have tried to develop other systems for NAB-IEF, such as (1) "stack" or "train" of free bases or acids "arrested by a deprotonation or protonation" mechanism, respectively (Chrambach and Hjelmeland, 1984); (2) "physically bonded" or "quasi-immobilized" pH gradients (Bier et al., 1984), (3) "steady-state rheoelectrolysis" (Rilbe, 1978).

We will analyze in depth some of these approaches, in particular the one developed by Bier's group which consists of highly sophisticated theories and models that show some striking similarities to notion of IPG. Their results are summarized in Fig. 13. Bier and his coworkers were able to generate "quite stable pH gradients formed using a simple system of a weak acid and a weak base (around neutrality), mixed in the proportion required to cover the desired pH range." In the simple case shown in Fig. 13, a gradient of a buffering acid (cacodylate, pK 6.2), varying linearly from 4 to 2 mM (anode to cathode) is titrated with a reciprocal linear gradient of buffering base (Tris, pK 8.3) ranging from 2 to 4 mM (anode to cathode). Although Bier and his coworkers claim that their system defies classification in terms of conventional modes of electrophoresis as it is not isoelectric focusing (i.e., not one of the components of the buffer are isoelectric) and not IPG as their buffers are not immobilized, close scrutiny of their data reveals that the buffers are a bit of both. The similarity with IPGs is striking. An analogous situation occurs in IPGs in the pH region 4.4–6.2, with Immobilines pK 4.4 (a weak acid) and pK 6.2 (a weak base), where the system is used under conditions in which the two components act simultaneously as buffer and titrant. As seen in Fig. 13A, the concentrations of the two are reciprocal, symmetrical linear gradients, generating a pH gradient from 6.21 (the pK of cacodylate, because the ratio [cacodylate]/[Tris] is 2:1) to pH 8.3 (the pK of Tris, because the ratio [Tris]/[cacodylate] is 2:1). However, the pH gradient is not linear but slightly sigmoidal, because the $\Delta pK = 2.09$, as predicted by our computer modeling (Gianazza et al., 1984a).

Such a situation was indeed fully predicted by our general theory on IPGs (Dossi et al., 1983), and we have simulated their data with our computer algorithm by assuming the two species are Immobilines. As shown in Fig. 14, we obtained the same results. The expected pH gradient is identical in the two cases, except that the deviation from linearity is quite high (maximum excursion, positive + negative, is 0.3 pH units, i.e., 15%

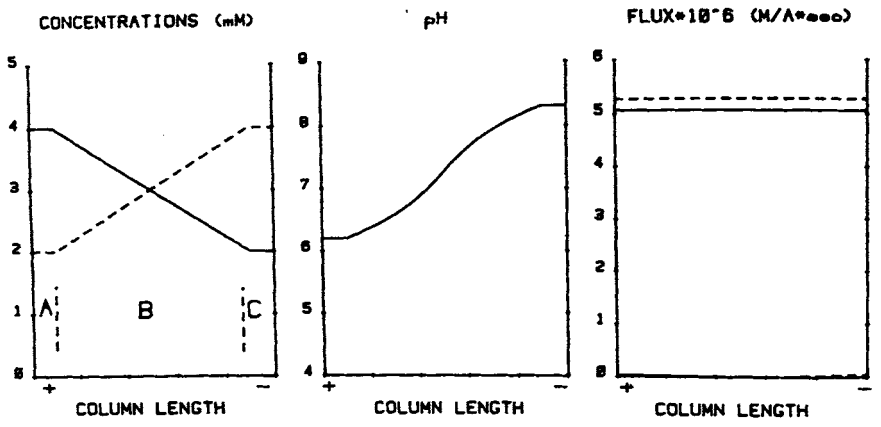

Fig. 13. Schematic presentation of the courses of the concentration of Tris-cacodylate and their respective fluxes and of the resulting pH gradient. Microcomputer calculated flux values are also plotted, assuming for Tris (dashed lines) a mobility of 2.42 cm^2/V-sec and a pK of 8.3, and for cacodylate (solid lines) a mobility of 2.31 cm^2/V—sec and a pK of 6.21. (From Bier et al., 1984. Reproduced with permission of the publisher.)

of the stated pH interval; for typical Immobiline gradients, both with narrow and extended ranges, the deviation can be contained within less than 1% of the pH span generated). We also simulated the β and I courses (Fig. 14*B*). As expected, they appear in the figure as two reciprocating, bell-shaped functions, with a minimum β power half way between the two peaks, corresponding to a maximum of ionic strength (by titrating the two species "inside" the two pKs, conditions of maximum ionization of the buffering groups are ensured).

Although with true Immobilines we can arrange for smoother β and I courses, the physicochemical parameters of Bier's system are acceptable and compatible with a well-functioning IEF setup. Of course it is true that the buffers here are not "chemically immobilized" but they nevertheless ensure a substantial stability of the system because they are immobilized according to physical laws. The fundamental requirement of Bier's gradients is that the flux of the two species is constant across the whole length of the column. In fact Bier and his coworkers have introduced a parameter, ρ, that is predictive of the stability of the system and is defined as

$$\rho = \frac{M^{A}_{a^-} M^{C}_{b^+}}{M^{A}_{b^+} M^{C}_{a^-}} \tag{4}$$

where M is the concentration of the acid (a−) and base (b+) in reservoirs

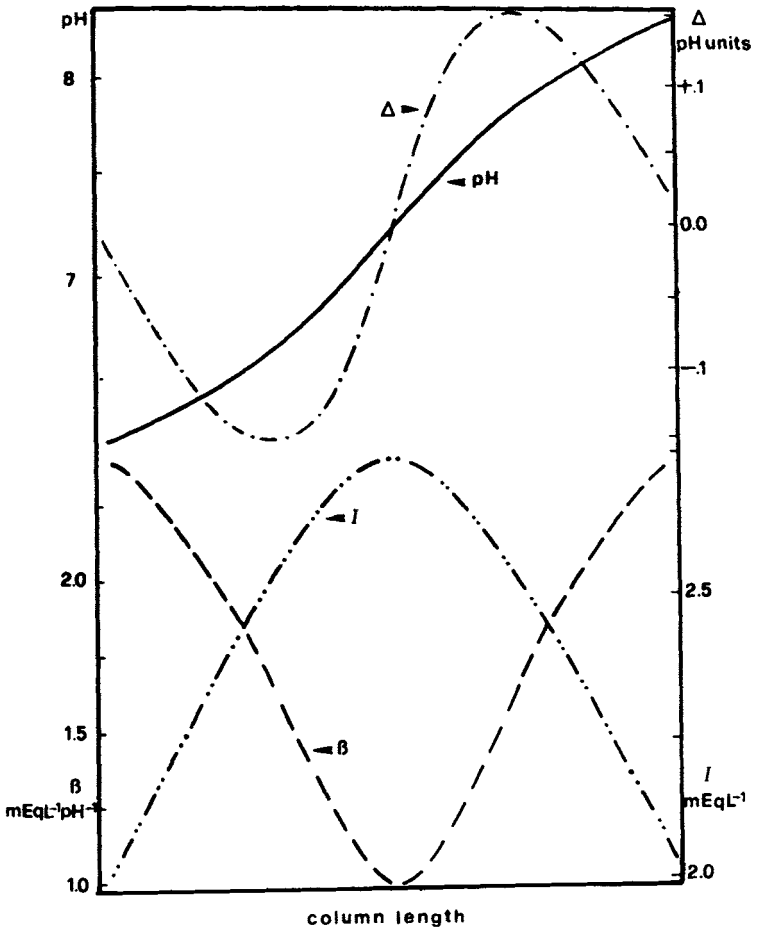

Fig. 14. pH gradient, deviation from linearity (Δ), buffering power (β) and ionic strength (I) of Bier's system of Fig. 13. Their data have been recalculated by using the same molarity and pK values and the same pH interval as in Fig. 13, except that Tris and cacodylate were assumed to be two Immobilines (i.e., with mobility = 0, flux = 0, diffusion coefficient = 0). Note that the shape of the expected pH gradient is identical in the two different computer models. Our computer simulation predicts that Bier's gradient is fully compatible with a well-functioning IEF system (ideally, however, we prefer to have an average β = 3 mequiv. $L^{-1}pH^{-1}$, so that the concentrations of the two species should be about doubled). (From Righetti and Gianazza, 1985. Reproduced with permission of the publisher.)

A and C. Only when ρ = 1 would there be perfect migrational stability, and this is one of the weaknesses of the system. As shown in Fig. 13*C*, the flux of Tris is slightly higher than the flux of cacodylate, and eventually the system is bound to decay.

The four modes of nonamphoteric buffer IEF summarized and compared clearly demonstrate that the system no longer depends on amphoteric species. However, a properly performing IEF system still has an absolute requirement the concept of "carrier." The carrier requires that the chemicals used to generate and stabilize the pH gradient behave as "good buffers" and "good conductors." Systems 2 and 3 discussed here (and IPGs of course) fulfill this fundamental requirement: in these three cases quasi-liner pH gradients are generated by titrating weak acids or weak bases symmetrically around their respective p*K*s, where they automatically provide the much needed buffering capacity and conductivity.

In the Chrambach "arrested stack" the system breaks down because the potential buffers are allowed to be stripped electrophoretically of counter ions and thus to collect in strongly acidic anodic layers or strongly basic cathodic zones, where they are deprived of their buffering and conducting powers. Although in Chrambach's system a natural pH gradient can still form (it is in fact a pH gradient generated by a stack of moving boundaries, as in isotachophoresis), it can hardly be controlled (for lack of buffering power) and can never be assumed to become stationary (for lack of immobilization). Indeed, the so-called arrested stack created by protonation of acids and deprotonation of bases is never quite arrested: it could only be so when the current in the system becomes zero, but at this point it would be quite meaningless still to speak in terms of "electrophoresis" (which, by definition, requires current flowing through the system). As for the other systems, although all three are based on sound and correct hypotheses, they are markedly different in operational terms.

Bier's system is subjected to two inherent disturbances: migrational instability (the parameter ρ very rarely will be unitary) and diffusional instability (decay of the boundaries). The two instabilities are additive and will ensure ultimate decay of the pH gradient. In Rilbe's system, again what theory predicts and what practice can achieve rapidly come into conflict: the predicted pH courses are only established in the absence of internal liquid flow (i.e., inside the electrophoresis cell). Unfortunately there is always a net liquid flow within electrolyzers, and this induces exponential and slowly decaying pH gradients.

VII. METHODOLOGY

1. Gel Casting with a Two-Vessel Gradient Mixer

For the cassette, the basic assembly is just as depicted in Fig. 15 (Immobiline gels usually have to be washed, so it is not feasible to cast them in glass cylinders). To the cover glass, for applying the sample in a free-liquid layer, we suggest binding pocket-forming strips (up to 20),

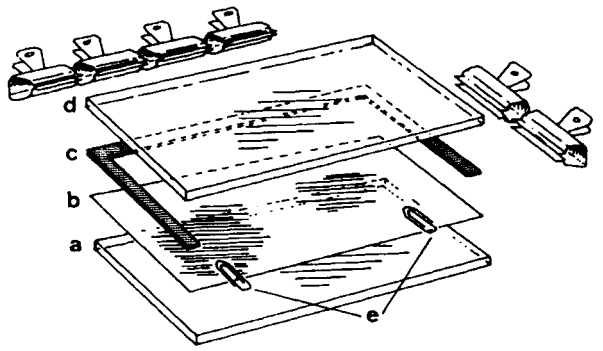

Fig. 15. Assembly of a gel cassette for casting IPGs. *(a)* Glass base plate (3 mm thick); *(b)* Gel Bond PAG foil; *(c)* U-gasket (in general silicone or rubber, often glued to the glass cover plate; usually 0.5 mm thick); *(d)* Template: 3 mm thick glass plate with pieces of self-adhesive Dymo tape (250 μm thick) for moulding of gel slots; *(e)* paper clips as temporary, additional spacers. (From Görg et al., 1978. Reproduced with permission of the publisher.)

cut out of adhesive embossing tape (Dymo), and then gluing the intact length of tape and cutting out and removing 3-mm-wide segments, perpendicular to it, so as to leave glued to the glass separate rectangles of tape. The depressions formed by the Dymo tape in the gel layer are about 250 μm deep and can usually accommodate volumes up to 10–12 μl. A double volume can be arranged by gluing two embossing strips on top of each other. It is always best, however, to make sure that, after opening the cassette, the pockets are sealed at the bottom by a thin film of polyacrylamide gel.

The final assembly is shown in Fig. 16. Notice that the two upper clamps on the top of the cassette are removed and that two paper clips are inserted instead. This greatly facilitates the insertion of the plastic tubing to convey the solution from the mixer to the chamber by forcing the top rims of the glass slabs to diverge and thus widen the 0.5 mm gap. The gradient mixer is positioned about 5–8 cm from the chamber top (the liquid will flow down by gravity) and is filled with the acidic and basic solutions. One should remember to fill only one chamber first and then to remove the air bubble from the channel connecting the two chambers by gently opening the central valve. The gel chamber stands vertically on a leveling table, and the capillary tubing is inserted in the middle. At this point stirring is started (500 rpm), the catalysts are added (TEMED and persulphate, in this order), both valves are opened, and the density (and pH) gradient is allowed to flow in the gel cassette. About 10 min pass before the onset of polymerization at 20°C, but in a hot room in summer

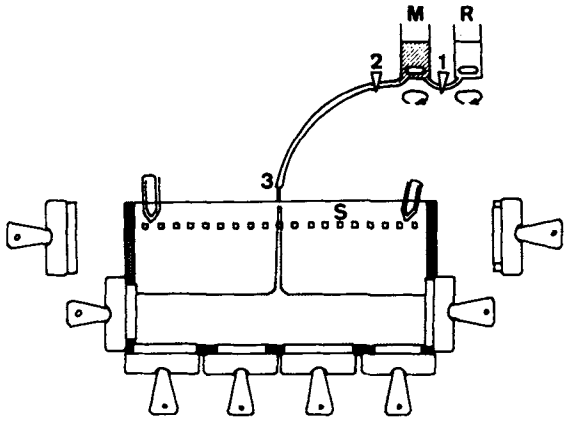

Fig. 16. Gel cassette and gradient mixer for casting an Immobiline gel. The basic, light solution is pipetted into the reservoir *(R)* of the microgradient mixer, while valves (1) and (2) are closed. The connection tube is filled by opening (1) for a brief moment. The acidic, heavy solution is pipetted into the mixing chamber *(M)*. The magnetic stirrer is started; (2) and (1) are opened. When the liquid surface has reached about two-thirds of the cassette height, the paper clips (temporary spacers) are cautiously removed without interruption of the filling procedure, and the two remaining upper clamps are placed on the cassette, so that the liquid rises to fill up the chamber. *S* = slot former; (1) connection valve; (2) outlet clamp; (3) tip of the outlet tube. (From Görg et al., 1983a. Reproduced with permission of the publisher.)

(and in 8 *M* urea) the reaction will be faster (2–3 min at temperatures higher than 30°C). Once all the gradient has been poured, the clips are quickly removed, and the two upper clamps are fastened in their position.

After standard polymerization (1 h, 50°C) the gel cassette is removed from the oven, the eight clamps are unfastened, and the supporting glass plate is gently pried open with the tip of a spatula. The Gel Bond PAG foil can now be lifted from one corner and gently peeled off, with the bound polyacrylamide gel layer, from the other plate closing the cassette. The first step at this point is weighing (after blotting any traces of liquid around the ridges of the foil) because as the gel is later washed, it will swell in water. It is well to mark the weight of the gel on the plastic backing. The gel is now washed in 1 liter of distilled water for 30–40 min for 0.5-mm gels (double this time for 1-mm gels). The washing step is essential: TEMED, persulfate, and 12–16% unpolymerized Immobilines must be removed; otherwise large plateaus of free acid and free base will form at the anode and cathode, respectively, and will prevent the protein from focusing. After washing, the gel should be blotted with soft tissue and

then, with the aid of a fan, reduced to its original weight. This step is essential because gels containing too much water will "sweat" during the IEF run and droplets of water will form on the surface. Now the Immobiline gel is ready for the electrophoretic run.

2. Gel Casting with Computer-Controlled, Step Motor-Driven Burettes

One of the main advantages of IPGs is the full control obtained of the environmental parameters during the electrophoretic run: β power, ionic strength, width, and slope of the pH gradient. Whereas the first two parameters depend solely on the initial molarities of the chosen Immobilines and on their incorporation efficiencies, the last two depend also on the casting equipment, such as the type of gradient mixer used and the gel cassette. Improper use of this equipment could result in alteration of the slope and width of the selected pH gradient, thus diminishing the full potential of the IPG technique.

For absolute reproducibility, Altland and Altland (1984) developed a program for computer-controlled cooperation of four commercially available step motor-driven burettes able to generate any type of density gradient and, in general, solute gradients. The slope of the gradients is defined by entering up to 200 endpoints of straight lines having as coordinates the percentage of the total volume and the concentration of the gradient-forming solute. The possible minimum increment of the discontinuous gradient is 0.5% of the total range. The gradients are obtained by mixing at variable flow rates the contents of two burettes containing the dense and light solutions, respectively, and of two additional burettes containing the two polymerization catalysts (TEMED and persulfate). The entire assembly is shown in Fig. 17, and the mixing chamber (having a dead volume of barely 200 μl) is depicted in Fig. 18. The entire equipment, including the computer program, is now available from Desaga, Heidelberg (GFR).

Although originally developed for porosity gradients in polyacrylamide and for centrifugation and chromatography gradients, the potential of this system for casting IPG gels is obvious. In collaboration with Dr. K. Altland, we have set up this equipment in our laboratory and have obtained extremely reproducible IPG gels. For such a purpose there is a need of only three burettes: one containing the dense solution, titrated to one pH extreme, another with the light solution buffered to the other end of the desired pH interval, and a third containing persulfate (TEMED being equally distributed in the former two). Another weak point in this system could be the casting cassette: after prolonged use, the rubber or

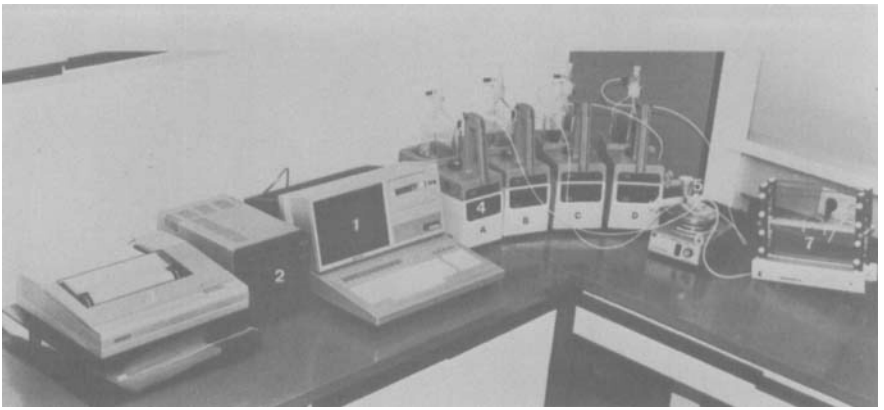

Fig. 17. The complete device for mixing an Immobiline gel gradient. (1)–(3) Computer, floppy disk station and matrix printer; (4) the four burettes, *A* to *D*; (5) the mixing chamber on a (6) magnetic stirrer; (7) a polymerization stand with two separation cells to be filled from the bottom. (From Altland and Altland, 1984. Reproduced with permission of the publisher.)

silicone grommet (in general 0.5 mm thick) could collapse, with a simultaneous decrement of the chamber volume; this in turn would produce a change in slope and width of the desired IPG interval. It is thus highly desirable to have chambers with rigid gaskets that will retain their thickness even after prolonged use.

3. Reswelling of Dried Immobiline Gels

For routine applications, especially when using the Altland and Altland (1984) casting technique, it is better to cast gels by a batch procedure and then store them dry for subsequent use. Gelfi and Righetti (1984) studied the gel-swelling kinetics as a function of the following variables: (1) solvent composition (plain water, 8 *M* urea, 2% Nonidet P-40 (British Drug House, Poole, England) and their mixture; Fig. 19); (2) gel composition (varying %T at fixed %C); (3) temperature (in the range 20–60°C); (4) gel thickness (from 0.5 to 2 mm; Fig. 20); and (5) operative pH interval (from the extreme acidic, pH 3.5–5, to the extreme alkaline, pH 8.5–10, ranges) under isoionic conditions. The following practical guidelines for gel drying should be observed: (1) the gels should have a low matrix content (e.g., 3%T); (2) they should have reduced thickness (0.5, max, 1 mm; for greater thicknesses, the swelling exponential becomes too steep); (3) alkaline gels should be dried in vacuo over silica, to prevent CO_2 adsorption; and (4) the gels should be extensively washed prior to drying.

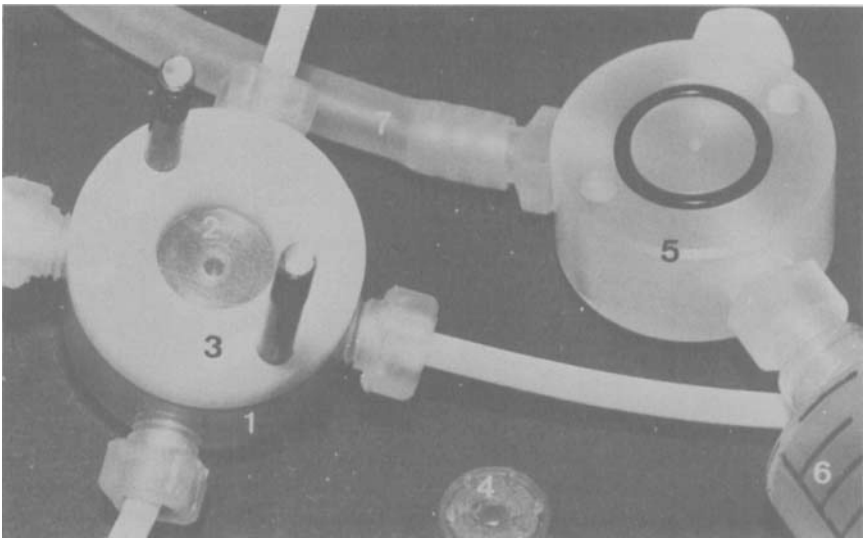

Fig. 18. The disassembled mixing chamber: *(a)* The X-connector with a central bore (2) and the four Teflon tubings from the burettes; (3) one of the exchangeable polyamide rings determining the internal volume of the mixing chamber; (4) the magnetic stirrer that fits into the mixing chamber to give a residual volume of 200, 400, and 1000 μl with appropriately sized polyamide rings (the chamber available from Desaga has a standard inner volume of 200 μl); (5) the Y-connector modified by a central bore and a *O*-ring as the upper part of the mixing chamber; (6) a plastic syringe fixed to the *Y*-connector which may be used to remove the rest of the gradient solution via the silicone tubing (7) into the separated cell. (From Altland and Altland, 1984. Reproduced with permission of the publisher.)

It has been found that the diffusion of water through Immobiline gels does not follow a simple Fick's law of passive transport from high (the water phase) to zero (the dried gel phase) concentration regions, but it is an active phenomenon: even under isoionic conditions, acidic ranges cause swelling 4–5 times faster than alkaline ones.

4. The Use of Plateaus

Plateaus, added at one or both ends of the IPG gels, introduce a new dimension in the Immobiline technique because they greatly enhance its versatility. There are three types of plateaus which can be utilized alone or in combination: (1) pH plateaus, (2) porosity plateaus, and (3) affinity ligand plateaus. For example, pH plateaus were first reported by Ek et al. (1983), their main purpose being salt removal from the IPG matrix. It is known that IPGs, being covalently bound to the gel matrix, are in principle unaffected by salt ions. There are, however, some practical limits to

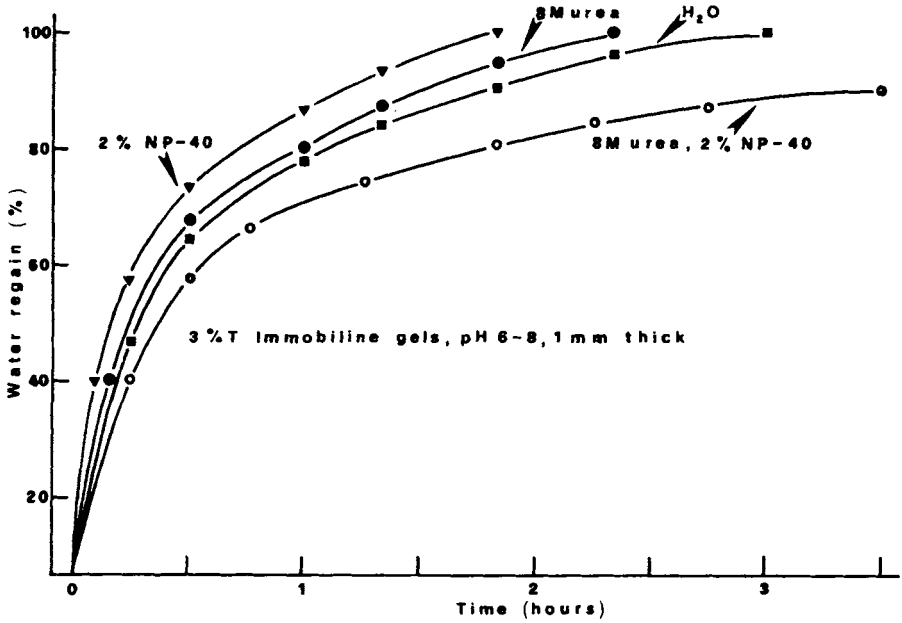

Fig. 19. Swelling kinetics of Immobiline gels. 1 mm thick, 3%T, 4%C Immobiline gels, pH 6–8, were dried and reswollen in the following solvents: plain distilled water (■), 8 *M* urea (●), 2% Nonidet P-40 (▼), and a mixture of 8 *M* urea and 2% NP-40 (○). The swollen gel weight, as taken just after polymerization, was subtracted from the tare (combined weights of Gel Bond PAG and of monomers) and the dried gel was reswollen to this net weight value. In the case of urea solutions, the solvent uptake was corrected for its density (i.e., the gel was allowed to reswell to 12% more weight, as solvent uptake was evaluated by weighing). (From Gelfi and Righetti, 1984. Reproduced with permission of the publisher.)

the amount of salt that can be tolerated even in IPGs, and they are due to the initial conductivity of the IPG gel and the generation of strongly acidic and strongly basic gel zones in proximity to the electrodes as a consequence of the physical separation of the salt ions. With respect to the first point, different amounts of salts can be tolerated in different pH ranges: at acidic pH (pH 3.5–5) as much as 10–15 μmol NaCl/ml gel solution can be tolerated, the corresponding amount in the pH range 9–10 being 3–4 μmol NaCl/ml gel solution. (It should be remembered that the free proton mobility is 350 $cm^2\ V^{-1}\ sec^{-1}$, whereas the corresponding OH^- mobility is only 85 $cm^2\ V^{-1}\ sec^{-1}$ at 25°C.) However, in the pH range 5.5–9, where the conductivity of the system is at a minimum and the contribution of free H^+ and OH^- quite small, the maximum tolerable amount is barely 0.5 μmol NaCl/ml gel solution.

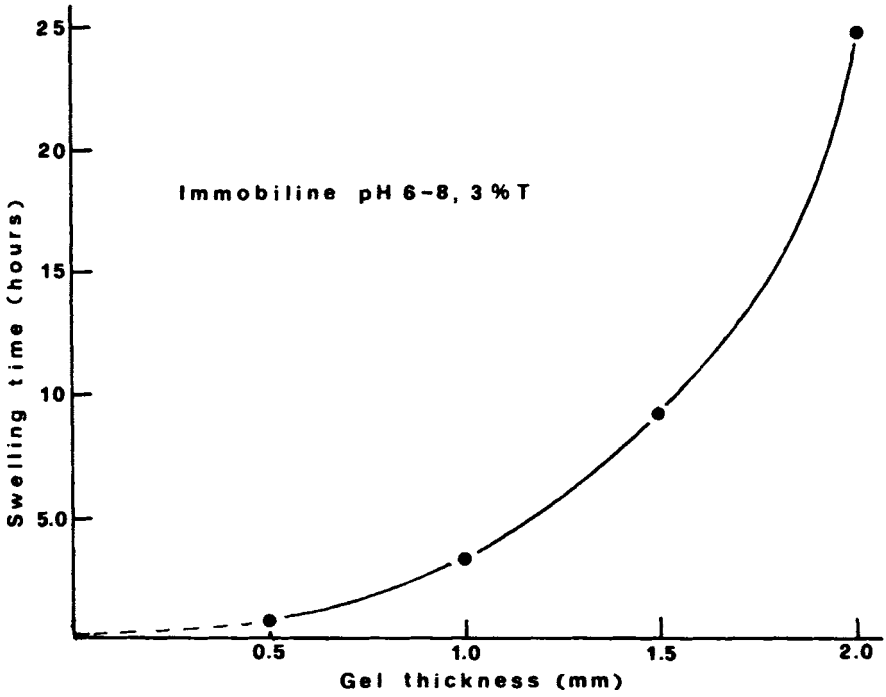

Fig. 20. Swelling kinetics of Immobiline gels. The equilibrium swelling times of gels of varying thicknesses have been plotted against gel thickness for 3%T, pH 6–8, Immobiline gels. Notice how the exponential becomes very steep above 1 mm thickness. (From Gelfi and Righetti, 1984. Reproduced with permission of the publisher.)

The second problem—collection of free cations and anions at the two electrodes, with formation of plateaus with extreme pH values—can be solved by elongating the gel with pH plateaus at the two extremes, where the ion components of the salt can collect just outside the Immobiline pH gradient. In this case it is best to polymerize a 50% longer gel (e.g., 15 cm instead of the 10 cm standard length). Enough of the acidic, dense solution, is injected in the chamber to form a 2.5-cm-long plateau, which is allowed barely to polymerize with the aid of a hot fan; over this is cast the desired Immobiline gradient, of standard 10-cm length. Then the remaining light, basic solution is gently floated over the gel to form a 2.5-cm-long cathodic plateau. The entire assembly is then polymerized under standard conditions, in the oven at 50°C for 60 min. During the run the anionic and cationic components of the salts in the sample will be seen as refractive lines moving out of the separation gel and collecting in the

two plateaus at the electrodes. At this point one can remove them by excision and repositioning of the electrode wires, thus continuing the experiment in a salt-free environment.

Porosity plateaus were first described by Righetti and Gelfi (1984) for strengthening the walls of the sample application trench during preparative runs in "soft" plyacrylamide gels. As described in Section VIII.3, low %T gels (e.g., 2.5–3%T) afford much higher sample loads than standard 5 or 6%T matrices. However, in such soft and thick gels, the wall of the trench will collapse, inhibiting the sample application to the matrix. Thus all the gel layer around the trench was cast as a more robust, 5%T zone, which also contained a more acidic pH plateau and a double ionic strength plateau to enhance the protein mobility in the loading zone. Even though porosity plateaus have been described only for this purpose, we can anticipate that a novel use could be to utilize them as sieves to eliminate some unwanted, higher Mr species, present in the sample mixture. Under these conditions a run with two simultaneous separation criteria (i.e., a mass coupled to a charge fractionation) would be carried out.

Affinity ligand plateaus have been run recently in our laboratory. They are very useful in coupling two independent separation parameters, namely an affinity prepurification step, based on a specific biological activity and followed by a charge fractionation in the IPG matrix proper. In the example shown in Fig. 21 a shelf was polymerized at the cathodic end of a wide-range Immobiline gel (pH 4–9) containing a gradient (perpendicular to the IPG gradient) of a specific human serum albumin ligand (Blue Dextran). It can be seen that, at the proper HSA/ligand ratio, practically all albumin is sequestered from the sample under analysis. This is a simple and elegant method to sequester HSA, an often unwanted component when analyzing human sera, as it often swamps and obliterates neighboring protein zones because its great concentration overwhelms other serum components. In our example, the immobilization of the ligands is simple, due to their entrapment in the gel fibers, caused by their extremely large size. In other cases the ligands will be bonded to the "affinity shelf," just like the Immobiline chemicals are.

5. Artifacts

All the possible artifacts of conventional IEF have been already comprehensively described (Righetti, 1983a). With a new technique it is important to define the range of validity within which the method behaves as predicted. Outside of these limits the method could give erroneous results leading to misinterpretation of the data. The IPG technique is no exception to this rule, although artifacts will occur by a different mechanism: as the charge density of the macromolecule to be separated approaches the

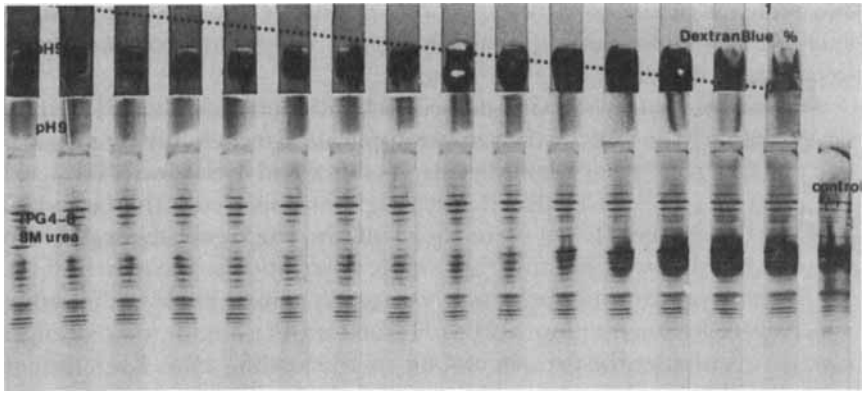

Fig. 21. An example of a ligand plateau coupled to an IPG gel. The plate includes three gel layers: lower, an IPG in the pH range 4–8, containing 8 *M* urea; middle: a constant pH gel, containing 10 m*M* Immobiline p*K* 9.3 and Immobiline p*K* 3.6 to a final pH = 9.0; upper: transverse (right to left) gradient 0–1% Dextran Blue in a constant pH gel, containing 10 m*M* Immobiline p*K* 9.3 and Immobiline p*K* 3.6 to a final pH = 9.1. The sample (5 μl straight serum) was applied in the 15 lanes of the upper gel; the plate was run 3 h at 750 V, with the pH 9.0 layer applied, gelly side down, as a bridge between the two gradients. The cathode was then moved at the alkaline edge of the IPG layer, 5 μl of serum applied on the 16th (control) lane, and the run continued overnight at 2000 V. (From Gianazza and Righetti, unpublished.)

charge density of the matrix, a strong interaction will occur, which will result in either total sample precipitation at the application point or extended smears covering a wide gel surface.

Righetti et al. (1983b) found that IPG matrices interact strongly with at least two classes of proteins, histones and the histonelike, "high mobility group" (HMG) chromatin proteins, forming insoluble complexes. The nature of these interactions has been demonstrated to be purely ionic: the complexes are split by high ionic strength (0.5 *M* NaCl) and/or by altering the pH (full disaggregation being obtained at pH 5.5 and 11.5). By preparing soluble homo-Immobiline polymers (polymerized in the absence of a cross-linker) formed by either a pure carboxyl or a pure amino surface, it was demonstrated that histones and HMGs bind preferentially with carboxyl Immobiline polymers (Fig. 22). Thus there are limitations to the IPG technique: nucleic acids, heparin, and polyanions are also not amenable to fractionation in IPG matrices, and produce a curtain of molecules smeared over the gel surface or simply precipitated at the application point.

Nevertheless, we have found that IPGs perform normally with all

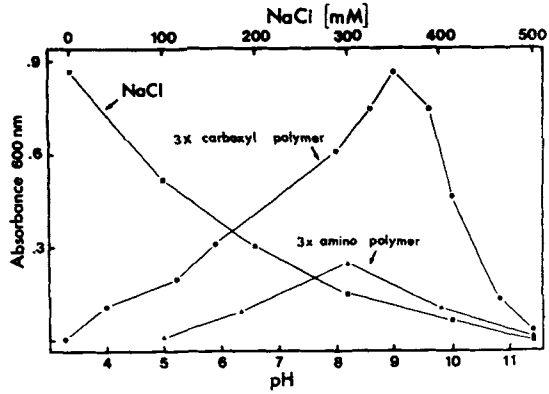

Fig. 22. Formation and disaggregation of complexes between soluble, carboxyl and amino Immobilines and histone like (HMG) proteins. Polymers with pure carboxyl and amino surfaces, having a threefold higher concentration of Immobilines than standard gels (approximately 30 m*M*), were used in this experiment, and the stability of their complexes with HMG proteins was studied as a function of pH. For the carboxyl polymer, the disaggregation of its complex with the HGM protein by increasing sodium chloride molarities is also plotted. (From Righetti et al., 1983b. Reproduced with permission of the publisher.)

proteins we have tested (having p*I*s in the pH range 3.5–10) except one: serum albumin (HSA). As seen in the separations of Görg et al. (1983b) and Cleve et al. (1982), HSA produces long smears betwen pH 4.7 and 5.2, instead of focusing regularly. It appears that HSA recognizes as ligands p*K* 4.4 and 4.6 Immobilines, which are unfortunately needed as buffers in the pH region in which HSA is isoelectric. These complexes are, however, sensitive to 8 *M* urea, so that practically normal patterns are obtained when running 2-D maps by the O'Farrell technique (Gianazza et al., 1984a).

VIII. PREPARATIVE ASPECTS

Now we consider some preparative aspects of IPGs. After IPGs' inception as an analytical technique, it soon appeared that their loading capacity in preparative work was also striking. The load ability of the IPG gels has been demonstrated to be at least 10 times higher than in conventional IEF, thus approaching or even passing the load limit of isotachophoresis (Gelfi and Righetti, 1983; Ek et al., 1983). The following aspects will be discussed in this section: (1) explorative runs aimed at defining the load

capacity, (2) optimization of experimental parameters (I, pH gradient width, gel thickness), (3) protein load as a function of %T in the matrix, (4) protein recovery from Immobiline gels into ion-exchange beads, and (5) small-scale protein recovery by the canal-Immobiline technique.

1. Theoretical Prediction of Acceptable Protein Loads in IPGs

An equation has been derived (Ek et al., 1983) correlating the maximum protein load in a single zone to the pI distance (ΔpI) from the nearest contaminant, to the gel cross-sectional area and to the slope of the pH gradient:

$$M = \left(\frac{\Delta \text{p}I}{d(\text{pH})/dx} - L \right) \cdot 2C_M \cdot A \tag{5}$$

where M = protein load in a single zone (major component) in mg; ΔpI = pI difference between major component and nearest contaminant (in pH units); d(pH)/dx = slope of the pH gradient along the separation track (pH units/cm); L = protein-free space between the major band and the impurity, which is needed to cut the gel without loss of protein or without carrying over the impurity (in general, 1 mm is an acceptable distance); C_M = average concentration in the focused zone of the major component (mg/ml); A = cross-sectional area of the gel perpendicular to the focusing direction (in cm^2).

It can be seen that protein load can be maximized by increasing A (the liquid volume available to the focused zone) and by decreasing the slope of the pH gradient (i.e., by focusing in ultranarrow pH gradients). As a practical guide line, a graph has been constructed correlating these three basic experimental parameters: protein load in a single zone, ΔpI between the band of interest and nearest contaminant and slope of the pH gradient along the separation axis [d(pH)/dx]. This graph is essentially a plot of equation (5), taking as a concentration limit (C_M) a common upper limit of 45 mg/ml experimentally determined. Figure 23 shows how the graph is constructed: the abscissa gives the ΔpI value (in pH units) and the ordinate the protein load (mg/cm^2) for a given A value. The ΔpI versus protein load plane is cut by lines of different slopes representing pH gradients of different widths along the IPG gel length. It is seen that ultranarrow pH gradients (e.g., 0.02 pH units/cm) allow extremely high protein loads (up to 80 mg/cm^2) while still retaining a resolution better than ΔpI = 0.01. At the opposite extreme broad pH gradients (e.g., 0.2 pH units/cm) would allow resolution of only ΔpI = 0.1 with a protein load of less than 40 mg/cm^2.

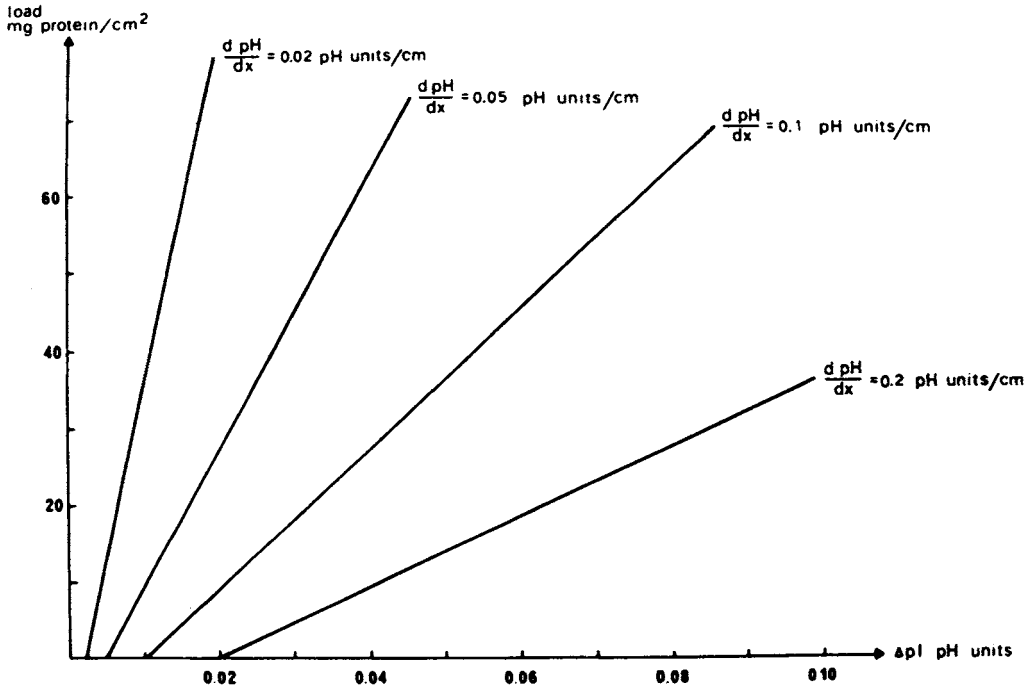

Fig. 23. Acceptable protein load as a function of ΔpI for different pH slopes plotted for a mean concentration of 45 mg/ml in the major protein zone. This is a graphical representation of equation (5). (From Ek et al., 1983. Reproduced with permission of the publisher.)

2. Optimization of Environmental Parameters

Gelfi and Righetti (1983) performed a thorough study on the optimization of environmental parameters (I, gel thickness, pH gradient width) for maximizing protein loads in Immobiline matrices. These aspects are summarized in Fig. 24. By increasing the ionic strength of the gel from 1.25 to 7.5 mequiv. Liter^{-1} a fourfold increment in load capacity is obtained; above this level a plateau is abruptly reached around 10–12 mequiv. Liter^{-1}. By increasing the gel thickness from 1 to 5 mm, a proportional fivefold increment in protein load ability is achieved. The system does not level off, but a 5-mm thickness seems to be optimal since thicker gels begin to develop thermal gradients in their transverse section, generating skewed zones. Finally, by progressively decreasing the width of the pH interval, there develops a linear increase in protein load capability. Here too the system does not reach a plateau. However, due to the

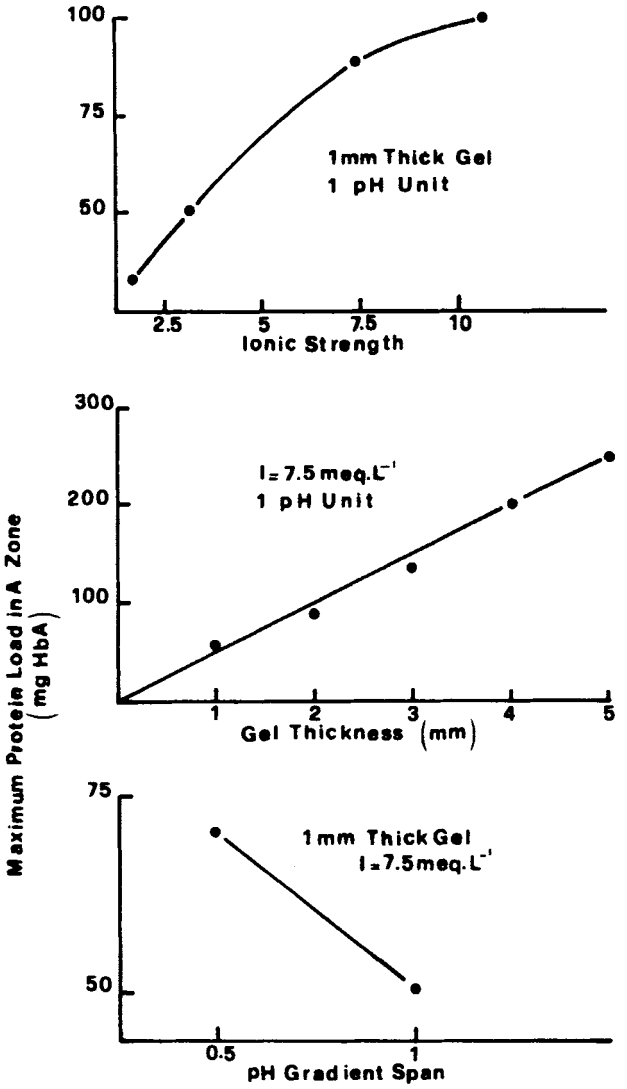

Fig. 24. Loading capacity of IPGs. The maximum load in a single protein zone is plotted: *(a)* as a function of ionic strength at constant gel thickness (1 mm) in a 1 pH unit span; *(b)* as a function of gel thickness at constant ionic strength in a 1 pH unit interval; *(c)* as a function of pH gradient width at constant ionic strength and constant gel thickness. (From Righetti, 1983b. Reproduced with permission of the publisher.)

very long focusing times required by narrow pH gradients, aggravated by the high viscosity of protein zones at high loads, it is probably unwise to attempt to fractionate large protein amounts in pH ranges narrower than 0.5 pH units.

We have seen in the previous section that IPGs have a load ability at least 10 times higher than conventional IEF. This is due most likely to the strong difference in ionic strength characteristic of the two systems. At the very low I values typical of IEF (ca. 1 mequiv. Liter^{-1}) macromolecules will have a very low solubility minimum and will tend to aggregate and flocculate. An increase in I, ca. 7–10 mequiv.L^{-1} as characteristic of IPGs, is thus beneficial since, according to the Debye-Hückel equation:

$$-\log \gamma = \log \left(\frac{S}{S_0}\right) = 0.51\, Z^2 \sqrt{I} \tag{6}$$

where γ is the activity coefficient of an ion of charge Z, S and S_0 are the solubilities of a protein at the pI at a given ionic strength and as extrapolated to zero ionic strength, respectively. Thus as the environmental I increases and the γ values of the ions (in both solution and the protein) decrease, the protein solubility increases: this is the well-known "salting-in" effect described in 1936 by Cohn. We are tempted to equate IPG gels to "salting-in" media and IEF gels to "salting-out" milieus. It might be argued that as long as the proteins precipitate at their pI, and this material is confined in the isoelectric zone, this should not affect the load capacity in gel matrices because the precipitated zone is gravitationally stable. However, in real cases this does not quite happen. As demonstrated by Gronwall (1942), the solubility curve of an isoionic protein, when plotted with respect to pH near the isoionic point, is a parabola, with a fairly narrow minimum at relatively high I but with progressively wider minima, on the pH axis, at decreasing I values. The latter case would thus depict conditions typical of conventional IEF, and the former condition would apply to IPGs. Therefore, in conventional IEF, what is detrimental in preparative runs is not isoelectric precipitation but near-isoelectric precipitation. The precipitate is not confined at the pI position but is usually smeared over as much as a 1/2 pH unit interval, thus being completely detrimental to the resolution of adjacent species.

3. Protein Load as a Function of %T

It turns out that the situation in preparative runs is more complex than what has just been described. It is apparent from Section VIII.1 that no matter how the experimental conditions are optimized and the ionic strength is increased, a common upper load limit for all proteins investi-

gated was found at 40–45 mg protein/ml gel solution. We have been intrigued by this limit and have explored ways to circumvent it. The key to this apparent "solubility limit" is to be found in Fig. 25 (Righetti and Gelfi, 1984): the amount of protein accepted by a gel matrix is directly related to its composition (%T). The limit of 40 mg protein/ml gel is only valid for a 5%T polyacrylamide matrix: as the concentration of fibers in the gel is decreased, progressively more protein can be loaded in the system, so that in a 2.5% T gel as much as 90 mg protein/ml gel can be applied. This has been interpreted as a competition for the available water between the two polymers, the polyacrylamide coils and the protein to be fractionated. This is an extraordinary amount of material to be carried by a gel phase, and thus IPG is by far the leading technique in any electrophoretic fractionation. However, such soft gels are quite difficult to handle: for easier manipulations a two-step casting procedure was described based on the formation of a %T step and a pH plateau around the application trench (to prevent collapse of the trench walls and to speed up the electrophoretic migration of the protein out of the application zone; see Section VII.4).

The highly diluted gels described here have two additional advantages: (1) by diluting the matrix, while keeping constant the amount of Immobiline (the conventional ca. 10 m*M* buffering ion), the charge density on the polymer coil is in fact increased, and this results in sharper protein zones and increased protein loading capacity; (2) below 3%T, the visco-elastic forces of the gel are weakened, allowing the osmotic forces in the protein zone to predominate and draw more water from surrounding gel regions: this results in a further increment in load ability within a given protein zone due to local gel swelling and concomitant increase in cross-sectional area.

4. PROTEIN RECOVERY IN DEAE- AND CM-SEPHADEXES

Although all the basic aspects of preparative IPGs have been described, it is still necessary to discuss appropriate ways of recovering purified protein zones from these matrices. The recovery would have to be electrophoretic for two reasons: (1) an IPG gel would behave as a weak ion-exchanger; (2) even extensively washed gels would still contain short, uncross-linked, polyacrylamide-Immobiline chains that would be coeluted with the protein if the latter were to be extracted directly from an excised and ground gel zone. Ek et al. (1983) had originally described a zone electrophoresis system for elution that embedded the excised Immobiline gel segment, containing the purified protein zone, into an

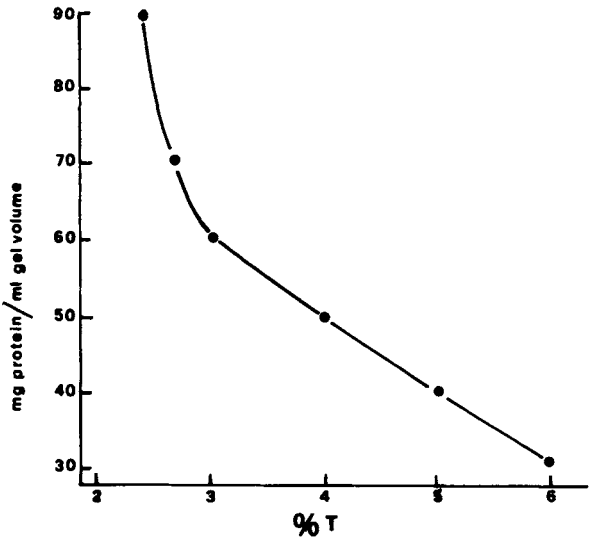

Fig. 25. Relationship between loading capacity (in terms of mg protein/ml gel volume) and %*T* (*T* = grams of acrylamide and cross-linker per 100 ml gel volume) value of the gel matrix. Notice that, though in the range 3 to 6%*T* the protein load decreases linearly, in softer gels (3%*T*) it increases exponentially. (From Righetti and Gelfi, 1984. Reproduced with permission of the publisher.)

agarose bed and then transferred it by electrophoretic retrieval into a layer of hydroxyapatite (HA) beads. Following this, the protein was recovered from HA crystals by elution with 0.2 *M* phosphate buffer, pH 6.8. However, although calcium phosphate crystals are an excellent ion-exchange material for separation of nucleic acids (Bernardi, 1971), for proteins they have relatively poor sorption capacity.

This transfer technique has been adopted from Ziola and Scraba (1976) and Guevara et al. (1982), but it was then realized that although it would work satisfactorily for small protein loads (in the mg/ml range), it would not perform properly on a larger scale (tens of mg/ml range), namely at loads compatible with Immobiline matrices. At these high loads, the HA grains would be quickly saturated, and the protein zone would cross the entire layer of resin and be lost in the anodal agarose layer embedding it. For this reason Casero et al. (1985) described a new transfer system based on electrophoretic recovery into true ion-exchangers utilized for protein separations. The IPG gel strip containing the zone of interest is transferred to a horizontal tray and embedded in 1%, low-gelling (37°C) agarose. For acidic to neutral proteins (up to p*I* 7.7) the

electrophoretic transfer is from the IPG strip into a layer of DEAE-Sephadex, buffered at pH 8.5 in 100 m*M* Tris-acetate (Fig. 26*A*). Recovery (better than 90% in all cases studied) was achieved by titrating the resin at pH 9.5, in 200 m*M* Tris-Gly buffer, containing 200 mM salt. For basic proteins (p*I* > 7.7) the electrophoretic retrieval is from the IPG strip into a zone of CM-Sephadex, buffered at pH 6.0, in 50 m*M* citrate (cathodic migration; Fig. 26*B*). Recovery (again better than 90%) is ac-

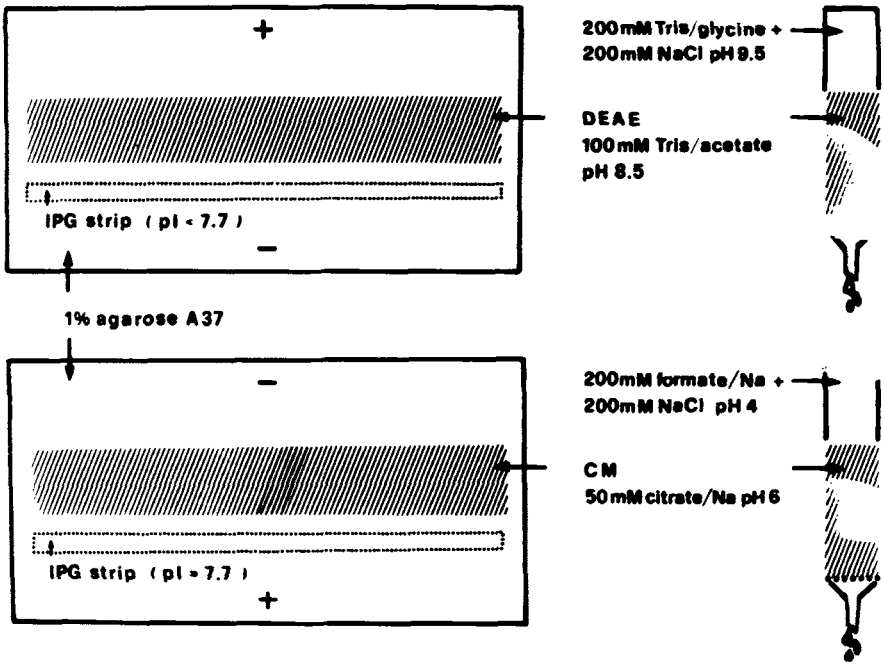

Fig. 26. Recovery of protein zones from IPG gels into ion-exchangers. Left side: after IEF, the IPG strip is cut out along the protein contour (still supported by the Gel Bond foil) and embedded in a 5 mm thick layer of 1% agarose A-37 (in the 250 × 110 mm size tray for preparative IEF in granulated gels). In front of it, a 2 cm wide, 22 cm long (or matching the length of the IPG strip) trench is dug into the gelled agarose, and filled with the ion-exchanger (the distance between the IPG gel and the resin should be barely 3–5 mm). For proteins with p*I*'s < 7.7, a CM-Sephadex in 50 m*M* Na-citrate, pH 6.0, is utilized for the electrophoretic retrieval (cathodic migration). The surrounding agarose layers are equilibrated in the corresponding buffers. Electrophoretic elution lasts in general 700 V × h. Right side: after electrophoresis, the resins are transferred to short columns or to plastic syringes, and the protein eluted with 200 m*M* Tris-Gly, pH 9.5 + 200 m*M* NaCl (anionic species) or with 200 m*M* Na-formate, pH 4 + 200 m*M* NaCl (cationic species).

complished by titrating the exchanger at pH 4.0, in 200 m*M* formate buffer, containing 200 mM NaCl. It has been demonstrated that Immobiline gels, even when incorporating five times the standard amount of buffer (75 m*M* Immobiline at pH=p*K*, i.e., 50 m*M* buffering ion and 25 m*M* titrant) exhibit, in the electric field, negligible ion-exchange properties, thus ensuring ideal supports for isoelectric focusing.

5. Protein Recovery by the Canal-Immobiline Technique

For small-scale protein loads in IPGs, an interesting method was described by Bartels and Bock (1984) who recovered the protein of interest focused in the Immobiline gel directly into gel filtration media: this was performed by collecting the protein of choice into a layer of Sephadex G-200, inserted into a channel cut into the IPG matrix.

How this is done is shown in Fig. 27*A* and *B*. The IPG plate is first run by applying the sample only in two lateral tracks (*C* and *C'* in Fig. 27*A*); after reaching equilibrium conditions, the two zones are cut away and stained for proteins. The developed analytical strips are then aligned back into their original position, and in the middle preparative area of the IPG gel, areas are selected where the protein bands of interest would focus. A channel is cut away with the aid of a scalpel and a spatula in these areas, and the trench is filled with a slurry of Sephadex G-200 equilibrated in distilled water. Then the sample for the preparative run is applied in tracks corresponding to the different cut out channels, and the IPG run is performed under the same conditions used for the analytical prerun. On reaching equilibrium, the desired protein will collect in the Sephadex-filled channel and will be forced to stay there by the electric field. At the termination of the run, the Sephadex grains are quickly removed from the different channels and individually transferred into suitable microcolumns, and the different protein zones are recovered by gel filtration.

The difference between the present method and the systems of Ek et al. (1983) and Casero et al. (1985) is that both the electrophoretic fractionation and the protein recovery are performed simultaneously in the same mixed Immobiline-Sephadex gel rather than sequentially in two different gel layers by two separate experiments. The efficiency of the separation is shown in Fig. 27*B*, here the fractions eluted in the (now empty) channels of Fig. 27*A* are rerun in the same Immobiline pH interval under analytical conditions, side by side with the unfractionated mixture as a control: fractions 1 to 4 appear as homogeneous, single-protein zones. We believe that the different techniques are indeed complementary: canal-Immobiline would be adequate for small-scale sample loads, whereas the

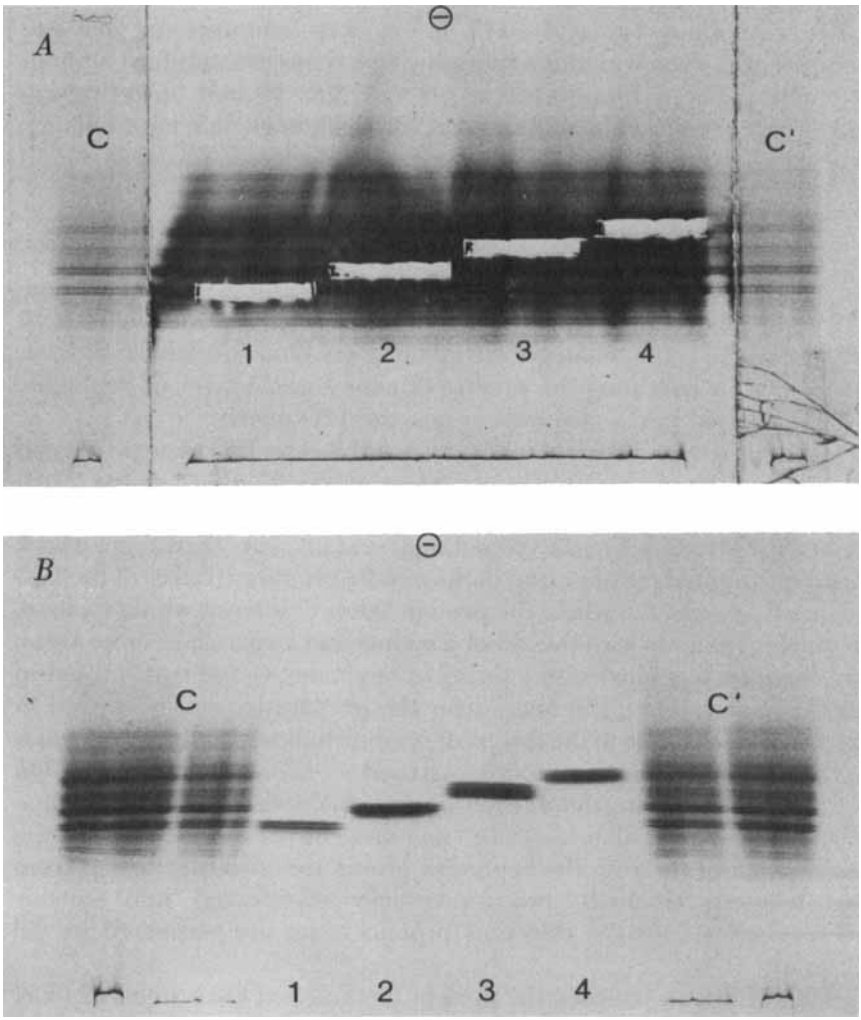

Fig. 27. *(A)* Immobiline-canal IEF of ovalbumin dissolved in water. Gel: 185 × 125 × 0.5 mm, pH gradient 4.3 to 5.3; 4°C; 8 kVh, max. 5W and 5 kV; fixing and staining in Coomassie Blue. *C* and *C'*: lateral edges for analytical prerun; 1–4: channels for the collection of proteins, filled with an aqueous slurry of Sephadex for IEF. The sample application trench is at the anode. *(B)* Refocusing of the four protein samples collected in the channels 1–4 of *(A)*; the IEF-Sephadex from the different channels of the previous gel was directly inserted into pockets at the anode and rerun under the same conditions of the analytical experiment. Lanes *C* and *C'*: control, unfractionated ovalbumin; channels 1–4: single fractions eluted from gel *(A)*. (From Bartels and Bock, 1984. Reproduced with permission of the publisher.)

two-step methodology of Ek et al. (1983) and Casero et al. (1985) is the only choice for large-scale preparations.

IX. TWO-DIMENSIONAL TECHNIQUES WITH IPGs

Two-dimensional maps have become increasingly important in all fields of life sciences. For the vast literature in the field, the reader is referred to some recent books and reviews: *Clinical Chemistry*, vols. 28 (No. 4, April 1982, pp. 737–1092) and 30 (No. 12, December 1984, pp. 1897–2108) representing the proceedings of two 2-D meetings organized by N. G. Anderson and N. L. Anderson at the Argonne National Laboratories (IL, USA); Celis and Bravo (1984a,b; the former a book devoted to 2-D techniques; the latter a review of cell biology applications); Dunn and Burghess (1983a,b; two fundamental reviews highly recommended; the first on methodology, the second on applications); Klose (1984; a systematic analysis of total cell proteins); Tracy et al. (1984; application of 2-D maps to clinical chemistry); Miller and Olson (1984; image acquisition analysis); Davidson (1984; electronic, autofluorographic aquisition of spots from 2-D maps); Righetti et al. (1983a; critical review of horizontal vs. vertical systems for generating 2-D maps).

We suggest the designation "IPG-DALT" for the sequence: isoelectric focusing in immobilized pH gradient-gel electrophoresis at right angles to each other in presence of sodium dodecyl sulfate (SDS; in analogy to the ISO-DALT acronym proposed by the Anderson's groups for conventional IEF followed by SDS-PAGE). Both narrow and wide range IPGs have been used for the first of the two-dimensional separations (Westermeier et al., 1983; Gianazza et al., 1984b; Gianazza et al., 1985c). When "open" systems were used, that is, when the run of the second dimension was performed in a flat bed apparatus, electroendosmosis caused trouble (vertical streaking). On the other hand, no such problem was noted with "submerged" systems, that is, when the second dimension step was run in a vertical apparatus. Marker proteins comigrated from either an IPG strip or a liquid phase showed the same apparent Mr.

The basic steps of an IPG-DALT run are illustrated in Fig. 28. Parallel lanes cut from a single gel slab (section 1) behave as completely independent tracks, like the individual gel rods used in conventional ISO-DALT protocols. With slab gels it is possible to apply the sample in any position along the pH gradient; if adequate, the area below and around the sample application pockets may be cast as a pH plateau (Section VII.4), and the whole width of the gradient can be moved to the same side as the sample slots. The latter procedure may be maintained or excised prior to the second-dimension step. The choice of a convenient strip width (usually 5

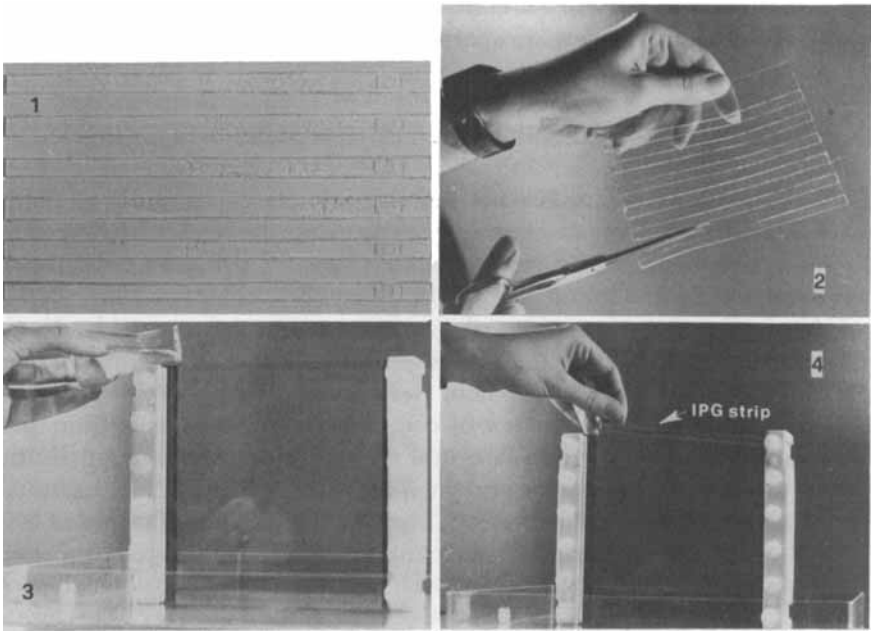

Fig. 28. Technical details for an IPG-DALT run. (1) The IPG slab is cut into parallel lanes (approximately 5 mm wide; each one mimicking a separate gel rod of conventional experimental setups). If the whole width of the gradient is to lie on the same side to the sample application pockets, a pH plateau is cast below and around them. (2) After an overnight run, the IPG slab is equilibrated for 15 min in SDS buffer (containing 2 ME). Each lane is cut into individual strips, flush with the gel at one side, having ca. 3 mm of protruding Gel Bond PAG film on the other side for easy handling. If required, the sample application slot and/or the underlying pH plateau is cut and discarted. (3) The SDS-PAG gradient gel is cast to fill the cassette for the second dimension to approximately 8 mm from the brim. The mold is warmed with buffer at 60°C. (4) 1% agarose (low electroendosmosis) is poured into the mold, and the IPG strip inserted and fused against the SDS-PAG gel (with the aid of two spacers, if required) (Gianazza and Righetti, unpublished.)

mm, although good results may be obtained up to 15 mm of gel width) allows for a quantitative transfer of the applied material to the second-dimension gel. The thickness of the IPG also has little effect on the outcome of the experiment. (We prefer, however, 1-mm gels supported

by 0.2-mm polyester foil to fit a 1.5-mm thick SDS gel.) On the contrary, it is important that the length of the IPG strip corresponds within at least 15% to the width of the SDS plate, to avoid slanted migration.

The sample is better applied without prerunning the gel as a low-viscosity, low-salt concentration solution. As already mentioned, the presence of excess 2ME affects the course of the alkaline portion of the gradient. The plate is usually run overnight at 2000 V. The gel is then equilibrated with electrode buffer containing SDS (no difference between concentrations >0.5%) and 2ME. Failure of equilibrating the gel or absence of a reducing agent in the equilibration medium results in irregular migration of alkaline and high Mr proteins, and double-banding of many spots. The duration of the equilibration step is 15 min for 5 × 140 × 1 mm strips, with shaking; the volume of the equilibration solution is 70 ml in a container 12 × 18 cm in size. The individual strips are then cut with scissors, flush with the gel at one side, leaving about 3 mm of free plastic support on the other for easy handling (Fig. 28, panel 2). It must be noted that the surface of the IPGs is extremely sticky and thus should be handled with wet fingers (or gloves, to avoid fingerprints at the silver stain level).

The SDS mold is warmed with electrode buffer at 60°C (Fig. 28, panel 3); it is then filled with melted 1% low electroendosmosis agarose in electrode buffer. The IPG strip is inserted and pressed on top of the SDS gel (with the aid of two spacers, or tweezers, if necessary (Fig. 28, panel 4), while squeezing the agarose from between the two gels. An intermediate layer of agarose or the presence of traces of liquid in the gap between the two gel phases results in severe lateral spreading of the spots.

The 2-D fractionation of human serum was studied in considerable detail. An interesting experiment is shown in Fig. 29. When the sample is treated in different ways before the IPG run, different patterns result. Of special interest is the amount of material precipitated at the application point. This appears minimal if the sample is simply diluted with 1–2 vol. of distilled water (dilution increases the migration from the application point, but the effect levels off at 1:2–1:3 ratios). To a lesser extent, elution is effective if the sample is added with 2ME immediately before use. Incubation of the reduced sample at room temperature results in massive precipitation of the proteins (the supernatant after 2 h is analyzed, Fig. 29, panel 2); the material left at the application point when the sample contains 2ME is likely to result from the early stages of such a process. Contrary to expectations, the poorest recovery is obtained in the presence of SDS, a widely used additive and highly effective solubilizing agent (Fig. 29, panel 7).

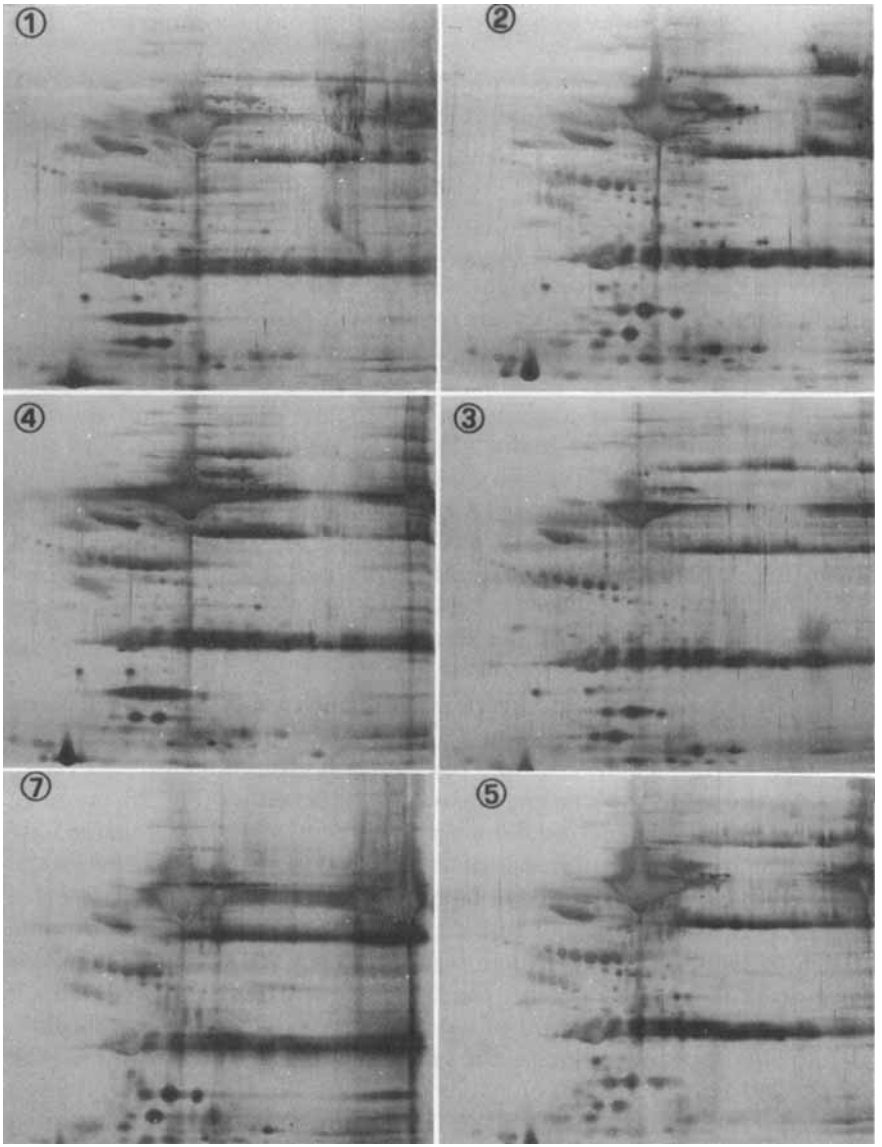

Fig. 29. Effect of sample pretreatment on the 2-D pattern of human serum. The sample (in all cases, a value corresponding to 1.5 μl of straight serum) was run on a nonlinear 4–10 IPG gel, equilibrated in 8 *M* urea. The second dimension was run on a 7.5–17.5% polyacrylamide gel gradient, with the discontinuous buffer system of Laemmli (1970). Silver stain according to Guevara et al. (1982a). The samples were pretreated as follows: (1) no additives; (2) with 2-ME just prior to the run; (3) incubated with 2-ME 2 h at room temperature and centrifuged; (4) added with urea to 8 *M* final concentration and incubated 2 h at room temperature; (5) added with 8 *M* urea, 2-ME and incubated 2 h at room temperature; (7) added with 2-ME and 2% SDS and incubated for 5 min at room temperature. (From Gianazza et al., 1985c. Reproduced with permission of the publisher.)

X. CONCLUSIONS

An attempt has been made to provide a broad view of what is very likely to be a technique of great importance. Owing to the extensive developments in the last two years, the IPG technique has had an extraordinary growth. In fact both its analytical and preparative aspects have already reached a considerable state of development and can now be used extensively. A highly porous matrix would be extremely useful, but it might take years of work to develop a practical one. At the moment the "soft" (highly diluted) polyacrylamide gels we have described will partially alleviate the problem.

We have not reviewed applications of IPGS. There are only a few now, but they can be expected to increase rapidly as the technique described is already in use in at least 50 other laboratories around the world.

Acknowledgments

This study was supported in part by a grant from Progetto Finalizzato "Chimica Fine e Secondaria," Tematica "Tecnologie di Supporto," from Consiglio Nazionale delle Ricerche (CNR, Roma). We are happy to mention friends and colleagues in Milan who have contributed to this project: Prof. F. Celentano, the late Dr. G. Dossi, Drs. C. Gelfi and P. Casero and two students in our laboratory, Misses S. Astrua-Testori and P. Giacon, who are developing 2-D maps as part of their Ph.D. dissertations. To colleagues abroad, Dr. B. Bjellqvist, Mrs. K. Ek (Bromma, Sweden), Dr. A. Görg (Munich, GFR), and Dr. K. Altland (Giessen, GFR) go our thanks for collaborations and for providing figures and material for the text.

Abbreviations and Symbols

Bis = N,N′-methylene bisacrylamide;
β = buffering power;
IEF = isoelectric focusing;
2-D = two-dimensional;
IPG = immobilized pH gradients;
ISO-DALT (or IPG-DALT) = 2-D maps developed by charge (isoelectric focusing) coupled ot mass (SDS electrophoresis) fractionation;
2ME = 2-mercaptoethanol;
mequiv. = milli equivalents;
μ, *I* = ionic strength;
NAB-IEF = nonamphoteric buffer isoelectric focusing;
PAGE = polyacrylamide gel electrophoresis;
p*I* = isoelectric point;
SDS = sodium dodecyl sulphate;
TEMED = *N*,*N*,*N*′,*N*′-tetramethyl ethylen diamine.

References

Altland, K., and Kaempfer, M. (1980), *Electrophoresis, 1*, 57–62.

Altland, K., and Altland, A. (1984), *Electrophoresis, 5*, 143–147.

Bartels, R., and Bock, L. (1984), in *Electrophoresis '84* (V. Neuhoff, ed.), Verlag Chemie, Weinheim, pp. 103–106.

Bernardi, G. (1971), in *Methods in Enzymology*, Academic Press, New York, Vol. 21, part D, pp. 95–140.

Bier, M., Mosher, R. A., Thormann, W., and Graham, A. (1984), in *Electrophoresis '83* (H. Hirai, ed.), de Gruyter, Berlin, pp. 99–107.

Bjellqvist, B., Ek, K., Righetti, P. G., Gianazza, E., Görg, A., Westermeier, R., and Postel, W. (1982), *J. Biochem. Biophys. Methods, 6*, 317–339.

Bjellqvist, B., Ek, K., Righetti, P. G., Gianazza, E., Görg, A., and Postel, W. (1983), in *Electrophoresis '82* (D. Stathakos, ed.), de Gruyter, Berlin, pp. 61–74.

Bos, E. S., Van Der Doelen, A. A., Van Der Struik, E., Bergink, E. W., and Schuurs, A. H. W. M. (1984), in *Electrophoresis '84* (V Neuhoff, ed.), Verlag Chemie, Weinheim, p. 93.

Brown, R. K., Caspers, M. L., Lull, J. M., Vinogradov, S. N., Felgenhauer, K., and Nekic, M. (1977), *J. Chromatogr., 131*, 223–232.

Casero, P., Gelfi, C., and Righetti, P. G. (1985), *Electrophoresis, 6*, 59–69.

Celis, J. A., and Bravo, R. eds. (1984a), *Two Dimensional Gel Electrophoresis of Proteins: Methods and Applications*, Academic Press, New York.

Celis, J. E., and Bravo, R. (1984b), in *Electrophoresis '84* (V. Neuhoff, ed.), Verlag Chemie, Weinheim, pp. 205–225.

Chrambach, A., and Hjelmeland, L. M. (1984), in *Electrophoresis '83*, (H. Hirai, ed.), de Gruyter, Berlin, pp. 81–97.

Cleve, H., Patutschnick, W., Postel, W., Weser, J., and Görg, A. (1982), *Electrophoresis, 3*, 342–345.

Davidson, J. B. (1984), in *Electrophoresis '84* (V. Neuhoff, ed.), Verlag Chemie, Weinheim, pp. 235–251.

Debye, P., and Hückel, E. (1924), *Physik, Z., 24*, 305–330.

Delincée, H., and Radola, B. J. (1978), *Anal. Biochem., 90*, 609–623.

Dossi, G., Celentano, F., Gianazza, E., and Righetti, P. G (1983), *J. Biochem. Biophys. Methods, 7*, 123–142.

Dunn, M. J., and Burghess, A. H. M. (1983a), *Electrophoresis, 4*, 97–116.

Dunn, M. J., and Burghess, A. H. M. (1983b), *Electrophoresis, 4*, 173–189.

Ek, K., Bjellqvist, B., and Righetti, P. G. (1983), *J. Biochem. Biophys. Methods, 8*, 134–155.

Gelfi, C., and Righetti, P. G. (1981a), *Electrophoresis, 2*, 213–219.

Gelfi, C., and Righetti, P. G. (1981b), *Electrophoresis, 2*, 220–228.

Gelfi, C., and Righetti, P. G. (1983), *J. Biochem. Biophys. Methods, 8*, 156–171.

Gelfi, C., and Righetti, P. G. (1984), *Electrophoresis, 5*, 257–262.

Gianazza, E., and Righetti, P. G. (1980), *J. Chromatogr., 193*, 1–8.

Gianazza, E., Dossi, G., Celentano, F., and Righetti, P. G. (1983a), *J. Biochem. Biophys. Methods, 8*, 109–133.

Gianazza, E., Artoni, F., and Righetti, P. G. (1983b), *Electrophoresis, 4*, 321–326.

Gianazza, E., Celentano, F., Dossi, G., Bjellqvist, B., and Righetti, P. G. (1984a), *Electrophoresis*, *5*, 88–97.

Gianazza, E., Frigerio, A., Tagliabue, A., and Righetti, P. G. (1984b), *Electrophoresis*, *5*, 209–216.

Gianazza, E., Astrua-Testori, S., and Righetti, P. G. (1985a), *Electrophoresis*, *6*, 113–117.

Gianazza, E., Giacon, P., Sahlin, B., and Righetti, P. G. (1985b), *Electrophoresis*, *6*, 53–56.

Gianazza, E., Astrua-Testori, S., Giacon, P., and Righetti, P. G. (1985c) *Electrophoresis*, *6*, 332–339.

Görg, A., Postel, W., and Westermeier, R. (1978), *Anal. Biochem.*, *89*, 60–70.

Görg, A., Weser, J., Westermeier, R., Postel, W., Weidinger, S., Patutschnick, W., and Cleve, H. (1983a), *Human Genet.*, *64*, 222–226.

Görg, A., Postel, W., Weser, J., Weidinger, S., Patutschnich, S., and Cleve, H. (1983b), *Electrophoresis*, *4*, 153–157.

Görg, A., Postel, W., and Johann, P. (1985), *J. Biochem. Biophys. Methods*, *10*, 341–350.

Gronwall, A. (1942), *C. R. Trav. Lab. Carlsberg, Ser. Chim.*, *24*, 185–195.

Guevara, J., Jr., Johnston, D. A., Ramagli, L. S., Martin, B. A., Capetillo, S., and Rodriguez, L. W. (1982a) *Electrophoresis*, *4*, 197–200.

Guevara, J., Jr., Chiocca, E. A., Clayton, F. C., von Eschenbach, A. C., and Edwards, J. J. (1982b), *Clin. Chem.*, *28*, 756–758.

Haglund, H. (1971), in *Methods of Biochemical Analysis* (D. Glick, ed.), Wiley-Interscience, New York, pp. 1–104.

Klose, J. (1984), in *Electrophoresis '84* (V. Neuhoff, ed.), Verlag Chemie, Weinheim, pp. 179–189.

Kolin, A. (1958), in *Methods of Biochemical Analysis* (D. Glick, ed.), Wiley-Interscience, New York, pp. 259–288.

Kolin, A. (1977), in *Electrofocusing and Isotachophoresis* (B. J. Radola, and D. Graesslin, eds.), de Gruyter, Berlin, pp. 3–33.

Låås, T., and Olsson, I. (1981), *Anal. Biochem.*, *114*, 167–168.

Laemmli, U. K. (1970), *Nature*, *227*, 680–683.

Miller, M. J., and Olson, A. D. (1984), in *Electrophoresis '84* (V. Neuhoff, ed.), Verlag Chemie, Weinheim, pp. 226–234.

Pietta, P., Pocaterra, E., Fiorino, A., Gianazza, E., and Righetti, P. G. (1985), *Electrophoresis*, *6*, 162–170.

Righetti, P. G., and Caravaggio, T. (1976), *J. Chromatogr.*, *127*, 1–28.

Righetti, P. G. (1980), *J. Chromatogr.*, *190*, 275–282.

Righetti, P. G., Tudor, G., and Ek, K. (1981a), *J. Chromatogr.*, *220*, 115–194.

Righetti, P. G., Gelfi, C., and Bianchi Bosisio, A. (1981b), *Electrophoresis*, *2*, 291–295.

Righetti, P. G., Tudor, G., and Gianazza, E. (1982), *J. Biochem. Biophys. Methods*, *6*, 219–227.

Righetti, P. G., (1983a), *Isoelectric Focusing: Theory, Methodology and Applications*, Elsevier, Amsterdam.

Righetti, P. G. (1983b), *Trends Anal. Chem.*, *2*, 193–196.

Righetti, P. G., Gianazza, E., and Bjellqvist, B. (1983a), *J. Biochem. Biophys. Methods*, *8*, 89–108.

Righetti, P. G., Delpech, M., Moisand, F., Kruh, J., and Labie, D. (1983b), *Electrophoresis, 4*, 393–398.

Righetti, P. G., Gianazza, E., Bjellqvist, B., Ek, K., Görg, A., and Westermeier, R. (1983c), in *Electrophoresis '83* (D. Stathakos, ed.), de Gruyter, Berlin, pp. 75–82.

Righetti, P. G. (1984), *J. Chromatogr., 300*, 165–223.

Righetti, P. G., and Gelfi, C. (1984), *J. Biochem. Biophys. Methods, 9*, 103–119.

Righetti, P. G., Ek, K., and Bjellqvist, B. (1984a), *J. Chromatogr., 291*, 31–42.

Righetti, P. G., Gianazza, E., and Gelfi, C. (1984b), in *Electrophoresis '84* (V. Neuhoff, ed.), Verlag Chemie, Weinheim, pp. 29–48.

Righetti, P. G., and Gianazza, E. (1985), *J. Chromatogr*, 334, 71–82.

Rilbe, H. (1978), *J. Chromatogr., 159*, 193–205.

Rochette, J., Righetti, P. G., Bianchi Bosisio, A., Vertongen, F., Schneck, G., Boissel, J. P., Labie, D., and Wajcman, H. (1984). *J. Chromatogr., 285*, 143–152.

Schumacher, E. (1957) *Helv. Chim. Acta, 40*, 221–228.

Svensson, H. (1961), *Acta Chem. Scand., 15*, 325–341.

Svensson, H. (1962), *Acta Chem. Scand., 16*, 456–466.

Tracy, R. P., Katzmann, J. A. and Young, D. S. (1984), in *Electrophoresis '84* (V. Neuhoff, ed.), Verlag Chemie, Weinheim, pp. 190–204.

Vesterberg, O. (1969), *Acta Chem. Scand., 23*, 2653–2666.

Westermeier, R., Postel, W., Weser, J., and Görg, A. (1983), *J. Biochem. Biophys. Methods, 8*, 321–330.

Ziola, B. R., and Scraba, D. G. (1976), *Anal. Biochem., 72*, 366–371.

Methods of Biochemical Analysis, Volume 32
Edited by David Glick
Copyright © 1987 by John Wiley & Sons, Inc.

METHODS OF BIOCHEMICAL ANALYSIS VOLUME 32

Assays for Superoxide Dismutase

JOE V. BANNISTER, *Biotechnology Centre, Cranfield Institute of Technology, Cranfield, Bedfordshire, England*
AND LILIA CALABRESE, *Institute of Biological Chemistry and CNR Centre for Molecular Biology, University of Rome, Rome, Italy*

I. GENERAL INTRODUCTION

The enzyme superoxide dismutase (EC 1.15.1.1) is unique in that it has three isozymes whose only similarity is that they catalyze the same reaction:- $2O_2^- + 2H^+ \rightarrow H_2O_2 + O_2$. There are not only different forms present in eukaryotes and prokaryotes, but different forms are present in eukaryotic cells. The main important difference between the three isozymes is that they contain different metals as the prosthetic group (Bannister and Rotilio, 1984; Parker et al., 1984). The eukaryotic species have two forms that contain either copper and zinc or manganese, although certain plant species have been found to have the main form present in prokaryotic species which is the iron-containing enzyme (Salin and Bridges, 1981). Prokaryotic species have either the iron- or the manganese-containing enzyme, and in some cases they can have both forms. Two

bacterial species have been found to have copper/zinc enzyme (Puget and Michelson, 1974; Steinman, 1982), whereas algal species more primitive than algae, such as protozoans and *Euglena* species, contain only the iron or the manganese form of the enzyme.

The iron- and manganese-containing forms are considered to be one class of enzyme. The main reason for this is the identity of structure, although this has only so far been inferred from the *N*-terminal region. It is as yet not possible to do a complete comparison because, though complete amino acid sequences have been determined for four manganese-containing superoxide dismutases, no complete primary structure has yet been determined for an iron enzyme and also, though the X-ray structure has been determined for two iron-containing enzymes (Ringe et al., 1983; Stallings et al., 1983), no complete X-ray structure has been determined for a manganese-containing enzyme. However, preliminary crystallographic data on the manganese enzyme indicate that the manganese and iron superoxide dismutases are structural homologs (Stallings et al., 1984) and have identical amino acid ligands to the metals (Barra et al., 1985). It has also been found that the anaerobic prokaryote *Propionibacterium shermanii* can synthesize either the manganese- or iron-containing enzyme depending on the culture conditions and that either form synthesized appeared to be identical at the *N*-terminal region (Meier et al., 1982). It has also been shown that it is possible to substitute the iron with manganese without loss of activity in the superoxide dismutase isolated from *Bacteroides gracilis* (Gregory and Dapper, 1983).

The copper- and zinc-containing form of superoxide dismutase is, however, different from the manganese- or iron-containing form. This isozyme has been considered to be present in the cytosol of eukaryotes, and some evidence has been presented that it is in the intermembranous space of mitochondria. However, recent experimental evidence has indicated that the copper/zinc enzyme is also associated with the lysosomes (Geller and Winge, 1982). The identity of structure between the various eukaryotic copper/zinc superoxide dismutases is firmly established (Parker et al., 1984; Rocha et al., 1984). The presence of a copper/zinc superoxide dismutase in the free living bacterium *Caulobacter crescentus* (Steinman, 1982) is as yet an unexplained anomaly. However, the presence of this isozyme in *Photobacterium leiognathi* (Puget and Michelson, 1974) has been considered to be a case of gene transfer from eukaryotes to prokaryotes (Martin and Fridovich, 1981). This is because this bacterium, although found free-living, is also a symbiont of ponyfish (Haneda, 1950). However, whereas gene transfer among prokaryotes is a well-documented phenomenon as also transfer from prokaryotes to eukary-

otes, gene transfer from eurkaryotes to prokaryotes has never been clearly documented. The amino acid sequence of *Photobacterium leiognathi* copper/zinc superoxide dismutase was found to have a low identity with other eukaryotic superoxide dismutases (Steffens et al., 1983). Therefore the hypothesis of gene transfer was discarded, and an independent evolutionary line was suggested for the presence of the copper/zinc enzyme in a bacterial species. This idea continued to be plausible when the sequence for a fish copper/zinc superoxide dismutase was determined and also showed low identity with the bacterial enzyme (Rocha et al., 1984). However, the *Photobacterium leiognathi* enzyme has similar molecular weight, subunit size, metal content, and catalytic activity as the eukaryotic copper/zinc enzymes. The single disulfide bridge, the seven metal ligands, and the two residues shown to be important in the mechanism of the bovine erythrocyte enzyme are all found in the bacterial enzyme in the correct sequence order. Also a very similar secondary structure is predicted for the bacterial, swordfish liver and bovine erythrocyte enzymes (Parker et al., 1984). Finally, analysis of the aligned sequences showed that more than half of the bacterial polypeptide chain has closely related or identical residues with the swordfish liver enzyme after deletions and insertions are excluded (Bannister and Parker, 1985). Clearly the evidence for a likely case of gene transfer is overwhelming. The manganese enzyme in eukaryotes is present in the mitochondrial matrix. Mitochondria are known to concentrate very efficiently both iron and manganese (Williams, 1982). The selection of manganese in favor of iron as the prosthetic group is wholly unclear.

The convergent property of any of the three superoxide dismutases is their ability to undergo redox cycling with superoxide radicals, O_2^-:

$$E\text{-}Me^{(n+1)} + O_2^- \xrightarrow{k_1} E\text{-}Me^{(n)} + O_2$$

$$E\text{-}Me^{(n)} + O_2^- + 2H^+ \xrightarrow{k_2} E\text{-}Me^{(n+1)} + H_2O_2$$

where Me is the metal and n is the oxidation state. The net result of the reaction is O_2^- dismutation into O_2 and H_2O_2. The rate constants k_1 and k_2 are usually comparable and neither O_2 nor H_2O_2 can kinetically compete with O_2^- for reoxidation of the reduced metal. In the case of the copper- and zinc-containing superoxide dismutase, the active metal has been shown to be the copper and a structural role has been proposed for the zinc. The rate constants for the dismutase of O_2^- by the copper/zinc, iron and manganese superoxide dismutases were first determined by

Forman and Fridovich (1973) using an indirect assay whereby O_2^- was generated either by the action of xanthine oxidase on xanthine or by the mechanical infusion of potassium superoxide in tetrahydrofuran. The generated O_2^- was allowed to react with ferricytochrome c or with tetranitromethane and the product formation was monitored spectroscopically. Details of the two assays are given in Section II.3. Addition of superoxide dismutase inhibits the formation of products. A rate constant of $2 \times 10^9\ M^{-1}\text{sec}^{-1}$ was determined for all three enzymes. This value agreed with the rate constant determined by pulse radiolysis for the copper/zinc enzyme (Klug-Roth et al., 1973; Fielden et al., 1974). The mechanism of action of the superoxide dismutases has been investigated by the technique of pulse radiolysis which is described in Section II.2. The bovine erythrocyte copper/zinc enzyme is the most studied form as far as the molecular and catalytic properties are concerned (Rotilio and Fielden, 1984). Pulse radiolysis investigations (Klug-Roth et al., 1973; Fielden et al., 1974) have shown that the enzyme carries out a very simple redox cycle of its copper:

$$E\text{-Cu(II)} + O_2^- \rightarrow E\text{-Cu(I)} + O_2$$

$$E\text{-Cu(I)} + O_2^- \rightarrow E\text{-Cu(II)} + H_2O_2$$

The rates for the two reactions are identical with the rate of the overall reaction which is around $3.5 \times 10^9\ M^{-1}\text{sec}^{-1}$ which is close to the diffusion limit (Fielden et al.; 1974). The ping-pong scheme outlined here is made possible by the slow reactivity of the bound copper to other redox reagents in particular H_2O_2 and O_2 (Rigo and Rotilio, 1980).

Although the general features of the dismutation reaction are well known, a detailed mechanism remains to be firmly established. This can be achieved when further information is obtained on (1) the steady-state titration of the copper site and the related problem of the possible interaction of the copper sites on different subunits, (2) the actual formation of an inner sphere copper-superoxide complex, (3) the role of the protein backbone, and finally (4) the role of the zinc. These points have been dealt in some detail in a recent review by Fielden and Rotilio (1984).

The dismutation of O_2^- by iron superoxide dismutase was found to be similar to that for the copper/zinc bovine superoxide dismutase. The results obtained by Lavelle et al. (1977) showed that catalysis of dismutation of O_2^- by the iron superoxide dismutase from *Photobacterium leiognathi* is first order with respect to substrate concentration for all ratios of substrate to enzyme concentrations reported. Although the enzyme is stable between pH 6.0 and 10.0, the value of the rate constant decreases as the pH increases. The second-order rate constant for the reaction be-

tween the iron superoxide dismutase, and O_2^- was found to be $k = 5.5 \times 10^8\ M^{-1}\text{sec}^{-1}$ at pH 8.0. This is an order of magnitude less than the constant obtained for the copper/zinc enzyme. However, as with the copper/zinc enzyme, no evidence for substrate saturation was found. The iron superoxide dismutase from *Escherichia coli* was found to have a turnover rate constant at $3 \pm 1 \times 10^8\ \text{M}^{-1}\text{sec}^{-1}$ at pH 7.4 (Fee et al., 1981). These investigations indicate that the iron redoxes in a similar way to the copper in the bovine erythrocyte copper/zinc enzyme:

$$\text{Fe(III) enzyme} + O_2^- \rightarrow \text{Fe(II) enzyme} + O_2$$

$$\text{Fe(II) enzyme} + O_2^- \xrightarrow{2H^+} \text{Fe(III) enzyme} + H_2O_2$$

This mechanism may not, however, be applicable to all the iron superoxide dismutases. This is because the iron enzyme from *E. coli* was found to exhibit saturation kinetics (Fee et al., 1981).

In contrast the manganese superoxide dismutase appears to exhibit complex kinetics. The simple scheme of one electron reduction and oxidation of the metal appears not to be applicable. Pick et al. (1974) investigating the manganese superoxide dismutase from *E. coli* suggested that not two but four oxidation-reduction reactions are involved and that each reaction is characterized by a different second-rate constant:

$$E + O_2^- \rightarrow E^- + O_2 \qquad k = 1.3 \pm 0.15 \times 10^9\ M^{-1}\text{sec}^{-1}$$

or (1)

$$(E + O_2^- + 2H^+ \rightarrow E^+ + H_2O_2)$$

$$E^- + O_2^- + 2H^+ \rightarrow E + H_2O_2 \qquad k = 1.68 \pm 0.6 \times 10^9\ M^{-1}\text{sec}^{-1}$$

or (2)

$$(E^+ + O_2^- \rightarrow E + O_2)$$

$$E^- + O_2^- \rightarrow E^{2-} + O_2 \qquad k \simeq 2 \times 10^8\ M^{-1}\text{sec}^{-1}$$

or (3)

$$(E + O_2^- \rightarrow E^- + O_2)$$

$$E^{2-} + O_2^- + 2H^+ \rightarrow E^- + H_2O_2 \qquad k \simeq 1 \times 10^{-1}\ M^{-1}\text{sec}^{-1}$$

or (4)

$$(E^- + O_2^- + 2H^+ \rightarrow E + H_2O_2)$$

where E^+, E, E^-, and E^{2-} may represent forms of the enzyme in which manganese (IV), manganese (III), manganese (II), and manganese (I) are, respectively, present. Three different oxidation states for the manganese are postulated in this mechanism and the apparent rate constant was found to be $1.5 \pm 0.15 \times 10^9\ M^{-1}\text{sec}^{-1}$ at pH 7.9. The reaction mechanism of manganese superoxide dismutase from *Bacillus stearothermophilus*

was also investigated by pulse radiolysis (McAdam et al., 1977a, b). A similar fast and slow reaction as that reported for the *E. coli* enzyme was also observed. McAdam et al. (1977b), however, suggested a different mechanism for the enzyme. They suggested a rapid one-electron oxidation-reduction cycle (the fast cycle) and concurrently a slower reaction giving a form of the enzyme that is essentially unreactive toward O_2^- but undergoes first-order decay to yield a fully active native enzyme (the slow cycle):

$$E_A + O_2^- \rightarrow E_B + O_2 \qquad k_1$$

$$E_B + O_2^- \xrightarrow{2H^+} E_A + H_2O_2 \qquad k_2$$

$$E_B + O_2^- \rightarrow E_c \qquad k_3$$

$$E_c \rightarrow E_A$$

Pulse radiolysis investigation of the manganese superoxide dismutase for *B. stearothermophilus* under conditions of low substrate to enzyme concentration (when the fast cycle predominates) showed that the enzyme activity decreases as the pH is increased from 6.5 to 10.2. The second-order rate constant at pH 8.0 was found to be $6.0 \times 10^8\ M^{-1}\text{sec}^{-1}$. The explanation as to why two pathways are present has been given by Sawyer and Valentine (1981), using an earlier observation of Howie and Sawyer (1976) that his (8-quinolato) manganese(II) complex is an effective catalyst for the disproportionation of O_2^- in aprotic media. The mechanism involves an manganese(III)-peroxide intermediate that oxidizes a second O_2^- to yield H_2O_2 and O_2 plus the original manganese(III)-enzyme:

$$M_{ox} + O_2^- \rightarrow [M_{ox}-O_2]^{2+}$$

$$[M_{ox}-O_2]^{2+} + O_2^- \xrightarrow{2H+} M_{ox} + O_2 + H_2O_2$$

This scheme has been proposed for the manganese superoxide dismutase from *Paracoccus denitrificans* (Teresch et al., 1983). This enzyme has been shown to exhibit saturation behavior by pulse radiolysis.

The best way of distinguishing between the various superoxide dismutases is to isolate the protein and characterize the metal present. However, it is also possible that the isozyme present can be identified in crude extracts. This is because each isozyme has been found to have a particular characteristic sensitivity toward a number of reagents. Cyanide was found to inhibit the copper/zinc superoxide dismutase but not the manganese superoxide dismutase (Weisiger and Freidovich, 1973; Kanematsu and Asada, 1978). Furthermore the product of the dismutation reaction, hydrogen peroxide, inactivates both the copper/zinc and iron but not the manganese-containing enzyme (Symonyan and

Nalbandyan, 1982; Hodgson and Fridovich, 1975; Asada et al., 1975), whereas azide inhibits the enzymes in the following order iron > manganese > copper/zinc superoxide dismutase (Misra and Fridovich, 1978). Diethyldithiocarbamate is another well-characterized inhibitor of the copper/zinc superoxide dismutase (Heikkila et al., 1977). It forms a complex with the copper and removes the metal from all the protein ligands. The copper-diethyldithiocarbamate complex can be separated without affecting the zinc content of the protein (Cocco et al., 1981).

With these methods it is therefore possible to distinguish between the various forms of superoxide dismutases. Asada et al. (1980) have extensively used this behavior of the three forms of the enzyme to distinguish which isozyme is present in a variety of plant and animal species. Other methods also based on selective inhibition have been applied. Geller and Winge (1983) treated crude extracts from eukaryotic species with 2% sodium lauryl sulphate at 37°C for 30 min. This treatment selectivity inactivates the mitochondrial manganese superoxide dismutase without affecting the copper/zinc activity; Kirby et al. (1980), on the other hand, applied the use of guanidine hydrochloride at low pH as a method for distinguishing between the manganese and iron superoxide dismutases. In this method apo enzymes are produced, and it was assumed that reactivation will only be carried out by the metal characteristic of the native enzyme. Therefore in crude extracts of prokaryotes, which may contain the iron or manganese isozyme, or both together, resolution can be obtained by treatment with iron(II) or manganese(II), or both, following inactivation with guanidine hydrochloride. Kirby et al. (1980) considered that it would be improbable that the apoenzyme would be reactivated by a metal other than that found in the native state. This is, however, now very debatable as Gregory and Dapper (1983) have been able to substitute manganese for iron without loss of activity in *Bacteroides gracilis* and the manganese and iron enzymes have been shown to have the same ligands to the protein (Barra et al., 1985).

All the inhibitions reported so far indicate that there is no known specific inhibitor for the manganese superoxide dismutase. The enzyme from *B. stearothermophilus* was found to be inhibited by cacodylate (Thornalley et al., 1982); however, the inhibition could only be observed in the xanthine/xanthine oxidase assay and not in the pulse radiolysis assay. No evidence was obtained that cacodylate could be competing with the enzyme for O_2^- because little or no inhibition was observed when the copper/zinc rather than the manganese enzyme was assayed in the presence of cacodylate. Further investigations revealed that the inhibitory effect is due to a cacodylate anion radical produced by the interaction of hydroxyl radicals (generated by the xanthine/xanthine oxidase reaction) and cacodylate anions. A radical of pamoic acid (4,4′-methylenebis-(3-

hydroxy-2-naphtoic acid)) was also found to be the cause of the observed inhibition of the copper/zinc superoxide dismutase (Hassan et al., 1980). In this case the pamoic acid did not inhibit the enzyme but decreased the sensitivity of the assays because it competed with the enzyme for the substrate.

II. ASSAYS FOR SUPEROXIDE DISMUTASE

1. Introduction

Enzyme activity measurements are usually based on the disappearance of the substrates or the appearance of products. The dismutation reaction

$$2O_2^- + 2H^+ \rightarrow H_2O_2 + O_2$$

is not easily followed by these criteria. The greatest complication arises from the nature of the substrate, the superoxide radical, O_2^-. The substrate is an unstable free radical which will spontaneously dismute. Also its lifetime is drastically shortened by transition metal ion catalysts that may be present in the reaction medium. Consequently the direct measurement of the disappearance of O_2^- often requires the use of sophisticated equipment that may not be present in all laboratories. They are therefore more useful for elucidating the mechanism of the reaction. However, a number of assays have been developed over the last 15 years since the discovery by McCord and Fridovich in 1969 that bovine erythrocuprein was in fact superoxide dismutase. All these assays have enabled not only the determination of the enzyme activity but also the concentration of the enzyme from a comparison of the activity with that of a pure enzyme. These assays have also been extensively used for the determination of which form of superoxide dismutase is present in cell extracts. In these assays, O_2^- can be generated enzymatically or nonenzymatically in the test medium which also contains an indicator that reacts with O_2^-. The reaction of the indicator with O_2^- is followed by a suitable method, generally spectrophotometrically. This type of assay is classified as an indirect negative assay and usually it records negative measurements, that is, the inhibition by superoxide dismutase of the spectrophotometrically measurable product resulting from the interaction between indicator and O_2^-. In only one case has an indirect assay resulted in positive measurements. This is the so-called dianisidine assay. Superoxide dismutase has been found to augment the formation of products. Indirect assays offer many advantages compared with direct methods for O_2^-; they do not require specialized equipment and are very sensitive. The scavengers that

trap O_2^- are used at concentrations that effectively compete with the dismutation reaction so that virtually all the O_2^- produced can be trapped and detected. Although direct assays of superoxide dismutase must be performed in the presence of ca. 10^{-5} *M* superoxide, indirect methods can be performed at steady-state levels of O_2^- in the range of $10^{-8}-10^{-13}$ *M* superoxide. The lower concentration will favor the enzyme in the competition for the dismutation reaction. The best-known direct and indirect assays are described in this section. Both forms of assays will indicate the activity of superoxide dismutase. They do not distinguish which form is being assayed. When more than one form of enzyme is present in the extract to be assayed, it is generally the case for the total superoxide dismutase activity to be determined and then the activity in the presence of a specific inhibitor. For tissue homogenates, cyanide is added to inhibit the copper/zinc enzyme activity and the activity determined is then that of the manganese enzyme. The copper/zinc enzyme activity is obtained by subtracting the manganese enzyme activity from the total activity. In the case of bacterial homogenates, the iron superoxide dismutase is inhibited by hydrogen peroxide and the activity determined is given that of the manganese enzyme. The iron superoxide dismutase activity is then obtained by subtracting the manganese enzyme activity from the total activity.

2. Direct Methods of Assaying for Superoxide Dismutase

There are two physical properties of O_2^- that can be used for its detection, paramagnetism, and ultraviolet absorption. Since the electron paramagnetic signal (epr) signal of O_2^- is not detectable at room temperature, direct assays are mostly based on the optical properties of O_2^-, which absorbs light maximally in the 240–260 nm range. The direct assays require a high enough concentration of O_2^- to be observed directly at around 250 nm, where the radical has a molar extinction coefficient of 2000. The simplest direct assay was described by Marklund (1976). Superoxide was generated from its potassium salt at alkaline pH where its stability increases. The decay at 250 nm in the presence and absence of superoxide dismutase is measured in a standard spectrophotometer. The assay is carried out in such a way that the rate of a decay in the presence of the enzyme is within the time response of the apparatus (Fig. 1). One unit of activity is arbitrarily taken as the enzyme activity that results in the dismutation of O_2^- at a rate of $0.1 sec^{-1}$. This rate of dismutation corresponds to 5.5 ng bovine copper/zinc superoxide dismutase and to 64.5 ng bovine manganese superoxide dismutase under the conditions described by Marklund (1976). The rate constants calculated for both enzymes were

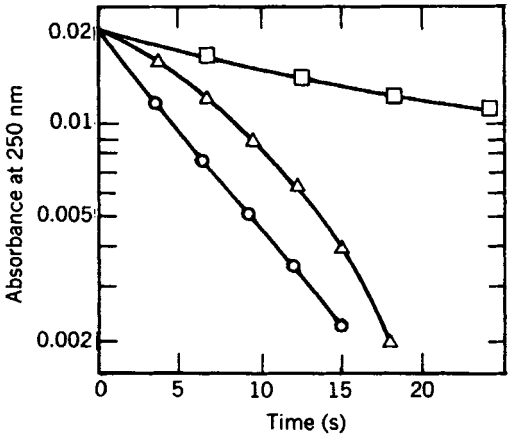

Fig. 1. The effect of cuprozinc and manganosuperoxide dismutase on the disproportionation of O_2^-. O_2^- stock solution was added to 50 m*M* 2-amino-2-methyl-1-propanol HCl, pH 9.5, + 0.2 m*M* diethylenetriamine pentaacetic acid + 100 n*M* catalase. The decay in A_{250} was followed in the absence and presence of superoxide dismutase: (□) spontaneous reaction; (○) 85 pM human cuprozinc superoxide dismutase; (△) 350 pM bovine manganosuperoxide dismutase. (Reprinted with permission from S. Marklund, *J. Biol. Chem.*, *251*, 7504–7507, 1976.)

found to be in agreement with the pulse radiolysis rate constants. Pure enzymes can be assayed by this method with high accuracy; however, crude solutions obtained from tissue homogenates and bacterial extracts can cause problems because of the high absorbance of the extracts in the ultraviolet region.

The generation of O_2^- from potassium superoxide was also applied to stop-flow procedures. In this method O_2^- was dissolved in dimethyl sulfoxide and stabilized in 18-crown-6-polyether. This method is useful for mechanistic studies; indeed, McClune and Fee (1976) were able to obtain catalytic rate constants for bovine copper/zinc superoxide dismutase as a function of pH in various buffers. More recently the mechanism of catalysis and of anion inhibition of iron superoxide dismutase from *E. coli* have been examined by this method using a specially constructed stop-flow spectrophotometer (Bull and Fee, 1985). A limitation of the method is that the pre-equilibrium state cannot be properly investigated because of the time resolution of the stop-flow equipment ($\simeq$ 5 msec).

The most important direct assay utilizes the technique of pulse radiolysis. Detailed studies on the mechanism of the three isozymes have been carried out using this technique (Klug-Roth et al., 1973; Fielden et

al., 1974, Pick et al., 1974; McAdam et al., 1977a, 1977b; Lavelle et al., 1977; Fee et al., 1981; Terech et al., 1983). Several accounts of pulse radiolysis equipment are documented in the literature (Willson, 1977). The technique can simply be described as the high energy analogue of flash photolysis where the flash lamp is replaced by a pulsed radiation source such as linear accelerator. The radiation pulse is of sufficiently high energy and intensity to generate radicals in detectable concentrations and the pulse length must be short (approx. 1 μsec or less) relative to the lifetime of the radicals under study. Absorption spectroscopy is used to detect the radicals formed since these absorb at wavelengths different from those of the compounds from which they are derived. An outline of the pulse radiolysis equipment in use at Brunel University, Uxbridge, Middlesex, England, is shown in Fig. 2. Superoxide radicals can be generated in the reaction mixture by a single pulse of ionizing radiation usually electrons in the 2–10 MeV range. The duration of the radiation pulse is in the range 10^{-8} to 10^{-6} secs. When the electron beam is passed through water it is absorbed, and a number of molecules are ionized:

$$H_2O \rightarrow OH\cdot, \quad e^-_{aq}, \quad H, \quad H_2, \quad H_2O_2$$

In the presence of an oxygenated solution and 100 m*M* formate or ethanol, the hydroxyl radical and the other reducing species are rapidly converted into superoxide radicals:

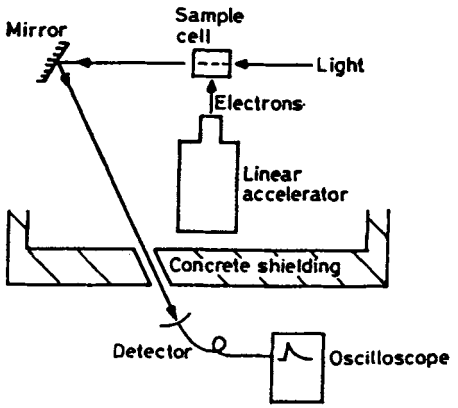

Fig. 2. Plan of pulse radiolysis equipment at Brunel University. (Reprinted with permission from R. L. Willson, *Chemistry and Industry*, *5*, 183–193, 1977.)

$$OH\cdot + HCOO^- \rightarrow H_2O + COO\cdot^-$$

$$COO\cdot^- \xrightarrow{O_2} O_2^- + CO_2$$

$$OH\cdot + CH_3CH_2OH \rightarrow H_2O + CH_3\dot{C}HOH$$

$$CH_3\dot{C}HOH \xrightarrow{O_2} CH_3\dot{C}HO_2OH$$

$$OH\cdot + CH_3CH_2OH \rightarrow H^+ + CH_3CHO + O_2^-$$

$$e^-_{aq} + O_2 \rightarrow O_2^-$$

$$H + O_2^- \rightarrow HO_2^- \rightleftharpoons O_2^- + H^+$$

All these reactions are rapid and a maximum concentration of O_2^- is reached within 5 μsec of the radiation pulse. The decay of O_2^- is followed spectrophotometrically at around 250 nm. The time resolution of pulse radiolysis is very high, and reaction times as short as 2×10^{-9} sec can be easily followed. In common with the direct assays that utilize the ultraviolet absorption of O_2^-, the problem of sample absorption in this region arises. Also the maximum single pulse yield of O_2^- (ca. 200 μ*M*) is less than that obtained from a solution of potassium superoxide. However, the technique has proved extremely useful for working with pure enzymes. The mechanisms decribed in Section I have all been obtained by this technique.

Another direct assay method is based on decay kinetics of pulse generated O_2^- (Takahashi and Asada, 1981). Superoxide was produced within 10 msec by a flash of light through the excitation of flavin mononucleotide in the presence of *N*,*N*,*N*′,*N*′-tetramethylethylenediamine and oxygen. The kinetics of O_2^- decay in the presence and absence of enzyme were followed at 240 nm. The catalytic rate constant for bovine erythrocyte copper/zinc superoxide dismutase was found to be $1.75 \times 10^9\ M^{-1}\text{sec}^{-1}$ in agreement with the pulse radiolysis determined rate constant.

Superoxide radical contains one unpaired electron (Neuman 1934) giving rise to an electron paramagnetic resonance (epr) spectrum that is unique and can be extracted even from a complicated set of overlapping signals (Knowles et al., 1969). Indeed, epr was used to furnish the most unequivocal evidence for one electron reduction of oxygen in biological systems (Bray et al., 1968, Nilsson et al., 1969, Orme-Johnson and Beinert, 1969). In frozen aqueous solutions at temperatures below 220°K, the radical exhibits an axial type of epr signal with a relatively broad g_{11} component with $g_{11} \simeq 2.1$. The signal parameters are sensitive to solvent and large variations are observed in the presence of alkaline metals, especially calcium, which affect the kinetic stability (Bray et al., 1977).

Unfortunately the epr spectrum of O_2^-, owing to fast relaxation, is well resolved only at low temperatures. As the temperature is raised the spectrum begins to broaden and is not observable in aqueous solutions at room temperature. This behavior negates any possibility of direct kinetic studies on samples under physiological conditions. However, O_2^- lifetime is such that it can be trapped by the rapid freezing method (Bray, 1961) and so studied in the frozen state.

Rapid freeze epr can be used as a direct assay of superoxide dismutase, as described in the earlier work by Ballou et al., (1969) who studied the effect of superoxide dismutase on the decay of the signal of O_2^-. Superoxide was trapped by rapid freezing during the reaction with oxygen of anaerobically reduced tetraacetyl riboflavin. The O_2^- available for reaction with superoxide dismutase was ca. 10^{-5} *M*, and under these experimental conditions, it was possible to estimate that the turnover rate number of superoxide dismutase was at least 3×10^6 min^{-1}. As a consequence of the difficulty inherent in the method, rapid freeze epr has not resulted in routine assay of superoxide dismutase. It has been used in a different approach for mechanistic studies (Fielden et al., 1974). In this case O_2^- was generated by pulse radiolysis, and the valence state of the enzyme estimated by epr.

Direct methods of assaying for superoxide dismutase have also been applied to the measurement of products. Superoxide dismutase like catalase can be assayed polarographically because the product of the reaction is molecular oxygen. Oxygen can be measured electrochemically with a variety of electrodes. However, a peculiar property of the electrodes used for polarographic assays of superoxide dismutases is that they are able to produce convenient amounts of O_2^- besides being sensitive to oxygen concentration. The electrodes are specifically modified to afford for the presence at the electrode surface of sufficiently high steady-state concentrations of O_2^- during the process of electroreduction of oxygen in aqueous solution. Rigo et al. (1975a) described a dropping mercury electrode that, when coated by a surfactant, was a very convenient source of millimolar concentrations of O_2^-. Although its sensitivity was very high (10^{-11} *M* enzyme could be assayed), it could only be utilized at pH values ≥ 10. Argese et al. (1983) found that the enzyme could also be assayed electrochemically by utilizing an appropriately modified rotating-disk electrode. Enzyme assays could, with this type of electrode, be carried out at neutral pH. The sensitivity was however found to be three orders of magnitude lower (10^{-8} *M* enzyme). Both methods are direct assays not limited by sample turbidity or high ultraviolet absorption. The rotating-disk electrode method is, however, not competitive in terms of sensitivity. It is therefore not suitable for assaying superoxide dismutase activity in

biological samples. It is particularly convenient for mechanistic studies of purified enzymes, especially the manganese and iron superoxide dismutases whose activities are pH sensitive, but also copper/zinc superoxide dismutases that show unusual pH dependence of activity (Argese et al., 1984). An additional advantage of the rotating-disk electrode method is its continuous and fast response, which permits monitoring of time-dependent process of the enzyme, such as inactivation, without repeated sampling as in a large interval of time (Argese et al., 1983).

The reduction of dioxygen in aqueous solution at the dropping of mercury electrode occurs according to the following mechanism (Kuta and Korita, 1965):

$$O_2 + e \rightarrow O_2^-$$
$$O_2^- + H_3O^+ \rightarrow HO_2^{\cdot} + H_2O$$
$$HO_2^{\cdot} + e \rightarrow HO_2^-$$
$$HO_2^- + H^+ \rightarrow H_2O_2$$

This is the proton catalyzed O_2^- dismutation which dominates the process if metal ion impurities are removed. When the dropping mercury electrode surface is covered by a monolayer of hydrophobic surfactant, such as α-quinoline or triphenylphosphine oxide, reduction to H_2O_2 is inhibited. The limiting current is controlled by the diffusion of oxygen to the electrode surface and is proportional to the O_2 concentration in solution. The addition of superoxide dismutase or lowering of the pH transforms, depending on the concentration of enzyme or H^+, the O_2^- present in the reaction layer into O_2 which, adding to the diffusive stream of O_2 from the solution to the electrode, will increase the cell current. When small aliquots of superoxide dismutase are added at a conveniently high pH (pH 9.8), small increments of current are obtained (Fig. 3). The full scale of current is set by obtaining complete dismutation of O_2^- through either addition of relatively concentrated enzyme ($\simeq 10^{-7}$ M in the cell) or by lowering the pH to the range 4–5. According to Rigo et al. (1975a), the superoxide dismutase concentration can be calculated from the Koutecky equation (Koutecky et al., 1953):

$$\left(7.42\,\frac{i}{i_d}\right) - \frac{7.42}{2.25} - 1.25\left(\frac{i}{i_d}\right) = KE \cdot tg$$

where i and i_d are the mean limiting current in the presence and absence of enzyme, respectively, E is the enzyme concentration, $K(M^{-1}\text{sec}^{-1})$ is the catalytic rate constant of the dismutation, and tg is the drop time of the

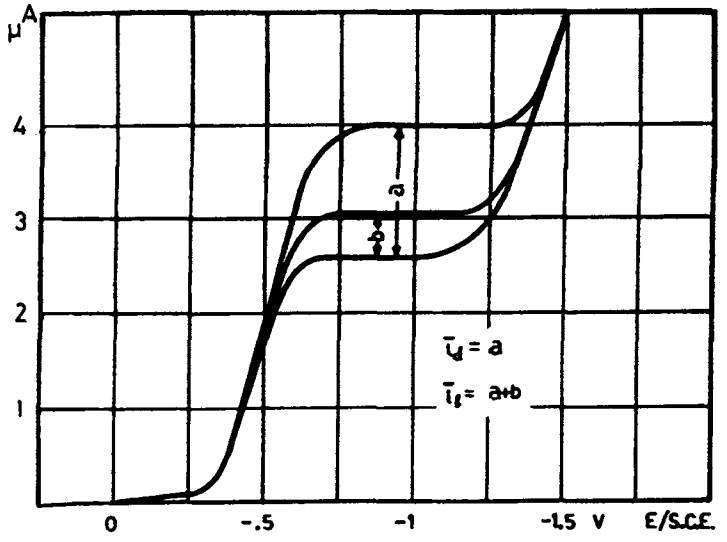

Fig. 3. Effect of concentration of bovine superoxide dismutase on oxygen wave at pH 9.76 in presence of triphenylphosphine oxide. (1) without superoxide dismutase; (2) superoxide dismutase = 1.4×10^{-9} *M*; (3) superoxide dismutase = 1.1×10^{-5} *M*. Air saturation sodium tetraborate 0.025 *M*; triphenylphoshine oxide 0.025% (wt.); pH = 9.76; temperature = 25°C, *tg* = 2.9sec *(a)* and *(a + b)* are, respectively, the diffusion and the limiting current relative to the fraction of O_2^- not spontaneously dismuted in the reaction layer. (Reprinted with permission from A. Rigo et al., *Electroanal. Chem. Interfac. Electrochem.*, *57*, 291–296, 1974.)

electrode (Fig. 4). From the slope of the plot and the drop time, the enzyme concentration can be calculated once *K* is known. This is obtained with pure enzyme under different conditions of inhibitors or denaturing agents or by varying the O_2^- concentration.

The method requires a three-electrode polarographic cell fitted with a dropping mercury electrode, a platinum counter electrode, and a saturated calomel electrode as reference. The apparatus is set at −1 V with *tg* = 3 sec. The polarographic solution is made up of 0.1 *M* borate buffer, pH 9.2; 5×10^{-4} *M* triphenylphosphine oxide and 5×10^{-4} *M* EDTA in a total volume of 4 ml. The solution is equilibrated with air. Suitable aliquots of the biological sample or purified enzyme under investigation are added 3–4 times to the polarographic solution in order to obtain a superoxide dismutase concentration in the range 10^{-11}–10^{-9} *M*. After each addition the cell current is recorded. The results are plotted according to the Koutecky equation. Small volumes, 1–50 μl of biological

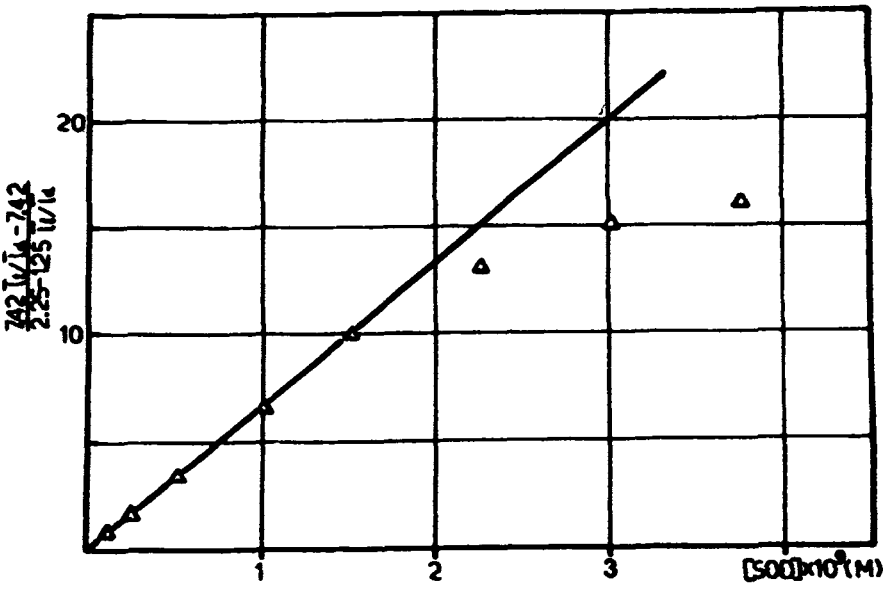

Fig. 4. Left side of Koutecky equation plotted versus the bovine superoxide dismutase concentration. Sodium tetraborate 0.025 *M*; triphenylphosphine oxide 0.025% (wt.); pH = 9.76; *tg* = 2.90sec; temperature = 25°C. (Reprinted with permission from A. Rigo et al., *Electroanal. Chem. Interfac. Electrochem.*, 57, 291–296, 1974.)

samples (2 μl of whole blood) are required for activity measurements. Blood plasma (0.1–0.2%) has to be added to the polarographic solution, in all cases except whole blood, to avoid the polarographic maximum which interferes with the determinations (Rigo and Rotilio, 1977). In the case of enzyme activity determinations the *K* value to be used to evaluate the enzyme concentration has to be standardized against the ionic strength of the polarographic solutions. This is necessary because the activity has been found to vary with the ionic strength (Rigo et al., 1975b). Measurements of the catalytic constant require subsequent additions of known concentrations of purified enzyme ($\simeq 3.5 \times 10^{-11}$ *M*) under various conditions. The method allows activity studies in the presence of urea, sodium lauryl sulfate, guanidine hydrochloride, and cyanide (Rigo et al., 1975a). Different O_2^- concentrations can be achieved by equilibrating the polarographic solution with N_2/O_2 mixtures (Rigo et al., 1975c).

In the rotating-disk method the thickness of the diffusion and reaction layers at the electrode surface is made less than at the dropping mercury electrode surface (Orsega et al., 1982). This reduces the extent of O_2^-

dismutation by H^+, thereby allowing considerable flow of O_2^- to be generated at pH values as low as 7.0. Besides this fundamental difference, the theoretical background and the operation procedure are the same as for the dropping mercury electrode method. A linear plot is obtained according to the following equation:

$$\left(\frac{i}{2i_d - i}\right)^2 = A + B\left(\frac{K}{\omega}\right)E$$

where i is the limiting current recorded under various conditions and $2i_d$ is the current recorded in the presence of complete O_2^- dismutation. A and B are constants, $K(M^{-1}\text{sec}^{-1})$ is the catalytic rate constant and ω(rad sec^{-1}) is the angular velocity of electrode rotation.

The rotating disk electrode requires a polarographic cell in which the dropping mercury electrode is replaced by a rotating disk electrode consisting of a 2 mm diameter platinum wire fitted into a Teflon rod rotated by a synchronous motor. The electrode surface is covered before each set of measurements by a thin mercury film by cathodic deposition from $Hg(CH_3COO)_2$ deareated solution (Argese et al., 1983). The polarographic solutions in 6 ml are borate buffer as for the dropping mercury electrode for pH values ≥ 9.0 or 100 mM Tris-perchlorate for pH values <9.0, 5×10^{-4} M triphenylphosphine oxide and 9×10^{-4} M EDTA. The solution is equilibrated with air. The experimental procedure is the same as that described for the dropping mercury electrode. Optimal plots of the preceding equation are obtained with 2.5×10^{-8} M copper/zinc superoxide dismutase and with around 10^{-6} M iron or manganese enzymes in 0.1 M Tris buffer pH 7.5 and with $\omega = 283$ rad sec^{-1}.

3. Indirect Methods of Assaying for Superoxide Dismutase

The indirect methods of assaying for superoxide dismutase are the most widely used routine assays because the reagents used are inexpensive, widely available, and usually very sensitive to detection. However, these types of assay are quite susceptible to interferences. Some of these interferences are unfortunately ignored, with the consequence that various discrepancies arise in the results obtained from the various laboratories. These assays can operate at a very low steady-state level of O_2^- and are considered to be indirect negative assays when superoxide dismutase inhibits the formation of products and indirect positive assays when the enzyme accelerates the formation of products. In the indirect assays a unit of enzyme activity is generally defined as the amount of the enzyme that inhibits the reaction by 50%.

In principle, all chemical methods for trapping of O_2^- are suitable for such indirect assays. An epr approach of this type is the spin-trapping technique, which can overcome many difficulties of detecting O_2^- by epr. This technique has been used as an approach to extend the lifetime of reactive paramagnetic species, thus enabling direct epr studies under steady-state conditions. Spin trapping is an integrative method in which the unstable free radical, in this case O_2^-, reacts with a scavenger, yielding a stable-free radical adduct which accumulates and can be measured by epr. The inhibition of the rate of spin adduct formation by superoxide dismutase can be developed as an assay provided that the spin trap does not interact (perturb) the system under investigation. The spin trapping agents used for O_2^- detection are usually nitrones. Much more conveniently assays have been developed from chromophoric systems for O_2^- detection.The simplest of the indirect negative assays are those in which O_2^- is produced during the autoxidation of a compound. The O_2^- produced acts as the chain-propagating species, and the end product is usually colored and can be followed spectroscopically. The effect of superoxide dismutase is to inhibit end product formation. The first documented autoxidation assay is that based on epinephrine. The copper(II) catalysis of epinephrine had earlier been explained by Borg (1965) on the basis of a free radical mechanism. An epinephrine solution, 3×10^{-4} *M* at pH 2.0 is added to 0.05 *M* carbonate buffer pH 10.2 containing 10^{-4} *M* EDTA, and the formation of adrenochrome was recorded at 480 nm (Misra and Fridovich, 1972). The absorbance change was found to be 0.025 per minute, and 50% inhibition was achieved by 46 ng/ml of bovine copper/zinc superoxide dismutase. The assay was found to be applicable to measuring the activity in crude extracts of yeast. It has a number of inherent defects, some of which have been considerably improved by Sun and Zigman (1978) who measured the autoxidation reaction at 320 nm rather than at 480 nm. The absorption of adrenochrome at 480 nm corresponds to a relatively weak and broad absorption band with an extinction coefficient of 4020 $M^{-1}cm^{-1}$ (Green et al., 1956). The absorption change to 320 nm was found to be about 6 to 10 times greater than that at 480 nm.

The autoxidation of hydroxylamine to nitrite also involves a radical chain process (Kono, 1978), and the reaction is carried out at high pH. The assay was originally utilized by Elstner and Heupel (1976) who initiated the autoxidation by O_2^- generated by the xanthine/xanthine oxidase reaction. Nitrite formation was determined colorimetrically at 530 nm by diazo coupling with α-naphthylamine and superoxide dismutase was found to inhibit end product formation. Kono (1978) developed the assay further by utilizing nitroblue tetrazolium as the

detection system. The reduction of nitroblue tetrazolium with O_2^- to form blue formazan is followed at 560 nm. Formazan tends to form colloids, and Kono (1978) overcame this problem by adding 0.03% (v/v) Triton X-100 to stabilize the formazan as recommended by Nishikimi (1975). Kono (1978) observed no autoxidation reaction below pH 8.0, and the maximum was observed at pH 10.2. The amount of spinach copper/zinc superoxide dismutase found to inhibit the reaction by 50% was 5.1 n*M*. Metals and hydrogen peroxide were found to interfere with the reaction (Kono, 1978), and Ernster and Heupel (1976) recommend dialysis of crude extracts to obviate possible superimposed effects from radical scavengers such as ascorbate.

The autoxidation of pyrogallol has the advantage of taking place at pH values near neutral. Pyrogallol autoxidizes to a yellow-brown product, with a spectrum showing a broad shoulder between 400 and 425 nm. The reaction has been utilized as an assay for superoxide dismutase (Marklund and Marklund, 1974). This has the advantage over the other autoxidation assays in that it is also useful for the manganese and iron isozymes which have a narrow pH range of activity. Maximum inhibition by superoxide dismutase of pyrogallol oxidation was found to be 99% in Tris-cacodylate buffer, pH 7.9, 93% at pH 9.0, and 15% at pH 10.6 Diethylenetriaminepentacetic acid was found to prevent interferences from redox metals. The rate of autoxidation is taken from the increase in absorbance at 420 nm which was found to be 0.020 min^{-1}. In the presence of 100 ng bovine copper/zinc superoxide dismutase, 50% inhibition was found to take place. A number of compounds interfere with the autoxidation, severely limiting its use for measuring the superoxide dismutase activity in crude extracts. Glutathione and ascorbate at 10^{-6} *M* concentration were found to inhibit the reaction by 20% and peroxidases interfered by accelerating the reaction. Interferences due to glutathione, ascorbate, and other low molecular weight compounds can be removed by dialysis.

A simple indirect negative assay is that based on the autoxidation of 6-hydroxydopamine (Heikkila and Cabbat, 1976). The autoxidation takes place at pH 7.4 and has the advantage of having no interferences from tissue extracts. Autoxidation of 6-hydroxydopamine results in the formation of quinoidal products (Heikkila and Cohen, 1973). The compound is prepared as a stock solution in water, and end product formation is monitored at 490 nm (Fig. 5). Superoxide dismutase inhibits the product formation.

The enzyme xanthine oxidase in the presence of its substrate xanthine is able to reduce oxygen univalently to O_2^-. The enzymatic generation of O_2^- and its ability to reduce cytochrome c formed the basis of the first

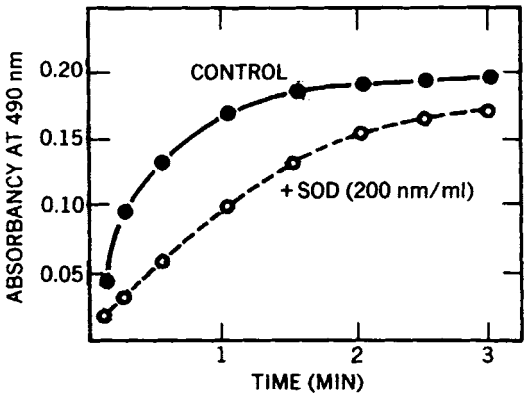

Fig. 5. The effect of superoxide dismutase (SOD, 200 ng/ml) on the autoxidation of 6-hydroxydopamine (10^{-4} *M*) as measured by the absorbance increase at 490 nm. (Reprinted with permission from R. E. Heikkila and F. Cabbat, *Anal. Biochem.*, *75*, 356–362, 1976.)

assay to be developed for measuring the activity of superoxide dismutase (McCord and Fridovich, 1969). The assay mixture consists of 1×10^{-5} *M* oxidized cytochrome c, 5×10^{-5} *M* xanthine, sufficient xanthine oxidase, and 100 m*M* phosphate buffer, pH 7.8 containing 10^{-4} *M* EDTA in a total of 3 ml. The reduction of cytochrome c is followed at 550 nm. One unit of superoxide dismutase is defined as the amount that causes 50% inhibition of the rate of reduction of cytochrome c. Cytochrome c is not the only detector that can be used with this assay. Nitroblue tetrazolium has also been used, although some caution about its use has been advised by Auclair et al. (1978). The dye provides the basis for an assay which is free of interference by other catalytic activities that may be present in crude extracts such as cytochrome oxidase and cytochrome c peroxidase capable of oxidizing ferrocytochrome c. Acetylation of the cytochrome c was found to diminish its ability to be utilized as a substrate following its reduction by O_2^-, (Azzi et al., 1975; Buchanan and Lees, 1976). Fresh xanthine oxidase should also be used as preparations that have been stored for long periods, frozen and thawed repeatedly, or exposed to high salt concentrations may be found contaminated with the deflavo derivative which will directly reduce cytochrome c (Fridovich, 1983).

The inhibition by superoxide dismutase of O_2^- dependent oxidation of sulfite first described by McCord and Fridovich (1969) was utilized by Tyler (1975) as the basis of a polarographic assay. Sulfite was measured polarographically during oxidation by O_2^- generated by the xanthine/

xanthine oxidase reaction. A reciprocal plot of sulphite oxidation rate against various amounts of either a rat liver fraction or purified bovine erythrocyte copper/zinc superoxide dismutase, added to the system, indicated that the inhibition of sulfite oxidation by the enzyme was strictly competitive.

Other systems generating O_2^- coupled to a detector are the so-called photochemical assays. Dyes that are electronically excited by absorption of a photon are more active oxidants than the same dyes in the ground state. When the dye is reduced to an autoxidizable semiquinone, O_2^- is generated on reoxidation. The photoreduction of flavins by EDTA was noted by Frisell et al. (1959) and was used by Massey et al. (1969) and Ballou et al. (1969) as a convenient source of O_2^-. Rapp et al. (1973) utilized the method, using nitroblue tetrazolium as the detector. Other assays developed used the interaction of molecular oxygen with tetrahydropteridine at physiological pH in the presence of Triton X-100 (Nishikimi, 1975), and illumination of solutions containing riboflavin, methionine, and nitroblue tetrazolium resulted in the accumulation of blue formazan (Beauchamp and Fridovich, 1971). In the absence of oxygen, superoxide dismutase was observed to have no effect on formazan formation, indicating that riboflavin can reduce the nitroblue tetrazolium directly. A similar effect was also noted when tetrahydropteridine was used as the dye. However, Nishikimi (1975) observed that only 7% of the nitroblue tetrazolium was reduced by an oxygen-independent pathway, and Fridovich (1983) reports that in air-equilibrated solutions, 80% of the nitroblue tetrazolium reduction is mediated by O_2^- generated by the xanthine/xanthine oxidase reaction.

An assay utilizing the dye-mediated O_2^- formation to reduce nitroblue tetrazolium has been applied to the detection of superoxide dismutase in crude extracts following polyacrylamide gel electrophoresis (Beauchamp and Fridovich, 1971). Gels are soaked in a solution of 2.45×10^{-3} *M* nitroblue tetrazolium for 30 min, followed by an immersion for another 30 min in a solution containing 0.028 *M* TEMED, 2.8×10^{-5} *M* riboflavin, and 0.036 *M* phosphate buffer pH 7.8. The gels are then placed in tubes and illuminated for 30 min. During illumination the gels become uniformly blue except at positions containing the enzyme activity. Scanning of gels containing crude extracts and of gels containing a known concentration of purified enzyme allows the concentrations to be determined from the relative peak heights. Cyanide or hydrogen peroxide are usually added to the phosphate buffer when various forms of the enzyme have to be distinguished on the gel. The high sensitivity of this method has been used by several investigators to demonstrate the presence of the various forms of the enzyme in crude extract. However, although the

enzyme could be detected by this technique in mouse liver (Salin and McCord, 1974), it could not be detected in rat liver (De Rosa et al., 1979). The enzyme has nevertheless been purified from this tissue, thereby confirming its presence (Salin et al., 1978).

Nishikimi et al., (1972) developed an assay for superoxide dismutase, using phenazine methosulfate which is structurally related to flavin. In this assay phenazine methosulfate is reduced by NADH, and on reoxidation, O_2^- was generated. The O_2^- was detected with nitroblue tetrazolium, and maximum inhibition of blue formazan formation by superoxide dismutase was 95% indicating that 5% of the reduction was due to direct interaction between the nitroblue tetrazolium and the reduced phenazine methosulfate. Addition of around 30 ng copper/zinc superoxide dismutase resulted in 50% inhibition of formazan formation. The assay was also used to locate the enzyme on polyacrylamide gels.

Riboflavin was observed to photosensitize the oxidation of dianisidine, and all the forms of superoxide dismutase were found to augment the oxidation (Misra and Fridovich, 1977a, b). This result (Fig. 6) has formed the basis of an assay that has been called an indirect positive assay. The oxidation measured at 460 nm proceeds by a mechanism in which ribofla-

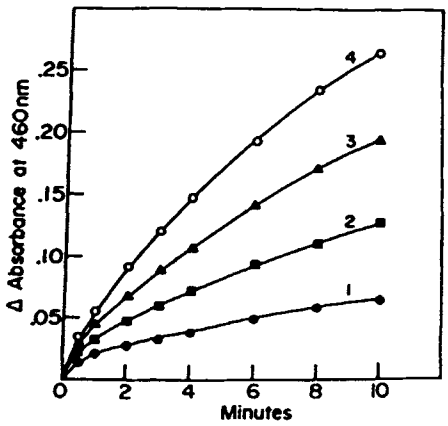

Fig. 6. The effect of superoxide dismutase on the photosensitized oxidation of dianisidine. The reaction mixture contained 2×10^{-4} *M* dianisidine, 1.3×10^{-5} *M* riboflavin and 0.01 *M* potassium phosphate, pH 7.5. The data on line 1 were observed in the absence of superoxide dismutase, and those on lines 2, 3, and 4 were observed in the presence of 0.2, 0.5, and 1.0 μg/ml of enzyme. (Reprinted with permission from H. P. Misra and I. Fridovich, *Arch. Biochem. Biophys.*, *181*, 308–312, 1977.)

vin absorbs a photon and becomes electronically excited. The excited state oxidizes the dianisidine, yielding the flavin semiquinone and a dianisidine radical which in the absence of competing reactions would dismute to yield the divalently oxidized dianisidine:

$$Rb^* + DH_2 \rightarrow RbH + DH^\cdot$$
$$DH^\cdot + DH^\cdot \rightarrow D + DH_2$$

However, the flavin semiquinone RbH can reduce oxygen to O_2^-, and the radical can in turn reduce the dianisidine radical $DH^\cdot$ preventing its oxidation:

$$RbH + O_2 \rightarrow Rb + H^+ + O_2^-$$
$$H^+ + O_2^- + DH \rightarrow DH_2 + O_2$$

Superoxide dismutase will scavenge the O_2^- formed and will therefore inhibit the reduction of the dianisidine radical by O_2^-. Consequently the dianisidine radical will dismute to yield the divalently oxidized dianisidine. In the presence of superoxide dismutase this reaction is augmented (Fig. 6). The possibility that O_2^- could reduce the final product of dianisidine oxidation and reverse the change in absorbance at 460 nm was tested and was excluded. The assay has been used to determine the rate constant for purified swordfish liver copper/zinc superoxide dismutase (Bannister et al., 1979) and could be applied to crude extracts. The assay was also found applicable to polyacryalmide gels (Misra and Fridovich, 1977c). Gels soaked in riboflavin plus dianisidine, and subsequently illuminated, developed stable brown bands. Peroxidases are also stained by this procedure due to the photochemical production of hydrogen peroxide. However, the development of bands due to peroxidase activity is much slower than the development of bands due to dismutase activity.

4. Assays for Superoxide Dismutase Not Based on Activity

Two rather unusual assays have been developed for superoxide dismutase. Both these assays do not reflect the catalytic activity of the enzyme. The first assay utilizes the unique effect of the metal centers on the relaxation rate of ^{19}F nucleus of fluoride which can be monitored by nuclear magnetic resonance, whereas the second assay is based on the antigenicity of the proteins.

The copper/zinc- and manganese-containing superoxide dismutases are the only metalloproteins that are able to enhance the nuclear magnetic relaxation rate of ^{19}F to an extent that makes this property detectable at the protein concentration usually present in most cells (Rigo et al., 1979).

An exception to this rule is galactose oxidase, also known to be a good ^{19}F relaxation probe, but this enzyme is present only in certain fungi (Marwedel et al., 1975). Since manganese and copper/zinc superoxide dismutase can be discriminated in mixtures containing both enzymes by the selective inhibition of the latter one by cyanide, the ^{19}F relaxation can in principle be used to measure both enzymes, even when they are both present. However, there are several limitations that recommend a cautious utilization of this technique, and in particular its application to the assay of copper/zinc superoxide dismutases only. The major points to be emphasized in this context are that the relaxation effect depends on the oxidation state of the metal, and this is not known for every biological sample to be assayed. Furthermore copper enhances the ^{19}F relaxation only in the copper(II) state, and all the copper/zinc superoxide dismutase of a given sample can be converted into the copper(II) form by a convenient incubation in air at pH values between 9 and 10, especially when the sample is first dialyzed to remove low molecular weight reductants. A further disadvantage of the method is its low sensitivity (10^{-7} to 10^{-8} *M*).

The advantages of the method are its physicochemical and chemical nature. In particular, ^{19}F has $I = \frac{1}{2}$, and therefore its signal is unaffected by quadrupole broadening. This increases the sensitivity of this method. Moreover the relaxation effect is seen at F^- concentrations that neither inhibit the enzyme activity nor change the electron paramagnetic resonance spectrum of the enzyme. From a biochemical view point the major advantage of the technique lies in its valence dependence. Once the total concentration of copper/zinc enzyme is known from other assays, the fraction of enzyme that, in a given tissue, is detectable by the ^{19}F NMR relaxation is the enzyme present as the copper(II) form (Viglino et al., 1981). This is particularly important when this fraction is found to be 50%. In fact this ratio can only be produced in the presence of usual concentration of oxygen, hydrogen peroxide, and reducing molecules available to ordinary cells, by an even moderate O_2^- flux. Superoxide is the only redox agent that reacts at the same very high rate with both reduced and oxidized copper/zinc superoxide dismutase (Fielden et al., 1974). The assay is really a spectroscopic method. However, it is as specific as an enzymatic assay. It may also be envisaged as a natural, nonperturbing, detection system for the actual production of O_2^- in biological samples (Rigo et al., 1981).

Paramagnetic metal ions usually enhance longitudinal and transverse relaxation rates ($1/T_1$ and $1/T_2$) of nuclear spins of ligand nuclei. The relaxation rates of a nucleus that experiences chemical exchange between the bulk of solution and a paramagnetic center are described by the

Luz-Meiboom equations (Luz and Meiboom, 1964, Mildvan and Cohn, 1970). Viglino et al., (1979) have studied the interaction of $^{19}F^-$, with the copper of bovine copper/zinc superoxide dismutase. They have shown that in this case the Luz-Meiboom equations can be written in a simplified form:

$$\frac{1}{q} \cdot \frac{1}{T_{1p}} = \frac{1}{(T_{1M} + \tau_M)}$$

$$\frac{1}{q} \cdot \frac{1}{T_{2p}} = \frac{1}{\tau_M}$$

where

$$q = \frac{[F^- \text{ bound}]}{[F^- \text{ total}]} = \frac{[SOD]}{(K_F^{-1} + [F^-])},$$

$1/T_{1p}$ and $1/T_{2p}$ are the paramagnetic contribution to longitudinal and transverse relaxation rates of $^{19}F^-$($1/T_1$ and $1/T_2$), T_{1M} is the longitudinal relaxation time of $^{19}F^-$ in the first coordination shell of the paramagnetic center, copper(II), τ_M the residence time that is the time a $^{19}F^-$ ion is bound to copper(II) before it exchanges and K_F (M^{-1}) is the stability constant of the superoxide dismutase-F^- complex.

The ^{19}F relaxation times depend on both copper(II) and F^- concentration. $1/T_{1p}$ is linearly dependent on the enzyme concentration between pH 7.8 and pH 10. $1/T_{2p}$ is independent of frequency between 7 and 56 MHz and strongly influenced by the temperature, a behavior typical of slow exchange condition. $1/T_{2p}$ is governed by the rate of chemical exchange of fluoride ions between the bulk and the binding site, whereas $1/T_{1p}$ is only partially dependent on τ_M.

^{19}F relaxation rates are strongly influenced by the presence of anions which compete with fluoride for the copper(II) site like cyanide, azide, and hydroxide. $1/T_{1p}$ measured at relatively high concentration of cyanide is practically equal to that measured for the copper-free enzyme.

The most convenient assay procedure involves measurements of ^{19}F T_{1p} of samples after addition of known amount of F^- (Rigo et al., 1979). T_1 measurements can be obtained by a conventional pulse nuclear magnetic resonance apparatus operating at 16 MHz and equipped with time averaging computer using the 90°-τ-90° sequence.

T_{1p}, the paramagnetic contribution to T_1 is calculated according to

$$\frac{1}{T_{1p}} = \frac{1}{T_1} - \frac{1}{T_{1o}}$$

being T_1 and T_{1_o} the $^{19}F^- - T_1$ of the sample and the buffer solutions, respectively.

For maximal sensitivity 0.1 ml of 2.5 *M* potassium fluoride in 0.1 *M* borate buffer, pH 9.8, containing 5×10^{-4} *M* EDTA, are added to 0.4 ml of sample to be assayed. The enzyme concentration can be calculated once *R*, the molar relaxivity of the enzyme, in the range $10^{-8} - 10^{-4}$ *M* enzyme, where ^{19}F relaxation rate is linearly dependent on enzyme concentration is known. *R*, a second-order kinetic rate constant ($M^{-1}sec^{-1}$), is calculated measuring the T_1 of ^{19}F in the presence of a known concentration of the oxidized form of a pure enzyme sample, according to the equation

$$R = T_{1_p} E^{-1}$$

Measurements of *R* are to be performed under controlled pH and F^-, since *R* is a function of both (Viglino et al., 1979).

The assay of superoxide dismutase from ^{19}F transverse relaxation time (T_2), although possible and even more sensitive on the basis of the results of Viglino et al. (1979), has only been preliminarily investigated (Rigo et al. 1979). In this case the method offers the advantage of being accessible to high resolution nuclear magnetic resonance spectrometers as T_2 can be easily evaluated by the ^{19}F linewidth measurements with high resolution nuclear magnetic resonance spectroscopy.

The nonidentity of the primary structure between the copper/zinc and manganese superoxide dismutases (Parker et al., 1984) indicates differences in their antigenic sites. This has led to the development of a number of radioimmunoassays for the two proteins. The assays are also highly specific, not only for the isozyme being investigated; no cross-reactivity is observed between species as well. The first radioimmunoassay was developed by Kelly et al. (1978) against bovine erythrocyte superoxide dismutase, and Del Villano and Tischfield (1979) and Holme et al. (1980) developed an assay against human erythrocyte superoxide dismutase. A radioimmunoassay against human liver manganese superoxide dismutase was developed by Baret et al. (1980). The assay of superoxide dismutase by radioimmunoassay is a very sensitive way of measuring the concentration of the enzyme. The assay was utilized by Joenje et al. (1979) to measure the levels of copper/zinc superoxide dismutase in Fanconi's anemia. The antigen-antibody reaction can also be monitored without the use of a radioactive tracer. Flohe and Otting (1984) described a Laurell and McKay (1978) electroimmunoassay measuring levels of superoxide dismutase.

5. Spin-Trapping Assays

Epr is considered to be the least ambiguous method for the detection of free radicals. However, even when concentrations of O_2^- exceed those normally required for detection (10^{-8} *M*), no epr spectrum is observed in aqueous solution under physiological conditions. This is because of the very short relaxation time of the O_2^- resonance (due to strong "spin orbital coupling"). A decrease in sample temperature may redress this effect, but it usually negates any physiologically significant kinetic and possibly structural aspects in the epr spectrum. However, spin trapping allows the formation of a stable free-radical product, thereby allowing their detection.

The method has the advantage of being qualitative as well as quantitative. The technique of spin trapping was developed, following research into nitroso/nitrone/nitroxide group chemistry, and was first called spin-trapping by Janzen and Blackburn (1969). The spin-trapping agents used for O_2^- detection are usually nitrones. The spin-trapping agents used are given in Table I and are usually obtained from the Aldrich Chemical Co. 5,5-Dimethyl-1-pyrroline-*N*-oxide (DMPO) as supplied

TABLE I

Spin Trapping Agents for Superoxide Radicals

5,5-Dimethyl-1-pyrroline-N-oxide (DMPO)	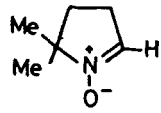
2,5,5-Trimethyl-1-pyrroline-N-oxide (TMPO)	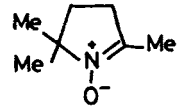
3,3,5,5-Tetramethyl-1-pyrroline-N-oxide (M_4PO)	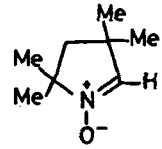
N-tert-Butyl-α-phenylnitrone (PBN)	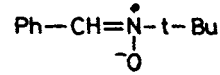

usually contains colored impurities. These can be readily removed either by double distillation (boiling point = 75°C at 0.4 mm Hg) or by stirring for 30 min at room temperature with activated charcoal a 10% solution of the nitrone in 10 m*M* sodium phosphate buffer, pH 7.4. The charcoal is filtered, and the filtrate is monitored by epr at high receiver gain (1×10^5) for nitrone impurities. The charcoal treatment is repeated until the filtrate is clear of free-radical impurities. The final solution is assayed for DMPO content at 234 nm, $\varepsilon = 7700\ M^{-1}cm^{-1}$ in ethanol (Bonnet et al., 1959). The spin-trapping agent 3,3,5,5-tetramethyl-1-pyrroline-*N*-oxide (M_4PO) is not commercially available and is synthesized from DMPO (Bonnet et al., 1959). M_4PO and the other agents 2,5,5-trimethyl-1-pyrroline-*N*-oxide (TMPO) and *N*-tert-butyl-α-phenylnitrone (PBN) are also further purified by charcoal treatment. The extinction for PBN in ethanol at 294 nm is 16,700 $M^{-1}cm^{-1}$ (Emmons, 1957). M_4PO, TMPO, and PBN are less water soluble than DMPO. All purified spin-trapping agents should be stored at −20°C in the dark.

A spin-trapping experiment simply involves performing the reaction in which superoxide production is suspected in the presence of a high concentration of a spin-trapping agent (e.g., 100 m*M* DMPO) within the cavity of an epr machine. For simple chemical oxidative processes and enzymatic reactions, the spin traps should be premixed with the reaction buffer, a chelating agent, usually 1 m*M* diethylenetriaminepentaacetic acid or desferrioxamine, and any other cofactor(s) prior to the initiation of the reaction. When superoxide production is measured in the presence of cellular systems, care should be taken to preserve the isotonicity of the supporting medium. Th Krebs-Ringer buffer in the presence of 100 m*M* DMPO should contain 500 m*M* less NaCl than normal. Typical spectrometer settings are: field set 3385 G, field scan 100 G, modulation frequency 10^5 Hz, modulation amplitude 0.5 G (or similar setting to avoid modulation broadening), receiver gain $1 \times 10^3 - 1 \times 10^5$, scan time 4×60 sec (or 1×24 sec if it is not possible to average the signal), time constant 0.128 sec (or 0.25 sec), microwave frequency 9.478 GHz, and microwave power 10 mW. Standard spin adduct spectra are given in Fig. 7. The *g* factors, hyperfine components, and splitting constants are measured for the spin adducts observed. The values for these parameters are given in Table II. Spin adduct concentrations may be computed from a calibrated double integral. Calibration of the integral is usually effected by comparison with the double integral of the epr spectrum of a known concentration of a persistent nitroxide such as 4-hydroxy-2,2,5,5-tetra-methylpiperidionooxy (Aldrich Chemical Co.). When noise in the experimental spectrum leads to erroneous results during double integration, the experimental spectrum may be simulated and the simulation used for integration.

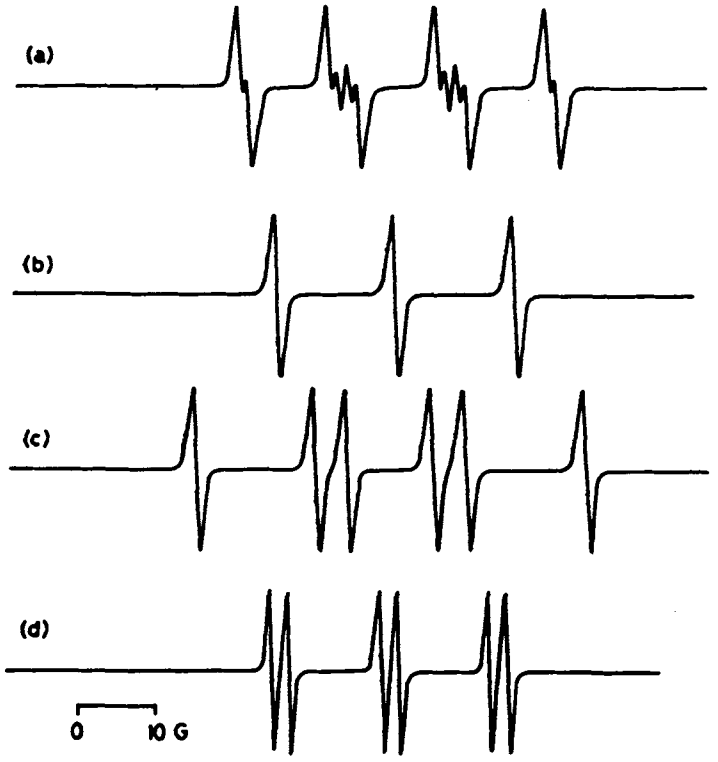

Fig. 7. Simulated superoxide spin adduct spectra. *(a)* DMPO-OOH, *(b)* TMPO-OOH, *(c)* M_4PO-OOH, and *(d)* PBN-OOH.

The kinetics of the reaction between superoxide and DMPO have been investigated by Finkelstein et al. (1980). The pH profile for the observed rate constant for the spin-trapping reaction, k_T, where

$$\frac{-d[O_2^-]}{dt} = k_T[O_2^-][\text{DMPO}]$$

can be resolved into two component rate constants for the spin trapping of superoxide (O_2^-) and hydroperoxyl ($HO_2^\cdot$) such that k_T (O_2^-) = 10 $M^{-1}\text{sec}^{-1}$ and k_T ($HO_2^\cdot$) = 6.6×10^3 $M^{-1}\text{sec}^{-1}$ at 298°K. At pH 7.8 and 298°K, k_T for the spin trapping of O_2^- by DMPO is around 10 $M^{-1}\text{sec}^{-1}$ and k_T for the spin trapping of O_2^- by TMPO under the same conditions is 7 $M^{-1}\text{sec}^{-1}$.

TABLE II

Superoxide Spin Adducts	Hyperfine Splitting Constants (aqueous solutions)			
	g	a_N	a_H^β	a_H^γ
5,5-Dimethyl-2-hydroperoxypyrrolidino-N-oxide (DMPO-OOH)	2.0061	14.3G	11.7G	1.25
2-Hydroperoxy-3,5,5-trimethylpyrrolidino-N-oxide (TMPO-OOH)	2.0060	15.6G	-	-
2-Hydroperoxy-3,3,5,5-tetramethylpyrrolidino-N-oxide (M$_4$PO-OOH)	2.0060	15.7G	20.0G	-
t-Butyl-α-hydroperoxybenzylnitroxide (PBN-OOH)	2.0057	14.3G	2.25G	-

The O_2^- spin adduct of DMPO, DMPO-OOH decays by a complex mechanism involving biomolecular and unimolecular kinetic pathways (Finkelstein et al., 1980). The bimolecular mechanism becomes significant at DMPO-OOH concentrations greater than 10 μM; below this concentration the decay is essentially unimolecular and pH dependent. The unimolecular half-life of DMPO-OOH at pH 3.0 and 9.0 is 90 and 30 sec, respectively (Buettner and Oberley, 1978). The O_2^- spin adduct of TMPO, TMPO-OOH decays relatively slowly, with a unimolecular half-life of around 1 h. TMPO would appear to be a good spin trap for O_2^-; however, the severe overlap and lack of distinguishing features in the epr spectra of TMPO spin adducts (nitroxide triplets with very small changes in hyperfine splitting constants) makes diagnostic analyses of TMPO spin adduct epr data very difficult. Some confusion appears to exist regarding the decay of the spin traps. Finkelstein et al. (1980) have observed that DMPO-OOH decays to DMPO-OH. However, Bannister et al., (1981) observed that neutrophil NADPH oxidase only produces DMPO-OOH, and no decay was observed. The inhibition of the rate of spin adduct formation by superoxide dismutase can be developed as a method for the enzyme. The method would nevertheless only be useful for pure enzymes as the spin trap may interact with the system under investigation and give erroneous results. Also as pointed out earlier, both TMPO and DMPO are inefficient scavengers, and a high concentration (60–200 mM) of spin trap is used to allow effective competition with spontaneous O_2 dismutation. Yet recently Rosen et al. (1982) observed that when a particular hydroxylamine 2-ethyl-1-hydroxy-2,5,5-trimethyl-3-oxazolidine

(OXANOH) reacts with superoxide to form its corresponding nitroxide, 2-ethyl-2,5,5-trimethyl-3-oxazolidinoxyl (OXANO) a stable product, the rate constant for the reaction is 6.7×10^3. OXANOH oxidation was used to detect O_2^- formation in a number of biological media, and no interferences were found. Product formation could be inhibited by superoxide dismutase leading to the development of an assay.

Acknowledgment

J.V. Bannister thanks the Medical Research Council for support.

Addendum

An X-ray structure for the manganese superoxide dismutase from *Thermus aquaticus* (Stallings, et al., 1985) and a complete amino acid sequence for the iron superoxide dismutase from *Photobacterium leiognathi* (Barra, et al., in press) confirm that the manganese and iron superoxide dismutases are homologous proteins.

References

Argese, E., DeCarli, B., Orsega, E., Rigo, A., and Rotilio, G. (1983), *Anal. Biochem. 132*, 110–115.

Argese, E., Rigo, A., Viglino, P., Orsega, E., Marmocchi, F., Cocco, D., and Rotilio, G. (1984), *Biochim. Biophys. Acta, 787*, 205–207.

Asada, K., Kanematsu, S., Okada, S., and Hayakawa, T. (1980), in *Chemical and Biochemical Aspects of Superoxide and Superoxide Dismutase* (J. V. Bannister and H. A. O. Hill, eds.), Elsevier, New York, pp. 136–153.

Asada, K., Yoshikawa, K., Takahashi, M., Maeda, Y., and Emmanji, K. (1975), *J. Biol. Chem., 250*, 2801–2807.

Auclair, C., Torres, M., and Hakim, J. (1978), *FEBS Letts., 89*, 26–28.

Azzi, A., Montecucco, C., and Richter, C. (1975), *Biochem. Biophys. Res. Commun., 65*, 579–603.

Ballou, D., Palmer, G., and Massey, V. (1969), *Biochem. Biophys. Res. Commun., 36*, 898–904.

Bannister, J. V., Anastasi, A., and Bannister, W. H. (1978), *Biochem. Biophys. Res. Commun., 81*, 469–472.

Bannister, J. V., Bellavite, P., Serra, M. C., Thornalley, P. J., and Rossi, F. (1982), *FEBS Lett., 145*, 323–326.

Bannister, J. V. and Parker, M. W. (1985), *Proc. Natl. Acad. Sci.* (USA), *82*, 149–152.

Bannister, J. V., and Rotilio, G. (1984), in *The Biology and Chemistry of Active Oxygen* (J. V. Bannister and W. H. Bannister, eds.), Elsevier, New York, pp. 146–189.

Baret, A., Schiavi, P., Michel, P., Michelson, A. M., and Puget, K. (1980), *FEBS Lett., 112*, 25–29.

Barra, D., Schinina, M. E., Bossa, F., and Bannister, J. V. (1985), *FEBS Lett., 179*, 329–331.

Barra, D., Schinina, M. E., Bannister, W. H., Bannister, J. V., and Bossa, F. J. (in press), *J. Biol. Chem.*

Beauchamp, C., and Fridovich, I. (1971), *Anal. Biochem., 44*, 276–287.

Bonnet, R., Brown, R. F. C., Sutherland, I. O., and Todd, A. (1959), *J. Chem. Soc.*, 2094–2102.

Borg, D. C. (1965), *Proc. Nat. Acad. Sci.* (USA), *53*, 633–639.

Bray, R. C. (1961), *Biochem. J., 81*, 189–193.

Bray, R. C., Knowles, P. F., Pick, F. M., and Gibson, J. F. (1968), *Hoppe-Seyler's Z. Physiol. Chem., 349*, 1591–1596.

Bray, R. C., Mautner, G. N., Fielden, E. M., and Carle C. I. (1977), in *Superoxide and Superoxide Dismutase* (A. M. Michelson, J. M. McCord, and I. Fridovich, eds.), Academic Press, New York, pp. 61–75.

Buchanan, A. G., and Lees, H., (1976), *Can. J. Microbiol., 22*, 1643–1646.

Buettner, G. R., and Oberley, L. W. (1978), *Biochem. Biophys. Res. Commun., 83*, 69–74.

Bull, C., and Fee, J. A. (1985), *J. Amer. Chem. Soc., 107*, 3295–3304.

Cocco, D., Calabrese, L., Rigo, A., Marmocchi, F., and Rotilio, G. (1981), *Biochem. J., 199*, 675–680.

Del Villano, B. C., and Tischfield, J. A. (1979), *J. Immunol. Methods, 29*, 253–262.

DeRosa, G., Duncan, D. S., Keen, C. L., and Hurley, L. S. (1979), *Biochim. Biophys. Acta, 566*, 32–39.

Elstner, E. F., and Heupel, A. (1976), *Anal. Biochem., 70*, 616–620.

Emmons, W. (1957), *J. Amer. Chem. Soc., 79*, 6522–6524.

Fee, J. A., McClune, G. J., O'Neill, P., and Fielden, E. M. (1981), *Biochem. Biophys. Res. Commun., 100*, 377–384.

Fielden, E. M., Roberts, P. B., Bray, R. C., Lowe, D. J., Mautner, G. N., Rotilio, G., and Calabrese, L. (1974), *Biochem. J., 139*, 49–60.

Fielden, E. M., and Rotilio, G. (1984) in *Copper Proteins and Copper Enzymes* (R. Lontie, ed.), CRC, Boca Raton, 27–61.

Finkelstein, E., Rosen, G. M., and Rauckman, E. J. (1980), *J. Amer. Chem. Soc., 102*, 4994–4998.

Flohe, L., and Otting, F. (1984), *Methods in Enzymol., 105*, 93–104.

Forman, H. J., and Fridovich, I. (1973), *Arch. Biochem. Biophys., 158*, 396–400.

Frisell, W. R., Chung, C. W., and Mackenzie, C. G. (1959), *J. Biol. Chem., 234*, 1297–1302.

Geller, B. L., and Winge, D. R. (1982), *J. Biol. Chem., 257*, 8945–8952.

Geller, B. L., and Winge, D. R. (1983), *Anal. Biochem., 128*, 86–92.

Green, S., Maxur, A., and Shorr, J. (1956), *J. Biol. Chem., 220*, 237–255.

Gregory, E. M., and Dapper, C. H. (1983), *Arch. Biochem. Biophys., 220*, 293–300.

Haneda, Y. (1950), *Pacific Sci., 4*, 214–227.

Hassan, H. M., Dougherty, H., and Fridovich, I. (1980), *Arch. Biochem. Biophys., 199*, 349–354.

Holme, E., Bankel, L., Lundberg, P. A., and Waldenstrom, J. (1980) in *Biological and Clinical Aspects of Superoxide and Superoxide Dismutase* (W. H. Bannister and J. V. Bannister, eds.), Elsevier, New York, pp. 262–270.

Heikkila, R. E., and Cabbat, F. (1976), *Anal. Biochem., 75*, 356–362.

Heikkila, R. E., and Cohen, G. (1973), *Science, 181*, 456–457.

Heikkila, R. E., Cabbat, F. S., and Cohen, G. (1976), *J. Biol. Chem., 251*, 2182–2185.

Hodgson, E. F., and Fridovich, I. (1975), *Biochemistry, 14*, 5294–5298.

Howie, J. K., and Sawyer, D. T. (1976), *J. Amer. Chem. Soc., 98*, 6698–6700.

Janzen, E. G., and Blackburn, B. J. (1969), *J. Amer. Chem. Soc., 91*, 4481–4490.

Joenje, H., Frants, K. K., Arwert, F., DeBriun, G. J. M., Kostense, P. J., Van De Kamp, J. J. P., De Koning, J., and Eriksson, A. W. (1979), *Scand. J. Clin. Lab. Invest., 39*, 759–764.

Kelly, C., Barefoot, C., Sehon, A., and Petkau, A. (1978), *Arch. Biochem. Biophys., 190*, 531–538.

Kirby, T., Blum, J., Kahami, I., and Fridovich, I. (1980), *Arch. Biochem. Biophys., 201*, 551–555.

Klug-Roth, D., Fridovich, I., and Rabani, J. (1973), *J. Amer. Chem. Soc., 95*, 2786–2790.

Kono, Y., (1978), *Arch. Biochem. Biophys., 186*, 189–195.

Koutecky, J., Brdicka, R., and Hanus, V. (1953), *Collect. Czech. Chem. Commun., 18*, 611–627.

Kuta, J., and Konita, J. (1965), *Collect. Czech. Chem. Commun., 30*, 4095–4101.

Lavelle, F., McAdam, M. E., Fielden, E. M., and Roberts, P. B. (1977), *Biochim. J., 161*, 3–11.

Laurell, C. B., and McKay, E. J. (1978), *Meth. Enzymol., 73*, 339–345.

Luz, Z., and Meiboom, S. J. (1964), *J. Chem. Phys., 40*, 2686.

Marklund, S. (1976), *J. Biol. Chem., 251*, 7504–7507.

Marklund, S., and Marklund, G. (1974), *Eur. J. Biochem., 47*, 469–474.

Martin, J. P., and Fridovich, I. (1981), *J. Biol. Chem., 256*, 6080–6089.

Marwedel, B. J., Kurland, R. J., Kosman, D. J., and Ettinger, J. J. (1975), *Biochem. Biphys. Res. Commun., 63*, 773–779.

Massey, V., Strickland, S., Mayhew, S. G., Howell, L. G., Engel, P. C., Matthews, R. G., Schuman, M., and Sullivan, P. A. (1969), *Biochem. Biophys. Res. Commun., 36*, 891–897.

McAdam, M. E., Fox, R. A., Lavelle, F., and Fielden, E. M. (1977a), *Biochem. J., 165*, 71–79.

McAdam, M. E., Lavelle, F., Fox, R. A., and Fielden, E. M., (1977b), *Biochem. J., 165*, 81–87.

McClune, G. J., and Fee, J. A. (1976), *FEBS Lett., 67*, 294–298.

McCord, J. M., and Fridovich, I. (1969), *J. Biol. Chem., 244*, 6049–6055.

Meier, B., Barra, D., Bossa, F., Calabrese, L., and Rotilio, G. (1982), *J. Biol. Chem., 257*, 13977–13980.

Mildvan, A. S., and Cohn, M. (1970) *Adv. Enzymol., 33*, 1–70.

Misra, H. P., and Fridovich, I. (1972), *J. Biol. Chem., 247*, 3170–3175.

Misra, H. P., and Fridovich, I. (1977a), *Arch. Biochem. Biophys., 181*, 308–312.

Misra, H. P., and Fridovich, I. (1977b), *Anal. Biochem., 79*, 553–560.

Misra, H. P., and Fridovich, I. (1977c), *Arch. Biochem. Biophys., 183*, 511–515.

Misra, H. P., and Fridovich, I. (1978), *Arch. Biochem. Biophys., 189*, 317–322.

Neuman, E. W. (1934), *J. Chem. Phys., 2*, 31–33.

Nilsson, R., Pick, F. M., Bray, R. C. and Fielden, E. M. (1969), *Acta Chem. Scand., 23*, 2554–2556.

Nishikimi, M. (1975), *Arch. Biochem. Biophys., 166*, 273–279.

Nishikimi, M., Rao, N. A., and Yagi, K. (1972), *Biochem. Biophys. Res. Commun., 46*, 849–854.

Orme-Johnson, W. H. and Beinert, H. (1969), *Biochem. Biophys. Res. Commun., 36*, 6–11.

Orsega, E., Argese, E., Viglino, P., Tomat, R., and Rigo, A. (1982), *J. Electroanal. Chem., 131*, 257–264.

Parker, M. W., Schinina, M. E., Bossa, F., and Bannister, J. V. (1984), *Inorg. Chim. Acta, 91*, 307–317.

Pick, M., Rabani, J., Yost, F., and Fridovich, I. (1974), *J. Amer. Chem. Soc., 96*, 7329–7333.

Puget, K., and Michelson, A. M. (1974), *Biochem. Biophys. Res. Commun., 58*, 830–838.

Rapp, U., Adams, W. C., and Miller, R. W. (1973), *Can. J. Biochem., 51*, 158–171.

Ringe, D., Petsko, G. A., Yamakura, F., Suzuki, K., and Ohmori, D. (1983), *Proc. Natl. Acad. Sci.* (USA), *80*, 3879–3883.

Rigo, A., and Rotilio, G. (1977), *Anal. Biochem., 81*, 157–166.

Rigo, A., Ugo, P., Viglino, P. and Rotilio, G. (1984), *FEBS Lett., 132*, 78.

Rigo, A., Viglino, P., Argese, E., Terenzi, M., and Rotilio, G. (1979), *J. Biol. Chem., 254*, 1759–1760.

Rigo, A., Viglino, P., and Rotilio, G. (1975a), *Anal. Biochem., 68*, 1–9.

Rigo, A., Viglino, P., and Rotilio, G. and Tomat, R. (1975b), *FEBS Lett., 50*, 86–88.

Rigo, A., Viglino, P., and Rotilio, G. (1975c), *Biochem. Biophys. Res. Commun., 63*, 1013–1018.

Rocha, H. A., Bannister, W. H., and Bannister, J. V. (1984), *Eur. J. Biochem., 145*, 477–484.

Rosen, G. M., Finkelstein, E., and Rauckman, E. J. (1982), *Arch. Biochem. Biophys., 215*, 367–378.

Salin, M. C., and Bridges, S. M. (1982), *Plant Physiol., 69*, 161–165.

Salin, M., Day, E. D., and Crapo, J. D. (1978), *Arch. Biochem. Biophys., 187*, 223.

Salin, M. L., and McCord, J. M. (1974), *J. Clin. Invest., 54*, 1005–1009.

Sawyer, D. T., and Valentine, J. S. (1981), *Acc. Chem. Res., 14*, 393–400.

Stallings, W. C., Pattridge, K. A., Strong, R. K., and Ludwig, M. L. (1984), *J. Biol. Chem., 259*, 10695–10699.

Stallings, W. C., Pattridge, K. A., Strong, R. K., and Ludwig, M. L. (1985), *J. Biol. Chem., 260*, 16424–16432.

Stallings, W. C., Powers, T. B., Pattridge, K. A., Fee, J. A., and Ludwig, M. L., (1983) *Proc. Natl. Acad. Sci.* (USA), *80*, 3884–3888.

Steffens, G. J., Bannister, J. V., Bannister, W. H., Flohe, L., Gunzler, W. A., Kim, S.-M.A., and Otting, F. (1983), *Hoppe-Seyler's Z. Physiol. Chem., 364*, 675–690.

Steinman, H. M. (1982), *J. Biol. Chem., 257*, 10283–10293.

Sun, M., and Zigman, S. (1978), *Anal. Biochem., 90*, 81–89.

Symonyan, M. A., and Nalbandyan, R. M. (1972), *FEBS Lett., 28*, 22–24.

Takahashi, M., and Asada, K. (1982), *J. Biochem., 91*, 889–896.

Terech, A., Pucheault, J., and Ferradini, C. (1983), *Biochem. Biophys. Res. Commun., 113*, 114–120.

Thornalley, P. J., Sarchet, A. W., Hill, H. A. O., Bannister, J. V., and Bannister, W. H. (1982), *Inorg. Chim. Acta, 67*, 75–78.

Tyler, D. D. (1975), *Biochem. J., 147*, 493–504.

Viglino, P., Rigo, A., Argese, E., Calabrese, L., Cocco, D., and Rotilio, G. (1981), *Biochem. Biophys. Res. Commun., 180*, 125–130.

Viglino, P., Rigo, A., Stevanato, R., Ranieri, G. A., Rotilio, G., and Calabrese, L. (1979), *J. Magnet. Res., 34*, 265–274.

Weisiger, R. A., and Fridovich, I. (1973), *J. Biol. Chem., 248*, 3582–3592.

Williams, R. J. P. (1982), *FEBS Lett., 140*, 3–10.

Willson, R. L. (1977), *Chem. Indust., 5*, 183–193.

Methods of Biochemical Analysis, Volume 32
Edited by David Glick
Copyright © 1987 by John Wiley & Sons, Inc.

METHODS OF BIOCHEMICAL ANALYSIS VOLUME 32

The Radiation Inactivation Method as a Tool to Study Structure-Function Relationships in Proteins

GUY BEAUREGARD, *Section de Génétique Médicale, Centre de Recherche Pédiatrique, Hôpital Sainte-Justine, Université de Montréal, Montréal, Canada,* ARLETTE MARET AND ROBERT SALVAYRE, *Laboratoire de Biochimie Médicale, Faculté de Médecine Purpan, Université Paul Sabatier, Hôpital Purpan, Toulouse, France,* AND MICHEL POTIER, *Section de Génétique Médicale, Centre de Recherche Pédiatrique, Hôpital Sainte-Justine, Université de Montréal, Montréal, Canada*

I. INTRODUCTION

A variety of physicochemical methods are available to determine the molecular size of proteins. Among them, the radiation inactivation method is unique since it does not require a purified or even a soluble protein preparation. Thus membrane proteins can be studied in their natural environment, in the absence of detergent. The principle of the method is to expose lyophilized or frozen protein preparations to high-energy ionizing radiations. The decay of biological activity or loss of protein integrity, due to radiation hits on individual molecules, is followed as a function of dose. The analysis of decay curves by target theory gives the size of the protein (Lea, 1955). Various terms have been employed, more or less interchangeably, to describe molecular size obtained by radiation inactivation: target size (Lea, 1955), functional unit (Kempner and Schlegel, 1979), and molecular weight (Lea, 1955; Kepner and Macey, 1968). The target theory allows us to define the target size as the mass of the protein whose integrity is destroyed following a direct hit by ionizing radiation. Later the term functional unit was introduced for oligomers, membrane proteins, and glycoproteins. It was defined as the minimal assembly of structures (subunits) required for the expression of a given biological activity (Steer et al., 1981). On the other hand, molecular weight refers to the whole molecule including all subunits, bound lipids, and covalently associated sugars when applicable. In the first part of this review, only all-polypeptide monomers will be discussed to establish the basic principles of the radiation inactivation method. The concept of functional unit, and experimental values of target size and molecular weight, will be considered as equivalent until more complex proteins are studied. They will then be distinguished and precisions concerning the basic principles will be given. Finally, we will discuss how each value can be measured or deduced and how the information can be used to establish structure-function relationships in oligomeric proteins.

Other review articles have been published on the radiation inactivation method (Pollard et al., 1955; Kempner and Schlegel, 1979), two of them recently (Jung, 1984; Harmon et al., 1985). Since we do not want to be repetitious, the theory and experimental procedure will only be described briefly, although enough details will be given to allow the reader to follow the discussion. We will focus our attention primarily on the basic concepts of target theory and protein inactivation.

II. PHYSICS AND CHEMISTRY OF PROTEIN INACTIVATION

1. Physics

The interaction of ionizing radiations (gamma rays, high-energy accelerated electrons, and X-rays) with matter and the mechanisms related to protein inactivation is not yet fully understood. However, we will provide an overall view of the basic physical and chemical phenomena involved. The direct effect of an ionizing radiation on a macromolecule such as a protein can be described as follows. When a high-energy ionizing radiation hits a protein, part of the incident particle energy is transferred to the polypeptide. This causes ionization of an atom leaving behind a positively charged protein. Due to the large amount of transferred energy, ionization does not depend on the nature of the atom (Dartinger and Jung, 1970) and on temperature (Lea, 1955; Augenstein and Mason, 1962). Besides ionization, an electron can be excited to higher-energy orbitals. The excitation energy is small, corresponds to an allowed electronic transition, and, contrarily to ionization, depends on chemical composition (Augenstein et al., 1964). A single hit by a radiation causes a primary ionization (Lea, 1955) or an excitation in about one picosecond (Jung, 1984); ionization and excitation occur nearly at equal frequencies (Augenstein et al., 1964).

2. Chemistry

The charge, or the excited electron energy, can migrate from atom to atom along the polypeptide chain (Patten and Gordy, 1960). In ionized proteins, a covalent bond is finally broken either at the point of impact or elsewhere along the polypeptide chain. Excited electrons in proteins can occasionally be ejected through valence reorganization, causing a rupture of a covalent bond. Such events precede the appearance of free radicals in the milliseconds (Jung, 1984). The breakage of a chemical bond in itself, or through an indirect effect on the secondary or tertiary structure, yields a damaged protein that completely loses its biological activity (Lea, 1955).

The inactivation process is completed within a period of seconds to hours following irradiation (Jung, 1984).

3. Classical Target Theory

The fundamental dogma of the target theory is that all single hits result in damaged and inactive protein molecules. There will be no partially active molecules after a direct hit, and those unhit molecules will maintain all their catalytic properties intact. Experimental evidence in favor of this conclusion has been provided by determining affinity constants, K_m or K_d of several enzymes and receptors, following exposure to increasing doses of radiation. In most proteins studied, the activity decreased with dose as expected but K_m or K_d values remained constant, indicating that the unhit active protein molecules had normal kinetic properties (Fluke, 1972; Steer et al., 1981).

With low linear-energy-transfer (LET) particles such as electrons, gamma, or X rays of about 1 MeV, ionizations or hits occur at a distance greater than 100 nm from each other. This distance is larger than protein diameters (about 4 to 15 nm) so that ionizations occur completely at random in the protein sample. The statistical Poisson distribution for the probability of no hit, $P(0)$, is applied for such independent events and expressed in a simplified form as

$$P(0) = \exp(-\mu D) \tag{1}$$

or in terms of the relative survival of intact molecules as

$$\frac{A_D}{A_0} = \exp(-\mu D) \tag{2}$$

where A_0 is the activity at zero dose and A_D is the activity at a dose D. The coefficient μ is directly proportional to the molecular weight of the protein independently of its shape (Lea, 1955) and represents the slope of the semilogarithmic plot of remaining activity versus dose. Such a linear relationship was observed experimentally for most proteins and is essential to validate the single-hit target theory as a method to interpret radiation inactivation data (Lea, 1955). Then, by definition

$$\mu = \frac{1}{D_{37}} \tag{3}$$

where D_{37} is the dose at which 37% of initial biological activity remains in the protein preparation.

Since the dose, D, is usually expressed in Mrad (10^8 ergs/g) or in kGray (kjoule/kg) and the product μD in equation (2) must be dimentionless,

then μ represents a mass per unit energy absorbed (Swillens and Dumont, 1981; Kempner and Miller, 1983). Until recently the common but erroneous practice in the literature was to express target size in volume units.

The proportionality factor between M_r and $1/D_{37}$ was established empirically by Kepner and Macey (1968) at 30°C:

$$M_r = \frac{6.4 \times 10^5}{D_{37}} \tag{4}$$

where D_{37} is expressed in Mrad. This empirical equation is widely used to calculate M_r of proteins from experimentally determined D_{37} values.

4. The Temperature Effect

Temperature affects the loss of biological activity versus dose curves of proteins (Fluke, 1966). About 2.9-fold more dose is required to inactivate a given proportion of the molecules in a preparation at −135°C than at 30°C. This observation is valid for all proteins studied, and the 2.9-fold correction factor was applied to obtain M_r from equation (4) when D_{37} was measured at −135°C (Kempner and Haigler, 1982).

The radiation inactivation process involves Q, the average amount of radiation energy required to inactivate one mole of protein (Kepner and Macey, 1968). Q for radical formation, one of the steps leading to protein inactivation, is temperature dependent (Müller, 1962). Beauregard and Potier (1985) proposed that the effect of temperature on Q is directly responsible for the temperature dependence of protein inactivation, as revealed by the variation of D_{37}, since the number of hits (or ionizations) per unit mass of the sample is temperature independent (Lea 1955; Augenstein and Mason, 1962). Thus the efficiency of a hit to result effectively in the inactivation of a molecule depends on the irradiation temperature. From Kepner and Macey (1968) and Jung (1984), we rewrite equation (4) to take the temperature into account:

$$M_r = \frac{10^{-8}Q(t)}{D_{37,t}} \tag{5}$$

This equation contained an algebric error in Beauregard and Potier (1985) also affecting $Q(30)$ and equation (6). It is valid at any temperature because the ratio $Q(t)/D_{37,t}$ is constant for a protein of a given M_r. By combining equations (3) and (5), μ in equation (1) and (2) is thus $(M_r/10^{-8}Q(t))$; the value of Q at 30°C is determined as 6.4×10^{13} erg/mol (Kepner and Macey, 1968). This represents enough energy to break 15 to 20 covalent bonds in a protein.

An expression of Q as a function of temperature can be obtained from

the compilation of data by Kempner and Haigler (1982) on D_{37} of proteins irradiated between −200 and +200°C. They reported a linear relationship between log $[D_{37,t}/D_{37,30}]$ (or log $[Q(t)/Q(30)]$ from equation (5)) and t in °C. From this relationship, the value of $Q(30)$, and equations (3) and (5), $Q(t)$ (in erg/mol of protein inactivated) can be calculated empirically for any temperature t (in °C) between −200 and +200°C (Beauregard and Potier, 1985):

$$\log Q(t) = 13.89 - 0.0028t \tag{6}$$

Combining equations (5) and (6), a more general form of equation (4), taking the irradiation temperature into account, is obtained:

$$\log M_r = 5.89 - \log D_{37,t} - 0.0028t \tag{7}$$

valid between −200 and +200°C.

The exact temperature-sensitive physical and chemical steps in the chain of events involved in protein inactivation after a hit are largely unknown. Ionization itself is not temperature dependent because of the large amount of energy deposited (Lea, 1955; Augenstein and Mason, 1962). On the other hand, charge or excited electron migration has been associated to covalent bond breakage (Patten and Gordy, 1960; Müller, 1962). Excited electrons by themselves considering the low energy involved are unlikely to cause breaks in the polypeptide chain or in the amino acid side chains (Lea, 1955). However, in combination with higher temperatures and more intense interatomic motion, these could damage the protein. Henricksen (1966) concluded that, for trypsin, radical formation and loss of activity are due to the expression of the same basic processes since their activation energies are identical. Other temperature-sensitive mechanisms can also be implicated such as a higher frequency of self-repairing events at low temperature (radical and/or electron recombination) (Pollard et al., 1955; Usatyi and Lazurkin, 1962). This could explain, at least in part, why Q for inactivation is higher at low temperature.

5. Criticism of the Target Theory

Some of the basic assumptions of the target theory have been challenged. Lea (1955), Pollard et al. (1955), and Usatyi and Lazurkin (1962) postulated that not all ionizations effectively result in permanent damage to structure and function of proteins. In some proteins two hits could be needed to inactivate a protein. Jung and Schüssler (1968) found altered amino acid contents of both active and radiation-denatured RNAse separated after irradiation. Their data suggest that even active enzyme mole-

cules, remaining after irradiation, are altered by radiations. This result contradicts the target theory which postulates a single-hit inactivation mechanism.

III. EXPERIMENTAL PROCEDURES

1. Radiation Sources

The ionizing radiations should be of sufficient energy to penetrate the whole thickness of the biological sample. Particles of at least 1 MeV, accelerated electrons from van de Graaff generators or linear accelerators, gamma rays from ^{60}Co sources, and X rays have been employed for radiation inactivation of proteins. All these radiations have in common that they are of the low LET type. High LET particles like protons and deuterons are currently less used and will not be discussed here. Relatively large radiation doses are needed to ensure sufficient decrease of biological activity to obtain a precise D_{37} value. Although the total dose needed varies with M_r of the protein of interest and temperature of irradiation, it must be around 15 Mrad at 30°C and 50 Mrad at −135°C. Electron accelerators deliver in the range of 1 to 2 Mrad/min and van de Graaff generators give about 1 Mrad per discharge (Jung, 1984). Gamma irradiators give lower dose rates, in the range of 0.1 to 3 Mrad/h, and the duration of radiation exposure must be increased accordingly.

Gamma irradiators present the advantage over electron sources that they are more readily available and much easier to use (Beauregard and Potier, 1982; Beauregard et al., 1983). The ^{60}Co source is calibrated with enzymes of known D_{37} values and the time (t_{37}) needed to decrease enzyme activity to 37% of initial value is determined. The dose rate of the equipment is obtained directly from D_{37}/t_{37} ratios of standard proteins: catalase (D_{37}, 2.78 Mrad; Norman and Ginoza, 1958), β-glucuronidase (D_{37}, 7.9 Mrad; Shikita and Hatano-Sato, 1973), rat liver cytosolic neuraminidase (D_{37}, 11.67 Mrad; Beauregard and Potier, 1982), and bovine erythrocyte acetylcholinesterase (D_{37}, 8.8 Mrad; Beauregard et al., 1980). Using standard proteins for calibration presents the advantage that proteins of unknown D_{37} are irradiated in the same conditions. Once the equipment is calibrated, the dose rate, R_t, can be obtained at any time by applying a simple correction for the radioactive decay of the ^{60}Co source (half-life, 5.26 years):

$$R_t = R_0 \times 10^{-0.301t/5.26} \tag{8}$$

where t is the time expressed in years since the initial calibration. In our

laboratory we have used three different Gammacell model 220 irradiators (built by the Atomic Energy of Canada, Ottawa), with dose rates varying between 0.1 and 3 Mrad/h. We have shown previously that there is a linear relationship between the amount of radioactive ^{60}Co in the Gammacell and the dose rate delivered by the equipment (Beauregard and Potier, 1986).

The dose rate varies significantly inside the cylindrical irradiation chamber of the Gammacell as shown by isodose curves (Curzio and Quaranta, 1982). Thus the tubes containing the protein samples for irradiation must be localized precisely in radial symmetry around the axis of the chamber. A special tube rack is used for this purpose, as described by Beauregard et al. (1983). We have now modified this rack to increase the capacity and to perform more irradiation experiments simultaneously. The sample tubes (Eppendorf 1.5 ml microcentrifuge) are placed on four plates instead of two, each plate containing two concentric rows of 16 tubes as previously described (Beauregard et al., 1983). Table I gives

TABLE I

Dose Rate at Different Positions Inside the Cylindrical Irradiation Chamber of a Gammacell Model 220 Irradiator, Expressed Relatively to Dose Rate at Geometric Center

X (cm)	*Y* (cm)	RELATIVE DOSE
0	0	1.000
5.25	−9.45	0.881
	−4.50	1.070
	+0.95	1.158
	+5.15	1.037
6.25	−9.45	0.909
	−4.50	1.124
	+0.95	1.209
	+5.15	1.103

Note: The positions are given in the plane containing the axis of the cylinder. This information was used to construct a special tube rack that localized the sample tubes for irradiation at the *X*, *Y* positions indicated. The rack was made of four circular plates containing two concentric rows of 16 holes to accept the sample tubes.

relative values of dose rate at the sample positions determined by this rack. This arrangement gives the possibility of performing eight experiments simultaneously at isodoses. Considerable precision in the determination of dose rate can be achieved with this procedure in Gammacell irradiators since the agreement between predicted dose rate, determined from isodose curves (Curzio and Quaranta, 1982), and experimental values at various positions inside the irradiation chamber was better than 2.7% (Beauregard et al., 1983). This equipment is also particularly suited for the study of large molecular weight proteins where accurate low doses are required (Noël et al., 1983).

High dose rate sources, such as electron accelerators and van de Graaff generators, need some temperature control during irradiation to avoid overheating and to keep frozen samples at a constant temperature (Levinson and Ellory, 1974; Kempner and Haigler, 1982). This is usually obtained with a flow of cold air, directed at the protein samples, or by keeping samples in close contact with a cold metal block during irradiation. These precautions are not required with gamma irradiators since the temperature inside the chamber is never higher than 38°C for the largest source we have tested (delivering about 3 Mrad/h). With lower dose rate equipment (<1 Mrad/h) the increase of temperature is negligible. In principle, it is possible to conduct radiation inactivation experiments at low temperature with Gammacell irradiators since an accessory for circulating liquid nitrogen inside the chamber is available from the manufacturer. However, to our knowledge, such a procedure has not yet been used.

2. Preparation of the Biological Samples

We routinely prepare 30 tubes (Eppendorf 1.5 ml microcentrifuge) each containing enough lyophilized material for performing one biological assay after irradiation. Tubes are irradiated in triplicate allowing 10 increasing doses to be given. Oxygen must be removed from the tubes or replaced by an inert gas such as nitrogen to avoid secondary inactivation of proteins (Butler and Robins, 1962). In our laboratory this is done by purging tubes with nitrogen in an inflatable glove box; however, the more usual procedure is to seal the glass ampoules under vacuum (Levinson and Ellory, 1974). The effect of oxygen, measured as D_{37} (air)/D_{37} (vacuo) depends on the enzyme studied and varies between 0.35 and 1 (Kepner and Macey, 1968). The protein preparation must be frozen or lyophilized to prevent secondary inactivations with diffusible radiolytic products of water. Although lyophilization does not remove all the water, this procedure is sufficient to achieve this goal. Proteins in water solutions

are about 100-fold more sensitive to ionizing radiations, and there is little or no discrimination between proteins on the basis of M_r. This is due to secondary inactivations that account for the majority of inactivations as compared to the primary effect.

For the study of membrane transport systems, where the membrane vesicles should remain intact for assay after irradiation, it is possible to freeze membrane preparations in a cryoprotective medium (e.g., containing glycerol) (Cuppoletti et al., 1981). Alternatively, the transport system can be extracted after irradiation and reincluded into fresh liposome membranes for assay. The latter method was used by Goldkorn et al. (1984) to study the lactose transport system of *E. coli*.

3. Dosimetry

Whatever the source of radiation used, the dose delivered to the biological samples is determined by the time of exposure to radiations. Thus the dose delivered by the radiation source must be measured with precision. Dosimetry can be performed with a ferrous sulfate solution (Fricke and Morse, 1927), thermoluminescent dosimeters, bleaching of films (Hart and Fricke, 1967), Perspex dosimetry (Berry and Marshall, 1969), or calibration with standard enzymes (Beauregard et al., 1980; Beauregard and Potier, 1982; Lo et al., 1982). In many laboratories, control enzymes with known D_{37} are added to protein preparations as internal standards so that any variation between experiments could be corrected for. Because of the better precision of dose rate in Gammacell irradiators, this precaution is not necessary.

When irradiating at low temperature, the temperature sensitivity of the various dosimeters must be taken into account to determine the dose rate. Thermoluminescent dosimeters are not affected by temperature, contrary to the other calibration methods (Kempner and Haigler, 1982; Jung, 1984).

IV. TARGET SIZE, RADIATION INACTIVATION SIZE, AND FUNCTIONAL UNIT OF PROTEINS

In their extensive review of literature data on proteins studied by radiation inactivation, Kempner and Schlegel (1979) noted that the size of several oligomeric proteins corresponded to that of their monomer, whereas others yielded the size of the whole oligomer. They suggested that with the latter proteins, the quaternary structure is necessary for the expression of biological activity and that the destruction of one monomer

causes the loss of activity of the whole oligomer. They also provided an alternative explanation for their observation; they postulated that the energy deposited after a hit in one monomer could be transferred to all other monomers, causing the destruction of all the active sites in a molecule. They introduced the concept of the "functional unit," instead of target size or of M_r, to describe such an interactive functional or structural assembly. Experimental evidence has now been provided that both explanations are valid with different proteins. Pursuing this line of thinking, we would like to propose a systematic approach and to clarify this problem of interpretation of experimental data obtained by radiation inactivation.

In order to discuss how radiation inactivation data could be used to obtain information on structure-function relationships in oligomeric proteins, it is necessary to define more precisely the terms employed to describe size measurements: target size and functional unit. We will also introduce a new term, the radiation inactivation size (RIS). Target size and RIS refer to experimentally determined values, whereas functional unit is a concept (Table II).

1. Target Size

This entity is the mass of one mole of the polypeptide(s) whose backbone chain(s) have been broken down as a result of a single direct hit by an ionizing radiation. In this definition we take into account that the energy may, or may not, be transferred between subunits in an oligomeric protein. If energy transfer occurs, the target size is the sum of the sizes of all the polypeptides in which the energy has been transferred. Thus the target size is a structural parameter.

Lea (1955) defined the target as "the molecule or structure in which an ionization has to be produced." He postulated that each ionization lead to a measurable inactivating event and that electron excitation had a negligible contribution to inactivation. The temperature effect suggests that it might not be the case. In fact temperature influences the number of

TABLE II

Classification of Rationalization and Experimental Values in the Analysis of Radiation-Inactivation Experiments

RATIONALIZATION	EXPERIMENTAL VALUE
Target	Target size
Functional unit	None
Size of target or functional unit	Radiation inactivation size

inactivated molecules per unit of dose. The definition of target size given in this chapter takes into account all factors that precede the irreversible end effect: the breakdown of the polypeptide. Although our definition is clearly different from that of Lea (1955), it has the advantage of being an experimental parameter.

The experimental method to determine target size is to irradiate a purified protein preparation with varying doses and to follow the remaining quantity of integral structure by electrophoresis on a SDS-polyacrylamide gel (Saccomani et al., 1981; McIntyre et al., 1983; Edwards et al., 1985). The target size (not M_r) is obtained from equation (4) or (7) by following the decrease of protein-specific dye-binding intensity or radioactivity (if the protein has been labeled with a radioactive precursor) as a function of dose. An example of a radiation inactivation experiment conducted with purified H^+-K^+ ATPase is shown in Fig. 1. The enzyme is composed of a unique monomer (M_r, 100,000) which loses structural integrity as a function of radiation dose with a target size of 250,000 (Fig. 1*A* and *B*). These results indicate energy transfer between subunits causing the destruction of three subunits for each hit. By this approach it is also possible to determine target sizes of proteins with no measurable biological activities such as the Ca^{2+} binding protein (Table III). This table lists all the proteins for which a target size has been determined. From now on, we will use the term "target size" according to the definition just given.

2. Radiation Inactivation Size

This entity (RIS) is a purely experimental parameter that we feel justified to introduce at this point of the discussion. It is the mass of one mole of protein structure(s) whose associated biological activity is abolished after a single hit by an ionizing radiation. It is obtained by plotting on a semi-logarithmic scale the relative initial biological activity of a protein as a function of dose and using equation (4) or (7) to calculate the RIS (not M_r). This parameter is used for a practical purpose since it makes no assumption on the functional unit or target size of a protein. It gives no indication of whether there has been energy transfer between subunits. Most radiation inactivation experiments that have been described in the literature resulted in the determination of a RIS. The RIS of various oligomeric proteins will correspond to the target size (structural) and/or the functional unit size (functional). For the H^+-K^+ ATPase, the RIS is similar to the target size (Fig. 1*C*). In the literature the distinction among target size, RIS, M_r and functional unit has not been fully appreciated.

The experimental error in the determination of RIS, obtained by

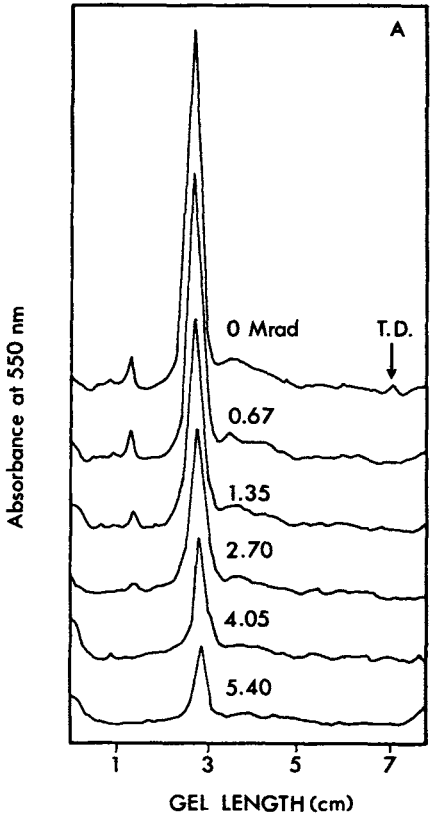

Fig. 1. Determination of target size and RIS of H^+-K^+ ATPase *(A)* electrophoregram of gastric ATPase before and after exposure to radiation. T. D., tracking dye. *(B)* semilogarithmic plot of the decrease in Coomassie blue staining of the M_r 100,000 polypeptide after irradiation showing a target size of 250,000. *(C)* inactivation data for Mg^{2+} ATPase (▲, △), K^+ ATPase (●, ○), and K^+ *p*-nitrophenylphosphatase (■, □) were plotted on a semilogarithmic scale as a function of radiation dose. A RIS of 270,000 was calculated for all three activities when gastric membranes were irradiated as frozen suspensions at −50°C (solid line and symbols). Similarly a RIS of 320,000 was obtained from the lyophilized samples irradiated at 23°C in vacuo (dashed line, empty symbols). Doses at −50°C are converted to their equivalent at 23°C (From Saccomani et al., 1981.)

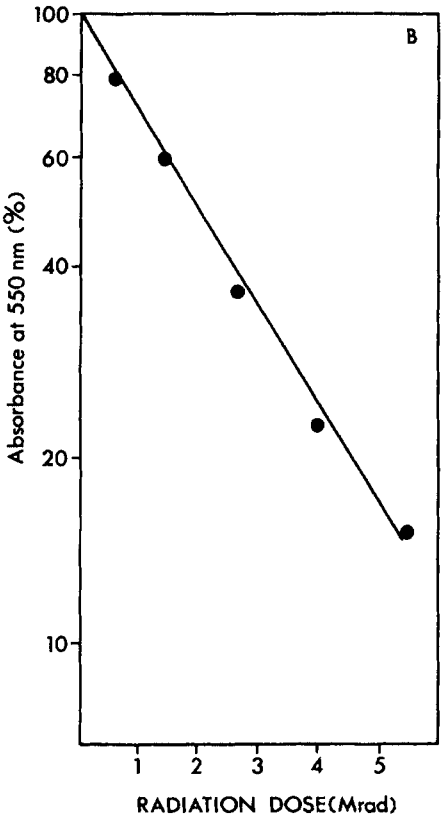

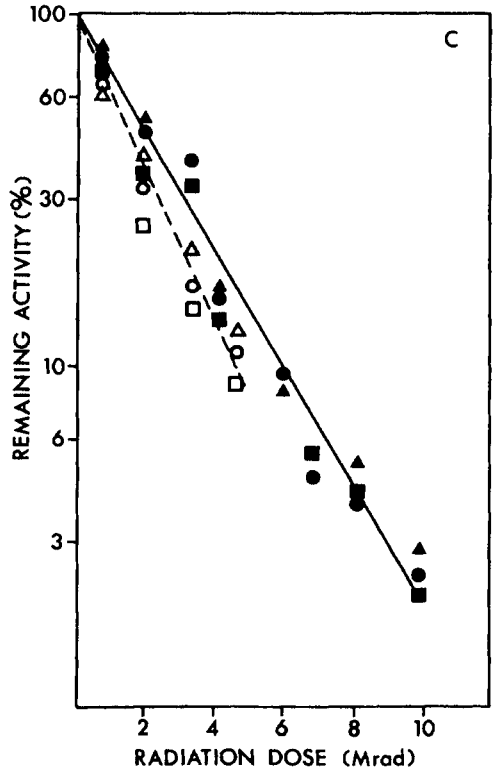

Fig. 1. *(Continued)*

TABLE III

Proteins with Known Target Size and Radiation Inactivation Size

PROTEIN	TARGET SIZE	RIS	MONOMER SIZE	REFERENCE
H^+-K^+ ATPase	250,000	270,000	100,000	Saccomani et al. (1981)
Ca^{2+} pump	229,000	213,000	110,000	Chamberlain et al. (1983)
Ca^{2+}-Mg^{2+} ATPase	230,000	214,000	120,000	Hymel et al. (1984) le Maire et al. (1976a, b)
H^+ ATPase	220,000	230,000	100,000	Bowman et al. (1985) Bowman and Slayman (1979)
Na^+-K^+ ATPase	128,000(α)	184,000	94,000 −121,000(α) 32,000 −43,000(β)	Karlish and Kempner (1984) Hayashi et al. (1983) Peters et al. (1981)
Na^+-dependent glucose transporter	298,000	343,000	85,000	Takahashi et al. (1985)
Ca^{2+} binding protein	49,500	—	44,000	Hymel et al. (1984) MacLennan and Wong (1971)
Acetylcholinesterase	220,000	260,000	70,000	Saccomani et al. (1981) Rosenberry et al. (1974)
β-Hydroxybutyrate dehydrogenase	104,000	119,000	31,000	McIntyre et al. (1983) Bock and Fleischer (1975)
Glutamate dehydrogenase	72,000	257,000	56,000	Kempner and Miller (1983) Hucho and Janda (1974)
3-Hydroxy-3-methyl glutaryl CoA reductase	98,000	202,000	97,200	Edwards et al. (1985) Chin et al. (1984)

comparing RIS of several proteins with accepted values of M_r in the literature, is around 14% (Kempner and Schlegel, 1979).

3. The Functional Unit

This concept has been introduced by Kempner and Schlegel (1979) and defined as "the *minimal* assembly of structures required for expression of a given biological activity" (Steer et al., 1981). The functional unit can be deduced in monomers or in oligomers that show no intersubunit energy transfer, including those proteins where the native quaternary structure is required for the expression of biological activity. In addition, with

proteins that manifest several biological activities, each associated to a putative protein domain such as the Na^+-K^+ ATPase (Ottolenghi and Ellory, 1983), the functional unit concept takes into account that the inactivation of each domain could occur independently of the others. Specific functional units smaller than the entire polypeptide chain could be defined from experimental RIS values. In the case of oligomers with intersubunit energy transfer, the functional unit cannot be deduced solely on the basis of radiation inactivation data. The possibility that each subunit is able to express biological activity by itself is masked by the destruction of all subunits through energy transfer.

4. Relationships between Experimental Data and Concepts

In this section we will discuss what could be learned from radiation inactivation experiments on structure-function relationships in oligomeric proteins. Initially only all-polypeptide monomers have been studied by radiation inactivation, and in this particular case, target size, RIS, functional unit, and M_r are identical. In more complex systems, however, these terms may have different meanings and correspond to different experimental values. We will now discuss each particular case and explain each definition in its context.

Table II distinguishes between concepts and experimentally determined values obtained by the radiation inactivation method. We use the terminology of boolean logic to explain various alternatives between experimental values and concepts corresponding to subunits or whole oligomer of proteins. In all the relations we develop, parameters on the left-hand side of the arrow are experimentally determined, and those on the right-hand side are deduced for each particular situation. We will describe the various possibilities that may be encountered when irradiating pure monomeric, homo-oligomeric, and hetero-oligomeric proteins of known M_r and subunit size.

A. MONOMERS

Target size and RIS are that of the monomer. The following relationship holds:

$$\mathrm{TS}m \vee \mathrm{RIS}m \longrightarrow \mathrm{FU}m \tag{9}$$

where TS*m* means that the target size is the monomer size, $\vee$ is the boolean operator "or," RIS*m* means that the radiation inactivation size is the monomer size, and FU*m* means that the functional unit is the monomer. This relation is trivial since for monomers, target size, RIS, and functional unit size all correspond to that of the monomer.

B. HOMO-OLIGOMERS

A homo-oligomeric protein with a RIS corresponding to the monomer size. The corresponding boolean relation is

$$\mathrm{RIS}m \longrightarrow \mathrm{TS}m \;\&\; \mathrm{FU}m \tag{10}$$

where & is the boolean operator "and." If the RIS is the monomer size, then the target size and functional unit necessarily correspond to the monomer. In this case it is deduced that the target size is the monomer since it cannot be larger than the RIS; that is, the structure destroyed by a hit cannot be larger than that supporting the activity. Although no formal determination of target size of such proteins has been published in the literature, there are several examples of homo-oligomeric proteins that yield RIS corresponding to the monomer (reviewed by Kempner and Schlegel, 1979). For all these proteins we predict that their target size will also be the monomer; the same holds true for monomeric proteins. It must also be noted that the radiation inactivation method, when applied to such proteins, gives an information difficult to obtain by other methods; that is, the subunit of these proteins is active per se in the native oligomeric structure.

The target size corresponds to the monomer but the RIS is a multiple of monomer size. The relation describing this situation is

$$\mathrm{TS}m \;\&\; -\mathrm{RIS}m \longrightarrow -\mathrm{FU}m \tag{11}$$

If the target size is the monomer and the RIS is the oligomer (the minus signs in front of TS*m*, RIS*m*, and FU*m* denotes that the proposition refers to the oligomer instead of the monomer), this implies that the functional unit size is that of the RIS that corresponds to the oligomer. Kempner and Miller (1983) reported that the target size of the homo-hexameric glutamate dehydrogenase corresponded approximately to the monomer, whereas the RIS was that of the whole enzyme (Fig. 2 and Table III). There is no intersubunit energy transfer in this enzyme, and the large RIS (that of the oligomer) means that the whole quaternary structure is required for enzymatic activity. In these homo-oligomers the target size is not equal to the RIS, in contradiction with target theory. This discrepancy will be explained in the conclusions.

The target size is a multiple of the monomer size. The following relation applies:

$$-TSm \longrightarrow -\mathrm{RIS}m \tag{12}$$

This means that there is energy transfer between subunits which are all destroyed following a single hit. Several examples of such proteins are

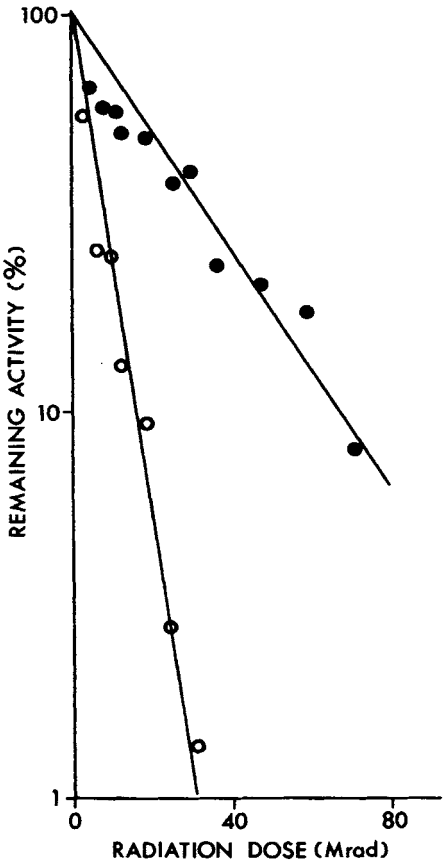

Fig. 2. Effects of high-energy electron irradiation at −135°C on frozen solutions of fluorescein isothiocyanate-coupled glutamate dehydrogenase. Surviving enzyme activity (○) (RIS) and intensity of Coomassie blue stain of the monomer subunit on the gel electrophoregrams (●) (target size) as a function of radiation exposure. (From Kempner and Miller, 1983.)

given in Table III. It must be pointed out that under these conditions the RIS necessarily corresponds to the oligomer size. No definite conclusion can be obtained on the functional unit size when the structure (target size) of the whole oligomer is destroyed. There are no means to determine, by the radiation inactivation method alone, the *minimal* assembly of structures required for the expression of biological activity. This conclusion differs from that of Kempner and Schlegel (1979) who believe that the

functional unit size is a parameter that could be determined for all proteins by the radiation inactivation method. This is due to the confusion between RIS and functional unit. This ambiguity has been resolved with the present rationalization. To illustrate our point, let us consider the muscle sarcoplasmic Ca^{2+}-Mg^{2+} ATPase (Table III), which is a homodimer of subunit M_r 120,000 by SDS-polyacrylamide gel electrophoresis. This enzyme is a good example of a protein where intersubunit energy transfer (target size is the dimer) masks a smaller functional unit size (the monomer) since after solubilization and dissociation in deoxycholate, the free subunits are active per se (le Maire et al., 1976a, b). In this example the value of RIS most likely reflects the target size, *not* the functional unit (Chamberlain et al., 1983).

The structural conditions required for intersubunit energy transfer are not completely understood. However, the study of Ca^{2+}-Mg^{2+} ATPase reveals that disulfide bridges are not necessary for energy transfer since a similar M_r of 120,000 was obtained by SDS-polyacrylamide gel electrophoresis of the pure enzyme in presence or in absence of mercaptoethanol (le Maire et al., 1976a, b). This result indicates that there is no disulfide bridge linking the two subunits; yet the target size corresponds to the dimer (Table III).

Relation (12) predicts that when the target size is oligomeric, the RIS cannot be monomeric.

C. HETERO-OLIGOMERS

For proteins composed of several subunits of varying sizes, the radiation inactivation method might help in defining which subunits are required for the expression of a given biological activity. We will describe various situations that may be encountered when studying such systems.

The RIS of an hetero-oligomer is that of one of the subunits. The functional unit size will correspond to that of the subunit responsible for the biological activity. However, confusion might occur if the same RIS is obtained by rearranging two or more smaller subunits in a manner to obtain a similar RIS value. In this case a target size analysis of all subunits with a purified system might help distinguish between the possibilities.

Intersubunit energy transfer occurs in the hetero-oligomer, and the RIS is larger than the smallest subunit size. The target size of the various subunits may be determined, and some information on the arrangement of subunits in the protein complex may be obtained. Physical proximity of subunits has to be assumed if energy transfer is observed. If two or more subunits are close together in the protein complex and energy transfer occurs, then, follow-

ing the decrease of each band intensity as a function of radiation dose will give an identical target size corresponding to the sum of the subunits sizes.

No intersubunit energy transfer occurs in the hetero-oligomer, and the RIS is larger than the smallest subunit size. If the target size of each subunit is equal to each subunit size determined by another method (e.g., SDS-polyacrylamide gel electrophoresis), then it can be deduced that the quaternary structure, involving two or more subunits, is mandatory for the expression of biological activity. The RIS will then represent the whole oligomer or the sum of the sizes of the subunits necessary for the activity. The RIS will then correspond to the functional unit. An example of such an hetero-oligomer is the pig kidney Na^+-K^+ ATPase where the catalytic subunit α has a M_r 94,000–121,000 and is associated with a 32,000–43,000 subunit β (Table III). The TS corresponds to subunit α whereas the RIS with ATP as substrate is the sum of both subunits, thus demonstrating an oligomeric functional unit for this enzyme.

V. WHAT CONSTITUTES TARGET SIZE AND/OR RADIATION INACTIVATION SIZE OF A PROTEIN

In the preceding discussion, we have established that the target size (or RIS) is not always identical to M_r. We will now discuss examples of (1) proteins associated to lipids, (2) membrane protein-detergent complexes, and (3) glycoproteins to show that associated lipids, detergents, or sugars are not part of the target size or RIS obtained by radiation inactivation.

1. Lipids

Two examples of membrane proteins physically associated to lipids will be discussed: bovine erythrocyte acetylcholinesterase and skeletal muscle sarcoplasmic reticulum Ca^{2+}-Mg^{2+} ATPase.

Bovine erythrocyte-membrane acetylcholinesterase readily solubilizes as a homo-dimer in hypotonic medium (monomer M_r, 72,000; Berman, 1973), with a partial specific volume of 0.811 ml/g suggesting the presence of associated lipids. The M_r of the lipid-protein complex, obtained from Stokes radius and sedimentation coefficient, is 210,000 (Beauregard and Roufogalis, 1979). The RIS is 144,000 for the dimer with associated lipids (Beauregard et al., 1980). Thus it is concluded that phospholipids are not part of the RIS of acetylcholinesterase even though they are part of the M_r.

The Ca^{2+}-Mg^{2+} ATPase is the major protein constituent of the skeletal muscle sarcoplasmic membranes. This enzyme can be solubilized

with detergents, purified, the detergent removed, and the enzyme reconstituted with various quantities of phospholipids (ratio of lipids to proteins, 0.14 to 0.32 by weight). Whatever the quantity of phospholipids bound to the enzyme, the RIS always corresponds to the target size, twice that of the monomer (Hymel et al., 1984; Table III). This enzyme is a homo-dimer in situ (Hymel et al., 1984) of monomer size 120,000 (le Maire et al., 1976a,b). Neither the target size nor the RIS correspond to the M_r, which is the sum of the polypeptide chains and bound lipids.

2. Detergents

Triton X-100 and other detergents are routinely used as a first step in the physicochemical characterization of a membrane protein. Although this treatment is necessary for solubilization, it could affect the aggregation state of the protein. Since detergents are so widely used, we have compared the RIS obtained by radiation inactivation of a variety of proteins bound to the membrane and in presence of sufficient quantities of detergent to solubilize the proteins (Beauregard and Potier, 1984). It was observed that the RIS determined in the presence of detergent must be diminished by a factor of 24% to obtain the RIS value. This applies only to membrane proteins, not to soluble proteins which bind little or no detergent (le Maire et al., 1980). This apparent increase in RIS is not proportional to the amount of detergent bound to the protein since steroid sulfatase and γ-glutamyltransferase bind more Triton X-100 than their equivalent weight and have an increased RIS of only about 24% (Beauregard and Potier, 1984). Although the mechanisms causing the increase in RIS value in presence of detergent is not completely understood, a possible explanation is that the detergent may favor secondary inactivations by formation of free radicals close to the proteins and/or by allowing greater diffusion of free radicals.

3. Carbohydrates

One glycoprotein, invertase, has been studied in detail by radiation inactivation. This glycoprotein is composed of two identical 120,000 monomers; each is made of a 60,000 polypeptide core, and the rest is carbohydrates (Trimble and Maley, 1977). The RIS is about 120,000 (Pollard et al., 1952; Lowe and Kempner, 1982). Removal of about 90% of the carbohydrates with endoglycosidase H reduced the M_r (determined by gel filtration) but had no effect on the RIS (Lowe and Kempner, 1982). It was concluded that a hit in the glycosylated portion of the invertase is not transferred to the polypeptide core, the sole part of the molecule apparently required for enzyme activity.

4. Conclusion

The experimental evidence presented suggests that the RIS and target size correspond to the size of the polypeptide portion of the molecule and not to associated structures such as lipids or carbohydrates, even though, as in the case of carbohydrates, these compounds are covalently bound to the protein. Therefore it is incorrect to state that the RIS obtained by the radiation inactivation method gives the M_r of lipid-associated proteins, detergent-associated proteins or glycoproteins.

VI. CONDITIONS INFLUENCING TARGET SIZE AND RADIATION INACTIVATION SIZE

1. Experimental Conditions

The interaction between subunits of an oligomeric protein could be polar, ionic, hydrophobic, or covalent. Any conditions that are likely to affect these interactions, such as buffer composition, pH, Triton X-100, or salt concentration, might affect the RIS value of oligomeric proteins. Genetic mutations that may affect protein conformation and/or subunit interactions are also likely to change RIS of proteins. Literature data on this subject are summarized in Table IV where it can be noted that, in most cases, effector-induced size changes are by a factor of about 2.

Change of buffer influences the RIS of erythrocyte acetylcholinesterases (Beauregard et al., 1980; Parkinson and Callingham, 1982). It is 73,000 or 144,000 depending on the type of buffer used (Beauregard et al., 1980). The presence of phosphate buffer transforms form α of acetylcholinesterase to form β which differs in its catalytic properties (Roufogalis and Beauregard, 1979): the RIS of form α corresponds to the size of the protein part of the dimer, and in form β to that of the monomer. However, the M_r of both forms, determined by hydrodynamic methods, was the same, indicating that the buffer change did not induce dissociation of subunits but only affected subunit interaction in the dimer.

Less information is available for the other proteins presented in Table IV than for the erythrocyte acetylcholinesterases. One exception is the eel acetylcholinesterase where the native tetramer actually splits down to dimers in Triton X-100 (Millar et al., 1973). This enzyme can be purchased from Sigma Chemical Co. (Saint Louis, MO) in two different forms. The type V has a RIS of 255,000 in Tris buffer (Levinson and Ellory, 1974), similar to its RIS and target size in phosphate buffer (Saccomani et al., 1981) (Table III). In contrast, type VI *eel acetylcholinesterase* in Tris buffer has a RIS of 71,000 (Levinson and Ellory,

TABLE IV

Effect of Experimental Conditions during Irradiation on Radiation Inactivation Size of Some Proteins

PROTEIN	AGENT	RIS	AGENT	RIS	REFERENCE
Buffers					
Bovine acetylcholinesterase	none	140,000	phos	73,000	Beauregard et al. (1980)
Human acetylcholinesterase	Tris	67,000	phos	131,000	Parkinson and Callingham (1982)
Chemicals					
E. Coli aspartokinase I	none	320,000	ammo	170,000	Kempner et al. (1980)
E. Coli homoserine dehydrogenase	none	270,000	ammo	140,000	Kempner et al. (1980)
E. Coli *lac* carrier	none	49,000	lact	87,000	Goldkorn et al. (1984)
Alkaline phosphatase	none	67,000	glyc	115,000	Turner and Kempner (1982) Takahashi et al. (1985)
Triton X-100					
Steroid sulfatase	none	533,000	trit	78,600	Noël et al. (1983)
Acetylcholinesterase	none	255,000	trit	150,000	Levinson and Ellory (1974)
β-glucosidase	none	97,800	trit	59,500	Maret et al. (1984)
Mouse neuraminidase	none	46,400	trit	111,500	Yan et al. unpublished
Insulin receptor regulator	none	350,000	trit	850,000	Harmon et al. (1980)
Ligand					
Benzodiazepin receptor	none	102,000	gaba	60,000	Doble and Iversen (1982)

Phos, phosphate buffer; Tris, tris(hydroxymethyl)aminomethane; ammo, ammonium sulfate; lact, D-lactate; glyc, glycerol; trit, Triton X-100; gaba, γ-aminobutyric acid.

1974) corresponding to the monomer (Rosenberry et al., 1974). It is interesting that both type V and type VI acetylcholinesterase are tetramers by hydrodynamic methods. Since the M_r and the subunit size of this enzyme are known, it is possible from relation (10) to deduce a target size of 71,000 for the type VI enzyme. Therefore we suggest that the different RIS observed for the two types of eel acetylcholinesterase is due to a modification of the target size. However, it is not possible to demonstrate that the monomer is active per se with the type V enzyme as it has been done with the type VI enzyme.

Recently Haigler et al. (1985) showed that an intersubunit disulfide bridge is responsible for radiation energy transfer in dimeric ricin. How-

ever, both human erythrocyte and eel acetylcholinesterase contain an intersubunit disulfide bridge (Ott et al., 1983; Rosenberry and Richardson, 1977), but they are not sufficient to cause intersubunit energy transfer in certain buffer conditions since the subunit size was obtained (Table IV and Levinson and Ellory, 1974). (See also Section IV,4,B).

2. Genetic Mutations

Genetic mutations can modify the RIS of oligomeric proteins by inducing modifications in the subunit interactions. This effect was observed with three different enzymes: human spleen glucosylceramide-β-glucosidase and membrane-bound nonspecific β-glucosidase, and liver neuraminidase from the mouse strain SM/J. Gaucher disease is characterized by a severe though incomplete deficiency of glucosylceramide-β-glucosidase activity. Determination of subunit M_r by SDS-polyacrylamide gel electrophoresis showed a similar subunit size in purified enzyme preparations from normal and Gaucher spleen: 66,000 in the normal and 57,000 in the Gaucher tissue (Pentchev et al., 1973). The RIS of normal spleen glucosylceramide-β-glucosidase was 67,000, corresponding approximately to the monomer, whereas in the type I Gaucher spleen the RIS was about double, around 125,000 (Maret et al., 1983). The corresponding radiation inactivation curves are presented in Fig. 3. The addition of Triton X-100 to remove the glucosylceramide-β-glucosidase from its lipid environment has no effect on the RIS of the enzyme. The mutation has modified the interaction between subunits of the enzyme so that it has altered either the target size or the functional unit size. The target size can be determined with a purified preparation of the enzyme, and the hypothesis of intersubunit energy transfer in the mutant enzyme could then be tested by this approach. This experiment remains to be done.

The membrane-bound nonspecific β-glucosidase showed a single component of RIS 97,500 in the normal whereas the Gaucher spleen had two components, one similar to the normal enzyme (101,000) and a larger one (557,000) (Maret et al., 1984). It is not known whether the larger β-glucosidase component observed in the Gaucher spleen is related to the Gaucher mutation. It is also not clear by which mechanism this modification in RIS occurs and why it persists in Triton X-100 (Maret et al., 1984).

The last example of a modification of RIS as a result of a mutation is that of liver neuraminidase in the SM/J mouse (Yan et al., unpublished work). The SM/J mouse is a mutant with a severe 4-methylumbelliferyl-α-D-*N*-acetylneuraminate neuraminidase deficiency in the liver (Potier et al., 1979). The residual neuraminidase activity in SM/J mouse liver is due to a thermostable component that differs in isoelectric point and RIS

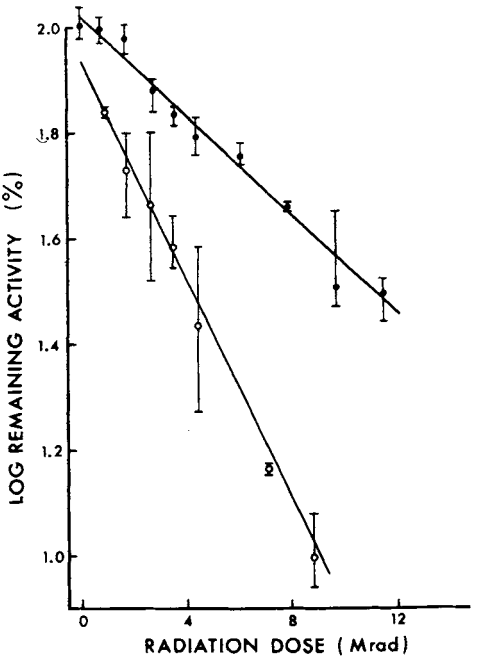

Fig. 3. Radiation inactivation size of acid β-glucosidase in normal (●) and Gaucher (○) spleens as determined at 22°C with NBD-glucosylceramide as substrate. (From Maret et al., 1983.)

from the corresponding component of normal liver of the control strain. The RIS of the SM/J enzyme was 46,400, whereas that of the control strain enzyme was 91,300. These results suggest a dissociation of two identical size subunits or at least a quaternary structure change affecting the RIS.

VII. LIMITATIONS IN THE INTERPRETATION OF EXPERIMENTAL DATA

In the absence of other structural data (M_r of subunit(s) or whole molecule) on the protein under study, the interpretation of RIS values obtained by radiation inactivation should be made with caution. Complex systems that do not yield a linear relationship between the logarithm of

residual biological activity and radiation dose are the most susceptible to errors of interpretation. It might be difficult, and even impossible, to assess linearity from considering uniquely the experimental data, as pointed out by Simon et al. (1982). The total dose applied to inactivate a given protein should be of sufficient magnitude to ensure that a linear relationship of log activity with dose is obtained. This is usually achieved by decreasing the biological activity by an order of magnitude of 2 to 3. In some practical situations, however, one could be limited by the amount of protein available and/or the sensitivity of the biological test to be applied after irradiation.

1. Effect of Regulatory Proteins: Inhibitors or Activators

Regulatory proteins, physically associated with enzymes or receptors, may interfere with the determination of biological activity in irradiated preparations and yield anomalous radiation-inactivation curves. In addition inhibitors or activators released during the homogenization procedure may interact with the enzyme or receptor of interest in the crude preparations. Simon et al. (1982) have proposed a general mathematical model simulating radiation inactivation of equilibrium regulatory protein-enzyme systems. Harmon et al. (1980) have described the radiation inactivation of the regulated insulin receptor of rat-liver plasma membranes. These authors observed an anomalous behavior with radiation exposure since the ligand binding increased at low radiation doses. They suggested that this unexpected effect was due to the presence of a large-M_r regulatory (inhibitory) protein closely associated with the receptor in the membrane. Since the target size of this inhibitory protein (M_r, 350,000) was greater than that of the receptor (M_r, 87,000), it was inactivated first under radiation exposure, thus explaining increased binding by the receptor at low radiation doses. Interestingly, increasing the insulin concentration in the receptor preparation prior to irradiation was reported by these authors to normalize the radiation inactivation curve, presumably by diminishing the amount of bound regulatory component (Harmon et al., 1980; 1981). Recently Potier and Giroux (1985) extended the model of Simon et al. (1982) to distinguish between competitive and noncompetitive inhibitors. Their approach used varying substrate concentrations in the assay medium after irradiation of a regulated enzyme system in order to modify radiation inactivation curves in an interpretable way. They showed that it is possible to distinguish the type of inhibition (competitive or noncompetitive) by examining the shape of the series of curves obtained at varying substrate concentrations. They also studied theoretically the effect of activators. Under certain conditions the radiation inactivation method could be used to characterize a regulated enzyme complex in

the membrane (type of inhibition and in certain cases inhibitor constants of the system in situ).

2. Radiation Inactivation of Complex Oligomeric Enzyme Systems

The interpretation of radiation inactivation of complex systems such as adenylate cyclase (Houslay et al., 1977; Martin et al., 1979; Nielsen et al., 1981) and phosphodiesterase (Kincaid et al., 1981) has been criticized by several authors (Swillens and Dumont, 1981; Ottolenghi et al., 1982; Simon et al., 1982; Verkman et al., 1984) who pointed out the lack of theoretical knowledge to apply the radiation inactivation method to such complex systems. Some efforts have been made to provide such a theoretical framework. Verkman et al. (1984) studied theoretically equilibrium and nonequilibrium homo-oligomer systems. Factors that influence radiation inactivation curves are (1) extent of reequilibration of the system at time of assay, (2) activity ratios of monomer versus oligomer, (3) presence of intersubunit energy transfer. A concave-upward inactivation curve suggests the presence of multiple independent functional units of distinct size and activity that do not interact with each others. Theoretical approaches to nonlinear radiation inactivation curves have been provided by Simon et al. (1982) and Potier and Giroux (1985). The difficulty with all these approaches is that they are almost impossible to use without detailed knowledge of the system under study because in most cases they do not allow a clear distinction between different models. For instance, concave-upward radiation inactivation curves can be either due to an oligomeric protein with several functional units (Verkman et al., 1984) or the interaction with an inhibitor or activator (Potier and Giroux, 1985).

VIII. CONCLUSIONS

The target theory is exclusively concerned with the polypetide(s) broken down by a single hit; target theory was incorrectly formulated through a secondary phenomenon: loss of biological activity. For regulated oligomers and those obeying relation (11), the loss of activity does not reflect polypeptide breakdown. The fundamental dogma of classical target theory is therefore incorrect. Activity decay versus dose (equation (2)) gives the RIS (equation (4), (5), or (7)) not the target size. We demonstrated that the functional unit is not an experimental parameter but can be deduced when the target size is monomeric.

The temperature effect has not been accounted for in classical target theory (Lea, 1955) because μ (equation (1)) was thought to be proportional to a single parameter, target size, which is insensitive to tempera-

ture. Beauregard and Potier (1985) found that μ represents the ratio of target size (rather than M_r) to $10^{-8}Q$ (referring to loss of intact structure rather than loss of activity), two parameters of target theory. Therefore, the temperature effect can theoretically be explained within the scope of target theory by changes in Q value with temperature as observed experimentally (Beauregard and Potier, 1985).

One advantage of the radiation inactivation method is that it is not required that the protein studied be purified or even solubilized, and the technique can be applied directly to partially purified membrane preparations. However, with a crude preparation, the target size cannot usually be determined, and this limits considerably the amount of information that can be obtained from radiation inactivation experiments. The determination of the RIS and target size allows assessment of the size of the functional unit or determination of the occurrence of radiation energy transfer between subunits of an oligomeric protein. This gives information on both the size of the structure needed for the expression of a given biological activity or on the physical proximity of subunits required for energy transfer to take place. This method is thus a tool to study quaternary structure-function relationships in proteins.

The target size and the RIS do not take into account associated structures such as phospholipids, carbohydrates, or detergents; thus these parameters do not necessarily reflect the M_r of a protein.

Although there are several unresolved problems in the application of the radiation inactivation method, this is a useful method in biochemistry particularly for the study of membrane and oligomeric proteins. Among the problems that should be approached, the most important is to determine which structural conditions are required to obtain intersubunit energy transfer in oligomeric proteins. Are the RIS changes observed for many proteins (Table IV) always associated to a change in target size as suggested for eel acetylcholinesterase, or due to reduction of disulfide bridges? Are the changes in RIS always associated with changes in kinetic properties as in the bovine erythrocyte acetylcholinesterase? Do the RIS changes have any functional role? The utilization of the radiation inactivation method is taking a new turn to approach these problems and should give an impulse to the study of subtle quaternary structure changes in proteins.

ACKNOWLEDGMENTS

The helpful comments and criticisms of Mohamed Aly Elkholy, Damian Labuda, and Suzanne Giroux are highly appreciated. The financial sup-

port of the Medical Research Council of Canada (Grant MT-5163) for some of the studies done in our laboratory is acknowledged.

References

Augenstein, L. G., and Mason, R. (1962), *Biological Effects of Ionizing Radiation at the Molecular Level*, International Atomic Energy Agency, Vienna, pp. 227–235.

Augenstein, L. G., Brustad, T., and Mason, R. (1964), *Adv. Radiat. Biol., 1*, 228–266.

Beauregard, G., and Potier, M. (1985), *Anal. Biochem., 150*, 117–120.

Beauregard, G., and Potier, M. (1986), *Receptor Biochemistry and Methodology*, Vol. 5 (J. C. Venter and C. M. Fraser, eds.), Alan R. Liss Inc., New York, in press.

Beauregard, G., and Potier, M. (1984), *Anal. Biochem., 140*, 403–408.

Beauregard, G., and Potier, M. (1982), *Anal. Biochem., 122*, 379–384.

Beauregard, G., and Roufogalis, B. D. (1979), *Biochem. J., 179*, 109–117.

Beauregard, G., Potier, M., and Roufogalis, B. D. (1980), *Biochem. Biophys. Res. Commun., 96*, 1290–1295.

Beauregard, G., Giroux, S., and Potier, M. (1983), *Anal. Biochem., 132*, 362–364.

Berman, J. D. (1973), *Biochemistry, 12*, 1710–1715.

Berry, R. J., and Marshall, C. H. (1969), *Phys. Med. Biol., 14*, 585–596.

Bock, H.-G., and Fleischer, S. (1975), *J. Biol. Chem., 250*, 5774–5781.

Bowman, B. J., Blasco, F., and Slayman, C. W. (1981), *J. Biol. Chem., 256*, 12343–12349.

Bowman, B. J., Berenski, C. J., and Jung, C. Y. (1985), *J. Biol. Chem., 260*, 8726–8730.

Butler, J. A. V., and Robins, A. B. (1962), *Radiat. Res., 17*, 63–73.

Chamberlain, B. K., Berenski, C. J., Jung, C. Y., and Fleischer, S. (1983), *J. Biol. Chem., 258*, 11997–12001.

Chin, D. J., Gil, G., Russel, D. W., Liscum, L., Luskey, K. L., Basu. S. K., Okayama, H., Berg, P., Goldstein, L., and Brown, M. S. (1984), *Nature, 308*, 613–617.

Cuppoletti, J., Jung, C. Y., and Green, F. A. (1981), *J. Biol. Chem., 256*, 1305–1306.

Curzio, O. A., and Quaranta, H. O. (1982), *Int. J. Appl. Radiat. Isot., 33*, 1–3.

Dartinger, H., and Jung, H. (1970), *Molecular Radiation Biology: The Action of Ionizing Radiation on Elementary Biological Objects*, Springer-Verlag, New York.

Doble, A., and Iversen, L. L. (1982), *Nature, 295*, 522–523.

Edwards, P. A., Kempner, E. S., Lan, S.-F., and Erickson, S. K. (1985), *J. Biol. Chem., 260*, 10278–10282.

Fluke, D. J. (1972), *Radiat. Res., 51*, 56–71.

Fluke, D. J. (1966), *Radiat. Res., 28*, 677–693.

Fricke, H., and Morse, S. (1927), *Am. J. Roentg., 18*, 426–430.

Goldkorn, T., Rimon, G., Kempner, E. S., and Kaback, R. (1984), *Proc. Natl. Acad. Sci.* (USA), *81*, 1021–1025.

Haigler, H. T., Woodbury, D. J., and Kempner, E. S. (1985), *Proc. Natl. Acad. Sci.* (USA), *82*, 5357–5359.

Harmon, J. T., Kahn, C. R., Kempner, E. S., and Schlegel, W. (1980), *J. Biol. Chem., 255*, 3412–3419.

Harmon, J. T., Kempner, E. S., and Kahn, C. R. (1981), *J. Biol. Chem., 256*, 7719–7722.

Harmon, J. T., Nielsen, T. B., and Kempner, E. S. (1985), *Methods Enzymol., 117*, 65–94.

Hart, E. J., and Fricke, H. (1967), in *Chemical Dosimetry-Radiation Dosimetry*, Vol. 2 (F. H. Attis and W. C. Roech, eds.), Academic Press, New York.

Hayashi, Y., Takagi, T., Maezawa, S., and Matsui, H. (1983), *Biochim. Biophys. Acta, 748*, 153–167.

Henriksen, T. (1966), *Radiat. Res., 27*, 694–709.

Houslay, M. D., Ellory, J. C., Smith, G. A., Hesketh, T. R., Stein, J. M., Warren, G. B., and Metcalfe, J. C. (1977), *Biochim. Biophys. Acta, 467*, 208–219.

Hucho, F., and Janda, M. (1974), *Biochem. Biophys. Res. Commun., 57*, 1080–1086.

Hymel, L., Maurer, A., Berenski, C., Jung, C. Y., and Fleischer, S. (1984), *J. Biol. Chem., 259*, 4890–4895.

Jung, C. Y. (1984), in *Receptor Biochemistry and Methodology*, Vol. 3 (J. C. Venter and C. M. Fraser, eds.), Alan R. Liss Inc., New York, pp. 193–208.

Jung, H., and Schüssler, H. (1968), *Z. Naturforschg., 23b*, 934–943.

Karlish, S. J. D., and Kempner, E. S. (1984), *Biochim. Biophys. Acta, 748*, 153–167.

Kempner, E. S., and Haigler, H. T. (1982), *J. Biol. Chem., 257*, 13297–13299.

Kempner, E. S., and Miller, J. H. (1983), *Science, 222*, 586–589.

Kempner, E. S., and Schlegel, W. (1979), *Anal. Biochem., 92*, 2–10.

Kempner, E. S., Miller, J. H., Schlegel, W., and Hearon, J. Z. (1980), *J. Biol. Chem., 255*, 6826–6831.

Kepner, G. R., and Macey, R. I. (1968), *Biochim. Biophys. Acta, 163*, 188–203.

Kincaid, R. L., Manganiello, V. C., and Vaughan, M. (1981), *J. Biol. Chem., 256*, 11345–11350.

Lea, D. E. (1955), *Actions of Radiations on Living Cells*, 2nd ed., Cambridge University Press, pp. 69–99.

le Maire, M., Møller, J. V., and Tanford, C. (1976a), *Biochemistry, 15*, 2336–2342.

le Maire, M., Jorgenson, K. E., Roigaard-Peterson, H., and Møller, J. V. (1976b), *Biochemistry, 15*, 5805–5812.

le Maire, M., Rivas, E., and Møller, J. V. (1980), *Anal. Biochem., 106*, 12–21.

Levinson, S. R., and Ellory, J. C. (1974), *Biochem. J., 137*, 123–125.

Lo, M. M. S., Barnard, E. A., and Dolly, J. O. (1982), *Biochemistry, 21*, 2210–2217.

Lowe, M. E., and Kempner, E. S. (1982), *J. Biol. Chem., 257*, 12478–12480.

MacLennan, D. H., and Wong, P. T. S. (1971), *Proc. Natl. Acad. Sci. (USA), 68*, 1231–1238.

Maret, A., Potier, M., Salvayre, R., and Douste-Blazy, L. (1983), *FEBS Lett., 160*, 93–97.

Maret, A., Potier, M., Salvayre, R., and Douste-Blazy, L. (1984), *Biochim. Biophys. Acta, 799*, 91–94.

Martin, R., Stein, J. M., Kennedy, E. L., Doberska, C. A., and Metcalfe, J. C. (1979), *Biochem. J., 184*, 253–260.

McIntyre, J. O., Churchill, P., Maurer, A., Berenski, C. J., Jung, C. Y., and Fleischer, S. (1983), *J. Biol. Chem., 258*, 953–959.

Millar, D. B., Grafius, M. A., and Palmer, D. A. (1973), *Eur. J. Biochem., 37*, 425–433.

Müller, A. (1962), *Biological Effects of Ionizing Radiation at the Molecular Level*. International Atomic Energy Agency, Vienna, pp. 61–71.

Nielsen, T. B., Lad, P. M., Preston, M. S., Kempner, E., Schlegel, W., and Rodbell, M. (1981), *Proc. Natl. Acad. Sci.* (USA), *78*, 722–726.

Noël, H., Beauregard, G., Potier, M., Bleau, G., Chapdelaine, A., and Roberts, K. D. (1983), *Biochim. Biophys. Acta*, *758*, 88–90.

Norman, A., and Ginoza, W. (1958), *Radiat. Res.*, *9*, 77–83.

Ott, P., Ariano, B. H., Binggeli, Y., and Brodbeck, U. (1983), *Biochim. Biophys. Acta*, *729*, 193–198.

Ottolenghi, P., and Ellory, J. C. (1983), *J. Biol. Chem.*, *258*, 14895–14907.

Ottolenghi, P., Ellory, J. C., and Klein, R. A. (1982), *FEBS Lett.*, *150*, 311–313.

Parkinson, D., and Callingham, B. A. (1982), *Radiat. Res.*, *90*, 252–259.

Patten, F., and Gordy, W., (1960), *Proc. Natl. Acad. Sci.* (USA), *46*, 1137–1144.

Pentchev, P. G., Brady, R. O., Hibbert, S. R., Gal, A. E., and Shapiro, P. (1973), *J. Biol. Chem.*, *248*, 5256–5261.

Peters, W. H. M., De Pont, J. J. H. M., Koppers, A., and Bonting, S. L. (1981), *Biochim. Biophys. Acta*, *641*, 55–70.

Pollard, E. C., Powell, W. F., and Reaume, S. H. (1952), *Proc. Natl. Acad. Sci.* (USA), *38*, 166–172.

Pollard, E. C., Guild, W. R., Hutchinson, F., and Setlow, R. B. (1955), *Progr. Biophys. Biophys. Chem.*, *5*, 72–107.

Potier, M., and Giroux, S. (1985), *Biochem. J.*, *226*, 797–801.

Potier, M., Yan, D. L. S., and Womack, J. E. (1979), *FEBS Lett.*, *108*, 345–348.

Rosenberry, T. L., and Richardson, J. M. (1977), *Biochemistry*, *16*, 3550–3558.

Rosenberry, T. L., Chen, Y. T., and Bock, E. (1974), *Biochemistry*, *13*, 3068–3079.

Roufogalis, B. D., and Beauregard, G. (1979), *Mol. Pharmacol.*, *16*, 189–195.

Saccomani, G., Sachs, G., Cuppoletti, J., and Jung, C. Y. (1981), *J. Biol. Chem.*, *256*, 7727–7729.

Shikita, M., and Hatano-Sato, F. (1973), *FEBS Lett.*, *36*, 187–189.

Simon, P., Swillens, S., and Dumont, J. E. (1982), *Biochem. J.*, *205*, 477–483.

Steer, C. J., Kempner, E. S., and Ashwell, G. (1981), *J. Biol. Chem.*, *256*, 5851–5856.

Swillens, S., and Dumont, J. E. (1981), *FEBS Lett.*, *134*, 29–31.

Takahashi, M., Malathi, P., Preiser, H., and Jung, C. Y. (1985), *J. Biol. Chem.*, *260*, 10551–10556.

Trimble, R. B., and Maley, F. (1977), *J. Biol. Chem.*, *252*, 4409–4412.

Turner, R. J., and Kempner, E. S. (1982), *J. Biol. Chem.*, *257*, 10794–10797.

Usatyi, A. F., and Lazurkin, Y. S. (1962), *Biological Effects of Ionizing Radiation at the Molecular Level*, International Atomic Energy Agency, Vienna, pp. 37–59.

Verkman, A. S., Skorecki, K., and Ausiello, D. A. (1984), *Proc. Natl. Acad. Sci.* (USA), *81*, 150–154.

Methods of Biochemical Analysis, Volume 32
Edited by David Glick
Copyright © 1987 by John Wiley & Sons, Inc.

METHODS OF BIOCHEMICAL ANALYSIS VOLUME 32

Immunoassay with Electrochemical Detection

WILLIAM R. HEINEMAN, H. BRIAN HALSALL, KENNETH R. WEHMEYER*, MATTHEW J. DOYLE,* AND D. SCOTT WRIGHT,** *Department of Chemistry, University of Cincinnati, Cincinnati, Ohio*

Our experiments reported in this chapter were supported by NSF Grants CHE 79-11872 and CHE-8217045 and NIH Grants 5 RO1 AI16753 and HD 13207

*Present address: Procter & Gamble, Miami Valley Laboratories, Cincinnati, Ohio

**Present address: Warner-Lambert, Ann Arbor, Michigan

I. INTRODUCTION

The immunoassay has become a preeminent tool for the detection and quantitation of physiologically important molecules at trace levels. This ascendency has been due to the very high level of selectivity that can be attained in the detecting antibodies, even in complex matrices. The original immunoassay (Yalow and Berson, 1959) used a radiolabel for quantitation. The past decade, however, has seen a progressively stronger interest in, and development of what have become known as "alternative immunoassays." In these, a nonradioactive labeling system is used, with the frequent design goal of providing an assay termed "homogeneous." This denotes a protocol with the convenience of lacking the separation step that is mandatory for the radioimmunoassay, a "heterogeneous" system. This chapter reflects our interest in developing homogeneous and heterogeneous immunoassays that employ electrochemical detection of some component in the assay system for the quantitation of analytes. The chapter is organized into discussions of enzymatically and nonenzy-

matically based electrochemical immunoassays. Within these divisions are described homogeneous and heterogeneous assays that we have developed that we have chosen to illustrate the broad applicability of the method, particularly its application to analyte molecular weight.

The discussion is restricted to immunoassays based on voltammetric electroanalysis, involving the application of a potential to an electrochemical cell and measurement of the current resulting from an oxidation or reduction at the electrode surface. Immunoassays based on potentiometric electrochemical techniques are also under active development. Additionally, electrochemical sensors in which immunological reactions provide the selectivity are being developed for a variety of purposes (*Proceedings*, 1983; Czaban, 1985).

II. ENZYME LABEL CATALYZING PRODUCTION OF ELECTROACTIVE PRODUCT

Enzymes may be used in electrochemical immunoassay as a label attached to the antigen or antibody to catalyze the production of an electrochemically detectable product. The rate at which the product is formed is then related to the concentration of the analyte in the sample. Enzyme immunoassays, whether electrochemically based or not, rely on the enzyme label for sensitivity through chemical amplification. This results from passing a substance through a catalytic, cycling, or multiplication mechanism, thereby generating a relatively large amount of product (Blaedel and Boguslaski, 1978). Thus a trace amount of an analyte may result in significantly higher product concentrations that can be more easily measured than the analyte itself.

1. Heterogeneous Enzyme Immunoassays

In general, heterogeneous enzyme immunoassays are based on the Enzyme Linked Immunosorbent Assay (ELISA) technique in which antibody (Ab) is typically immobilized on the walls of small volume ($\sim$ 500 μl) plastic cuvettes. The general procedure is outlined in Fig. 1 for the determination of antigen (Ag), which will represent the analyte in this and other examples (Heineman and Halsall, 1985). Reagent cuvettes are prepared by attaching specific Ab to the inside walls by passive adsorption or covalent bonding. The cuvettes are then rinsed with a nonionic surfactant such as Tween 20 to cover any exposed surface between Ab molecules and remove weakly bound Ab. Reagent cuvettes of this type can be prepared in advance and stored. The protocol now adopted will depend

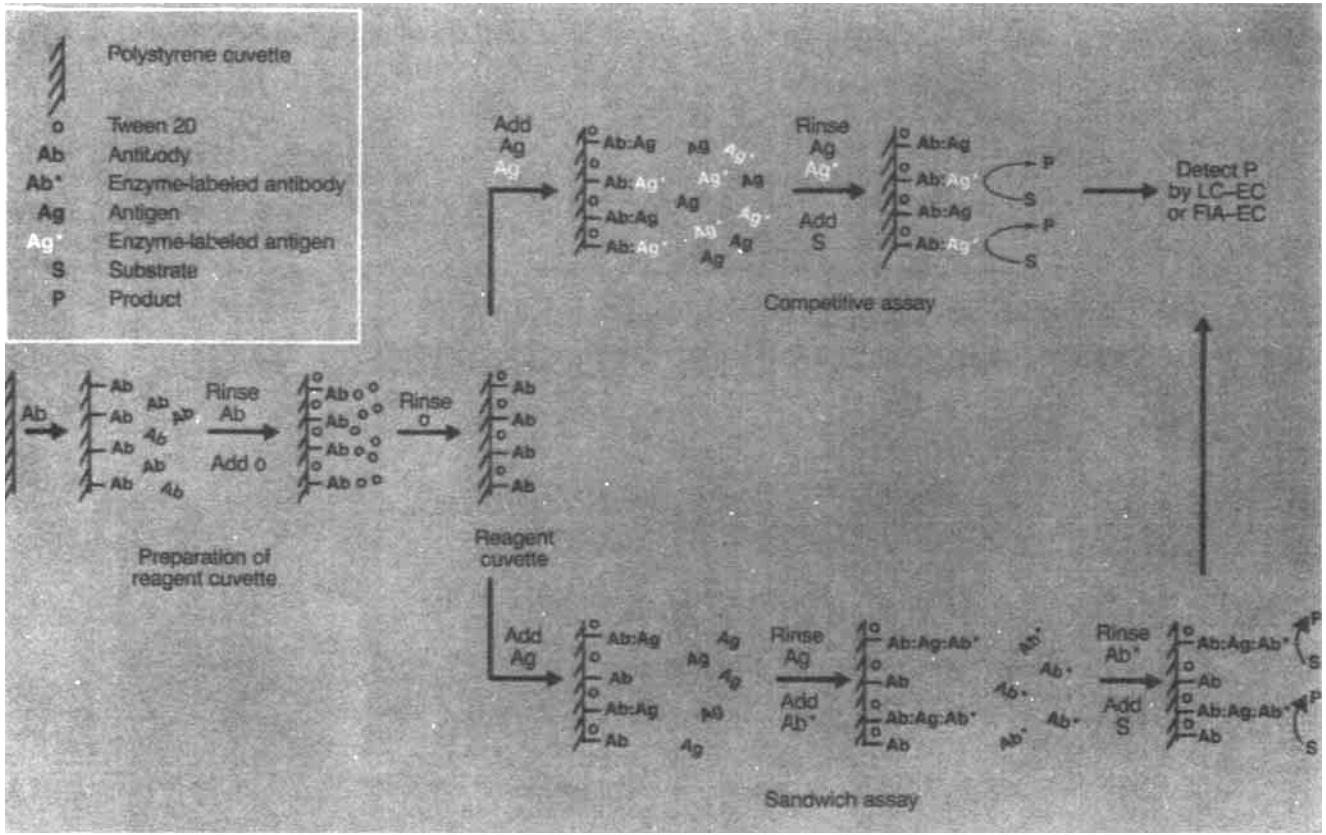

Fig. 1. General protocol for heterogeneous enzyme immunoassay: preparation of reagent cuvettes by coating Ab, competitive assay format, and sandwich assay format. (Reprinted with permission from Heineman and Halsall, 1985. Copyright 1985, American Chemical Society.)

on whether a "competitive" or "sandwich" assay is desired. These are also depicted in Fig. 1 and described in Sections II.1.C and II.1.D.

A. ENZYME LABEL

An enzyme suitable for use as a label must meet several important criteria. For detection at very low levels the formation of a chemically, physically, and mechanically stable adduct, and the retention of a high specific activity by the enzyme in the adduct are most important. The products of the enzymatic reaction should be nontoxic and easily detected at low levels. For widespread use the enzyme should be inexpensive and commercially available in high purity. A number of enzyme systems that meet these criteria have been utilized as labels for immunoassay (Jarvis, 1979; Sharpe et al., 1976). Several generate electroactive product from an electroinactive, and therefore noninterfering, substrate and are ideally suited for use in electrochemical immunoassay (Wehmeyer et al., 1983).

Alkaline phosphatase (AP) meets these requirements. It may be used to catalyze the conversion of an electroinactive substrate (phenylphosphate) to an electroactive product (phenol), as shown here:

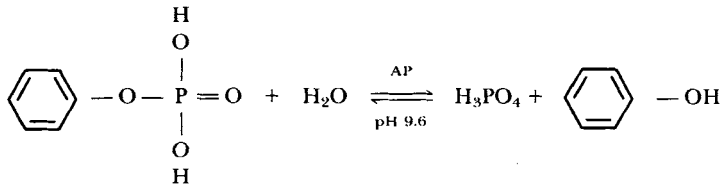

B. ELECTROCHEMICAL DETECTION OF PHENOL

Phenol can be detected electrochemically by oxidation at a carbon paste electrode (Wehmeyer et al., 1983). A convenient means of determining a low concentration of phenol in a small volume of sample is by liquid chromatography with electrochemical detection (LCEC). A diagram of the LCEC system is shown in Fig. 2. The sample is injected by means of 20-μl sample loop into a 5-cm column slurry-packed with 10-μm C_{18} stationary phase. The column serves to separate the peak for phenol from other assay constituents in order to achieve a better detection limit. The phenol is detected by oxidation in a thin-layer electrochemical cell with a carbon paste working electrode.

A typical chromatogram for the detection of phenol is shown in Fig. 3. Note that the detector responds to both the phenol, which is undergoing oxidation, and the other components in the assay buffer. Even though these components are electroinactive, injection of the buffer without

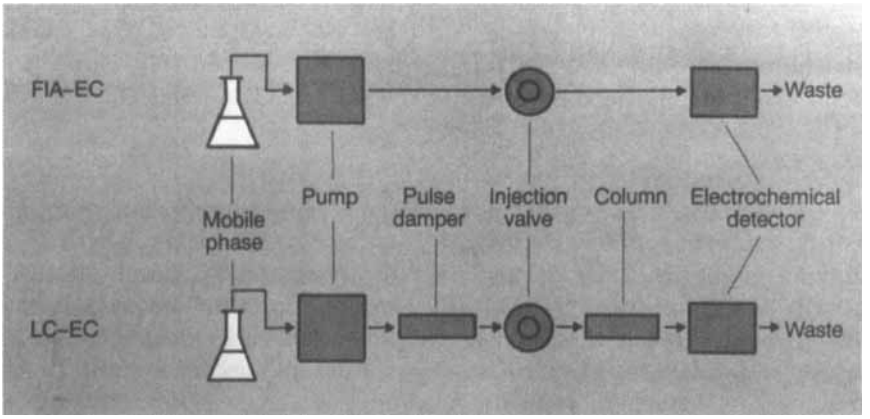

Fig. 2. Schematic diagram of instrumentation for FIAEC and LCEC.

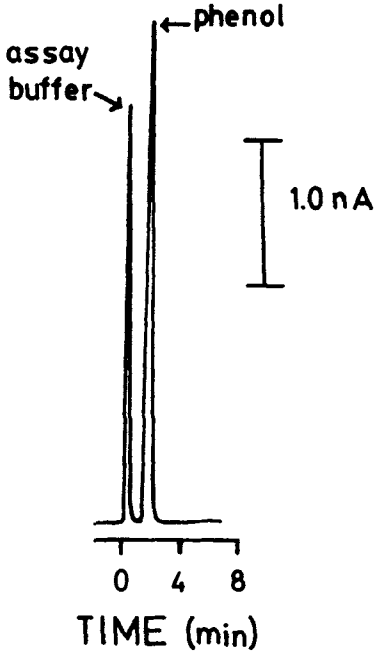

Fig. 3. LCEC chromatogram of 5.3×10^{-7} *M* phenol in 0.05 *M* carbonate buffer. Flow rate, 1.2 ml/min; eluent, 0.1 *M* phosphate buffer (pH 7.0); 20 µl injection. (From Wehmeyer et al., 1983, with permission.)

phenol gives rise to this capacitive current peak because of the matrix difference between the substrate solution and the mobile phase, which contains no phenylphosphate or $MgCl_2$.

The variation in peak height for the phenol signal as a function of the potential applied to the electrochemical cell is shown by the hydrodynamic voltammogram in Fig. 4. Maximum sensitivity for phenol detection is achieved at a potential of +850 mV versus Ag/AgCl, or greater. Our experiments were conducted at a potential of +870 mV.

The LCEC detection of phenol is linear over the considerable range of between 9.0×10^{-9} *M* and 9.6×10^{-6} *M* (slope = 0.57 nA/n*M*, $b = -0.30$ nA, $r = 0.999$). This approach represents a simple, sensitive, and precise method for the detection of AP-generated phenol. No evidence of electrode fouling is observed over this concentration range. The LCEC system can be operated continuously for up to three months before column replacement or electrode resurfacing is necessary.

Phenol can also be determined by flow injection analysis with electrochemical detection (FIAEC). In FIAEC the sample is injected directly into

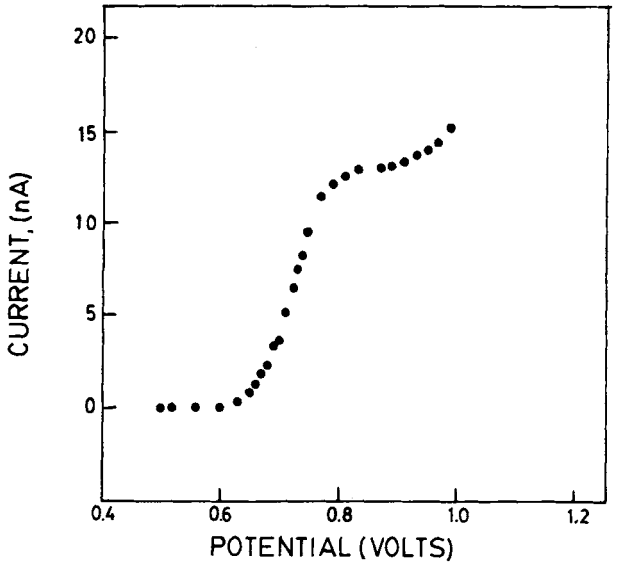

Fig. 4. Hydrodynamic voltammogram of 7.0×10^{-7} *M* phenol. See conditions for Fig. 3. (From Wehmeyer et al., 1983, with permission.)

the thin-layer amperometric detector by means of the apparatus shown in Fig. 2. Since the sample does not pass through a column, the phenol signal is not separated from the capacitance response (i.e., blank signal) of the components in the assay buffer. Consequently the detection limit for phenol by FIAEC is limited by the blank signal to approximately 1.5×10^{-7} *M*. FIAEC detection of phenol at +870 mV versus Ag/AgCl has a linear dynamic range of $1.5 \times 10^{-7} - 2.8 \times 10^{-5}$ *M* ($r = 0.999$). Representative current-time responses for the injection of blank substrate solution and two solutions of substrate with phenol concentrations near the detection limit are shown in Fig. 5. The absence of a column results in a very fast response to phenol. By comparison, the LCEC method offers a 100-fold lower detection limit for phenol than FIAEC, but at the expense of a longer analysis time, approximately 2.5 min for LCEC compared to 25 sec for FIAEC.

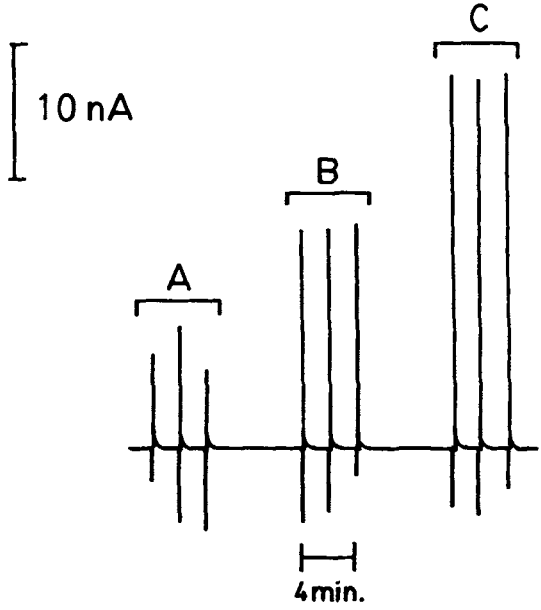

Fig. 5. FIAEC traces for 20 μl injection of 0.05 *M* sodium carbonate buffer containing 9.2×10^{-4} *M* phenyl phosphate, 1.5×10^{-3} *M* magnesium chloride and *(A)* 0, *(B)* 1.5×10^{-7}, and *(C)* 2.9×10^{-7} *M* phenol. (Reprinted with permission from Wehmeyer et al., 1986. Copyright 1986, American Chemical Society.)

C. COMPETITIVE ELECTROCHEMICAL IMMUNOASSAY

In its most common form, a competitive solid phase or saturation analysis immunoassay involves the competition between labeled (Ag*) and unlabeled antigen for a limited number of matrix bound antibody binding sites (Fig. 1). The source of Ag may be standards or samples, and equilibration may require several minutes or hours, depending on the analyte and the configuration of the reaction used. Adequate results may be obtainable before equilibrium is reached. Unbound Ag and Ag* are rinsed from the tubes and substrate(s) added. Samples are withdrawn at known times and analyzed for electroactive product, *P*. Since a greater concentration of Ag in the sample results in less Ag* being bound to adsorbed Ab, a typical standard plot of current from the electrochemical measurement of *P* versus concentration of Ag standard shows the electrochemical signal diminishing with increasing Ag concentration. By mass action, the bound to free ratio *(B/F)* is proportional to the concentration of Ag originally present in the solution.

These assays are applicable to both large (protein) and small (drug) molecules. During the development of competitive immunoassay it is critical to ascertain the optimum conditions for each stage of the procedure. The heterogeneous enzyme assay requires the evaluation of the antigen/antibody incubation interval, the antibody coating concentration, and the enzyme-conjugate dilution. Optimizations are routinely performed in a "checkerboard" fashion, where one parameter is varied while the other two are held constant. Alternatively, simplex optimization algorithms are available that can greatly facilitate this process (Morgan and Deming, 1974).

In general, ideal immunoassay curves should exhibit the greatest sensitivity (Δ response/Δ concentration) over the concentration range of interest and the lowest limit of detection. Several theoretical treatments of immunoassay optimization have appeared (Yalow and Berson, 1964, 1971; Ekins and Newnan, 1970). Assay sensitivity can be tailored to cover a specific dynamic range within limits governing the amounts of Ab which can be sorbed to the solid phase. It is generally advisable to work at the lowest range possible, maximize assay sensitivity, and dilute the analyte to meet those conditions. We will describe in this section competitive assays for the small molecule, digoxin (Wehmeyer et al., 1986) and the macromolecule, orosomucoid (Doyle et al., 1984).

A large number of clinically important substances (therapeutic drugs, hormones, steroids) have molecular weights of less than 5,000 amu. As an example of the application of electrochemical competitive immunoassay to small molecular weight species, digoxin was chosen as a model com-

pound. Digoxin, a steroidal cardiac glycoside, is used in the treatment of chronic heart disease to enhance the force and frequency of contractions. Precise control of plasma digoxin levels is important as it exhibits a relatively narrow therapeutic range (0.5–2.0 ng/ml). In addition to small molecular weight compounds, there are a significant number of large molecular weight (> 5000 amu) molecules such as TSH, insulin, and immunoglobulins, which are of diagnostic interest. The antigen that was chosen for these model studies was human serum orosomucoid (OMD, α_1-acid glycoprotein). This is a small, acute-phase glycoprotein whose serum concentration rises during inflammation (Jamieson et al., 1972), pregnancy (Adams and Wacher, 1968), and certain malignancies (Gendler et al., 1982; Rashid et al., 1982). Altered OMD-drug-binding affinities correlate directly with metastatic progression (Abramson, 1982; Jackson et al., 1982), and the diagnostic value of OMD as a tumoral marker has been suggested (Vea-Martinez, 1982). Quantitative methods for the determination of OMD are quite tedious and often insensitive.

a. Digoxin.

1. Results. The general assay protocol is shown in Fig. 1. Ag represents digoxin in the sample or standard and Ag* represents digoxin labelled with alkaline phosphatase. The phenol produced by the enzyme reaction is quantitated by LCEC. Representative LCEC assay chromatograms for digoxin standards in plasma are shown in Fig. 6. The peak current is proportional to the amount of phenol produced by the antibody bound digoxin-enzyme conjugate, which is inversely proportional to the amount of digoxin present in the standard, as expected.

The LCEC method in conjunction with the optimal assay parameters resulted in a very sensitive immunoassay for digoxin in plasma throughout its therapeutic range, with a detection limit of 50 pg/ml. A standard curve is shown in Fig. 7. The relative standard deviation of i_p obtained for any given digoxin standard ranged from 4% to 12% on various days and is comparable to results ordinarily obtained by other heterogeneous enzyme immunoassays. Approximately 20 samples can be injected per hour.

Samples from patients receiving digoxin therapy were analyzed by the heterogeneous immunoassay LCEC method. Samples were diluted 5/1 with pooled human plasma in order to eliminate an observed antibody matrix effect. Digoxin standards in pooled human plasma were treated similarly and a standard curve constructed. Digoxin levels in patient samples were determined by reference to the standard curve. The values obtained for the samples by the electrochemical enzyme immunoassay method were compared to those obtained by radioimmunoassay. The results for the 54 samples analyzed are presented in Fig. 8. A good correlation was obtained between the two methods ($r = 0.93$).

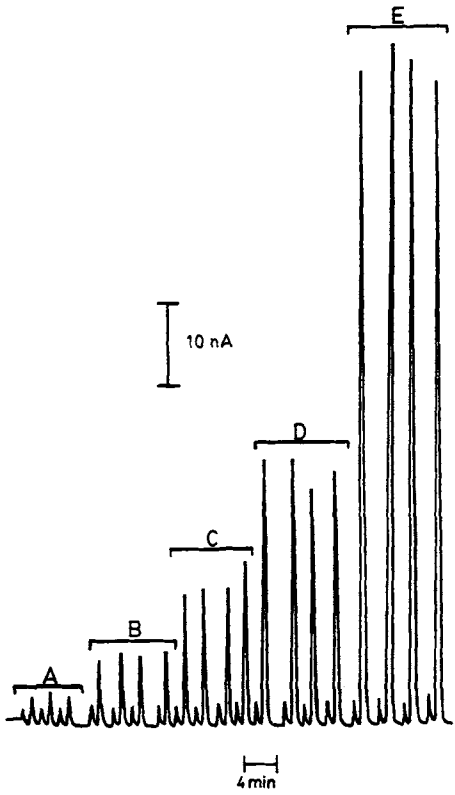

Fig. 6. Heterogeneous enzyme immunoassay with LCEC detection for a series of digoxin standards in plasma solutions. Concentration of digoxin in plasma samples: *(A)*, 5.0, *(B)* 2.0, *(C)* 1.0, *(D)* 0.5, and *(E)* 0 ng/ml. Assay conditions: 10 μg/ml antibody coating concentration, 1/125 digoxin-alkaline phosphatase conjugate dilution, 4 h antigen/antibody incubation interval, and 40 min substrate reaction time. (Reprinted with permission from Wehmeyer et al., 1986. Copyright 1986, American Chemical Society.)

A sufficient concentration of phenol was generated under assay conditions that measurements could be made by FIAEC. A representative current-time response for a series of digoxin standards in pooled human plasma is shown in Fig. 9. Although only 17 samples were analyzed, a good correlation ($r = 0.95$) between FIAEC immunoassay and RIA was found.

2. Materials and Methods. For liquid chromatography and flow injection analysis with hydrodynamic amperometric detection, a prototype

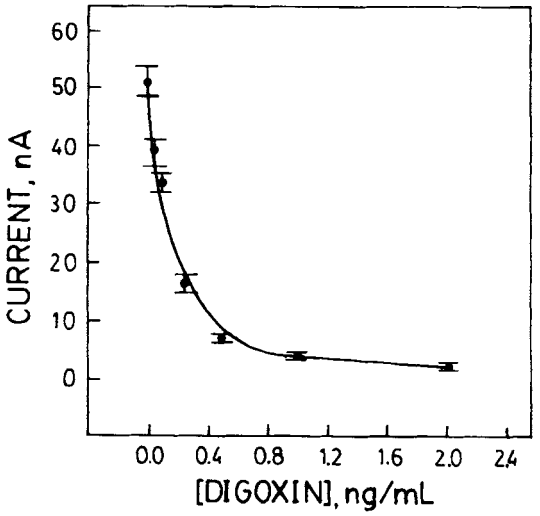

Fig. 7. Standard plot for digoxin standards in human plasma. Assay conditions are the same as in Fig. 6. (Reprinted with permission from Wehmeyer et al., 1986. Copyright 1986, American Chemical Society.)

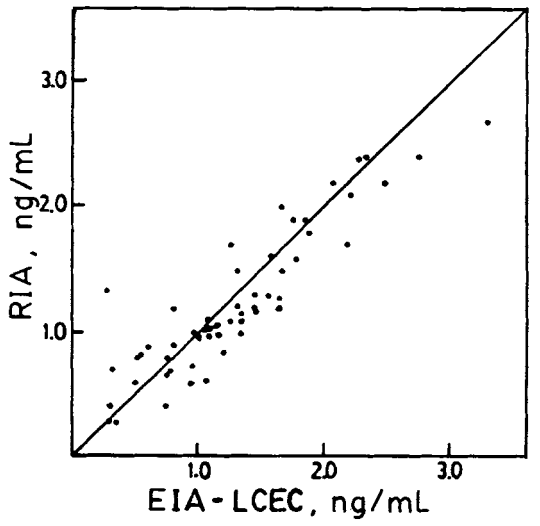

Fig. 8. Correlation between digoxin concentration in patients by RIA and competitive heterogeneous enzyme immunoassay liquid chromatography/electrochemistry (EIA-LCEC). A perfect correlation is represented by the solid line. (Reprinted with permission from Wehmeyer et al., 1986. Copyright 1986, American Chemical Society.)

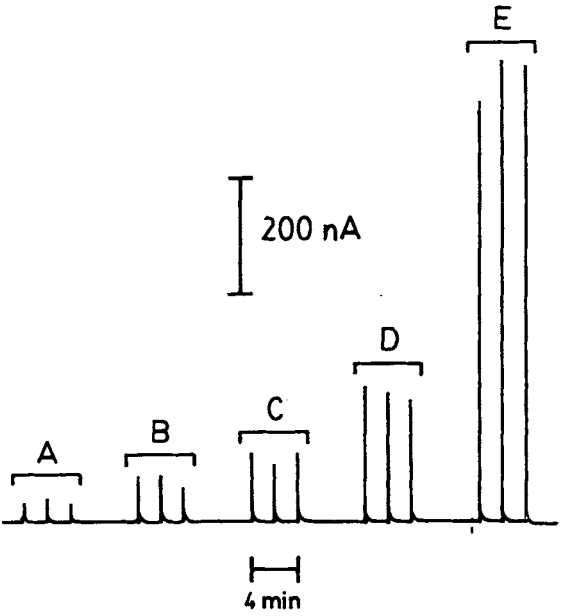

Fig. 9. Heterogeneous enzyme immunoassay with FIAEC detection for a series of digoxin standards in pooled human plasma. Concentrations of digoxin in plasma: *(A)* 5.0, *(B)* 2.0, *(C)* 1.0, *(D)* 0.5, and *(E)* 0 ng/mL. Conditions are the same as in Fig. 6. (Reprinted with permission from Wehmeyer et al., 1986. (Copyright 1986, American Chemical Society.)

electrochemical immunoassay system (Bioanalytical Systems, Inc.) was used. The working electrode was paraffin oil-based carbon paste, the reference electrode was silver/silver chloride (Ag/AgCl) with 3 *M* KCl, and the auxiliary electrode was a stainless-steel block that comprised one-half of the thin-layer cell. A slurry-packed 5 cm × 2 mm precolumn with 10-μm irregularly shaped RSiL material (Alltech Associates) was used in LCEC to separate phenol from the components of the assay buffer. A 12 cm × 4 mm Knauer column dry-packed with 37- to 44-μm pellicular C_{18} packing material (Alltech Associates) was placed between the pump and the injection valve to saturate the mobile phase and thereby extend the lifetime of the RSil column. In all hydrodynamic amperometric analyses the mobile phase was phosphate buffer (0.1 *M*, pH 7.0) containing 0 to 40 ml of methanol per liter, the flow rate was 1.0 to 1.6 ml/min, and the applied potential was +870 mV versus Ag/AgCl. A fixed 20 μl injection loop was used.

All buffer solutions were prepared from distilled/deionized H_2O of at least 10^6 Ω resistivity using ACS grade chemicals obtained from MCB or

Fisher Scientific. The 0.15 *M* phosphate buffered saline (PBS, pH 7.4) and 0.05 *M* carbonate (pH 9.6) buffers were prepared by using the appropriate sodium and ammonium salts, respectively. Tween 20 solutions (Fisher) were prepared as 0.5 ml of Tween 20 in 1 liter of 0.15 *M* PBS.

Substrate solutions (always prepared just prior to use to prevent nonenzymatic hydrolysis), consisted of 0.0146 g of phenyl phosphate (Calbiochem-Behring Corp.) and 0.0055 g of $MgCl_2 \cdot 6H_2O$ (Baker, Phillipsburg, NJ) in 25 ml of 0.05 *M* carbonate, pH 9.6.

Digoxin (Sigma Chemical Co.) standards (0 ng/ml–5 ng/ml) were prepared in phosphate buffer or pooled human plasma (University Hospital, Cincinnati, OH). An antibody coating solution of 10 μg/ml was prepared by dissolving the appropriate amount of digoxin specific antibody (Center for Disease Control, Atlanta, GA) in carbonate buffer containing 0.02% sodium azide. Digoxin-alkaline phosphatase conjugate (Immunotech Corp.) was diluted with an appropriate amount of PBS-Tween. For analysis of patient samples both the samples and standards were diluted with pooled human plasma.

Polystyrene cuvettes were coated with digoxin-specific antibody by passive adsorption according to a reported procedure (Parsons, 1981). In this procedure 375 μl of the digoxin standard or sample and 25 μl of a conjugate dilution were added at the same time to the antibody coated cuvettes. The assay solutions were incubated at room temperature for 4 h. The contents of the cuvettes were aspirated, and the cuvettes washed consecutively, twice with PBS Tween, once with PBS Tween (5 min), and twice with carbonate buffer. Following the washing step, 300 μl of the enzyme substrate solution were added to each cuvette and incubated at room temperature for a timed interval. The enzyme reaction was then stopped by the addition of 25 μl of 5.5 *M* NaOH. Immediately before chromatographic injection 25 μl of 5.5 *M* HCl were added to each sample. This step reduced the slowly decaying capacitive current observed on the injection of the more alkaline solution. Following the HCl addition, 20 μl of the substrate solution were injected into the chromatograph.

b. Orosomucoid. The assay protocol employed is outlined in Fig. 1 and is similar to that discussed for small molecules. Alkaline phosphatase was the labeling enzyme, and the product of the subsequent enzymatic reaction was determined by LCEC.

1. Results. Chromatograms for a series of OMD standards appear in Fig. 10. The concentration of phenol, and hence peak current, is inversely proportional to the concentration of OMD in the test solution, as predicted. Nonspecific adsorption was not apparent under these test condi-

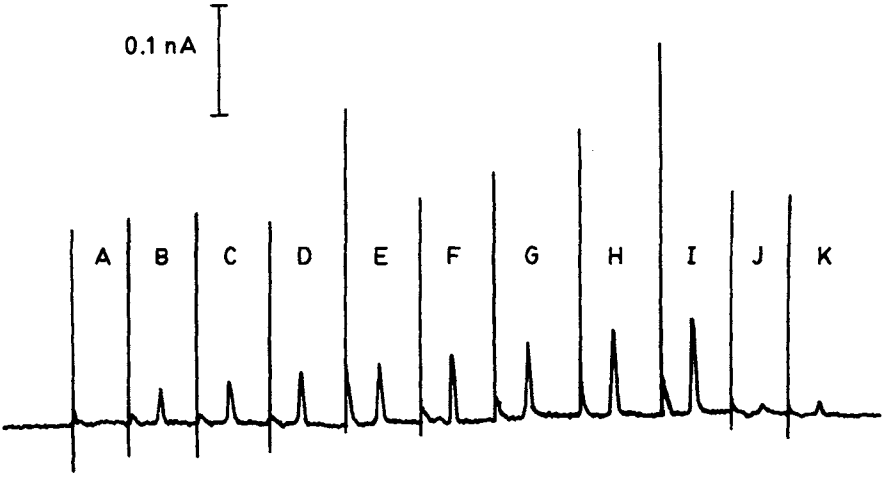

Fig. 10. Heterogeneous enzyme immunoassay with LCEC detection for a series of OMD standards: *(A)* 0.05 *M* carbonate, *(B)* 200, *(C)* 100, *(D)* 60, *(E)* 10, *(F)* 5.0, *(G)* 2.5, *(H)* 1.0, and *(I)* 0.75 ng/ml. The addition of AP alone *(J)* or OMD-AP in cuvettes coated with nonspecific IgG *(K)* show little activity and hence minimal nonspecific adsorption. (Reprinted with permission from Doyle et al., 1984. Copyright 1984, American Chemical Society.)

tions (Fig. 10*J*, *K*). A plot of peak current versus OMD concentration indicated that the assay is most sensitive in the region between 1.0 and 10.0 ng/ml (Fig. 11). The percent relative standard deviation for a 4 ng/ml OMD standard by LCEC was 3.7% ($n = 9$), much improved over conventional immunoassay protocols.

Rate methods can be employed to minimize error due to competing side reactions or quantitate analyte in the presence of interfering constituents. A plot of i_{pa} versus substrate incubation time for a 5 ng/ml OMD standard following the assay was linear with a slope of 0.0228 nA/min. This indicates that the substrate incubation period may be shortened to 10–20 min without a loss in sensitivity, since a detectable amount of phenol is reproducibly generated in that time span.

2. Materials and Methods. Measurements of phenol were made with the same LCEC apparatus described for the digoxin assay.

Human orosomucoid (OMD, α_1-acid glycoprotein) and bovine intestinal AP (Type VII) were obtained from Sigma Chemical. Coupling of OMD to AP as well as the purification and characterization of the resulting conjugate have been previously discussed in detail (Doyle et al., 1984).

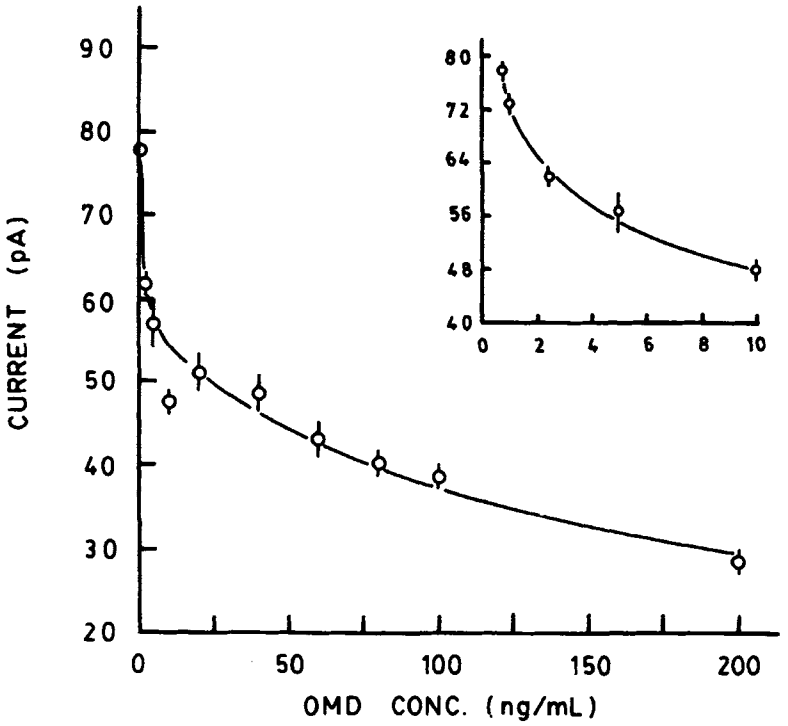

Fig. 11. Standard plots for OMD standards. (Reprinted with permission from Doyle et al., 1984. Copyright 1984, American Chemical Society.)

All standard OMD and enzyme conjugate solutions were diluted with PBS/Tween to minimize nonspecific interactions. Antibody coating solutions were prepared in 0.05 *M* carbonate buffer by adding the appropriate amount of antiserum.

Typically cuvette coating involved the incubation of 0.6 ml of OMD antiserum solution (1.0 μg/ml) or nonspecific IgG (10.0 μg/ml) in each cuvette at 37°C for 24 h. Each well was then aspirated dry and rinsed twice with PBS/Tween for 15 min and once rapidly. Rinsing with surfactant removes excess protein and minimizes nonspecific adsorption by coating unoccupied sites. Cuvettes can be conveniently stored at 4°C or used directly.

An OMD-containing solution (0.4 ml) was mixed with 0.1 ml of a 1/100 dilution of the enzyme conjugate and allowed to equilibrate with the Ab solid phase. Following a 12 h incubation period, the cuvettes were aspirated dry, again rinsed twice with PBS/Tween for 15 min, once with

PBS/Tween quickly, and once using 0.05 *M* carbonate. The wells were aspirated dry, and 0.5 ml of substrate solution were added to each. Cuvettes were allowed to stand at room temperature for 1 h, and the enzymatic reaction was stopped by transferring the substrate solutions from each well into corresponding poly(propylene) microbeakers. The product of the enzymatic reaction was determined amperometrically. LCEC samples were diluted as follows: 10 μl of each solution were mixed with 1.0 ml of 0.05 *M* carbonate, and 20 μl of this diluted sample were injected into the chromatograph.

D. SANDWICH ELECTROCHEMICAL IMMUNOASSAY

A second form, the sandwich immunoassay, is based on noncompetitive binding and involves two separate Ag/Ab interactions (Wisdom, 1976). Typically Ab is attached to a solid support and exposed to a sample containing the Ag of interest as depicted in Fig. 1. The amount of Ag bound to the solid phase-Ab is determined following incubation with a second ligand-specific labeled Ab (Ab*). In contrast to a competitive assay, the amount of Ab-bound Ag, and therefore the amount of enzyme label, is proportional to the Ag concentration in solution.

Sandwich assays require an Ag to contain at least two distinct antigenic sites and as a result are only applicable to large molecular weight compounds. Optimization of the sandwich assay parameters is also commonly done by a "checkerboard" approach. This is not a saturation assay, free Ab binding sites must remain after the adsorption of Ag.

a. Rabbit Immunoglobulin G. Rabbit immunoglobulin G was selected as a model compound to evaluate the electrochemical sandwich immunoassay (Wehmeyer et al., 1985).

1. Results. Figure 12 shows typical sandwich-type assay chromatograms for rabbit IgG standards in PBS Tween. The peak current is proportional to the amount of phenol produced, which in turn is directly proportional to the amount of rabbit IgG in the standard solution, as expected. Figure 13 shows results for the sandwich-type assay, carried out under optimized conditions and allowing 20 min for reaction with substrate. Concentrations of rabbit IgG ranged from 250 to 0 μg/l, with a detection limit of 0.1 μg/l. The coefficient of variation for the peak current for 10 repetitions of the 10 μg/liter standard was 3.8%. A 60-min substrate reaction time and the preceding assay conditions lowered the detection limit to 50 ng/liter (Table 1), which could be further improved to 10 ng/liter by increasing the antigen/antibody incubation interval to 10 h, each with a 60-min substrate reaction interval (Table 1). Table 1

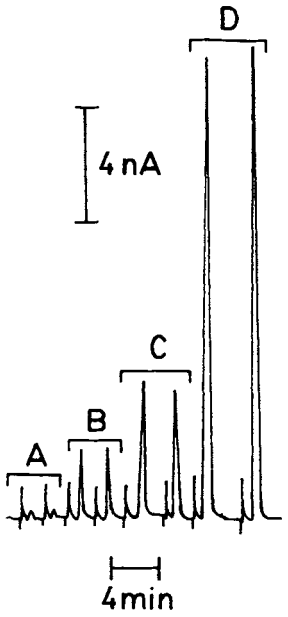

Fig. 12. Sandwich enzyme immunoassay with LCEC detection for a series of rabbit IgG standards in PBS Tween. Concentrations of IgG: *(A)* 0, *(B)* 1.0, *(C)* 2.0, and *(D)* 6.0 ng/ml. (From Wehmeyer et al., 1985, with permission.)

also shows results of a 30-min antigen/antibody incubation interval in conjunction with a 60-min substrate reaction interval. In this shortened assay the detection limit was 100 ng/liter.

Under both optimum and shortened assay conditions the labeled antibody bound by the lowest detectable rabbit IgG standard sufficed to produce a phenol concentration in the 10 to 100 nmol/liter range. Phenol concentrations in these ranges did not strain the detection capabilities of the electrochemical technique. For both the optimum and shortened assays the detection limit was not set by the ability to quantitate the phenol produced by the enzyme, but rather by the amount of nonspecific adsorption of the antibody-enzyme conjugate demonstrated by the 0 ng/liter standard. This nonspecific binding corresponded to a phenol concentration in the 10 nmol/liter region.

2. Materials and Methods. The apparatus was identical to that described for the digoxin assay.

Rabbit IgG (Sigma Chemical Co) standard solutions were prepared from a 10 mg/ml stock solution by appropriate dilution with PBS Tween. Goat antiserum to rabbit IgG (Sigma Chemical Co), received lyophilized

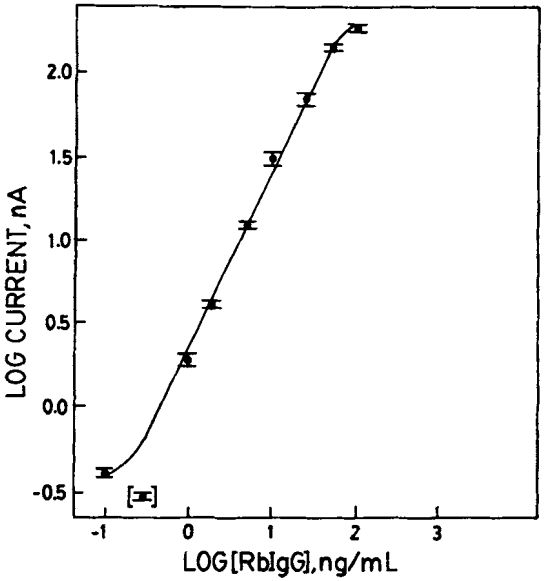

Fig. 13. Log/log plot of LCEC peak current versus rabbit IgG concentration in PBS Tween for the sandwich immunoassay. The brackets denote the 0 ng/ml standard. n = 5 each. (From Wehmeyer et al., 1985, with permission.)

TABLE I

Results of Sandwich-Type Immunoassay for Rabbit IgG

RABBIT IgG (NG/LITER)	i_p(nA) MEAN	SD
3 h incubation of Ag/Ab		
0	0.18	0.01
50	0.34	0.01
100	0.59	0.07
500	2.96	0.21
1000	8.35	0.17
30 min incubation of Ag/Ab		
0	0.23	0.01
100	0.33	0.04
500	0.87	0.06
1000	1.78	0.06
2000	11.36	—

Source: From Wehmeyer et al. (1985), with permission.
Note: Both assays included 60 min incubation of assay mixture with substrate solution. i_p = peak current, nA = nanoamperes, Ag = antigen, Ab = antibody.

in individual vials, was reconstituted with 2.0 ml of carbonate buffer and diluted 1000-fold with carbonate buffer. Goat (anti-rabbit IgG) antibody-alkaline phosphatase conjugate (Sigma Chemical Co) was diluted 1000-fold with PBS-Tween.

Polystyrene cuvettes were coated with the goat antibody by passive adsorption from 500 μl of carbonate buffer. After coating, the cuvettes were washed three times with PBS Tween, allowing the PBS Tween to remain in the cuvettes for 10 min during each wash. Then 400 μl of the rabbit IgG standards were added to the cuvettes and incubated at room temperature. Following incubation, the cuvettes were aspirated and washed three times with PBS Tween. After washing, 375 μl of the enzyme-labeled goat antibody solution were added to each cuvette, again incubated at room temperature, and the cuvettes washed consecutively with PBS Tween (twice) and carbonate buffer (twice). Following this step, 300 μl of the enzyme substrate solution were added to the cuvettes, incubated at room temperature and the substrate reaction stopped by the addition of 25 μl of 5.5 *M* NaOH. Immediately before chromatographic injection, 25 μl of 5.5 *M* HCl were added to the sample, and 20 μl of the subsequent reaction mixture were injected into the chromatograph. The peak heights obtained for the oxidation of phenol were used to construct a standard curve.

b. Immunoreactor. Enzyme immunoassays can also be based on an immunoreactor with electrochemical detection of the column effluent as developed by de Alwis and Wilson (1985). In this technique antibody is immobilized on a chromatography column (immunoreactor). Sample or standard Ag is injected into the immunoreactor where binding occurs. Enzyme-labeled Ab* is then injected. The amount of enzyme label retained in the reactor is then measured by injecting substrate. The amount of electroactive product formed is proportional to the amount of Ab* bound to the column, which is proportional to the amount of Ag in the sample. The electroactive product flows through a thin-layer detector where it is oxidized/reduced and quantitated from the area of the resulting current peak. A switching valve is then used to pass an acidic buffer through the column to displace bound Ag and Ab* in preparation for the next sample. The flow injection/chromatography mode enables carefully controlled conditioning of the immunosorbent (e.g., washing) which is essential to good experimental precision. The immunosorbent columns are stable for at least three months (500 assays). It has been demonstrated that the immunoaffinity column can be used to perform a sandwich assay for IgG with a detection limit of 1 femtomole in less than 30 min. The second antibody is a glucose oxidase-goat anti-IgG conjugate. Following

injection of glucose into the affinity column, peroxide is detected by oxidation at a platinum electrode.

E. CONCLUSIONS

The LCEC detection of phenol provides a rapid, simple, and extremely sensitive method of quantitating alkaline phosphatase activity and can be applied to heterogeneous immunoassay methodology using this enzyme as the label. The assay may be devised in either a competitive or a sandwich format and may be applied to both small and large molecular weight molecules. The precision and limits of detection achieved using amperometric based assays are equivalent to or better than conventional immunoassay techniques for similar antigens.

The lowest detectable amount of analyte achievable via a competitive format is limited by the ratio of the experimental error to the magnitude of the antibody binding constant. Assuming a constant level of experimental error, the quality of the antisera, and not the activity of the label, will determine the detection limit. Conversely, an increase in the specific activity of the label will generally result in lower detection limits for the sandwich assay. At zero nonspecific binding and infinite label-specific activity, the detection limit of the sandwich assay is 1 molecule of antigen (Ekins, 1981). Therefore the signal amplification advantages of enzyme labels are more fully exploited when the sandwich immunoassay form is employed.

2. Homogeneous Enzyme Immunoassays

Immunoassays of the homogeneous type rely on a change in the intensity of the label signal that occurs when Ag* binds with Ab to form Ab-Ag*. The general equilibrium scheme for a homogeneous immunoassay is shown in Fig. 14. The ability to distinguish between Ag* and Ab:Ag* enables the immunoassay to be done without a separation step.

When the label is an enzyme, the immunoassay relies on a reduction in the rate of enzyme catalysis occurring when the antibody binds to the enzyme-labeled antigen. The enables free Ag* to be distinguished from Ab:Ag* on the basis of the rate of production of product. As shown in the equilibrium scheme in Fig. 14, Ag* catalyzes, for example, the reduction of NAD^+ to NADH, whereas the catalytic activity of Ab:Ag* is substantially diminished as a consequence of steric hindrance, conformational change, and/or limited substrate access. Since a larger concentration of Ag results in more Ag* being in the unbound and consequently more active form, a calibration plot can be based on the rate of NADH formation versus Ag concentration. An assay of this type is called an Enzyme

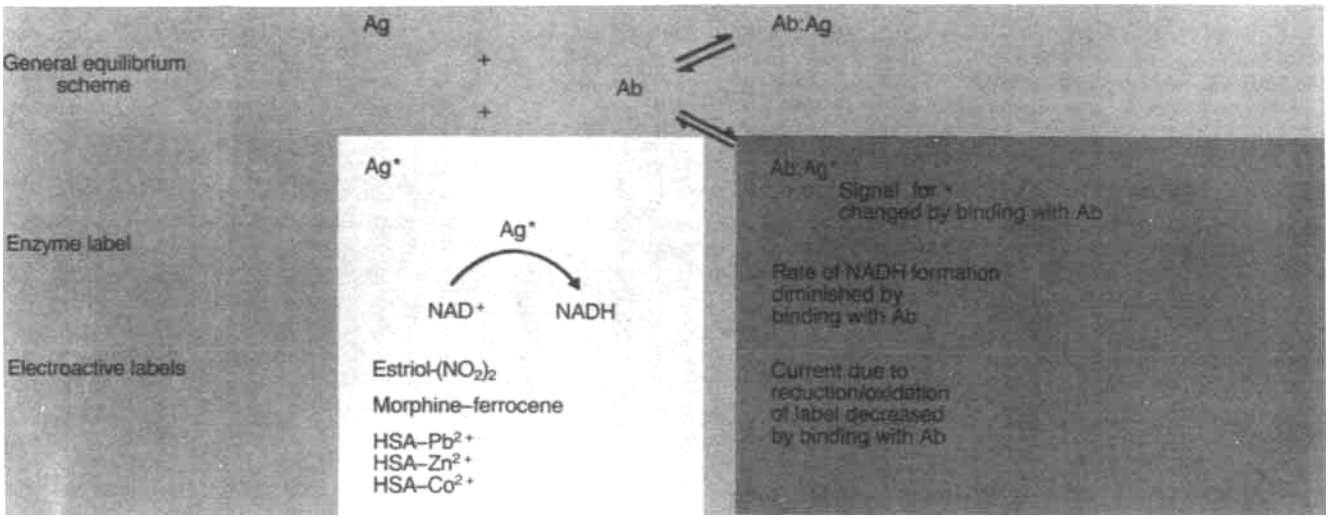

Fig. 14. General reaction scheme for homogeneous immunoassay with examples of enzyme and electroactive labels. (Reprinted with permission from Heineman and Halsall, 1985. Copyright 1985, American Chemical Society.)

Multiplied Immunoassay Technique (EMIT™) and is commonly used with spectrophotometric detection of NADH (Rosenthal et al., 1976).

The discussion that follows describes the adaptation of commercially available immunoassay kits for digoxin and phenytoin which were originally intended for use in such a spectrophotometric assay.

A. ELECTROCHEMICAL DETECTION OF NADH

NADH is oxidized via a single-step two-electron and one-proton loss (Bresnahan et al., 1980; Elving et al., 1982) with the nicotinamide moiety as the electroactive center. The hydrodynamic voltammogram in Fig. 15 shows that NADH is oxidized at a carbon paste (paraffin oil) electrode at potentials more positive than ca. 500 mV versus Ag/AgCl. The voltammogram indicates that the operating potential for maximum sensitivity would be on the limiting current plateau at about 1200 mV, however, for baseline stability and improved selectivity a much lower constant operating potential of 750 mV versus Ag/AgCl is used. At this potential, a calibration plot for NADH determination by LCEC is linear ($r = 0.999$) over the range of 0.23 μM to 295 μM with a detection limit of 0.06 μM at a signal to noise ratio of 2.

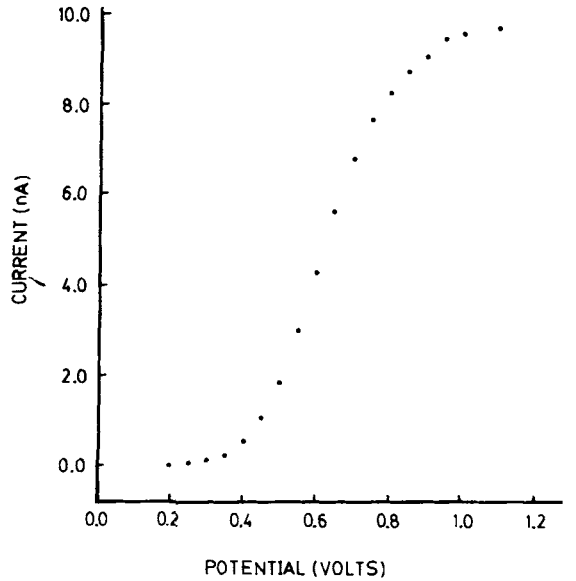

Fig. 15. Hydrodynamic voltammogram of 20 μM NADH in 0.1 M phosphate buffer, pH 7.4. Potential versus Ag/AgCl.

B. IMMUNOASSAY FOR DIGOXIN

In this scheme the major feature is that high performance liquid chromatographic (HPLC) column switching (Apffel et al., 1981; Erni et al., 1981) is used to transfer selectively a chromatographic zone(s) from one column to another. An aliquot of the serum sample-immunoassay reaction mixture is injected into an HPLC column switching system in which a heart-cut is performed. The NADH zone is routed from a precolumn (microparticulate gel filtration) to an analytical column (reversed phase C_{18}) in-line with an amperometric detector; earlier- and later-eluting zones that contain electrochemical interferences are routed from the precolumn to waste. This procedure permits repetitive injections of sample-immunoassay reaction mixtures into the chromatograph while maintaining the working electrode as a stable sensor for NADH.

a. Removal of Electrochemical Interferences. Human serum is an extremely complex matrix and contains a great many electroactive components. A consequence of this is that it is difficult to find an electroinactive "window" where an indicator analyte such as NADH can be measured relatively free from interferences. In serum, interference to NADH measurement occurs both electrochemically and by passive adsorption at the electrode surface. HPLC column switching provides a convenient and precise on-line sample clean up, which removes electrochemical interferences prior to amperometric detection of NADH. The serum biomatrix is the most severe interference source, and readily passivates the working electrode. Table 2 indicates working electrode passivation after several blank human serum injections into a unidimensional HPLC system (C_{18} or Lichrosorb-DIOL column). Triplicate NADH injections were made before and after blank serum injec-

TABLE II

Working Electrode Passivation by Injection of Blank Human Serum into HPLC System with Amperometric Detection at 750 mV versus Ag/AgCl

REVERSED-PHASE C_{18}[a]		LICHROSORB DIOL[b]	
NUMBER OF INJECTIONS	REDUCTION IN NADH PEAK (%)	NUMBER OF INJECTIONS	REDUCTION IN NADH PEAK (%)
1	39	1	18
2	52	3	36
7	70	13	57

[a]Blank human serum diluted by 1/2.
[b]Blank human serum diluted by 1/9.

tion(s) and the extent of electrode passivation was measured as a percent reduction in mean NADH peak height. For example, one serum injection (1/2 dilution factor) into the C_{18} system reduced the mean NADH peak height by 39%. Seven serum injections resulted in a 70% reduction. Similar results were obtained for injections of serum into a Lichrosorb-DIOL, column and a human serum albumin (HSA) solution into both HPLC systems. Neither the C_{18} packing nor the Lichrosorb-DIOL packing alone protected the working electrode from passivation by the serum. However, the Lichrosorb-DIOL column offers an efficient procedure for separation of proteins from NADH and other small molecules (Buchholz et al., 1982; Roumeliotis and Unger, 1979; Schmidt et al., 1980), since the diol portion of the packing minimizes adsorption to the packing material while the small particle size of the packing provides a rapid and highly efficient separation on the basis of size-exclusion.

Uric acid, a serum component having a maximal normal level of 6 mg/100 ml (Orten and Neuhaus, 1982), is a major electroactive interference. A hydrodynamic voltammogram for uric acid displayed an $E_{1/2}$ of 430 mV versus Ag/AgCl. Consequently potential selection could not be used to resolve NADH from the more easily oxidizable uric acid. Immunoassay reagents were also sources of electrochemical interference.

It is important to select column switching times carefully in order to produce an effective sample cleanup. The selection was made by characterizing the Lichrosorb-DIOL precolumn and conducting a switching time survey. As a general guide to the column switching time selection procedure, we describe next in some detail the methods we used for this assay. The details of course will vary from system to system.

The precolumn was first characterized by evaluating the retention times of NADH and the known electrochemical interferences. Spectroscopic detection was used for this, since the electrode passivators (IgG, HSA), uric acid, and NADH absorb at 280 nm, and IgG and HSA are electroinactive at 750 mV versus Ag/AgCl. Figure 16 shows a chromatogram of a blank human serum—NADH mixture which was injected into the Lichrosorb-DIOL precolumn. The first peak (retention time of 113 sec) was primarily composed of IgG and HSA. The second peak (173 sec) was NADH; the shoulder that appears at approximately 190 sec was uric acid. Therefore a heart-cut should be from 150 sec (to remove the macromolecular fraction) to 185 sec (to remove the late-eluting uric acid among other possible interferences).

Switching time surveys were performed to find optimal column switching times, that is, when during the assay the precolumn was to be switched in and out of line with the analytical column. The switching time set of 162/182 sec was chosen for the digoxin immunoassay, since it

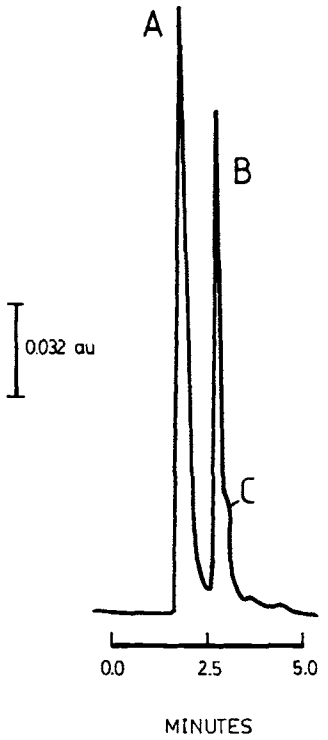

Fig. 16. Chromatogram of blank human serum calibrator-NADH mixture. Lichrosorb-DIOL column, flow rate 1.1 ml/min, detection by absorbance at 280 nm *(A)* HSA and IgG, *(B)* NADH, and *(C)* uric acid.

maximizes the time distance from the HSA retention time and also eliminates most of the uric acid. The timing interval was also surveyed between 10 and 90 sec with the 20 sec interval producing the least electrode fouling and most precise data. An electronically switched valve system would be an obvious advantage here.

The C_{18} analytical column was chosen to separate NADH from possible coeluting interferences and a disturbance resulting from the switching process. Thus no switching was required to cut the NADH peak from the C_{18} outflow prior to presentation to the electrode surface. This column-switching scheme was effective in removing electroactive and electrode-passivating interferences. No reduction in mean NADH peak height was observed after 44 injections of serum-enzyme reaction mixtures; no deterioration in chromatographic performance was observed after 176 serum injections.

The precision of the HPLC column-switching–amperometric system was consistently excellent. For example, 11 injections of a 5.28×10^{-6} *M* NADH solution gave a relative standard deviation of 0.3% (x = 9.65 nA; s = 0.03 nA).

b. Enzyme Immunoassay. The EMIT kit for digoxin produces quantities of NADH easily detectable electrochemically in short periods of time. This is the result of the glucose-6-phosphate dehydrogenase providing a large amplification quotient (NADH:digoxin). For digoxin at 7.05×10^{-10} *M*, the quotient is 3.7×10^4 at 5 min and 1.6×10^5 at 38 min.

A two-point kinetic method (2 and 7 min) was used to provide a simple rate measurement for NADH production. These times were chosen for convenience and precision, and the procedure eliminates the effects of trace interferents that may coelute with the NADH on the C_{18} column. Figure 17 is a chromatogram of six digoxin calibrators (0–7.5 ng/ml) with two injections for each calibrator. The number above each bracketed set of peaks is the digoxin calibrator concentration (ng/ml). The starred peaks represent NADH generated enzymatically after 2 and 7 min. As expected, the NADH peak increases with both increasing digoxin concentration and time. Similar peak sets were produced for each unknown. The unmarked small peaks were a result of residual uric acid and the column switching process.

Figure 18 is a digoxin standard curve encompassing the therapeutic range, using the EMIT modified logit-log data transformations (Dietzler

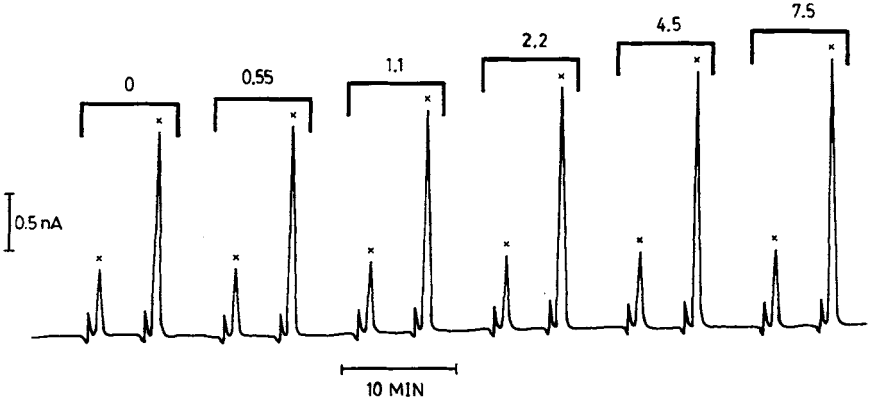

Fig. 17. Homogeneous enzyme immunoassay with column switching LCEC for digoxin calibrators of marked concentration in ng/ml. *–NADH peaks. Enzyme reaction sampled at 2 and 7 min for each calibrator.

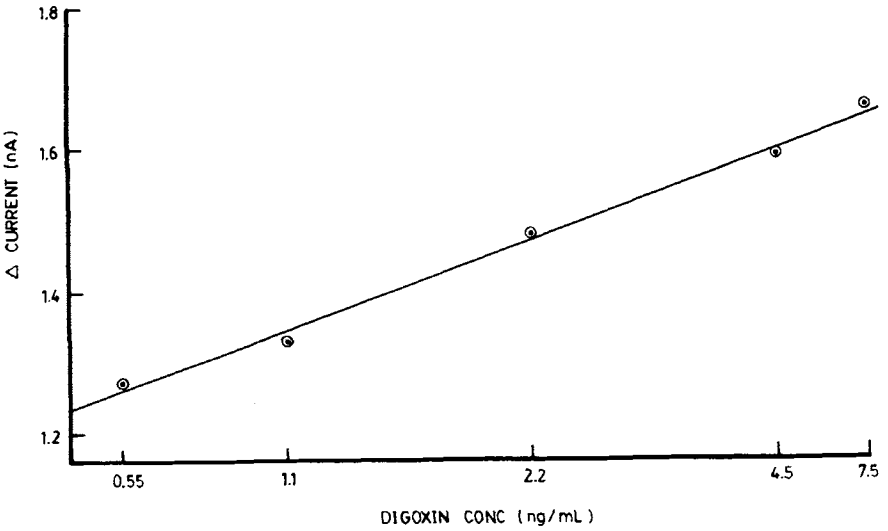

Fig. 18. Digoxin calibration plot (log-logit).

et al., 1980; Wellington, 1980). This was generated by plotting the difference in peak heights (nA) for each calibrator versus digoxin concentration. The ordinate, representing the rate of NADH production, was arbitrarily scaled with respect to the change in current (nA/5 min). the abscissa is logarithmic with respect to the digoxin concentration. Note that the plot is linear over the range of 0.55 to 7.5 ng/ml.

The ability of the antibody to inhibit enzyme activity of the enzyme labeled digoxin is poor, and a substantial blank yield of NADH is obtained. This high blank yield is the major contributor to the detection limit obtained, and therefore a high degree of precision for the whole procedure is needed for a usable assay. The within-run precision for this immunoassay using the amperometric HPLC column-switching system was good. For the assay of six digoxin calibrator #3 replicates (2.2 ng/ml), the relative standard deviation of the amperometric response was 2.3% (x = 2.15 nA; s = 0.05 nA) which is slightly better than those reported for the spectrophotometric or other modifications of the assay, which range from 2.7 to 7.1% (Linday and Drayer, 1983; Rumley et al., 1980; Brunk and Malmstadt, 1977; Eriksen and Andersen, 1978; Rosenthal et al., 1976). Under the conditions used, this amperometric method requires only one sixth of the enzyme incubation time, resulting in an overall assay shortening by two-thirds.

Precision studies of an aqueous mixture of NADH and uric acid were

run before and after the digoxin immunoassay to evaluate both the condition of the columns and the working electrode with respect to retention times and mean peak height. No significant changes resulted, and the HPLC column-switching system was considered stable and effective in removing interferences.

*c. **Comparison with Radioimmunoassay.*** Accuracy of the amperometrically based enzyme immunoassay was evaluated by comparison with a commercially available digoxin radioimmunoassay (ARIA HT digoxin system). Forty-eight human serum samples were assayed by both methods; two of the sample results were rejected as outliers by the *Q*-test at the 99% confidence level. The correlation plot in Fig. 19 summarizes the results of the comparison. The range of digoxin concentrations evaluated by RIA was 0.3–4.1 ng/ml. Correlation analysis yielded a correlation coefficient of 0.942 between the two methods.

*d. **Materials and Methods.*** A block diagram of the HPLC column-switching system is shown in Fig. 20. Two high-pressure solvent delivery pumps (Milton Roy Laboratory Data Control model 396-31 and model 396-57) were used to provide flow rate stability upon column switching.

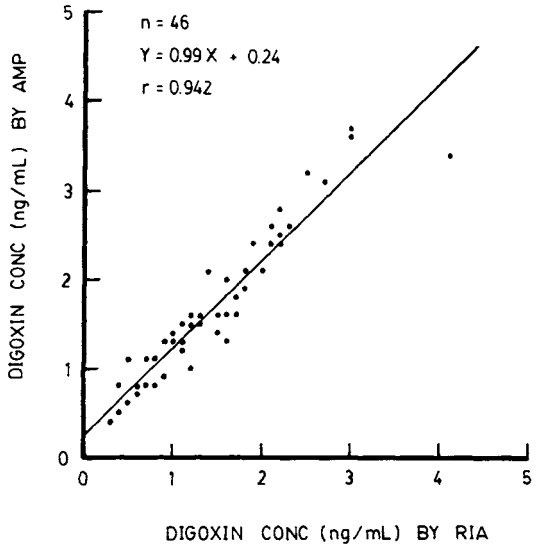

Fig. 19. Correlation between digoxin concentrations in patients by RIA and LCEC. Line is a simple linear regression of the paired data.

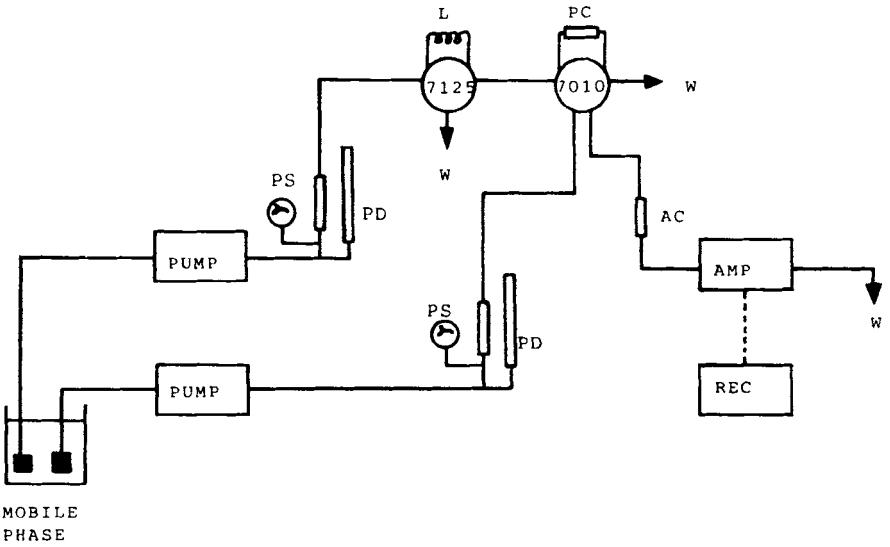

Fig. 20. Block diagram of HPLC column switching system with electrochemical detection. *L*, sample loop; 7125 and 7010, injection valves; *W*, waste; *PC*, precolumn; *AC*, analytical column; *AMP*, electrochemical detector; *REC*, strip chart recorder; *PD*, pulse dampers; *PS*, presaturator columns.

Both pumps delivered mobile phase from a common reservoir at 1.15 ml/min. Each pump flow line was supplied with a standing-air column pulse damper, a high-pressure gauge, and a presaturator column. Both presaturator columns contained Vydac pellicular C_{18}. Two Rheodyne sample injection valves were used for column switching: model 7125 (20 μl sample loop) syringe-loader and model 7010. The switching columns included a precolumn (10 μm Lichrosorb DIOL; 25 cm × 4.6 mm, Knauer) which was positioned where the sample loop would normally be in the 7010 injection valve, and an analytical column (10 μm RSiL C_{18} HL; 2 cm × 2.0 mm, Upchurch). A stop watch was used to time the manual switching of the injection valves.

Amperometric detection included a BAS (Bioanalytical Systems, Inc.) LC-4B amperometric detector, a BAS TL-3 thin-layer amperometric flow cell (5 mil spacer), and an RC-2A reference compartment. The flow cell contained a carbon paste-paraffin oil working electrode, a silver/silver chloride reference electrode (RE-1), and a stainless steel auxiliary electrode. A BAS RYT strip-chart recorder was used.

The EMIT Digoxin Assay is a commercially available kit from the Syva

Company (Palo Alto, CA). Immunoassay reagents and calibrators were prepared as prescribed in the kit instruction manual. Six digoxin calibrators (0–7.5 ng/ml in human serum) were provided.

NADH and goat IgG were purchased from the Sigma Chemical Co.; uric acid from MCB; human serum albumin from Miles Laboratories, Inc., as a lyophilized preparation. The mobile phase (0.1 *M* phosphate buffer at pH 6.6) was prepared from Na_2HPO_4 and Na_2HPO_4 (Fisher Scientific Co.). Phosphate buffer (0.1*M* pH 7.4) was used to prepare solutions of NADH, uric acid, immunoglobulin G, and human serum albumin.

The EMIT protocol was followed through the production of NADH. The 50 μl of the NADH-containing reaction mixture was diluted 11:1 with 0.1 *M* phosphate pH 7.4, vortexed, and sampled by HPLC. Under the conditions used the NADH residence time on the Knauer column was 2 min 47 sec. Tubes were processed every 12 min in this manner.

C. OTHER IMMUNOASSAYS

An enzyme immunoassay based on the production of NADH has also been developed in our laboratory for phenytoin, an antiepileptic drug (Eggers et al., 1982). The assay is of the EMIT format with glucose-6-phosphate dehydrogenase as the enzyme label. As such, this assay for phenytoin is in most respects similar to that described for digoxin. The therapeutic level for phenytoin is 2.5–3.0 μg/ml, which is about 1000-fold higher than the level for digoxin. This high concentration of analyte caused correspondingly higher levels of NADH production in the same time frame as for digoxin. Consequently, samples were diluted 121-fold immediately before injection into the HPLC in order to reduce the NADH level to the optimum range for its detection. This dilution step also lowered the concentrations of interfering uric acid and adsorbable proteins to a level at which an LCEC system as shown in Fig. 2 with a C_{18} chromatography column sufficed to protect the electrode. Good correlation (correlation coefficient = 0.99, slope = 0.98, *y*-intercept = 0.01) for samples from patients on phenytoin maintenance was obtained between the electrochemical and spectroscopic detection of NADH.

A homogeneous enzyme immunoassay based on antibody inhibition of enzyme conversion from the apo- to the holo- form has been developed for DNP-aminocaproic acid, DNP-ACA (Ngo et al., 1985). A competitive equilibrium is established between the analyte DNP-ACA and DNP-conjugate apoglucose oxidase, DNP-CAGO, which is the labeled hapten. Flavin adenine dinucleotide, FAD, added to the mixture binds to free DNP-CAGO to give DNP-CAGO:FAD, which is enzymatically active and

catalyzes the production of H_2O_2 from O_2. Since FAD cannot bind to Ab:DNP-CAGO, the rate of H_2O_2 generation is a measure of the concentration of free DNP-CAGO, which in turn reflects the concentration of DNP-ACA in the sample. The rate of production of H_2O_2 is measured amperometrically by oxidation at 700 mV. This assay has a range of approximately 2–40 μg/ml.

III. NONENZYMATIC ELECTROACTIVE LABELS

A second major class of electrochemical immunoassays involves labeling an antigen with a group that renders the antigen electroactive. The labeled antigen (Ag*) would be reducible or oxidizable in a potential range over which Ag is electroinactive, thereby enabling Ag* to be electrochemically distinguishable from Ag.

1. Homogeneous Assays

The homogeneous assay is based on a competitive equilibrium between Ag and Ag* for a limited amount of antibody as described (see Fig. 14 and Section II.2). The assay relies on a decrease in the current signal for the reduction/oxidation of Ag* when bound to Ab. Since all of these assays have no enzyme multiplication feature, the detection limits are generally much higher. In the model assay that follows, the free, equilibrium concentration of electroactively labeled estriol is determined by differential pulse polarography at a dropping mercury electrode (Wehmeyer et al., 1982). The peak current from the polarographic reduction of Ag* is then proportional to the concentration of Ag present. The separation of Ab:Ag* from Ag* is unnecessary because of the attenuation of the Ab:Ag* reduction.

A. ELECTROCHEMICAL DETECTION

Differential pulse polarography (DPP) is a sensitive method for the trace (detection limit of 10^{-6}–10^{-8} M) determination of electroactive organic compounds (Kissinger, 1984; Brooks, 1984). In this technique the sample is introduced into an electrochemical cell for which the working electrode is a dropping mercury electrode (DME). A polarogram is obtained by scanning the potential of the DME and measuring the resulting current. Reduction of an electroactive analyte in the cell is signaled by a peak-shaped current response, the peak height being proportional to the analyte concentration. The low detection limit of DPP is obtained by pulsing the electrode potential late in the lifetime of each mercury drop

and making a precisely timed differential current measurement that discriminates against interference from electrode charging (Kissinger, 1984). Continuous renewal of the electrode surface of the DME by formation of a new drop every few seconds is advantageous for protein-containing solutions that are prone to foul electrode surfaces.

Introducing two nitro groups into the A ring of estriol produces an electroactive labeled hapten that is electrochemically distinguishable from the unlabeled hapten. The dinitroestriol (DNE) is electroactive with two distinct reduction waves with peak potentials of −422 mV and −481 mV versus Ag/AgCl (Fig. 21). The peak current is linear with concentration from 60 ng/ml to 3.7 μg/ml. In order to detect the nitro label on the estriol, the other assay components should be electroinactive in the potential region where this group is reduced. This situation exists for solutions of estrogen-specific antibody, estriol, and phosphate buffer, which are electroinactive in the potential range −200 to −1000 mV versus Ag/AgCl. Thus this relatively large "potential window" is available for the observation of the labeled material without interference.

B. ANTIBODY-DNE BINDING

The effect of a specific antibody on the reduction of DNE is readily seen when polarograms are recorded before and after the addition of successive aliquots of the estrogen antibody (Fig. 22). As DNE is bound by an antibody, there is a sequential decrease in the reduction peak current.

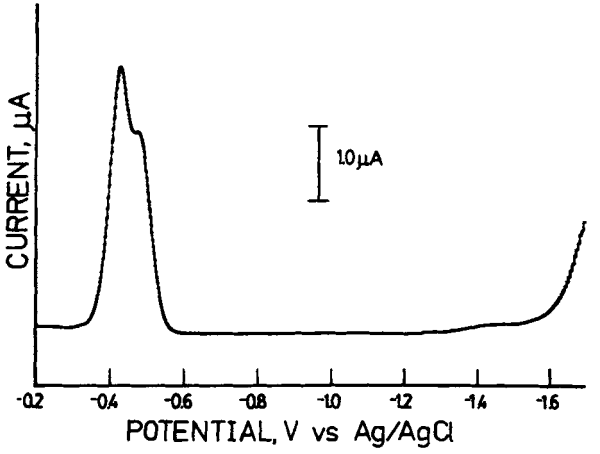

Fig. 21. Differential pulse polarogram of 7.3 μ*M* dinitroestriol, 0.1 *M* phosphate buffer. (From Wehmeyer et al., 1982, with permission.)

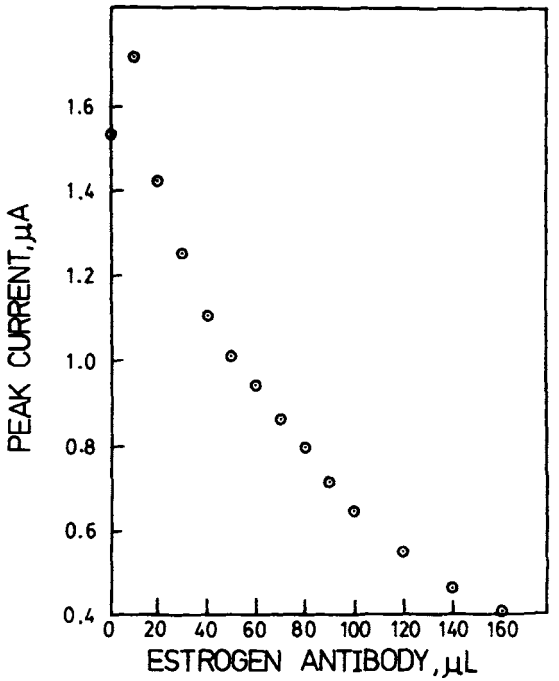

Fig. 22. Plot of differential pulse polarogram peak currents for 4.6 ml of phosphate buffer solution containing dinitroestriol (7.7 μM) versus microliters of estrogen-specific antibody added to the dinitroestriol solution. (From Wehmeyer et al., 1982, with permission.)

Two major possibilities exist for this decrease in peak current. The antibody binding of DNE may sequester the electroactive nitro groups from the electrode surface by burying them in the binding site. The DNE-Ab complex would be electroinactive, and the decrease in peak current would therefore be due to a decrease in the concentration of the reducible solution species. It is also possible, however, that the DNE-Ab complex is still electroactive, in which case the decrease in peak current would be due to the large decrease in the diffusion coefficient of the DNE-Ab complex as compared with that of free DNE. The diffusion coefficients of globular proteins of M_r 150 000–160 000 in aqueous media are about 10^{-7} cm^2/sec, whereas those of small organic compounds such as estriol are about 10^{-5} cm^2/sec. In polarography, since the peak current is directly proportional to the square root of the diffusion coefficient of the electroactive species, the decrease therefore could be

attributable to a change in diffusion coefficient on binding. In either case the effect of binding is clearly measurable without separation of the bound-labeled from the free-labeled species. The increase in peak current observed for the addition of the first aliquot of antiserum is probably due to some type of adsorption phenomenon at the electrode surface.

C. CONSIDERATIONS FOR IMMUNOASSAY

We have not developed this general scheme into a functional immunoassay for estriol at the clinical level because of the inadequate detection limit, unlike previous sections. However, we have explored those features of such an assay that would be applicable to other analytes. It is particularly important with an electrode such as the DME that readily adsorbs proteins to demonstrate that the results obtained are not artifactual. It is also important to determine whether the labeled Ag has radically different properties from unlabeled Ag that might be detrimental to assay development.

a. Reversible Binding. For any antigen-antibody reaction to serve as a functional competitive-type analytical method, the bound labeled hapten must be reversibly displaced from the antibody by unlabeled hapten, and the amount of displaced labeled hapten should be proportional to the concentration of unlabeled hapten in the standard or sample to be analyzed. This can be tested by recording first a polarogram for a solution of DNE plus antibody and then for this solution after the addition of aliquots of estriol. A plot of the resulting peak current is shown in Fig. 23. The reversibility of the displacement of DNE from the Ab binding sites is demonstrated by the sequential increase in peak current with successive aliquots of unlabeled estriol. The displacement increases the concentration of free DNE capable of being reduced and correspondingly decreases the concentration of bound DNE. An immunoassay based on DPP would rely on the quantitative detection of this reversible displacement.

b. Ab Selectivity. Estrone and estradiol were also able to displace antibody-bound DNE, as would be expected from the reported cross reactivity with these steroids of the antisera used. Progesterone, however, did not displace DNE from the antibody-binding sites, indicating that estrogen specificity has not been lost. In a similar way nonspecific interactions between DNE and Abs other than anti-DNE-Ab were assessed using nonspecific bovine Ab. Aliquots of a bovine Ab solution were added successively to a solution of DNE and the polarograms recorded. Figure 24 shows a plot of normalized peak current versus concentration of bovine Ab.

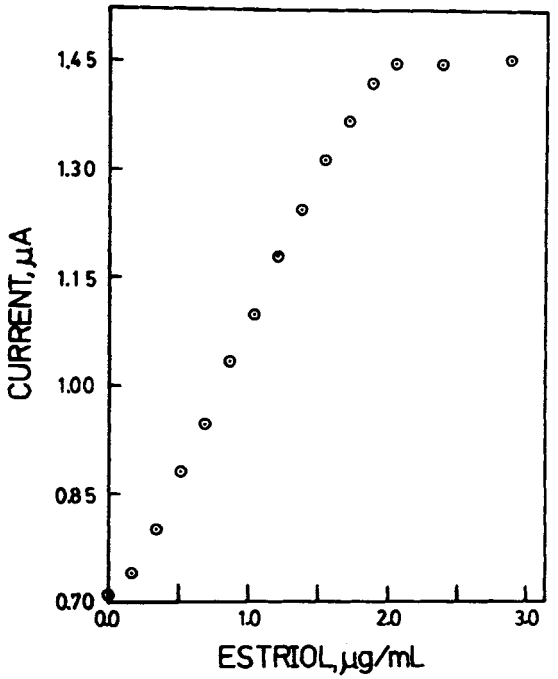

Fig. 23. Plot of differential pulse polarogram peak currents of 5.5 ml of phosphate buffer solution containing dinitroestriol (5.6 μmol/l) plus 150 μl of estrogen-specific antibody versus estriol added to the solution. (From Wehmeyer, et al., 1982, with permission.)

With the addition of successive aliquots of the Ab, the normalized peak current decreased to a limiting value, after which further aliquots of bovine Ab produced no further decrease in normalized peak current. Subsequent addition of an aliquot of an unlabeled estriol solution to the DNE-bovine IgG solution failed to increase the normalized peak current (Fig. 24). This initial decrease in the normalized peak current is the result of protein coating or "fouling" of the electrode surface.

The addition of successive aliquots of estrogen antisera to a solution of DNE containing bovine Ab caused incremental decreases in the normalized peak current, whereas further additions of a bovine Ab solution resulted in no significant decrease in normalized peak current. Also the addition of an aliquot of estriol to a solution of DNE containing estrogen antisera plus bovine Ab increased the normalized peak current, in contrast to the addition of estriol to the DNE solution containing bovine Ab

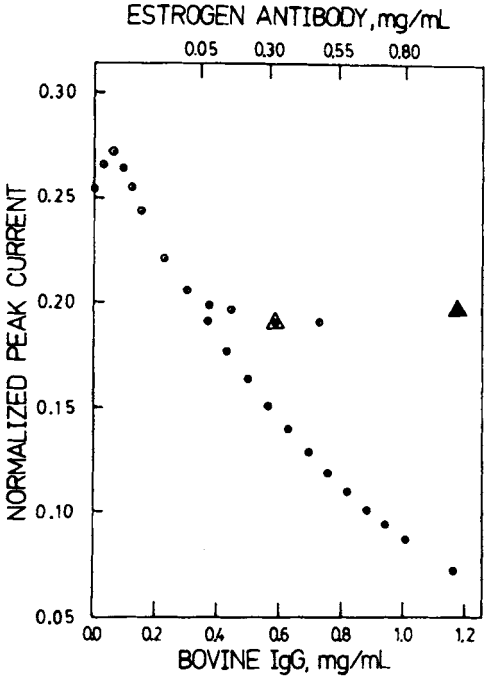

Fig. 24. Plot of normalized peak current [(peak current)/(concentration DNE)] from differential pulse polarograms of 5.0 ml of phosphate buffer solution containing dinitroestriol (DNE), bovine IgG, estriol, and (or) estrogen-specific antisera. ⊙, DNE 7.0 μ*M* plus bovine IgG as shown on bottom scale; Δ, DNE 7.0 μ*M* plus bovine IgG (0.7 g/liter) and estriol (74 μ*M*); ●, DNE 8.8 μ*M* plus bovine IgG (0.3 g/liter) and estrogen-specific antisera as shown on top scale; ▲, DNE 8.8 μ*M* plus bovine IgG (0.3 g/liter), estrogen-specific estriol (0.9 g/liter), and estriol (6.0 μ*M*). (From Wehmeyer et al., 1982, with permission.)

only (Fig. 24). These results indicate that a specific hapten-antibody interaction is responsible for the decrease in peak current observed for DNE/estrogen antisera combination, but not for the small decrease observed with the DNE/bovine Ab combination.

c. Effects of Clinical Matrices. The effects of urine and plasma were determined by using high concentration "spikes" of estriol in these fluids. Binding and displacement of DNE from Ab sites by estriol were readily observable in urine, but not in plasma. This is probably due to a high amount of nonspecific binding by the serum albumins, an observation in common with other assays for this hydrophobic analyte.

In summary, the use of DPP and an electroactive label resulted in a competitive homogeneous immunoassay with a detection limit in the 100 ng/ml range. Although application to estriol is not feasible, the direct analysis of urinary samples for other analytes in this concentration range would be possible. The analysis of plasma analytes may or may not require a cleanup step, depending on the analyte involved.

D. MATERIALS AND METHODS

Estriol, estradiol, and bovine Ab were of the highest available purity (Sigma Chemical Co.). Estrogen-specific monoclonal antiserum was a gift from New England Nuclear. Water was doubly distilled and passed through an ion-exchange column. All other chemicals were reagent grade or better.

The supporting electrolyte was potassium phosphate buffer, 0.1 *M*, pH 7.4. The analysis buffer was purged with N_2 for 1 h and then preelectrolyzed over a mercury pool electrode maintained at −1.3 V versus SCE for at least 48 h to remove trace-metal impurities. The Ab fraction was isolated by use of a Sephacryl 200 (Pharmacia) column, using 0.1 *M* potassium phosphate buffer (pH 7.4) as the eluent. It was then dialyzed overnight against the same buffer and lyophilized. The lyophilized Ab fraction was reconstituted with deionized water, and this solution was used as the antiserum in this study.

For DPP we used a Model 174A polarographic analyzer (Princeton Applied Research Corp.) with a Model 2000 x-y recorder (Houston Instruments), a Model 303 static mercury drop electrode (PARC), a saturated Ag/AgCl reference electrode, and a platinum auxiliary electrode. All polarography was with these scan conditions: range of scan, −200 to −1700 mV versus Ag/AgCl; pulse amplitude, 25 mV; scan rate, 10 mV/sec; drop time, 1.0 sec; medium mercury drop (0.186 μl). Solutions were purged for 5 to 12 min, with nitrogen passed through vanadous chloride deoxygenating towers. They then were blanketed with nitrogen while recording polarograms. Polarograms were repeated three times to obtain average values. The solution volumes used in this study were about 5.0 ml, although smaller volumes can be routinely tested. Protein solutions were deoxygenated at a slow N_2 flow rate to prevent frothing.

Estriol was nitro-labeled in the 2 and 4 positions by the procedure of Konyves and Olsson (1964). The product was separated from an impurity by column chromatography on silica gel 60 and elution with acetone/chloroform (l/l, by vol.). The isolated product melted at 225°C. The labeled estriol was dissolved in ethanol/water (l/l, by vol.) solution and used as a standard solution.

E. OTHER LABELS

Electroactive labels have been used by other workers in systems such as morphine labeled with ferrocene that was detected by FIAEC at a glassy carbon electrode (Weber and Purdy, 1979), ovalbumin labeled with electroactive diazotized *p*-aminobenzoic acid that was detected polarographically by reduction at a DME (Breyer and Radcliff, 1951, 1953), *p*-(*p*-aminophenylazo)-phenylarsonic acid that was monitored by cathode-ray polarography (Schneider and Sehon, 1961), and estriol labeled with mercuric acetate detected by differential pulse polarography (Heineman, et al., 1979). As pointed out in Section III.1.B, homogeneous immunoassays of this type are apparently based in part on the difference in diffusion coefficient between the free labeled antigen and the labeled antigen bound to the much larger antibody (Steinhardt and Reynolds, 1969). Consequently this is a general approach that should be applicable when the antigen is sufficiently smaller than the Ab to give a large difference in diffusion coefficient.

Immunoassays for human serum albumin (HSA) have been based on HSA labeled with Pb^{2+} (Alam and Christian, 1982), Co^{2+} (Alam and Christian, 1984), and Zn^{2+} (Alam and Christian, 1985). The metal ion bound to the HSA can be detected with differential pulse polarography by reduction at a mercury electrode. The peak current for the labeled HSA decreases on binding with Ab, which is the basis for the immunoassay.

An electrochemical luminescence-based immunoassay has been presented with HSA labeled with the aromatic hydrocarbon amino-pyrene (Ikariyama et al., 1985). The pyrene-labeled HSA luminesces during reduction at a platinum electrode, and on binding to Ab, the intensity of luminescence is decreased. A detection limit of 10^{-6} *M* for HSA was obtained. Labels with greater luminescence efficiency should provide lower detection limits.

These latter two assays rely more on steric hindrance of access of the electroactive groups to the electrode surface than changes in diffusion coefficient upon binding to Ab. Thus their sensitivity is dependent on careful placement of the electroactive species with respect to the Ab binding site(s) on the Ag.

2. Heterogeneous Assays

A releasable electroactive metal ion may be used as the label for a heterogeneous assay (Doyle et al., 1982). Release of the metal ion label after competitive equilibration with antibody enables the very sensitive tech-

nique of differential pulse anodic stripping voltammetry (DPASV) to be used as the electroanalytical method (Heineman et al., 1984; Wang, 1985). In^{3+} is used as a label for this purpose since it is easily determined by DPASV and forms strong complexes with bifunctional chelates such as diethylenetriaminepentaacetic acid (DTPA), which can be used to attach the label to an antigen (Doyle et al., 1982). In^{3+} is as yet unfound in human tissue, and hence in clinically relevant analyses interference from the sample itself is avoided.

This strategy is described here using human serum albumin (HSA). Indium-labeled HSA consists of HSA to which DTPAHD is covalently attached. DTPAHD strongly complexes the In^{3+} label ($K_f = 10^{29}$), yielding the labeled albumin, (i.e., *H*SA-*D*TPA-*I*n^{3+}, HDI). The assay procedure is outlined in Fig. 25. After equilibration with HSA and Ab (which in this case is adsorbed to insolubilized protein A of *Staphylococcus aureus*), Ab:HDI is separated by centrifugation of the immunoadsorbent complex. The In^{3+} label is then released by acidification and determined by DPASV. A calibration curve shows peak height of the stripping wave for In^{3+} decreasing as increasing concentrations of HSA displace more HDI from Ab.

The heterogeneous electrochemical procedure described here is widely applicable to protein antigens due to the universal nature of the DTPA coupling reaction. Recently a similar heterogeneous immunoassay protocol has been made commercially available by LKB using Eu-DTPA complex as a tracer (LKB News, 1984). The europium label is released following acidification and detected by fluorescence spectroscopic methods. The popularity of this class of immunoassays should continue to grow as chelate-coupled macromolecules become readily available. In addition the utilization of a "sandwich" format and longer deposition times for DPASV should result in a series of assays with even lower limits of detection.

A. ELECTROCHEMICAL DETECTION

Anodic stripping voltammetry (ASV) is ideally suited to the determination of metal ions that are reducible to mercury-soluble metals (Heineman et al., 1984; Wang, 1985). The technique consists of two steps. First, a fraction of the sample metal ion is deposited as amalgamated metal by reduction at a mercury electrode such as a hanging mercury drop electrode (HMDE). This is accomplished by applying a potential that is sufficiently negative to reduce the sample metal ion for a carefully measured time. This step, often called the "deposition" step, serves to preconcentrate sample as metal in the small mercury drop by what is

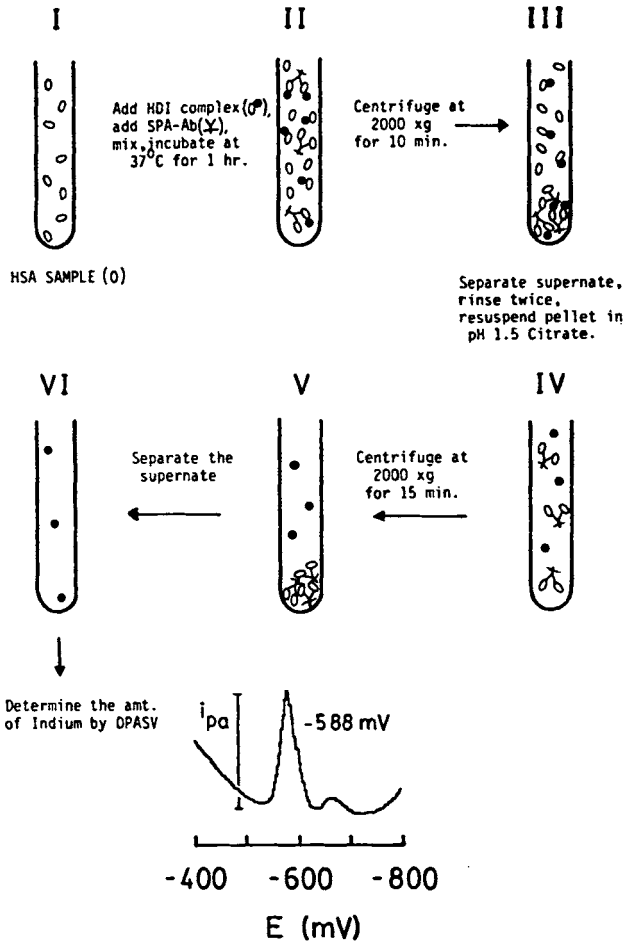

Fig. 25. An outline of the heterogeneous DPASV immunoassay protocol using the SPA-αHSA complex as an immunoadsorbent for labeled and unlabeled antigen. (Reprinted with permission from Doyle et al., 1982. Copyright 1982, American Chemical Society.)

essentially an electrochemical extraction. It is this preconcentration feature that enables detection limits as low as 10^{-10}–10^{-11} M to be achieved. Second, a positive potential scan is then applied to the mercury electrode. This scan causes oxidation of the deposited metal which is signaled by a peak-shaped anodic current response. The peak height is proportional to the concentration of metal ion in the sample. Detection

limits are improved by using a differential pulse technique which discriminates against electrode charging current (see Section III.1) for the positive potential scan. This method is termed differential pulse anodic stripping voltammetry (DPASV).

Preliminary experiments with DPP and DPASV confirmed that In^{3+} could be released from the HDI complex by acidification. Released In^{3+} was preconcentrated by reduction to In^0 (Losev and Moledov, 1976) at a HMDE at a potential of −0.8 V versus SCE maintained for 5 min with a stirred solution. The stripping peak for indium occurred at −0.588 mV. Assay conditions were optimized with respect to pH to achieve maximal current response and maintain the highest degree of selectivity for the determination of indium (Doyle et al., 1982).

B. MINIMIZATION OF PROTEIN ELECTROSORPTION

The HMDE is highly susceptible to fouling by protein adsorption. This problem can be surmounted by removing interfering protein from solution prior to electrochemical investigation. This is done conveniently using a solid phase immunoadsorbent such as protein A, which is specific for a single antigen when complexed with the appropriate antibody, and permits the ready separation of protein by centrifugation. These principles were used in a competitive heterogeneous immunoassay, which removed HDI and HSA from solution and retained them so that the indium could be detected at the electrode surface in an interference-free manner. The kinetics of antigen dissociation in the presence of salt are slow (Hardie and van Regenmortel, 1977) compared to the equilibria governing indium release from DTPA upon acidification. Thus the possibility of antigen leaching is unlikely, and any residual protein remaining in the supernate is of such low concentration that current attenuation is not a problem. After the separation step the total protein concentration of each tube is identical and only the ratios of bound HSA/HDI differ. Thus any depression in current response due to adsorption is reflected equally throughout the assay. Other approaches designed to remove interfering protein complexes (i.e., chromatography) could also be developed.

C. IMMUNOASSAY BY ANODIC STRIPPING VOLTAMMETRY

Following the assay protocol summarized in Fig. 25, a characteristic anodic wave corresponding to released indium appears at −588 mV as seen in Fig. 26. The wave at −633 mV, which also appears in blank analysis, is attributable to trace cadmium associated with the commercial immunologic reagents. The wave at −588 mV is resolvable in the presence of that at −633 mV, and HSA effectively displaces HDI bound to the

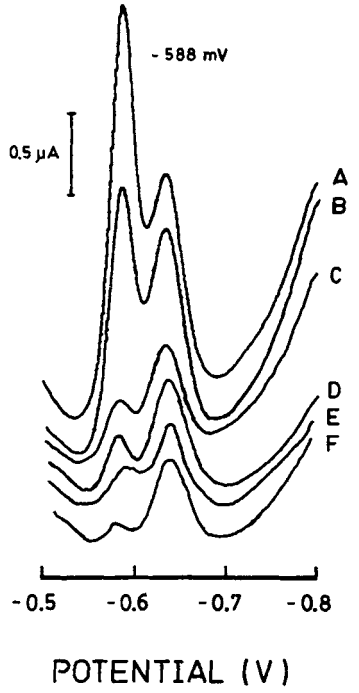

Fig. 26. Differential pulse anodic stripping voltammograms of a series of HSA standard solutions of increasing concentrations *(A–F)* in 0.1 citrate. (Reprinted with permission from Doyle et al., 1982. Copyright 1982, American Chemical Society.)

SPA-Ab adsorbent phase. Decreasing amounts of released indium are observed as the amount of HSA in the original analytical solution increases. Consequently a progressive decrease in anodic peak current (i_{pa}) for the indium wave results with HSA standards of increasing concentration (Fig. 26*A–F*). A plot of this peak current versus HSA concentration generates a smooth standard curve, which can be utilized for unknown sample analysis (Fig. 27).

The controlled release of indium, simply by adjusting solution pH, coupled with the removal of protein, enables one to detect the tracer in an essentially interference-free environment. This approach eliminates any possibility of competing equilibria, as has been reported by others (Alam and Christian, 1982, 1984, 1985; Svoboda, 1981), which might seriously compromise the utility of the assay.

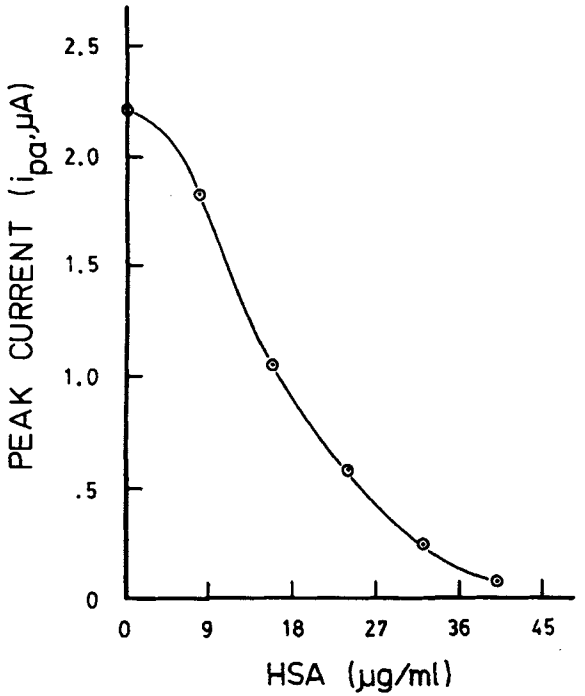

Fig. 27. Plot of anodic peak current for indium vs concentration of HSA in a series of standard solutions. (Reprinted with permission from Doyle et al., 1982. Copyright 1982, American Chemical Society.)

D. COMPARISON WITH MICROBIURET METHOD

Analytical methods employed for the quantitation of serum proteins vary widely depending on the analyte concentration. The microbiuret assay was chosen as the most appropriate technique to compare with the electrochemical method, primarily because their applicable concentration ranges overlap. Further the microbiuret assay is frequently used for HSA quantitation when precision is required. Since the microbiuret assay measures the UV absorption of a complex formed between peptide nitrogens and Cu^{2+} in an alkaline $CuSO_4$ media (Itzhaki and Gill, 1964), it is relatively nonspecific and suffers from interferences including bile pigments and ammonia (Bradford, 1976) which may be present as a pathological consequence.

The electrochemical method, on the other hand, is highly specific for the analyte of interest and free from endogenous interferences. A corre-

lation plot obtained for the analysis of a common set of solutions by the electrochemical immunoassay and the microbiuret assay yielded a correlation coefficient of 0.998 over a 20–100 μg/ml range.

E. MATERIALS AND METHODS

Citrate buffer and saline (MCB) solutions were preelectrolyzed for 24 h at −1100 mV versus SCE to remove metal ion impurities. Acetonitrile (MCB) was redistilled and stored over molecular sieves. DTPA (Aldrich), triethylamine (Aldrich), and isobutylchloroformate (Sigma) were of the highest available purity. HSA (essentially globulin free) and rabbit IgG specific for HSA (Sigma) were obtained in the lyophilized form. Indium was obtained as anhydrous, ultrapure $InCl_3$ (Alfa Products). All solutions were prepared from distilled/deionized H_2O of at least 10^6 Ω resistivity. Protein A from *Staphylococcus aureus* (SPA, Enzyme Center) was employed as an immunoadsorbent. It was obtained as a 10% (w/v) suspension with a 1.47 mg/ml binding capacity for immune complexes. 2-mercaptoethanol, sodium dodecyl sulfate, and acrylamide reagents were all of electrophoretic grade (Bio-Rad).

The equipment described in Section III.1.D was used for DPASV measurements. Analyses by DPASV were done with a large hanging mercury drop (0.372 μl). Indium was preconcentrated using a deposition time of 5 min at a potential of −800 mV. The potential range between −800 mV and 0 V was then scanned positively at a 2 mV/sec scan rate, with a 25 mV pulse height of 0.5 sec duration. pH measurements were made with a Fisher Model 610A pH meter (Fisher Scientific) with a glass-body microcombination pH electrode mounted in the electrode housing of the SMDE, enabling pH monitoring during the course of the experiment. Electrophoretic studies employed a Polyanalyst disk gel apparatus (Buchler Inst.).

A modification (Doyle et al., 1982) of the four-step mixed anhydride procedure of Krejcarek and Tucker (1977) was used to couple DTPA to HSA. A 17-fold molar excess of In^{3+} was added to the cooled HSA-DTPA solution, and the mixture stirred for 35 min. The pH was adjusted to pH 4.50 with 1.0 *M* NaOH, and the solvent was sequentially replaced by ultrafiltration using a 10,000 MWCO membrane, against 200 ml of 0.15 *M* NaCl and then 400 ml of 0.1 *M* citrate buffer (pH 5.50) and dialyzed once against 1 liter of 0.1 *M* citrate buffer (pH 5.50) to remove any unbound In^{3+} or noncovalently attached DPTA. The HDI complex was shown to be monodisperse by gel chromatography and electrophoresis, immunoreactive via Ouchterlony radial immunodiffusion, and contained 3–5 mol In^{3+}/mol HDI as determined by plasma emission spectroscopy (Doyle et al., 1982).

The immunoadsorbent was prepared as follows: 2.0 ml of SPA solution were mixed with 35 μl of rabbit IgG (82 mg/ml) specific for HSA. The SPA has a high molecular weight ($>10^6$) and is insoluble. The SPA-αHSA complex retains specific affinity for HSA and HDI, and the resulting SPA-αHSA-HDI/HSA complexes are easily separated from solution by centrifugation. A series of HSA solutions, ranging in concentration from 0 to 40 μg/ml, in 0.1 *M* citrate (pH 7.50) was prepared.

The assay protocol is outlined in Fig. 25. Briefly 110μl of HDI (1.038 mg/ml stock) and 36 μl of SPA-αHSA are added in order to a 5.0 ml HSA sample, mixed in 12 × 75 mm polystyrene serological tubes and incubated at 37°C for 1 h. The tubes are centrifuged for 20,000 g-min, and the supernate discarded. This supernate contains excess protein, and only HSA or HDI bound to SPA remains within the tubes. The pellets are rinsed with 0.1 *M* citrate (pH 7.50) and resuspended in 0.1 *M* citrate (pH 1.50) which releases In^{3+} bound in the HDI complexes. The tubes are centrifuged a second time for 30,000 g-min to pellet the SPA-HSA-Ag complexes. The free In^{3+} concentration in the supernatant liquid is then determined by DPASV.

IV. CONCLUSIONS

The combination of antibody selectivity with the low detection limits of modern electrochemical techniques results in a powerful analytical tool. Electrochemical methods are free from problems of sample turbidity, quenching, and interferences from the many absorbing and fluorescing compounds in typical biological samples that interfere with spectroscopic techniques. Although electrode fouling is generally a problem with samples of biological origin, this potential difficulty has been effectively circumvented in the assays described here. The relatively simple instrumentation requirements for LCEC and FIAEC are advantageous compared to other types of immunoassays. Automation of these systems would substantially decrease the analyst's time by allowing most of the assay protocol to be implemented unattended. Detection levels in the low pg/ml range on 20 μl samples ($\sim 10^{-18}$ mol of analyte) have been achieved for both large and small molecules. In these cases the limit of detection was restricted by factors such as the antibody antigen binding constant and nonspecific adsorption of the labeled compound, rather than the electrochemical technique. Consequently even lower detection levels should be possible.

References

Abramson, F. B. (1982), *Clin. Pharmacol. Ther., 32*, 652.

Adams, J. B., and Wacher, A. (1968), *Clin. Chem. Acta, 21*, 155.

Alam, A. I., and Christian, G. D. (1982), *Anal. Lett., 15*, 1449–1456.

Alam, A. I., and Christian, G. D. (1984), *Fr. Z. Anal. Chem., 318*, 33–36.

Alam, A. I., and Christian, G. D. (1985), *Fr. Z. Anal. Chem., 320*, 381–384.

Apffel, J. A., Alfredson, T. V., and Majors, R. E. (1981), *J. Chromatogr., 206*, 43–57.

Blaedel, W. J., and Boguslaski, R. C. (1978), *Anal. Chem., 50*, 1026–1032.

Bradford, M. (1976), *Anal. Biochem., 72*, 248–254.

Bresnahan, W. T., Moiroux, J., Samec, Z., and Elving, P. J. (1980), *Bioelectrochem. Bioenerg., 7*, 125–155.

Breyer, B., and Radcliff, F. J. (1951), *Nature, 167*, 79.

Breyer, B., and Radcliff, F. J. (1953), *Austral. J. Exp. Biol., 31*, 167–172.

Brooks, M. A. (1984), in *Laboratory Techniques in Electroanalytical Chemistry* (P. T. Kissinger and W. R. Heineman, Eds.), Dekker, New York, chap. 21.

Brunk, S. D., and Malmstadt, H. V. (1977), *Clin. Chem., 23*, 1054–1056.

Buchholz, K., Godelmann, B., and Molnar, I. (1982), *J. Chromatogr., 238*, 193–202.

Czaban, J. D. (1985), *Anal. Chem., 57*, 345A–356A.

de Alwis, W. U., and Wilson, G. S. (1985), *Anal. Chem., 57*, 2754–2756.

Dietzler, D. N., Weidner, N., Tieber, V. L., Mcdonald, J. M., Smith, C. H., Ladenson, J. H., and Leckie, M. P. (1980), *Clin. Chem. Acta, 101*, 163–181.

Doyle, M. J., Halsall, H. B., and Heineman, W. R. (1982), *Anal. Chem., 54*, 2318–2322.

Doyle, M. J., Halsall, H. B., and Heineman, W. R. (1984), *Anal. Chem., 56*, 2355–2360.

Eggers, H. M., Halsall, H. B., and Heineman, W. R. (1982), *Clin. Chem., 28*, 1848–1851.

Ekins, R. P., and Newnan, G. B. (1970), *Acta Endocrinol., 147*, 11.

Ekins, R. (1981), in *Monoclonal Antibodies and Developments in Immunoassay: Proceedings of the 3rd International Conference on Radioimmunoassay* (A. Albertini and R. Ekins, eds.), Elsevier, Amsterdam, p. 3.

Elving, P. J., Bresnahan, W. T., Moiroux, J., and Samec, Z. (1982), *Bioelectrochem. Bioenerg., 9*, 365–378.

Eriksen, P. B., and Andersen, O. (1978), *Clin. Chem., 25*, 169–171.

Erni, F., Keller, H. P., Morin, C., and Schmitt, M. (1981), *J. Chromatogr., 204*, 65–76.

Gendler, S. J., Dermer, A. B., Silverman, L. M., and Tokes, Z. A. (1982), *Cancer Res., 42*, 4567.

Hardie, G., van Regenmortel, M. H. V. (1977), *J. Immunol. Methods, 15*, 305–314.

Heineman, W. R., Anderson, C. W., and Halsall, H. B. (1979), *Science, 204*, 865–866.

Heineman, W. R., and Halsall, H. B. (1985), *Anal. Chem., 57*, 1321A–1328A.

Heineman, W. R., Mark, Jr., H. B., Wise, J. A., and Roston, D. A. (1984), in *Laboratory Techniques in Electroanalytical Chemistry* (P. T. Kissinger and W. R. Heineman, eds.), Dekker, New York, chap. 19.

Ikariyama, Y., Kunoh, H., and Aizawa, M. (1985), *Biochem. Biophys. Res. Commun., 128*, 987–992.

Itzhaki, R. F., and Gill, D. M. (1964), *Anal. Biochem.*, *9*, 401–410.

Jackson, P. R., Tucker, G. T., and Woods, H. F. (1982), *Clin. Pharmacol. Ther.*, *32*, 295.

Jamieson, J. C., Ashton, F. E., Frieson, A. D., and Chou, B. (1972), *Can. J. Biochem.*, *50*, 871.

Jarvis, R. F. (1979), *Antibiotics Chemother.*, *26*, 105.

Kissinger, P. T. (1984), in *Laboratory Techniques in Electroanalytical Chemistry* (P. T. Kissinger and W. R. Heineman, eds.), Dekker, New York, pp. 152–154.

Konyves, I., and Olsson, A. (1964), *Acta Chem. Scand.*, *18*, 483–487.

Krejcarek, G. E., and Tucker, K. L. (1977), *Biochem. Bipohys. Res. Commun.*, *77*, 581–585.

Linday, L., and Drayer, D. E. (1983), *Clin. Chem.*, *29*, 175–177.

LKB News (1984), spring.

Losev, V. V., and Moledov, A. I. (1976), in *Encyclopedia of Electrochemistry of the Elements* (A. J. Bard, ed.), Vol. 6, Dekker, New York.

Morgan, S. L., and Deming, S. N. (1974), *Anal. Chem.*, *46*, 1170.

Ngo, T. T., Bovaird, J. H., and Lenhoff, H. M. (1985), *Appl. Biochem. Biotech.*, *11*, 63–70.

Orten, J. M., and Neuhaus, O. W. (1982), in *Human Biochemistry*, 10th ed., C. V. Mosley, St. Louis, p. 437.

Parsons, G. H. (1981), in *Methods of Enzymology* (J. J. Langone and H. Van Vunakis, eds.), Academic Press, New York.

Proceedings of the International Meeting on Chemical Sensors, Fukuoka, Japan, Sept. 19–23, 1983. Kodanasha: Tokyo, 1983.

Rashid, S. A., O'Quigley, J., Axon, A. T. R., and Cooper, E. H. (1982), *Br. J. Cancer*, *45*, 390.

Rosenthal, A. F., Vargas, M. G., and Klass, C. S. (1976), *Clin. Chem.*, *22*, 1899–1902.

Roumeliotis, P., and Unger, K. K. (1979), *J. Chromatogr.*, *185*, 445–452.

Rumley, A. G., Trope, A., Rowe, D. J. F., and Hainsworth, I. R. (1980), *Ann. Clin. Biochem.*, *17*, 315–318.

Schmidt, Jr., D. E., Giese, R. W., Conron, D., and Karger, B. L. (1980), *Anal. Chem.*, *52*, 177–182.

Schneider, H., and Sehon, A. H. (1961), *Trans. N. Y. Acad. Sci.*, *24*, 15–22.

Sharpe, R. I., Cooreman, W. M., Bloome, W. J., and Leakeman, G. M. (1976), *Clin. Chem.*, *22*, 733.

Steinhardt, J., and Reynolds, J. A. (1969), *Multiple Equilibria in Proteins*, Academic Press, New York, p. 58.

Svoboda, G. J. (1981), Ph.D. Dissertation, Duke University.

Vea-Martinez, A., Gatell, J. M., Sequra, F., Heiman, C., Elena, A., Ballsta, A. M., and Mundo, M. R. (1982), *Cancer*, *50*, 1783.

Wang, J. (1985), *Stripping Analysis*, VCH Publishers, Deerfield Beach.

Weber, S. G., and Purdy, W. C. (1979), *Anal. Lett.*, *12*, 1–9.

Wehmeyer, K. R., Doyle, M. J., Wright, D. S., Eggers, H. M., Halsall, H. B., and Heineman, W. R. (1983), *J. Liq. Chromatogr.*, *6*, 2141–2156.

Wehmeyer, K. R., Halsall, H. B., and Heineman, W. R. (1982), *Clin. Chem.*, *28*, 1968–1972.

Wehmeyer, K. R., Halsall, H. B., and Heineman, W. R. (1985), *Clin. Chem.*, *31*, 1546–1549.

Wehmeyer, K. R., Halsall, H. B., Heineman, W. R., Volle, C. P., and Chen, I.-W. (1986), *Anal. Chem.*, *58*, 135–139.

Wellington, D. (1980), in *Enzyme Immunoassay* (E. T. Maggio, ed.), CRC Press, Boca Raton, FL, chap. 12.

Wisdom, G. B. (1976), *Clin. Chem.*, *22*, 1243.

Yalow, R. S., and Berson, S. A. (1959), *Nature (London)*, *184*, 1649–1658.

Yalow, R. S., and Berson, S. A. (1964), in *The Hormones* (G. Pincus and K. V. Thiamin, eds.), Academic Press, New York.

Yalow, R. S., and Berson, S. A. (1971), in *Principles of Competitive Protein-Binding Assays* (W. D. Odell and W. H. Daugherty, eds.), Lippincott, Philadelphia.

Methods of Biochemical Analysis, Volume 32
Edited by David Glick
Copyright © 1987 by John Wiley & Sons, Inc.

Author Index

Methods of Biochemical Analysis, Volume 32
Edited by David Glick
Copyright © 1987 by John Wiley & Sons, Inc.

Subject Index

Methods of Biochemical Analysis, Volume 32
Edited by David Glick
Copyright © 1987 by John Wiley & Sons, Inc.

Cumulative Author Index, Volumes 1–32 and Supplemental Volume

Methods of Biochemical Analysis, Volume 32
Edited by David Glick
Copyright © 1987 by John Wiley & Sons, Inc.

Cumulative Subject Index, Volumes 1–32 and Supplemental Volume